

'Devourer of Gods'

The palaeoecology of the Cretaceous pliosaur

Kronosaurus queenslandicus

A dissertation by

Colin Richard McHenry B.Sc.(Hons)

submitted for the degree of

Doctor of Philosophy

University of Newcastle

April 2009

This thesis contains no material which has been accepted for the award of any other degree or diploma in any university or other tertiary institution and, to the best of my knowledge and belief, contains no material previously published or written by another person, except where due reference has been made in the text. I give consent to this copy of my thesis, when deposited in the University Library, being made available for loan and photocopying subject to the provisions of the Copyright Act 1968.

Colin Richard McHenry

Contents

	Preface and acknowledgements	ii
1	An introduction to big pliosaurs, and the question of what they ate?	1
2	Methods: using biomechanics to reconstruct palaeoecology in fossil carnivores	51
3	Geological context: palaeoenvironment, palaeofauna, and taphonomy of marine reptile fossils in the Great Artesian Basin	87
4	Form and function in <i>Kronosaurus queenslandicus</i> , part 1: Form (2-D)	167
5	Form and function in <i>Kronosaurus queenslandicus</i> , part 2: Form (3-D)	287
6	The anatomy, taxonomy, and ecology of body size in large pliosaurs	357
7	Form and function in <i>Kronosaurus queenslandicus</i> , part 3: Function	461
8	The palaeoecology of <i>Kronosaurus queenslandicus</i>	539

The large pliosaur *Kronosaurus queenslandicus* is known from numerous specimens from the Early Cretaceous marine sediments of the Australian Great Artesian Basin. The preservation of these specimens in nodular limestone generally lacks pronounced taphonomic distortion, allowing the three-dimensional shape of the osteology, in particular the skull, to be inferred with confidence. Three-dimensional geometry is critical data for the functional analyses that can form the basis for reconstruction of palaeoecology, in particular, approaches based in computational biomechanics that make use of high resolution Finite Element Modelling. These techniques have been used successfully to infer diet and feeding behaviour in various species of extinct carnivore, and are here applied to a species of large pliosaur for the first time.

The cranial anatomy of *Kronosaurus queenslandicus* is here summarised for the first time, and outstanding questions concerning the taxonomy of the relevant material are addressed as fully as possible given available data. Overall body proportions and size are estimated in the context of other known material from specimens of large pliosaurs. The material examined supports the hypothesis that there is one species of large pliosaur in the Late Albian the Great Artesian Basin, and this material is referred to *Kronosaurus queenslandicus* Longman 1924. Material from the Late Aptian of the Great Artesian Basin is also *Kronosaurus*, and is presently referred to *Kronosaurus queenslandicus* Longman 1924: however questions about the anatomy of *Kronosaurus boyacensis* Hampe 1992 mean that further examination of material to hand, or recovery of new specimens from the Late Aptian, may require the taxonomic status of the Late Aptian material to be reviewed. *Kronosaurus* is a member of the Brachaucheniidae Williston 1925. Maximum size is 10.5 metres total length and approximately ~11,000 kg body mass.

Biomechanical analysis of the skull of *Kronosaurus* shows that it had a high bite force, comparable to that predicted for a hypothetical similar sized saltwater crocodile *Crocodylus porosus*. The magnitude of its maximum bite force, around

30,000 Newtons, was likely exceeded by *Tyrannosaurus rex* and *Carcharocles megalodon*. Finite element modelling of the skull, compared with the skull of a 3.1 metre *Crocodylus porosus*, suggests that the skull of *Kronosaurus* carried more strain under loads simulating feeding on large prey. Accordingly, maximum prey size, relative to predator body size, is interpreted as lower in *Kronosaurus* than for a 3.1 metre *C. porosus*, although the magnitude of this limit is unknown due to incomplete data on the feeding ecology of *C. porosus*. Other evidence, from functional morphology, taphonomy, and comparison with extant aquatic carnivores suggests that *Kronosaurus* was the apex predator of the Australian Early Cretaceous inland seas. Relatively small prey were likely to be an important component of the diet of *Kronosaurus*, although certain morphological features of the skull appear to have permitted predation upon larger prey when available. Several of these morphological features may constitute evolutionary adaptations to the conflicting mechanical demands of feeding on small and large prey.



Kronosaurus, by John Conway

Preface and acknowledgements

The work presented in this thesis is the culmination of a prolonged attempt to come to grips with the remarkable fossils of *Kronosaurus queenslandicus*, combined with an interest in how large marine animals make their living in that fascinating environment. My pathway to this point has perhaps been unconventional (but are not all Ph.D.s unique?); I have had two attempts at completing a Ph.D. on *Kronosaurus*, the first at the University of Queensland during the 1990s, and the second (described herein) at the University of Newcastle in more recent years. The first attempt, which aimed to provide a ‘traditional’ account of the anatomy of this species, was thwarted by a combination of the logistics of the fossil material (the two main specimens took several years to reassemble and did not cooperate with attempts to prepare them) and my own naivety, but it was during this time that I started to wonder about how the palaeoecology of fossil species might be reconstructed from morphological data. That curiosity led to an interest in biomechanics as a possible means of investigating the link between anatomy and ecology, an area which I started to explore whilst in Queensland but which I was able to develop more fully after I started work at the University of Newcastle in 2003. That work in turn led to the approach that I have sought to apply to the *Kronosaurus* material in this thesis.

Of course, doing it this way around has had its share of frustrations, for myself but undoubtedly more so for my long-suffering family, but it has also been an interesting learning experience – the convoluted pathway that I have followed has exposed me to a large range of science and scientists who are linked with research into palaeontology, marine science, ecology, geology, anatomy, biomechanics, and so forth. Throughout, I have been amazed by the good will of the many people who have offered their help, whether logistical or technical, who have been prepared to share their knowledge and patiently explain things to me, and who

have simply offered encouragement. Although it is impossible to list all of these people here, I am very grateful to everyone who have provided such assistance to this work.

Tony Thulborn gave me the opportunity for the first attempt to do a Ph.D. on the Queensland material, and the staff and students the Dept. Zoology at the University of Queensland provided a stimulating environment for this work; in particular, I'd like to thank Kate Arnold, Maurizio Bigazzi, Damien Broderick, Cullum Brown, Carol Burrow, Anne Cameron, Sonia Clegg, Terry Dyer, Nancy Fitzgibbon, Joanne Ford, Craig Franklin, Tom Gorringe, Kathryn Green, Gordon Grigg, Les Hall, Mark Hamman, Andrew Hugal, Tim Jessop, Peter Kind, Louise Kuchel, Janet Lanyon, Petra Lundgren, Ian Owens, Russell Palmer, Mark Read, Chloe Schäuble, Frank Seebacher, David Souter, Joanna Sumner, Mel Venz, Robbie Wilson, and Louise Wynan. Peter Dwyer and Tim Hamley did an effective job of challenging my preconceptions on how evolutionary biology and palaeontology work, and Tony Tucker provided much of the early stimulus in thinking about the functional morphology of crocodiles. At the same time, the help and support of the staff at the Queensland Museum was invaluable, especially that of Peter Arnold, Alan Bartholomai, Laurie Beirne, Nat Camalleri, Bernie Cooke, Patrick Cooper, Jeanette Covacevich, Heather Janetzki, Phil Lawless, Ralph Molnar, Don McKenzie, Sue Turner, Mary Wade, and Jo Wilkinson. The Australian Vertebrate Palaeontology community is a small one, but they made me feel welcome; Mike Archer, Ross Damiani, Ben Kear, Robert Jones, Noel Kemp, John Long, Caroline Northwood, Tom Rich, John Scanlon, Anne Warren, Paul Willis, and Adam Yates all provided assistance at different times and I am grateful to them.

One of the many joys of this type of work is the opportunity to spend time in 'the field'; in this case, the spectacular landscape of north and western Queensland. In the course of this work I've had the chance to meet some of the characters who

are a large part of the charm of this landscape, and without them much of the work contained in this thesis would have been impossible. They are too many to list, but I'd like to thank especially Margaret and Hugh Dick, Marlin Entriiken, Robbie Ievers, Ian Ievers, Ninian and Ann Stewart-Moore, and John Towning.

Another joy of this work has been the opportunity (excuse?) to visit some collections in museums around the world, and although this is hard work usually undertaken without sufficient funds, it is an incredible experience for any student. Without assistance from a lot of people, though, it would be impossible: the help and support of Pat Holroyd, John Hutchinson, Kevin Padian, Jim Parham, and Sam Welles at UCMP Berkeley; Peter Robinson at Boulder and Ken Carpenter and Logan Ivy at Denver; Arthur Cruickshank and John Martin at Leicester; Michael Benton and Roger Clark in Bristol; Sandra Chapman, Colin McCarthy, and Angela Milner at the Natural History Museum in London; Leslie Marcus and Mark Norrell at the AMNH in New York; Farish Jenkins and Charles Schaff at the MCZ in Harvard; Mike Brett-Surman, Jim Mead, and Andy Ross at the Smithsonian; Steve Salisbury and Dino Frey at Karlsruhe; Rupert Wilde at Stuttgart; Mike Everhart, Greg Liggett, and Bruce Schumacher at the Sternberg Museum; and Olivier Rieppel, Bill Simpson, and Kenshu Shimada in Chicago. In addition to access to specimens, many of these provided meals and floor space, for which I am especially grateful, as I am to Rich and Brigitte Crawley, Pete Edwards, Hank Guarisco, Julia Howard, Guy Hills-Spedding, and Paul Wilson.

Part of the journey of this Ph.D. has been from student to 'proper' scientist (whatever that is), and I would like to acknowledge several people who have played an important role in that journey. My early interest in biology and the sea I owe to my father, Felix McHenry, no doubt fuelled by a diet of David Attenborough's work. The Biology Dept. at King's College Taunton, led by Jim Scott and Roger Poland, fanned the flames of this interest, and the students and staff at the University of Southampton converted it into a professional pathway;

John Allen, Keith Anderson (and the denizens of the Pastry Lab), Frank Bisbey, Michael House, Rory Putman, Tom Sherratt, and Michael Sleigh are gratefully acknowledged in this respect. In particular, Michael House suggested doing a Ph.D. in Australia, and Jeremy Rayner was supportive of this wild idea.

One of the most enjoyable parts of science are the animated discussions about arcane subjects, often in association with late nights and beer, and the wide scope of this thesis means that I've been able to do this with a lot of different people who deserve thanks for their patience and generosity: Of course, the 'Plesiosaur' people figure strongly in such a list; David Brown, Ken Carpenter, Arthur Cruickshank, Pat Druckenmiller, Mark Evans, Richard Forrest, Marcela Gomez, Oliver Hampe, Hilary Ketchum, Espen Knutsen, Dave Martill, Adam Morrell, Betsy Nicholls, Leslie Noè, Adam Smith, Glen Storrs, Michael A. Taylor, and Bill Wahl. Patrick Vignaud and Jean-Michel Mazin organised the first symposium of Secondary Adaptation of Tetrapods to the Water in Poitiers, which allowed me to meet some of the amazing people working in marine palaeontology and biology, and many of these have been very kind with their help, especially Paul Brodie, Daryl Domning, and Frank Fish. Within the wider vertebrate palaeontology community Chris Brochu, Jeff Liston, David Norman, and David Unwin provided discussion and entertainment. The kindness, encouragement, and support of Arthur Cruickshank, Jim Farlow, Ewan Fordyce, Chris McGowen and Mason Meers is especially appreciated, as is the generosity of Adam Britton in providing materials and sharing expertise: the same thanks go to Tim Rowe and the DigiMorph staff. Similarly, the 'Biomechanics' people have provided much necessary enlightenment and discussion; Mike Bennett, Betsy Dumont, Ian Jenkins, Keith Metzger, Paul O'Higgins, Emily Rayfield, Ryan Ridgely, Callum Ross and Larry Witmer. Bill Daniel enabled my first foray into the delights of FEA, and Holger Preuschoft, Eric Snively, Jeff Thomason, and Ulrich Witzel have provided much needed advice and encouragement.

Of course, in the internet age discussion by correspondence is an important part of staying in touch with the field, and many of the people who I have met on line (mainly, through the Dinosaur Mailing List) have since become friends as well as colleagues; in particular, Jim Cunningham, John Conway, Darren Naish, Mike P. Taylor, and Dan Varner. Many others in the online 'vert-paleo' community have helped with copies of hard-to-get papers and pdfs, and this help, along with the library staff at the different institutions that I have worked at, is much appreciated; Tracey Ford and Corey Sullivan especially went out of their way to provide this assistance. Chris Sloan and Richard Ellis helped me to understand how my scientific efforts might be of interest to the wider community, and Ernie Lundelius is thanked for random acts of kindness.

I am particularly grateful to Ron Boyd for the opportunity to have another crack at *Kronosaurus* at the University of Newcastle: I am also very appreciative of the encouragement and assistance I have received from my colleagues there; Richard Bale, Katherine Boyachuk, Alan Brichta, Bob Callister, John Clulow, Claudia Diaz, Gary Ellem, Dean Ferry, Peter Garfoot, Doug Gillespie, Ian Goodwin, Karel Grezel, Liz Huxtable, Josh Kautto, Shane Keys, Erich Kisi, Bill Landenburger, Kira Mileham, Mike Mahony, Bill McBride, Anna McConville, Geoff McFarlane, Robin Offler, Tina Offler, Phil Peady, Lea Petrovic, Tim Rolph, Graeme Murch, and Jenny Wandsworth. To John Rodger I am especially grateful for his invaluable help and support. During this phase of my work various people in Queensland were most helpful, including Christina Cook, Chris and Kathy Glen, Scott Hocknull, Kristen Spring, and Paul Stumkat. Being able to develop this work as part of a vital and engaging research group has been a privilege and a pleasure, and I thank my colleagues and students in the CBRG; especially Karen Moreno for her help with the programming, and Janet Ingle and Frith McLellan for generating data that was very useful to Chapters 7 and 8 of this thesis. Eleanor Cunningham and the staff of the CT unit at the Newcastle Mater Hospital have very kindly

provided the access to their facilities which has made much of the work herein possible.

This work would not have been possible without my advisory committee; in addition to reading through drafts of chapters and so forth, Alex Cook helped me to understand the palaeontology of the Great Artesian Basin, Phil Clausen and Steve Wroe helped with the biomechanical modelling, and Ron Boyd provided sage advice on structure and scope. To Alex, Phil, and Steve I owe particular thanks for their constant help and support over the years.

This thesis is, in the main part, an inter-disciplinary work, and so I have tried to write it so that it can be understood by readers from a range of disciplines. Unfortunately, this goal often requires more words, and so has exacerbated my tendency to long-windedness. I am therefore very grateful to my wife, Sarah, for valiantly proof reading the whole thing, although of course any remaining errors are entirely my responsibility, and to my children Finn and Cormac and their grandmother Inez for providing various forms of incentive to finish this thesis. To all of my family, thanks for your patience, and to my mother Rionagh, thanks for the inspiration.

Newcastle, April 2009.

For
Sarah, Finn, and Cormac
and
Rionagh.

In Memory of
Tim Hamley
Sorely missed but never forgotten.

Nov 25

9 1192

A. Crombie Esq

Dear Sir

I have to day
received the fossil of which you
write and for which I venture to
anticipate the formal thanks of
the Trustees; from your letter I
concluded that I should have to
record a new locality for fossils of
the age of the Darling Downs drifts
but my expectations are exceeded
it dates from a much more remote
time when the flood and most of
the western and northern country
was at the bottom of the Cretaceous
sea - It is a piece of the snout of one
of the great fish-lizards of those times
- an Enaliosaurus - the tail of this
reptile are quite new to me, you
may judge therefore that I place
great value

This specimen and shall carefully preserve it
unfortunately your request that I should write an
account of it for the public journals is just at present
difficult to comply with I am in the midst of
being up for removal to new quarters a work which
scarcely demands my whole time and thought
with therefore ask you to excuse me until I get settled
at Bowen Park

Yours very truly

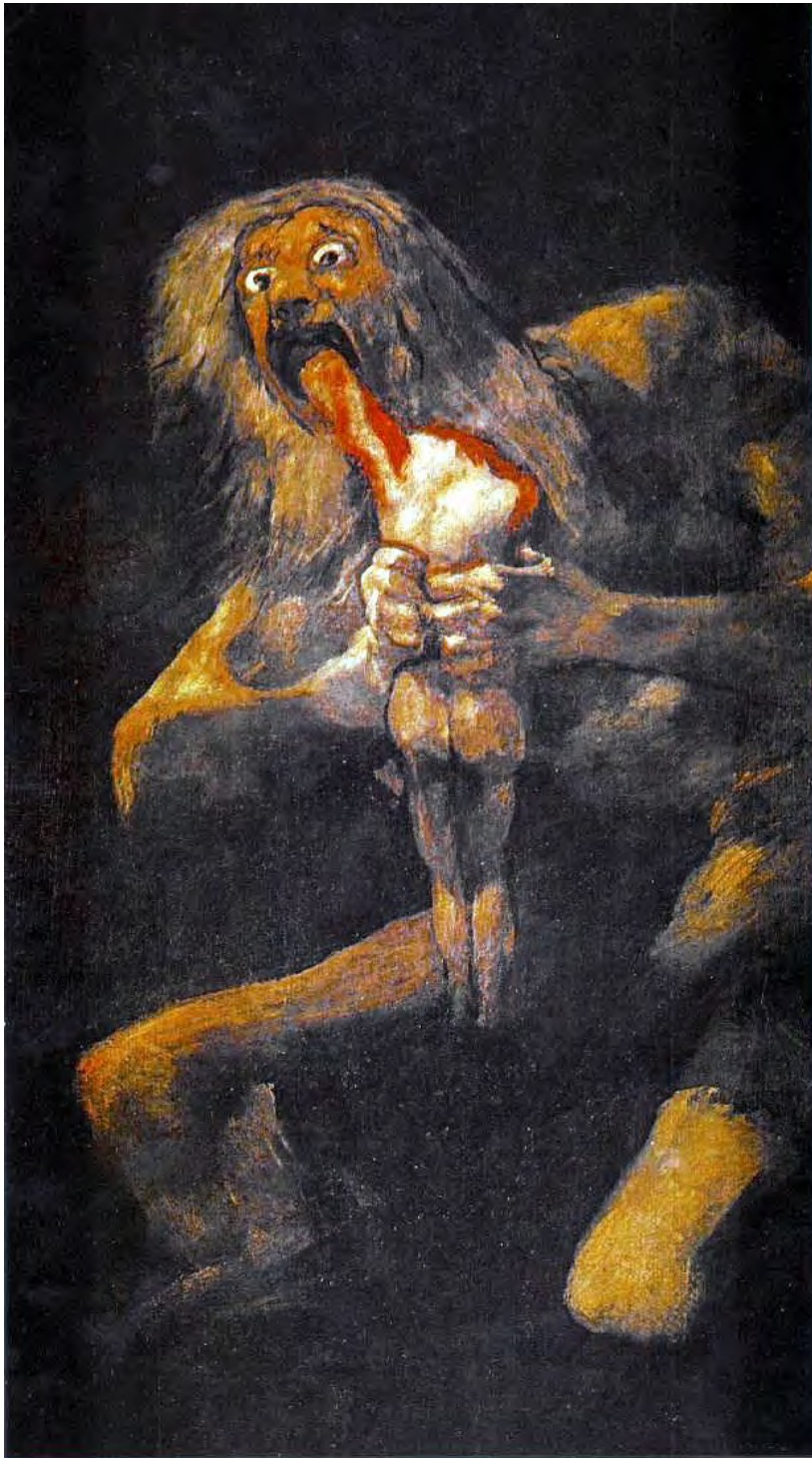
C. de Vis

Barator

The selenite contents of the tooth cavities are
very interesting and uncommon

Letter from Charles de Vis to Andrew Crombie, acknowledging receipt of the specimen that was to become the holotype of *Kronosaurus queenslandicus*. The letter was sent in 1899 (Queensland Museum Archives).

1. Big pliosaurs



Kronos devouring his son: Francisco Goya, 1819

“Many were increasingly of the opinion that they'd all made a big mistake in coming down from the trees in the first place. And some said that even the trees had been a bad move, and that no-one should ever have left the oceans”.

Douglas Adams, *The Hitchhiker's Guide to the Galaxy*.

1.1 **The return to the sea: a history of big pliosaurs**

The evolution of the amniotes, the first group of vertebrates able to live their entire lives out of water, is seen as a pivotal point in the evolution of life on Earth. The key physiological innovations that permitted a terrestrial lifestyle were the development of a water-tight skin, efficient kidneys that minimised water loss, and a water-tight egg – the latter a property of the eponymous amniotic egg membrane. Once the beach-head on the dry land had been secured by about 350 million years ago, the amniotes diversified into two major lines; the synapsids (mammals and their ancestors), and the sauropsids. The latter are better known by their old English name, the reptiles.

At this point most accounts then focus upon the events leading to the dawn of the great ‘Age of the Reptiles’, also known by its technical name, the Mesozoic Era. Commencing 251 million years ago with the dawn of the Triassic Period, the story of the Mesozoic follows the recovery of global ecosystems from the Great Dying of the end-Permian extinctions (Erwin 1991), through the rise of the most famous reptile group of all, the dinosaurs, in the Triassic and Jurassic Periods, and finishes with another extinction – one that killed off the dinosaurs at the end of the Cretaceous Period some 65 million years ago and which set the stage for the rise of our own group, the mammals. It’s a version of events that, having established the link between the reptiles and their water-bound ancestors, tends to focus upon the terrestrial story. And while there are many amazing aspects of this story, it misses one very important and recurring theme of amniote evolution – the return to an aquatic existence.

Almost as soon as they relinquished their dependence on the aquatic environment, the amniotes started to move back into it. Unlike their amphibian ancestors, their water-proof skin and improved osmoregulatory physiology enabled them to make a

Big pliosaurs

living in the salt-laden environment of the world's oceans; indeed, one of the consistent themes of amniote history is the frequency with which they returned to the sea (Ellis 2003, Williston 1914). Few lineages made the transition prior to 250 million years ago, but during the Mesozoic the reptiles made numerous independent reinvasions of the sea or freshwater (Benton 1990). Since the Cretaceous, most of the aquatic incursions have been made by various groups of those highly specialised reptiles, the birds, but they have been joined by numerous groups of synapsids, with several mammalian lineages going back to the seas and streams (Jefferson et al. 1993).

Of all the groups that returned to the sea, arguably the most successful - and perhaps the most bizarre to our eyes - were the plesiosaurians, a sauropterygian order which achieved a prolonged dominance of the oceans for most of the Jurassic and Cretaceous. Most groups of marine reptiles and mammals are remarkable because they resemble one of two basic body forms - either tunniform in shape, resembling a tuna fish or a lamnid shark (e.g. ichthyosaurs, cetaceans, phocids, sirenians); or crocodylian with an elongate torso and tail (e.g. mesosaurs, crocodiles, nothosaurs, askeptosaurs, mososaurs). In these cases the limbs are much reduced, the hind limbs of cetaceans and sirenians becoming completely atrophied. In contrast with these more usual patterns, the body form of the plesiosaurians is rather unique; the tail is greatly shortened, the torso short but rotund, and both pairs of limbs are greatly enlarged into huge paddles. What takes many species of plesiosaur from unusual to bizarre is a tiny skull set atop a neck so long that in many cases it exceeds the length of the rest of the skeleton – seen in its most extreme form in the ultra long-necked Cretaceous family *Elasmosauridae*.

A major plesiosaurian group, the 'pliosaurs', resemble the long-necked plesiosaurs from the tail to the shoulder, but instead of the long neck and small head they have an enormous skull at the end of a greatly reduced neck. Indeed the skull of the largest pliosaurs are so huge only the skulls of large cetaceans and some species of ceratopsian dinosaur are bigger. This robust skull held rows of large caniniform teeth, and the pliosaurs are interpreted as the major marine predators for much of the Mesozoic.

If longevity is any measure of success, then the pliosaurs must count as one of the most successful groups of vertebrate of all. From the beginning of the Jurassic Period until at least half way through the Cretaceous – a period of 115 million years – pliosaurs were a consistent component of marine ecosystems, occupying the same set of niches worldwide. Their obscurity belies the fact that they were one of the first groups of fossil reptiles to be recognized by modern science, and is all the more surprising given that the particular niche that they held down for all that time was that of apex predator, a role that looms large in popular imagination – consider the instant recognition of the pliosaurs' terrestrial counterparts, *Tyrannosaurus rex* and the sabre-toothed cat.

In many ways, pliosaurs were the Mesozoic equivalent of modern toothed whales, matching odontocetes in the range of body sizes (from 2 metres for the smallest to 15-18 metres for the largest) and geographical distribution, but greatly exceeding the 30 million years that toothed whales have managed so far. Their story is one that is rarely told, but it is a good one. In one sense, it started nearly two centuries ago, just as science was starting to come to grips with both the enormity of geological time and the monstrosity of the creatures that had preceded our modern world. Since pliosaurs arguably embody each of these qualities better than any other reptile, they are an especially apt guide to the beginnings of modern palaeontology, deep in the rooms of a London hall some 180 years ago....

The first Enaliosaurs

In 1821 Henry De la Beche and the Reverend William Daniel Conybeare gave the learned gentlemen of the Geological Society of London "notice of the discovery of a new fossil animal forming a link between the *Ichthyosaurus* and the crocodile" (De la Beche and Conybeare 1821). The fossils of *Ichthyosaurus*, recording an animal with the gross form of a large fish but the osteological details of a reptile, had been described by Sir Everard Home some years previously (Home 1814), and its name ('fish-lizard') described the opinion of the time that it formed some link between fish and reptiles. As the title of their first communication reveals, De la Beche and Conybeare believed that the new form was even closer to the crocodiles; the name they gave it, *Plesiosaurus*, means "near reptile". The structure of its limbs, which were developed into large paddles like those of *Ichthyosaurus*, revealed that it too was a

Big pliosaurs

water living creature. In 1824 Conybeare offered a further paper detailing the first complete fossil of the *Plesiosaurus* (the previous material, though diagnostic, was not complete). The new specimen (Figure 1-1) showed that, instead of being flattened from side to side as was *Ichthyosaurus*, *Plesiosaurus* was flattened from top to bottom, like the sea turtles of recent times (Conybeare 1824). The torso was not elongated, and showed the limbs had been modified into paddles; again, a pattern similar to that of turtles, a slight deviation being that in the extinct form all four limbs were of equal size. There the similarities seemed to end - *Plesiosaurus* bore no shell or armour, but most remarkable of all was the neck, which it was composed of 40 vertebrae and exceeded in length the rest of the vertebral column put together. The head, being relatively tiny in size, also distinguished the creature from the fish-lizards and the crocodiles, but when Conybeare gave the first name to this species he named it after its most noticeable feature - *Plesiosaurus dolichodeirus* means "long-necked near reptile"¹.



Figure 1-1: The spectacular type specimen of *Plesiosaurs dolichodeirus*. This specimen was the first insight afforded to modern science of the bizarre (but evidently successful) plesiosaurian bodyplan.

¹ Like others of their time, these gentlemen believed that the Creator had ordered living beings according to a grand *Scala Naturala*, a chain of being upon which the whole spectrum of life could be placed between the simplest forms (such as the unicellular microscopic organisms) and the most complex (unanimously agreed to be Mankind) in an orderly linear sequence. The discovery of this Scale was held to be the correct purpose of the Naturalist-Theologian, a purpose well illustrated by the title of the Reverend Buckland's work on Natural Theology; "The Bridgewater Treatises on the Power, Wisdom, and Goodness of God as Manifested in His Creation" (Buckland, 1836).

Yet even as he christened the first species of plesiosaurian, Conybeare drew attention to some bones that were common in the Kimmeridge Clay, a strata much younger than the Liassic rocks of Lyme Regis that preserve *Plesiosaurus dolichodeirus*. This other form, known only to Conybeare from small sequences of vertebrae, bore many resemblances to that of *Plesiosaurus*, and Conybeare declared them to belong to that genus (Conybeare, 1824). They were much larger, but the chief difference was that the vertebrae from the neck region were much shorter than those from the neck of the Lyme Regis animal, even though the bones of the former were much greater in diameter. He also mentioned a fossil of a similar animal, from Market Ramsen in Lincolnshire, that had just been procured by the Rev. Buckland. Conybeare concluded that, when found, the younger and larger form would differ from the genoholotype in having a shorter neck, and dubbed it *Plesiosaurus giganteus*.

In 1841 Sir Richard Owen gave account of the Market Ramsen fossil, a partial skeleton from the Kimmeridge Clay (Owen 1841)². He described an animal that shared with *P. dolichodeirus* the general form of the torso, limbs, and tail; where it differed was not only in the comparative shortness of the neck (as Conybeare had surmised) but in the huge size of its head, teeth, and jaws. Owen named the Market Ramsen specimen *Plesiosaurus brachydeirus*, which means "short-necked near reptile", but considered that the new species was sufficiently different from *P. dolichodeirus* to warrant its inclusion in a separate sub-genus or genus, for which he proposed the name '*Pliosaurus*'³ (Owen 1840-1845). Since this distinction describes a fundamental difference in body form between those plesiosaurians with long necks and small heads, and those with short necks and large heads, these species are considered to be the types of the two great subdivisions within the Order Plesiosauria, the Plesiosauroidea and the Pliosauroidae.

Just how different pliosaurs were to their long-necked cousins was made evident when Owen published a review of the Kimmeridgian plesiosaurs (Owen 1869),

² There is some confusion over the correct citation dates for several of Owen's publications during the 1840s – see the range of dates offered for *Odontography* – and the date (and page numbers) of this report is an example; it is given by several authors as 'Owen (1942) Report on British fossil reptiles, Part II. Report of the British Association of the Advancement of Science, London, pp 60-204'.

³ Owen originally spelt this as "Pleiosaurus", but the name was modified afterwards to the modern spelling.

Big pliosaurs

including a 1:1 scale lithograph of the 30 cm teeth of *Pliosaurus grandis* (Figure 1-2). Judging by its dental equipment, *Pliosaurus* was the most powerful of the Mesozoic reptiles known at that time. Conybeare (1824) had contrasted the mode of life of *Plesiosaurus* with that of *Ichthyosaurus*. The latter, with its streamlined body form, like that of a shark or a dolphin, was believed to be an active hunter of the fish and cephalopods that swam in the Liassic seas. The 'weakness' of the plesiosaurians small head and teeth was according to Conybeare compensated for by the long neck, which gave the animal sufficient manoeuvrability to catch its prey. He seemed to believe that the larger skull and jaws of the ichthyosaur would offer it an advantage over *Plesiosaurus*. Similar logic was later used to infer that *Pliosaurus*, with its massive skull and caniniform teeth, was a predator of the other reptiles.

Sauropterygian taxonomy

The Sub-class of reptile to which Plesiosaurs belong, the Sauropterygia (Owen 1860), include the amphibious Triassic forms commonly known as the 'nothosaurs' and the placodonts. The Order Plesiosauria was erected by De Blainville (1835) to include the Family Plesiosauridae Gray 1825 [Conybeare had earlier (1821) created the Order Enaliosauria to include both plesiosaurs and ichthyosaurs, but by the turn of the century these groups were believed to be of separate origin within the reptiles]. Victorian taxonomists were fond of creating new species, doing so with almost every new specimen found, but were reluctant to create new genera - their concept of the genus probably equates with our modern concept of the family. This forbearance is exemplified by Owens' remarks concerning a specimen which he referred to *Pliosaurus trochanterius*; "I have neither respect nor inclination for undue multiplication of genera; but the degree of difference in the number of mandibular teeth and extent of the symphysis tempts to a view of the present evidence of *Pliosaurus trochanterius* as testifying to something more than specific distinction from the *Pliosaurus grandis*. I leave, however, the opening for a "name" to any labourer in gattungsmackery who may yield to the temptation" (Owen 1869; p 8 – but in a final irony the specimen he was discussing is actually a crocodile). Thus the earliest named species were initially placed within Conybeare's *Plesiosaurus*, but as more forms were described from an increasing number of horizons it became difficult to force them all into one genus.

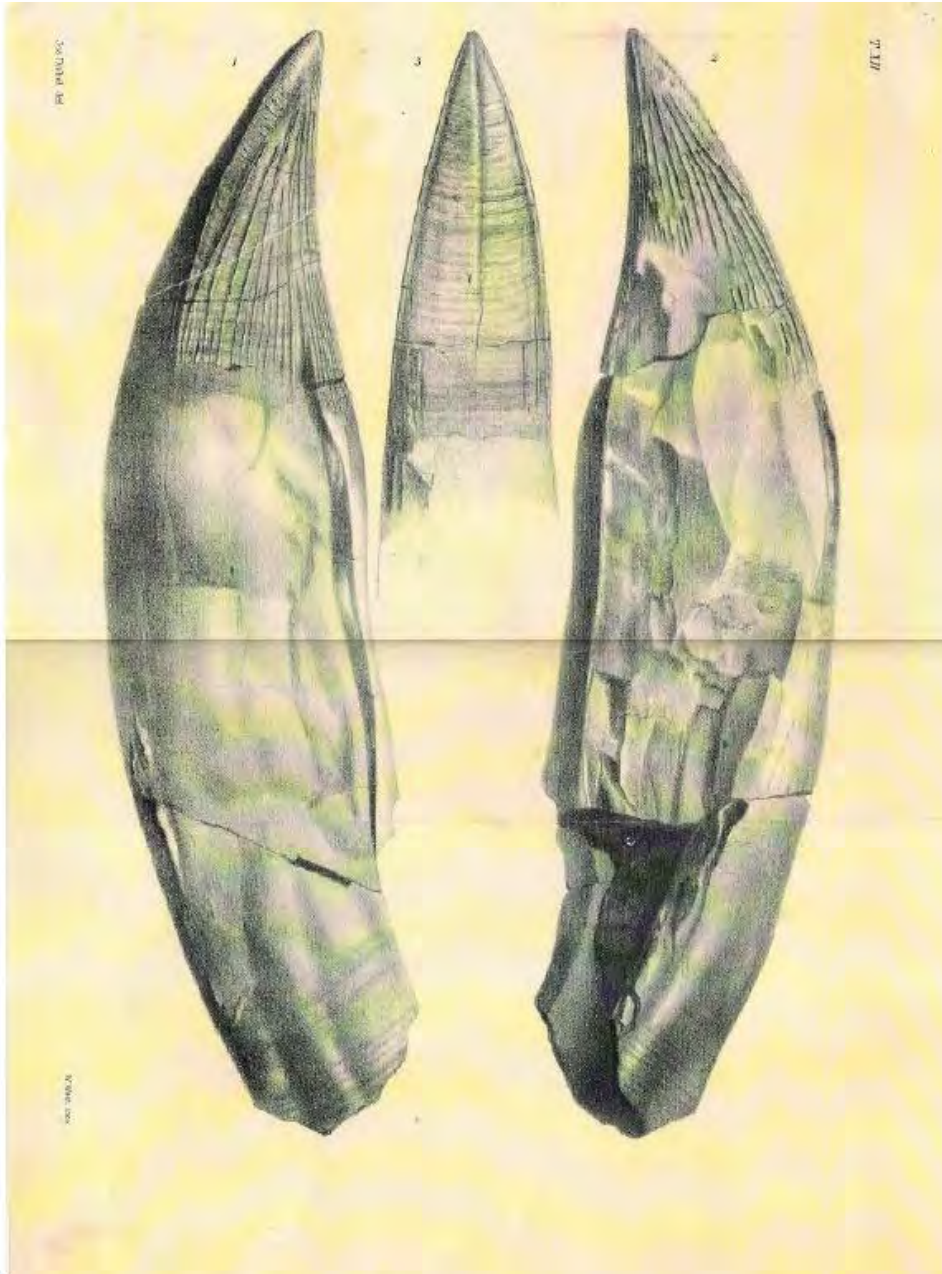


Figure 1-2: The teeth of '*Pliosaurus grandis*', as figured by Owen (1869). The tooth was figured at actual size – a length of 33cms, although 2/3 of this is the root. Presuming that this was the largest tooth in the maxillary row, the minimum length of the animal would have been ~10 metres – slightly longer than large modern killer whale.

By 1874 Seeley had used the familial name Pliosauridae to distinguish those forms similar to Owen's *Pliosaurus* (Seeley 1874), and in 1943 Welles proposed the Superfamilies Plesiosauroidea (to include the Families Plesiosauridae and Elasmosauridae) and Pliosauroidae (then including the Families Pliosauridae and Polycotylidae) – at that point he recognised a total of 35 genera within the Order Plesiosauria, an indication of the diversity of form contained therein (Welles 1943). Brown (1981) recognised three families of plesiosauroid; the Plesiosauridae Gray

Big pliosaurs

1825, the Cryptoclididae Williston 1925, and the Elasmosauridae Cope 1869, although Bakker (1993) has suggested that the Jurassic elasmosaurids of Brown may actually form a distinct family, the Muraenosauridae White 1940. Five families of pliosauroid (the Rhomaleosauridae Nopsca 1925, the Pliosauridae Seeley 1874, the Leptocleididae White 1940, the Brachaucheniidae Williston 1925, and the Polycotylidae Williston 1908) have been discussed by Hampe (Hampe 1992, Hampe and Leimkuhler 1996). Recently the monophyly of each superfamily has been questioned; Carpenter (1996, 1997, 1999) has drawn attention to a number of features shared by the Elasmosauridae and the Polycotylidae. Bakker (1993) took this as indicating that the elasmosaurids are in reality pliosauroids which have independently acquired the plesiosauroid body form, whilst Carpenter's own interpretation is that Polycotylids are large-headed plesiosauroids (Carpenter 1996, 1997, 1999), a view supported in some more recent cladistic analyses (O'Keefe 2001, Ketchum 2008) but not others (Druckenmiller 2006, Druckenmiller and Russell 2008, Smith and Dyke 2008).

The Linnaean system of nomenclatural hierarchy, devised to organise and assist understanding of the group, often serves to confuse in the case of the Plesiosauria because so many of the levels have identical roots, differing only in the suffix. Thus *Plesiosaurus* is at once a plesiosaurid (i.e. a member of the Family Plesiosauridae Gray 1825), a plesiosauroid (i.e. belonging to the Superfamily Plesiosauroidea Welles 1943, which includes those families with long necks and small heads), and a plesiosaurian (i.e. belonging to the Order Plesiosauria de Blainville 1835, which includes both the Plesiosauroidea and the Pliosauroidae). Similarly *Pliosaurus* is a pliosaurid pliosauroid plesiosaurian. This confusion is only magnified by the imprecision and inconsistency with which the vernacular terms 'plesiosaur' and 'pliosaur' are used. The most common use for 'plesiosaur' at the moment seems to be in description of the entire order, i.e. as an equivalent of 'plesiosaurian', whilst for 'pliosaur' it appears to be specify membership of the Superfamily Pliosauroidae. This unfortunate practice serves to confuse (pliosaurs are also plesiosaurs), leaves the Plesiosauroidea without a vernacular name less clumsy than 'plesiosauroid', and places the more elegant term 'plesiosaurian' in danger of redundancy. A more agreeable situation would be the reservation of 'plesiosaur' as equivalent to 'plesiosauroid', introducing a modicum of consistency within the vernacular appellations, but in the current state it seems

prudent to specify each grouping by its proper name. In the context of this thesis, the vernacular term 'pliosaur' is used as equivalent to the Pliosauroida *sensu* Welles 1943.

Early plesiosaurs - the Liassic forms

The contrast between the two forms – pliosauroid and plesiosauroid – reaches its most extreme manifestation in the younger Cretaceous species, but the split is apparent in the oldest rocks that preserve plesiosaurians. The Liassic rocks around Street, in Somerset, record the Triassic - Jurassic boundary, including the very top of the Rhaetian (Triassic) and the very base of the Hettangian (Jurassic). They include two species of plesiosaurian; the long necked form *P. hawkinsi* Owen 1838 [now placed in its own genus, *Thalassiodracon* (Storrs and Taylor 1996)], and the short necked *P. megacephalus* Stutchbury 1846 [currently referred to the genus *Rhomaleosaurus* Seeley 1874 (Cruickshank 1994)]. In the table given by Sollas, *T. hawkinsi* is listed as having 31 vertebrae in the neck, whilst *R. megacephalus* is stated to have 30 - not a huge difference in number, but the short nature of each individual cervical vertebrae in the latter species means that the neck of *R. megacephalus* is less than half of the length of its body (Figure 1-3), while the neck of *T. hawkinsi* is more than one and a half times the length of its torso (Sollas 1881). Concurrent with the difference in neck length is the change in the opposite direction of head size - skull length in *R. megacephalus* is more than half the length of the body, whereas in *T. hawkinsi* the head is equivalent to less than half of the length of the trunk. This trend is not only present in the younger Liassic strata - the rocks of Lyme Regis, as we have seen, contain many specimens of *Plesiosaurus dolichodeirus*, in which the neck is even longer (it contains 40 or more cervical vertebrae) and the head even shorter than is the case in *Thalassiodracon hawkinsi*. Similarly the pliosauroid present at Lyme Regis, *P. rostratus* (now referred to *Archaeonectrus* Novozhilov 1964) continues the trend slightly further in the opposite direction. The Upper Lias of Whitby has produced fossils of *P. homalospondylus* Owen 1865 (now placed within *Microcleidus* Watson 1909), in which the head is the smallest and the neck the longest of all Liassic plesiosaurians, and *Rhomaleosaurus zetlandicus* Phillips 1854, a pliosauroid where the skull is massively developed compared with other Liassic forms.

Big pliosaurs

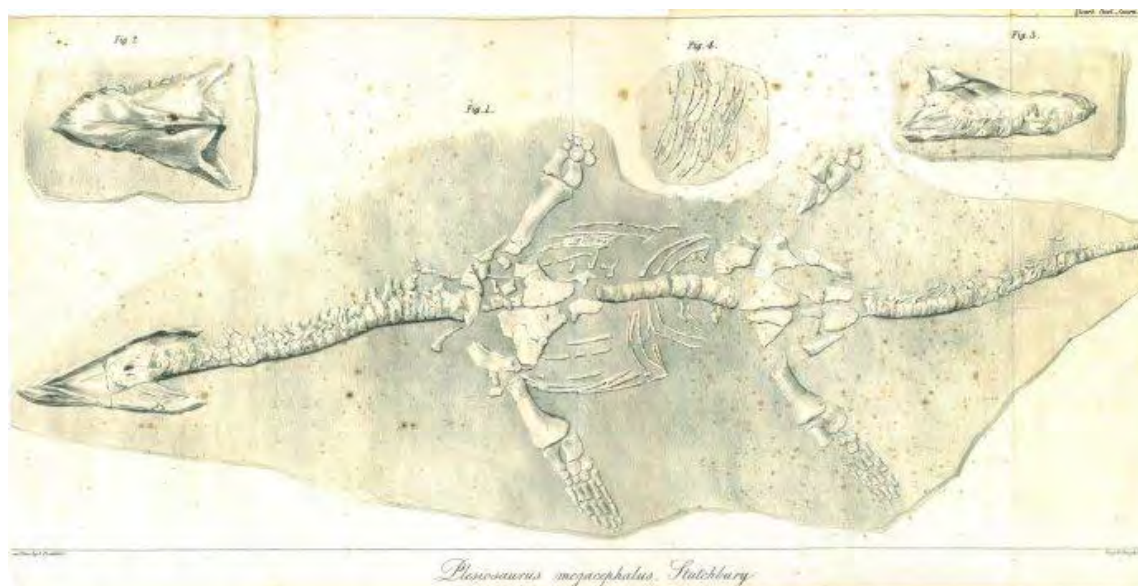


Figure 1-3: *Rhomaleosaurus megacephalus* (from Owen 1840).

In spite of the clear dichotomy in body form the significance of these trends within the Liassic have taken a long time to become clear. This is due mainly to the long standing confusion concerning Liassic plesiosaurs; literally hundreds of species have been named from the Lias, most of which have been founded on scrappy material. During the last century opinion meandered through a journey of believing first neck length, then vertebral dimensions, and then pectoral girdle morphology to be of primary importance in the taxonomy of plesiosaurs. Compounding these difficulties are both the early Victorian habit of swelling genera, particularly *Plesiosaurus*, to include many tens of species, and the lack of attention given to skulls (which are rare) – the state of knowledge of Liassic plesiosaurians inherited by 20th Century workers was so confused and seemingly intractable that only recently (Cruickshank 1994, 1996, Smith and Dyke 2008, Storrs 1997, Storrs and Taylor 1996, Taylor 1992b) has attention turned back to these species. Most of the recent work has been concerned with reviewing the taxonomy and redescribing key specimens, but two recent papers have concerned themselves with pliosauroid biology. Taylor's description of the skull of *Rhomaleosaurus zetlandicus* included a functional analysis of the skull's mechanical properties (Taylor 1992a), whilst Computed Tomography (CT) scan of a skull of *Rhomaleosaurus megacephalus* has revealed a nasal region that seems to be hydraulically optimised, i.e. providing an acute sense of smell underwater (Cruickshank et al. 1991).

Plesiosaurs of the Oxford Clay, and an acquaintance with Peloneustes

In the second half of the 19th Century studies of marine reptiles concentrated upon the Middle Jurassic Oxford Clay fauna, culminating in Andrews' review of the Leeds Collection (Andrews 1910a, 1913), which benefited from many excellent specimens from this Callovian lagerstätten, and the taxonomic and descriptive work has been less confused than with the Liassic forms. Of particular significance was the comprehensive and meticulous collection of material by Alfred Leeds in the brick pits of the Peterborough region; much of which was donated to British Museum of Natural History and formed the basis for Andrews' descriptive catalogue. The plesiosauroids are included in Brown's review of the Upper Jurassic forms, and the genera *Tricleidus*, *Cryptoclidus*, and *Muraenosaurus*, named over 100 years ago, are considered to reflect the extent of generic diversity in this deposit (Brown 1981). It is true that all plesiosaurians in the Oxford Clay are instantly recognisable as being of either plesiosauroid or pliosauroid type – the distinguishing features of each superfamily are more clearly shown here than in the Liassic forms, the dolichodeiran condition being taken to an extreme in *Muraenosaurus* with 44 elongate cervical vertebrae. The cryptoclidids *Tricleidus* and *Cryptoclidus* show a new variant of the long-necked form – the neck is not as elongate and the skull is proportionately larger than in *Muraenosaurus* (or even the Liassic *Microcleidus*), the cryptoclidids having greater numbers of less robust teeth. Brown (1981) has suggested that they took small shoaling animals in large numbers.

Similarly, the first Oxford Clay fauna included an number of pliosauroid taxa. The first to be named was *Plesiosaurus philarchus* (Seeley 1869), later placed in its own genus, *Peloneustes*, by (Lydekker 1889). It is a medium sized pliosaur, commonly reaching lengths of 3.5 metres but occasionally exceeding 4 metres, and is the most commonly member of the superfamily found in the Oxford Clay. It is known from many fine specimens, including at least one almost complete skeleton (Andrews 1910b – Figure 1-4) and an abundance of skulls, the descriptions by Andrews (1895, 1913) are of high quality, and it has recently been reviewed in detail (Ketchum 2008). As it clearly shows many typical pliosauroid features, the skull of *Peloneustes philarchus* may serve as an introduction to the cranial anatomy of post-Liassic pliosaurs; the following outline provides a brief acquaintance with this species, dwelling only slightly upon those areas of particular relevance or controversy.

Big pliosaurs

The head is slightly less than a fifth of the overall length, and has the form of a finely tapered cone; at the back of head the skull and mandibles taken together are about as tall as the skull is wide, the length of the skull exceeding its width by a factor of 2.5 and giving a very streamlined appearance. The upper jaw holds six conical teeth in each premaxilla and 28-30 teeth in the maxillaries (Andrews 1895, 1913) - the 3rd, 4th, 5th, and 6th maxillary teeth are larger than the others. The lower jaws hold about 40 teeth in each dentary; 14-16 of these lie within the mandibular symphysis, of which the anteriormost seven teeth are larger and caniniform - these are held in a spatulate broadening of the symphysis. The teeth are all circular in cross section, recurved, and about half their length is taken up by the root. The crown is ornamented with a number of ridges - the very tip of the tooth is free of them, a small number originate below the tip, and their number increases towards the base of the crown not by bifurcation but the appearance of new, shorter ridges. There are no carinae, and teeth of *Peloneustes* rarely show any sign of wear at the tips. The orbits are situated well back on the skull, defining a long rostrum, and the temporal fenestra behind them are roughly circular in shape and are very large, as is typical of plesiosaurians.

On the dorsal surface the premaxillary bones send narrow processes posteriorly along the midline of the skull - these processes entirely separate the maxillary bones and form pronounced ridge along the length of the rostrum. They meet the anterior

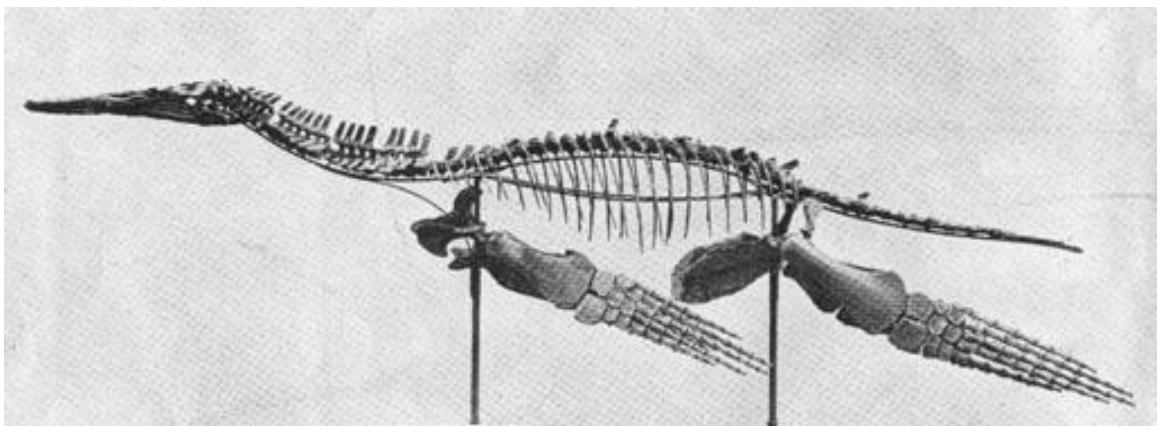


Figure 1-4: *Peloneustes philarchus*, from Andrews (1910).

process of the fused parietal bones in a complex interdigitate suture which is underlapped by a ventro-medial growth of the frontal bones, which on the dorsal surface lie lateral to the parietal/premaxillary joint. Though considered by many authors to be important in determining relationships between species, the topology of the bones in this region has been difficult to characterise in many species of pliosaur - the three dimensional complexity renders it prone to errors of interpretation, a problem exacerbated by the frequency with which this part of the skull is crushed or abraded. There are a number differing opinions relating to whether the premaxillaries meet the parietals on the dorsal surface (or whether they are instead excluded by a midline suture between the frontals) in various pliosaurs (Andrews 1895, 1913, Carpenter 1996, Druckenmiller and Russell 2008, Ketchum 2008, Taylor and Cruickshank 1993, Williston 1907) but it is likely that the condition seen *Peloneustes* is typical of many of the other species.

The post-orbital bar, separating the orbit from the temporal foramen, is formed from the postorbital laterally and the postfrontal. The former attaches to the jugal and an anterior ramus of the squamosal, which together make up the cheek bar. The medial surface butts onto the parietal and the frontal. The frontals bound the inner margin of the orbit and the prefrontals form the forward margin (Ketchum 2008) – both bones send processes down which contact the palate and form a wall separating the nasal cavity from the orbit. Between the prefrontal and that part of the maxilla that together with the jugal forms the outer margin of the orbit is what appears to be a lacrimal. The nasal bone is often considered to be absent in plesiosaurians (Brown 1981, Druckenmiller and Russell 2008, Storrs 1993), but Andrews (1913: p42) mentions that "there is some indication that the posterior and outer borders are formed by a small distinct element, which, if actually present, must be regarded as a nasal". The external nares lie slightly forward of the orbits as is usual in plesiosaurians. Anterior to the external nares the rostrum is triangular in section, being buttressed by the posterior prongs of premaxillaries along the dorsal apex. A section through the rostrum reveals a very large nasal cavity, the mass of bone being rather small in this region.

The palatal surface of the skull reveals a number of uniquely plesiosaurian features. The premaxillaries meet along the midline for most of their length, but the

Big pliosaurs

maxillaries are separated by the vomers anteriorly - these fused bones run posteriorly until a point level with the 7th or 8th maxillary alveolus. The internal nares lie level with the 6th and 7th maxillary alveoli and are bounded by the maxillaries externally and the vomers medially, anteriorly and posteriorly (according to Andrew's 1913 reconstruction). This topology is shared by another Oxford Clay pliosaur, *Liopleurodon ferox* (Andrews 1913), in addition to the Kimmeridgian *Pliosaurus brachyspondylus* (personal observation of 'Westbury #2' skull, BRSMG Cc332) but contrasts with that of the Liassic *Rhomaleosaurus megacephalus*, where the vomers form the internal and anterior borders of the nares, the posterior edge being formed by the more posterior palatal bones. In truth the dorso-ventral crushing of many specimens from the Oxford Clay makes this region of the skull rather difficult to interpret - Andrews' later interpretation differs from the one he offered in 1895. In any case the position of the internal nares is considerably anterior to that of the external nares - a decidedly unusual situation and one seemingly at odds with any requirement for breathing with all but the top of the head submerged. The recent reinterpretation of the function of the nasal passages as underwater olfactory organs (Cruickshank et al. 1991) offers a plausible explanation of this configuration, although it does raise the problem of how pliosaurs did ventilate their lungs⁴.

Behind the vomers lie the palatines and the pterygoids. The palatines lie medial to the maxillaries, extending back to a position roughly equivalent to the middle of the orbit. The pterygoids are very well developed and complex in pliosaurs; they are triradiate, with an anterior ramus which runs forward of the line of the orbits, lying medial to the palatines for most or all of the latter's length; a lateral (transverse) ramus which runs along the rear line of the orbits to meet the jugal, ectopterygoid, and perhaps the maxilla in a complex joint; and a posterior ramus that extends underneath the braincase and runs back to the suspensorium. Posterior to the orbits

⁴ Most animals breathe only through their nose, not their mouth - cetaceans are incapable of breathing through their mouth, and will suffocate if the nares are blocked. The nasal and buccal systems are less well separated in turtles; they are capable of olfaction underwater, and routinely ventilate their lungs through their mouth (pers. obs.). However the turtle has to raise most of its skull above the surface to avoid drowning. The skull of a pliosaur is much longer than that of a turtle, and the largest species would have had to raise at least 1.5 metres of skull out of the water every time they wanted to breathe. It is possible that a pliosaur could restrict breaths to coincide with porpoising (a form of rapid locomotion where most or all of the body leaves the water, reducing drag for part of the swimming cycle; it becomes efficient above a threshold speed) as do many dolphins and sea-lions, but this does not assist them at slower speeds, or when they may wish to avoid the noise of porpoising for fear of alerting potential prey to their presence.

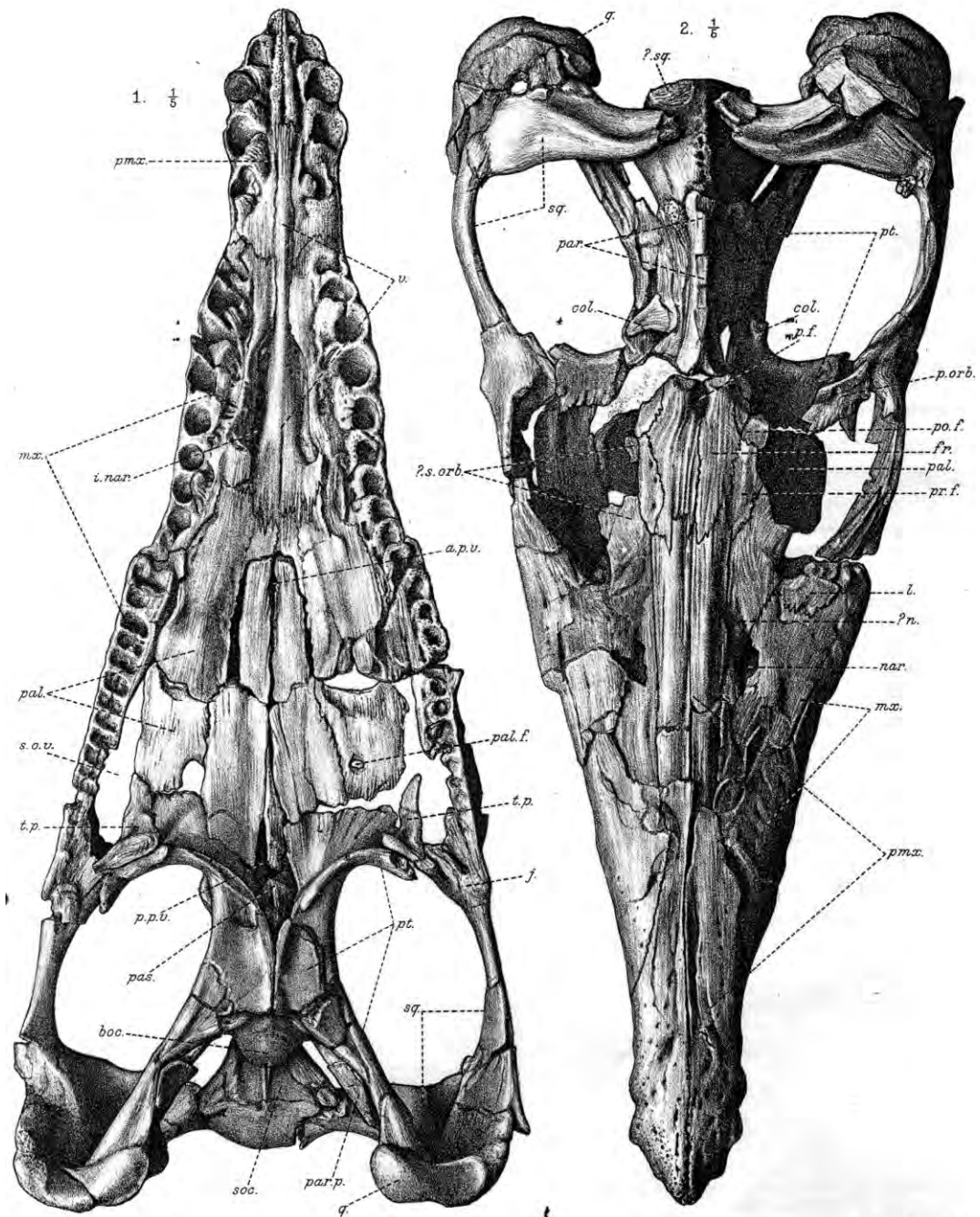
there is a well marked vacuity between the two pterygoids (the posterior inter-ptyergoid vacuity *sensu* Andrews 1913), revealing the ventral surface of the parasphenoid. The suture of the parasphenoid with the basisphenoid is just visible before the pterygoids again join in a strong midline suture that underlies the basicranium - this arrangement is unique to pliosaurs. From this region there is a process that runs laterally and posteriorly to meet the quadrate and the squamosal, helping to reinforce the hinge of the lower jaw.

The exact configuration of the pterygoids and palatines at the front of the palate, just behind the vomers, has also been subject to a number of differing interpretations. Andrews (1895) states that no specimen of *Peloneustes* shows the extent of the palatines clearly, but thought that the anterior ramus of the pterygoids contacted the vomers, the pterygoids thereby separating the palatines completely. He offered the same interpretation for *Liopleurodon ferox* - however in some specimens of *Liopleurodon ferox* it appears that the anterior process of the pterygoid rises slightly dorsally as it runs forward, so that the anterior parts of the palatines may underlie them and meet along the ventral midline (pers. obs.). If this interpretation is correct the contact between the palatines, vomers, and pterygoids may be three-dimensionally complex, and thus prone to the vagaries of preservation and interpretation. The surface bone may also show significant topological variation that belies any consistency in the relations between the greater parts of the bones.

A notable feature of the pterygoids of *Peloneustes* is that the anterior processes of the pterygoids are separated by a narrow vacuity for most of their length. This condition has also been reported in *Liopleurodon ferox* and *Pliosaurus brachyspondylus*.

Posterior to the orbital region the parietals form a tall narrow sagittal crest which is connected to the pterygoids beneath them by the columnar epipterygoids and then the opisthoics and supraoccipital at the rear of the skull. The parietals join onto the medial ramus of the squamosals in a complex suture which is often so well fused that no trace of it is visible. The squamosals unite with the quadrates, the quadrate being visible from an internal perspective but being mostly covered by a ventral projection of the squamosal externally. The articulations with the lower jaw lie wholly upon the ventral surface of the quadrate which takes the form of a curved sheet of bone, the

Big pliosaurus



G.M.Woodward del. et lith.

PLIOSAURUS FEROX.

West, Newman im

Figure 1-5: The skull of *Liopleurodon ferox* (plate from Andrews, 1913).

concave surface facing anteriorly. The suspensorium is abutted by the paroccipital process, which projects laterally and posteriorly from the opisthotic. The exoccipitals are fused with the opisthoics, and form columnar processes joining to the basisphenoid, which is a large bone bearing the occipital condyle.

The Callovian pliosaur fauna

It soon became clear that *Peloneustes* was not the only pliosaur in the shallow, subtropical seas in which the Oxford Clay had been deposited some 160 million years ago. Some very large pliosaur teeth were being found in England and in France, and in 1873 Sauvage created a new genus and species for these, *Liopleurodon ferox* (Sauvage 1873). The validity of the new genus was argued for some time - as fossils of the skull and postcranium were discovered, it became clear that the overall form of the species resembled that of Owen's *Pliosaurus* and when Andrews compiled his descriptions of the material at the British Natural History Museum he referred the species to *Pliosaurus*. The new species had a massive wedge-shaped skull, flattened like that of a crocodile (Figure 1-5) – but the head length (tip of the snout to the rearmost part of the lower jaws) was much larger at 1.5 metres, and the overall length of the animal was 8-9 metres.

Another large pliosaur was named by Andrews himself (Andrews 1909). Although not as large as *Liopleurodon/Pliosaurus ferox*, it shared some features that distinguished both of these, together with *Peloneustes*, from the earlier species of the Liassic pliosaur fauna. Most notably, neck length was shorter (about 22 vertebrae) in the Callovian species vs 32 in the Liassic; head length as a proportion of body length was greater in the Callovian forms, and the femur is a consistently greater length than the humerus in the more recent species. Compared with *P. ferox*, the skull of Andrew's new species was shorter but the teeth, especially at the front of the snout, were at least as robust (Figure 1-6) and Andrews duly christened it *Simolestes vorax* – the 'voracious snub-nosed robber'.

Most of the plesiosaurians described in the 19th Century endured the vagaries of Victorian taxonomy – almost a new species for every specimen – only to move straight into indifference in the early part of the 20th Century as research into Mesozoic reptiles went very out of fashion. The Oxford Clay fauna was fortunate to be the subject of a comprehensive descriptive catalogue by Andrews, in which they were beautifully illustrated and carefully described (Andrews 1910a, 1913). Andrews' taxonomic review of the pliosaur fauna is still used by workers today, with one exception: in his own review of the Upper Jurassic⁵ pliosaurs, Tarlo (1960) decided

⁵ Although the title of both Tarlo's (1960) and Brown's (1981) reviews specified the Upper Jurassic

Big pliosaurs

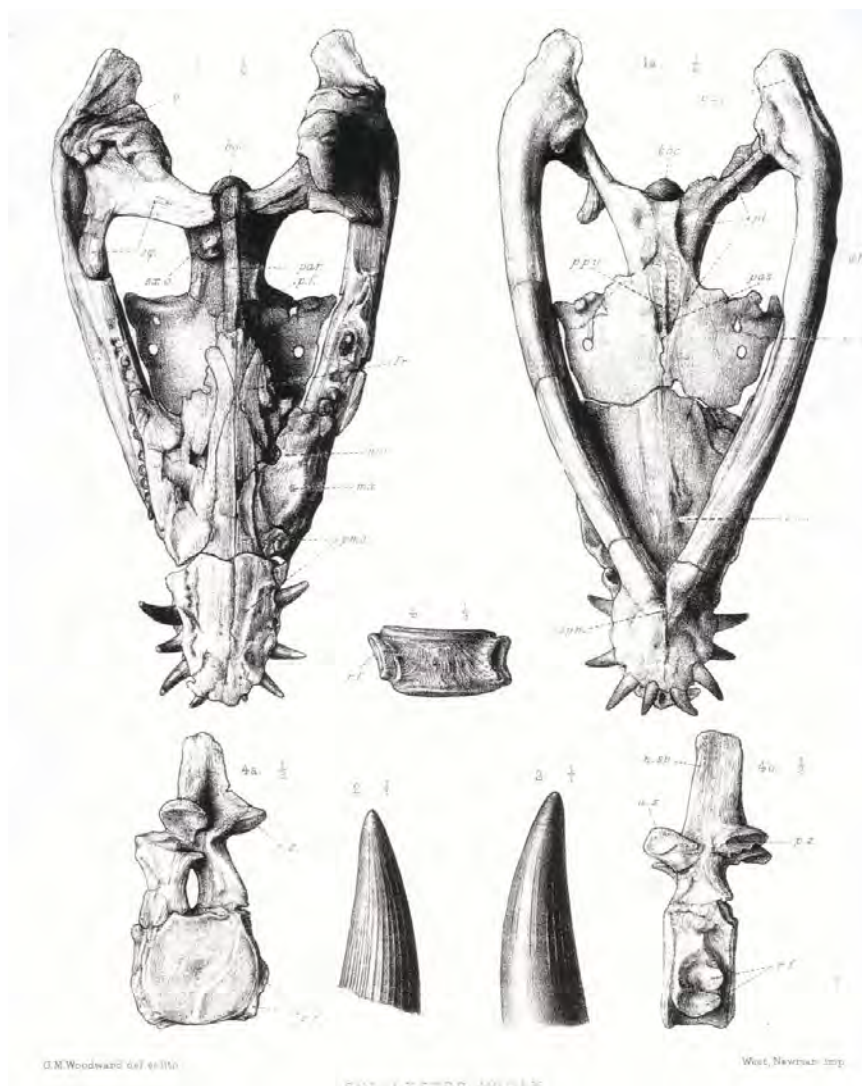


Figure 1-6: The skull, teeth, and a neck vertebrae from the holotype specimen (NHM R3319) of *Simolestes vorax* Andrews 1909 (plate from Andrews 1913).

that the Oxford Clay 'Pliosaurus' *ferox* differed sufficiently from the Kimmeridgian species of *Pliosaurus* to warrant placement in a different genus and resurrected the name Sauvage had originally created: since Tarlo's review, the species has been known as *Liopleurodon ferox*. In distinguishing the various genera and species of Callovian and Kimmeridgian pliosaur, Tarlo (1960) emphasised two traits as being of taxonomic significance; the length of the mandibular symphysis (Figure 1-7), and the shape and ornamentation of the teeth (Figure 1-8). One of his reasons for separating

they each included the Oxford Clay forms because of the Oxfordian age assigned to the Clay at that time. It is now believed to be Upper Callovian in age, placing it at the top of the Middle Jurassic – ironically, this means that no pliosaur species are known from the Oxfordian, despite the most speciose fauna occurring in the Oxford Clay.

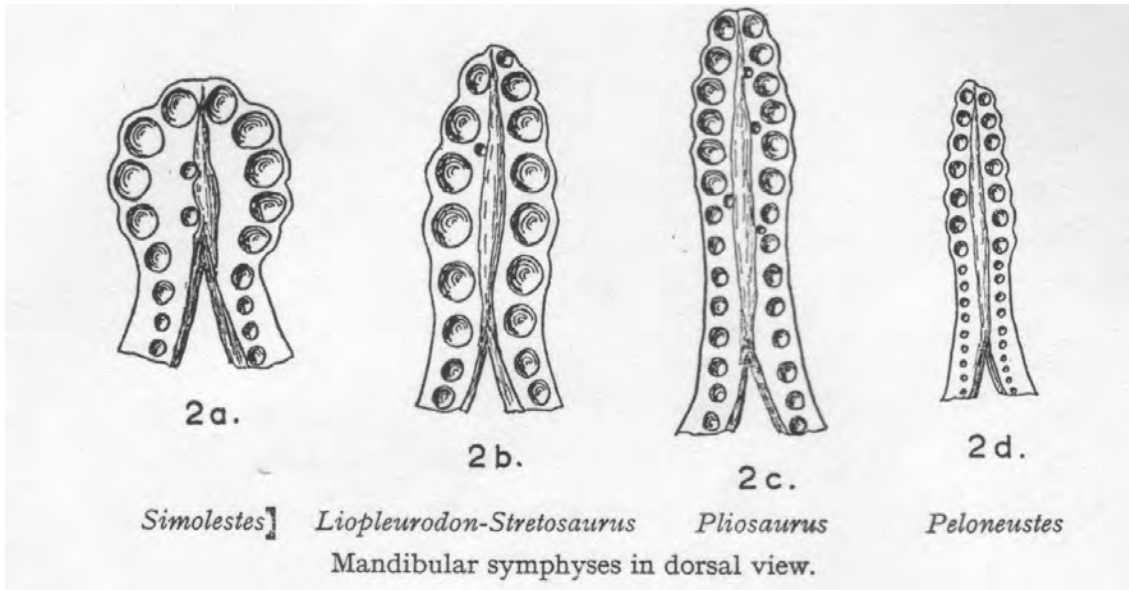


Figure 1-7: Mandibular symphyses of Callovian and Kimmeridgean pliosaur taxa, as figured by Tarlo (1960).

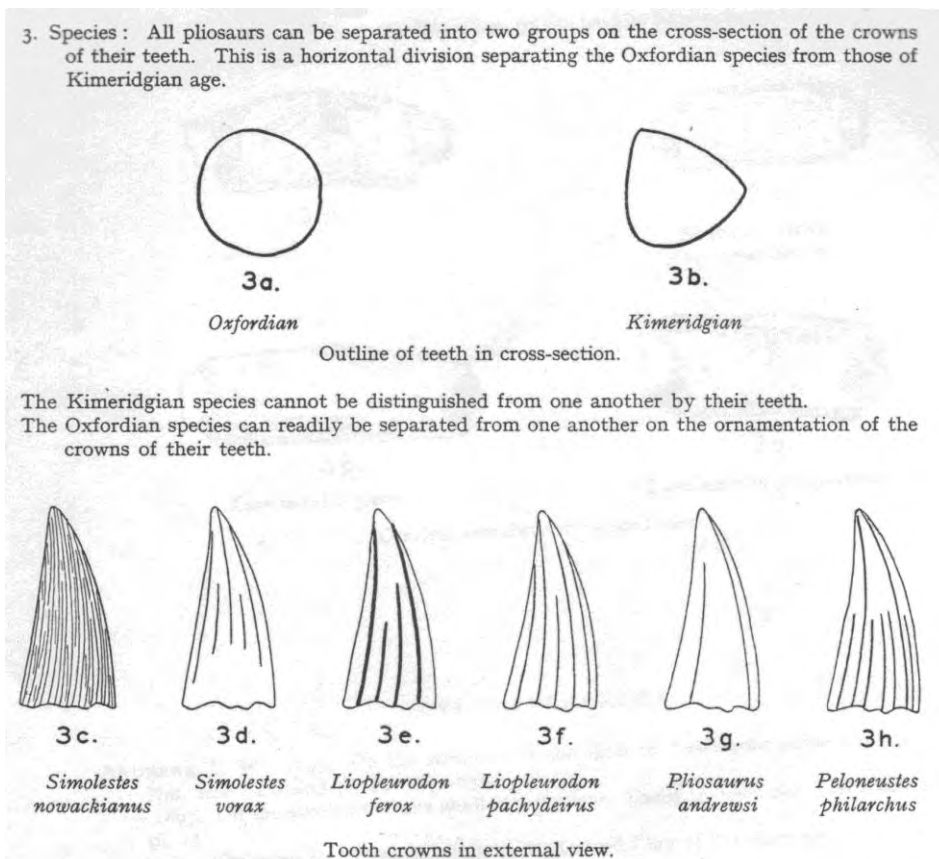


Figure 1-8: The part of Tarlo (1960)'s key to 'Upper' Jurassic (Callovian and Kimmeridgean) pliosaurs relating to tooth section and ornamentation. Note that, of the 'Oxfordian' (=Callovian) species, *Simolestes nowackianus* is a teleosaurid crocodile (Bardet and Hua 1996), and *Liopleurodon pachydeirus* is not considered to be a valid taxon (junior synonym of *L. ferox*: Noè, 2001).

Big pliosaurs

L. ferox from *Pliosaurus* was that the former has a short (6-7 teeth) symphysis with teeth that are circular in cross section, whilst the latter have a longer symphysis and teeth with a sub-triangular section.

How so many species of large pliosaur co-occurred in the seas of the Oxford Clay has been one of the few palaeoecological questions tackled in connection with pliosaurs: Massare (1987) used tooth morphology to separate different marine reptiles into guilds and on this basis assigned *Peloneustes*, *Liopleurodon* and *Simolestes* to different parts of the trophic web. Consistent with ecological niche theory, the different species do show some diversity in body size and patterns of tooth shape and wear. The most common species, the medium sized *Peloneustes* (body length of 3 to 4 metres) has slender teeth that rarely show signs of wear, a feature of modern fish- and squid-eating dolphins such as *Delphinus* and *Tursiops*. At 5-6 metres long *Simolestes* was not much larger than *Peloneustes*, but the skull is much more robust, and the large teeth show obvious signs of the wear that results from macrophagy⁶. The largest predator known from reasonably complete specimens is *Liopleurodon* – large well-preserved skulls are around 1.8 metres total head length, and as with *Simolestes*, many *Liopleurodon* teeth show the sort of wear that indicates predation on large animals. The discovery of yet another species of Oxford Clay pliosaur, *Pachycostasaurus dawnii* (Cruickshank et al. 1996), further complicated the composition of the guild and Noè (2001) offered an emended version of Massare's trophic chart in which *Pachycostasaurus* and *Liopleurodon* occupied the 'Cut' sub-guild, specialising on large fish and marine reptiles – they were presumably separated within this guild by body size, as *Pachycostasaurus* is much smaller than *Liopleurodon* – and *Peloneustes* was placed within the 'Pierce II' sub-guild, specialising on fish. Noè's work in revising *Simolestes* led him to the conclusion that *Simolestes* sat somewhere in the overlap between these two (Noè 2001).

⁶ Living macrophagous (literally, 'eating big') marine carnivores include killer whales (*Orcinus*), false killer whales (*Pseudorca*) and the larger members of crocodylian species such as *Crocodylus niloticus* or *Crocodylus porosus*. In this species, the teeth are often broken and re-worn as a result of feeding on large prey. By analogy, fossil teeth exhibiting this pattern of wearing can be used as an indication of macrophagous habits in their owners.

The age of chalk

The Cretaceous Period, named after the Greek word for the abundant chalk deposits that characterise rocks of this age in Europe, is the longest division of the Mesozoic Era and is currently dated between 144 and 65 million years ago. It was a time when ‘middle life’ was at its most diverse and infamous: during this age animals such as *Tyrannosaurus*, *Triceratops*, and *Velociraptor* played their respective roles in the terrestrial ecosystems. At the start of the Cretaceous, the continents were still grouped together as northern and southern super-continent: by the end of this period, the land masses had started to assume a recognisably modern configuration. The drift towards our modern world was reflected in the biology of the age; flowering plants first appeared together with many of the great insect orders that co-depend on them; modern groups of fast swimming teleost fish – especially the clupeiformes (herrings et al.) – became abundant in the seas; and the first examples of the lamniform (whites and makos) and carcharhiniform (whalers) sharks appeared alongside early skates and rays.

Despite this emerging modernity, the marine ecosystems of the Cretaceous were at the same time still in a Mesozoic ocean, and groups such as ammonites, belemnites, and holostean fishes were still abundant. And feeding upon all of these were the marine reptiles, with the plesiosaurs the most abundant of these.

Preservation of Jurassic marine fossils in Europe is remarkable, with three highly fossiliferous deposits – the Lias, the Oxford Clay, and the Kimmeridge Clay – in England alone. Germany has two Jurassic lagerstätten – Holzmaden and Solnhofen – which preserve fossils in exquisite detail, including details of soft tissue, and which have provided insight into the body form and reproductive mode of ichthyosaurs, and the evolution of feathers within small theropod dinosaurs. In contrast, the first 45 million years of the Early Cretaceous are almost without any record in Europe, and so our knowledge of how plesiosaurians, and in particular pliosaurs, survived the minor mass extinction and faunal turnover at the end of the Jurassic Period is very poor.

That pliosaurs did survive the Jurassic was first confirmed by Owen’s description of some scrappy material from the Cambridge Greensand (Owen 1840-1845), a deposit

Big pliosaurs

that lies near the boundary between the Early and Late parts of the Cretaceous and which is approximately 95–90 million years old (Albian–Cenomanian) (Unwin 2001). Owen first named this pliosaur after some isolated teeth that had heavy, ridged ornament along the crowns: *Polyptychodon* means ‘many ridged tooth’. Subsequently, some fragments of skull were found in association with this type of tooth and the pliosaur identity of *Polyptychodon* was confirmed. Owen named two species – *P. continuous*, in which the ridges ran the whole length of the tooth, and *P. interruptus*, where the ridges stopped short of the tip. The material is so incomplete that both species may end up being considered invalid taxa, but they at least confirm the survival of pliosaurs until at least the Albian Age of the Early Cretaceous.

A far better indication of the form of Cretaceous pliosaurs was provided by Williston, who described a remarkable fossil that had been recovered from the Niobrara Chalk of Kansas (Williston 1903). Comprising a skull and an articulated set of 35 vertebrae with ribs, the holotype of *Brachauchenius lucasi* is one of the most remarkable pliosaur fossils known (Figure 1-9) and affords an important insight into the anatomy of these animals. The discovery of a second specimen from Texas, made up of skull, some vertebrae, and limb bones, provided further information on the species (Williston 1907). In both specimens, the skull was a little under 1 metre long, suggesting a medium sized pliosaur. The holotype has 13 cervical (neck) vertebrae, far fewer than any of the Jurassic pliosaurs, and the vertebral centra lack the nutritive foramina on their ventral surface that otherwise characterise the Plesiosauria⁷.

It is remarkable that Williston, who wrote some of the best accounts of North American fossils ever published, was working at the same time as Andrews, whose descriptions of marine reptiles set a new standard within European palaeontology. The taxonomic relationships of *Brachauchenius* were the subject of some discussion between these two: Williston at first considered it to belong to the Pliosauridae, the family which at that time was considered to contain all of the pliosaurs thus far described from the European Jurassic (Williston 1903, 1907). Andrews (1913) pointed out that *Brachauchenius* differed from *Pliosaurus* in the shortness of the neck, the configuration of the palatal bones, and the morphology of the cervical ribs, and

⁷ Known as ‘sub-central’, or more correctly ‘infra-central’, foramina, these small holes on the under-surface of plesiosaurian vertebrae are quite distinctive and are often the quickest way to identify plesiosaur specimens in the field.

that Williston's "definition would exclude the type genus from the family", suggesting further that "Probably the North-American reptiles corresponding to the Pliosaurus of Europe will be found to constitute a distinct family, in which the characteristics common to the two groups are the consequence of parallel modifications" (Andrews 1913: p2). Williston appeared later to accept this view, placing *Brachauchenius* as the sole member of a new family of pliosaurs, the Brachaucheniidae (Williston 1925).



Figure 1-9: *Brachauchenius lucasi*, Holotype (from Williston, 1907).

Australian enaliosaurs

In 1899 – about the time that Williston was first coming to grips with the Kansas *Brachuchenius* – a small fossil was sent to the Queensland Museum in Brisbane by a Mr Andrew Crombie in 1899, and was received by Charles deVis, who was at that time director of the museum. The specimen represented a fragment of mandibular symphysis, and deVis assigned it to the Enaliosauria, the group which at that time included both the Ichthyosaurs and the Plesiosaurs, but his mention in the letter of the English translation of Ichthyosaur, 'fish lizard', suggests that he believed the specimen to an example of *Ichthyosaurus australis*. He did, however, make note of the large thecodont dentition, unusual for an ichthyosaur. No locality information exists for that specimen, but it was described by Heber Longman, the next director of the Museum, who mentioned that Mr Crombie came from Hughenden, a small farming town in the Rolling Downs of Central Western Queensland, and presumably the fossil was found near the town. Longman astutely recognised that the fragment of symphysis belonged to a large pliosaur, which he christened *Kronosaurus queenslandicus*⁸ (Longman 1924)⁹. This specimen, the designated holotype, holds the Queensland Museum collection number QM F1609.

That Longman managed to identify the specimen to family despite never having seen any comparative material, either in Australia or overseas (at that time there were no identified pliosaurs from Australia, and Longman was never able to travel abroad), is testament to his abilities as a palaeontologist. In 1930 he published a description of some more fragments of bone, including the proximal ends of a pair of huge propodial bones which he identified as pliosaurian (suggesting that they were humeri), and referred them to *Kronosaurus* (Longman 1930). On the basis of these bones (QM F2137) Longman suggested that *Kronosaurus queenslandicus* may have been the largest pliosaur yet recorded, the dimensions of the propodials exceeding those reported for Knight's *Megalneusaurus rex* a few years before (Knight 1895, 1898).

⁸ cf. Frontspiece – named after the Greek Titan Kronos, whom legend held devoured his children (including Zeus). Kronos is not to be confused with Aeon, or Chronos, the God of Time: the name does not mean 'Time Reptile', although that would be an appropriate description of doing a PhD on the taxon.

⁹ 100 years after Conybeare named *Plesiosaurus dolichodeirus*

As is presumed for the holotype, the postcranial material described by Longman in 1930 was from a locality two miles to the south of Hughenden. The rocks in this area are of the Toolebuc Formation of the late Albian stage of the Lower Cretaceous, which are currently dated at 102 million years old, and it is believed that QM F1609 and QM F2137 are both from the Toolebuc.

In 1932 an expedition from the Museum of Comparative Zoology of Harvard University was collecting examples of extant and extinct fauna from Australia. W.E. Schevill, a member of that expedition, was in the Rolling Downs when he collected two specimens of large pliosaur from properties to the north of Richmond, a town 110 km west of Hughenden. The first specimen, MCZ 1284, included a well preserved piece of the anterior rostrum tightly joined to the entire mandibular symphysis, in addition to several other pieces of scrap, and was collected from a property called Grampian Valley. The second specimen (MCZ 1285), found on the neighbouring Army Downs, comprises several tonnes of material and included a few large portions of skull, a long sequence of vertebral column, and a few pieces of girdle and limb bone. Schevill and his assistant, an itinerant British Army major¹⁰, collected the larger specimen using dynamite to break the largest block into several smaller, more manageable pieces, packed the specimen in bales of sheep's wool, and shipped it back to Massachusetts. The cranial material from both specimens was described by Theodore White, who referred the new material to Longman's *Kronosaurus queenslandicus*, drawing "attention to the remarkable acumen of Mr Longman in allocating this species to the Pliosauridae" (White 1935). White diagnosed the species as a "giant pliosaur with four teeth in the premaxillary" (a situation that can be observed clearly in MCZ 1284 and which at that time was unique amongst described pliosaurs¹¹). The other characters he mentioned in his diagnosis are general to pliosaurs, except for his report of "no median palatal vacuity"

¹⁰ Known by the locals as 'The Maniac' (Thulborn and Turner, 1993).

¹¹ A premaxillary tooth count of 5 is considered primitive for the Plesiosauria and the pliosauroids, and the early pliosaurs, such as the Lower Jurassic *Rhomaleosaurus* (Taylor 1992, Cruickshank 1994, 1996) and the Middle Jurassic *Simolestes* (Noè, 2001), and *Liopleurodon* (Andrews 1913) all have 5 teeth in the premaxilla. Exceptions to this generality have increased tooth counts - both the Middle Jurassic *Peloneustes* (Andrews 1895) and the Upper Jurassic *Pliosaurus* (pers. obs., contra Taylor and Cruickshank 1993) have 6 teeth in the premaxillary. Of the Cretaceous pliosaurs, *Brachauchenius* (Carpenter 1996) and *Kronosaurus boyacensis* (Hampe 1992) both have 5 premaxillary teeth, whilst the count in *Plesiopleurodon* is not reported but appears to be 5 (Carpenter 1996).

Big pliosaurs

(presumably equivalent to the anterior inter-pterygoid vacuity of Andrews, 1913), which was at that time an absence seen only in *Brachauchenius* (Williston 1903).

Both the properties that Schevill collected from lie on the Doncaster member, an Upper Aptian sequence which lies below the Toolebuc and is approximately 112 million years old. In 1935 the Queensland Museum collector J. Edgar Young collected more pieces of large pliosaur from the younger Toolebuc rocks of Telemon station, 30 km west of Hughenden. The material was collected within a small area and is mostly scrap, and it is uncertain how many individuals are represented in this haul: they are registered in the Queensland Museum catalogue under the QM numbers; F2446, F2447, F2449, F2450, F2454, and F2455. The most important specimen of these is QM F2446, which includes one piece with an occipital condyle and the back of the braincase, and another large section of middle skull which includes the external nares and most of the orbits. QM F2454 has several very crushed pieces of skull, the tooth sockets of which indicate a very large animal, and a reasonably intact mandibular glenoid.

The next important collection was in 1979, when Alan Bartholomai of the Queensland Museum was called to Toronto station, just north of Richmond, by the owner of the property who had just found some very large bones. This specimen included a large amount of cranial and postcranial material, mostly well preserved, from a very large pliosaur, and it was taken back to the museum at Brisbane where it is registered as QM F10113; it too comes from the Toolebuc Formation.

A decade later there was then a rush of new discoveries; in 1989 Telemon station produced more pliosaur material, found by the family who own it and the neighbouring property of Dunluce. QM F18762 is a nearly complete skull, the first of such found, although it is fairly crushed and covered in a hard limestone matrix – it was collected by Mary Wade and Don Mackenzie, both of the Queensland Museum. In June 1990 Charles Robinson of Canary station, some 60 kms south-east of Boulia (which lies on a section of Toolebuc Formation 500 km to the south-west of Richmond), found a skull and a pair of propodial heads, which Wade and MacKenzie collected and registered as QM F18154. And then in July of that same year a very large, mostly uncrushed and nearly complete skull was found on the airstrip at

Lucerne station, which like Toronto is situated on the Toolebuc just to the north of Richmond. The owner notified the museum and the skull, found broken up into several nodules lying in the black soil, was collected and registered as QM F18827.

All of these specimens, save the two collected by Schevill in 1932 and taken back to Harvard, are from the Toolebuc, and it was not until 1994 that further material was found in the Doncaster; Robert Ievers was prospecting for ammonites on Grampian Valley (the property that yielded Schevill's MCZ 1284) and found a number of large plesiosaurian vertebrae. Personnel from the Queensland Museum and the University of Queensland (including myself) excavated the site in 1995 and recovered a series of vertebrae and a section of middle torso including gut contents. This specimen is registered as QM F33574.

The most recent acquisition of *Kronosaurus* material by the Queensland Museum came in 1996, when Alex Cook of the Queensland Museum noticed a small section of skull in the collections of the James Cook University Geology Museum. The specimen lacks any collection data, but the matrix is consistent with that of the Toolebuc Formation from the Hughenden region, near the property Dunraven, and the fossil represents an exceptionally well example of the orbital region of a pliosaur skull. The specimen was transferred to the Queensland Museum collection, where it is registered as QMF51291.

In none of the material was there any compelling evidence for more than one species, and so it was all referred to Longman's *Kronosaurus queenslandicus*, in spite of the wide stratigraphic range (more than 10 My) from which the various specimens were collected. And despite the abundance of material, very little in the way of formal description was ever performed on it. White's 1935 work established a preliminary description of the skull, but the remainder of the material at the Museum of Comparative Zoology was left unstudied on the collection shelves because the resources (time and space, in abundant quantities!) required to study such a large specimen adequately were in short supply. Whatever chances existed of that specimen ever being described disappeared in the mid-50's, when the Director of the Museum, the near-legendary Alfred Sherwood Romer, was approached by a wealthy Boston gentleman, named Godfrey Cabot, whose family had a history of sighting

Big pliosaurs

sea-serpents in the coastal waters around that city. He was interested in assisting research into these sea-serpents, and Romer informed him that he had "the mother and father of all sea-serpents" sitting in the basement of the museum. Cabot promptly made a rather generous donation, and work started mounting the pliosaur material for display. It is well known that Romer's primary interest was in the synapsid ancestors of the mammals, and pliosaurs fall well outside this interest; it would not then be unfair to say that Romer held little concern for the material as a subject of scientific study. The fossil was incorporated into the display, and was rather crudely 'improved' with liberal applications of Plaster-of-Paris to give the impression of a complete, well preserved specimen. Even White's original restoration of the skull seems to have been ignored, for the finished restoration of the skull on the display bears little resemblance to White's illustrations. Romer published a brief account of the material (Romer & Lewis, 1959), but it appears that much of the information he reported must have come to him second hand as it contains a number of errors and inconsistencies. This is compounded by the problem that the material had been sitting on shelves for over 20 years, and the person who had collected the material was long gone to another institution. Despite the attention that has been directed at this mount since the display opened, with the reconstructed animal measuring nearly 13 metres and for a long time bearing the title of the largest marine reptile ever recorded, the "Harvard *Kronosaurus*" is a rather disappointing restoration of what must have been an excellent fossil specimen.

The same problems of space and time were not unique to the Museum of Comparative Zoology; the Queensland Museum was also forced to leave the material it was collecting unprepared and unstudied because of similar logistical considerations. In his review of Australian fossil reptiles Molnar figured the large section of skull included with QMF 2446, noting that it differed from the MCZ restoration. Recalling that the Harvard material was from the Doncaster member of the Wallumbilla Formation, a unit stratigraphically older than the rocks that had yielded both the holotype of *Kronosaurus queenslandicus* and the referred specimen QMF 2446, Molnar suggested that the Harvard material might represent a different species to *K. queenslandicus* (Molnar 1991).

Brachaucheniids in South America...

So far, the Toronto specimen recovered by Bartholomai is probably the most complete specimen of *Kronosaurus queenslandicus* known to date, but Queensland was not the only place producing large pliosaur fossils during the 1970s. Perhaps the most complete specimen of any large pliosaur yet found – certainly the best from the Cretaceous – was unearthed near the village of Leiva, in the Boyaca Provenance of Colombia in 1977, from rocks of Aptian age. Notice of the discovery was published soon after (Acosta et al. 1979), and Hampe (1992) published a preliminary description in which he named the new specimen *Kronosaurus boyacensis*. This specimen remains in the ownership of the village near to which it was found – it has not been moved, but was placed on public display by constructing a shed over the top of it – but whether the specimen will survive for long in the absence of curation in a temperature and humidity controlled environment is questionable (O. Hampe, pers. comm.).

When Hampe was studying the Colombian *Kronosaurus*, the only comparison he could make with *K. queenslandicus* was with the Harvard mount. *K. boyacensis* certainly differs from that reconstruction, but then so does *K. queenslandicus*. Although it seems that the two species are far more similar than Hampe initially suspected, some of the details he described from the Colombian fossil – in particular, a premaxillary tooth count of five – do suggest that the Boyaca pliosaur is a different species to Longman's *K. queenslandicus*. Premaxillary tooth counts have long been emphasised in pliosaur alpha taxonomy (Noè et al. 2004, Tarlo 1960 – see discussion in Chapter 6), and a different count between *K. queenslandicus* and *K. boyacensis* could arguably indicate a genus-level distinction between the two species, but when the jaws are preserved in tight occlusion, as they are in *K. boyacensis* holotype, this feature can be difficult to interpret and may need revisiting. Hampe did note that the number of cervical vertebrae (12-13) and the lack of infra-central foramina were features that *K. boyacensis* shared with *Brachauchenius lucasi*, and referred the new species to Williston's Brachaucheniidae (Hampe, 1992).

...and polycotyliids in the North

That this taxonomic decision by Hampe was the first use of Williston's family in the 68 years since it was created is somewhat indicative of the attention given to Cretaceous large pliosaurs during the 20th Century. This is not to say that Chalk Age plesiosaurs were completely ignored during this time: if the European Jurassic was the focus of plesiosaur publications during the 19th Century, then the American Cretaceous was the primary focus of the 20th, largely due to the work of Welles, who wrote extensively on the plesiosaur fossils from the Western Interior and California Basins of North America. Welles' attention was held by the spectacular elasmosaurs – those with the impossibly long necks – and the another group of small plesiosaurs, the polycotyliids.

Although not closely connected to the large pliosaurs, the Polycotylidae nevertheless represent an interesting radiation of the plesiosaurian body plan that became very common in Late Cretaceous rocks worldwide. In some ways, they seem to mark a third way in plesiosaur evolution: instead of having either a short skull + long neck (plesiosauroids) or a long skull + short neck (pliosauroids), polycotyliids combine a relatively long neck with an elongated skull reminiscent of the ichthyosaurs. By the Late Cretaceous the ichthyosaurs had disappeared from oceans worldwide, and the polycotyliids have been suggested as a move into that vacant ecomorph by the plesiosaur lineage. Whatever the true story behind their evolution, the nature of Polycotylidae evolution, together with that of the contemporaneous elasmosaurs, was the subject of several papers by Welles. In 1963 Welles did turn his attention briefly to the larger pliosaurs, describing some material from the Turonian of Texas that he and his co-author referred to Owen's *Polyptychodon*. The material is scrappy but was considered sufficient to warrant creation of a new species, *Polyptychodon budsoni* (Welles and Slaughter 1963). A rather more complete specimen, also from the Texas Turonian, was described by Storrs (1981) and referred to Welles and Slaughter's new species.

Owen had originally referred *Polyptychodon* to the Pliosauridae, but that referral was made when all short-necked plesiosaurians were placed in that one family. When Williston created the Brachauchenidae to hold *Brachauchenius*, the taxonomic status of *Polyptychodon* was not reviewed and its familial placement was allowed to stand

without any serious consideration of how many families of large pliosaur were actually present in the Cretaceous. Indeed, most workers seem simply to have ignored Williston's Brachaucheniidae until Hampe placed *Kronosaurus* within it (Hampe, 1992). Soon thereafter, Carpenter reviewed the short necked plesiosaurians from the Western Interior Basin of North America: in addition to clarifying the taxonomic status of various polycotylids (which, in contrast to the wisdom of the time, he suggested were actually derived plesiosauroids), he described a new, complete skull of *Brachauchenius lucasi* that was on display at the Fort Hays Sternberg Museum in Kansas (Carpenter, 1996). He also described a new species based upon a specimen held at the Pittsburgh Museum. Carpenter named this new animal *Plesiopleurodon wellsi*, in honour of Welles' work on American plesiosaurs and to draw attention to a perceived similarity to the Jurassic *Liopleurodon* (Carpenter 1996). Although the paper in which this new species was christened places *Plesiopleurodon* within the Brachaucheniidae, this was a typographical error and Carpenter intended to refer the species to the Pliosauridae (K. Carpenter, pers. com.).

In the last decade, work on the large Cretaceous pliosaurs has included; the recovery of another pliosaur specimen from the Colombian Aptian, possibly representing a new species (M. Gomez, pers. com.); relocation of the type locality of *Brachauchenius lucasi* (Schumacher and Everhart 2005); description of new brachaucheniid material from the Barremian of Colombia (Hampe 2005), which represents the earliest large pliosaur known from the Cretaceous; and the identification of fragments of a large pliosaur from the Late Cretaceous of Japan (M. Everhart, pers. com.).

1.2 The feeding ecology of large pliosaurs

Even amongst aficionados of big carnivores, the large pliosaurs hold a special place in the unofficial ‘premier league’ of super-predators (Forrest 2008). Although not as well studied as their dinosaurian contemporaries or their mammalian successors, the sheer size and power of a large pliosaur skull is hard to ignore. Ever since Conybeare first commented in print on the existence of these monsters, their place at the top of the Mesozoic marine food chains has more or less been assumed, and the ‘godzillaisation’ of *Liopleurodon* in recent popular accounts has drawn further attention (Ellis 2003).

The assumption of ferocity is understandable, given the large, robust skull and the big caniniform teeth, and there have been some attempts to evaluate pliosaur ecology using scientific approaches. Massare reviewed the tooth morphology of the Oxford Clay pliosaurs and demonstrated similarities between *Liopleurodon* and a modern apex marine predator, the killer whale *Orcinus* (Massare 1987). A broad diet, also typical of apex carnivores, is suggested by fossilised stomach contents of Middle and Upper Jurassic pliosaurs (Martill 1992, Taylor et al. 1993). Marks on the bones of long necked plesiosaurs have been interpreted as bite marks from large pliosaurs (Clarke and Etches 1991, Thulborn and Turner 1993).

The skull of large pliosaurs count amongst the largest known for any (presumed) macrophagous predator. However, having a large skull does not indicate predatory power *per se*. As the apex carnivore of modern marine ecosystems (Pauly et al. 1998), *Orcinus* has a much shorter skull, in both absolute and relative terms, than those of the baleen whales such as *Balaenoptera*, the sperm whale *Physeter*, or Shepherd’s beaked whale *Tasmacetus*. *Orcinus* also has, relative to body size, a snout that is shorter and broader than that of other delphinids such as the bottlenose dolphin *Tursiops*. In another group of living aquatic predators, the crocodiles, a robust, broad snout is also linked with feeding on large prey. Conversely, more elongated snout proportions, in both odontocetes (toothed whales) and crocodiles is linked with a diet of smaller, agile prey such as fish. The skulls of large pliosaurs appear to be both robust and relatively elongate (Figure 1-5), which complicates attempts to infer diet from overall skull proportions.

The tooth morphology of the biggest pliosaurs – *Liopleurodon*, *Pliosaurus*, and *Kronosaurus* – may provide a clearer indicator of their feeding ecology. The caniniform teeth of *Liopleurodon* and *Kronosaurus* have a robust conical shape, with enlarged crowns and deep set roots, are very similar to those of *Orcinus* and the larger, macrophagous species of *Crocodylus*. The trihedral section of the teeth of *Pliosaurus*, which combine the strength of the conical section with the cutting ability of a more flattened, blade-like tooth, may indicate an even greater ability to feed on large prey. In all of these pliosaurs, the caniniform ‘fangs’ are often broken at the tips, with the broken surface reworn smooth: a similar pattern of breakage and wear can be seen in the teeth of large *Crocodylus* and in *Orcinus* and in these is understood to result from feeding on large prey with robust bones (Massare 1987). However, like skull size, tooth size and shape does not necessarily indicate prey size; the largest conical teeth of any modern predator are the lower jaw teeth of the sperm whale *Physeter*, and yet sperm whales feed predominantly on squid and fish and are not believed to routinely feed on marine reptiles or mammals (Clarke et al. 1993, Clarke and Paliza 2001). Sperm whales are able to feed on the largest species of squid, including giant squid *Architeuthis* and colossal squid *Mesonychoteuthis* (Clarke 1996), but the functional relationships between tooth morphology and teuthivory in odontocetes are poorly understood because many teuthivorous species (e.g. the beaked whales Ziphiidae) lack functional feeding teeth (Pauly et al. 1998), and stomach contents from individual sperm whales that lack teeth indicate that those animals were still able to feed. Functional inferences are difficult given that little is understood about how sperm whales actually find and catch squid (Fristrup and Harbison 2002), but it is clear that sperm whales do not use their teeth to catch large vertebrate prey, as fish form a minor part of the diet and the species taken tend to be small (Clarke 1996, Clarke et al. 1993, Clarke and Paliza 2001).

Sperm whales are not the only odontocete that possess large, caniniform teeth, but which do not appear to routinely target marine mammals or reptiles. Relative to jaw size, the teeth of the false-killer whale *Pseudorca* are perhaps the largest of any odontocete (with the exception of the enlarged tusk of the narwhal *Monodon*), but marine mammals seem to form a minor part of its diet and most prey are fish and squid (Stacey et al. 1994). Even with the killer whale *Orcinus*, there appear to be

Big pliosaurs

populations that feed almost exclusively on fish and which may be reproductively isolated from those animals that prey upon marine mammals (Jefferson et al. 1991); both forms, however, have the large caniniform teeth characteristic of the species.

In addition to enlarged, caniniform teeth, many species of crocodylian also display anisodonty, where there is appreciable variation in size of the teeth along the tooth row (Iordansky 1973), and the degree of anisodonty appears to be greatest in the most macrophagous species. However, as with toothed whales, the link between tooth shape and predation upon large mammals or reptiles does not always hold for crocodylians, either: although species such as *Crocodylus niloticus*, *C. palustris*, *C. porosus*, and *Melanosuchus* certainly prey upon large animals, there are many other species that have similar robust, conical teeth and anisodontic dentition, but which appear to feed mostly on fish; *Caiman crocodylus*, *Crocodylus acutus*, *C. intermedius*, *C. mindorensis*, *C. moreletti*, and *C. novaeguinae*, and this list does not include the longirostrine taxa that are believed to be specialised piscivores (Ross and Garnett 1989). Even for the modern crocodile with one of the fiercest reputations, the saltwater crocodile *Crocodylus porosus*, has resided in Australia for a period of at least 30,000 years, between the Pleistocene extinction of the marsupial megafauna and the Recent introduction of the feral Asian water buffalo (Wroe 2002, Wroe et al. 2006), with no available large prey, and yet appears to have prospered regardless (Molnar 1991).

Comparative anatomists, and particularly palaeontologists, have long sought to explain the function of structures in poorly known animals by identifying analogues in species where the function is better understood: in the case of plesiosaurs, this dates back to the first description of *Plesiosaurus dolichodeirus* by Conybeare (1824). However, the conflicting signals between skull shape, tooth morphology, and feeding ecology in living aquatic predators make this a somewhat complicated task in the case of large pliosaurs. The situation is made even more difficult by the fact that (a) pliosaurs, plesiosaurs, and even sauropterygians are a completely extinct group of reptiles with no close living relatives, and (b) in terms of their anatomy, they seem to be a mish-mash of different aspects of modern animals; the skull looks a bit

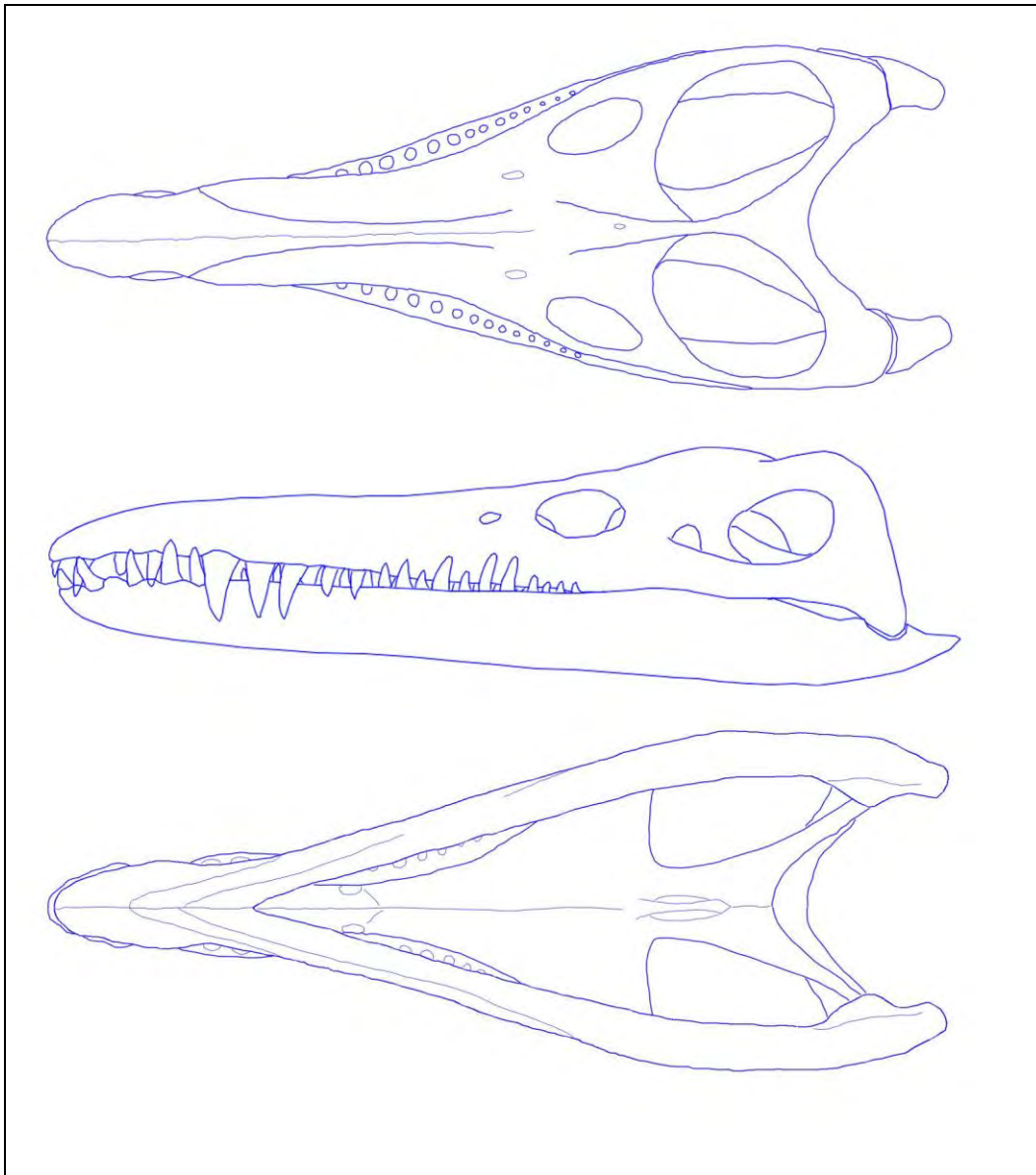


Figure 1-10: Preliminary reconstruction of the skull of *Kronosaurus queenslandicus*, in (top) dorsal, (middle) lateral, and (bottom) ventral view, from data collected in 1997 (see Chapter 4). Compare the dorsal view with the crocodylian skulls in Figure 1-11.

like that of a crocodile, but also shares features of some mammals and even birds (McHenry et al. 2006). If, given a rough idea of skull shape in a large pliosaur such as *Kronosaurus* Figure 1-10, we were asked to pick the most similar looking crocodile Figure 1-11 on the basis of overall skull proportions, the best choice might be the skull of the Orinoco crocodile *Crocodylus intermedius*. In the case of odontocetes, the bottlenose dolphin might be a better match, in terms of snout proportions, than a killer whale – and yet, in aspects of the dentition, *Kronosaurus* certainly resembles killer

Big pliosaurs

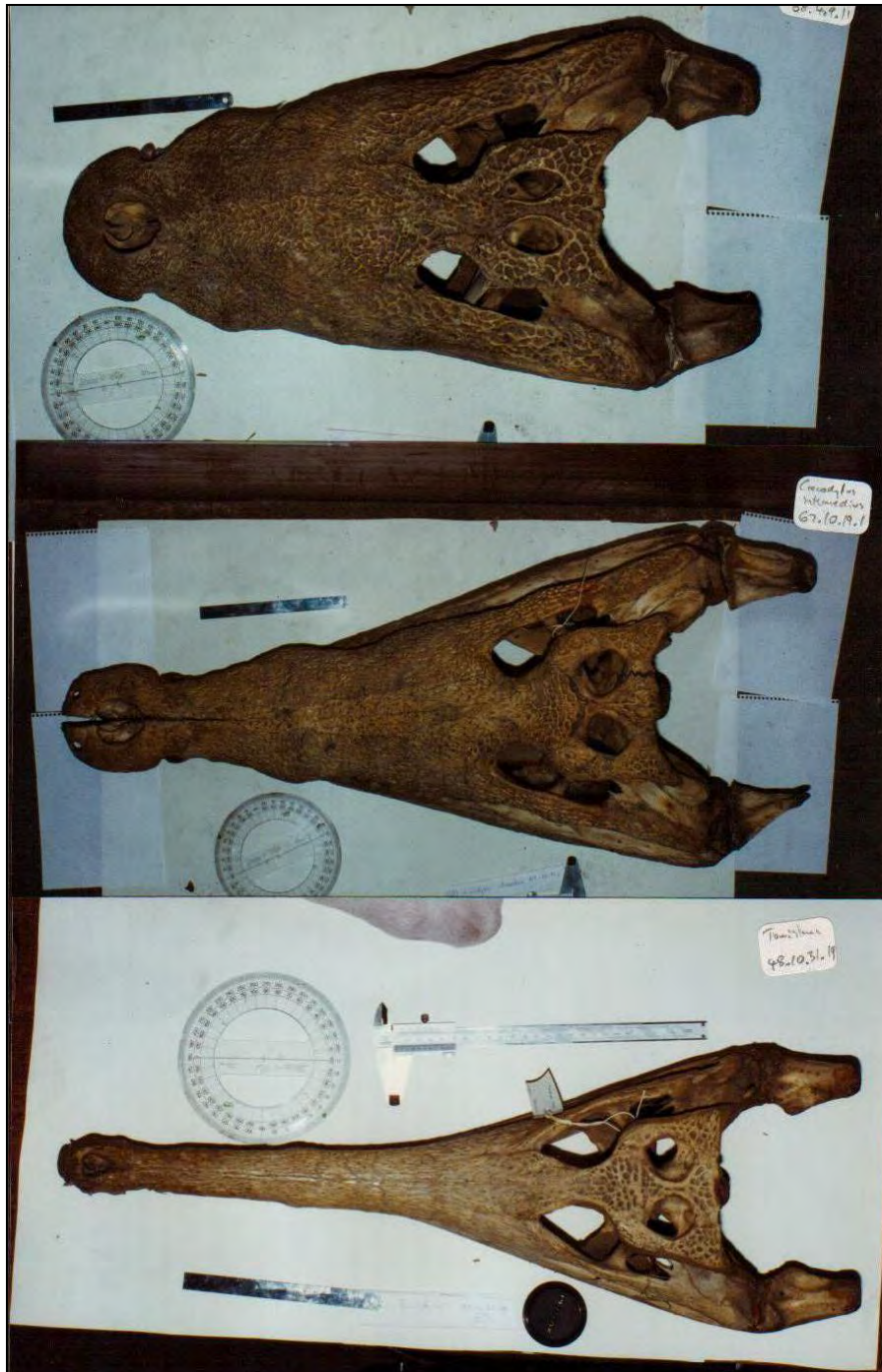


Figure 1-11: The skulls of three modern crocodylians in dorsal view: from top to bottom, the mugger *Crocodylus palustris* (similar to *C. niloticus* or *C. porosus*); the Orinoco crocodile *C. intermedius*; and the false gharial *Tomistoma schlegelii*.

whales and saltwater crocodiles Figure 1-12. And yet both of those species can survive perfectly well on a diet of fish – and at the same time, are capable of taking the largest prey by any mammal or reptile respectively. How then, in the face of this confusion, are we to attempt an accurate reconstruction of the ecology in a group of

predators that are, in terms of geological longevity, the most important marine carnivores in the history of life on Earth?

Stomach contents and other form of trace fossil evidence can provide an invaluable window into the lives of ancient animals, especially with plesiosaurs (McHenry et al. 2005), but are too rare to provide a full picture. Most fossils provide direct information on structure but not behaviour and, as noted above, palaeontologists have relied extensively on the our understanding of the relationship between structure and function (Thompson 1917) in living organisms to reconstruct the biology of extinct species. One branch of biology in particular, functional

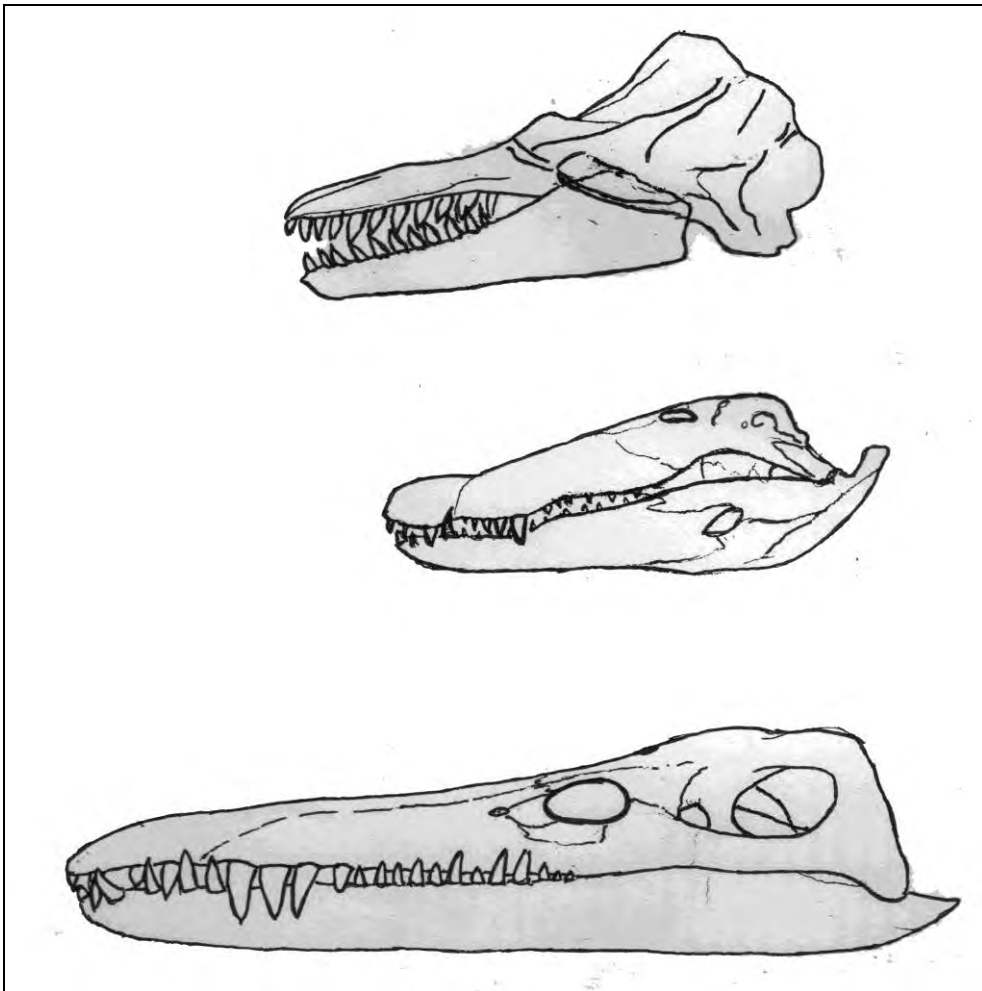


Figure 1-12: The skulls of a Killer whale *Orcinus orca* (top), a saltwater crocodile *Crocodylus porosus* (middle), and the pliosaur *Kronosaurus queenslandicus* (bottom – preliminary reconstruction), viewed in left lateral aspect. The skulls are reproduced to scale.

morphology, has provided much of the methodologies and techniques used in studying palaeobiology (Thomason 1995). Although functional morphology is a broad collection of methods which includes phylogenetic-based techniques, more traditional approach of explanation by analogy, and quantitative morphometric approaches (Plotnick and Baumiller 2000), recent advances in the application of computational methods to biomechanical approaches offer the possibility of assessing the mechanical behaviour of complex structure for which no obvious modern equivalent exists (McHenry et al. 2007, Wroe et al. 2005). Biomechanical approaches can provide the opportunity to experimentally test palaeobiological hypotheses, and combine a traditional comparative approach with techniques based upon the application of physics and mechanics: the fundamental approach would have been familiar to D'Arcy Thompson (Thompson 1917), but the most recent analyses exploit modern computational capability to increase the power of the approach. One methodology in particular, finite element analysis (FEA) can be used to model the mechanical behaviour of very complex shapes such as the vertebrate skull (Rayfield 2007), and the consequences of different biological behaviours (hypothetical or observed) can be evaluated using this data (Daniel and McHenry 2001, Dumont et al. 2005, Jenkins et al. 2002, McHenry et al. 2006, Metzger et al. 2005, Pierce et al. 2008, Rayfield 2005, Rayfield et al. 2001, Ross et al. 2005, Snively and Russell 2002, Strait et al. 2005).

Since 2003 an Australian based group of researchers (the Computational Biomechanics Research Group¹², of which I am a proud member) have developed a set of techniques for modelling the biomechanics of the skull in fossil and extant species of a wide range of taxa that allow rapid construction and testing of models using realistic features such as heterogeneous material properties, cranial-mandibular and cranial-cervical articulation, and highly resolved 3D geometry of the jaw musculature (Bourke et al. 2008, Clausen et al. 2008, McHenry et al. 2007, Moreno et al. 2008, Wroe 2007, Wroe et al. 2007a, Wroe et al. 2008, Wroe et al. 2007b). These methods provide the opportunity to test, for the first time, the biomechanics of the pliosaurian skull using accurate complex computer-based simulations. However, these 3D modelling techniques require accurate information of the 3D geometry of

¹² www.compbio mech.com

the skull, data which is not available for many specimens of large pliosaur because of taphonomic distortion.

The fossil material of large pliosaurs from the Early Cretaceous of the Australian Great Artesian Basin, all of which is currently referred to *Kronosaurus queenslandicus* Longman 1924, is remarkable for the frequent high quality of its three dimensional preservation, apparently a consequence of preservation in nodular limestone. As detailed above, a great deal of material has been collected, including numerous skulls, providing the opportunity to accurately describe the three dimensional geometry of a large pliosaur to the level of detail required for finite element analysis. Despite the abundance and quality of the material, however, the anatomy and taxonomy of *Kronosaurus queenslandicus* have not been studied in any detail: before the geometry of the skull can be reconstructed, a basic level of knowledge of these is required. Three-dimensional reconstruction of the skull geometry of *K. queenslandicus* will allow the skull biomechanics to be assessed using finite element analysis: data from that analysis can then provide the basis for a reconstruction of the palaeoecology in this species of large pliosaur.

1.3 Aims and structure of this thesis

This thesis will attempt to:

- Review the material currently assigned to *Kronosaurus queenslandicus* Longman 1924 currently held in the collections of the Queensland Museum (QM) and the Museum of Comparative Anatomy (MCZ), and assess the skull anatomy and taxonomy to the level required for reconstruction of the geometry of the skull.
- Use the available anatomical information to create a three-dimensional reconstruction of the skull geometry, taking into account the taphonomic context of each specimen.
- Conduct a biomechanical analysis of the skull of *Kronosaurus*, in comparative context with the skull of a modern large aquatic carnivore (*Crocodylus porosus*), using high resolution finite element analysis.
- Describe the functional morphology of *Kronosaurus queenslandicus*, based around the biomechanical analysis of the skull but including other types of anatomical data, and placed within the context of predator body size.
- Augment data from analysis of functional morphology with available taphonomic evidence of feeding ecology.
- Place these into a palaeoenvironmental context to provide a reconstruction of feeding ecology in *Kronosaurus queenslandicus*.

The biomechanical analysis of the skull will form the core of the work, and is based around the techniques using finite element analysis developed in collaboration with the other members of the Computational Biomechanics Research Group (Bourke et al. 2008, Clausen et al. 2008, McHenry et al. 2007, Moreno et al. 2008, Wroe 2007, Wroe et al. 2007a, Wroe et al. 2008, Wroe et al. 2007b). A comparative approach is used, whereby the biomechanical response of the skull in *Kronosaurus* is modelled along that of an extant predator with similar overall skull proportions, *Crocodylus porosus*: ecological interpretation of results is made in light of described feeding behaviour for *C. porosus* and similar taxa.

To complete these tasks, the thesis will be organised as follows;

- Chapter 2: A summary of the issues and methods relevant to Finite Element Analysis (as conducted in this thesis).
- Chapter 3: The geological context of the fossil material, including the palaeoenvironmental data required for interpretation of palaeoecology, and a summary of the taphonomic processes that have distorted the geometry of the specimens of *Kronosaurus queenslandicus*.
- Chapter 4: An assessment of the taxonomy and basic anatomy (but not including detailed osteology) of the *Kronosaurus* specimens that preserve useful skull material, accounting for taphonomic distortion and augmented by data from other pliosaurs as appropriate, and leading to a 2-dimensional reconstruction of skull anatomy in *Kronosaurus queenslandicus*.
- Chapter 5: Three-dimensional reconstruction of skull anatomy in *Kronosaurus queenslandicus*, using the data generated in the preceding chapter in combination with 3-D imaging from CT scan data of one specimen that shows minimal taphonomic distortion.
- Chapter 6: A reconstruction of body size in *Kronosaurus* and other large pliosaurs, a review of the ecological implications of large size in marine amniotes, and an assessment of their taxonomy based upon cranial and post-cranial data.
- Chapter 7: A comparative biomechanical analysis of the skull in *Kronosaurus queenslandicus* and *Crocodylus porosus*, using data compiled in the previous chapters.
- Chapter 8: The reconstruction of the palaeoecology of *Kronosaurus queenslandicus*, combining data from biomechanics, functional morphology, taphonomy, and the described ecology of modern large aquatic predators.

1.4 References

- Acosta, C., G. Huertas, and P. Ruiz. 1979. Noticia preliminar sobre el hallazgo de un presunto *Kronosaurus* (Reptilia: Dolichorhynchopidae) en el Aptiano Superior de Villa de Leiva, Colombia. *Lozania (Acta Zoologica Colombiana)* 28:1-7.
- Andrews, C. W. 1895. On the structure of the skull of *Peloneustes philarcus*, a pliosaur from the Oxford Clay. *Annals and Magazine of Natural History* 16(6):242-256.
- Andrews, C. W. 1909. On some new Plesiosauria from the Oxford clay of Peterborough.
- Andrews, C. W. 1910a. A descriptive catalogue of the marine reptiles of the Oxford Clay. Part 1. *Brit. Museum Nat. Hist. London*.
- Andrews, C. W. 1910b. Note on a mounted skeleton of a small pliosaur, *Peloneustes philarchus* Seeley. *Geological Magazine Lond.* 7:110-112.
- Andrews, C. W. 1913. A descriptive catalogue of the Marine Reptiles of the Oxford Clay, Part II. *BM(NH), London*.
- Bakker, R. T. 1993. Plesiosaur extinction cycles - events that mark the beginning, middle, and end of the Cretaceous. *Geological Association of Canada Special Paper* 39:641-664.
- Bardet, N., and S. Hua. 1996. *Simolestes nowackianus* Huene, 1938 from the Upper Jurassic of Ethiopia is a teleosaurid crocodile, not a pliosaur. *Neues Jahrbuch für Geologie und Paläontologie Monatshefte* 1996(2):65-71.
- Benton, M. 1990. The reign of the reptiles. *Quarto*.
- Bourke, J., S. Wroe, K. Moreno, C. R. McHenry, and P. D. Clausen. 2008. Effects of Gape and Tooth Position on Bite Force in the Dingo (*Canis lupus dingo*) using a 3-D Finite Element Approach. *PLoS ONE* 3(5e2200):1-5.
- Brown, D. S. 1981. The English Upper Jurassic Plesiosauroidea (Reptilia) and a review of the phylogeny and classification of the Plesiosauria. *Bulletin of the British Museum (Natural History), Geology series* 35(4):253-347.
- Buckland, W. 1836. Treatise VI; Geology and Mineralogy Considered with Reference to Natural Theology. *In* The Bridgewater Treatises, On the Power Wisdom and Goodness of God as Manifested in The Creation. William Pickering, London.
- Carpenter, K. 1996. A review of short-necked plesiosaurs from the Cretaceous of the Western Interior, North America. *Neues Jahrbuch für Geologie und Paläontologie Abhandlungen* 201:259-287.
- Carpenter, K. 1997. Comparative cranial anatomy of two North American Cretaceous plesiosaurs. Pp. 191-216. *In* J. M. Calloway, and E. L. Nicholls, eds. *Ancient Marine Reptiles*. Academic Press.
- Carpenter, K. 1999. Revision of North American elasmosaurs from the Cretaceous of the Western Interior. *Paludicola* 2:148-173.
- Clarke, J. B., and S. Etches. 1991. Predation amongst Jurassic marine reptiles. *Proceedings of the Dorset Natural History and Archaeology Society* 113:202-205.

- Clarke, M. R. 1996. Cephalopods as Prey. III. Cetaceans. Philosophical Transactions of the Royal Society of London, Series B 351:1053-1065.
- Clarke, M. R., H. R. Martins, and P. Pascoe. 1993. The diet of sperm whales (*Physeter macrocephalus* Linnaeus 1758) off the Azores. Philosophical Transactions of the Royal Society of London, Series B 339:67-82.
- Clarke, R., and O. Paliza. 2001. The food of sperm whales in the southeast Pacific. Marine Mammal Science (17):2.
- Clausen, P., S. Wroe, C. McHenry, K. Moreno, and J. Bourke. 2008. The vector of jaw muscle force as determined by computer generated three dimensional simulation: A test of Greaves' model. Journal of Biomechanics 41(15):3184-3188.
- Conybeare, W. D. 1824. On the Discovery of an almost perfect skeleton of the Plesiosaurus. Transactions of the Geological Society, Second Series 1:381-389.
- Cruickshank, A. R. I. 1994. Cranial anatomy of the Lower Jurassic pliosaur *Rhomaleosaurus megacephalus* (Stutchbury) (Reptilia: Plesiosauria). Philosophical Transactions of the Royal Society, London B 343:247-260.
- Cruickshank, A. R. I. 1996. Cranial anatomy *Rhomaleosaurus thorntoni* (Reptilia: Plesiosauria). Bulletin of the Natural History Museum Of London (Geology) 52(2):109-114.
- Cruickshank, A. R. I., D. Martill, and L. F. Noè. 1996. A pliosaur (Reptilia, Sauropterygia) exhibiting pachyostosis from the Middle Jurassic of England. Journal of the Geological Society London 153:873-879.
- Cruickshank, A. R. I., P. G. Small, and M. A. Taylor. 1991. Dorsal nostrils and hydrodynamically driven underwater olfaction in plesiosaurs. Nature 352:62-64.
- Daniel, W., and C. McHenry. 2001. Bite force to skull stress correlation: modelling the skull of *Alligator mississippiensis*. Pp. 135-143. In G. Grigg, F. Seebacher, and C. Franklin, eds. Crocodylian biology and evolution. Surrey Beatty, Chipping Norton.
- De Blainville, M. H. 1835. Description de quelques espèces de reptiles de la Californie précédée de l'analyse d'un système général d'érpetologie et d'amphibiologie. Nouvelles Annales du Museum d'Histoire Naturelle de Paris 3:233-272.
- De la Beche, H., and W. D. Conybeare. 1821. Notice of the discovery of a new fossil animal forming a link between the Ichthyosaurus and the Crocodile, together with general remarks on the osteology of the Ichthyosaurus. Transactions of the Geological Society of London 5:559-594.
- Druckenmiller, P. S. 2006. Early Cretaceous plesiosaurs (Sauropterygia: Plesiosauria) from northern Alberta: palaeoenvironmental and systematic implications. PhD Thesis, University of Calgary.
- Druckenmiller, P. S., and A. P. Russell. 2008. A phylogeny of Plesiosauria (Sauropterygia) and its bearing on the systematic status of *Leptocleidus* Andrews, 1922. Zootaxa 1863:1-120.
- Dumont, E. R., J. Piccirillo, and I. R. Grosse. 2005. Finite-element analysis of biting behaviour and bone stress in the facial skeleton of bats. Anatomical Record 283A:319-330.

- Ellis, R. 2003. *Sea Dragons: predators of the prehistoric oceans*. Kansas University Press.
- Erwin, D. H. 1991. The mother of all mass extinctions. *Palaios* 6(6):517-518.
- Forrest, R. 2008. The Plesiosaur Site. www.plesiosaur.com.
- Fristrup, K. M., and G. R. Harbison. 2002. How do sperm whales catch squids? *Marine Mammal Science* 18(1):42-54.
- Hampe, O. 1992. Ein grosswuchsiger Pliosauridae (Reptilia: Plesiosauria) aus der Unterkreide (oberes Aptium) von Kolumbien *Courier Forsch.-Inst. Senckenberg* 145:1-32.
- Hampe, O. 2005. Considerations on a *Brachauchenius* skeleton (Pliosauroida) from the lower Paja Formation (late Barremian) of Villa de Leyva area (Colombia). *Mitt. Mus. Nat.kd. Berl., Geowiss. Reihe* 8:37-51.
- Hampe, O., and C. Leimkuhler. 1996. Die Anwendung der Photogrammetrie in der Wirbeltierpalaontologie am Beispiel eines *Kronosaurus*-Fundes in Kolumbien. *Mainzer geowissenschaftliche Mitteilungen* 25:55-78.
- Home, E. 1814. Some account of the fossil remains more nearly allied to the fishes than any other classes of animals. *Philosophical Transactions of the Royal Society of London* 104:571-577.
- Iordansky, N. N. 1973. The skull of the Crocodilia. Pp. 201-262. *In* C. Gans, ed. *Biology of the Reptilia*, vol. 4. Academic Press, New York.
- Jefferson, T., S. Leatherwood, and M. A. Webber. 1993. *FAO species identification guide. Marine mammals of the world*. FAO, Rome.
- Jefferson, T., P. J. Stacey, and R. W. Baird. 1991. A review of Killer Whale interactions with other marine mammals: predation to co-existence. *Mammal Review* 21(4):151-180.
- Jenkins, I., J. J. Thomason, and D. B. Norman. 2002. Primates and engineering principles: applications to craniodental mechanisms in ancient terrestrial predators. *Senckenbergiana Lethaea* 82:223-240.
- Ketchum, H. F. 2008. The anatomy, taxonomy, and systematics of three British Middle Jurassic pliosaurs (Sauroptrygia: Pleiosauria) and the phylogeny of Plesiosauria. Unpublished Ph.D. Thesis. University of Cambridge.
- Knight, W. C. 1895. A new Jurassic plesiosaur from Wyoming. *Science* 2(449).
- Knight, W. C. 1898. Some new Jurassic vertebrates from Wyoming. *American Journal of Science* 4:378-381.
- Longman, H. A. 1924. A new gigantic marine reptile from the Queensland Cretaceous. *Memoirs of the Queensland Museum* 8:26-28.
- Longman, H. A. 1930. *Kronosaurus queenslandicus* A gigantic Cretaceous Pliosaur. *Memoirs of the Queensland Museum* 10(1):1-7.
- Lydekker, R. 1889. On the remains and affinities of five genera of Mesozoic reptiles. *Quarterly Journal of the Geological Society of London* 45:41-59.
- Martill, D. 1992. Pliosaur stomach contents from the Oxford Clay. *Mercian Geologists* 13(1):37-42.
- Massare, J. A. 1987. Tooth morphology and prey preference of Mesozoic marine reptiles.

Journal of Vertebrate Paleontology 7:121-137.

- McHenry, C. R., P. D. Clausen, W. J. T. Daniel, M. B. Meers, and A. Pendharkar. 2006. The biomechanics of the rostrum in crocodylians: a comparative analysis using finite element modelling. *Anatomical Record*, 288A:827-849.
- McHenry, C. R., A. G. Cook, and S. Wroe. 2005. Bottom-Feeding Plesiosaurs. *Science* 310:75.
- McHenry, C. R., S. Wroe, P. D. Clausen, K. Moreno, and E. Cunningham. 2007. Supermodeled sabercat, predatory behavior in *Smilodon fatalis* revealed by high-resolution 3D computer simulation. *Proceedings of the National Academy of Sciences* 104(41):16010-16015.
- Metzger, K. A., W. J. T. Daniel, and C. F. Ross. 2005. Comparison of beam theory and finite element analysis with in vivo bone strain data from the alligator cranium. *Anatomical Record* 283A:331-348.
- Molnar, R. E. 1991. Fossil Reptiles of Australia. Pp. 605-701. In P. Vickers-Rich, J. M. Monaghan, R. F. Baird, and T. H. Rich, eds. *Vertebrate Palaeontology of Australasia*.
- Moreno, K., S. Wroe, P. D. Clausen, C. R. McHenry, D. C. D'Amore, E. J. Rayfield, and E. Cunningham. 2008. Cranial performance in the Komodo dragon (*Varanus komodoensis*) as revealed by high-resolution 3-D finite element analysis. *Journal of Anatomy* 212(6):736-746.
- Noè, L. F. 2001. A Taxonomic and Functional Study of the Callovian (Middle Jurassic) Pliosauroida (Reptilia, Sauropterygia). Unpublished PhD Thesis. University of Derby.
- Noè, L. F., D. T. J. Smith, and D. I. Walton. 2004. A new species of Kimmeridgian pliosaur (Reptilia; Sauropterygia) and its bearing on the nomenclature of *Liopleurodon macromerus*. *Proceedings of the Geologists' Association* 115:13-24.
- Owen, R. 1840. Report on British fossil reptiles. Report of the British Association for the Advancement of Science, London 9:43-126.
- Owen, R. 1840-1845. *Odontography, or a treatise on the comparative anatomy of the teeth; their physiological relations, mode of development and microscopic structure in the Vertebrate Animals*. Hippolyte Bailliere.
- Owen, R. 1841. Report on British fossil reptiles, Part II. Report of the British Association for the Advancement of Science, London:60-65.
- Owen, R. 1860. Report of the Twenty-ninth meeting of the British Association for the Advancement of Science. John Murray.
- Owen, R. 1869. Monographs on the British fossil Reptilia from the Kimmeridge Clay. no.111, containing *Pliosaurus grandis*, *P. trochanterius* and *P. portlandicus*. Monograph of the Palaeontographical Society, London:1-12.
- Pauly, D., A. W. Trites, E. Capuli, and V. Christensen. 1998. Diet composition and trophic levels of marine mammals. *ICES Journal of Marine Science* 55(467-481).
- Pierce, S. E., K. D. Angielczyk, and E. J. Rayfield. 2008. Patterns of Morphospace Occupation and Mechanical Performance in Extant Crocodylian Skulls: A Combined Geometric Morphometric and Finite Element Modeling Approach. *Journal of*

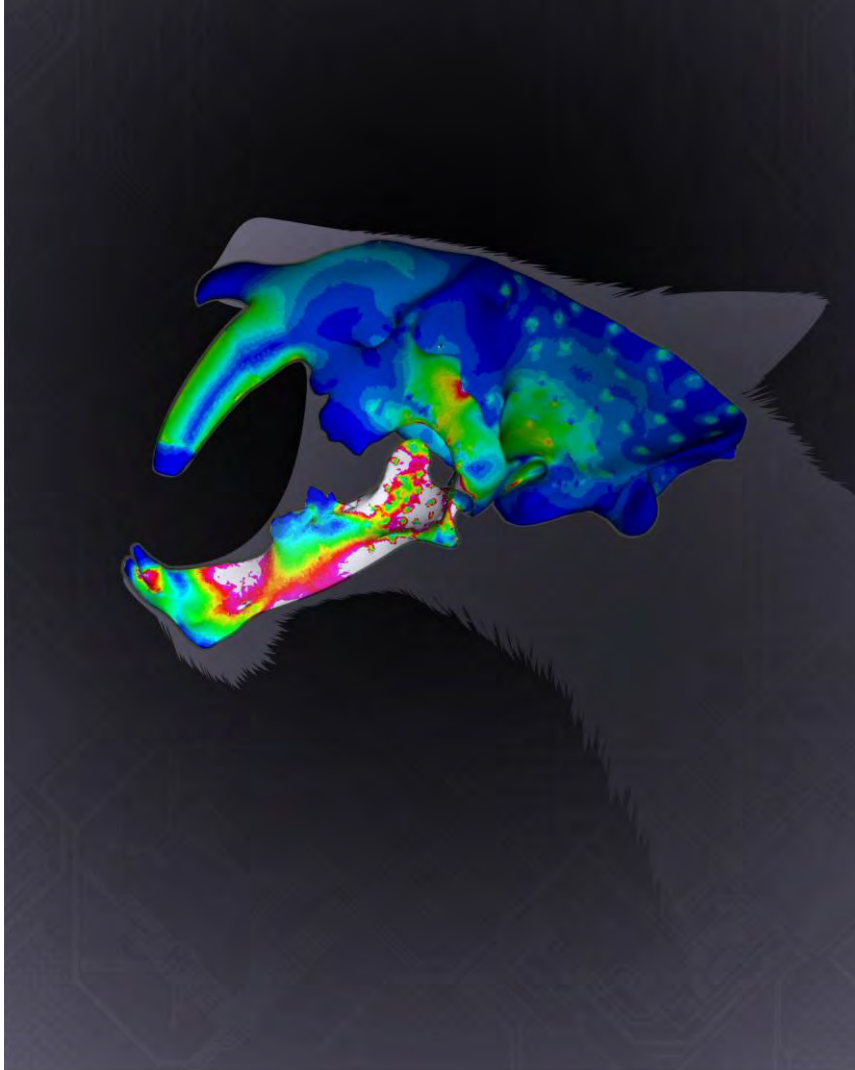
- Morphology 269:840-864.
- Plotnick, R. E., and T. K. Baumiller. 2000. Invention by Evolution: Functional Analysis in Paleobiology. *Paleobiology* 26(4):305-323.
- Rayfield, E. J. 2005. Aspects of comparative cranial mechanics in the theropod dinosaurs *Coelophysis*, *Allosaurus* and *Tyrannosaurus*. *Zoological Journal of the Linnean Society* 144:309-316.
- Rayfield, E. J. 2007. Finite Element Analysis and Understanding the Biomechanics and Evolution of Living and Fossil Organisms. *Annual Review of Earth and Planetary Sciences* 35:541-576.
- Rayfield, E. J., D. B. Norman, C. C. Horner, J. R. Horner, P. M. Smith, J. J. Thomason, and P. Upchurch. 2001. Cranial design and function in a large theropod dinosaur. *Nature* 409(6823):1033-1037.
- Ross, C. A., and S. Garnett, eds. 1989. Crocodiles and alligators. Facts on file, New York.
- Ross, C. F., B. A. Patel, D. E. Slice, D. S. Strait, P. C. Dechow, B. G. Richmond, and M. A. Spencer. 2005. Modeling Masticatory Muscle Force in Finite Element Analysis: Sensitivity Analysis Using Principal Coordinates Analysis. *Anatomical Record* 283A:288-299.
- Sauvage, H. E. 1873. Notes sure les reptiles fossils. *Bulletin de la Societe Geologique de France (Paris)* 3(1):365-380.
- Schumacher, B. A., and M. J. Everhart. 2005. A stratigraphic and taxonomic review of plesiosaurs from the old "Fort Benton Group" of Central Kansas: a new assessment of old records. *Paludicola* 5(2):33-54.
- Seeley, H. G. 1869. Index to the fossil remains of Aves, Ornithosauria, and Reptilia from Secondary System of Strata arranged in the Woodwardian Museum. Deighton, Bell & Co., Cambridge.
- Seeley, H. G. 1874. Note on some of the generic modifications of the plesiosaurian pectoral arch. *Quarterly Journal of the Geological Society of London* 30:436-449.
- Smith, A. S., and G. J. Dyke. 2008. The skull of the giant predatory pliosaur *Rhomaleosaurus cramptoni*: implications for plesiosaur phylogenetics. *Naturwissenschaften* DOI 10.1007/s00114-008-0402-z.
- Snively, E., and A. P. Russell. 2002. The tyrannosaurid metatarsus: bone strain and inferred ligament function. *Senckenbergiana Lethaea* 82:35-42.
- Sollas, W. J. 1881. On a new species of plesiosaur (*P. conybeari*) from the Lower Lias of Charmouth: with observations on *P. megacephalus*, Stutchberry, and *P. brachycephalus*, Owen. *Journal of the Geological Society London* 37:472-481.
- Stacey, P. J., S. Leatherwood, and R. W. Baird. 1994. *Pseudorca crassidens*. *Mammalian Species* 456:1-6.
- Storrs, G. W. 1981. A review of occurances of the Plesiosauria (Reptilia: Sauropterygia) in Texas with description of new material. University of Texas, Ph.D. Thesis
- Storrs, G. W. 1993. Cranial anatomy of a plesiosaur form the Triassic/Jurassic Boundary of Street, Somerset, England.

- Storrs, G. W. 1997. Morphological and taxonomic clarification of the genus *Plesiosaurus* Pp. 145-190. In J. M. Callaway, and E. L. Nicholls, eds. Ancient Marine Reptiles. Academic Press.
- Storrs, G. W., and M. A. Taylor. 1996. Cranial anatomy of a new plesiosaur genus from the lowermost Lias (Rhaetian/Hettangian) of Street, Somerset, England. *Journal of Vertebrate Paleontology* 16:403-420.
- Strait, D. S., Q. Wang, P. C. Dechow, C. F. Ross, B. G. Richmond, M. A. Spencer, and B. A. Patel. 2005. Modeling elastic properties in finite-element analysis: how much precision is needed to produce an accurate model? *Anatomical Record* 283A:275-287.
- Tarlo, L. B. 1960. A review of the Upper Jurassic pliosaurs:.. *Bulletin of the British Museum (Natural History), Geology series* 4:145-189.
- Taylor, M. A. 1992a. Functional anatomy of the head of the large aquatic predator *Rhomaleosaurus zetlandicus* (Plesiosauria, Reptilia) from the Toarcian (Early Jurassic) of Yorkshire, England. *Philosophical Transactions of the Royal Society, London B* 335:247-280.
- Taylor, M. A. 1992b. Taxonomy and taphonomy of *Rhomaleosaurus zetlandicus* (Plesiosauria, Reptilia) from the Toarcian (Early Jurassic) of the Yorkshire coast.
- Taylor, M. A., D. B. Norman, and A. R. I. Cruickshank. 1993. Remains of an ornithischian dinosaur in a pliosaur from the Kimmeridgian of England. *Palaeontology* 36(2):357-360.
- Taylor, M. A. D., and A. R. I. Cruickshank. 1993. Cranial anatomy and functional morphology of *Pliosaurus brachyspondylus* (Reptilia: Plesiosauria) from the Late Jurassic of Westbury, Wiltshire. *Philosophical Transactions of the Royal Society London. B* 341:399-418.
- Thomason, J. J. 1995. *Functional Morphology in Vertebrate Paleontology*. Cambridge University Press.
- Thompson, D. W. 1917. *On Growth and Form*. Cambridge University Press.
- Thulborn, T., and S. Turner. 1993. An elasmosaur bitten by a pliosaur. *Modern Geology* 18:489-501.
- Unwin, D. 2001. An overview of the pterosaur assemblage from the Cambridge Greensand (Cretaceous) of Eastern England. *Mitt. Mus. Nat.kd. Berl., Geowiss. Reihe* 4(1):189-221.
- Welles, S. P. 1943. Elasmosaurid Plesiosaurs with description of new material from California and Colorado. *Memoirs of the University of California* 13(3):125-254.
- Welles, S. P., and B. H. Slaughter. 1963. The first record of the Plesiosaurian genus *Polyptychodon* (Pliosauridae) from the New World. *Journal of Paleontology* 37(1):131-133.
- White, T. 1935. On the skull of *Kronosaurus queenslandicus* Longman. *Boston Soc. Natural History, Occ. Papers* 8:219-228.
- Williston, S. W. 1903. North American Plesiosaurs (Part 1). *Field Columbian Museum, Publ.* 73, *Geological Series* 2(1):1-79.
- Williston, S. W. 1907. The skull of *Brachauchenius*, with special observations on the

relationships of the plesiosaurs.

- Williston, S. W. 1914. *Water Reptiles of the Past and Present*. University of Chicago Press.
- Williston, S. W. 1925. *The Osteology of the Reptiles*. Harvard University Press, Cambridge, Mass.
- Wroe, S. 2002. A review of terrestrial mammalian and reptilian carnivore ecology in Australian fossil faunas, and factors influencing their diversity: the myth of reptilian domination and its broader ramifications. *Australian Journal of Zoology* 50:1-24.
- Wroe, S. 2007. High-resolution 3-D computer simulation of feeding behaviour in marsupial and placental lions. *Journal of Zoology* 274:332-339.
- Wroe, S., P. Clausen, C. McHenry, K. Moreno, and E. Cunningham. 2007a. Computer simulation of feeding behaviour in the thylacine and dingo: a novel test for convergence and niche overlap. *Proceedings of the Royal Society Series B* 274:2819-2828.
- Wroe, S., J. Field, and D. K. Grayson. 2006. Megafaunal extinction: climate, humans and assumptions. *Trends in Ecology and Evolution* 21(61-62).
- Wroe, S., D. R. Huber, M. Lowry, C. McHenry, K. Moreno, P. Clausen, T. L. Ferrara, E. Cunningham, M. N. Dean, and A. P. Summers. 2008. Three-dimensional computer analysis of white shark jaw mechanics: How hard can a great white bite? *J. Zoology* 276(4):336-342.
- Wroe, S., C. McHenry, and J. Thomason. 2005. Bite club: comparative bite force in big biting mammals and the prediction of predatory behaviour in fossil taxa. *Proceedings of the Royal Society of London, Series B* 272:619-625.
- Wroe, S., K. Moreno, P. Clausen, C. McHenry, and D. Curnoe. 2007b. High-resolution computer simulation of hominid cranial mechanics. *The Anatomical Record* 290A:1248-1255.

2. Methods



A biomechanical model of the sabre-toothed cat *Smilodon fatalis*, visualised using finite element analysis (John Conway). At the time that it was produced, this model was the most complex of its kind ever produced for a vertebrate skull (from McHenry et al., 2007)

“I just want to know where to put the damned callipers!”.

Attributed to Jim Farlow (M. Meers, pers. com.)

2.1 **Functional morphology – peering dimly into the past**

In living animals, our knowledge of a predator’s feeding ecology is based largely on direct evidence, such as observed hunting behaviours, analysis of stomach contents and faeces, and in some cases isotope analysis of epidermal structures such as fur and feathers (Emslie and Patterson 2007). These lines of evidence can also apply to fossil predators: traces of feeding behaviour, such as tooth marks preserved on the bone of the prey animal (Carpenter 2000, Clarke and Etches 1991, Erickson et al. 1996, Farlow and Holtz 2002), are well known from the fossil record, stomach contents and coprolites are known from a variety of predator groups (Brown 1904, Chin et al. 2003, Chin and Kirkland 1998, Cicimurri and Everhart 2001, McHenry et al. 2005, Northwood 2005, Williston 1904), and isotopic analysis may offer useful data in some circumstances, although diagenesis is a limitation. For fossils, however, these direct lines of evidence are imperfect and may not be available for many species; reconstructions of feeding ecology for many species of extinct predators must therefore rely on indirect evidence, of which the most commonly used is functional morphology.

Functional morphology is a loose term encompassing a range of techniques and approaches that seek to explain biological structures (morphology) in terms of the way they are used by organisms (function). In the present context of reconstructing palaeoecology, these techniques are classified as indirect evidence for behaviour, because they are largely based upon using general patterns to make specific predictions about feeding ecology. A simple example is the observation that many mammals that possess large shearing teeth are carnivorous; on this basis, a fossil specimen of a previously unknown species of mammal, which does not preserve stomach contents or any other direct evidence of diet, may be inferred to be a carnivore due to the possession of shearing post-canine teeth. The prediction of

feeding ecology in the new specimen may be further refined by considering other features of the skull and postcranium.

Both phenomenological and mechanistic approaches can be applied to functional morphology. With the former, it is not necessary to explain the reasons why certain morphologies predict particular ecologies, only to establish a statistically robust link between them, and phenomenological approaches focus on comparing high quality ecological data with morphometric information in order to establish those links (Wroe and Milne 2007). Conversely, mechanistic approaches seek to explain the reasons why a morphology is associated with a specific ecology from first principles, and are based thus almost entirely upon the application of principles from physics and engineering to biological contexts – hence, biomechanics.

In practice, many studies in functional morphology draw on aspects of both approaches to varying degrees (Busbey 1995, Pierce et al. 2008). Whether the approaches used are mainly phenomenological or mechanistic, their application to palaeoecology is similar; relationships between morphology and function are established using data from extant organisms, and then applied to the extinct forms in order to predict ecology. This asymmetry in the use of neontological and palaeontological data can lead to frustration for palaeontologists wishing to use functional morphology to interpret ecology in particular fossil groups; often, the data required from suitable comparative living organisms is lacking. The logistical demands of collecting detailed ecological and morphological / biomechanical data on living species are significant – even so, suitable comparative datasets are surprisingly rare. Partly, this might be a question of motivation; neontologists do not need to employ indirect techniques to describe ecology in living forms because more direct lines of evidence are available to them, whereas for palaeontologists functional morphology is the principle method of reconstructing feeding ecology in many taxa – many studies that use functional morphology do so within a palaeontological context. Unfortunately, the level of direct data on feeding ecology that evidently satisfies neontological curiosity is often an inadequate basis for establishing robust predictions of feeding ecology under a functional morphology approach, compounding the frustration associated with this method and leading to the

observation that palaeontologists have all the questions, but neontologists have all the data.

In terms of the broad methodological framework, functional morphology is almost always applied within a comparative context and is thus part of a rich tradition of comparative biology. Furthermore, functional morphology implicitly assumes a strong relationship between structure and function; the philosophical nature of structure–function relationships in biology is a subject of ongoing debate that dates back to the work of Aristotle (Russell 1916, Shaw 1972), and the preposition that a particular structure precisely predicts a specific function has been rejected by many workers as being an approach that requires a too strongly deterministic concept of the relationship between structure and function – see Gould (2002) for an overview. Even weaker forms of structural determinism, i.e. that particular structures *tend* to predict specific functions, have been challenged by some workers; for example, Lauder considered that the plasticity of behaviour is such that attempts to make any predict of function based upon structure alone are ‘optimistic’ (Lauder 1995).

These criticisms of the assumptions that underlie functional morphology are certainly valid in some cases, as there have been many instances where functional morphology has been narrowly interpreted in a strongly deterministic context. However, to deny that structure has any predictive power with respect to function may be an over-reaction to such excesses. It is true that, in biology, individual structures operate as components of an organism’s anatomy, and that behavioural flexibility means that a structure can, and often does, perform a number of different roles over the course of an organism’s lifetime, but this does not necessarily invalidate the ‘functionalist’ approach. A gentler form of the argument underlying functional morphology is simply that, whatever use a organism makes of a structure, it can not exceed the mechanical capabilities of that structure; that the basic physical properties of the structure sets limits on the range of behaviours it can be employed in. The difference between framing structure–function arguments in this way, as opposed to attempts to discover the optimal use of a structures, has been summarised by Plotnick and Baumiller as asking what a structure *could* have done, rather than what it *did* do (Plotnick and Baumiller 2000). Establishing those limits sets boundaries to the possible range of behaviours, and thus the ecology, available to the organism in

question and can still provide valuable insight, even if it does not tell us precisely what the organism's behaviour actually is/was. Problems of optimality-driven hypotheses notwithstanding (Plotnick and Baumiller 2000), functionalist approaches may also provide insight into the optimal behaviour/ ecology for a certain morphology (Ferry-Graham et al. 2002); however, much caution is needed as optimality, like functionalism, can be problematic if it is applied in too deterministic a fashion (Pierce and Ollason 1987).

Pros and cons of different approaches to functional morphology

Because they are founded on a statistical relationship between ecology and morphology in living organisms, phenomenological approaches work well when they are being applied to fossil species that closely resemble living forms. The diversity of extant form is, however, merely a subset of the range of form that has existed over time and there are myriad examples of structures in fossil species that have no clear analogue amongst the living; a well known example is the sabre-tooth ecomorph, which arose several times amongst various groups of mammals – in particular, the nimravids and cats – but which is absent in modern ecosystems. In such instances, mechanistic approaches can still be informative because, even without any clear modern analogues, the extinct form remains subject to physical and mechanical constraints in the same way that the extant form is, and behavioural-ecological hypotheses can thus be tested using a biomechanical approach, as shown by recent analyses of form and function in the sabre-toothed cat *Smilodon fatalis* (McHenry et al. 2007).

The absence of suitable modern analogues is not necessarily linked with phylogeny; with the above example of sabre-toothed mammals, the extinct sabre-toothed cats have many close living relatives, but these do not share the critical morphological feature (hypertrophied upper canines) that define the ecomorph and thus the ecology of modern cats offers little insight into the palaeoecology of sabre-toothed cats. Indeed, predictive relationships between structure and function that are robust for extant felids can produce highly misleading results if applied to closely related but morphologically distinct species (Wroe et al. 2005), whilst better functional insight can be gained from phylogenetically more distant groups – specifically, the

postcranial skeleton of sabre-toothed cats is more similar to that of bears and this similarity underlies morphological constraints on sabre-toothed cats' ecology (Wroe et al. 2008b). Conversely, useful insight into the palaeoecology of species with no close living relatives might be gained from unrelated living species that possess analogous morphology; for example, the feeding ecology of extinct allosaurid dinosaurs has been reconstructed with reference to the functional morphology of certain species of large varanid lizards (Moreno et al. 2008). This is noteworthy because many modern studies that describe themselves as 'comparative biology' emphasise phylogenetics as a primary context for the data, to the point where 'comparative' techniques are explicitly linked with phylogenetic analysis (Harvey and Pagel 1991), and leading to the development of numerically based methods that are referred to as Phylogenetic Comparative Methods. This has resulted in some confusion, with oft repeated claims that all palaeobiological analysis must be performed within a phylogenetic framework; however, the importance of phylogenetic context within functional morphology has, in some instances, been overstated and 'non-historical' (or 'ahistorical') studies that do not explicitly frame analysis within a phylogenetic context remain valid (Wu and Russell 1997, Padian 1995). In particular, because they are based upon principles of physics and engineering that are independent of phylogenetic relationships, biomechanical approaches do not depend primarily on the availability of a phylogenetic context.

Both of these factors – lack of clear modern structural analogues, and lack of modern phylogenetic relatives – apply to the reconstruction of palaeobiology in pliosaurs. Pliosaurs are a member an important group of reptiles, the Sauropterygia, which are completely extinct and which have no close modern relatives. Recent phylogenetic analysis place sauropterygians within the Diapsida (O'Keefe 2001), but this is a very broad phylogenetic context that spans crocodylians, birds, lizards, snakes, and tuataras, and which does not in any case include any species that are even broadly comparable, ecologically, to a 10 tonne marine reptile. Morphologically, pliosaurs do have superficial similarities with crocodylians, but they also show similarities with delphinid odontocetes (especially killer whales), lobodontine seals (in particular, leopard seals), and even some groups of aquatic birds (for example, kingfishers) (McHenry et al. 2006), and it is difficult to know *a priori* which of these similarities

are of functional importance with respect to feeding behaviour – this is a significant problem for phenomenological approaches.

An additional problem is that, even if extant crocodylians were to be adopted as an appropriate analogue for pliosaurs such as *Kronosaurus*, the data on feeding ecology in extant crocodylians is very patchy (McHenry et al. 2006) and whilst diet has been described in quantitative terms for some species [e.g. *Crocodylus niloticus* – see Cott (1961)], for most species descriptions of feeding ecology are highly qualitative and are inadequate as a basis for establishing detailed statistical relationships between morphology and diet.

The aim of this work is to provide a reconstruction of feeding ecology in the pliosaur *Kronosaurus queenslandicus*. Because pliosaurs have no close modern relatives, no clear modern morphological analogues, and because the most obvious group for comparison, the crocodylians, do not have adequate ecological data, a phenomenological approach is considered problematic. As mechanistic approaches can be applied in the absence of clear modern analogues or relatives, this study will therefore use a biomechanical approach to the question; what was the feeding ecology of *Kronosaurus queenslandicus*?

Biomechanics as a tool for investigating structure-function relationships in biology

Like functional morphology and comparative biology, biomechanics has a long tradition in the biological sciences, and texts such as ‘On Growth and Form’ (Thompson 1917) contain many of the essential elements of the biomechanical approach. The use of biomechanics as a tool in functional morphology has been referred to as ‘comparative biomechanics’ (Vogel 2003) to distinguish it from the medical context of biomechanics, but both versions of the term are based upon the application of concepts from physics and engineering to biological situations; its application to palaeontology has increased significantly following the work of Alexander (1989, 2003).

Although classical approaches to the subject – in particular, Thompson (1917) – were successful in identifying many of the basic physical principles that shape biological

form, the application of mechanics to specific biological questions faces many obstacles. Biological structures tend to be geometrically complex, much more so than most man-made objects, and classical analytical techniques, such as beam theory, are difficult to apply to objects that have complex/ irregular geometries. Biological materials are also complex: for instance, stiff skeletal structures are often composite materials formed from lattices of inorganic minerals set within an organic matrix with several hierarchical levels of organisational complexity – vertebrate bone being a notorious example (Ferretti et al. 2003, Schnitzler 2003) – whilst soft connective tissues often have viscoelastic properties. In addition, the materials that engineers are most familiar with have Hookerian properties, whilst biological materials are more often non-Hookerian and are both unfamiliar and more complex to analyse for traditionally trained engineers (Vogel 2003).

These challenges have often thwarted attempts to investigate specific examples of biological structure using biomechanics, and the application of mechanics to biology has for a long time been limited to general explanations of the physical limitations on biological form. More recently, however, the advent of desktop computing has enabled the basic principles of mechanics to be applied to vastly more complex problems. Perhaps the most important of the engineering tools developed in the computer era has been Finite Element Analysis: this technique discretises complex shapes into a number of smaller, regular shapes (elements). Mechanical behaviour can be modelled in each element using classical analytical mechanics, and the overall behaviour of the complex shape is thus modelled by summing the behaviour of the individual elements. This approach allows engineers to simulate the mechanics of complex structures and, harnessing the number-crunching power of modern computers, is widely used in the design of many man-made objects, including aeroplanes, cars, buildings, and bridges. The ability of Finite Element Analysis (FEA) to be applied to the mechanics of geometrically complex shapes has encouraged its use by life scientists (Plotnick and Baumiller 2000), and FEA is being used increasingly in biomechanical studies, both in ‘comparative’ (Bourke et al. 2008, Clausen et al. 2008, Daniel and McHenry 2001, Dumont et al. 2005, Jenkins et al. 2002, McHenry et al. 2006, McHenry et al. 2007, Metzger et al. 2005, Rayfield 2005, 2007, Rayfield et al. 2007, Rayfield et al. 2001, Snively and Russell 2002, Strait et al. 2005, Witzel and Preuschoft 2005, Wroe 2007, Wroe et al. 2007a, Wroe et al. 2008a)

and biomedical (Bosisio et al. 2007, Takada et al. 2006, Verhulp 2006, Zhang et al. 2004) contexts.

Plotnick and Baumiller (2000) considered that the use of biomechanics to address questions of functional morphology in a palaeontological context was important enough to coin a new term, 'palaeobiomechanics'. In a review of functional-morphology approaches to palaeobiology, they observed that, because palaeobiology is so dependent upon functional morphology to reconstruct the biology of extinct forms, it requires a different emphasis, where the capability of fossil structures to perform hypothesised functions can be tested using mechanical approaches. An extension of this logic is that the use of functional morphology in palaeontology forms the ultimate test of understanding of the relevant principles and data, and this perhaps explains the particular enthusiasm shown for the application of FEA to palaeobiological questions. Some of the details of the use of FEA within palaeobiomechanical studies are considered in detail below.

Within the broader context of functional morphology, however, an additional point about the potential use of biomechanical approaches is worth noting. Taking measurements from fossil specimens is often complicated by the quality of preservation in various specimens, and even their geographic location in different collections, and taking large sets of measurements from each specimen is often impossible and is at best logistically difficult. A common goal for many palaeoecologists is to identify a small set of measurements that contain the maximum amount of ecological data. Whilst statistical approaches can be used to identify these measurements, it is also possible that biomechanical approaches can be used to identify mechanically important measurements – where to put the callipers – and in this way biomechanics may augment more statistically oriented approaches.

2.2 Finite Element Analysis in Palaeobiomechanics

The application of finite element analysis within palaeontology has developed markedly in the last decade. Many of the developments concern methodological issues; these involve the modelling of geometry, material properties, boundary conditions, loads, and joints. The following summary is not intended to be an exhaustive review: instead, it concentrates on studies that have modelled skull mechanics, as these are of the greatest relevance to biomechanical analyses of feeding behaviour, and in particular on the modelling techniques developed as part of collaborative work with the other members of the Computational Biomechanics Research Group (Clausen et al. 2008, McHenry et al. 2007, Moreno et al. 2008, Wroe et al. 2007a, Wroe et al. 2008a, Wroe et al. 2005, Wroe et al. 2007b). For a broader account of the use of FEA in functional morphology analyses, including historical context, see Rayfield (2007).

Geometry

The complex shape of the biological structure being modelled must be input into the finite element analysis software. As many studies – for example, those focusing upon the vertebrate skull – involve shell structures, both internal and external geometry is required and for this reason CT scan data has been widely used as a primary data source from which the model's geometry is created. Techniques for creating 3D geometry from CT data can be manual, where the coordinates of nodes representing the geometry are specified individually (Daniel and McHenry 2001, Jenkins et al. 2002, McHenry et al. 2006, Rayfield and Milner 2008), or automatic, where specialist software is used to convert the CT data into a 3D 'mesh' that approximates the geometry of the original object and which can then be imported into the FE modelling software (Dumont et al. 2005, McHenry et al. 2007, Moazen et al. 2009, Moreno et al. 2008, Wroe 2007, Wroe et al. 2007a, Wroe et al. 2008a, Wroe et al. 2007b): specific software packages that can perform this step include AMIRA, GEOMAGIC, and MIMICS.

The complex geometry of many biological structures was a substantial obstacle for initial attempts to utilise FEA in biomechanics, with manually constructed models requiring weeks to months to build relatively low resolution models (Daniel and

McHenry 2001, McHenry et al. 2006). Progress in this area, however, has been rapid and current techniques allow the rapid construction of models with a resolution of several million elements (the current record is around four million elements for models of whole skulls) from CT data (McHenry et al. 2007, Wroe et al. 2007b). The highest resolution model that I am aware of to date is a ~90 million element model of the proximal human femur (Verhulst 2006).

In 'surface-based' approaches, the packages used to process the CT data into a 3D model generally create what is known as a surface mesh of the object (Rayfield 2007): the software creates nodes at intervals across the surface (external and internal) of the skull, and connects these nodes into a series of triangles so that the surface geometry is approximated by a polygonal mesh. No nodes are created within the thickness of the structure, i.e. between the internal and external surfaces, so the surface mesh is actually a warped two dimensional surface that occupies 3D space, as with a torus. Finite elements analysis, however, generally requires a solid mesh, where three dimensional elements fill the space between the internal and external surfaces, and many FEA packages are capable of producing a solid mesh based upon a surface mesh. This step requires that the surface mesh is 'watertight' and is of sufficient geometric quality for the solid meshing algorithms to work. Specific FEA packages will produce different solid meshes for a given surface mesh; the polygons that form the surface mesh become the external surfaces of the outermost solid elements. Because commercially available FE packages are geared towards 'traditional' engineering applications, i.e. the use of homogenous, Hookerian materials in man made structures, the solid meshing algorithm may be optimised to reduce bandwidth by using much larger elements internally than are represented by the geometry of the surface polygons. This, however, can be a problem for biomechanical FEA if a 'solid, heterogeneous' approach is being taken to modelling bone (see below), and it may be preferable to have internal elements with edges of a similar size to those on the original surface mesh. An alternative mesh generation technique creates the solid model geometry directly from the voxels of the CT scan, and is thus termed 'voxel-based' meshing (Pfeiler et al. 2007, Rayfield 2007).

In finite element modelling, the elements themselves can be 'low order', which have nodes only at the corners of each element, or 'high order', where there are additional

nodes on each edge. Thus, a low order tetrahedral element has four nodes, whilst a high order tetrahedral element has at least ten. Low order elements use linear equations to describe the element's shape, function and hence behaviour, whereas high order elements use at least quadratic equations for the shape function and therefore more accurately describe the element's response to load (Cook 1995). Thus, finite element models comprising high order elements are considered to give more accurate results than those made from low order elements, but require considerably more bandwidth to solve due to the increase in the number and complexity of equations involved. However, the modelling benefits of high order elements are approximated by increases in resolution; since, with biomechanical models, a high resolution (i.e. large number of elements) model is generally preferred, in order to adequately capture the original geometry, the relative benefits of using high order elements are expected to diminish and Dumont and colleagues found convergence in the results of high order and low order models above a resolution of 200,000 elements (Dumont et al. 2005). For models comprising 1–2 million elements, the relative performance of high order vs low order element models has yet to be quantified, but is not expected to be significant (P. Clausen, pers. comm.).

Likewise, finite element modelling theory predicts higher accuracy with hexahedral elements, which require a surface mesh based upon quadrilateral elements. However, my own experience with the meshing process suggests that surface meshes based upon triangles (the precursor for a tetrahedral element solid mesh) approximate the original geometry with considerably more accuracy than the meshes required to generate hexahedral based models. Although sensitivity analysis of the two mesh types in a biomechanical context are few, there is some evidence that a triangle-based geometry does give more accurate modelling results (Pfeiler et al. 2007).

Algorithms that produce a 3D mesh from CT data typically include smoothing functions, which increases mesh quality (from a computational perspective), but introduces inaccuracies in the geometry of the mesh compared with the original object. For studies that assume homogeneous material properties, this represents only a small source of error, but for 'heterogeneous' approaches that assign material properties to each element on the basis of the CT density of the corresponding voxel (see below), the smoothing produces important errors due to volume averaging of

Methods

surface elements with the surrounding space. This can lead to elements at the surface of the bone being assigned a density that is too low, and where material properties are calculated from density, these surface elements will then have a too-low elastic modulus. After the model is solved, stress in these elements will be artificially low (because they are too weak to carry significant loads), whilst strain will be artificially high (because they have low stiffness and are easily deformed) (McHenry et al. 2007). This error particularly affects surface elements at concavities, where the smoothing functions (which effectively ‘cut the corner’) result in the inclusion of too much empty space within the relevant voxels. Although increasing model resolution can go some way towards reducing this source of error, it is difficult to produce a workable mesh without some use of smoothing functions, and this volume averaging effect remains an unsolved problem. One strategy is to select surface elements likely to be affected by volume averaging, and to manually assign them densities that are more typical of cortical bone (Wroë 2007).

Material properties

Thus far, most applications of FEA to biomechanics have focussed upon the structural mechanics of the hard skeleton, with an emphasis on vertebrates. The modelling of the material properties of bone are therefore an important part of the overall analysis. Bone is a remarkable material; it is a composite of hydroxyapatite crystals and fibrous organic molecules (predominately collagen), capable of self-repair and adaptive remodelling, with a complex, hierarchical organisation encompassing micro-, meso-, and macroscopic scales (Ferretti et al. 2003, Schnitzler 2003). It is also anisotropic; the overall anisotropy of a bony element is a product of material and structural anisotropy at several different scales (Schnitzler 2003).

All of these fundamental properties are at odds with a finite element approach – bone is not organised around the discretised pattern that makes up finite element models. Homogeneous, Hookerian materials can be modelled with reasonable accuracy using FEA because with these the boundaries between elements are simply a modelling convenience and do not represent the fundamental structure of a material such as steel: at the scale represented by individual elements in the model, the material properties of steel and many other commonly used man-made materials

can be modelled without loss of accuracy. In contrast, at a macroscopic scale, bone is a heterogeneous material and the organisation of that heterogeneity does not match the geometric organisation of elements within a finite element model. At the mesoscopic level, various regions of an element such as a femur differ in the basic growth type of bone present (cortical vs spongy), and in the degree of mineralisation. Spongy bone in particular has a complex geometry, being a porous solid of varying porosity, and to accurately model spongy bone requires an extremely high resolution model comprising elements so small that they accurately reconstruct the geometry of individual trabeculae. One attempt to model spongy bone in this fashion required nearly 100 million elements, and demanded significant computational resources to solve; namely, an array of dedicated workstations and many months of CPU time (Verhulp 2006). Although these models did account for the structural heterogeneity resulting from the porous structure of spongy bone, they did not account for the tissue heterogeneity that results from the variable mineralisation of bone, assuming a uniform set of material properties throughout the model. In reality, the degree of mineralisation in bone varies between cortical and spongy bone, within both cortical and spongy bone, between different elements within an organism, with the age of an organism, and between species: the degree of mineralisation has a strong effect on the material properties of bone, with highly mineralised bone having high stiffness at a cost to strength (Currey 2004).

All models necessarily involve simplifications and assumptions, and various authors have attempted to incorporate some aspects of the complex material properties of bone into biomechanical FEA. One technique is to model the bone, not as a porous solid, but as a solid of minimal porosity but highly variable density (McHenry et al. 2007, Moreno et al. 2008, Wroe et al. 2007a). In this approach, the two forms of true variation in density – from the structural heterogeneity of trabecular struts and trabecular spaces within spongy bone, and the tissue heterogeneity of variable mineralisation – is reduced to one parameter of variation in density between elements. In the model construction process, the density of an element is assigned on the basis of the X-Ray attenuation of the corresponding voxel within the CT scan dataset, and does not discriminate between structural and tissue heterogeneity. At very high resolutions, such as the 100 million element models used by Verhulp (2006), the difference between these two components of heterogeneity would be less

important because individual elements represent either empty trabecular space or a small volume of bone of very precise density: however, heterogeneous models of this complexity have yet to be attempted, and in practice much lower resolution models, of a maximum of four million elements, have been employed (Wroe et al. 2007b); in these, an individual element may include both trabecular struts and spaces, as well as a range of different tissue densities, within its volume and as such volume averaging effects are likely to be significant (McHenry et al. 2007, Wroe et al. 2007b). Even so, modelling bone in this fashion is potentially far more accurate than assuming uniform, homogeneous material properties through an entire bone, or even a skull. As yet, however, no attempts have been made to benchmark the accuracy of these ‘coarse heterogeneous’ versus homogeneous approaches against empirical data. In addition, fundamental questions remain about the precise relationship of CT density, absolute density, and basic material properties such as Young’s modulus of elasticity; even for a comparatively well studied and economically important organism such as *Homo sapiens*, there remains considerable disagreement in the literature, with some authors arguing that Young’s modulus of bone is essentially a function of density (i.e. mineralisation), whilst others argue for additional qualitative differences between spongy bone and cortical bone on top of the variation caused by mineralisation (Bensamoun et al. 2004, Bosisio et al. 2007, Kaneko et al. 2004, Rho et al. 1995, Rice et al. 1988, Turner et al. 1999).

The material anisotropy of bone is an additional challenge for FE modelling; although bone is well known to have anisotropic properties, precise measurement of these is problematic and empirical studies have yielded variable results (Kosmopoulos et al. 2008, Rho et al. 1995, Rice et al. 1988, Turner et al. 1999, Wang and Dechow 2006, Wang et al. 2006). Even without this uncertainty, the question of how to incorporate the geometry of anisotropic properties into a finite element model is far from clear, with the result that very few FE models have attempted to include anisotropy – see Strait et al. (2005) for a notable exception.

Thus, while some aspects of the problems surrounding the material properties may yield to further improvements in model resolution and geometry, fundamental questions concerning the details of material properties in bone – and almost all other

biological materials – remain and this is a significant challenge for future improvements in the application of FEA to biomechanics.

Boundary conditions

These refer to the manner in which the modelled structure is held in space. Real organisms are held in position by combinations of gravity, buoyancy, friction, reaction forces, and muscular forces, all of which may operate differentially across the entire organism. Including all of these in a finite element model would be a very complex exercise. Biomechanical finite element analyses that have focused on whole skulls can restrain nodes at the jaw joint (Daniel and McHenry 2001, Dumont et al. 2005), or at the occipital condyle (Bourke et al. 2008, Clausen et al. 2008, Moreno et al. 2008, Wroe 2007, Wroe et al. 2007a, Wroe et al. 2007b); the latter is intended to replicate the way that the skull is held by the neck. For each of these, restraining individual nodes can be methodologically preferable but is biologically unrealistic, as it tends to concentrate reaction forces at individual nodes, and several studies use a network of thin but strong beam elements, tessellated upon the mesh around the restraint point, to spread these forces and avoid point artefacts (Moreno et al. 2008, Wroe et al. 2007a, Wroe et al. 2007b); however, the validity of these approaches remains untested against empirical data. In some cases, the model includes the neck, and the restraints are placed at the posterior end of the neck assembly (McHenry et al. 2007). Where only a portion of the skull, such as the rostrum, is modelled, restraints may be placed along the ‘cut’ edge of the model (McHenry et al. 2006, Rayfield and Milner 2008), but this approach is problematic as it introduces unrealistic constraints upon the model (McHenry et al. 2006).

The other component of boundary conditions involve the manner in which the structure is loaded (this is a separate question to the magnitude and direction of those loads – see below). For example, with the skull of a predator that is biting on a prey item using the force applied by the jaw muscles, the teeth are resisted by the prey’s hard and soft tissues; this situation can be complicated by the failure of the prey’s tissues, which introduce non-linear fracture mechanics, and the way that the prey is itself held (or moving) in space. In terms of finite element modelling, this is a highly complex scenario to model accurately, and most analyses have taken the

cruder, but logistically easier, path of simply restraining the teeth (Dumont et al. 2005, McHenry et al. 2006, McHenry et al. 2007, Rayfield et al. 2001, Wroe 2007, Wroe et al. 2007a, Wroe et al. 2008a, Wroe et al. 2007b) in a manner similar to the restraints on e.g. the occipital condyle described above. These restraints can be partially-fixed (McHenry et al. 2007) or fully-fixed (Wroe et al. 2007b); in neither case, however, has there been any attempt to investigate how well this approach simulates the actual mechanics of an animal biting on a food item.

Loads

The loads experienced by the skull of a predator result from (1) the weight of the predator's own tissues, as well as that of anything being held in the jaws, (2) the tensile forces of the predator's muscles acting upon the skull, as well as reaction forces from joints and objects in contact with the skull, and (3) the action of any prey animal being held in the jaws that has a different velocity to that of the predator. In finite element modelling, the effects of gravity are generally ignored as the effect of self-weight is assumed to be negligible, and only the loads resulting from muscular action are considered here.

From the viewpoint of animal behaviour, the forces generated by a dog shaking a rabbit, or from a varanid gripping part of a large carcass in its teeth and pulling back, may seem different from the forces that result from the violent struggles of a buffalo that is being bitten on the hindquarters by a lion. In terms of modelling the biomechanics, however, all of these scenarios involve forces generated outside of the predator's skull and which apply loads to the skull; for an FE model of the skull alone, it makes little difference if the forces are generated by the predator's own postcranial musculature, or by the muscles of the prey animal. Because of their 'external' nature, these have been classed as 'extrinsic' loads in some analyses (McHenry et al. 2007, Wroe 2007, Wroe et al. 2007a). They are contrasted with the loads resulting from the predator biting into the prey, where the forces generated by the jaw musculature¹ adduct the jaws and force the teeth into the prey; because bites are powered by the musculature of the skull, they are termed 'intrinsic' loads.

¹ McHenry et al. (2007) included the neck-driven bite used by some felids as an intrinsic load, even though the neck muscles that power this bite are anatomically extrinsic to the skull, because they are similar to jaw-driven bites in that they act to force the predator's teeth into the prey, and can be used to augment jaw-driven bites.

In modelling terms, the extrinsic loads can be applied as forces or moments to nodes at the teeth or any other part of the skull. As outlined in the discussion of the boundary conditions above, loads applied to single nodes can cause modelling artefacts: a force can be divided and applied to a number of neighbouring nodes, or applied to a single node and a network of interconnected beams used to distribute the load as described above. Loads representing predator shaking a prey, or a predator being shaken by a prey, can be modelled as a laterally directed force acting on the teeth, whilst the loads that result from a predator pulling against the prey (or the prey pulling against the predator) can be modelled by an anteriorly directed force acting on the teeth (McHenry et al. 2007, Moreno et al. 2008, Wroe 2007, Wroe et al. 2007a). It is generally simplest to apply a moment to a single node; where the moment is being applied to a number of the teeth these can be connected by very stiff beams, and the moment applied to these (McHenry et al. 2007, Wroe 2007, Wroe et al. 2007a).

There is very little data on the magnitude of extrinsic loads that may be encountered by a predator's skull: Preuschoft and Witzel calculated that a dog shaking a 2 kg rabbit induces similar loads to the dog's own predicted bite forces (Preuschoft and Witzel 2005), and in modelling the action of extrinsic loads upon mammalian carnivores various studies have assumed that extrinsic loads are at least equal to intrinsic loads (see below). One advantage of comparative studies is that, in many cases, the accuracy of the load in absolute terms is not as important as gauging the mechanical performance of different skulls relative to each other. Comparative studies are complicated when the skulls in question are a different size; although many of the specific behaviours that generate extrinsic loads can be approximated by standard engineering equations (see Chapter 7), these scale in a number of different ways. Some studies assume that the extrinsic loads scale linearly with predator mass (Wroe 2007, Wroe et al. 2007a): an alternative approach is to simply ignore the difference in size between two predators and apply the same loads to each (McHenry et al. 2007) – the hypothesis being tested then becomes, in effect, one concerning the ability of the predators to tackle prey of a similar absolute size, as opposed to a similar relative size. Yet another approach is to scale the skull models to the same volume (Tseng 2009), which allows results to be framed in terms of mechanical

Methods

efficiency – i.e., mechanical performance for a given amount of structural material – but which can complicate biological interpretation if, for example, the species under study have different head sizes relative to body size. Given that most specimens included in a comparative study are likely to be of differing size, the choices made with respect to scaling loads (or models) are important, as different strategies allow some types of questions to be addressed, but preclude others.

Intrinsic loads – bite forces – can be modelled as simple forces applied to the bite points (i.e., teeth) (McHenry et al. 2006), but this approach does not include the forces produced by the jaw musculature acting on the attachment to the cranium and mandible, which can dominate the loads in the adductor chamber of the skull (Herring and Teng 2000). Many studies, therefore, have included the action of the jaw muscles upon the bones as an integral part of the finite element model. One method of achieving this is to assign forces that act directly on the sites of muscle attachment in the cranium, with the force vector replicating the line of action of the jaw muscle (Dumont et al. 2005, Rayfield et al. 2001); these forces can be subdivided and applied to a number of nodes which are spatially equivalent to the area of the muscle attachment on the skull, which avoids point artefacts (Daniel and McHenry 2001, Ross et al. 2005). If the cranium is restrained at the jaw joint surface and at the bite points, the model simulates the mechanics of a jaw muscle driven bite, including the loads induced by the muscles pulling on the muscle attachments, and the reaction forces produced at the jaw joint and teeth – this approach is biomechanically realistic and has been used by a number of different studies (Daniel and McHenry 2001, Dumont et al. 2005, Rayfield et al. 2001, Ross et al. 2005).

The realism of the model can be increased by including the jaw mechanism; the mandible is articulated with the skull by means of a hinge that replicates the action of the jaw joint (see below), and the skull is restrained at the teeth and at the occiput. The action of the muscles can then be replicated by beams that connect the nodes at either end of the muscle, at the ‘origin’ and ‘insertion’ points of the muscle: assigning a pretension to these beams produces the required forces at either end of the muscle, inducing a torque upon the jaw hinge and resulting in a bite reaction force at the restrained teeth (Bourke et al. 2008, Moreno et al. 2008, Wroe 2007, Wroe et al. 2007a, Wroe et al. 2008a, Wroe et al. 2007b). Using multiple pretensioned beams for

each muscle more closely replicates the 3D geometry of the real muscle, and minimises point artefacts. Alternatively, forces can be applied directly to the nodes representing the muscle attachments on both the cranium and mandible, and as long as these forces are balanced the effect is similar to using pretensioned beams. Because the structural properties of the beams used with the ‘pretension’ technique can affect the net force – the beams effectively absorb some of the pretension force – the latter technique offers some advantages (Clausen et al. 2008); in models that involve the action of muscles across a series of joints, the pretension technique produces substantial artefacts and applying forces directly to nodes at muscle attachment sites is preferable (McHenry et al. 2007).

As with extrinsic loads, the magnitude of the intrinsic loads should be biologically realistic, and although there are more data on bite forces than for extrinsic loads, empirical data on bite force is lacking for all but a few taxa. Many studies of *in vivo* bite force involve studies of jaw kinematics in primates [e.g. Hylander and Johnson (1993) – see Ross et al. (2005) for a FE modelling perspective], but measurement of bite force in non-primates is patchy and for taxa relevant to the biomechanics of large predators data is very rare; Binder and Van Valkenburgh (2000) measured bite force in spotted hyaena *Crocuta crocuta*, Erickson et al. (2003) measured bite force in the American alligator *Alligator mississippiensis*, and Ellis et al. (2008) in domestic dogs *Canis lupus familiaris*.

The physiology of force production by muscle is reasonably well understood, and empirical studies have found that the stress exerted by muscle lies within a consistent range of between 147 and 392 kPa (Rayfield et al. 2001). For an intermediate value of, for example, 300 kPa (Weijs and Hillen 1985), this is equal to a force of 30 Newtons per square centimetre of muscle cross sectional area; various studies have thus derived muscle forces by direct measurement (usually, through dissection) of the physiological cross-sectional area² (PCSA) of the relevant muscles and multiplying

² The relevant measurement of cross-sectional area is normal to the axis of the muscle fibres, but since muscle fibres in non-parallel muscles (i.e. pennate organisation, which characterises most jaw muscles) are not aligned with the axis of the whole muscle, a simple measurement of the cross-sectional area of the entire muscle will not provide an accurate assessment of the force-production capability of the muscle. For this reason, the cross sectional area of individual fibres (or fibre bundles) are measured and summed for the entire muscle – this measurement is termed the Physiological Cross-Sectional Area.

Methods

the result by an estimate of muscle tension (Daniel and McHenry 2001, Moreno et al. 2008, Rayfield et al. 2001, Ross et al. 2005, Strait et al. 2005, Wroe et al. 2008a). An alternative approach was developed by Thomason (1991), who devised criteria for measuring the cross sectional area available within the skull to contain the major muscle groups within the adductor chamber / temporal arcade. In addition to being logistically simpler than direct measurement of PCSA, Thomason's technique has the advantage of being applicable to specimens that do not preserve intact jaw musculature – since this includes most museum specimens and all fossils, Thomason's 'dry skull' method has been employed by palaeobiomechanists to derive estimates of bite force from a large number of extinct and extant taxa (Christiansen 2007a, b, Christiansen and Adolfssen 2005, Christiansen and Wroe 2007, Thomason 1991, Wroe et al. 2005). The estimate of muscle force from the dry skull method can be input directly into a FE model of the skull, and the 3D geometry of the muscle attachment points and vectors may provide an improved estimate of the effective moment arm (inlever) of the jaw muscles, compared with the simpler estimate used in 2D estimates of bite force with the dry skull approach (McHenry et al. 2007, Wroe 2007, Wroe et al. 2007a).

Although very useful for comparative analyses, the dry skull method is a modelling technique and may not accurately predict the actual bite forces generated by the jaw musculature. In a comparison of dry skull predictions of bite force with *in vivo* data taken from the same specimens, Ellis et al. (2008) found that the dry skull method consistently underestimated the *in vivo* measurements. Thomason recognised that measurement of the cross-sectional area of the adductor chamber is likely to underestimate PCSA of the pennated jaw muscles, and used data from dissection of jaw muscles in a range of carnivoran species to derive a regression relationship between the dry-skull estimate of bite force and corrected estimates that account for PCSA (Thomason 1991). Some of the patterns arising from this correction factor, the *in vivo* data collected by Ellis et al. (2008), and the improved estimates of muscle inlever dimensions provided by 3D modelling, are discussed further in Chapter 7.

An important point is that, in many instances, animals may not use all of the available muscle force in an individual bite (Wroe et al. 2005), and indeed many detailed empirical studies of mastication in various mammals, particularly primates,

demonstrate that the pattern of jaw muscle activation during mastication are complex (see, for example, Hylander and Johnson 1993, Ross et al. 2005). However, modelling the actual complexity of jaw muscle activity as part of a 3D finite element model is a logistically difficult task. One recently developed approach that can account for the kinematics of different skeletal parts along a temporal dimension is multibody dynamics analysis (MDA) (Curtis et al. 2008, Moazen et al. 2008a), and some recent studies have combined MDA with FEA (Moazen et al. 2008b) – this is likely to be an important tool in the future development of techniques to more accurately model the action of the jaw muscles upon the skull.

Of course, muscles have many physical properties that make them difficult to model satisfactorily in commercially available FEA software. For example, the maximum force produced by a muscle changes with its length. Although most instances of muscle produced force are correlated with contraction of the muscle, muscles can still exert tensional forces whilst their length is being increased (for example, by the actions of weight or agonistic muscles acting across a joint), or even without any change in length. These latter instances are often described as the ‘bracing’ of a joint or a bone by the muscle, i.e. the tendency of some force to displace a bone or create movement around a joint is counteracted by the bracing effect of the muscle.

Biomechanically, this aspect of muscular action is very important; bracing of the skeleton by the musculature serves to keep the displacement or rotations of joints within permissible ranges, and to distribute loads more evenly across the skeleton, thereby preventing injury to hard and soft-tissues, as well as controlling movement. To replicate the bracing effect of muscles upon a skull within a finite element model is not a straightforward task: one approach has been to use the beams that represent the jaw muscle fibres (see above), but instead of assigning a pretension to these that would simulate muscle contraction, the elastic modulus of the beam elements is increased so that they have sufficient strength to resist movement. This has been used specifically to simulate the bracing action of the jaw muscles on the skull when the teeth are subjected to extrinsic loads (McHenry et al. 2007, Wroe 2007, Wroe et al. 2007a). Determining a realistic value for modulus is a problem, as there are very little empirical data that can be applied to this aspect of muscle mechanics, but some data indicates a modulus of approximately 15 MPa for muscle tissue under rigor (de Winkel et al. 1994).

A final problem in modelling muscles comes from the simple observation that muscle fibres do not run in a straight line from origin to insertion points; instead, the muscles bend around hard and soft-tissue structures. The relevant force vectors imposed by the muscle therefore vary, not only during the contraction and movement of that muscle, but with the contraction of all the other muscles surrounding it. In addition, as muscles wrap around other skeletal structures, they exert loads upon those structures as they contract. All of these can cause significant effects upon the force vectors and effective leverage of different jaw muscles – especially, as we shall see in Chapter 7, the crocodilian pterygoidus muscle – and represent further modelling challenges. One useful approach has been to calculate the tensile, normal, and tangential components of muscle load that act upon skeletal structures using purpose-written software (Grosse et al. 2007). The role played by fascia in aligning and transmitting muscle generated forces, particularly with the mammalian temporal fascia (Preuschoft and Witzel 2002) but potentially also with the fascia associated with the reptilian temporal fenestra(e) and suborbital fenestra, is predicted on biomechanical principles to be significant, but has yet to be incorporated in to FEA of skulls – with the exception of Ross et al. (2005).

Joints

The vertebrate skull contains a large number of joints, mostly fibrous (sutures) but with a small number of synovial joints (jaw joints, cranio-cervical joint).

The mechanical effect of sutures has received some attention (Herring and Teng 2000, Rayfield 2004, 2005) – see Moazen et al. (2008b) for a summary. Growth of the various skull bones is located at sutural contacts (Sun et al. 2004), but the joints are mechanically weaker than bone (Rayfield 2004). Under certain mechanical environments, sutures would be expected to fuse once the requirement for continued growth has finished: this has been suggested for the nasals of *Tyrannosaurus rex*, which fuse at early adulthood and thereby increase the capacity of the facial region to carry torsional loads (Snively et al. 2006). However, many cranial sutures remain patent well after growth as slowed or stopped, and various authors have suggested that the sutures play a role in absorbing stresses within the skull [Jaslow (1990) – see also Moazen et al. (2008b), Rayfield (2004) for a summary from a modelling perspective].

Incorporating sutures into a finite element model of the skull requires high resolution CT data; for large skulls, many medical CT scanners do not provide sufficient resolution. Even with suitable CT data, the geometry of the sutural contacts is difficult to identify using automated techniques and requires intensive manual manipulation of the data. Nevertheless, some studies have started to incorporate sutural joints into FE models of the skull (Moazen et al. 2008b, Rayfield 2004). At present, there is not a great deal of data on the material properties of the soft-tissues within the joints (Moazen et al. 2008b), and it is also not clear how these should be modelled: fibrous structures are predicted to carry more stress in tension along the long axes of the fibres than in compression or shear, and modelling materials in this manner using FEA requires non-linear solutions, which are computationally intensive. An additional complication is that, when the apposing surfaces of bone at the sutural contact are interdigitated – which many sutures in the skull are to some degree – the geometry of fibre orientation within sutures is complex. The question then becomes, from a modelling perspective, whether the complex structure of the sutures demands models that capture this complexity in detail – which would require more complex models than are currently possible – or whether the overall mechanical behaviour of the sutures can be approximated at larger scales. Much more work is required to address this issue.

In terms of their fundamental anatomy and mechanics, synovial joints are more complicated than sutures; they include a fluid-filled, sealed joint space, joint surfaces covered in low-friction cartilage that move substantial distances relative to each other as part of the normal functioning of the joint, a complex arrangement of capsular and accessory ligaments, and in many cases articular discs or menisci that lie with the joint capsule. A detailed mechanical model of such a mechanism would thus require component of linear solid mechanics (sufficient to model the bone), non-linear / viscoelastic solid mechanics (for modelling the cartilaginous and ligamentous components) and fluid dynamics (for modelling the hydrostatic behaviour of the synovial fluid sac). No detailed models of this kind have been attempted, although some analyses have attempted simplified models of derived (non-fluid) joints such as the mammalian inter-vertebral joint, which is of considerable biomedical importance (Baroud et al. 2004, Martinez et al. 1997).

Methods

Despite the detailed complexity of synovial joints, however, their large-scale mechanical properties tend to be simple enough to comprehend using relatively unsophisticated models. The joints transmit forces evenly between the bones involved, and the range of movement that they allow correlates well with the shape of the joint surfaces (Williams and Warwick 1980). In the mammalian jaw joint, the range of movement can be complex: however, the jaws of predators, such as many carnivorans, require fewer degrees of freedom than those of herbivores which must grind their food, and for the purposes of a linear static FE model of a simple bite, rotation around a single jaw axis (aligned more or less in the transverse axis of the skull) is sufficient. Thus, the jaw joint can be modelled as a transversely oriented beam that allows rotation about its long axis; when each end of the beam is connected, via very stiff beams, to the cranial and mandibular joint surfaces respectively, the basic mechanics of the joint are captured in the model, i.e. the ability to allow rotation about a single hinge axis, and to transmit loads across the joint to apposing bones (Bourke et al. 2008, Clausen et al. 2008, McHenry et al. 2007, Wroe 2007, Wroe et al. 2007a, Wroe et al. 2008a, Wroe et al. 2007b). If anything, the reptilian jaw joint has even fewer degrees of freedom than in carnivorous mammals, and this modelling approach can be used for finite element models of reptilian predators as well (Moreno et al. 2008). However, there has yet to be any experimental assessment of how accurately this technique does model the large-scale mechanical properties of synovial joints: in addition, given the potential biomedical benefits of being able to model the soft-tissues of various joints in more detail, it is likely that this aspect of the models will see considerable attention in future research.

Many species of squamates, birds, and fish have kinetic joints within the skull and mandible; these can be 'loose' fibrous joints, or may even be synovial (Metzger 2002). Some attempts have been made to assess the mechanical importance of these joints using FEA (Rayfield 2004, 2005), whilst others have used static models to assess the tendency of the structure to concentrate stress at the points in the skull thought to have kinetic joints (Moreno et al. 2008). From a modelling perspective, the technical issues involved with incorporating kinetic joints into finite element analysis of skulls are similar to those outlined above for sutural and synovial joints, with the likely addition of techniques such as MDA to account for the potential importance of the musculature in controlling skull kinesis (Moazen et al. 2008b).

Measuring mechanical performance

There are many ways of assessing the effects of loads upon a structure: physiologists are familiar with strain, because it can be measured experimentally *in vitro* or *in vivo*. Engineers also make use of stress to assess the capacity of a structure to carry load, and in addition concepts such as energy density can be useful in different circumstances. Both stress and strain can be given in terms of principle stress/ strain, which measures the vectors of compression or tension in the structure, as well as shear stress/ strain. Other measures combine the compression, tension, and shear upon the structure, allowing overall levels of stress or strain to be visualised – a commonly used measure is von Mises stress and strain. In some instances, the most useful results may simply be those that show the raw displacement experienced by the structure under load (Cook 1995).

These different measurements are suitable for different types of question. Stress is useful because it shows the load carried by a structure, whilst strain shows how much deformation the structure experiences under that load. For biologists, strain is often considered a useful output, as it can be compared directly with experimental output from strain gauges [see, for example, Metzger et al. (2005)], and because yield strength of bone is understood to be controlled by strain rather than stress (Currey 2004).

Principle strains are of interest to many workers because many of the questions in biomechanics developed before the use of high resolution, 3D finite element models concerned the functional significance of different morphologies in resisting compressive and tensile components of bending and torsional loads (Busbey 1995, Thomason 1991, Thomason and Russell 1986). However, principal strains (and stresses) are calculated with respect to spatial axes and in a 3D model this requires the results of principal strain/stress to be output in three different axes, making interpretation difficult. Often, the principal strain at the external surface of the structure is of interest, particularly if comparing with experimental results from strain gauges, but the surfaces in the model will mostly not be aligned with the global axis system of the model, or even with the local axis system of 3D elements. In these situations, the use of 2D elements as virtual strain gauges may be warranted, but in many cases the mechanical performance of the structure can be more easily

Methods

visualised by using a measure, such as von Mises strain/stress, that is independent of spatial axes. A disadvantage of von Mises is that it does not directly identify the compressive, tensile, or shear components of the stress or strain affecting the structure.

Many studies make use of the graphical output from the finite element software to show results visually. However, statistical analysis is also possible – most FE packages will output the desired measure (e.g. strain/strain, principle/von Mises, etc) as data arrays which can be exported as text files and analysed in a statistics package. However, the statistical measurement must be chosen carefully, as complex FE models, no matter how carefully constructed, contain artefacts such as point loads and distorted elements, and these can produce artificially high measurements of strain in a small number of elements. For this reason, the maximum statistical value of e.g. strain is usually not a reliable indicator of maximum strain in the structure, and other measurements, such as 95% values, medians, quartiles, or means may be preferable (Bourke et al. 2008, McHenry et al. 2007, Moreno et al. 2008, Wroe 2007, Wroe et al. 2007a). For visual and statistical analyses of FE results, regions of the model known or suspected to be affected by artefacts – for example, because of the boundary conditions of restraining the skull at a particular node – are avoided for the purposes of data collection, with recourse to St. Venant's principle.

Measurement of mechanical performance can also be made in terms of reaction forces, for example at teeth during biting, or at joints during simulated behaviours (Bourke et al. 2008, Clausen et al. 2008). Although the results can be affected by boundary conditions, e.g. the mode of restraint upon bite points, these offer a means of testing hypotheses that have been generated from 2D / beam theory analyses (Greaves 2000, Therrien 2005).

2.3 Skull biomechanics of *Kronosaurus queenslandicus*

In using a functional-morphology approach to reconstruct feeding ecology in *Kronosaurus*, this study will aim to generate a 3D finite element model that can be used as part of a comparative biomechanical analysis. Whilst analyses that encompass a broad range of extant taxa are preferable, logistics limit the number of comparative models that can be used. The present analysis will use the saltwater crocodile, *Crocodylus porosus*, as the extant comparative taxon; overall skull proportions in *C. porosus* are broadly comparable to those of *Kronosaurus queenslandicus*, the two species are understood to be aquatic predators, and the described feeding behaviour in *C. porosus* and related species provides a context for interpretation of the results from the biomechanical analysis.

The biomechanical modelling is based around techniques using finite element analysis developed in collaboration with the other members of the Computational Biomechanics Research Group³ (Bourke et al. 2008, Clausen et al. 2008, McHenry et al. 2007, Moreno et al. 2008, Wroe 2007, Wroe et al. 2007a, Wroe et al. 2008a, Wroe et al. 2007b), for which the preceding summary provides a context. Specific details relating to modelling methods are given in the relevant section (Chapter 7).

A major challenge for the biomechanical analysis of *Kronosaurus queenslandicus* is the nature of the fossil material. Unlike the specimens to which biomechanical FE analyses have been applied to date, there are no complete, undistorted specimens of *Kronosaurus* upon which to base a FE model. Instead, the available material is either incomplete, distorted, or – most often – both. In order to generate an FE model, this material needs to form the basis of a reconstruction of the 3D geometry of the skull: however, this requires descriptive data on the anatomy that is preserved in the specimens, and interpretation of the variation – intraspecific, interspecific, allometric, taphonomic, or otherwise – that they represent. In particular, taphonomic distortion of the original geometry is a critical aspect and the pattern and process of the taphonomic context of these specimens is considered in the subsequent chapters.

³ www.compbio mech.com

Methods

The taphonomic history of the material referred to *Kronosaurus queenslandicus* specimens is part of the geological context of these specimens. Details of the palaeoenvironment relating to *Kronosaurus*, especially the palaeofauna in which it lived, are also part of the relevant geological information; these are outlined in the following chapter.

2.4 References

- Alexander, R. M. 1989. Dynamics of Dinosaurs and Other Extinct Giants. Columbia University Press, New York.
- Alexander, R. M. 2003. Modelling approaches in biomechanics. *Philosophical Transactions of the Royal Society of London* 358:1429-1425.
- Baroud, G., J. Nemes, P. Heini, and T. Steffen. 2004. Load-shift in the intervertebral disc after a vertebroplasty: a finite-element study. *European Spine Journal* 12(421-426).
- Bensamoun, S., M.-C. Ho Ba Tho, S. Luu, J.-M. Gherbezza, and J.-F. de Belleval. 2004. Spatial distribution of acoustic and elastic properties of human femoral cortical bone. *Journal of Biomechanics* 37(4):503-510.
- Binder, W. J., and B. Van Valkenburgh. 2000. Development of Bite Strength and Feeding Behaviour in Juvenile Spotted Hyenas (*Crocuta crocuta*). *Journal of Zoology* 252:273-283.
- Bosisio, M. R., M. Talmant, W. Skalli, P. Laugier, and D. Mitton. 2007. Apparent Young's modulus of human radius using inverse finite-element method. *Journal of Biomechanics* 40(9):2022-2028.
- Bourke, J., S. Wroe, K. Moreno, C. R. McHenry, and P. D. Clausen. 2008. Effects of Gape and Tooth Position on Bite Force in the Dingo (*Canis lupus dingo*) using a 3-D Finite Element Approach. *PLoS ONE* 3(5e2200):1-5.
- Brown, B. 1904. Stomach stones and food of plesiosaurs. *Science* 20(184-185).
- Busbey, A. B. 1995. The structural consequences of skull flattening in crocodylians. Pp. 173-192. *In* J. Thomason, ed. *Functional morphology in vertebrate paleontology*. Cambridge University Press, Cambridge.
- Carpenter, K. 2000. Evidence of predatory behaviour by carnivorous dinosaurs. *Gaia* 15(135-144).
- Chin, K., D. A. Eberth, M. H. Schweitzer, T. A. Rando, W. J. Sloboda, and J. R. Horner. 2003. Remarkable preservation of undigested muscle tissue within a Late Cretaceous tyrannosaurid coprolite from Alberta, Canada. *Palaios* 18(3):286-294.
- Chin, K., and J. I. Kirkland. 1998. Probable herbivore coprolites from the Upper Jurassic Mygatt-Moore Quarry, Western Colorado. *Modern Geology* 23:249-275.
- Christiansen, P. 2007a. Comparative bite forces and canine bending strength in feline and sabretooth felids: implications for predatory ecology. *Zool. J. Linn. Soc.* 151:423-437.
- Christiansen, P. 2007b. Evolutionary implications of bite mechanics and feeding ecology in bears *J. Zoology* 272:423-443.

- Christiansen, P., and S. Adolfssen. 2005. Bite forces, canine strength and skull allometry in carnivores (Mammalia, Carnivora). *Journal of Zoology*, London 266:133-151.
- Christiansen, P., and S. Wroe. 2007. Bite forces and evolutionary adaptations to feeding ecology in carnivores. *Ecology* 88:347-358.
- Cicimurri, D. J., and M. J. Everhart. 2001. An elasmosaur with Stomach Contents and Gastroliths from the Pierre Shale (Late Cretaceous) of Kansas. *Transactions of the Kansas Academy of Science* 104(3-4):129-143.
- Clarke, J. B., and S. Etches. 1991. Predation amongst Jurassic marine reptiles. *Proceedings of the Dorset Natural History and Archaeology Society* 113:202-205.
- Clausen, P., S. Wroe, C. McHenry, K. Moreno, and J. Bourke. 2008. The vector of jaw muscle force as determined by computer generated three dimensional simulation: A test of Greaves' model. *Journal of Biomechanics* 41(15):3184-3188.
- Cook, R. D. 1995. *Finite Element Modelling for Stress Analysis*. Wiley, USA.
- Cott, H. B. 1961. Scientific results of an inquiry into the ecology and economic status of the Nile crocodile (*Crocodylus niloticus*) in Uganda and Northern Rhodesia. *Transactions of the Zoological Society of London* 29:211-357.
- Currey, J. D. 2004. Tensile yield in compact bone is determined by strain, post-yield behaviour by mineral content. *Journal of Biomechanics* 37(4):549-556.
- Curtis, N., K. Kupczik, P. O'Higgins, M. Moazen, and M. J. Fagan. 2008. Predicting skull loading: applying multibody dynamics analysis to a macaque skull. *Anatomical Record* 291:491-501.
- Daniel, W., and C. McHenry. 2001. Bite force to skull stress correlation: modelling the skull of *Alligator mississippiensis*. Pp. 135-143. *In* G. Grigg, F. Seebacher, and C. Franklin, eds. *Crocodylian biology and evolution*. Surrey Beatty, Chipping Norton.
- de Winkel, M. E., T. Blange, and B. W. Treijtel. 1994. High frequency characteristics of elasticity of skeletal muscle fibres kept in relaxed and rigor state *J. Muscle Res. Cell. Mot.* 15(3):130-144.
- Dumont, E. R., J. Piccirillo, and I. R. Grosse. 2005. Finite-element analysis of biting behaviour and bone stress in the facial skeleton of bats. *Anatomical Record* 283A:319-330.
- Ellis, J. E., J. J. Thomason, E. Kebreab, and J. France. 2008. Calibration of estimated biting forces in domestic canids: comparison of post-mortem and *in vivo* measurements. *Journal of Anatomy* 212:769-780.
- Emslie, S. D., and W. P. Patterson. 2007. Abrupt recent shift in $\delta^{13}\text{C}$ and $\delta^{15}\text{N}$ levels values in Adélie penguin eggshell in Antarctica. *Proceedings of the National Academy of Sciences* 104:11666-11669.

- Erickson, G. M., A. K. Lappin, and K. A. Vliet. 2003. The ontogeny of bite-force performance in American alligator (*Alligator mississippiensis*). *Zool Lond* 260:317–327.
- Erickson, G. M., S. D. Van Kirk, J. Su, M. E. Levenston, W. E. Caler, and D. R. Carter. 1996. Bite force estimation for *Tyrannosaurus rex* from tooth-marked bones. *Nature* 382:706-708.
- Farlow, J. O., and T. R. Holtz. 2002. The fossil record of predation in dinosaurs. *Paleontological Society Special Papers* 8:251-265.
- Ferretti, J. L., G. R. Cointy, and R. Cappozza. 2003. Noninvasive Analysis of Bone Mass, Structure, and Strength. Pp. 145-167. *In* Y. H. An, ed. *Orthopaedic Issues in Osteoporosis*. CRC Press.
- Ferry-Graham, L. A., D. I. Bolnick, and P. C. Wainwright. 2002. Using Functional Morphology to Examine the Ecology and Evolution of Specialisation. *Intergrative and Comparative Biology* 42(265-277).
- Gould, S. J. 2002. *The Structure of Evolutionary Theory*. Belknap Press.
- Greaves, W. S. 2000. Location of the Vector or Jaw Muscle Force in Mammals. *Journal of Morphology* 243:293-299.
- Grosse, I., E. R. Dumont, C. Coletta, and A. Tolleson. 2007. Techniques for modeling muscle-induced forces in finite element models of skeletal structures. *Anatomical Record* 290(9):1069-88.
- Harvey, P. H., and M. D. Pagel. 1991. *The comparative method in evolutionary biology*. Oxford University Press, Oxford.
- Herring, S. W., and S. Teng. 2000. Strain in the braincase and its sutures during function. *American Journal of Physical Anthropology* 112:575-593.
- Hylander, W. L., and K. R. Johnson. 1993. Modelling relative masseter force from surface electromyograms during mastication in non-human primates. *Archives of Oral Biology* 38:233-240.
- Jaslow, C. R. 1990. Mechanical properties of cranial sutures. *Journal of Biomechanics* 23:313-321.
- Jenkins, I., J. J. Thomason, and D. B. Norman. 2002. Primates and engineering principles: applications to craniodental mechanisms in ancient terrestrial predators. *Senckenbergiana Lethaea* 82:223-240.
- Kaneko, T. S., J. S. Bell, M. R. Pejcic, J. Tehranzadeh, and J. H. Keyak. 2004. Mechanical properties, density and quantitative CT scan data of trabecular bone with and without metastases. *Journal of Biomechanics* 37(4):523-530.
- Kosmopoulos, V., C. Schizas, and T. S. Keller. 2008. Modeling the onset and propagation of trabecular bone microdamage during low-cycle fatigue. *Journal of Biomechanics* 41(3):515-522.
- Lauder, G. V. 1995. On the inference of function from structure. Pp. 1-18. *In* J. J. Thomason, ed. *Functional Morphology in Vertebrate Paleontology*. Cambridge University Press.

- Martinez, J., V. O. A. Oloyede, and N. D. Broom. 1997. Biomechanics of load-bearing of the intervertebral disc: an experimental and finite element model. *Medical Engineering and Physics* 19(2):145-156.
- McHenry, C. R., P. D. Clausen, W. J. T. Daniel, M. B. Meers, and A. Pendharkar. 2006. The biomechanics of the rostrum in crocodylians: a comparative analysis using finite element modelling. *Anatomical Record*, 288A:827-849.
- McHenry, C. R., A. G. Cook, and S. Wroe. 2005. Bottom-Feeding Plesiosaurs. *Science* 310:75.
- McHenry, C. R., S. Wroe, P. D. Clausen, K. Moreno, and E. Cunningham. 2007. Supermodeled sabercat, predatory behavior in *Smilodon fatalis* revealed by high-resolution 3D computer simulation. *Proceedings of the National Academy of Sciences* 104(41):16010-16015.
- Metzger, K. A. 2002. Cranial kinesis in Lepidosauria: Skulls in Motion. *In* P. Aerts, D. Aouf, A. Herrel, and R. Van Damme, eds. *Topics in Functional and Ecological Vertebrate Morphology*. Shaker Publishing.
- Metzger, K. A., W. J. T. Daniel, and C. F. Ross. 2005. Comparison of beam theory and finite element analysis with *in vivo* bone strain data from the alligator cranium. *Anatomical Record* 283A:331-348.
- Moazen, M., N. Curtis, S. E. Evans, P. O'Higgins, and M. Fagan. 2008a. Rigid-body analysis of a lizard skull: Modelling the skull of *Uromastix hardwickii*. *Journal of Biomechanics* 41(6):1274-1280.
- Moazen, M., N. Curtis, S. E. Evans, P. O'Higgins, and M. J. Fagan. 2008b. Combined finite element and multibody analysis of biting in a *Uromastix hardwickii* lizard skull. *Journal of Anatomy* 213(5):499-508.
- Moazen, M., N. Curtis, P. O'Higgins, M. Jones, S. Evans, and M. J. Fagan. 2009. Assessment of the role of sutures in a lizard skull - a computer modelling study. *Proceedings of the Royal Society Series B* 276:39-46.
- Moreno, K., S. Wroe, P. D. Clausen, C. R. McHenry, D. C. D'Amore, E. J. Rayfield, and E. Cunningham. 2008. Cranial performance in the Komodo dragon (*Varanus komodoensis*) as revealed by high-resolution 3-D finite element analysis. *Journal of Anatomy* 212(6):736-746.
- Northwood, C. 2005. Early Triassic coprolites from Australia and their palaeobiological significance. *Palaeontology* 48(1):49-68.
- O'Keefe, F. R. 2001. A cladistic analysis and taxonomic revision of the Plesiosauria (Reptilia: Sauropterygia). *Acta Zool. Fennica* 213:1-63.
- Padian, K. 1995. Form versus function: evolution of a dialectic. Pp. 264-277. *In* J. J. Thomason, ed. *Functional Morphology in Vertebrate Paleontology*. Cambridge University Press.
- Pfeiler, T. W., D. S. Lalusha, and E. G. Loba. 2007. Semiautomated finite element mesh generation methods for a long bone. *Computer Methods and Programs in Biomedicine* 85:196-202.

- Pierce, G. J., and J. G. Ollason. 1987. Eight reasons why optimal foraging theory is a complete waste of time. *Oikos* 49(1):111-118.
- Pierce, S. E., K. D. Angielczyk, and E. J. Rayfield. 2008. Patterns of Morphospace Occupation and Mechanical Performance in Extant Crocodylian Skulls: A Combined Geometric Morphometric and Finite Element Modeling Approach. *Journal of Morphology* 269:840-864.
- Plotnick, R. E., and T. K. Baumiller. 2000. Invention by Evolution: Functional Analysis in Paleobiology. *Paleobiology* 26(4):305-323.
- Preuschoft, H., and U. Witzel. 2002. Biomechanical investigations on the skulls of reptiles and mammals. *Senckenbergiana Lethaea* 82:207-222.
- Preuschoft, H., and U. Witzel. 2005. Functional Shape of the Skull in Vertebrates: Which Forces Determine Skull Morphology in Lower Primates and Ancestral Synapsids? *Anatomical Record* 283A:402-413.
- Rayfield, E. J. 2004. Cranial mechanics and feeding in *Tyrannosaurus rex*. *Proceedings of the Royal Society Series B* 271:1451-1459.
- Rayfield, E. J. 2005. Aspects of comparative cranial mechanics in the theropod dinosaurs *Coelophysis*, *Allosaurus* and *Tyrannosaurus*. *Zoological Journal of the Linnean Society* 144:309-316.
- Rayfield, E. J. 2007. Finite Element Analysis and Understanding the Biomechanics and Evolution of Living and Fossil Organisms. *Annual Review of Earth and Planetary Sciences* 35:541-576.
- Rayfield, E. J., and A. C. Milner. 2008. Establishing a framework for archosaur cranial mechanics. *Paleobiology* 34(4):494-515.
- Rayfield, E. J., A. C. Milner, V. B. Xuan, and P. G. Young. 2007. Functional Morphology of Spinosaur 'Crocodile-Mimic' Dinosaurs. *Journal of Vertebrate Paleontology* 27(4):892-901.
- Rayfield, E. J., D. B. Norman, C. C. Horner, J. R. Horner, P. M. Smith, J. J. Thomason, and P. Upchurch. 2001. Cranial design and function in a large theropod dinosaur. *Nature* 409(6823):1033-1037.
- Rho, J. Y., M. C. Hobatho, and R. B. Ashman. 1995. Relations of mechanical properties to density and CT numbers in human bone. *Medical Engineering and Physiology* 17:347-355.
- Rice, J. C., S. C. Cowin, and J. A. Bowman. 1988. On the dependence of the elasticity and strength of cancellous bone on apparent density. *Journal of Biomechanics* 21(2):155-168.
- Ross, C. F., B. A. Patel, D. E. Slice, D. S. Strait, P. C. Dechow, B. G. Richmond, and M. A. Spencer. 2005. Modeling Masticatory Muscle Force in Finite Element Analysis: Sensitivity Analysis Using Principal Coordinates Analysis. *Anatomical Record* 283A:288-299.
- Russell, E. S. 1916. *Form and Function: A Contribution to the History of Animal Morphology*. University of Chicago Press, Chicago.

- Schnitzler, C. M. 2003. Histomorphology of Osteoporosis. Pp. 19-37. In Y. H. An, ed. Orthopaedic Issues in Osteoporosis. CRC Press.
- Shaw, J. R. 1972. Models for Cardiac Structure and Function in Aristotle. *Journal of the History of Biology* 5(2):355-388.
- Snively, E., D. M. Henderson, and D. S. Phillips. 2006. Fused and vaulted nasals of tyrannosaurid dinosaurs: implications for cranial strength and feeding mechanics. *Acta Palaeontologica Polonica* 51:435-454.
- Snively, E., and A. P. Russell. 2002. The tyrannosaurid metatarsus: bone strain and inferred ligament function. *Senckenbergiana Lethaea* 82:35-42.
- Strait, D. S., Q. Wang, P. C. Dechow, C. F. Ross, B. G. Richmond, M. A. Spencer, and B. A. Patel. 2005. Modeling elastic properties in finite-element analysis: how much precision is needed to produce an accurate model? *Anatomical Record* 283A:275-287.
- Sun, Z., E. Lee, and S. W. Herring. 2004. Cranial sutures and bones: Growth and fusion in relation to masticatory strain. *The Anatomical Record Part A: Discoveries in Molecular, Cellular, and Evolutionary Biology* 276A(2):150-161.
- Takada, H., S. Abe, Y. Tamatsu, S. Mitarashi, H. Saka, and Y. Ide. 2006. Three-dimensional bone microstructures of the mandibular angle using micro-CT and finite element analysis: relationship between partially impacted mandibular third molars and angle fractures. *Dental Traumatology* 22:18-24.
- Therrien, F. 2005. Feeding behaviour and bite force of sabretoothed predators. *Zoological Journal of the Linnean Society* 145(3):393-426.
- Thomason, J. J. 1991. Cranial strength in relation to estimated biting forces in some mammals. *Canadian Journal of Zoology* 69:2326-2333.
- Thomason, J. J., and A. P. Russell. 1986. Mechanical factors in the evolution of the mammalian secondary palate - a theoretical analysis. *Journal of Morphology* 189:199-213.
- Thompson, D. W. 1917. *On Growth and Form*. Cambridge University Press.
- Tseng, Z. J. 2009. Cranial function in a late Miocene *Dinocrocuta gigantea* (Mammalia: Carnivora) revealed by comparative finite element analysis. *Biological Journal of the Linnean Society* 96:51-67.
- Turner, C. H., J. Rho, Y. Takano, T. Y. Tsui, and G. M. Pharr. 1999. The elastic properties of trabecular and cortical bone tissues are similar: results from two microscopic measurement techniques. *Journal of Biomechanics* 32(4):437-441.
- Verhulp, E. 2006. *Analyses of Trabecular Bone Failure*. PhD Thesis, University of Technology, Eindhoven
- Vogel, S. 2003. *Comparative Biomechanics: Life's Physical World*. Princeton University Press.

- Wang, Q., and P. C. Dechow. 2006. Elastic properties of external cortical bone in the craniofacial skeleton of the rhesus monkey. *American Journal of Physical Anthropology* 131(3):402-415.
- Wang, Q., D. S. Strait, and P. C. Dechow. 2006. A comparison of cortical elastic properties in the craniofacial skeletons of three primate species and its relevance to the study of human evolution. *Journal of Human Evolution* 51(4):375-382.
- Weijjs, W. A., and B. Hillen. 1985. Cross-sectional area and estimated intrinsic strength of the human jaw muscles. *Acta Morphol. Neerl. Scand.* 23:267-274.
- Williams, P. L., and R. Warwick, eds. 1980. *Gray's Anatomy*, 36th Edition. Churchill Livingstone, Philadelphia.
- Williston, S. W. 1904. The stomach stones of the plesiosaurs. *Science* 20:565.
- Witzel, U., and H. Preuschoft. 2005. Finite-Element Model Construction for the Virtual Synthesis of the Skulls in Vertebrates: Case Study of *Diplodocus*. *Anatomical Record* 283A:391-401.
- Wroe, S. 2007. High-resolution 3-D computer simulation of feeding behaviour in marsupial and placental lions. *Journal of Zoology* 274:332-339.
- Wroe, S., P. Clausen, C. McHenry, K. Moreno, and E. Cunningham. 2007a. Computer simulation of feeding behaviour in the thylacine and dingo: a novel test for convergence and niche overlap. *Proceedings of the Royal Society Series B* 274:2819-2828.
- Wroe, S., D. R. Huber, M. Lowry, C. McHenry, K. Moreno, P. Clausen, T. L. Ferrara, E. Cunningham, M. N. Dean, and A. P. Summers. 2008a. Three-dimensional computer analysis of white shark jaw mechanics: How hard can a great white bite? *J. Zoology* 276(4):336-342.
- Wroe, S., M. B. Lowry, and A. Anton. 2008b. How to build a mammalian superpredator. *Zoology* 111(196-203).
- Wroe, S., C. McHenry, and J. Thomason. 2005. Bite club: comparative bite force in big biting mammals and the prediction of predatory behaviour in fossil taxa. *Proceedings of the Royal Society of London, Series B* 272:619-625.
- Wroe, S., and N. Milne. 2007. Convergence and remarkably consistent constraint in the evolution of carnivore skull shape. *Evolution* 61:1251-1260.
- Wroe, S., K. Moreno, P. Clausen, C. McHenry, and D. Curnoe. 2007b. High-resolution computer simulation of hominid cranial mechanics. *The Anatomical Record* 290A:1248-1255.
- Wu, X.-C., and A. P. Russell. 1997. Functional Morphology. Pp. 258-268. *In* P. J. Currie, and K. Padian, eds. *Encyclopedia of Dinosaurs*. Academic Press.
- Zhang, Q. H., S. H. Tan, and S. M. Chou. 2004. Investigation of fixation screw pull-out strength on human spine. *Journal of Biomechanics* 37(4):479-485.

3. Geology



The Late Albian Allaru Formation, seen from the Flinders Highway between the townships of Hughenden and Richmond in central-west Queensland (looking south – the road is actually straight). Several significant marine reptile finds, including some of the *Kronosaurus* specimens detailed in Chapter 4, come from within 10 km of this point, preserved in the limestone nodules that float to the surface of the blacksoil plains.

“Billiard-table topography...”

Technical description of the Australian landscape west of the Great Divide, Telstra Corporation

3.1 **Geology and palaeoecology**

Documenting the ecology of living animals can be an intensive and demanding exercise requiring many different types of information. Some of these – records of diet and foraging behaviour, ranges of spatial and temporal distribution and activities – are focused upon particular ecological relationships that centre upon the species in question: this aspect is termed the autecology of that particular species. As the science of an organism’s relationships with its environment, however, ecology also involves the physical and biological context of that species, and an understanding of the ecosystem (synecology) in which it lives is also required.

As outlined in the previous chapter, the direct evidence used to document ecology in extant species is very patchily preserved for fossil species, and reconstructing ecology from indirect evidence is often used: functional morphology is one such form of indirect evidence and will be used in this thesis to reconstruct aspects of the autecology in *Kronosaurus queenslandicus*. Specifically, this thesis will utilise a biomechanical approach that is based upon 3D modelling, and for this the geological context of the specimens is important: fossilisation alters almost all aspects of a specimen, and the original shape is often significantly distorted by the taphonomic processes that affect it. In order to conduct 3D modelling of *Kronosaurus queenslandicus*, it is necessary to account for the taphonomy in reconstructing the original 3D shape of the specimens, and the details of taphonomy lie in the geological context of the relevant specimens.

Kronosaurus queenslandicus did not live in isolation, of course, and its feeding behaviour was determined as much by the potential prey that lived alongside it as its physical abilities to catch and kill animals of difference sizes and types. The geological context of the specimens thus provides the synecological setting for *Kronosaurus*; the other

organisms that made up the ecosystem in which it lived, and the oceanographic context of water temperature, productivity, currents, depth, and all the other factors that are important to all marine organisms.

The following summary aims to list the relevant information on the palaeoenvironment, in terms of the biotic and abiotic components, of *Kronosaurus queenslandicus*, and the taphonomic processes that are relevant to the fossil specimens. The palaeofauna and palaeo-oceanography of the Great Artesian Basin, from which all specimens currently assigned to *Kronosaurus queenslandicus* are known, is summarised below but has been documented in the literature and the reader is referred to primary references for specific details. However, the taphonomic processes that are relevant to these specimens have not, to my knowledge, been considered in detail; no attempt is made here to present any original data on the taphonomy of the specimens, but in the hope that future work on the palaeontology of marine reptiles from the Great Artesian Basin will place a greater emphasis on taphonomy, an expanded summary of the relevant processes is attempted below, including summaries from actuopalaeontology of recent marine mammal specimens.

The general information on the taphonomic processes summarised here will form the basis for reconstructions of the specific taphonomic circumstances of each specimen in the following chapter, as part of the attempted reconstruction of the 3D morphology of the skull of *Kronosaurus queenslandicus*. This will in turn form the basis for the functional morphology analysis of feeding behaviour in *Kronosaurus*, and final assessment of the palaeoecology of *Kronosaurus queenslandicus* will combine that data with the palaeoenvironmental data summarised in the following section.

3.2 Depositional context and regional geology

All of the fossils that have been referred to *Kronosaurus queenslandicus* come from the Great Artesian Basin (GAB), which during the Cretaceous Period was intermittently covered by a series of shallow inland seas. Itself composed of three major basins, the Surat, the Carpentaria, and the Eromanga (and thus more correctly termed a superbasin), the GAB is a very large geological structure, with an approximate area of 1,761,200 km² (Day 1969), that covers much of the north-eastern part of the Australian craton¹.

The marine strata in which *K. queenslandicus* fossils are found date to the latter part of the Early Cretaceous, approximately between 115 and 100 million years in age, and spanning the Aptian and Albian stages². At this time, Australia formed most of the Eastern Peninsular of the supercontinent Gondwana (Figure 3-1) and was united to Antarctica along its present southern margin. As Antarctica was, at this time, located close to its current position at the South Pole, the epeiric seas covering the GAB were at high latitudes of 65°–45° (compared with the present latitude of the GAB, 30°–10°) (Figure 3-2). During the late Aptian-late Albian the continent underwent significant anticlockwise rotation (Frakes et al, 1987, Veevers 2006.).

The basement rocks of the GAB are heterogeneous, overlain by Jurassic terrestrial sequences that were deposited as part of extensive riverine and lacustrine systems. Oscillations in sea level between 125 and 98 million years ago led to at least four major incursions of the sea over the GAB and other Australian continental basins. The sequence and shore-line topography of these inland seas has been reconstructed by Frakes et al. (1987) and along with data from Cook and McKenzie (1996) can be summarised (see also Table 3-1);

¹ 'Craton' refers to a region of continental-type rocks; it is similar (but not identical) to the geographical concept of a continent.

² The Early Cretaceous spans from about 140 million years ago (140 Ma) to 95 Ma – the Aptian Stage is the time from 114 Ma to 107 Ma, and the Albian Stage is from 107 Ma to 95 Ma. Thus the Aptian and Albian between them cover the last part of the Early Cretaceous.

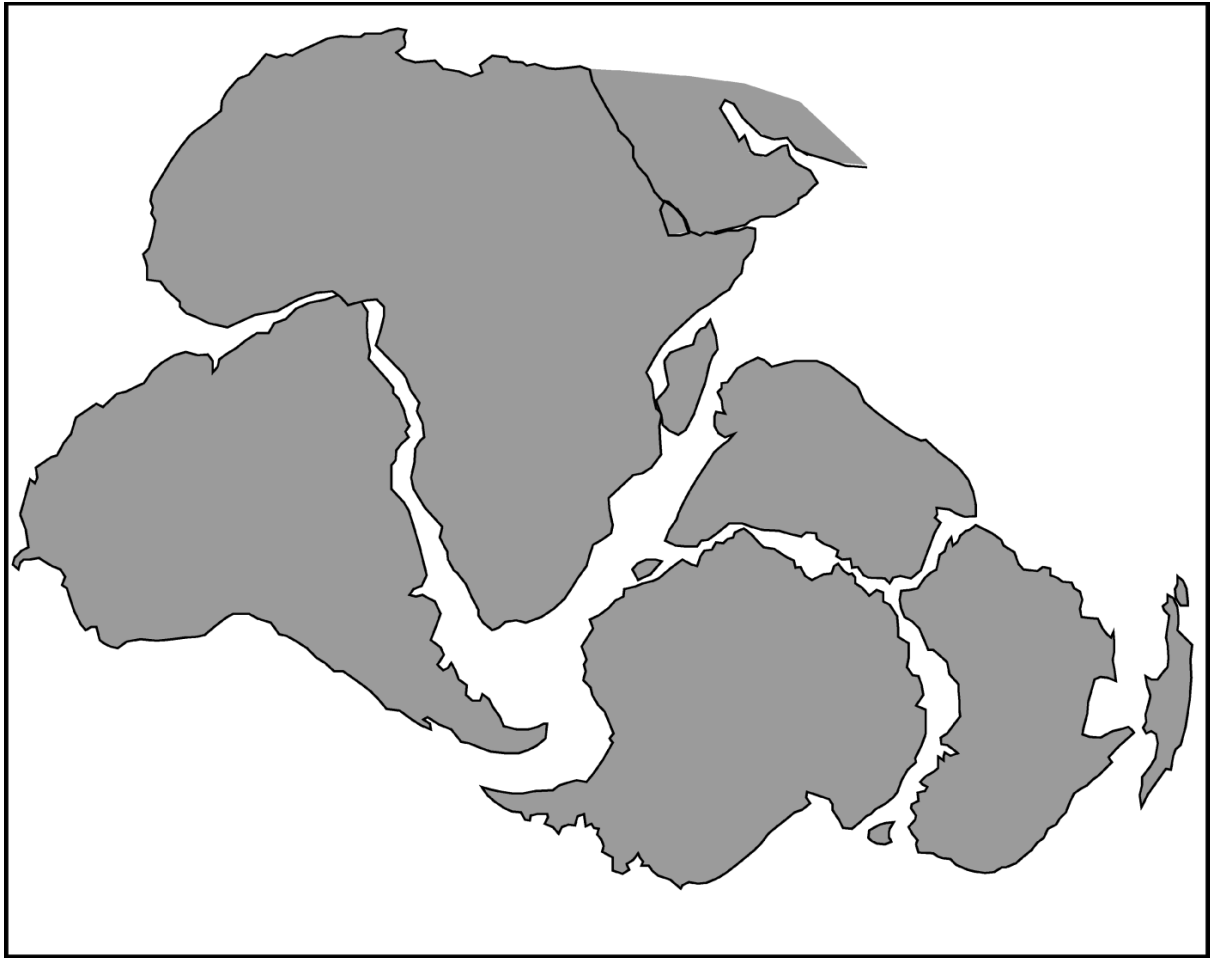


Figure 3-1: The southern supercontinent Gondwana, showing the approximate disposition of the modern continents during the Middle Jurassic (~160 Ma), prior to the initiation of breakup. The position of Antarctica is similar to its current location at the South Pole; the coastlines shown are modern and do not indicate palaeoshorelines. From McDougall (2008), ex Powell et al. (1980).

1. Barremian–Early Aptian (125–120 Ma): an extensive inundation which covered most of the GAB: the Canning Basin in Western Australia was also submerged in this time. This Early Aptian sea connected with the ocean to the north (via the Carpentaria Basin) and possibly to the east (via the Surat and Maryborough Basins). Geologically, it is principally represented by the Nullawurt and Minmi members of the Bungil Formation, which is part of the mainly Neocomian Blythesdale Group, all of which are minimally exposed.
2. Late Aptian (117–112 Ma): the most extensive of the inland seas, covering the entire GAB and connecting with the inundated Canning Basin via the present Nullabor Plain and the adjacent parts of central Australia. The sea

also connected with the ocean to the north and east via the Carpentaria and Maryborough Basins respectively, and possibly to the south via the Murray Basin. Geologically, this sea is represented in Queensland by the 220 m thick Doncaster Formation and the overlying Jones Valley Member. The underlying Gilbert River Formation has been interpreted as Early Aptian (Day 1969), but in the northern part of the Eromanga Basin the Doncaster Formation sits conformably on this unit and it therefore represents in part at least an early transgressive phase of the Late Aptian Sea. The geology of the opal bearing Cretaceous rocks of White Cliffs in New South Wales is problematic, but these also appear to be Late Aptian in age (see Kear et al. 2003b). In South Australia, the Bulldog Shale is equivalent to the Doncaster Formation. The various Late Aptian units are exposed widely throughout the GAB and have produced many fossils

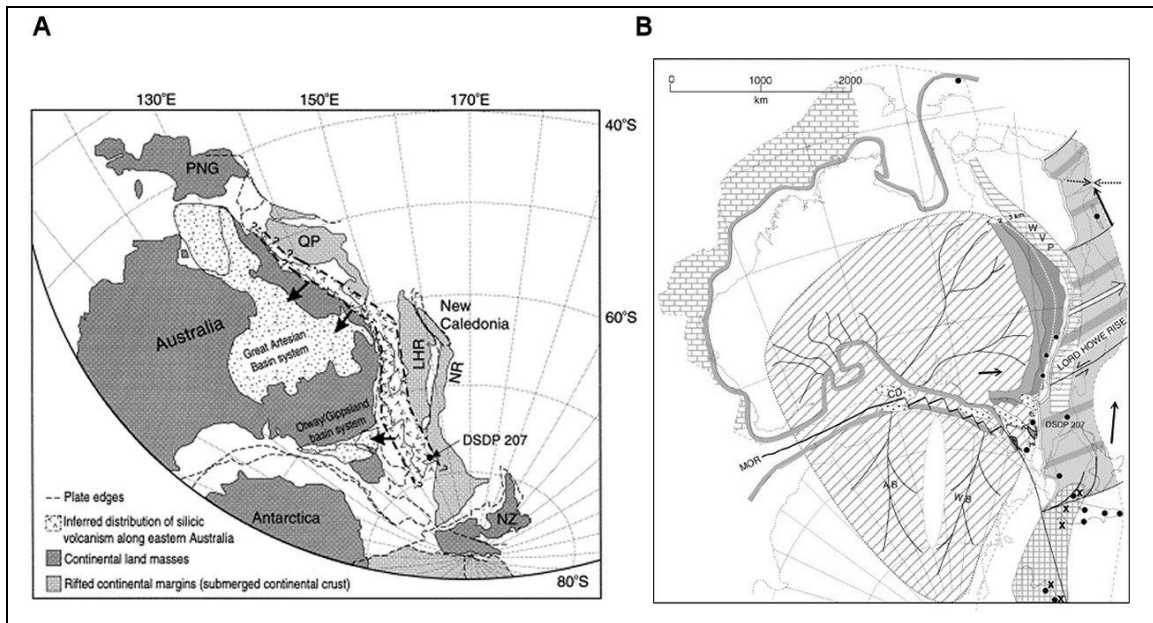


Figure 3-2: Mid-Cretaceous tectonic context of eastern Australia, from two recent studies: A, from Bryan et al. (1997); B, from Veevers (2006). Each shows the extent of the Whitsunday Volcanic Province along the present-day east coast (stippled region in A, ‘WVP’ in B), and the location of rifting between southern Australia and Antarctica. The area labelled ‘Great Artesian Basin system’ in A corresponds approximately with the extent of the Early Albian inland sea, whilst the palaeo-shoreline (heavy grey line) in the Cape York – Carpentaria region in B corresponds approximately with the mid-Albian regressive phase, with a hypothesised southwards draining terrestrial basin covering southern Australia and the apposite part region of Antarctica. Palaeolatitudes at 100 Ma are show in A.

Ma	Age	Sea	Eromanga Basin			Carpentaria Basin		Surat Basin	
			north, west	central, east	south-west	west	east	south	north
			Qld (Boulia–Richmond–Hughenden)	Qld (Tambo–Winton)	South Australia	NW Qld	NE Qld	NSW	S Qld (Roma)
100	Cenomanian			Winton Fm		Normanton Fm			
	Albian	Late Albian	Mackunda Fm						
			Allaru Fm		Woolridge M	Kamileroi LS	Trimble Fm		
		Early Albian	Ranmoor M	Coreena M	Coorikiana M			Griman Creek Fm	
110								Coreena M	
	Aptian	Late Aptian	Jones Valley M						
			Doncaster Fm		Bulldog Shale		Doncaster Fm	'White Cliffs'	
			Blantyre Beds				Gilbert River Fm	Doncaster Fm	
120		Early Aptian	Blantyre Beds				Gilbert River Fm	Bungil Fm	
130	Neocomian						Blythesdale Group		
	Hauterivian								
	Valanginian								
140	Berriasian								
	Tithonian								

Table 3-1: Major Cretaceous geological units of the Great Artesian Basin. Shaded rows indicate the four separate marine inundations discussed in the text (i.e. the ‘Early Aptian’, ‘Late Aptian’, ‘Early Albian’, and ‘Late Albian’ Seas); darker shade indicates preserved marine units, lighter shade shows inferred marine sequences that lack preserved strata. Unshaded cells indicate inferred (unnamed) or preserved (named; i.e. Winton Formation) terrestrial phases, dashed lines denote significant stratigraphic uncertainty. Note: (1) the retreat of the Late Albian Sea to the north is preserved as the marine sequences of the Normanton Formation that are in part contemporaneous with the terrestrial Winton Formation of the Eromanga Basin; (2) The Gilbert River Formation is a collection of marginal marine deposits for which stratigraphic control is poor; parts of it lie conformably below the Doncaster Formation and thus represent an early transgressive phase of the Late Aptian Sea, but other sections may represent part of the Early Aptian Sea (Oosting 2004) – a similar situation applies to the Blantyre Beds (A. Cook, pers. comm.); (3) the White Cliffs locality likely represents the Late Aptian Sea but stratigraphic control is poor – Kear (2005a), citing Burton and Mason (1998), assigns it to the Doncaster Formation; (4) The ‘Early Aptian’ Sea is shown here as mainly Late Barremian, but age control of the relevant units is poor; (5) The Blythesdale Group includes several poorly understood strata with minimal biostratigraphic control: potentially, it may preserve one or even two additional marine inundations of the GAB during the Neocomian. Geological abbreviations: Ma, million years ago; Fm, Formation; M, Member; LS, Limestone.

3. Early–Mid Albian (108–105 Ma): this inland sea was less extensive than its predecessors and connected to the ocean only via the Carpentaria Basin to the north, although it covered most of the Eromanga and Surat Basins as well. Geologically, it is represented by the Ranmoor and Coreena Members of north and central Queensland, the Coorikiana Member of the Oodnadatta Formation in South Australia, and the Grimman Creek Formation of southern Queensland and northern New South Wales: the latter is famous for the opal deposits of Lightning Ridge.

4. Late Albian (102–98 Ma): this was the last and possibly the smallest of the inland seas, covering only the Eromanga and Carpentaria Basins. The single connection with the ocean was to the north. Nevertheless, the rocks laid down from this inland sea are exposed widely throughout the GAB and contain an abundant fossil fauna. The oldest unit, the Toolebuc Formation, is a thin (< 35 m) band of carbonates and organic shales with large outcrops in the Hughenden – Richmond region of Central-West Queensland, and which has produced a large number of marine reptile fossils, including most of the *Kronosaurus queenslandicus* specimens that are discussed in this thesis. It is overlain by the Allaru Formation, which has a maximum thickness of 250 m; this in turn is overlain by the Mackunda Formation, which is of a similar thickness. The Wooldridge Limestone Member of the Oodnadatta Formation in South Australia may be equivalent to the Toolebuc Formation. The Allaru and Mackunda Formations represent the gradual infilling of the GAB with siliclastic sediments derived from extensive volcanism of the Whitsunday Igneous province to the East (see below) and the final retreat of the inland sea from the craton.

After the Early Cretaceous transgressions, backfill of the basin followed the erosion of the Whitsunday Igneous province and the Great Dividing Range to the east, allowing the development of a large vegetated basin, and which has produced fossils of various terrestrial fauna and flora, including sauropod dinosaurs (Cook and McKenzie 1996). The unit deposited during this time, the Winton Formation, comprises terrestrial sands and shales and is up to 200 m thick. Sedimentation

decreased markedly by the latest Cretaceous, but persistence of the subtropical forest led to three phases of deep weathering of the underlying rocks until at least the Miocene. After this point overlying vegetation changed from wet forest to drier woodland and finally the modern scrub-grasslands – erosional processes dominated during this time (Cook and McKenzie 1996).

Flexure near the junction between the Eromanga and Carpentaria Basins, brought about by collision of the Australian and Indonesian plates and the associated uplift of the New Guinea Highlands during the late Miocene / Pliocene, reversed drainage from its previous northerly direction towards the Gulf of Carpentaria to the current southerly direction. Depression at the southern margins of the SuperBasin at Lake Eyre, together with reductions in overall drainage volumes resulting from the reduction in Australian rainfall post Miocene, mean that drainage now remains within the Eyre Basin so formed. However, the Diamantina appears to represent a once large main channel and may even mark the position of the major northerly drainage in pre-Miocene times (A. Cook, pers. comm.).

Since the increase in erosion after the Miocene, much of the Winton Formation has been eroded, and over large parts of the GAB the rocks laid down during the sequence of Early Cretaceous marine transgressions are now exposed. In Queensland, these rocks are collectively known as the Rolling Downs Group, and comprise 5-6 major units (see above). They are widely covered by black soil plains, vast areas of smectic clay-rich soils that are themselves a result of weathering of the volcanically-derived sediments of the Rolling Downs Group and localised Neogene basalt flows.

Early Cretaceous Palaeoenvironments

Reconstruction of palaeoenvironment in the Cretaceous inland seas are determined by their relatively high latitudes, in combination with three other factors; global climate, regional tectonics, and basin oceanography:

Global climates: The Cretaceous Period was part of an extended 'greenhouse' phase in global climate history (Barron 1983), with data pointing to average temperatures

exceeding modern ones at all latitudes. Although the Cretaceous polar latitudes have previously been interpreted as ice-free, more recent evidence points to glacial episodes throughout the Early Cretaceous (Alley and Frakes 2003, Stoll and Schrag 1996) and extending into the Late Cretaceous (Miller et al. 2003). Against a background trend of warming from minimal global temperatures in the Berriasian³ (Alley and Frakes 2003), rising to maximal hothouse conditions in the Cenomanian/Turonian⁴ (Kuypers et al. 1999, Wilson et al. 2002), glacial episodes appear to have led to rapid and frequent oscillations in eustatic sea levels. In Australia, these oscillations led to a series of between four and six separate transgressive events, where shallow epicontinental seas covered most or all of the GAB and neighbouring basins (Cook and McKenzie 1996, Frakes et al. 1987, Veevers 2006).

Even during the Berriasian, polar ice sheets were less extensive than their modern distribution (Alley and Frakes 2003) and, taken together with the higher equatorial average temperatures, it seems likely that the temperature climate zone was located at higher latitudes, and had a more condensed latitudinal range, than the current temperate zone. The southern part of the GAB, and the more southerly Gippsland/Otway Basins, seems to have experienced cool climates during the Aptian and Albian, with sedimentological evidence for seasonal ice cover (Constantine et al. 1998, Kear 2003). The northern part of the GAB appears to have been significantly warmer, with stromatolites present in the Aptian of the Carpenteria Basin (pers. obs., 1999), and colonial scleractinian coral in the Albian of the Eromanga Basin (Cook and McKenzie 1996). In addition to the effects of latitude, Albian temperatures in the GAB are thought to have been warmer than Aptian (Day 1969); since northwards movement of the craton between these times was minimal, this appears to have been a result of increasing average global temperatures in the latter part of the Lower Cretaceous (Kuypers et al. 1999, Wilson et al. 2002).

Regional tectonics: The Early Cretaceous shows the onset of the rifting between southern Australia and Antarctica that was to lead to the separation of these continents and the northerly movement of Australia in the Late Cretaceous and

³ The earliest part of the Cretaceous Period, approximately 140 million years ago.

⁴ 95–90 million years ago.

Cainozoic (McDougall 2008). Evidence of rifting is present in the Otway and Gippsland Basins of Victoria throughout the Aptian and Albian. The contemporary presence of a large igneous provenance (Figure 3-2) along the eastern margin of Australia, exemplified by the Whitsunday volcanics, has been interpreted as a passive plate margin associated with the breakup of Eastern Gondwana (Bryan et al. 1997, McDougall 2008). Volcanic activity associated with this igneous provenance peaked during the Aptian and Albian, and was a major source of sediment for all of the major basins in eastern Australia: the GAB alone is estimated to have received more than 1 million km³ of volcano-clastic sediment during this time (Bryan et al. 1997).

Basin oceanography: Epicontinental seas are necessarily shallow; modern examples, such as the North Sea and Hudson Bay, are generally less than 200 m deep and over most of their extents are considerably shallower: the average depth of the North Sea is ~50 m (Couper 1989). Sea level likely varied for the successive Aptian and Albian versions of the inland sea covering the GAB, but maximum depth is believed to be less than the storm base and depths may have ranged from 30 to 120 m (Cook and McKenzie 1996). At these depths, the sea floor would lie within the photic zone, at least during the summer months.

Oxygenation of the water column is likely to have been controlled by large scale currents, which probably correlated with the extent of interconnections with surrounding oceanic waters. Thus, the inland seas of the Aptian, with oceanic connections to the north, east, west, and perhaps south, probably had much greater circulation than the much more enclosed Albian seas. The sea-floor of the Late Albian Sea preserved in the Toolebuc Formation is regarded as an extensive, anoxic benthic community (Henderson 2004), and the reduced connection of the Late Albian sea to the ocean may be comparable to the modern Black Sea, which is meromictic⁵ with extensive deep water anoxia. In contrast, the Doncaster Formation of the Late Aptian Sea has been interpreted as better oxygenated environment (Day 1969), corresponding with the greater connectivity of that sea with oceanic waters, although there is evidence of localised areas of low oxygen levels at the sea floor

⁵ In meromictic water bodies the surface and bottom waters can remain unmixed for several years at a time.

even with this high oceanic connectivity. Anoxic bottom waters in the Toolebuc are likely to have been an important factor in the excellent preservation of marine reptiles from this unit (Henderson 2004).

Nutrient input and sedimentation are strongly associated with the extensive volcanism of the Whitsunday Igneous Province (Bryan et al. 1997). Volcanic flows commenced in the Barremian (127 Ma) and continued until the Early Cenomanian (95 Ma), with the main extensive outflows occurring in the Late Aptian through to the Early Albian – a time associated with the large volumes of the Doncaster Formation and Coreena and Ranmoor Members of the Wallumbilla Group (Table 3-1). Similarly, the thickness of the Allaru and Mackunda Formations of the Late Albian Sea are testament to large volumes of volcanoclastic flow into the GAB; as reworked sediment in the case of the Allaru, but more directly from the volcanic source in the Mackunda (Cook and McKenzie 1996). In contrast, the Toolebuc Formation is much thinner, and has a greatly reduced siliclastic component, compared with the under- and overlying units. A possible interpretation is that the Toolebuc Formation represents a period of reduced volcanic activity in the Whitsunday Igneous Province, with reduced siliclastic sedimentary input into the sea and therefore a concentration of organically derived shales and carbonate deposition (Henderson 2004). However, Henderson emphasises that the increased organic fraction in the Toolebuc is not simply a consequence of lowered siliclastic input into the Basin, interpreting photosynthetic production in the Toolebuc to have been especially high, fed by the flow of nutrients (rather than sediments) derived from the Whitsunday volcanics.

Photosynthetic production would have been restricted to the oxygenated upper waters of the water column, with the other components of the ecosystem based upon this. At the high latitudes of the Aptian–Albian seas, the phytoplankton blooms may have been seasonal, and if so this may have influenced the life cycles of the rest of the fauna. The low levels of diversity of the benthic fauna over large parts of the Toolebuc Formation are consistent with low oxygen levels at the sea-bed, although

regions of heavily bioturbated sediment⁶ indicate that the benthos was oxygenated at least occasionally, and it is possible that any seasonal patterns of ice cover and productivity may have affected oxygen levels.

The interactions between the strong seasonal variation of sunlight experienced at high latitudes, the extent of possible ice cover in the southern part of the sea, and the apparently elevated temperatures in the northern part of the GAB are likely to have been complex and reconstruction of the various inland seas as basically homogenous waterways may be overly simplistic. At present, additional oceanographic factors, such as stratification of the water column and possible variation in salinity, are poorly understood.

Palaeofauna

Invertebrates

The various Early Cretaceous marine units of the Great Artesian Basin preserve abundant invertebrate fossils, although there is variation in faunal composition between each of the four inland seas. Recorded diversity is highest in the units corresponding to the Late Aptian and Late Albian seas (Day 1969): this is to be expected, given the much greater exposure of these rocks throughout the GAB. In terms of species turnover, the most noticeable difference is between the Late Aptian and the Early Albian invertebrate faunas, reflecting global faunal turnover between the Aptian and Albian: for example, for the northern Eromanga Basin, only 20% of the species of invertebrates known from the Late Aptian Doncaster Formation and Jones Valley Member are present in the Early Albian Ranmoor Member (Table 3-2, Day 1969).

The nektonic faunal component of the Aptian and Albian inland seas is dominated by cephalopods; predominantly ammonites, with several species of belemnites and squid. The ammonites and belemnites are generally small: for most species, the maximum linear dimensions are less than 50 cm, but fossils of both groups are

⁶ Note that, in the Toolebuc, the layers containing large vertebrate fossils are not visibly bioturbated and this process seems not to be involved in the taphonomy of the marine reptile carcasses discussed in the next section.

	Early Aptian	Late Aptian	Early Albian	Late Albian
cephalopods	1 (1)	12 (11)	9 (8)	17 (13)
protobranch bivalves	2 (2)	5 (4)	2 (1)	4 (0)
eulamellibranch bivalves	12 (12)	17 (7)	12 (6)	10 (5)
pteriomorph bivalves	8 (8)	14 (8)	7 (6)	14 (9)
gastropods	2 (2)	2 (0)	4 (3)	9 (7)
scaphopods	0 (0)	1 (1)	1 (0)	2 (1)
brachiopods	1 (1)	2 (1)	0 (0)	1 (0)
crinoids	0 (0)	1 (1)	0 (0)	0 (0)
decapods	0 (0)	1 (1)	0 (0)	3 (3)
glass sponges	0 (0)	0 (0)	0 (0)	0 (0)
tube worms	0 (0)	0 (0)	0 (0)	1 (1)
total	26 (26)	55 (34)	35 (24)	58 (36)
extinction at end of stage	19%	80%	37%	-

Table 3-2: Species counts for major invertebrate fossil groups over the four transgressive events in of the Early Cretaceous Great Artesian Basin (GAB). Numbers in each column indicate numbers of species in the fossil record for each stage; numbers in brackets indicate the number of those species that appear in the fossil record of that stage for the first time within the GAB. Percentage extinction is calculated as the component of the species in the following stage that do have an earlier record, as a proportion of the total species for a stage, i.e. for the Late Aptian, as $100 - [(35-24)/55]$. Data tabulated from Day (1969) and Cook (A. Cook, pers. comm.).

abundant throughout the GAB. Squid fossils are much rarer, but several species are known from the Toolebuc Formation, including *Boreopeltis* and *Trachyteuthis* (Wade 1993). The preserved gladius lengths of these are 1.3 m and ~1 m respectively; depending on the ratio of gladius to mantle length, this may indicate a mantle length of at least 1 metre and perhaps exceeding 2 metres, although the gladius to mantle length ratio in *Trachyteuthis* may not be much more than 1 (Donovan et al. 2003). Mantle lengths between 1 and 2 metres are comparable to the large modern deepwater species of big squid such as *Dosidicus*, *Taningia*, *Onykia*, *Kondakavia*, *Galiteuthis*, *Megalocranchia*, and even the giant squid *Architeuthis* has a mantle length of 2.5 m, although is greatly exceeded by the largest known squid, the colossal squid *Mesonychoteuthis*.

The benthic communities are dominated by bivalve molluscs: the highest diversity is in the Late Aptian Sea (36 spp.), but diversity in the Late Albian Sea is also significant with 28 species (Day 1969). The eulamellibranchs (clams and allies: veneroids, myoids, and anomalodesmoids) appear to be equally diverse in all four of the inundations, whilst the pteriomorphs (oysters, mussels, and scallops) are more diverse in the Late Aptian and Late Albian strata.

Gastropods are a less common part of the fauna, achieving maximum diversity in the Late Albian Sea (9 spp). Other minor parts of the fauna include protobranchs (primitive bivalves), crinoids, scaphopod molluscs, decapod crustaceans, brachiopods, tube worms (polychaetes), and the glass sponge *Purisiphonia*.

Several authors have noted that, in contrast to the overlying Allaru Formation, the Toolebuc Formation is characterised by low diversity of benthic invertebrates (Cook and McKenzie 1996, Day 1969, Henderson 2004). A small number of pteriomorph bivalve taxa are extremely common throughout the Toolebuc Formation; these are mainly the large, oyster like form *Inoceramus*, along with the smaller *Aucellina*. Both of these bivalves are believed to be tolerant of hypoxic conditions, an interpretation consistent with the hypothesised low oxygen benthic conditions during deposition of the Toolebuc. Henderson has reconstructed the sea-bed during Toolebuc times as hypoxic but rich in microbial activity, thus providing a food source that the inoceramids were able to exploit thanks to their tolerance of hypoxic conditions and ability to cope with soft substrates (Henderson 2004). In many layers in the Toolebuc, inoceramid shells form extensive coquinas, where most of the rock is composed of their characteristically prismatic shell. The coquinas are interspersed with layers of organic shale which lack inoceramid fossils entirely, and bioturbated facies where inoceramid fossils comprise a much smaller fraction of the sediment: these are interpreted as, respectively, completely anoxic periods where even inoceramids could not survive (Henderson 2004), and relatively well oxygenated periods where the substrate was tunnelled by large crustaceans and inoceramid biomass was substantially reduced.

Although benthic invertebrates – with the exception of the inoceramids – are rare during the Toolebuc, the diversity of nektonic forms such as cephalopods and, as we shall see below, ray-finned fishes, sharks, and reptiles, is high. This suggests that, although bottom waters may have been oxygen poor, the upper waters were adequately aerated and the high level of nutrient input inferred for the Toolebuc sea (Henderson 2004) supported a diverse and abundant nektonic fauna, probably based upon productivity from plankton.

Bony fishes

Fish remains are rare in the Aptian strata of the GAB, but are abundant in the Albian, particularly in the Late Albian (Bartholomai 2004, 2008). The Toolebuc Formation is noted for extensive beds that consist largely of fish ‘hash’: teeth, bone, and scales from small herring-sized osteichthyian (bony) fishes. Articulated fossils of these are so far unknown, but they may indeed represent pelagic clupeiforms (i.e. herrings and allies), which diversified in the Early Cretaceous (Carroll 1988). Clupeiforms are a major component of the pelagic fauna in modern ecosystems, and the abundant shoaling species such as herring, sardines, and anchovy are planktonivorous: they thereby constitute a major trophic link between the plankton and the larger predators in pelagic ecosystems. It seems likely that the fish preserved in the Toolebuc ‘fish hash’ beds formed a similar link in the ecosystem of the inland Late Albian inland sea.

Larger, predatory bony fishes are known from articulated fossils and several species have been described. The aspidorhynchid *Richmondichthys sweeti* (previously assigned to *Belonostomus*) (Bartholomai 2004), with its elongate rostrum and armour of heavy scales, looks similar to the extant holostean garfish *Lepisosteus*, although aspidorhynchids may have been basal teleosts (de Pina 1996). Another holostean / basal teleost, the pachycormid *Australopachycormus burleyi*, has been described from the Toolebuc of the Boulia region (Kear 2007a); with a head length of 45 cm, this species may have exceeded 2 m in length. The Pachycormidae include the Jurassic giant *Leedsichthys*, which exceeded 12 m and has been reconstructed as a planktonivore (Liston 2004, 2007): perhaps the reduced maxillary dentition reported in *Australopachycormus* is suggestive of a comparable diet.

Described teleostean taxa include the elopiform *Flindersichthys* (Longman 1932), as well as several large clupeiformes. Although elopiforms are closely related to the eels, their overall body shape resembles clupeiforms and modern species include the predatory tarpons *Megalops*. The clupeiform taxa consist of the ichthyodectid *Cooyoo australis*, a smaller relative of the notorious Late Cretaceous *Xiphactinus*, and the pachyrhizodontid⁷ *Pachyrhizodontus marathonsensis*. All of these species – *Flindersichthys*, *Cooyoo*, *Pachyrhizodontus* – can be reconstructed as large, active predatory fishes: in addition to the tarpon, a potential modern analogue is the enigmatic wolf herring *Chirocentrus* (Bardack 1965), a large chirocentrid clupeiform that is reported to exceed 3 metres⁸ (Migdalski and Fichter 1976, Whitehead 1985) and which is described as a ‘voracious predator’ of herring, sardines, and other small pelagic clupeiforms (Froese and Pauly 2007).

A large osteoglossomorph is known from freshwater sediments of the Cenomanian Winton formation near Isisford, but there is no record of this taxon from marine sediments and the extant species of this group of fishes are entirely freshwater in habit (Migdalski and Fichter 1976). The distinctive tooth plates of ceratodid lungfishes are found in near-shore marine and lower catchment (lacustrine and fluvial) freshwater deposits throughout the GAB, predominantly in the Early Albian Griman Creek Formation and the Late Albian Winton Formation, with some rarer finds in the Coreena and Mackunda Formations (Kemp 1991a). At least three species of *Ceratodus* are present (although only two are sympatric in any one deposit), and fossils of *Ceratodus wollastoni* in particular are abundant in certain beds. Also present, although rarer, are two species of *Neoceratodus*, including the living Queensland lungfish *Neoceratodus fosteri*, identified on the basis of some fragmentary tooth plates from the Early Albian Griman Creek Formation of Lightning Ridge. Living *Neoceratodus* are thought to be entirely dependent on freshwater, but *Ceratodus* may have been capable of excursions into marine environments, as suggested by its

⁷ Although Shimada, Schumacher et al. (2006) list the Pachyrhizodontidae within the Elopiformes.

⁸ However, Bardack (1965) considers these reports to be exaggerated, and states that the true length is closer to 1 metre. The latter size corresponds with the records for the two extant species, *Chirocentrus dorab* and *C. nudus*, in FishBase (Froese and Pauly, 2007).

occasional presence in the shallow marine Coreena and Mackunda units (Kemp 1991a).

Since living *Neoceratodus fosteri* are reported incapable of breeding in temperatures less than 10°C, the presence of lungfishes in the GAB and in the more southerly Gippsland and Otway Basins has been interpreted as a palaeoenvironmental indicator: however, whether *Ceratodus* had the same environmental requirements as its living relative is unknown (Molnar 1991).

Sharks and rays

As with the bony fishes, fossils of sharks are rare in the Aptian seas but are much more widespread in the Albian, especially in the Late Albian Sea. Most specimens of course consist of isolated teeth, although several specimens comprising vertebrae are known. Although the fossils are widespread, systematic studies of the GAB shark fauna are confined to a review by Kemp (1991b); the summary presented here is based upon this in conjunction with preliminary results from ongoing work by N. Kemp and D. Ward (N. Kemp, pers. comm.).

Confirmed Aptian species currently consist only of the callorhynchid chimaera *Edaphodon eyrensis*, from the Late Aptian Bulldog Shale of South Australia (Kemp 1991b). In contrast, the Late Albian shark faunas are diverse, with records of more than 20 species in 8 orders and 15 families (Kemp 1991b, N. Kemp, pers. comm.). This fauna is dominated by lamniforms, especially the cretoxyrhinids but also odontaspids (sand-tigers / grey-nurse sharks), mitsukurinids (goblin sharks), anacorids, and an eoptolamnid. The cretoxyrhinids include the Late Cretaceous species *Cretoxyrhina mantelli*, a large shark of comparable size to the modern white shark *Carcharodon*; the teeth are large and blade-shaped, inviting further comparison with *Carcharodon* as a possible ecological analogue (Shimada 1997a, b). However, if *Cretoxyrhina* is present in the Australian Early Cretaceous, it was a rare component of the fauna; Kemp identified “a number of fragmentary teeth” from the Toolebuc Formation as having the robust morphology characteristic of *Cretoxyrhina* (Kemp 1991b), and as these teeth are not common relative to the other cretoxyrhinids it seems that the Late Albian fauna may represent an early phase in its distribution.

Cretoxyrhina mantelli has been the subject of intensive study in recent years, and some conclusions from this work are worth mentioning here because of the potential importance of this species as an apex predator. Several nearly complete, articulated specimens are known from the L. Coniacian–Santonian⁹ Smokey Hill Chalk Member of the Niobrarra Chalk (Shimada 1997c), indicating a total size of ~4.5 m. Other less complete specimens indicate that maximum size was 6.4–7 m (Corrado et al. 2003, Shimada 2008), comparable to maximum size in *Carcharodon*. Overall body proportions are similar to *Carcharodon*, and preserved tail regions suggest a high aspect-ratio, lunate caudal fin, similar to the morphology of the tail in high speed, active predatory lamnids, scrombroids, and ichthyosaurs (Ellis 2003, Lingham-Soliar and Plodowski 2007, Shimada et al. 2006a).

Despite the similarity in body size and shape between *Cretoxyrhina* and *Carcharodon*, tooth morphology in *Cretoxyrhina* is more similar to that of the mako *Isurus*: although robust, the teeth are not as blade-like as those of *Carcharodon* and lack the serrated edges that characterise the teeth of white sharks (Shimada 1997a). Tooth morphology is considered to be an important correlate of diet in sharks, and while large individual *Isurus oxyrinchus* are known to prey upon marine mammals, makos are predominantly predators of fish and squid: the shortfin mako *I. oxyrinchus* regularly takes large scrombroid fishes, whilst the longfin mako *I. paucus* seems to target smaller schooling fishes and squid (Compagno 1984). As with other lamnid species, including white sharks, mako teeth become more robust with increasing size (Kemp 1991b), suggesting that larger individuals may take a higher proportion of relatively larger prey.

Living makos do not exceed 4 metres, but it is possible that *Cretoxyrhina* was similar to a hypothetical 6-7 m mako. Predation by *Cretoxyrhina* upon *Xiphactinus audax*, itself a large and voracious predator, appears to have occurred in the Niobrarra Chalk; at least one *Cretoxyrhina* fossil contains *Xiphactinus* and these have been interpreted as stomach contents (Shimada 1997b, Shimada and Everhart 2004), perhaps paralleling the shortfin mako's reported taste for the large and potentially dangerous istiophorid

⁹ Late Cretaceous, approximately 85 million years old.

and xiphiid billfishes (Last and Stevens 1994). However, records of predation by *Cretoxyrhina* on marine reptiles, particularly mosasaurs, are more common: a specimen of *Clidastes* shows evidence of healing after an attack by a *Cretoxyrhina* (the specimen exhibits infectious spondylitis and contains an embedded tooth from *C. mantelli*), as well as tooth marks, whilst a series of vertebrae from a sub-adult *Platecarpus?* shows tooth marks and an embedded *C. mantelli* tooth from which the mosasaur did not recover (Shimada 1997b). Everhart reports several additional mosasaur specimens showing evidence of feeding by *Cretoxyrhina* (Everhart 1999), and two specimens of the giant protostegid sea turtles *Protostega gigas* have been described with tooth marks and, in one case, embedded teeth from *Cretoxyrhina* (Shimada and Hooks 2004). Interestingly, *Carcharodon* is known to prey upon the largest living sea turtle, the leatherback *Dermochelys* (Witzell 1987).

Whether these fossils represent scavenging or predatory attacks by the shark is of course difficult to determine, but several of the specimens reported by Everhart (1999) are from mosasaurs as large or larger than the maximum size for *Cretoxyrhina*. The one case that is definitely not scavenging, the *Clidastes* that shows healing, is a smaller species of mosasaur with a maximum size of 3–4 metres. White sharks scavenge carcasses of large whales, but do not hunt live animals of that size: if *Cretoxyrhina* hunted smaller mosasaurs but only scavenged larger reptiles, then the relative prey size would be consistent with the mako-type tooth morphology, considering the larger absolute size of *Cretoxyrhina*. However, if *Cretoxyrhina* actively preyed upon mosasaurs as large or even slightly larger than itself, its behaviour would be more akin to that of *Carcharodon*: in a comprehensive analysis of the palaeoecology of *Cretoxyrhina*, Shimada concluded that *Carcharodon* is the most appropriate ecological analogue (Shimada 1997b). As noted above, white shark teeth are more robust and blade-like, features that have been interpreted as adaptations to predation on marine mammals, and that this morphology is lacking in *Cretoxyrhina* is intriguing. Perhaps the tooth morphology of white sharks is specific to the type (i.e. mammalian, in the case of *Carcharodon*) as well as the relative size of their preferred prey. Alternatively, *Cretoxyrhina* may have been more similar to *Isurus*, hunting prey smaller than itself but scavenging larger carcasses when these were available.

Far more common in the Late Albian of the GAB are the smaller cretoxyrhinids *Archaeolamna kopingensis* and *Cretalamna appendiculata*. Like *Cretoxyrhina*, these are also known from the Late Cretaceous of N. America and Europe, but they are smaller species with less robust teeth. The teeth of *Cretalamna* are comparable to that of modern piscivorous lamniforms such as the sand-tiger ('grey-nurse') sharks *Carcharias* and *Odontaspis*, or the goblin shark *Mitsukurina*, while those of *Archaeolamna* are more robust and superficially are more like the teeth of the thresher sharks *Aliopas*, or even younger individuals of the mako *Isurus* and the porbeagle *Lamna* [see illustrations of tooth morphology in Kemp (1991b), Shimada (2005), Shimada et al. (2006b)]. All of these modern taxa are predominantly piscivorous, and *Archaeolamna* and *Cretalamna* thus seem to have been predators of small to medium sized fishes. Modern goblin and thresher sharks are noted for unusual body shapes, i.e., the enlarged rostrum and highly mobile jaws of goblin sharks, and the very long upper tail fin of thresher shark, and sand-tiger sharks are noted for their generally 'sleepy' nature when not hunting – in Australian waters, grey nurse sharks appear to concentrate foraging to restricted areas in coastal waters over a period of days to weeks, migrating between foraging grounds (Otway and Burke 2004, Otway et al. 2003). The overall body proportions of *Archaeolamna* and *Cretalamna* have not been described in detail, but if similar to those of *Cretoxyrhina* then these species may have been more active open water predators, more comparable to makos and porbeagles than to the modern odontaspid sand-tiger sharks. Perhaps the slightly more robust teeth of *Archaeolamna* indicate a preference for larger fish, or the hard-shelled ammonites – the latter would certainly seem to constitute an abundant potential food source for a predator capable of breaching the shell. Both *Archaeolamna* and *Cretalamna* are known from the Toolebuc, Allaru, and Mackunda Formations; in addition, *Cretalamna* teeth have been recovered from the Coreena Member, indicating the presence of this species in the Early Albian Sea.

The Odontaspidae are represented by at least two species of *Carcharias* in the Toolebuc and the Mackunda Formations (but not, so far, the Allaru). The palaeoecology of this species is presumed to be similar to that of the living species, the grey-nurse shark *Carcharias taurus*, i.e. mainly fish and squid, but also smaller sharks and even benthic crustaceans (Compagno et al. 1989, Froese and Pauly 2007).

Another lamniform family with a similar tooth morphology to the odontaspids is the goblin sharks, Mitsukurinidae, and Kemp noted that teeth from the Allaru formation, which he referred to the mitsukurinid genus *Scapanorhynchus*, may in fact be odontaspid (Kemp 1991b). Although the teeth of goblin sharks may be similar to those of odontaspids, the head shape is very different: the living species *Mitsukurina* has a elongated rostrum and highly protrusible jaws which give it its rather bizarre appearance. The rostrum is covered with a large number of electro-sensory organs, which may allow the goblin shark to forage in the deep waters where it is found (Compagno 1984, Compagno et al. 1989), but most encounters with this species have been made as bycatch in deep water trawls and very little is known about its behaviour.

Fossilised teeth from goblin sharks are known through the Late Cretaceous and Cainozoic, and whole body fossils of *Scapanorhynchus* indicate that the overall body proportions are similar to the extant *Mitsukurina*, complete with the 'paddle-fish' like rostrum (Cappetta 1980). *Mitsukurina* teeth are more slender than those of *Carcharias* (Shimada 2005), but the teeth of various species of *Scapanorhynchus* are more robust, resulting in potential confusion with odontaspid teeth, and in some species are similar to those of the shortfin mako (Bourdon 2008); this suggests a preference for slightly larger prey in these fossil goblin sharks. Even more robust are the teeth of another mitsukurinid, *Anatomodon*, which are known from near Aramac; these may be Toolebuc but the exact stratigraphy is not clear. Given that the living goblin shark inhabits waters more than 1000 m deep, the ecology of two Albian species inhabiting an epicontinental sea must have been quite different.

Another important Cretaceous family of lamniforms were the anacoracids, which have no living members but which were common in the Late Cretaceous and which have been compared, in ecological terms, to the modern carcharhinid sharks, especially the tiger shark *Galeocerdo* (Shimada 1997b). Two species have been described from the Late Albian of the GAB, both from the Toolebuc; *Microcorax*, and *Pseudocorax* (Kemp 1991b). Carcharhinids are the most abundant and important large predators in many modern marine ecosystems, and the suggested ecological parallel

between these and anacoracids is interesting. The species present in the GAB appear to have been small, generalised predators/ scavengers.

Leptostyrax is a small lamniform with teeth that may also indicate a generalised diet. Although traditionally considered a member of the Cretoxyrhinidae, it has recently been assigned to new family, the Eoptolamnidae, along with *Protolamna* and *Eoptolamna* (Kriwet et al. 2008). The Eoptolamnidae are known from Upper Cretaceous and Aptian – Albian rocks in the northern hemisphere, but are also widespread in Neocomian (i.e. pre-Aptian Early Cretaceous) strata, and are considered to be basal lamniforms (Kriwet et al. 2008).

Modern lamniforms are generally open water predators of the upper water column. In addition to the Lamniformes, the rocks of the Late Albian GAB also preserve species of shark from orders which are considered, on the basis of their living species, to be 'bottom dwelling'. These include the hexanchiform seven-gill shark *Notorhynchus*, several species of the Orectolobiformes (carpet sharks), two species of the saw-shark *Pristiophorus*, and two species of the *Squaliformes* (dog-sharks) (Kemp 1991b; N. Kemp, pers. comm.). One of the squaliforms, the bramble shark *Echinorhinus*, is of particular interest because the extant members of this genus are noted for their preference for the sea floor in deep water (up to 900 m) habitats (Bourdon 2008); their teeth are abundant in the Toolebuc Formation, perhaps suggesting a tolerance of hypoxic bottom conditions and a consequent ability to scavenge carcasses lying on the sea-floor (N. Kemp, pers. comm.). Although not described in living bramble sharks, such a behaviour is known for another squaliform, the sleeper shark *Somniosus* (Smith 2005 – see below), which may constitute an appropriate ecological analogue for the Albian *Echinorhinus*.

The Late Albian shark fauna of the GAB also includes two species of palaeospinacids, a family of synechodontiform which first appear in the Triassic and which appear to be basal neoselachians, i.e. close to the origin of the modern sharks (Underwood 2006). Also present is a tooth from a batoid ray.

The Late Albian shark fauna thus includes some members of 'primitive' groups, but in many respects is similar to a modern fauna. The diversity of the fauna, in a high latitude sea that is of limited size and which lacks deep water habitats, is also impressive. In contrast, diversity in the Early Aptian, Late Aptian, and Early Albian seas is restricted to one or two species. There are several possible reasons for this pattern; the reduced exposure of Early Albian and Early Aptian rocks can be expected to bias diversity estimates downwards, but this reason cannot explain the reduced diversity of the Late Aptian fauna, from which large exposures of the Doncaster Formation and the Bulldog Shale are known. A similar point can be made with respect to the actinopterygian fauna, which also lacks diversity and abundance prior to the Late Albian. If the Late Albian Sea does represent an appreciably more temperate habitat than the Aptian seas (Cook and McKenzie 1996, Day 1969, Kear 2006b), then it seems possible that the abundance and diversity of bony and cartilaginous fishes was controlled at least partly by climatic factors. However, the Early Cretaceous was an important time in the early diversification of both teleosts and neoselachians, and the Aptian–Albian phase in particular seems to have been a critical period. It is likely that, to some degree, the marked increase in diversity in the Late Albian seas reflects the macro-evolutionary history of these both of these groups, which between them dominate modern marine fish faunas.

Turtles

Fossils of sea turtles are very common in the Late Albian rocks of the GAB, but are so far unknown from the older strata. Only one family is present, the extinct Protostegidae, which includes the famous very large Late Cretaceous *Archelon* and which appears to have been the dominant family of sea turtles in the Cretaceous. Nearly of the fossils are from the Toolebuc, and most belong to *Notochelone*, a relatively small species that does not exceed 1 metre carapace length (Molnar 1991). Fossils of *Notochelone* are common throughout the Toolebuc, and Molnar considers it to have been the most common reptile in this formation (Molnar 1991). Fossilised gut contents and coprolites assigned to *Notochelone* indicate a diet of inoceramid bivalves (Kear 2006a).

A recently described species from the Toolebuc, *Bouliachebys* (Kear and Lee 2006), is described as a larger species than *Notochelone*, although the authors did not provide an estimate of absolute size. The enigmatic species *Cratochelone*, known only from a single fragmentary specimen, represents a very large protostegid, possibly of a similar size to *Archelon* (Kear 2006d, Molnar 1991).

Plesiosauroids

The long-necked plesiosaurs are a constant component of marine reptile communities throughout the Jurassic and Cretaceous, and many fossils from this important group are known from Australian Early Cretaceous. One family, the Elasmosauridae, appears to dominate Cretaceous faunas worldwide, and most of the Australian finds appear to represent this group, but so far identification of species and even genera has proved difficult. In part, this reflects long term confusion regarding the alpha taxonomy of elasmosaurids worldwide: even in the North American Late Cretaceous, where several taxa are represented by nearly complete specimens that include cranial material, attempts to provide a taxonomy have yielded inconsistent results (Brown 1981, Carpenter 1999, Welles 1943, 1952, 1962, Williston 1906). Many specimens of elasmosaurid are preserved without any part of the skull, and traditional taxonomies emphasised postcranial characters that are now considered to be unreliable; only recently have cranial characters been emphasised and a more stable taxonomy (but not necessarily phylogeny) of the Late Cretaceous material begun to emerge (Carpenter 1999, Sato 2002).

Unfortunately, although elasmosaurid material is relatively common in both the Late Aptian and Late Albian of the GAB, most of it is frustratingly incomplete and cranial material is extremely rare; as a result, even basic questions, such as how many species are represented in the GAB, cannot yet be answered. Several species have been erected, but these are mostly founded on indeterminate material and are most likely invalid. The first species to be named, apparently from the Late Albian, were *Plesiosaurus sutherlandi* and *Plesiosaurus macrospondylus*, but these are now considered to be indeterminate elasmosaurids (Kear 2003, Persson 1960, Welles 1962). Persson named *Woolungasaurus glendowerensis* on the basis of associated vertebral and appendicular material, including a pectoral girdle, from the Late Aptian Doncaster

Formation of Hughenden (Persson 1960), but while this is certainly an elasmosaur it is also regarded as indeterminate and the name is considered to be invalid (Kear 2003, Welles 1962). Another taxon, *Cimoliasaurus maccoyi*, from the Late Aptian of White Cliffs, is most likely another indeterminate elasmosaurid (Kear 2003).

Only one complete elasmosaurid skull is known, from the Toolebuc Formation of Queensland (Persson 1960), but even this specimen is problematic due to severe taphonomic distortion; apparently, it was bitten by a large pliosaur and is extremely crushed (Thulborn and Turner 1993). Nevertheless, it was used by Kear to establish a new genus, *Eromangasaurus* (Kear 2005b, 2007c), although the severe distortion and the lack of postcranial elements make determination of its relationships with the other Australian elasmosaurid material difficult. However, it seems comparable to the Aptian South American elasmosaur *Callawayasaurus*, which is known from cranial and postcranial material (Carpenter 1999, Ketchum 2008, Welles 1962).

Despite the taxonomic uncertainty, the material to hand is sufficient for a palaeoecological summary to be made. Elasmosaurid material is widespread in the in Bulldog Shale (Late Aptian) and Oodnadatta Formation (unspecified Albian) (Kear 2006b) of South Australia, the Doncaster Formation of both the Eromanga and Carpentaria Basins in Queensland, the Late Aptian of White Cliffs in New South Wales, and the Late Albian of the Eromanga Basin in Queensland (Kear 2003, 2005a, Molnar 1991, Persson 1960). Several isolated teeth from the Griman Creek Formation of Lightning Ridge may also be elasmosaurid, potentially indicating a presence in the Early Albian sea as well (Kear 2003, 2006b). In Queensland, the Late Albian material appears to indicate a larger maximum body size than for the Late Aptian (pers. obs.), although none of the specimens are as large as the biggest taxa from the Late Cretaceous. Stomach contents are known from several specimens; these commonly include gastroliths, but an Aptian and an Albian specimen also preserve traces of diet and these indicate predation on benthic and nektonic invertebrates (McHenry et al. 2005). This latter observation is of interest as, based upon preserved stomach contents from Late Cretaceous specimens, and general interpretations of the functional morphology of the teeth and especially the very long neck, a diet of nektonic cephalopods and fish is emphasised in most accounts

(Cicimurri and Everhart 2001, Ellis 2003, Massare 1987, Welles 1962). Both of the Queensland specimens were small (> 1,000 kg) and may have been young animals, suggesting that diet might have varied with ontogeny (Wiffen et al. 1995): alternatively (or perhaps even commensurately), the elasmosaur neck was a far more flexible feeding organ than has commonly been supposed.

Until recently, all plesiosauroid material from the GAB has been referable to the Elasmosauridae¹⁰. However, a specimen from the Late Aptian Bulldog Shale of Andamooka (Kear 2006b) preserves several features, notably in the dentition, the proportions of the cervical vertebrae, and the pectoral girdle, that are inconsistent with traditional concepts of the Elasmosauridae and which instead are more typical of cryptoclidoids (Druckenmiller and Russell 2008a, Kear 2006b, Ketchum 2008). Kear erected the new species *Opallionectes andamookaensis* for this specimen, and although he declined to assign it to a family, it seems unlikely that this species is an elasmosaurid; *Opallionectes* thus constitutes the first good evidence for a non-elasmosaurid species of long-necked plesiosaur from the Australian Early Cretaceous. The fine, needle-like teeth are similar to those of cryptoclidoids, and this morphology has been interpreted as an adaptation to gulp feeding on small shoaling prey (Brown 1981, Cruickshank and Fordyce 2002, Kear 2006b), a feeding strategy that may be analogous to use of multi-cusped teeth by the modern Antarctic crabeater seal *Lobodon* to capture euphausiids (krill) (Bargagli 2005, Jefferson et al. 1993). Interestingly, a large number of gastroliths are known from the type specimen (Kear 2006b). The implications of this species for the higher taxonomy of plesiosauroids are discussed below.

Leptocleidoids

This taxon has been coined recently as a grouping for various smaller Cretaceous pliosaurs, specifically the polycotylids and the leptocleidids (Druckenmiller 2006, Druckenmiller and Russell 2008a). Leptocleidids are known from Early Cretaceous deposits worldwide, and although traditional accounts placed all of the specimens

¹⁰ This includes the material referred to the Cimoliosauridae Delair, 1959: that family is founded on invalid taxa and, *sensu* Persson (1960), is no longer regarded as valid (Brown, 1960); although it was resurrected by O'Keefe (2001) to contain several aberrant Cretaceous cryptocleidoid taxa (see text). Much of the Australian material that was identified as cimoliosaurid *sensu* Persson is elasmosaurid (Kear, 2003).

into the single genus *Leptocleidus* (Andrews 1922, Cruickshank 1997, Cruickshank and Long 1997), more recent studies suggest that the taxonomic diversity of these species has been underestimated (Druckenmiller 2006, Sato 2002): the group of small pliosaurs that are similar to *Leptocleidus* seem to represent their own family, the Leptocleididae (White 1940), and this pattern is supported by recent analyses (Druckenmiller 2006, Druckenmiller and Russell 2008a, Ketchum 2008, Smith and Dyke 2008). A notable feature of leptocleidid palaeontology is the occurrence of the fossils in strata indicating marginal marine or even freshwater habitats (Andrews 1922, Cruickshank and Long 1997), suggesting a paralic lifestyle for this group perhaps comparable to modern river dolphins, or even harbour seals or harbour porpoises.

The presence of leptocleidids in the GAB was first indicated by a remarkable fossil from the Late Aptian opal fields of Cooper Pedy in South Australia, which consists of a nearly complete 2 metre animal that is entirely preserved in opal. The specimen has been used to establish a new species, *Umoonasaurus demoscyllus* (Kear et al. 2006); some gut contents, including gastroliths and small fish vertebrae, are also preserved. Additional leptocleidid material from the South Australian Late Aptian comprises a small specimen from the Bulldog Shale that has been interpreted as a juvenile, but which is of indeterminate species (Kear 2007b).

Various non marine deposits of the Otway/ Gippsland Basins, and the Griman Creek Formation of Lightning Ridge, have produced plesiosaur remains and these appear to be mainly attributable to the Leptocleididae (Kear 2006c). The presence of leptocleidids in non-marine environments is of interest in the light of previous finds of this family (see above); however, the Griman Creek Formation consists of interbedded freshwater and marginal marine deposits, and not all of the plesiosaur fossils from Lightning Ridge are necessarily from freshwater habitat. Additionally, some of the isolated teeth from Lightning Ridge are consistent with the morphology of non-leptocleidoid taxa, i.e. long-necked plesiosauroids and even large pliosauroids cf *Kronosaurus* (see below).

As with the leptocleidids, the presence of the Polycotyliidae in the GAB basin was first confirmed with the discovery of a spectacular fossil, in this case a from the Late Albian Allaru Formation near Richmond. Representing a new taxon, QM F18041¹¹ is a complete, minimally distorted polycotyliid; although as yet undescribed, morphological data from this specimen has been incorporated into recent phylogenetic analyses and, as might be expected from its stratigraphic position, it appears to be a basal member of the family (Druckenmiller 2006, Druckenmiller and Russell 2008a, Ketchum 2008). However, it is not the oldest polycotyliid specimen from the GAB as indeterminate polycotyliid material is known from the Late Aptian; from the Bulldog Shale of South Australia (Kear 2006b), the Doncaster Formation of the Carpenteria Basin (pers. obs. of QM F43871), and as material from White Cliffs previously assigned to *Cimoliasaurus leucoscopus* (Kear 2003, 2005a, Molnar 1991, Persson 1960).

Polycotyliids are an important group of plesiosaurs in the Late Cretaceous, and show a derived morphology compared with other pliosaurs including a longer neck and an elongate rostrum that is similar to the rostral proportions of extant longirostrine crocodylians, such as the false gharial *Tomistoma* and the freshwater crocodile *Crocodylus johnstoni*. Several authors have speculated that the polycotyliids may have filled the niche vacated by the ophthalmosaurid ichthyosaurs during the mid Cretaceous (e.g. Bakker 1993): given that ichthyosaurs are regarded as being effective predators of Mesozoic cephalopods (McGowan 1991), reports of ammonite remains in the stomach content of a polycotyliid from the Late Cretaceous of Japan are of particular interest (Sato and Tanabe 1998).

Recent analyses that have found a close relationship for leptocleidids and polycotyliids within the Leptocleidoidea indicate that the Early Cretaceous species are of an intermediate morphology: the placement of *Umoonasaurus*, *Edgarosaurus*, QM F18041, and another Early Cretaceous specimen that represents a new taxon, TMP 94.122.01¹², lies between *Leptocleidus* and the Late Cretaceous polycotyliids, with the

¹¹ Widely referred to as the 'Richmond pliosaur'.

¹² Designated as the holotype of a new taxon, *Nichollsia borealis*, by Druckenmiller and Russell (2008b): however, *Nichollsia* is preoccupied, requiring a new genus name for this species (P. Druckenmiller, pers. com.)

precise topology varying between analyses (Druckenmiller 2002, 2006, Druckenmiller and Russell 2008a, Ketchum 2008, Smith and Dyke 2008). The intermediate nature of the Early Cretaceous taxa is exemplified by TMP 94.122.01 (Druckenmiller and Russell 2008b); Druckenmiller initially thought this to be an animal very similar to *Leptocleidus*, but eventually found it to group closer to the Late Cretaceous polycotylids (Druckenmiller 2006, Druckenmiller and Russell 2008a). A leptocleidoid specimen from the Toolebuc Formation, QM F12719, that represents a new taxon also shows some 'intermediate' leptocleidid–polycotylid features; it is currently under study by C. Glen (Glen 2002).

Brachaucheniiidae

The large pliosaur *Kronosaurus queenslandicus* was named on the basis of material from the Late Albian Toolebuc Formation of Hughenden (Longman 1924), and a large amount of material collected from the Toolebuc since that time has been referred to this taxon (Longman 1930, 1935, Molnar 1991). Additional specimens from the Late Aptian Doncaster Formation have also been referred to *Kronosaurus* (Romer and Lewis 1959, White 1935), although whether the Doncaster material represents the same species as that from the Toolebuc has been questioned (Kear 2003, Molnar 1991, Thulborn and Turner 1993). A similar species from the Early Aptian of Colombia has been referred to a new species, *Kronosaurus boyacensis* (Hampe 1992), although the features that distinguish the two species have not been clarified in the scientific literature. Originally referred to the Pliosauridae, *Kronosaurus* is very similar morphologically to the North American Late Cretaceous taxon *Brachauchenius*, and Hampe has placed *Kronosaurus* together with *Brachauchenius* within the family Brachaucheniiidae Williston, 1925 (Hampe 1992, 2005). The taxonomy of the various specimens referred to *Kronosaurus* is considered in detail in following sections of the present thesis (see Chapters 4 and 6).

Teeth from large pliosaurs are distinctive and have been collected from the Late Aptian Bulldog Shale of South Australia (Kear 2006b), and from White Cliffs in New South Wales (Kear 2005a). Some of the isolated teeth from the Early Albian Griman Creek Formation of Lightning Ridge, figured by (Kear 2006c), resemble the teeth of a large pliosaur and are described as have broken and reworn tips, a feature

characteristic of large macrophagous pliosaurs (Massare 1987, Noè 2001). The morphology of these isolated teeth is consistent with that of *Kronosaurus*, and there is currently no evidence of more than one genus of large pliosaur from the GAB.

Ichthyosaurs

Fossils of ichthyosaurs are known from the Late Aptian Bulldog Shale (Kear 2006b) and White Cliffs (Kear 2005a), and are especially common in the Late Albian Toolebuc Formation: to date, only a single species, *Platypterygius longmani*, has been described (Kear 2003, Molnar 1991, Wade 1990). One of the geologically youngest ichthyosaur taxa known, *Platypterygius longmani* was a medium to large sized animal of at least 5 metres and perhaps as much as 7 metres total length. Within the Toolebuc formation, it is second only to *Notochelone* in abundance and was probably the most common large animal in the Late Albian Sea. For example, in the Boulia area scattered outcrops of the Toolebuc Formation have yielded over 120 individual ichthyosaurs (R. Suter pers. comm.). Comparison with similar sized extant odontocetes suggests a mass of between 1 and 2 tonnes, and the long, thin jaws are filled with numerous small teeth, suggesting a diet of fish, squid, and belemnites. One remarkable specimen preserves gut contents of a hatchling turtle, an enantiornithine bird (to date, the only record of that group in the Australian Early Cretaceous) and fish, perhaps indicating that *Platypterygius* was an opportunistic predator: the same specimen also contains a large embryo skull and was evidently a gravid female (Kear et al. 2003a). The Late Aptian material is indeterminate but, given the generally low levels of ichthyosaur diversity in the Cretaceous, can be assumed to represent the same species.

Archosaurs

In addition to the ingested bird remains mentioned above, several specimens of archosaur are known from marine strata within the GAB. These include rare fossils of pterosaurs, which can nevertheless be reconstructed as sea living reptiles, and representatives of several groups of dinosaur, which are less likely to have been marine reptiles. The dinosaurs are all fragmentary remains of large animals, and seem likely to represent 'bloat and float' carcasses from terrestrial habitats adjoining the seas: they include the basal ankylosaur *Minmi*, known from both the Early Aptian

Minmi Member of the Bungil Formation (Molnar 1991) and the Late Albian Allaru Formation; the ornithopod *Muttaborrasaurus*, known from the Late Albian Toolebuc and Mackunda formations (Molnar 1991); and various remains of titanosaurid sauropods, including *Austrasaurus*, from the Allaru Formation (Molnar 1991), as well as several indeterminate fragments from the Toolebuc Formation. The Early Albian Griman Creek Formation of Lightning Ridge preserves several smaller taxa, including theropods, but these are most likely from the terrestrial strata that are interbedded with the marginal marine layers of this unit. Evidently, carcasses of smaller dinosaurs were not large enough to be floated out to the offshore marine facies.

Pterosaurs are well known from marine and marginal marine sediments throughout the Cretaceous, and many species are regarded as maritime predators analogous to various modern sea birds. Although they are expected to have been present in the various Australian Early Cretaceous seas – the Santana Formation of S. America is of a similar age as preserves numerous specimens of several species – fossils are rare in the GAB and so far all known specimens are highly fragmentary. An isolated pelvis is known from the Toolebuc Formation of Bouliá (Molnar 1991), and a partial snout from the Toolebuc of Hughenden has been used to found a new taxon, *Mythunga* (Molnar and Thulborn 2007). Another specimen, also from the Toolebuc of Hughenden, also preserves an incomplete snout. The Queensland material indicates a small pterosaur, of ~2 m wingspan, and has been compared to the better known *Ornithocheirus*, although the rostral fragments lack the rostral crest evident in some species of that genus and the taxonomy of the Australian pterosaurs remains uncertain.

Evolutionary and palaeobiological implications

The Aptian–Albian plesiosaur fauna of the GAB is interesting from the perspective of plesiosaur systematics, which are in a state of flux. Although O’Keefe recovered *Kronosaurus* as a basal pliosaurid only distantly related to the American Cretaceous taxon *Brachauchenius* (O’Keefe 2001), his analysis was based mainly upon published descriptions: several more recent analyses are based upon first-hand observation of the relevant material, or unpublished data from the present thesis, and these find *Kronosaurus* as either to be either a derived pliosaurid (Druckenmiller and Russell

2008a) that is a sister group to *Brachauchenius* (Ketchum 2008), or in a clade with *Brachauchenius* as the sister group of the Pliosauridae (Smith and Dyke 2008). If the latter topology is supported by further analyses, then the Brachaucheniidae Williston 1925 *sensu* Hampe (1992) is a valid family of large pliosaurs that is distinct from the Jurassic pliosaurids. However, Ketchum's result, of *Kronosaurus* and *Brachauchenius* as derived Cretaceous pliosaurids, is part of an analysis that was primarily focussed upon the Pliosauridae and if her result is supported then Williston's Brachaucheniidae is more appropriately regarded as the Brachaucheniinae Williston, 1925 (*sensu* Ketchum 2008).

The precise taxonomic context of *Kronosaurus* is of interest in the context of this thesis, but given that *Kronosaurus* and *Brachauchenius* are sister taxa, it is probably of little consequence to most workers whether they are a sister group of the Pliosauridae or instead lie within that family. However, several other parts of the GAB pliosaur fauna may have more important implications for higher level plesiosaur systematics. Of particular interest is the suggestion by Kear that the long necked Late Aptian taxon *Opallionectes* is not an elasmosaurid (Kear 2006b). The presence of non-elasmosaurid families of long-necked plesiosaurs in the Cretaceous is controversial, although there are certainly several taxa that have very aberrant morphologies compared with the 'typical' elasmosaurids known from the North America Late Cretaceous. In particular, the Late Cretaceous forms *Aristonectes* from South America and Antarctica, and *Kaimbekea* from the New Zealand, have enlarged skulls, a large number of needle-like teeth, and relatively shortened cervical vertebrae: these tooth and neck features are shared with the Jurassic cryptoclidids and several authors have suggested that *Aristonectes* and *Kaimbekea* are late survivors of a Cretaceous radiation of the cryptoclidids in the Southern Hemisphere (Brown 1981, Cruickshank and Fordyce 2002, Cruickshank et al. 1999). However, other analyses have found *Aristonectes* to be an elasmosaurid (Gasparini et al. 2003, Ketchum 2008), or have found the Cretaceous 'cryptoclidid' like forms to represent a different family, to which the name Cimliosauridae (Delair 1959) has been applied¹³ (O'Keefe 2001). Ketchum found that *Kaimbekea* may be a distant relative of the Cryptoclididae within

¹³ See above – this family was originally created by Delair (1959) and used by Persson (1960) as a home for the N. America Cretaceous *Cimoliasaurus*, which is widely regarded as an invalid taxon (see Brown, 1981).

the superfamily Cryptoclididae (Ketchum 2008). In light of the confusion surrounding Cretaceous plesiosauroid systematics in general, and elasmosaurid systematics in particular, the status of *Aristonectes* as an elasmosaurid is perhaps best treated with an open mind pending further analysis. Given the patchy Cretaceous record of the relevant taxa and the potential importance of Early Cretaceous taxa, data from *Opallionectes*, in conjunction with the enigmatic Berriasian *Brancaesaurus*, may yet prove to be critical in establishing the validity (or not) of the enigmatic and decidedly weird Cimoliasauridae (*sensu* O'Keefe, 2001).

The Early Cretaceous is also likely to be a critical stage in the evolution of the Polycotylidae and thus data from Aptian–Albian polycotylids is potentially very valuable in establishing the currently controversial higher level relationships of this important family. Polycotylids are well known from the Late Cretaceous of North America, and have generally been assumed to represent a relatively long-necked form of pliosauroid, but several workers have suggested that they shared a number of features with the long-necked plesiosauroids and may thus represent a convergence upon the 'pliosaur' body form (Carpenter 1996, Carpenter 1997, 1999, O'Keefe 2001, O'Keefe 1999). In particular, O'Keefe found the polycotylids to be a sister group to the Cryptoclididae. Conversely, a number of authors have noted similarities between the polycotylids and the leptocleidids (A. Cruickshank, pers. comm., (Cruickshank 1997, Cruickshank et al. 1999, Cruickshank and Long 1997), suggesting that the Late Cretaceous polycotylids may have descended from these small, Early Cretaceous pliosaurs. The Polycotylidae are an important part of Late Cretaceous marine faunas, but the Late Cretaceous forms are highly derived, complicating attempts to resolve their evolutionary relationships. The inclusion of data from Early Cretaceous members of the family would be expected to clarify this situation, and both Druckenmiller and Ketchum have recovered the Leptocleididae as the sister group to the Polycotylidae with datasets that include data from Early Cretaceous taxa (Druckenmiller 2006, Druckenmiller and Russell 2008a, Ketchum 2008): this grouping has been termed the Leptocleididae (Druckenmiller 2006). However, the two analyses do not agree on the placing of the leptocleidids: Ketchum (2008) found them to be plesiosauroids closely related to the cryptoclidids, while Druckenmiller and Russell (2008a) found them to be pliosauroids that are a sister

group to the Pliosauridae. Despite the profound difference between these results, the situation is, at present, not so much controversial as it is confusing, since these analyses were based upon very similar datasets (Druckenmiller, pers. comm.).

Although both Druckenmiller's and Ketchum's analyses included data from two Early Cretaceous GAB taxa – *Umoonasaurus*, and QM F18041 – it is possible that some of the other material discussed above, in particular QM F12719, will prove to be an important part of this perplexing puzzle.

In several papers dealing with the leptocleidid material from the southern part of the GAB, Kear has adopted O'Keefe's (2001) assignment of *Leptocleidus* to the Rhomaleosauridae: given that this family is otherwise known only from the Early to Middle Jurassic, the consequent status of the Australian 'leptocleidid' material as 'archaic' has been emphasised. However, all of the more recent analyses (Druckenmiller 2006, Druckenmiller and Russell 2008a, Ketchum 2008, Smith and Dyke 2008) have failed to find any close relationship of *Leptocleidus* and related taxa to the Rhomaleosauridae, and this important Jurassic family is therefore not represented in the Early Cretaceous of the GAB (*contra* Kear 2003, 2006b, 2007b, Kear et al. 2006).

Kear notes that plesiosaurs dominate the Late Aptian fauna, but that ichthyosaurs and turtles are more abundant in the Late Albian, and suggests that this may correlate with a greater tolerance for plesiosaurs for cold water habitats (Kear 2005a, Kear et al. 2006). The occurrence of plesiosaurs at high latitudes in other parts of the world has been noted by other authors (Cruickshank and Fordyce 2002, Cruickshank et al. 1999). Kear has also emphasised that the South Australian and New South Wales records of elasmosaurids and leptocleidids in the Late Aptian comprise a large proportion of small individuals, and has postulated that the southern extreme of the Late Aptian Sea may have served as a breeding ground or a preferred habitat for juvenile animals (Kear 2005a, 2006b, 2007b).

Summary

In comparison with other well studied Mesozoic marine reptile faunas – for example, the Early Jurassic Lias, the Middle Jurassic Oxford Clay, and the Upper Cretaceous

Niobrarra Chalk – the Early Cretaceous GAB marine reptile fauna is not particularly diverse. However, individual species appear to be reasonably abundant, particularly in the Late Aptian and Late Albian and especially in the Toolebuc Formation, although this remains a qualitative assessment. As noted above, in this respect the reptile fauna differs from the bony fish and shark faunas, which are not diverse until the Late Albian. At present, understanding of macroevolutionary trends for the various marine reptile groups during the Early Cretaceous is poor and whether the observed patterns of diversity are a function of intrinsic evolutionary processes at that particular time, or instead are controlled by more extrinsic factors such as climate and ecosystem productivity, is at present unclear. Of course, all of these may be relevant in different cases.

In broad terms, the inland seas appear to have been productive high latitude marine ecosystems that contained reasonable levels of invertebrate and vertebrate diversity, given their nature as restricted epicontinental waterways. A key point is that, although apparently less diverse than modern oceanic ecosystems, the Cretaceous inland seas were much smaller than an oceanic system. It is unclear just how important the restricted connectivity between the inland seas and the ocean was in determining diversity, but that the Albian seas in particular had only a single connection to the ocean, which may have been in a substantially different climatic zone to the majority of their waters, is probably relevant. Modern analogues for the inland seas are difficult to identify, partly because of uncertainty about the Cretaceous climate but also because there are not many modern epicontinental seas. The Caspian and Black seas are possibilities, but are even more cut-off from the ocean than the GAB inland seas. The Mediterranean Sea is of a somewhat greater area to the GAB, is much deeper, and lies in a subtropical climate zone: these issues also apply to the Gulf of Mexico, although it has much greater connectivity to the Atlantic Ocean than does the Mediterranean. Hudson Bay is a similar area and depth, and may even be climatically comparable to some stages of the Early Cretaceous in the GAB: the connectivity to the ocean is probably similar to the Albian inland seas, but overall it is probably too cold. Perhaps a better analogue is the North Sea; shallow, of a similar area, and even a similar climate, although its connectivity to the ocean would be more akin to the Late Aptian Sea than the Late Albian inundation.

3.3 **Through the taphonomic window: the distortion of fossil form**

The aim of this thesis is to investigate the cranial biomechanics of *Kronosaurus queenslandicus*. The mechanical properties of any structure are determined by two attributes: its shape (geometry), and the properties of the material(s) from which it is constructed. With both of these, there are problems for the reconstruction of skull biomechanics in fossil species: the original geometry of the skull is almost always distorted (with some rare and notable exceptions) by the processes involved with death, burial, exposure, and even scientific study, and the skeletal materials are always altered by fossilisation. Any attempt to model palaeobiomechanics must therefore deal with two hurdles: the anatomical information preserved in the fossil specimen must be understood, and the preserved anatomy then adjusted to take into account the taphonomic distortions to which it has been subjected. The hoped-for result is a reconstruction which approximates the original geometry and material properties of the biological structure as it appeared in life.

The processes of taphonomy – everything that happens to an organism following death – act as a filter, preventing much anatomical information from ever being collected scientifically, and distorting that which does get collected. The most obvious effect of this filter is that, usually, only hard parts are preserved: although some fossils do preserve information on soft-tissues, they are rare and for most fossil species the anatomy of soft tissues much be guessed. For a biomechanical analysis of the skeletal system, this means that the muscular, tendinous, ligamentous, and cartilaginous components of the system are not based upon direct evidence – a major deficiency. Furthermore, although the hard (i.e. teeth and bone) parts of the skeleton are preserved, they are usually incomplete and are often badly distorted. Each individual specimen represents a unique episode of taphonomy, but some generalities do exist and it is important to understand the manner by which specimens are altered through taphonomy – this information is crucial when the reconstruction of the original structure is being attempted.

The different stages of taphonomy

For any organism, taphonomic processes can be divided into a basic scheme as follows:

1. Death: not all organisms meet a violent end, but plenty do and the violence of death often represents the first change inflicted upon the structure of the organism relative to its normal live condition. Bite marks are a common example, and a powerful bite by an attacker can crush bones. The sites of injury often in turn set up local taphonomic micro-environments that can alter the details of the taphonomic process in the anatomical region surrounding the injury (for example, by allowing iron-rich blood to pool in a haematoma) or even the whole animal (e.g. by piercing the body wall and thus preventing a build up of gases later in the decomposition process).
2. Post-mortem / pre-depositional phase: In many cases, there is a considerable period between death and the onset of burial. What happens to the carcass in this phase has a significant effect upon the final condition of the fossilised specimen, and although details are specific to each case, are largely determined by the basic environment in which the animal dies, i.e. marine or terrestrial. During this phase the carcass can be disturbed by scavengers, transported by currents, and exposed to the elements, all of which affect the state of the carcass when burial eventually commences.
3. Deposition: The basic nature of the depositional environment has obvious effects on the final outcome of the taphonomic processes. The nature of the matrix – carbonate, sandstone, mudstone, etc – which will later surround the fossil is a function of the depositional environment, as is the ‘energy’ of depositional site (e.g. high energy shorelines and river channels vs lower energy floodplains, lakes, and marine benthos). However, there are some subtler aspects of this process: deposition is not necessarily uniform around the preserved skeletal elements. Complete burial of a carcass can take an appreciable period of time, and during this period the shape and nature of the carcass may change as different soft-tissues decompose. If the nature of the sediment burying the carcass changes as well, then there is potential for differential burial of the specimen – for example, the choanae (nasal passages)

may become infilled with sediment before the tissues enclosing the nasal cavity break down, so that when the nasal cavity does become infilled it might be with a different sediment (if the sedimentary profile varies over the course of burial), allowing the position of the nasal passages to be inferred. The process of infilling, as well, can lead to differences in sediment size inside and outside of a structure: the micro-environment inside a structure such as a nasal cavity is generally of a lower energy than the surrounding environment, leading to smaller particle sizes in the infilled component. These variations in sediment type and particle size across the depositional phase can be important because (1) the mechanical properties of matrix alter with particle size, and thus heterogeneity in matrix can lead to differential compression of the specimen in the following post-depositional phase, and (2) a marked division between two types of sediment in the absence of an obvious barrier can be used to infer the presence of a soft-tissue barrier at the start of deposition.

4. Post-depositional phase: Once the remains of the carcass have been entombed in sediment, it is subject to a range of processes that alter and distort the structure and which are collectively referred to as 'diagenesis'. Diagenetic processes include: geochemical alteration of the remains, vertical compression due to weight of overburden, and even minor tectonic alteration. Of these, the first two are particularly important and are responsible for much of the physical alteration of the original structure.
5. Exposure: After millions of years of burial, the specimen – now a fossil – is exposed through weathering of overlying rock: we are thus talking about an erosional landscape. In different soil/rock profiles, the weathering horizon extends below the surface by up to several metres, and so the final stages of diagenetic alteration merge into the initiation of weathering, with the latter tending to be a far more rapid process. The most obvious effect of weathering is the physical abrasion of preserved organic structures, and the fragmentation of the fossil as the blocks of matrix containing it are split into smaller pieces, but chemical alteration often accompanies this phase. As this process continues, the remains of the fossil can become dispersed through the action of water, wind, and gravity – even where the rock containing the fossil is not exposed directly – as parts gradually are worked to the surface through

fragmentation of the upper layer and movement of the overlying soil, and different parts of the fossil can end up being separated before they come to the surface.

6. Collection, curation, preparation, and study: The effects of these on the final state of the fossil should not be underestimated. Ideally, every part of the fossil should be collected, along with carefully recorded information on the position of each fragment and its immediate sedimentological context: but often, this does not happen. Parts of the fossil may be left in the field, accidentally or intentionally, and detailed surveys of sites are time-consuming and are often side-stepped. The result can be a museum shelf full of a fossil/matrix jigsaw pieces, with no picture to work from and key pieces missing. Once in the collection, specimens may be mixed up, mislabelled, lost, stolen, or placed on display. Preparation, whether mechanical or chemical, invariably results in some damage, and display can involve the specimen being painted, glued, covered in lacquer, covered in plaster, and drilled with holes for fixation to supporting structures: and, in addition to the hazards of deliberate actions, accidental breakage is common. Finally, the study of the specimen is limited by logistics, the skill of the researcher, and the methodologies used. If this seems like an overly pessimistic list, they are all involved to varying degrees with the *Kronosaurus* specimens that will be considered later in this chapter.

Taphonomy, then, thwarts attempts to reconstruct the structure of fossil forms. If we are to have any chance of reconstructing the life appearance of a species known only through fossil remains, we must understand the taphonomic history of that specimen so that we can take account of it in the reconstruction. In particular, the processes that are specific to the marine environment are an important part of the taphonomic context for *Kronosaurus* fossils. One field of the geological sciences, actuopalaeontology, seeks to describe the predepositional and early depositional phases that apply to Recent organisms, in order to provide data for the reconstruction of taphonomy in fossil forms. The following section summaries the actuopalaeontology relevant to the taphonomy of large vertebrates in marine environments.

Death at sea: floaters, floaters, and the remarkable phenomenon of whale-fall

The post-mortem processes that affect terrestrial vertebrates have been well documented, with a view to quantifying taphonomic bias in their fossilisation. In contrast, the equivalent processes that affect marine vertebrates have not received a great deal of attention. An important exception is Schäfer's account of marine actuopalaeontology in the North Sea, based upon observations of the death, decay, and burial of various species: the vertebrates for which data is provided include cetaceans, seals, birds, and fish (Schäfer 1972). For these, the pattern of the pre-depositional phase is largely determined by two key factors; whether the carcass spends any time floating on the surface of the water, and whether any part of this phase occurs on land (i.e. washed up on a beach).

The fate of a cetacean carcasses in the North Sea illustrates the relevant features of Schafer's studies. Most cetaceans, whether whales or dolphins, that die at sea sink immediately: the exceptions are those species of whale with sufficient blubber to float even when dead; the so-called 'right' whales, Balaenidae, named because this feature made them suitable for hunting by land-based whalers, the sperm whale *Physeter*, and some balaenopterids that are hunted late in the summer when their fat reserves are high (Allison et al. 1991). In the North Sea, the carcass then floats when a sufficient volume of gas has been produced by decomposition. Schäfer (1972; p.20) states that carcasses that sink into ocean basins with anaerobic bottom waters do not produce sufficient gases to refloat the carcass, and that this is a result of the water being unfavourable for microbial activity: however, the North Sea is generally shallow and the bottom waters are well oxygenated. When afloat, the carcass drifts for a period of days to weeks, and in a restricted basin the size of the North Sea there is a good chance that it will be washed ashore during that time. If it remains afloat, the carcass gradually disintegrates, shedding elements over a wide area: in the case of dolphins and seals, the mandibles soon come loose from the head and the various bones of the cranium start to disarticulate. In the seal, the tympanic bullae drop away relatively early – presumably, the even denser bullae of dolphins do likewise but this data is not recorded. Of interest to students of marine reptiles, the forelimbs of the

seal start to disintegrate well before the hindlimbs, the distal elements of the manus (which are in life held together in a collagenous matrix) being lost whilst the pes elements are still held together by ligaments and tendons, raising the possibility that the patterns of forelimb preservation in marine reptile fossils may provide information on the soft-tissue anatomy of these organs if the taphonomic context can be established.

Eventually, the head and limbs are lost, leaving a floating carcass comprising of the trunk section and limb girdles. In Schäfer's own words, describing a seal carcass 48 days after death: "The fur is now torn at both ends of the body, but it still contains the vertebral column with the rib cage, the shoulder blades, the pelvis, and the thighs. The carcass continues to float". After 57 days, "Only a few pieces of fur are drifting about. The last skeletal parts have separated and, one by one, have dropped from the integument to the sea floor" (Schäfer 1972; pp 33-4). It appears that, in the North Sea at least, the chances of a floating carcass being buried whole, or even semi complete, are slim.

The situation is very different with carcasses that wash ashore or are the result of strandings. These carcasses may be floated and refloated due to tide and wave action, but there is a good chance that they will eventually end up on a beach out of reach of the ensuing cycle of waves and tides. The drying action of the wind and sun can mummify the skin, and the concentration of oily secretions from the decomposition of the blubber can protect remaining parts from the action of maggots and bacteria. The gases of decomposition inflate and straighten out the body – if buried in this state, the skeleton will appear to be 'laid out' as if by an undertaker. Eventually, the body wall ruptures and the gases escape, and after this point the body may become twisted: even so, elements remain in much closer association than with a floating carcass. Schäfer notes that, once exposed to the sun, the bones quickly lose their periosteum, marrow, and organic (i.e. the collagen fibres from the bone matrix) components of the bone: he further states that the spongy bone becomes visible, implying that the outer cortical layer is quickly eroded (Schäfer 1972). The action of wind-blown sand may be important in removing cortical bone, and it is also likely that cortical bone layers in marine mammals are thinner than in their terrestrial

counterparts due to the reduced requirement for weight-bearing by the skeleton. Perhaps if this removal of cortical bone proves to be characteristic of a terrestrial component of the pre-depositional phase, the resulting patterns of exposed spongy bone can provide information on the decompositional setting of marine mammal and reptile fossils, provided that it can be distinguished from post-depositional erosion of the fossilised specimen?

Schäfer could not observe the fate of carcasses that sink and remain on the ocean floor, but such carcasses have been discovered and their progress of decay monitored. Smith et al. (1989) described a carcass of a ~20 m balaenopterid whale, discovered by the ALVIN submersible in 1987, at a depth of 1280 m in the Santa Catalina Basin in the north-east Pacific, and identified on the basis of size as either a Blue (*Balaenoptera musculus*) or Finn (*B. physalus*) whale. The discovery provided a rare opportunity to document the processes of decay in a large amniote carcass in deep water, and were revisited in 1988 and 1991 (Allison et al. 1991, Bennett et al. 1994). Oxygen content of the water at the sediment/water interface was low, and the muddy sediment was completely anoxic below a depth of 10 cm. The skeleton was incompletely buried in mud, ventral side up, and the skull and vertebral column are preserved in a nearly straight line. About half of the expected number of ribs were visible, and these were in more-or-less natural positions: the other ribs as well as the limb elements and some skull bones were not visible and were presumed to have been completely buried in the mud (Bennett et al. 1994). Both mandibles are present and the posterior ends are lying close to the location of the jaw articulation with the skull: the anterior ends have separated at the symphysis and are slightly displaced to the left relative to the skull. Only a few bones showed evidence of displacement, and these are assumed to have been moved by the vortices generated by the submersible.

Of particular interest was the state of the bones. Where they were exposed above the sediment, they were 'corroded', with the spongy bone clearly visible. The portions of the bone that were covered by sediment, however, were intact. This observation was consistent across the entire skeleton, although some exposed bones were more heavily corroded than others. In the bones that were recovered to the laboratory, the buried, intact parts showed high levels of iron sulphite deposition within the

trabecular bone, indicative of activity by chemoautotrophic (in this case, sulphate reducing) bacteria. The bones and the sediment immediately surrounding them were encrusted with bacterial mats, tube worms, bivalves, and gastropods. The bacterial mats are thought to be sulphite and methane oxidisers (utilising the oxygen in the water column and the metabolic products of the anaerobic chemoautotrophs within the bones and sediment). The molluscs included species of limpet thought to be grazing on the bacteria mats, and species of mussels (Mytilidae) and clams (Vesicomidae) known to contain endosymbiotic chemoautotrophic bacteria. The fauna shows taxonomic and structural similarities with vent fauna, leading to speculation that carcasses such as this are involved with the dynamics of that community (Allison et al. 1991, Bennett et al. 1994, Smith et al. 1989). The corrosion of the bones above the sediment surface may be a result of grazing by the gastropods, metabolism by the bacterial mats, or chemical dissolution assisted by a halo of lowered pH surrounding the carcass (Allison et al, 1991).

The carcass is thought to have sunk immediately after death, and to have remained on the bottom without refloating. In contrast to Schäfer's interpretation of lowered oxygen levels leading to reduced bacterial activity, lowered gas production, and hence permanent sinking of the carcass, Allison et al. point out that many of the bacteria involved in decomposition are necessarily anaerobic and thus low oxygen levels should not be expected to determine whether or not a carcass re-floats. They suggest that pressure may be more important, both in reduced levels of bacterial activity, but more importantly in increasing the amount of gas required to produce sufficient volume to refloat the carcass. According to some basic calculations that assume all of the available soft-tissue are decomposed bacterially, the depth of water required to prevent possible refloating of a whale carcass such as the Santa Catalonia Basin specimen is 1500m if decay is dominated by fermentation – if decay is mainly by methanogenesis, the minimum depth will be greater (Allison et al. 1991). The Santa Catalonia Basin specimen is at 1240 m and yet did not refloat, implying that a portion of the tissues were not available for bacterial decomposition, perhaps as a result of scavenging by relatively large animals such as hagfish and sharks, or that the body wall was perforated before a sufficient quantity of gas could build up. Presumably both factors were at play, but the orientation of the skeleton on its back implies that

gas built up within the abdominal cavity was sufficient to roll the carcass belly-up before the body wall failed. Additional factors that may retard gas production are cool temperatures, and the increased dissolution of gases into the water column at high pressure (Allison et al. 1991).

Subsequent monitoring of artificially sunken Gray whale (*Eschrichtius robustus*) carcasses in deep waters on the California slope revealed successional phases in the composition of the decomposer community (Smith 2005, Smith and Baco 2003). In the early stages of decomposition, significant amounts of soft tissues are removed by 'mobile scavengers', which include hagfish, sleeper sharks (*Somniosus*) and macrophagous invertebrates (Smith 2005); flesh was removed at ~60 kg per day, leading to skeletonisation of a 35 tonne carcass in 18 months (Smith 2005). This is then followed by an 'enrichment opportunist' stage, where the nutrient enriched bones and surrounding sediment are colonised by polychaetes and crustaceans and which is thought to last between months and years, and a 'sulphophilic stage', which can last for decades and which appears to be the stage at which the Santa Catalonia Basin carcass was first encountered. Finally, there may be a 'reef stage', where the nutrient value of the carcass, including the bones and surrounding sediment, has been fully exploited, and the bones serve as hard substrate for filter feeding benthic taxa (Smith and Baco 2003).

The fate of large whale carcasses in shallower shelf waters is less clear. Smith (2005) mentions two such carcasses: a Gray whale lying in 150 m deep water off the Alaskan coast, and a Fin whale placed on the sea-floor in 90 m depth in the Strait of San Juan de Fuca (near Vancouver Island). Whether the former was a natural fall, and the degree of completeness, is not recorded, but assuming that partial carcasses are less likely to be discovered accidentally, if the Alaskan Gray whale was a natural fall then it does imply that carcasses in shallower water can remain on the sea-floor without refloating, or, if refloating does occur, it is for a period too short for major disarticulation of the carcass to occur. The action of larger scavengers may be important in both scenarios – if feeding by *Somniosus* and other benthic scavenging sharks is at a comparable rate to that reported for the deep water whale-falls (Smith 2005), then it is possible that the body wall of the carcass is disrupted at an early stage of decomposition, before a volume of gas sufficient to refloat the carcass has

built up. The species of sleeper shark that is most common at these carcasses, *S. pacificus*, exceeds 4 metres in size and specimens of 7 m have been reported (Compagno 1984); it is also widely distributed in temperate and sub-polar waters (Compagno and Niem 1998). Conversely, carcasses of large whales floating at the surface attract considerable attention from pelagic sharks, including large species such as blue sharks (*Prionace*), tiger sharks (*Galeocerdo*), Great Whites (*Carcharodon*), as well as larger species of *Carcharhinus* (Smith 2005). A sperm whale carcass that washed up on Merewether Beach, Newcastle in 2006 showed extensive signs of feeding by sharks, and although it is unclear how long the carcass had been afloat, it was long enough to putrify (pers. obs.). Given that fresh sperm whale carcasses float due to their high blubber content, it is unclear whether floatation in this instance was 'primary', secondary (due to gas build-up), or a combination of both, but it is possible that sperm whales and right whales may continue floating for a long time even after scavengers break through the body wall. How long a refloated carcass belonging to one of the less buoyant species will tend to float is unknown: it is possible that the extended floatation period recorded by Schäfer (1972) for dolphin and seal carcasses is partly a reflection of the sparse populations of pelagic sharks in the North Sea. Refloated carcasses in areas with higher shark populations *might* tend to sink following disruption of the body wall before the skeleton becomes substantially disarticulated – but there is little available data to guide us.

Marine reptile taphonomy in the GAB: predepositional phases

Although fragmentary fossil remains are common, the GAB is remarkable for the number of partially to nearly complete marine reptile specimens in the Aptian and Albian sequences, particularly the Doncaster and Toolebuc Formations. Fourteen significant specimens of *Kronosaurus* have been recovered, of which five include complete or nearly complete skulls and two of these are associated with a large proportion of the pre-caudal skeleton. In addition, a large number of elasmosaurid, leptocleidoid, and ichthyosaurian specimens of similar or superior quality are known: many of these specimens are preserved with substantial articulation of the cranial and postcranial components. The taphonomy of these species has yet to be analysed quantitatively, but the qualitative patterns can be summarised as follows;

- Most specimens are preserved in limestone nodules, but some are found associated directly with laminar shales.
- Bulkier, fleshy body regions are preserved more often than extremities such as distal limb elements, posterior caudal vertebrae, and, in the case of the long-necked elasmosaurids, the anterior cervical vertebrae and head.
- A large proportion of specimens, especially the elasmosaurids, preserve stomach contents.
- Many of the reptile fossils are associated with numbers of bivalve molluscs, especially inoceramids and auctellinids, that appear to have been epifaunal on the carcass.
- In pliosaurs, the mandibles are often preserved in association or even in articulation with the cranium.
- Reptile teeth preserved with the rest of the carcass are usually partially or completely recrystallised in calcite. In some cases, they are preserved only as external moulds in the surrounding matrix. Generally, only isolated teeth (i.e. shed by a living animal or dropped from a floating carcass) are preserved without substantial recrystallisation.

The degree of completeness of many of these specimens suggests that they sunk upon death or, if they did refloat, that this was only for a short time and they sank before the specimen became disarticulated. At the same time, that most of these specimens are only partially complete may suggest that most specimens did float for a short time, long enough to become at least partially disarticulated. But, if this was the case, why did the specimens not float until completely disarticulated, as was the case for the seal carcasses tracked by Schäfer (1972) in the North Sea? Is scavenging by pelagic predators at an early stage of decomposition a key factor in sinking the carcass, as outlined above? How well does the 'bloat and float' model of predepositional taphonomy apply to the GAB marine reptile specimens. In the context of these fossils, several oceanographic factors may be relevant and these are considered below.

To sink or float – factors affecting carcass buoyancy

Depth: In many ways, the Eromanga Basin is more similar to the North Sea than the Santa Catalonia Basin: maximum depth in the North Sea is 700 m but the mean depth is 95m and large areas, such as the Dogger Bank, are between 15-30 m. This contrasts with the Santa Catalonia Basin and other deep-water whale fall sites in the North-East Pacific, where the minimum depth was 960 m (Smith and Baco 2003) – the fact the Eromanga Basin preserves an epicontinental seaway precludes depths of that magnitude. Just how deep the seaways were during deposition of the Doncaster and Toolebuc Formations is not clear, however: the seafloor in these episodes was almost certainly deeper than 30 metres, but may have been much more, perhaps even greater than 100 metres. Depths between 100 m and 150 m would be comparable to the deeper parts of the North Sea and the mid to outer parts of the continental shelf off SE Australia (Boyd et al. 2004). Whether these depths would be sufficient to prevent refloatation of a sunken amniote carcass is unclear – Schäfer (1972) states not, and Allison et al. (1991) calculate that decomposition of only 1.5–7.3% of soft tissue mass would be enough to refloat a 20m balaeopterid carcass at depths of 100 m, if the body wall had not been disrupted.

Temperature: water temperature may have had some role in affecting the refloatation potential of marine reptile carcasses in the Eromanga seaways. Palaeolatitudes for the northern part of the Basin, where the *Kronosaurus* specimens are derived from, are much higher than modern latitudes: 55°S during the Aptian (Day 1969), when the Doncaster Formation was deposited, and perhaps 50-45°S during the deposition of the Toolebuc Formation during the Albian. As we have seen, these latitudes do not necessarily mean that water temperatures were low: climate in the Cretaceous was generally far warmer than modern times, and palaeotemperatures in the Aptian have been described as suggesting “cool climatic conditions, rather than frigid ones” (Day 1969; p.65), with sea surface temperatures estimated at between 13° and 17°C, comparable to modern cool temperate seas between 35° and 40° latitude. Sea floor temperatures would obviously have been much lower than these figures, but exactly how low is unknown: in the modern Santa Catalonia Basin, they are 4.1°C (Bennett et al. 1994). Palaeotemperatures in the Albian may have been significantly warmer – between 15° and 25°C (Day 1969). This warming may be partially due to the northerly progress of the Australian continent following the onset of rifting between

southern Australia and Antarctica, but is also associated with a global warming episode throughout the Albian.

Benthic oxygen levels: The Albian warming event may be partly responsible for the ‘anoxic’ bottom conditions reported for the Toolebuc Formation. Ocean circulation is largely maintained by the polar ‘pump’, where cool waters at the poles sink and move towards the equator in deep water currents – this in turn causes the movement of surface waters towards the poles, and is the major factor in oxygenating a large portion of the water column. Episodes of global warming shut down this pump by reducing the capacity of the poles to cool surface waters. However, other factors were probably important in determining benthic oxygen levels of the Eromanga Basin.

Despite differences in absolute depths, there are some similarities between the Santa Catalina Basin and the Cretaceous Eromanga Sea. Despite its oceanic setting, the Santa Catalina Basin is a partially restricted waterway: with a maximum depth of 1300 m, it is surrounded by a ridge that rises to 943 m depth. Thus the lowermost 200-300 metres of the Basin are effectively cut-off from the predominantly horizontal currents of the surrounding ocean, resulting in poor circulation and ultimately leading to reduced levels of dissolved oxygen in the benthic waters. Although at absolutely shallower depths, the Eromanga Basin is comparable – even where the Basin connected with oceanic waters, the edges of the Basin were shallow and this would have restricted exchange of its bottom waters with those of the adjacent oceanic systems. Shallow epicontinental basins lack the deep water and upwelling currents which mix bottom and surface waters in oceans, and if deep water is only occasionally disturbed by storms then it can become relatively stagnant, with substantially lowered oxygen levels relative to the surface waters.

The Aptian inland sea of the Doncaster Formation had multiple connections with oceanic waters – to the north (Carpentaria Gulf), the south east (Brisbane), and the south-west (via present day Central Australia). Combined with lower temperatures, which reduce the degree of stratification resulting from thermoclines, this led to benthic oxygen levels that, while low, were not as anoxic as in the Toolebuc. The

Albian inland sea of the Toolebuc had only one connection to the ocean, via the Carpenteria Gulf to the north, and the warmer conditions would have increased thermocline-induced stratification, both of which are expected to reduce bottom water oxygen levels. Consistent with this interpretation, the Toolebuc preserves both dark muddy shales (suggestive of low-oxygen levels) and oil-shales (suggestive of benthic water anoxia).

Scavenging: In both the Doncaster and especially the Toolebuc Formations, circulation of the deep waters was probably low, leading to low temperatures and hypoxic to anoxic conditions. Both of these may have acted to suppress microbial activity in marine reptile dead-falls, reducing the tendency for carcasses to refloat by providing a longer window for the mobile scavengers to remove large portions of tissue and/or perforate the body wall before sufficient gas had built up to refloat the carcass. Low oxygen levels do not necessarily inhibit bottom dwelling scavengers such as sleeper sharks and hagfishes: bottom waters at the Santa Catalina Basin carcass have 8% of the mean dissolved oxygen level for surface waters. Many of these fishes are characterised by sluggish movements and, presumably, low metabolisms, which may increase their tolerance of hypoxic conditions.

Blubber content: If carcasses did refloat, however, then additional factors may have meant that they often sank again before the skeleton became dissociated. Pelagic scavenger activity may have been higher than in the modern North Sea, where refloats seals and dolphins tend to refloat until completely dissociated. But the phylogenetic differences between the carcasses may also have played a role: seals and dolphins are both marine mammals with high metabolic rates and which thus use thick layers of low density blubber for insulation. Blubber can be a significant factor in determining the buoyancy of a carcass, and it possible that blubber content in plesiosaurs and ichthyosaurs was lower than in modern cetaceans and phocids. This is not to say that we should assume that, simply because plesiosaurians and ichthyosaurs are reptiles, that they had low metabolic rates and small amounts of subcutaneous fat: this may true of those groups of reptile that are alive today, but both plesiosaurs and ichthyosaurs are only distantly related to lizards, snakes, crocodiles, and turtles, and were highly specialised to a very different environment.

The Extant Phylogenetic Bracket approach can be useful in reconstructing soft-tissue anatomy in extinct groups (Witmer 1995), but where the fossil group diverge markedly in life habit from the extant bracketing species care should be taken with this approach. Of the living reptiles, only the marine turtles (Chelonia) are ecologically comparable with respect to habitat, and whilst most of the living species are tropical–warm temperature, the leatherback turtle *Dermochelys* is commonly found in cool temperate waters, likely of similar temperatures to those reconstructed for the Eromanga Seas. *Dermochelys* is noted for a number of physiological characters that are interpreted as adaptations to tolerating cooler waters, including a countercurrent exchange system between peripheral arterial and venous supply, a relatively high (compared to other turtles) resting metabolic rate, and thick layers of subcutaneous fat. Ichthyosaurs are regarded as the most anatomically specialised of all marine reptile to the aquatic habit, and plesiosaurs were also highly specialised: given the abundance of plesiosaur fossils from high palaeolatitudes, especially in the Cretaceous, it is certainly possible and perhaps even likely that members of both groups displayed physiological adaptations to cold water environments at least comparable to those of *Dermochelys*.

Although we should be generous in envisaging physiological / soft-tissue adaptations in plesiosaurs, it does not necessarily follow that they shared all of the features seen in modern odontocetes. Even by mammalian standards, the subcutaneous fat layers of cetaceans and phocids are thick, and blubber may warrant regard as a highly specialised tissue in its own right. We can accept that ichthyosaurs and plesiosaurs were highly specialised to marine environments, even to cool temperate waters, without necessarily requiring that they too had blubber comparable to that of Antarctic seals. Sea-lions (Otariidae) are also highly adapted to the marine environment, and may species live in sub-polar and polar waters, but the subcutaneous fat layer is not as thick as in seals. Whether otariid carcasses sink earlier than phocid carcasses is unknown, but data would provide some clues on the possible post-mortem buoyancy of marine reptile carcasses.

Integument: One final factor may have affected the period for with which marine reptile carcasses may have remained afloat. The subdermal connective tissue sheath

(perhaps a form of superficial fascia, lying internal to the blubber layer) of cetacean is notably tough and has a high collagen content. Some authors have speculated that this allows elastic recovery of energy during locomotion (Brodie 2001, Wainwright et al. 1985), in a manner similar to that proposed for sharks (Wainwright et al. 1978). The mechanics and even the feasibility of this are unclear (Fish and Hui 1991), but if a thickened sub-dermal, collagenous sheath of fascia is involved with increased axial undulatory-oscillatory mode of swimming seen in dolphins, tuna, and sharks, then it may apply to marine reptiles with a similar gait. Ichthyosaurs are one such group, and rare fossils that preserve dermal features suggest a strong, fibrous ‘corset’ that might be equivalent to the fascia sheath in dolphins and sharks (Lingham-Soliar 1999, 2001). In contrast, plesiosaurs are paraxial swimmers, meaning that they use their limbs to generate propulsive forces, rather than their axial skeleton, and thus the sub-dermal fascia may not be as strong as in the axial swimmers – theoretically, there is less need to recover energy elastically, in paraxial swimmers, and studies of the sub-dermal layers of modern paraxial swimmers such as sea-lions and penguins may be informative in this.

As far as taphonomy goes, a strong sub-dermal layer could have various effects. It may increase the pressure required to burst the body wall, or the time taken for the body wall to fail: each of these may increase the float time of the carcass. It may hinder dissociation of the carcass, leading to a higher level of completeness when the floating carcass eventually does sink. Or, it may increase the ‘stiffening’ effect of the pressure build-up of the decomposition gases, leading to a straightening of the skeleton as reported for stranded cetacean carcasses (Schäfer 1972).

Patterns of association – a measure of predepositional flotation?

Some of the patterns of preservation of the marine reptile fossils seems to suggest that, if the carcasses were afloat, it wasn’t for long. Of the 13 specimens listed in Table 3-3, 11 include material from the head skeleton, and of these only one (the holotype, QMF1609) comprises a mandible with no associated skull material. All of the specimens that include skull material are associated with at least fragments of mandibles, and in most cases the mandibles are articulated and adducted to the skull with minimal displacement. Schäfer (1972) records that, in floating North Sea

Specimen (year of recovery)	Provenance, Age, Stratigraphy, Region	cranium	mandible	postcranium	stomach contents	matrix
QM F1609 (1899)	Eromanga, Albian, ?Toolebuc, Hughenden		partial symphysis			nodular limestone
QM F2137	Eromanga, Albian, Toolebuc, ??			propodial heads		nodular limestone
QM F2446 (1935)	Eromanga, Albian, Toolebuc, Telemon	orbital region, occiput	partial, adducted to cranium			nodular limestone
QM F2454 (1935)	Eromanga, Albian, Toolebuc, Telemon	>50%	partial, articulated to quadrate			nodular limestone
QM F10113 (1979)	Eromanga, Albian, Toolebuc, Toronto	>50%	partial, articulated to quadrate, anterior end slight displaced	complete articulated pre- caudal axial column, prox. appendicular.	prey (turtle); one gastrolith?	nodular limestone, high iron levels
QM F18154 (1989)	Eromanga, Albian, Toolebuc, Canary	>50%		partial cervical and pectoral elements, prox. humerus	two gastroliths	nodular limestone,
QM F18726 (1989)	Eromanga, Albian, Toolebuc, Dunluce	>90%	nearly complete, articulated to cranium			nodular limestone
QM F18827 (1991)	Eromanga, Albian, Toolebuc, Lucerne	>90%	>50%, adducted to cranium	partial cervical and pectoral elements, prox. humerus		nodular limestone
QM F33574 (1995)	Eromanga, Aptian, Doncaster, Grampian			partial trunk	prey (plesiosauroid)	nodular limestone
QM F51291	Eromanga, Albian, Toolebuc?, Hughenden	orbital region	partial, adducted to cranium			nodular limestone
QM F52279 (1964)	Eromanga, Albian, Toolebuc, Lydia Downs	orbital region	partial, associated	fragments		nodular limestone, high iron levels
MCZ1284 (1932)	Eromanga, Aptian, Doncaster, Army Downs	ant. rostrum	symphysis, adducted to cranium			nodular limestone
MCZ1285 (1932)	Eromanga, Aptian Doncaster, Grampian	3 large blocks?	adducted to cranium?	complete, articulated pre- caudal series, some ant. caudals, prox. appendicular elements		nodular limestone

Table 3-3: Preservation of fossils referred to *Kronosaurus queenslandicus* from the Eromanga Basin.

dolphin and seal carcasses, the mandibles become dissociated from the skull early in decomposition. Jaw joints in reptiles have deeper cotylar sockets and a tighter ‘fit’ with the condylar heads than is the case with most mammals, but the joint is ultimately held together by soft tissues and, were the carcasses afloat, it is

questionable whether the jaw would have dropped from the rest of the carcass significantly later in decomposition. The common association of skull and mandible suggests that the carcasses were on the sea-floor at an early stage of decomposition.

The high frequency of carcasses with stomach contents – two specimens of *Kronosaurus*, and several species of elasmosaurid (Table 3-4) from the same deposits – likewise suggests that, if they were afloat, the carcasses did not sink at a late stage of decomposition.

Conversely, the rarity of fossils preserving distal limb elements, even when proximal elements are preserved, might support the idea that these carcasses were afloat for at least some time: the distal elements of seal forelimbs are recorded to dissociate at a relatively early stage in this situation (Schäfer 1972). In the case of seal carcasses, the pattern of dissociation is related to the soft-tissues that hold those elements: cartilage in the forelimb, tendon and ligament in the hind, with the hind-limb remain intact for longer. If the plesiosaur carcasses are interpreted as having been afloat for only a short period, and the distal elements have nevertheless become dissociated, then that would suggest the distal limb elements are held together by a tissue such as cartilage, rather than tendon and ligament: the exact nature of the soft tissues has implications for analysis of locomotion in these animals.

Specimen (year of recovery)	Provenance, Age, Stratigraphy, Region	preservation	stomach contents	matrix
QM F420	Eromanga, Albian, ?, Charlotte Plains	partial anterior trunk	35 gastroliths	nodular limestone
QM F2100	Eromanga, Albian, Allaru, Dartmouth	trunk, girdles	prey (crustacean); 135 gastroliths	nodular carbonate-mudstone
QM F14934	Eromanga, Toolebuc, Albian, Canary	partial trunk?	2 gastroliths	Limestone matrix
QM F33037 (1994)	Carpentaria, Aptian, Doncaster, Walsh	trunk, post. cervicals, prox. limb	prey (molluscs, teleost); 35 gastroliths	nodular limestone
Richmond: 'Grampian' (1995)	Eromanga, Aptian, Doncaster, Grampian	axial column, ribs, girdles, prox. limb	–	shale
QM F51069 ('Dave') (1999)	Carpentaria, Aptian, Doncaster, Walsh	axial column, ribs, girdles, prox. limb	–	greensand

Table 3-4: Preservation of selected plesiosauroid (c.f. Elasmosauridae) specimens from the GAB.

Burial and diagenesis

While predepositional and early stages have significant control on how much of a carcass is preserved together, the taphonomic stage that has the main effect on the distortion of the individual elements is the time in between burial and exposure, when the fossil is overlain by hundreds of metres of rock.

The forces that distort sedimentary rocks and the fossils they contain can be summarised as (1) tectonic forces, that result from movement of tectonic plates relative to each other, and (2) compaction forces, which result from the accumulated weight of rock above the layer in question. Compaction forces have a vertically oriented vector, whilst that of tectonic forces usually involves a significant horizontal component. Tectonic forces are an important component of the geophysical history of fold belts, and are currently active at the northern ('leading') edge of the Australian plate (where the New Guinea highlands are being uplifted by collision with South East Asia), but Great Artesian Basin has been subjected to very low levels of tectonic forces since the Jurassic, and so these have played a very minor role in the alteration of the Basin's Cretaceous sedimentary rocks.

The compaction forces caused by the weight of overlying rock is, however, a far more significant cause of distortion of fossils in the GAB. Each of the Doncaster, Allaru, Mackunda, and Winton formations are well over 200 m thick in places. The forces that result from the accumulated weight of these are potentially significant; for example, consider a hypothetical fossil at the base of the Doncaster Formation. Although it may be at the surface now, by the weathering of the overlying strata in the last 15 million years, for most of its 115 million year history it has been overlain by up to (or perhaps even more than) 1,000 metres of rock. Sedimentary rocks, such as limestones, sandstones, and shales have a range of densities between 2,200 and 2,800 kg/m³. Assuming an average density 2,500 kg/m³, each square metre of the rock containing the fossil has been subjected to 2.5 tonnes per metre of overlying rock thickness: if the overburden is 1,000 metres thick, that equates to 25,000,000 Newtons of force being applied to 1 square metre of fossil containing layer, i.e. a pressure of 25 MegaPascals.

The mechanical response of a large vertebrate fossil to this pressure is primarily dependant upon the type of sediment it is buried within. With respect to resilience against compaction forces, different sediments have very different mechanical properties; mud is often compressed into a shale whose thickness is often less than half that of the original mud layer. Even more extreme is the compaction of sediments with large quantities of organic matter – peats can be compacted into coals that have less than 10% of the original thickness of the sediment (Chan and Archer 2003). Sands are mechanically stronger than muds and as a result sandstones are typically compacted far less than are shales (Prothero and Schwab 1996).

The fossils preserved in the marine sediments of the GAB are buried in carbonate rocks. The geology of carbonate deposition is complex, but a simplified scheme is adequate for the present analysis. Some carbonate rocks are formed from silicate sediments that are cemented by calcium carbonate; if the silicate sediment is a mud or a clay, the resulting rock is a carbonaceous shale, if a glauconitic sand then the rock is classed as a greensand. The source of the calcium carbonate cement is usually biological, i.e. from the skeletons of plankton that settle on the sea bed, or from coralline algae. Where the deposition rate of siliceous sediment is low, the biogenic calcium carbonate can accumulate on the sea bed and be cemented by the precipitation of dissolved carbonate; this results in a rock that is mostly composed of calcium carbonate and which is termed a limestone.

Text book accounts of the deposition of carbonate rocks emphasise warm temperatures and low pressures, hence the focus on tropical shelf waters as sites of major carbonate production (Prothero and Schwab 1996), but carbonate deposition is not limited to shallow, low latitude environments. In modern systems, extensive carbonate deposition occurs in mid to high latitudes such as the Shetland Shelf of the North-East Atlantic (Light and Wilson 1998), the Lord Howe rise of the South West Pacific (Kennedy and Woodroffe 2004), and the South East Australian shelf (Boyd et al. 2004). In the latter example, bathymetry shows a latitudinal gradient in the depth where carbonates are the primary depositional feature; from approximately 120 m depth at 33°S to 60 m depth at 29°S (Boyd et al. 2004).

The majority of reptile fossils in the GAB are preserved in large limestone nodules. The formation of limestone nodules is imperfectly understood; in modern day environments, carbonate nodules have been observed forming as the result of the growth of carbonaceous encrusting organisms (foraminifera and algae) and gentle repositioning by wave action – a sort of ‘snowball’ growth (Prager and Ginsberg 1989). However, the limestone nodules in the GAB are thought to have formed within the sediment after burial, rather than on the surface of the sea-bed, and the chemical microenvironment produced by the buried carcass is thought to play an important role. There are many questions about the details of this process, but a basic model is as follows (A. Cook, pers. comm.): in the later stages of decay, i.e. equivalent to the ‘sulphophilic’ stage described for modern whales carcasses (Smith and Baco 2003), the carcass becomes buried in fine siliciclastic sediment. Continued reduction of organic tissues, in particular lipids, by sulphate reducing chemoautotrophic Bacteria and Archea results in the formation of iron sulphite (pyrite). During the early stages of diagenesis (i.e. within the first few decimetres of burial, perhaps representing 10^5 to 10^6 years after death), the pyrite is altered to iron carbonate (siderite), which is in turn altered to calcium carbonate (calcite). The calcite is deposited as micro-crystals, producing a micritic limestone that forms in an expanding ‘halo’ around the original source of sulphate: the result is a spheroidal or sub-spheroidal limestone nodule. Nodule size may be related to the size of the original source of sulphates: thus, large carcasses such as an adult *Kronosaurus* are interred in large nodules. The siliceous sediment in between nodules, where the chemistry is not suitable for this process, lithifies to a black shale.

In addition to the determining the extent to which the fossil can resist sedimentary compaction (see below), this process may also be a factor in the pattern of association of a vertebrate carcass, especially with respect to the non-preservation of distal elements: if the mass of organic tissue (particularly lipids) surrounding bones such as phalanges, posterior caudals, or even anterior cervicals in the case of long-necked plesiosaurs, is not sufficient to initiate the diagenetic pathway described above, then these elements may not be preserved within nodules. Whether they become fossilised in the surrounding shale, or whether diagenesis removes them completely, is unknown.

Calcium carbonate is mechanically strong and, when cemented chemically in the form of a limestone nodule, provides very good protection against sedimentary compression. A comparison between two similar fossils, one preserved in a carbonaceous shale or clay, the other in nodular limestone, is an impressive demonstration of this point, and such an example exists for pliosaur skulls; specimens of the medium sized pliosaur *Peloneustes* are common in the Middle Jurassic Oxford Clay, and as most of the fossils are preserved in the soft shales of this unit, specimens of *Peloneustes* are often very flattened and extensively cracked. In contrast, rarer skulls that are preserved in nodules preserve the 3-dimensional shape of the skull, which is actually quite tall for its width [see Figure 3-3, illustrations in Ketchum (2008), and Section 3.4 below]. In addition to the lack of vertical crushing, the anatomy in nodule-preserved specimen is less obscured by cracks, and this reveals an important feature about the way that the clay-preserved species have been distorted: cracks are a result of brittle deformation, which occurs when the strain rate of compression is relatively high (i.e. the sedimentary compaction occurs over a relative short time span), and when there is a marked difference in the mechanical properties of the material being fossilised and those of the surrounding matrix.

Compared with clay- or shale-preserved specimens, fossils in carbonate nodules can appear undistorted, but it is rare that they will be free of any distortion. Marine reptile fossils from the GAB are typically far less cracked than those from the Oxford Clay, but this does not necessarily mean that they are free of compaction: if strain rates are low, particularly when the material comprising the fossil is mechanically similar to that of the surrounding matrix, then deformation can be plastic rather than brittle; this leaves far fewer cracks but nevertheless does alter the original shape of the fossil. Plastic deformation can be difficult to quantify: potentially, it can be gauged by measuring the shape of any structure thought to have originally been a sphere, and the occipital condyle of pliosaurs is perhaps of use in this respect. An alternative method may be to compare the shapes of commonly preserved structures (such as ammonite fossils) that are lying in a variety of orientations with respect to the vertical axis, although to my knowledge this has yet to be assessed for the limestones of the GAB. For the *Kronosaurus* fossils that are the



Figure 3-3: Preservation of *Peloneustes philarchus* crania; NHM R4058 (above), preserved in a pyritic carbonate nodule, and NHM R3803, preserved in a clay bed. Both specimens are from the Oxford Clay of England, and are of similar size. The extent to which the clay-preserved specimen is flattened in the vertical axis is apparent from comparison with the specimen preserved in the nodule.

subject of the present work, however, the extent of plastic deformation to which the specimens have been subjected is assessed qualitatively by comparing the 3-D shape of similar parts in the various specimens, and by documenting the degree to which the assumption of bilateral symmetry is violated.

The fact that many of the marine reptile fossils known from the GAB have been preserved in nodular limestone affords a remarkable opportunity to document the 3-D shape of the skull in a pliosaur. Even though they are not completely free of distortion, the *Kronosaurus* material that is described in the next chapter is less

compressed than pliosaur skulls from the European Jurassic or the North American Cretaceous (see Section 3.4 below).

Exposure

The final step in the taphonomy of *Kronosaurus* specimens in the GAB comes approximately 100 million years after they were first buried, when the overlying sediments have been eroded away and the rock containing the fossils is eventually brought within range of the sub-soil weathering horizon – a depth of perhaps a couple of metres. The weathering loosens the nodules from the shale bed in which they have been lying, and the cycling of the soil brings the nodules to the surface by the same process that causes Brazil nuts marble to float to the top of a packet of mixed nuts if the system is shaken lightly, a phenomenon that has been dubbed the ‘Brazil-nut effect’ (Möbius et al. 2001, Rosato et al. 1987)¹⁴. Only nodules float to the soil surface, and bigger nodules float faster than smaller ones, and this might be an additional mechanism that might explain why smaller, peripheral elements do not end up being recovered with the rest of the fossil (see above). Whether the recently reported ‘reverse Brazil-nut effect’ (Shinbrot 2004), where the system exhibits paradoxical behaviour under certain conditions, has any affect on limestone nodules in soil is unknown.

The very last stages of this process also have a strong potential effect on the separation of a once-intact carcass. Often, all of the parts of a fossil that are exposed are simply not collected. This is not necessarily a case of simple neglect by field workers, as fossils become exposed over a long period of time – up to hundreds of years – and there are many opportunities for smaller, peripheral fragments to be removed from the site by the same processes that erode landscapes, in particular water flow and disturbance by animals. Probably all of the specimens listed in Table 3-3 and Table 3-4 have been incompletely collected, for whatever reason. Where the fossils are preserved in nodules, the primary evidence for incompletely collected material are freshly broken faces of fragments/blocks that have no counterpart.

¹⁴ In the case of nodules floating to the surface of blacksoil, the agitation of the soil system comes from repeating cycles of wetting and drying of the soil, which cause the clay within it to expand and contract, rather than shaking.

Summary of distortions

The general taphonomic distortions that seem to apply to marine reptile fossils in the Great Artesian Basin are thus as follows;

1. Damage incurred at the time of death: this is usually bite marks and/or fractures.
2. Incompleteness of the bony skeleton: a result of disassociation during the decay of the carcass.
3. Diagenetic obliteration of morphological structures: for example, the removal of teeth and replacement by large calcite crystals. Both this and the preceding stage are also affected by dissolution of bone surfaces during diagenesis. Fossils from the western side of the Basin appear to be prone to recrystallisation in gypsum.
4. Sedimentary compression during diagenesis: this leads to distortion of the structure, by either ductile (plastic) or brittle deformation.
5. Differential preservation and incorporation into nodules: smaller, peripheral elements such as phalanges may not be included within the nodules, which can lead to these elements having a different fate in subsequent taphonomic phases.
6. Working of nodules out of the bedrock and up to the soil surface: this can move some parts of the skeleton and leave others behind, move different parts at different rates and thus introduce differences in exposure to surface weathering, and alter the relative position of different parts of the skeleton.
7. Surface weathering, transport, and collection: all of the above steps can result in only one part of a fossil being exposed at the surface at a particular point in time. This in turn can result in parts of the fossil being weathered / transported / collected whilst other parts remain in the ground.

The result of all of these is a fossil that, relative to its original morphology, is incomplete and distorted. The fossil itself represents an individual animal that itself lay within a range of variation – allometric, sexual, or otherwise – particular to its species. Our challenge is to try and cut through all of these sources of variation and produce a reconstruction that can be used to analyse the biomechanics of that species.

3.4 **An example of taphonomic induced confusion: the circum-orbital region of the pliosaur skull roof**

Specimens of large pliosaurs (with a reconstructed total body length greater than five metres) are known from Jurassic and Cretaceous sediments worldwide, and have variously been sorted into the families Rhomaleosauridae (Nopsca 1928), Pliosauridae (Seeley 1874), and Brachaucheniidae (Williston 1925). Although many of these specimens include good skull material, the topology of dermal elements in the orbital region of the skull roof has been difficult to interpret in many cases because of poor preservation. Many of the most complete and historically important skulls come from the Jurassic shales and clays of England, and because these specimens were largely described by British workers during the initial growth of modern vertebrate palaeontology their descriptions have become the foundation for studies of pliosaur cranial anatomy.

In particular, the descriptions by C. W. Andrews of specimens from the Oxford Clay of Peterborough, held as part of Leeds Collection in the British Natural History Museum, have provided a framework for understanding pliosaur anatomy that has been largely followed by workers since. In a series of publications Andrews described in detail the cranial anatomy of the Middle Jurassic pliosaurs *Peloneustes phylarchus*, *Liopleurodon ferox*, and *Simolestes vorax* (Andrews 1895, 1897, 1911, 1913). Although much of the dermal skull elements are preserved in these specimens there is considerable post-depositional deformation, mainly as a result of sedimentary compression. Consequently, some of the original three-dimensional structure has been lost and the skulls exhibit a characteristic preservation where, having generally been orientated in the sediment with the frontal plane in the horizontal, they are squashed almost flat with the fossilised bone subject to deformation and extensive cracking (Figure 3-3). In some parts of the skull, such as the anterior rostrum, this is only a minor inconvenience and the anatomy can still be reconstructed with confidence. However, the orbital region of the skull appears to have been prone to extensive taphonomic deformation and the collapse and cracking of the bones in this

region have made the topology of its dermal elements difficult to identify with confidence.

Andrews himself made reference to this problem on several occasions (Andrews, 1897:183; Andrews, 1911:160; Andrews 1913:8, 40) and refined his interpretation of the orbital region over the course of his studies – his reconstructions of this part of the skull in *Peloneustes philarchus* and *Liopleurodon ferox* in particular changed between the times of his initial descriptive accounts (in 1895 and 1897 for these taxa respectively) and his later reviews (in 1911 and 1913). Much of his uncertainty centred upon the relationship between the parietal, frontal, and premaxillary bones in the ‘brow’ of the skull (i.e. the median part of skull roof that lies between the orbits). In 1897, in a description of a complete skull of *Liopleurodon ferox* (NMH R2680) he reconstructed the frontal bones with a substantial median contact on the dorsal surface of the skull roof in front of the pineal foramen, so that the united frontals between them separated the anterior part of the parietals from the posterior facial processes of premaxillae on the dorsal surface (Andrews, 1897). In 1911 he published an account of a *Peloneustes philarchus* specimen that showed good preservation of this part of the skull and which persuaded him that, although the frontals could be seen united in the midline on the ventral surface of the skull roof (Figure 3-4), on the dorsal surface the parietals extended some way in front of the pineal foramen and formed the extensive, interdigitate joints with the facial processes of the premaxillae. In this interpretation the frontals were thereby excluded from meeting in the midline of the dorsal surface, although each frontal was exposed on the skull roof lateral to the anterior part of the parietal, in front of the position of the pineal foramen. By 1913, in the second part of his descriptive catalogue of the Oxford Clay marine reptiles, he had incorporated this re-interpretation of the dorsal skull surface into the plate illustrating *Peloneustes philarchus* (reproduced as Figure 3B of Andrews, 1913), and although the plate of the same volume illustrating *Liopleurodon ferox* (Figure 3-5) was labelled according to his original interpretation of the osteology he had corrected himself in the accompanying text. Thus, by 1913, he had shown that the frontals in *Peloneustes philarchus* were excluded from a median contact on the dorsal surface by overgrowths of the parietals and premaxillae, but that the frontals did meet on the midline underneath the dorsal surface, and had cautiously reinterpreted the relations

of these elements *Liopleurodon ferox* to agree with the pattern seen in *Peloneustes philarchus*.

With the median skull roof elements interpreted thus, the circum-orbital series was reconstructed in a pattern that closely matches the traditional topology given for the basic tetrapod skull. With respect to *Liopleurodon ferox*, the element lying lateral to the parietal and forming the postero-medial margin of the orbit on the dorsal surface of the roof was identified as the postfrontal (Andrews 1913). Andrews had identified in his Plate 1 the ?supra-orbital as being the element contacting the front of the postfrontal on the dorso-medial edge of the orbit, forming the antero-medial margin of the orbit on the dorsal surface, and lying antero-lateral to the ‘outcropping’ of the frontal on the dorsal surface – this was re-interpreted in the text as the prefrontal (Andrews, 1913). In front of the orbital margin this element extended forward to form the postero-medial margin of the external naris – Andrews suggested that this anterior part of the element might be the nasal bone fused to the prefrontal. He was less equivocal about the presence of a separate element which, lying lateral to the prefrontal, formed the anterior margin of the orbit on the dorsal surface and which

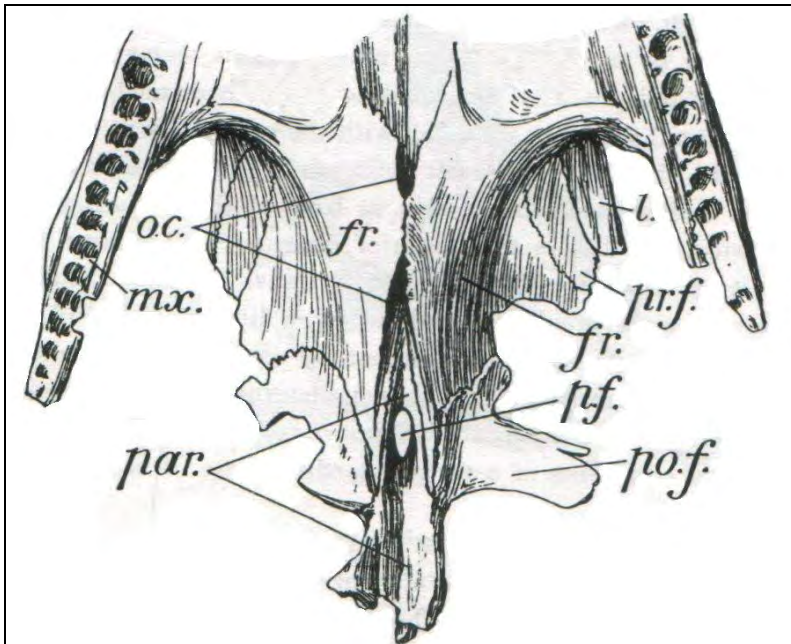


Figure 3-4: Part of the skull roof of *Peloneustes philarchus*, reproduced from Andrews (1911). The original caption read; “Fig. 1. Inner face of the middle portion of the skull roof in *Peloneustes philarchus*. (About one-third natural size.) *fr.* frontals ; *l.* lachrymal ; *mx.* maxilla ; *o.c.* channel enclosed by the downgrowths of the frontals ; *par.* parietals ; *p.f.* pineal foramen ; *po.f.* post-frontal ; *pr.f.* pre-frontal.” Note the use of a variant spelling of ‘lacrimal’.

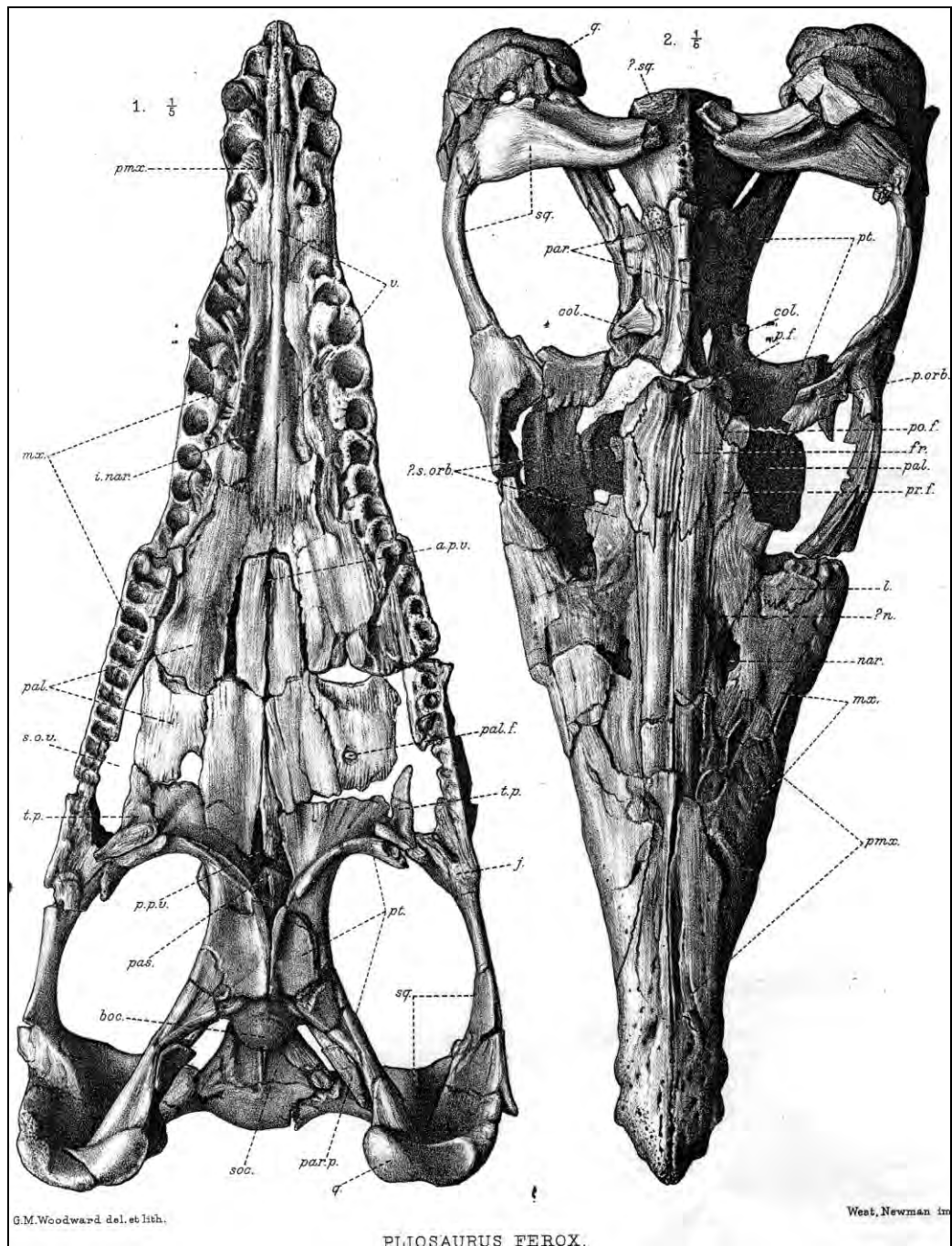


Figure 3-5: Reproduction of plates from Andrews' Catalogue of Marine Reptiles from the Oxford Clay, Volume II (1913). Plate I, Fig.2; NHM R2680, *Liopleurodon ferox*, in dorsal view (right) and ventral view (left) – in the taxonomy used by Andrews *Liopleurodon ferox* was retained within the genus *Pliosaurus*. Key to labels (spelling and terminology as in original); *col.*, columella cranii (epipterygoid); *fr.*, frontal; *j.*, jugal; *l.*, lachrymal; *mx.*, maxilla; *?n.*, ?nasal; *nar.*, external nares; *par.*, parietal; *p.f.*, pineal foramen; *pmx.*, premaxilla; *po.f.*, postfrontal; *p.orb.*, postorbital; *pr.f.*, prefrontal; *pt.*, pterygoid; *q.*, quadrate; *?s.orb.*, ?supraorbital bone; *sq.*, squamosal. Note that the skull elements in the orbital region are labelled according to Andrews' (1897) previous interpretation of these – however, in the main text accompanying these plates he had corrected his interpretation. The extensive cracking affecting the specimen is visible in the region around and in front of the orbits in both dorsal and ventral views. See text and Noè (2001) for discussion.

was distinct from the maxilla; he identified this as ‘probably’ being the lacrimal. He identified the lateral margin of the orbit as being formed by the jugal, and described that element as contacting the postorbital, which formed the postero-lateral margin of the orbit and thus completed the circum-orbital series (Andrews, 1913). He was not able to identify the relationship of the medial part of the post-orbital with neighbouring bones.

At roughly the same time that Andrews was describing the Oxford Clay pliosaurs, Williston published descriptions of skull material from two specimens of the Upper Cretaceous pliosaur *Brachauchenius lucasi* (Williston 1903, 1907). This material was preserved in the limestones and chinks of the Western Interior Basin in Kansas and Texas, and was evidently subject to less sedimentary compression than the material from the Oxford Clay, although there both specimens are crushed and cracked to some extent. The holotype of *Brachauchenius lucasi* (USNM 4989) in particular includes a well preserved skull as well as an articulated axial skeleton and is one of the more remarkable fossils from the Kansas chalk, and although the referred specimen (USNM 2361) does display some pyritisation of the fossil bone Williston was able to reconstruct the orbital anatomy of *Brachauchenius lucasi* based upon these specimens. In his second paper on this species (Williston, 1907) he provided an interpretation of the dorsal surface of the orbital region that agreed closely with Andrews’ later re-interpretation of the anatomy in *Peloneustes philarchus* and *Liopleurodon ferox*. Indeed, Williston discussed the position of the frontals at length, showing that in *Brachauchenius lucasi* these elements were excluded from a median union on the dorsal surface by the anterior overgrowths of the parietals to the premaxillae, and strongly suggested that this would be found to be the pattern in *Liopleurodon ferox* also. It is possible that Williston’s interpretation was a factor in Andrew’s re-examination of this question between 1897 and 1911.

Williston was also quite definite about the presence of lacrimals in *Brachauchenius lucasi*, going so far as to state that “the presence of a lachrymal as a distinct bone in the plesiosaurs may finally be set at rest” (Williston, 1907: 481). In essence, the topology of skull roof elements on the dorsal surface that Williston described for *Brachauchenius lucasi* agreed closely with that detailed by Andrews in 1913 for

Liopleurodon ferox, except that the slightly better preservation of the surface bone in the former taxon allowed Williston to be even more positive about his interpretation on some points (such as the position of the frontals and the presence of a lacrimal). The only point of difference between these two descriptions concerned the nasal – neither was able to identify it as a distinct element. Andrews (1913) raised the possibility that it was fused to the prefrontal – Williston (1907) suggested that it may be fused to the frontal. In most other respects, their interpretations coincided.

These descriptions by Andrews and Williston set a standard of descriptive anatomy that has rarely been matched within the anatomical literature on pliosaurs. In this context, it is interesting to note that recent analyses, which are based in part upon anatomical data from pliosaurs such as *Liopleurodon ferox* and *Brachauchenius lucasi*, have largely ignored or directly contradicted the anatomical interpretations put forward by Andrews (1913) and Williston (1907). Many of these more recent studies discuss the anatomical data in connection with systematic reviews of the Plesiosauria. Storrs (1991) asserts that the lacrimal is absent in the Plesiosauria, a view followed by other authors (Carpenter 1996, O'Keefe 2001). How this view is reconciled with Williston's very definite identification of a lacrimal in *Brachauchenius lucasi* is addressed only by Carpenter, who in briefly discussing a third skull of that taxon (FHSM VP321) held that Williston "was apparently misled by cracks in the orbital region of his specimen" (Carpenter, 1996: 262). The confusion is not limited to the presence or absence of the lacrimal; while Storrs (1991) considers the nasal to be absent in all post-Triassic plesiosaurs, O'Keefe (2001) states that it is present in various pliosaurs. Carpenter's (1996) discussion of *Brachauchenius lucasi* does not mention a nasal, but instead states that the frontals are united on the dorsal surface of the skull roof, between the parietals and the premaxillae, and that the frontals are pierced by the pineal foramen. He further interprets the frontal and postfrontal of Williston (1907) as the prefrontal and postorbital respectively. O'Keefe (2001), in contrast, accepts Andrews' (1911, 1913) and Williston's (1907) interpretation of the frontals' morphology in *Peloneustes philarchus* and other pliosaurs.

That this continuing confusion is not merely of academic importance is demonstrated by O'Keefe's (2001) extensive cladistic analysis of plesiosaurian

phylogenetics. Of a data matrix incorporating 166 characters, 16 relate to the topology of the elements discussed above, and there are several more characters for which scoring may be affected by the interpretation of elements in the orbital region. The potential for phylogenetic hypotheses to be profoundly affected by incorrect interpretation of the anatomy in this region is therefore high.

Noè (2001) has provided the first detailed anatomical examination of the Oxford Clay pliosaurs since the work of Andrews (1913). Although he did not examine *Peloneustes philarchus*, Noè did review the *Liopleurodon ferox* and *Simolestes vorax* specimens described by Andrews in addition to new material referable to these taxa. Noè found that two specimens of *Liopleurodon ferox* preserved a lacrimal, but that it could not be identified as a separate element in *Simolestes vorax* – however, he showed that in the latter species the prefrontal included a ‘ventral process’ which formed the anterior margin of the orbit on the dorsal surface, and which may represent the fused lacrimal (Noè 2001). Noè also confirmed the presence of the nasal as a separate element in adult specimens of both *Liopleurodon ferox* and *Simolestes vorax*; in both species, the nasal forms the postero-medial margin of the external nares and, antero-medial to the orbit, forms complex contacts with premaxillae and frontals. Noè noted that in both species the nasal had a small outcropping on the dorsal surface but that, as with the situation described above for the frontal bone, had a greater extent within the bony roof of the posterior rostrum and brow region. He further noted that in some specimens of *Liopleurodon ferox* the nasal was fused posteriorly to the frontal. In other respects, Noè’s (2001) reconstructions of the osteology in the orbital region broadly confirmed those of Andrews (1913), with some differences in detail. Further work by Ketchum (2008) on *Peloneustes* supported Andrew’s (1913) interpretation of frontal-parietal topology on the dorsal surface of the skull roof: Ketchum also suggested the lacrimal is present in *Peloneustes*, although she did not identify the nasal as a separate element.

The situation can be summarised thus; Andrews and Williston are regarded as two of the finest anatomists to have published upon plesiosaurs, and yet the confusion surrounding the bones of the orbital region evidently survived even their attempts to resolve the anatomy. Noè (2001) has provided the most thorough analysis of pliosaur

cranial anatomy since the work of Andrews (1913) and Williston (1907), and was able to confirm and in some cases (i.e. the presence of the nasal) clarify their interpretations of the orbital region anatomy in pliosaurs, but confusion about the presence and topology of these elements persists in the phylogenetic literature. The current state of opinion with regard to the circum-orbital anatomy of the pliosaur skull has been reviewed and expanded in recent work by Druckenmiller and by Ketchum, each of whom have made reference to the (relatively undistorted, nodule-preserved) *Kronosaurus* material that is described within this thesis (Druckenmiller 2006, Druckenmiller and Russell 2008a, Ketchum 2008), demonstrating the potential value of relatively undistorted specimens in providing osteological data.

The focus of the present work is structural biomechanics, and since the methodological tools I will be using do not at present allow for the structural effects of sutures to be included in the analysis, the confusion over the topology of specific bones and the position of sutures does not directly affect us here. But the reasons behind the confusion in the roof bone topology of pliosaur orbits also affect our knowledge of that structural geometry, arguably to an even greater degree. Skull bone topology can be reconstructed, even when the preservation has ‘pancaked’ the skull: but the geometry of the skull cannot be resurrected from this without knowledge of the basic 3-D template of the skull’s morphology. For useful biomechanical models, the geometry of both the external and internal surfaces is critical. External geometry can be estimated, but with the sort of preservation that is typical for the British and North American pliosaur skulls discussed above, the internal geometry is largely unknown. In the rostrum and the braincase, internal geometry can be estimated based upon the thickness of bone preserved at the cross sections exposed by fragmentation of the fossil. Around the orbital region, however, the potential complexity of the internal anatomy¹⁵ means that good, three-dimensional preservation is required.

Why is the anatomy of the orbital region so important for a biomechanical model? Mechanically, this part of the skull forms the connection between the snout and the temporal region: during biting, the mechanics of the former is predicted to be

¹⁵ Recall the confusion surrounding the external anatomy in this region.

dominated by the loads applied to the teeth, whilst the latter should be dominated by the forces applied by the jaw muscles (Popowics and Herring 2007, Rafferty and Herring 1999). The orbital region is the part of the skull where these two sets of loads meet, and the way in which bending moments from the rostrum are transmitted to the posterior part of the skull is potentially critical to the mechanical response of the entire skull. In crocodylians, the structural complexity of the orbital regions involves the following components: the median inter-orbital bar ('brow'), the skull roof bones of the anterior orbital margin, the underlying palatal bones, the bar on the lateral side of the orbit, the postorbital bar, and the prefrontal column that forms a vertical connection between the brow and the palate at the anterior-medial corner of each orbit. The precise geometry of these components can be expected to have important consequences for the mechanics of the whole skull (Busbey 1995, McHenry et al. 2006): the same is likely to be true for pliosaurs.

In this context, the information contained in a series of pliosaur specimens that exhibit relatively little crushing and preserve the orbital region of a species of large pliosaur is of considerable interest, not just for the description of the anatomy of that species, but for understanding of pliosaur cranial anatomy in general. However, the main focus of the present work is the exploration of skull biomechanics using finite element analysis (see Chapter 2), and because of the preservation in nodular limestone, the various specimens of *Kronosaurus* that preserve cranial material provide the opportunity to reconstruct the 3-dimensional geometry of the skull in this pliosaur to the level of detail required for high resolution finite element modelling. The details of these specimens, and the reconstructions of skull geometry that can be generated from them, are the subject of the following two chapters.

3.5 **References**

- Alley, N. F., and L. A. Frakes. 2003. First known Cretaceous glaciation: Livingston Tillite Member of Cadna-owie Formation, South Australia. *Australian Journal of Earth Sciences* 50(2):139-144.
- Allison, P. A., C. R. Smith, H. Kukert, J. W. Deming, and B. A. Bennett. 1991. Deep-water taphonomy of vertebrate carcasses; a whale skeleton in the bathyal Santa Catalina Basin. *Paleobiology* 17(1):78-89.
- Andrews, C. W. 1895. On the structure of the skull of *Peloneustes philarcus*, a pliosaur from the Oxford Clay. *Annals and Magazine of Natural History* 16(6):242-256.
- Andrews, C. W. 1897. On the structure of the skull of a pliosaur. *Quarterly Journal of the Geological Society London* 53:177-185.
- Andrews, C. W. 1911. On the Structure of the Roof of the Skull and of the Mandible of *Peloneustes*, with some remarks on the Plesiosaurian Mandible generally. *Geological Magazine* 8(4):160-164.
- Andrews, C. W. 1913. A descriptive catalogue of the Marine Reptiles of the Oxford Clay, Part II. BM(NH), London.
- Andrews, C. W. 1922. Description of a new plesiosaur from the Weald Clay of Berwick (Sussex). *Quarterly Journal of the Geological Society of London* 78:285-298.
- Bakker, R. T. 1993. Plesiosaur extinction cycles - events that mark the beginning, middle, and end of the Cretaceous. *Geological Association of Canada Special Paper* 39:641-664.
- Bardack, D. 1965. Anatomy and evolution of chirocentrid fishes. *The University of Kansas Paleontological Contributions: Vertebrata* 10:1-88.
- Bargagli, R. 2005. *Antarctic Ecosystems: Environmental Contamination, Climate Change, and Human Impact*. Springer.
- Barron, E. J. 1983. A Warm, Equable Cretaceous: the Nature of the Problem. *Earth-Science Reviews* 19:305-338.
- Bartholomai, A. 2004. The large aspidorhynchid fish, *Richmondichthys sweeti* (Etheridge Jnr and Smith Woodward, 1891) from Albian marine deposits of Queensland, Australia. *Memoirs of the Queensland Museum* 49(2):521-536.
- Bartholomai, A. 2008. Lower Cretaceous chimaeroids (Chondrichthys: Holocephali) from the Great Artesian Basin, Australia. *Memoirs of the Queensland Museum* 52(2):1-xx.
- Bennett, B. A., C. R. Smith, B. Glaser, and H. L. Maybaum. 1994. Faunal community structure of a chemoautotrophic assemblage on whale bones in the deep northeast Pacific Ocean *Marine Ecology Progress Series* 108:205-223.

- Bourdon, J. 2008. The Life and Times of Long Dead Sharks. www.elasmo.com.
- Boyd, R., K. Ruming, and J. J. Roberts. 2004. Geomorphology and surficial sediments of the southeast Australian continental margin. *Australian Journal of Earth Sciences* 51(5):743-764.
- Brodie, P. F. 2001. Feeding mechanics of rorquals (*Balaenoptera* sp.). Pp. 345-352. In J.-M. Mazin, and V. de Buffrenil, eds. *Secondary Adaptation of Tetrapods to Life in Water*. Verlag Dr. Friedrich Pfeil, Munchen.
- Brown, D. S. 1981. The English Upper Jurassic Plesiosauroidea (Reptilia) and a review of the phylogeny and classification of the Plesiosauria. *Bulletin of the British Museum (Natural History), Geology series* 35(4):253-347.
- Bryan, S. E., A. E. Constantine, C. J. Stephens, A. Ewart, R. W. Schön, and J. Parianos. 1997. Early Cretaceous volcano-sedimentary successions along the eastern Australian continental margin: Implications for the break-up of eastern Gondwana. *Earth and Planetary Science Letters* 153(1-2):85-102.
- Burton, G. R., and A. J. Mason. 1998. Controls on opal localisation in the White Cliffs area. *Quarterly Notes, Geological Survey of New South Wales* 107:1-11.
- Busbey, A. B. 1995. The structural consequences of skull flattening in crocodylians. Pp. 173-192. In J. Thomason, ed. *Functional morphology in vertebrate paleontology*. Cambridge University Press, Cambridge.
- Cappetta, H. 1980. Les sélaciens du Crétacé supérieur du Liban. 1: Requins. *Palaeontographica Abteilung A* 168:69-148.
- Carpenter, K. 1996. A review of short-necked plesiosaurs from the Cretaceous of the Western Interior, North America. *Neues Jahrbuch für Geologie und Paläontologie Abhandlungen* 201:259-287.
- Carpenter, K. 1997. Comparative cranial anatomy of two North American Cretaceous plesiosaurs. Pp. 191-216. In J. M. Calloway, and E. L. Nicholls, eds. *Ancient Marine Reptiles*. Academic Press.
- Carpenter, K. 1999. Revision of North American elasmosaurs from the Cretaceous of the Western Interior. *Paludicola* 2:148-173.
- Carroll, R. 1988. *Vertebrate paleontology and evolution*. W. H. Freeman, New York.
- Chan, M. A., and A. W. Archer. 2003. *Extreme Depositional Environments: Mega End Members in Geologic Time*. Geological Society of America.
- Cicimurri, D. J., and M. J. Everhart. 2001. An elasmosaur with Stomach Contents and Gastroliths from the Pierre Shale (Late Cretaceous) of Kansas. *Transactions of the Kansas Academy of Science* 104(3-4):129-143.
- Compagno, L. J. V. 1984. *FAO species catalogue. Vol. 4. Sharks of the world. An annotated and illustrated catalogue of shark species known to date. Part 1 - Hexanchiformes to Lamniformes*. FAO Fish. Synop. 125:1-249.
- Compagno, L. J. V., D. A. Eberth, and M. J. Smale. 1989. *Guide to the sharks and rays of southern Africa*. New Holland, London.

- Compagno, L. J. V., and V. H. Niem. 1998. Squalidae. Dogfish sharks. Pp. 1213-1232. FAO Identification Guide for Fishery Purposes. The Living Marine Resources of the Western Central Pacific. FAO, Rome.
- Constantine, A. E., A. Chinsamy, T. H. Rich, and P. Vickers-Rich. 1998. Periglacial environments and polar dinosaurs. *South African Journal of Science* 94:137-141.
- Cook, A. G., and E. D. McKenzie. 1996. *The Great Artesian Basin*. M'Choinneach Publishers.
- Corrado, C. A., D. A. Wilhelm, K. Shimada, and M. J. Everhart. 2003. A new skeleton of the Late Cretaceous lamniform shark, *Cretoxyrhina mantelli*, from western Kansas. *Journal of Vertebrate Paleontology* 23(Supplement to Number 3):43A.
- Couper, A. D., ed. 1989. *Atlas and Encyclopedia of the Sea*. Times Books.
- Cruikshank, A. R. I. 1997. A Lower Cretaceous Pliosauroid from South Africa. *Ann. S. Afr. Mus.* 105:207-226.
- Cruikshank, A. R. I., and E. Fordyce. 2002. A new marine reptile (Sauropterygia) from New Zealand: further evidence for a Late Cretaceous austral radiation of cryptoclidid plesiosaurs. *Palaeontology* 45:557-575.
- Cruikshank, A. R. I., E. Fordyce, and J. Long. 1999. Recent developments in Australian Sauropterygian palaeontology. *Records of the Western Australian Museum (Supplement)* 57:23-36.
- Cruikshank, A. R. I., and J. A. Long. 1997. A new species of pliosaurid reptile from the Early Cretaceous Birdrong Sandstone of Western Australia.
- Day, R. W. 1969. The Lower Cretaceous of the Great Artesian Basin. Pp. 140-173. *In* K. Campbell, ed. *Stratigraphy and Palaeontology: Essays in honour of Dorothy Hill*. ANU Press, Canberra.
- de Pina, M. C. C. 1996. Teleostan monophyly. *In* S. M. L. J. e. al., ed. *Interrelationships of Fishes*. Academic Press, New York.
- Delair, J. B. 1959. The Mesozoic reptiles of Dorset. Part 2. *Proceedings of the Dorset Natural History and Archaeology Society* 80:52-90.
- Donovan, D. T., L. A. Douguzhaeva, and H. Mutvei. 2003. Two pairs of fins in the Late Jurassic Coleoid *Trachyteuthis* from Southern Germany. *Berliner Paläobiol. Abh.* 3:91-99.
- Druckenmiller, P. S. 2002. Osteology of a plesiosaur from the Lower Cretaceous (Albian) Thermopolis Shale of Montana. *Journal of Vertebrate Paleontology* 22:29-42.
- Druckenmiller, P. S. 2006. Early Cretaceous plesiosaurs (Sauropterygia: Plesiosauria) from northern Alberta: palaeoenvironmental and systematic implications. PhD Thesis, University of Calgary.
- Druckenmiller, P. S., and A. P. Russell. 2008a. A phylogeny of Plesiosauria (Sauropterygia) and its bearing on the systematic status of *Leptocleidus* Andrews, 1922. *Zootaxa* 1863:1-120.

- Druckenmiller, P. S., and A. P. Russell. 2008b. Skeletal anatomy of an exceptionally complete specimen of a new genus of plesiosaur from the Early Cretaceous (Early Albian) of northeastern Alberta, Canada. *Palaeontographica Abt. A* 283:1-33.
- Ellis, R. 2003. *Sea Dragons: predators of the prehistoric oceans*. Kansas University Press.
- Everhart, M. J. 1999. Evidence of feeding on mosasaurs by the late Cretaceous lamniform shark, *Cretoxyrhina mantelli*. *Journal of Vertebrate Paleontology* 17(Supplement to No 3):43A-44A.
- Fish, F. E., and C. A. Hui. 1991. Dolphin swimming-a review. *Mammal Review* 21(4):181-195.
- Frakes, L. A., D. Burger, M. Apthorpe, J. Wiseman, M. Dettmann, N. Alley, R. Flint, D. Gravestock, N. Ludbrook, J. Backhouse, S. Skwarko, V. Scheibnerova, A. McMinn, P. S. Moore, B. R. Bolton, J. G. Douglas, R. Christ, M. Wade, R. E. Molnar, B. McGowran, B. E. Balme, R. A. Day, and A. C. P. Group). 1987. Australian Cretaceous shorelines, stage by stage. *Palaeogeography, Palaeoclimatology, Palaeoecology* 59:31-48.
- Froese, R., and D. Pauly. 2007. FishBase. www.fishbase.org.
- Gasparini, Z. B., N. Bardet, J. E. Martin, and M. Fernandez. 2003. The elasmosaurid *Aristonectes* Cabrera from the latest Cretaceous of South America and Antarctica. *Journal of Vertebrate Paleontology* 23(104-115).
- Glen, C. 2002. A new pliosaur from the Albian of Central Queensland. Unpublished undergraduate thesis, University of Queensland.
- Hampe, O. 1992. Ein grosswuchsiger Pliosauridae (Reptilia: Plesiosauria) aus der Unterkreide (oberes Aptium) von Kolumbien *Courier Forsch.-Inst. Senckenberg* 145:1-32.
- Hampe, O. 2005. Considerations on a *Brachauchenius* skeleton (Pliosauroida) from the lower Paja Formation (late Barremian) of Villa de Leyva area (Colombia). *Mitt. Mus. Nat.kd. Berl., Geowiss. Reihe* 8:37-51.
- Henderson, R. A. 2004. A Mid-Cretaceous Association of Shell Beds and Organic-rich Shale: Bivalve Exploitation of a Nutrient-Rich, Anoxic Seafloor Environment. *Palaios* 19:156-169.
- Jefferson, T., S. Leatherwood, and M. A. Webber. 1993. FAO species identification guide. *Marine mammals of the world*. FAO, Rome.
- Kear, B. P. 2003. Cretaceous marine reptiles of Australia: a review of taxonomy and distribution. *Cretaceous Research* 24:277-303.
- Kear, B. P. 2005a. Marine reptiles from the Lower Cretaceous (Aptian) deposits of White Cliffs, southeastern Australia: implications of a high latitude, cold water assemblage. *Cretaceous Research* 26(769-782).
- Kear, B. P. 2005b. A new elasmosaurid plesiosaur from the Lower Cretaceous of Queensland, Australia. *Journal of Vertebrate Paleontology* 25(4):792-805.

- Kear, B. P. 2006a. First gut contents in a Cretaceous sea turtle. *Biology Letters* 2(1):113-115.
- Kear, B. P. 2006b. Marine reptiles from the Lower Cretaceous of South Australia: elements of a high-latitude cold water assemblage. *Palaeontology* 49(4):837-856.
- Kear, B. P. 2006c. Plesiosaur remains from Cretaceous high-latitude non-marine deposits in southeastern Australia. *Journal of Vertebrate Paleontology* 26(1):196-199.
- Kear, B. P. 2006d. Reassessment of *Cratochelone berneyi* Longman, 1915, A giant sea turtle from the Early Cretaceous of Australia. *Journal of Vertebrate Paleontology* 26(3):779-783.
- Kear, B. P. 2007a. First record of a pachycormid fish (Actinopterygerii: Pachycormiformes) from the Lower Cretaceous of Australia. *Journal of Vertebrate Paleontology* 27(4):1033-1038.
- Kear, B. P. 2007b. A juvenile pliosauroid plesiosaur (Reptilia: Sauropterygia) from the Lower Cretaceous of South Australia. *Journal of Paleontology* 81(1):154-164.
- Kear, B. P. 2007c. Taxonomic clarification of the Australian elasmosaurid genus *Eromangasaurus*, with reference to other Austral elasmosaur taxa. *Journal of Vertebrate Paleontology* 27(1):241-246.
- Kear, B. P., W. E. Boles, and E. T. Smith. 2003a. Unusual gut contents in a Cretaceous ichthyosaur. *Proceedings of the Royal Society Series B* 270(Suppl. 2):S206-S208.
- Kear, B. P., R. J. Hamilton-Bruce, B. J. Smith, and K. L. Gowlett-Holmes. 2003b. Reassessment of Australia's oldest freshwater snail, *Viviparus* (?) *albascopularis* Etheridge, 1902 (Mollusca: Gastropoda: Viviparidae), from the Lower Cretaceous (Aptian, Wallumbilla Formation) of White Cliffs, New South Wales. *Molluscan Research* 23:149-158.
- Kear, B. P., and M. S. Y. Lee. 2006. A primitive protostegid from Australia and early sea turtle evolution. *Biology Letters* 2(1):116-119.
- Kear, B. P., N. I. Schroeder, and M. S. Y. Lee. 2006. An archaic crested plesiosaur in opal from the Lower Cretaceous high-latitude deposits of Australia. *Biology Letters* 2(4):615-619.
- Kemp, A. 1991a. Australian Mesozoic and Cainozoic Lungfish. Pp. 465-496. *In* P. Vickers-Rich, J. M. Monaghan, R. F. Baird, and T. H. Rich, eds. *Vertebrate Palaeontology of Australasia*.
- Kemp, N. R. 1991b. Chondrichthyans in the Cretaceous and Tertiary of Australia. Pp. 497-568. *In* P. Vickers-Rich, J. M. Monaghan, R. F. Baird, and T. H. Rich, eds. *Vertebrate Palaeontology of Australasia*.
- Kennedy, D. M., and C. D. Woodroffe. 2004. Carbonate sediments of Elizabeth and Middleton Reefs close to the southern limits of reef growth in the southwest Pacific. *Australian Journal of Earth Sciences* 51(6):847-857.

- Ketchum, H. F. 2008. The anatomy, taxonomy, and systematics of three British Middle Jurassic pliosaurs (Sauropterygia: Pleiosauria) and the phylogeny of Plesiosauria. Unpublished Ph.D. Thesis. University of Cambridge.
- Kriwet, J., S. Klug, J. I. Canudo, and G. Cuenca-Bescos. 2008. A new Early Cretaceous lamniform shark (Chondrichthyes, Neoselachii). *Zoological Journal of the Linnean Society* 154:278-290.
- Kuypers, M. M., R. D. Pancost, and J. S. Sinninghe Damsté. 1999. A large and abrupt fall in atmospheric CO₂ concentration during Cretaceous times. *Nature* 399:342-345.
- Last, P. R., and J. D. Stevens. 1994. *Sharks and Rays of Australia*. CSIRO, Australia.
- Light, J. M., and J. B. Wilson. 1998. Cool-water carbonate deposition on the West Shetland Shelf: a modern distally steepened ramp. *Geological Society, London, Special Publications* 149(1):73-105.
- Lingham-Soliar, T. 1999. Rare soft tissue preservation showing fibrous structures in an ichthyosaur from the Lower Lias (Jurassic) of England. *Proceedings of the Royal Society, London, Series B* 266:2367-2373.
- Lingham-Soliar, T. 2001. The ichthyosaur integument: skin fibers, a means for a strong, flexible and smooth skin. *Lethaia* 34(4):287-302.
- Lingham-Soliar, T., and G. Plodowski. 2007. Taphonomic evidence for high-speed adapted fins in thunniform ichthyosaurs. *Naturwissenschaften* 94:65-70.
- Liston, J. J. 2004. An overview of the pachycormiform *Leedsichthys*. Pp. 379-390. *In* G. Arratia, and A. Tintori, eds. *Mesozoic Fishes 3 – Systematics, Paleoenvironments and Biodiversity*.
- Liston, J. J. 2007. *A Fish Fit For Ozymandias?: The Ecology, Growth and Osteology of Leedsichthys (Pachycormidae, Actinopterygii)*. PhD Thesis, University of Glasgow.
- Longman, H. A. 1924. A new gigantic marine reptile from the Queensland Cretaceous. *Memoirs of the Queensland Museum* 8:26-28.
- Longman, H. A. 1930. *Kronosaurus queenslandicus* A gigantic Cretaceous Pliosaur. *Memoirs of the Queensland Museum* 10(1):1-7.
- Longman, H. A. 1932. A new Cretaceous fish. *Memoirs of the Queensland Museum* 10(2):89-97.
- Longman, H. A. 1935. Palaeontological Notes. *Memoirs of the Queensland Museum* 10(5):236-239.
- Massare, J. A. 1987. Tooth morphology and prey preference of Mesozoic marine reptiles. *Journal of Vertebrate Paleontology* 7:121-137.
- McDougall, I. 2008. Geochronology and the evolution of Australia in the Mesozoic. *Australian Journal of Earth Sciences* 55(6):849-864.
- McGowan, C. 1991. *Dinosaurs, Spitfires and Sea Dragons*. Harvard University Press.

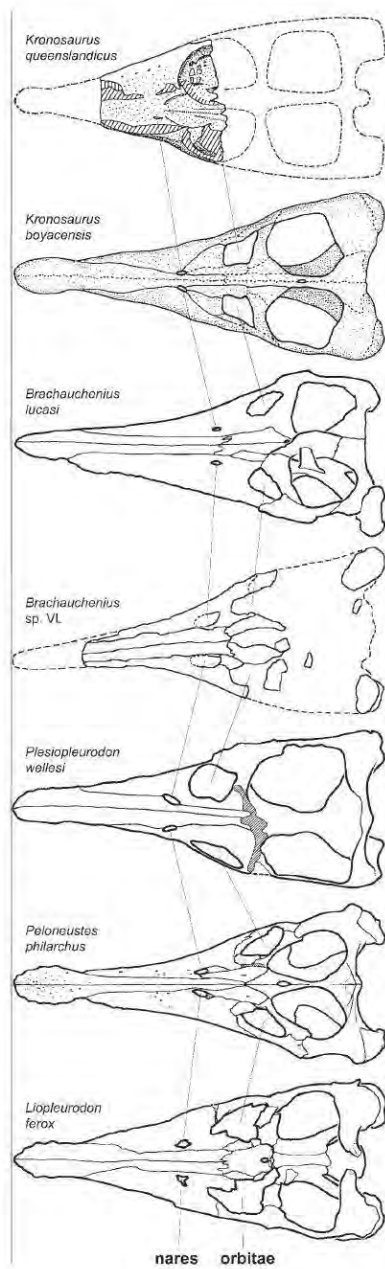
- McHenry, C. R., P. D. Clausen, W. J. T. Daniel, M. B. Meers, and A. Pendharkar. 2006. The biomechanics of the rostrum in crocodylians: a comparative analysis using finite element modelling. *Anatomical Record*, 288A:827-849.
- McHenry, C. R., A. G. Cook, and S. Wroe. 2005. Bottom-Feeding Plesiosaurs. *Science* 310:75.
- Migdalski, E. C., and G. S. Fichter. 1976. The fresh & salt water fishes of the world. Knopf, New York.
- Miller, K. G., P. J. Sugarman, J. V. Browning, M. A. Kominz, J. C. Hernández, R. K. Olsson, J. D. Wright, M. D. Feigenson, and W. Van Sickle. 2003. Late Cretaceous chronology of large, rapid sea-level changes: Glacioeustasy during the greenhouse world. *Geology* 31(7):585-588.
- Möbius, M. E., B. E. Lauderdale, S. R. Nagel, and H. M. Jaeger. 2001. Size separation of granular particles. *Nature* 414(270).
- Molnar, R. E. 1991. Fossil Reptiles of Australia. Pp. 605-701. *In* P. Vickers-Rich, J. M. Monaghan, R. F. Baird, and T. H. Rich, eds. *Vertebrate Palaeontology of Australasia*.
- Molnar, R. E., and R. A. Thulborn. 2007. An incomplete pterosaur skull from the Cretaceous of north-central Queensland, Australia. *Arquivos do Museu Nacional, Rio de Janeiro* 65(4):461-470.
- Noè, L. F. 2001. A Taxonomic and Functional Study of the Callovian (Middle Jurassic) Pliosauroida (Reptilia, Sauropterygia). Unpublished PhD Thesis. University of Derby.
- Nopsca, F. 1928. The genera of reptiles. *Palaeobiologica* 1:163-188.
- O'Keefe, F. R. 2001. A cladistic analysis and taxonomic revision of the Plesiosauria (Reptilia: Sauropterygia). *Acta Zool. Fennica* 213:1-63.
- O'Keefe, R. 1999. Phylogeny and convergence in the Plesiosauria. *Journal of Vertebrate Paleontology* 19 (Supplement to No. 3):67A.
- Oosting, A.M. 2004. Palaeoenvironmental and climatic changes in Australia during the Early Cretaceous. Ph.D. Thesis, Utrecht University, 206 pp.
- Otway, N. M., and A. L. Burke. 2004. Mark-recapture population estimate and movements of grey nurse sharks. NSW EA Project No. 30786. P. 53. NSW Fisheries Final Report Series No 63. NSW Fisheries.
- Otway, N. M., A. L. Burke, N. S. Morrison, and P. C. Parker. 2003. Monitoring and identification of NSW Critical Habitat Sites for conservation of grey nurse sharks. NSW EA Project No. 22499. P. 62. NSW Fisheries Final Report Series No 47. NSW Fisheries.
- Persson, P. O. 1960. Lower Cretaceous plesiosaurs (Reptilia) from Australia.
- Popowics, T. E., and S. W. Herring. 2007. Load transmission in the nasofrontal suture of the pig, *Sus scrofa*. *Journal of Biomechanics* 40(4):837-844.
- Powell, C. M., B. D. Johnson, and J. J. Veevers. 1980. A revised fit of east and west Gondwanaland. *Tectonophysics* 63:13-29.

- Prager, E. J., and R. N. Ginsberg. 1989. Carbonate nodule growth on Florida's outer shelf and its implications for fossil interpretations. *Palaios* 4(4):310-312.
- Prothero, D. R., and F. Schwab. 1996. *Sedimentary Geology: An Introduction to Sedimentary Rocks and Stratigraphy*. Freeman.
- Rafferty, K. L., and S. W. Herring. 1999. Craniofacial sutures: Morphology, growth, and in vivo masticatory strains. *Journal of Morphology* 242(2):167-179.
- Romer, A. S., and A. D. Lewis. 1959. A mounted skeleton of the giant plesiosaur *Kronosaurus*. *Brevoria Museum of Comparative Zoology* 112:1-15.
- Rosato, A., K. J. Strandburg, F. Prinz, and R. H. Swendsen. 1987. Why the Brazil nuts are on top: Size segregation of particulate matter by shaking. *Physical Review Letters* 58(10):1038-1040.
- Sato, T. 2002. Description of plesiosaurs (Reptilia: Sauropterygia) from the Bearpaw formation (Campanian - Maastrichtian) and a phylogenetic analysis of the Elasmosauridae. Ph.D. Thesis, University of Calgary.
- Sato, T., and K. Tanabe. 1998. Cretaceous pliosaurs ate ammonites. *Nature* 394:629-630.
- Schäfer, W. 1972. *Ecology and Palaeoecology of Marine Environments*. The University of Chicago Press.
- Seeley, H. G. 1874. Note on some of the generic modifications of the plesiosaurian pectoral arch. *Quarterly Journal of the Geological Society of London* 30:436-449.
- Shimada, K. 1997a. Dentition of the Late Cretaceous lamniform shark *Cretoxyrhina mantelli*, from the Niobrara Chalk of Kansas. *Journal of Vertebrate Paleontology* 17(2):269-279.
- Shimada, K. 1997b. Paleocological relationships of the Late Cretaceous Lamniform Shark, *Cretoxyrhina mantelli* (Agassiz). *Journal of Paleontology* 7(5):926-933.
- Shimada, K. 1997c. Skeletal anatomy of the Late Cretaceous lamniform shark, *Cretoxyrhina mantelli*, from the Niobrara Chalk in Kansas. *Journal of Vertebrate Paleontology* 17(4):642-652.
- Shimada, K. 2005. Phylogeny of lamniform sharks (Chondrichthyes: Elasmobranchii) and the contribution of dental characters to lamniform systematics. *Palaeontological Research* 9(1):55-72.
- Shimada, K. 2008. Ontogenetic parameters and life history strategies of the Late Cretaceous lamniform shark, *Cretoxyrhina mantelli*, based on vertebral growth increments. *Journal of Vertebrate Paleontology* 28(1):21-33.
- Shimada, K., S. L. Cumbaa, and D. Van Rooyen. 2006a. Caudal fin skeleton of the Late Cretaceous lamniform shark, *Cretoxyrhina mantelli*, from the Niobrara Chalk of Kansas. *Bulletin of the New Mexico Museum of Natural History* 35:185-192.

- Shimada, K., and M. J. Everhart. 2004. Shark-bitten *Xiphactinus audax* (Teleostei: Ichthyodectiformes) from the Niobrara Chalk (Upper Cretaceous) of Kansas. *The Mosasaur* 7:35-39.
- Shimada, K., and G. E. Hooks. 2004. Shark-bitten protostegid turtles from the Upper Cretaceous Morreville Chalk, Alabama. *Journal of Paleontology* 78(1):205-210.
- Shimada, K., B. A. Schumacher, J. A. Parkin, and J. M. Palermo. 2006b. Fossil marine vertebrates from the lowermost Greenhorn Limestone (Upper Cretaceous: Middle Cenomanian) in southeastern Colorado. *Journal of Paleontology Memoir* 63:1-45.
- Shinbrot, T. 2004. The brazil nut effect — in reverse. *Nature* 429:352-353.
- Smith, A. S., and G. J. Dyke. 2008. The skull of the giant predatory pliosaur *Rhomaleosaurus cramptoni*: implications for plesiosaur phylogenetics. *Naturwissenschaften* 95(10): 975-980.
- Smith, C. R. 2005. Bigger is Better: The Role of Whales as Detritus in Marine Ecosystems. *In* J. Estes, ed. *Whales, Whaling and Marine Ecosystems*. University of California Press.
- Smith, C. R., and A. R. Baco. 2003. Ecology of Whale Falls at the Deep-Sea Floor. *Oceanography and Marine Biology: an Annual Review* 41:311–354.
- Smith, C. R., H. Kukert, R. A. Wheatcroft, P. A. Jumars, and J. W. Deming. 1989. Vent fauna on whale remains. *Nature* 341:27.
- Stoll, H. M., and D. P. Schrag. 1996. Evidence for Glacial Control of Rapid Sea Level Changes in the Early Cretaceous. *Science* 272:1771-1774.
- Storrs, G. W. 1991. Anatomy and relationships of *Corosaurus alcovensis* (Diapsida: Sauropterygia) and the Triassic Alcova Limestone of Wyoming. *Bulletin of the Peabody Museum of Natural History* 44:1-151.
- Thulborn, T., and S. Turner. 1993. An elasmosaur bitten by a pliosaur. *Modern Geology* 18:489-501.
- Underwood, C. J. 2006. Diversification of the Neoselachii (Chondrichthyes) during the Jurassic and Cretaceous. *Paleobiology* 32(2):215-235.
- Veevers, J. J. 2006. Updated Gondwana (Permian-Cretaceous) earth history of Australia. *Gondwana Research* 9(3):231-260.
- Wade, M. 1990. A review of the Australian longipinnate ichthyosaur *Platypterygius* (Ichthyosauria, Ichthyopterygia). *Memoirs of the Queensland Museum*, 28:115-137.
- Wade, M. 1993. New Kelaenida and Vampyromorpha: Cretaceous squid from Queensland. *Memoirs of the Australasian Association of Palaeontologists* 15:353-374.
- Wainwright, S. A., D. Pabst, and P. F. Brodie. 1985. Form and function of the collagen layer underlying cetacean blubber. *American Zoologist* 25(146A).

- Wainwright, S. A., F. Vosburgh, and J. H. Hebrank. 1978. Shark Skin: Function in Locomotion. *Science* 202(4369):747-749.
- Welles, S. P. 1943. Elasmosaurid Plesiosaurs with description of new material from California and Colorado. *Memoirs of the University of California* 13(3):125-254.
- Welles, S. P. 1952. A review of the North American Cretaceous Elasmosaurs. *University of California Publications in Geological Sciences* 29(3):46-144.
- Welles, S. P. 1962. A new Species of Elasmosaur from the Aptian of Colombia and a review of the Cretaceous Plesiosaurs.
- White, T. 1935. On the skull of *Kronosaurus queenslandicus* Longman. *Boston Soc. Natural History, Occ. Papers* 8:219-228.
- White, T. 1940. Holotype of *Plesiosaurus longirostris* Blake and the classification of the plesiosaurs. *Journal of Paleontology* 14:451-467.
- Whitehead, P. J. P. 1985. FAO species catalogue. Vol. 7. Clupeoid fishes of the world (suborder Clupeoidei). An annotated and illustrated catalogue of the herrings, sardines, pilchards, sprats, shads, anchovies and wolf-herrings. Part 1 - Chirocentridae, Clupeidae and Pristigasteridae. *FAO Fish. Synop.* 125(7/1):1-303.
- Wiffen, J., V. d. Buffrenil, A. d. Ricqles, and J.-M. Mazin. 1995. Ontogenetic evolution of bone structure in Late Cretaceous Plesiosauria from New Zealand. *Geobios* 28(5):625-640.
- Williston, S. W. 1903. North American Plesiosaurs (Part 1). *Field Columbian Museum, Publ.* 73, *Geological Series* 2(1):1-79.
- Williston, S. W. 1906. North American Plesiosaurs: *Elasmosaurus*, *Cimoliasaurus*, and *Polycotylus*. *American Journal of Science*, 4th Series 21(123):221-236.
- Williston, S. W. 1907. The skull of *Brachauchenius*, with special observations on the relationships of the plesiosaurs.
- Williston, S. W. 1925. *The Osteology of the Reptiles*. Harvard University Press, Cambridge, Mass.
- Wilson, P. A., R. D. Norris, and M. J. Cooper. 2002. Testing the Cretaceous greenhouse hypothesis using glassy foraminiferal calcite from the core of the Turonian tropics on Demerara Rise. *Geology* 30:607-610.
- Witmer, L. 1995. The Extant Phylogenetic Bracket and the importance of reconstructing soft tissues in fossils. Pp. 19-33. *In* J. J. Thomason, ed. *Functional Morphology in Vertebrate Paleontology*. Cambridge University Press.
- Witzell, W. N. 1987. Selective predation on large cheloniid sea turtles by tiger sharks (*Galeocerdo cuvier*). *Japanese Journal of Herpetology* 12(1):22-29.

4. Form (2-D)



Reconstructions of pliosaur palaeobiology depend upon accurate reconstructions of morphology – but this is complicated by taphonomic distortion and ontogenetic variation. The basic taxonomy of Cretaceous pliosaur (represented here by the upper five skulls) is affected by both of these factors (from Hampe 2005).

4.1 **The problem of shape**

“We are jigsaw pieces.... interlocked by a missing piece”

Marillion

The aim of this thesis is to investigate the cranial biomechanics of *Kronosaurus queenslandicus*: the purpose of this chapter is to produce a reconstruction of the skull (using 2D techniques) as a first step in that process. This reconstruction will be based upon the morphological data preserved in eight specimens that have been collected from the Rolling Downs Group of Queensland, most of which are held in the collections of the Queensland Museum.

The descriptions that follow are slightly different to the more usual descriptive accounts in vertebrate palaeontology. The goal of many authors is to describe the osteology – the bones present in the skull, and their topological relationships – preserved in a fossil, often with the intention of providing data for phylogenetic or other palaeobiological analyses. The goal of the present study, however, is biomechanical analysis: although the position and nature of fibrous joints (sutures) between skull bones is undoubtedly of mechanical consequence, present techniques do not provide a way of incorporating these into models and thus the exact position of sutures is of secondary interest. In the following account, I am more concerned with shape and overall structure, and the identity of the bones that form that structure are not of primary concern. Although many of the fossils discussed below do preserve osteological data – some in better detail than any pliosaur material that I have seen – a comprehensive account of the osteology of these specimens is beyond the scope of the present work. I hope to address the osteological details of these specimens in future work. Osteological information will be presented where appropriate, where it serves (1) as a convenient description of form, or (2) bears upon current areas of uncertainty / controversy in pliosaur palaeontology, but the present study is focused upon reconstructing the overall geometry of the skull rather than the details of osteology, and the descriptions that follow will focus on the taphonomic distortion affecting each fossil as much as they do traditional aspects of osteology.

The specific goals of this chapter are to:

- Describe the geometry and summarise the anatomy of specimens preserving skull material referable to *Kronosaurus queenslandicus* (Section 4.2).
- Describe the geometry and summarise the anatomy of comparative material that preserves features missing in the *Kronosaurus queenslandicus* material (Section 4.3)
- Assess the validity and alpha taxonomy of the material referred to *Kronosaurus queenslandicus* (Section 4.4).
- Produce reconstructions, using 2D techniques, of skull geometry in *Kronosaurus queenslandicus* based upon the above analyses (Section 4.5).
- Provide estimates of skull size in the different specimens of *Kronosaurus queenslandicus* that can inform assessment of ontogenetic and allometric variation, as well as palaeoecology (Section 4.6).

4.2 **The skull of *Kronosaurus*: specimens preserving cranial and mandibular material.**

Since Longman first named *Kronosaurus queenslandicus* in 1924, a large amount of material referable to this taxon has been collected from the Aptian and Albian marine strata of the Rolling Downs Group in the Great Artesian Basin. Most of this material is held in the collections of the Queensland Museum (QM), with two additional significant specimens held at the Museum of Comparative Zoology (MCZ) at Harvard University in Massachusetts. The material considered here represents all of the specimens in these two collections that preserve skull material, with two exceptions: MCZ 1285, which is currently on mounted display, and in which the cranial material is obscured by plaster used to augment the display (see Chapter 6), and QM F18726, a skull from the Toolebuc Formation of the Hughenden area which may be the most completely preserved specimen of a *K. queenslandicus* skull known, but which is largely obscured by the hard limestone matrix typical of that region. It is likely that many of the points of uncertainty that are highlighted below could be resolved by careful study of this specimen, but the logistics of preparing QM F18726 are beyond the current study.

For the purposes of the description of the material detailed in Section 4.2 below, the taxonomic assignment to *Kronosaurus queenslandicus* Longman (1924) is accepted. The validity of those taxonomic assignments is reviewed in Section 4.4.

Specimen preparation

For fossils preserved in carbonate matrix, two forms of preparation can be used: mechanical, or acid. Acid preparation has yielded remarkable results with some specimens, even from the Rolling Downs Group within the Great Artesian Basin, but initial attempts to prepare QM F18827 did not yield useable results: the acid often preferentially attacked the fossil bone. Despite numerous attempts to consolidate the fossilised bone, using products such as Bedacryl™ or Paraloid™, a satisfactory protocol was not found, whether the consolidate was dissolved at high or low concentrations in acetone or methanol; at various concentrations of the acid and the amount of buffer used; and whether the specimen was placed in an acid bath, or

the acid was dripped onto a specific area of interest. Whatever protocol was used, the level of damage to the bone was unacceptably high and eventually attempts to prepare QM F18827 using acid treatment were abandoned. Some acid preparation of QM F10113 was also attempted, but the increased level of iron in the matrix of this specimen seemed to resist the action of the acid and progress was too slow to be of use.

Mechanical preparation can be used, but it is slow, carries a high probability of damage to the specimen, and raises significant OH&S issues for the preparator¹. With specimens of the size of *Kronosaurus*, there are severe logistical limitations in this technique. Some parts of QM F18827 were prepared using a hand-held pneumatic drill, but the size of this specimen thwarted significant progress. The only specimen upon which mechanical preparation was used with some effect was QM F51291, where the siderite covering the prefrontal surface on both sides of the skull, and parts of the limestone matrix within the orbits, were removed by Joanne Wilkinson of the Queensland Museum, resulting in significant new anatomical data; however, this specimen was one of the smaller in this study and this smaller size is of considerable benefit to the logistics of preparation.

Assembly

Reptile fossils from the Rolling Downs Group are typically preserved as fragmented nodules ('blocks') of matrix and fossilised bone (see Chapter 3), and the more complete skulls of *Kronosaurus queenslandicus* are each preserved in many pieces – more than 10, and in one specimen approaching 100 individual fragments. In order to describe the geometry of the skull, these must be put together precisely to produce the correct shape of the fossil. In practical terms, this requires assembling a three dimensional jigsaw with irregular surfaces, and the fossil needs to be assembled on a substrate that is strong enough to provide mechanical support, but which can be moulded to the shape of the fossil it is supporting: hence the use of sand-boxes. The different fragments are then lined up with apposing surfaces in contact ('click-fits'). Even tiny amounts of slip between apposing surfaces of adjacent fragments produce

¹ I ended up with 'carpel tunnel' in both wrists after mechanically preparing large parts of the braincase in QM F18827.

errors in the overall geometry: these errors are compounded with each extra fragment that is put into place. However, forcing surfaces of rock against each other in tight click-fit damages the fossil bone exposed on the surface, and during the course of the study repeated assemblies of individual specimens were avoided as much as possible.

Imaging

The staple of vertebrate palaeontology is descriptive anatomy, where the osteology is described in words and supported by figures. In many instances, the choice of the image used is determined simply by whatever best illustrates the anatomy being described. For the preparation of 2D reconstructions of the skull – which are made in orthogonal views, i.e. dorsal, ventral, lateral, anterior, posterior – the images of the fossil that will form the basis of the reconstruction need to be taken, as close as is possible, in the relevant orthogonal axes.

Palaeontology has always made use of illustrations – for example, the initial description of *Plesiosaurus dolichodeirus* was illustrated by a stunning lithograph (Conybeare 1824) – and photography has been extensively used throughout the 20th Century. The rise of digital photography has in many ways offered many advantages to the student who must extract useable images from poorly lit collection facilities: the capacity to instantly review images, and to retake photographs as necessary, means that the experience of receiving a entire roll of unusable film from the developers, taken in an institution that is now on the other side of the world, is one that the emerging generation of palaeontologists need not worry about.

Digital photography does have its own challenges, however, and although a detailed account of the differences between digital and film photography is beyond the scope of the present study, one aspect that deserves attention here is the focal lengths ('zoom') of modern digital cameras lenses, because the focal length setting for each shot determines the degree by which the resulting image is distorted by parallax. With film photography, which predominantly used the 35 mm format, the effects of different focal lengths upon the parallax affecting photographs was well understood and a 50 or 55 mm lens was often considered as a standard length: these offered a

useable field of view without producing the parallax distortion of a shorter ‘fish-eye’ lens².

The advent of digital photography has complicated this aspect of photographing specimens. Until recently digital SLR cameras have been expensive and many researchers have been using compact digital cameras: for the last six to eight years these have offered a good combination of image quality and price, and most of the images shown in this chapter were taken with this class of camera. In keeping with their intended versatility, many of these cameras have a zoom lens that provides a range of focal lengths that is often equivalent to 35–110 mm in the 35 mm film format. Unlike the old film SLR cameras, however, there is very little feedback on the focal length being used for each photograph; and the zoom lens is operated by a toggle switch, rather than allowing the focal length to be set to a predetermined value as was possible in most 35 mm SLR cameras. The result is that, in most cases, the photographer has very little immediate sense of the focal length being used: typically, the images must be downloaded and their properties interrogated on the computer before the focal length of any particular shot is known.

For the majority of users of digital cameras, perhaps even amongst palaeontologists, this is not an important issue, but for the purposes of the present study it is potentially important. Since the aim here is to derive a reconstruction of geometry from photographic data, parallax distortions in the photographs are an unwelcome source of error. For each of the photographs used below to compose the orthogonal views of each specimen, the focal length is stated so that, if required, the degree of parallax affecting each image can be quantified. This is further complicated by the fact that in digital compact cameras, the relevant focal length measurements mean very different levels of zoom and parallax to (1) the same measurements for a 35mm SLR camera, and (2) the same measurement in different models of digital cameras. Table 4-1 provides a list of the ‘35mm equivalents’ for the different focal lengths of the digital cameras used in the present study.

² Lenses with longer focal lengths have less parallax, but the field of view is so narrow that for many specimens the camera needs to be at least several meters away from the specimen; where the flash unit is mounted directly on the camera, lighting then becomes an issue, and in addition many collection facilities simply do not have the space to set up a camera much more than a couple of meters away from a specimen.

35 mm SLR	40	50	60	70	80	90	100	110	FLM
Powershot A95	8.2	10.3	12.3	14.4	16.4	18.5	20.5	22.6	4.87
Powershot 720	6.6	8.3	9.9	11.6	13.3	14.9	16.6	18.2	6.03

Table 4-1: Focal lengths for the two models of compact digital camera used in this study, listed against the equivalent focal length for a 35 mm film SLR. All values in mm, except for Focal Length Multiplier (FLM), which is the conversion ratio for each camera model.

In addition to all of these issues, the photography of very large specimens presents a set of unique challenges. Put simply, the entire skull of an adult *Kronosaurus* does not fit within the field of view unless the camera is positioned a long way from the specimen, or a wide-angle lens is used. For a 35 mm SLR with a 50 mm lens, the camera needs to be at least 6–7 metres away in order to fit a 2.3 metre skull within the field of view. In many collection facilities, there is not enough space next to whatever surface the skull has been assembled upon to manage this shot. Added to this, the assembled skull is usually very difficult to manipulate, so that if it has been assembled, for example, dorsal-side up, the camera needs to be 6–7 metres above the skull to take an orthogonal dorsal shot. The two large skulls considered below – QM F18127 and QM F10113 – cannot be assembled on their sides, and it was not possible to place the camera far enough above the fossils to fit the entire skulls in one shot.

The solution used here was to take the e.g. dorsal shots as a series of photographs along the length of the skull: for example, with QM F18827 the camera was set on a tripod that was placed on a small bench that was then placed upon the larger bench holding the fossil, so that the smaller bench straddled the specimen. This raised the camera to ~1.5 metres above the dorsal surface of the skull, and provided a field of view sufficient to capture an ~50 cm length of the skull in each shot. With overlap between adjacent shots, this gave a total of six photographs that between them covered the entire length of the skull in dorsal view. These can then be manipulated digitally to produce a photo-composite, or photo-mosaic, of the whole skull.

The digital manipulation brings with it a further set of issues. Firstly, any variation in the focal length of the camera, or the distance of the camera from the specimen, will

result in different images of the mosaic being at different scales, and so that the final image is not distorted each of the individual photographs need to be scaled to a consistent size. This is not a simple procedure, even if a scale bar is being used, because any inconsistency in the relative positions of camera, scale bar, and specimen between shots will produce inconsistent results. Secondly, the rectangular image produced from a photograph is relatively undistorted near the middle of the image, but the extent of distortion increases to the edges: this complicates the juxtaposition of photographs, or parts of photographs, when compiling the photo-mosaic. Thirdly, and perhaps most significant, the differences due to parallax at the apposing edges of adjacent shots, that result from the movement of the camera along the length of the skull, are very noticeable and produce enormous complications for the construction of photo-mosaics that seek not to distort the shape of the skull.

One strategy that can partially compensate for the parallax affecting the edges of adjacent shots is to concentrate on parts of each photograph from near the centre of the image; these parts can be masked digitally and used to construct the photo-mosaic. The result is that the apposing edges between the masked central parts of adjacent photographs are less distorted by parallax: but of course this approach only works if there is sufficient overlap between consecutive photos in the series. This approach offers a further advantage when dealing with specimens such as the *Kronosaurus* material; when the whole specimen comprises many fragmented blocks that must be assembled, like a 3D jigsaw, in order to take the photographs. Often, it is difficult or impossible to get perfect apposition ('click-fit') between each of the blocks during assembly of the specimen: this results in small gaps between adjacent blocks which, along the total length of the specimen, can add up to a substantial error in the specimen's dimensions. Digitally masking individual blocks and constructing a photo-composite from those can offset this problem.

An example of the practical consequences of different approaches to constructing photo-composites is shown in Figure 4-1, for QM F18827. Note that the 'simple' composite has been aligned to the midline of the dorsal surface, and that there are distortions away from this axis. Also, there are noticeable gaps between different blocks. In the masked photo-composite, the distortions away from the midline axis have been partially removed, and the gaps between adjacent blocks closed: but the



Figure 4-1: Two photo-mosaics of QM F18827 in dorsal view. Left, 'basic' mosaic composed directly from photographs. Right, 'digital' mosaic composed by masking and aligning images in Paintshop Pro. In the digital mosaic, the rule used as a scale bar in each component image has been masked and rescaled as for the fossil in each respective image: aligned, these show the variation in rescaling of individual photographs; the distance between the lines marked **a** and **b** is 10 cm for each rule.

rescaling of different masked blocks required to produce a coherent image is illustrated by the resulting discrepancies in the size of the scale bars from each of the original photographs. It is unlikely that all of this discrepancy can be explain by

variation in the positions of the camera, scale bar and specimens between different shots, and this highlights the problems with relying on digital editing to compensate for photographic distortion.

The photographs used to illustrate Figure 4-1 were taken in 1997 as part of the preparation and assembly of that specimen, rather than specifically for the present project. By the time that data was being collected specifically for the current work, experience with some of these issues led to the development of some different techniques for taking photographs of large specimens. The skull of QM F10113 is of a similar size to that of QM F18827, and can be assembled from its component blocks in a sand-tray. A sand-tray designed to fit on a fork-lift palette was used: the camera was fixed to a tripod that was strapped to a 4 metre ladder with sufficient span so that the palette, with the sand-tray on top, could be placed between the legs of the ladder directly under the camera (Figure 4-2). A sequence of photographs were taken, with the exposure, lighting, and focal length settings of the camera kept constant: between each shot, the palette was moved along a pre-determined set of positions using a palette-jack, giving a series of photographs with the required amount of overlap between each.

The sand-tray was 1.5 metres long, which is not enough to assemble the entire skull in one go, but the design of this set-up allowed enough consistency to allow assemblies of the front and rear halves of the skull to be photographed to consistent specifications. The resulting photographs were all taken at a constant scale, with lower distortion from parallax due to the increased height of the camera, and were much easier to digitally manipulate into a photo-composite of the whole skull. An example of one of the resulting photo-composites, of a dorsal view of the skull, is shown in Figure 4-3.

Morphological descriptions

In the following sections, each of the referred *Kronosaurus queenslandicus* specimens is considered in turn: the geological context, relevant collection data, and preparation history are listed, the taphonomic alteration affected the specimen is interpreted, and the particulars for the photography given. Although the primary purpose is to



Figure 4-2: Camera set-up for photography of articulated skull fragments of QM F10113. Top, the fossils are 'jigsawed' together in a sand-box that is placed on a pallet, which is moved into position with a palette-jack. The camera is fixed on an armature, which is fixed to the top of the ladder to give a consistent field of view and camera position between shots. Below, images of different parts of the skull can then be superimposed to provide an image of the whole skull, even though the whole skull does not fit on the sand-tray.

describe the geometry, osteological features of particular interest are summarised for each specimen.

The dentition is described using the positions of teeth/ alveoli along the tooth row, from front to back, according to the bone that bears the tooth. Thus, the third tooth position, from the front, in the premaxilla is denoted as 'Pmx3', the first maxillary tooth position as 'M1', and the fifth dentary tooth as 'D5'.



Figure 4-3: Photo-composite of QM F10113 skull in dorsal view. The original images were taken at a wide angle (see Figure 4-2) and aligned digitally (using Paintshop Pro v8 – see text).

QM F18827

Specimen summary

This specimen derives from the Late Albian Toolebuc Formation: it was collected in 1990 by Ralph Molnar (then of the Queensland Museum) and colleagues, from the airstrip on Lucerne Station, north of Richmond. The specimen comprises a large, nearly complete skull (Figure 4-5), articulated anterior cervical vertebrae, and associated cervical and pectoral elements, including parts of the girdle and the proximal head of a humerus. It was donated to the Queensland Museum by the owner of Lucerne Station, Mr. Marlin Entriken.

From field notes and photographs, the skull was lying as a series of weathered nodules in the soil: it had been displaced from the host bedrock. The nodules had started to break up, and were plaster jacketed for transport to the Queensland Museum in Brisbane. The material was removed from the jackets at the University of Queensland (by the author) and the skull reassembled.

The specimen is preserved in a light grey limestone matrix. Extensive attempts were made to prepare the matrix from the bone in the orbital, occipital, and temporal regions of the skull, using acid and mechanical preparation techniques (see above). Although large volumes of matrix were removed, exposure of the surface bone was problematic – the different techniques all caused unacceptable levels of damage to the bone – and was eventually abandoned. Exposed bone has been consolidated with Paraloid™. The summary description of the skull presented here is based largely upon the ‘natural’ exposure of the bone by weathering and fragmentation of the nodules.

Apart from QMF18726 (which is not included in the present analysis), the ‘Lucerne’ skull is the most complete specimen of *Kronosaurus* cranial material in the Queensland Museum collections. Although the preservation of the fossil makes description of the osteology difficult, the 3D geometry is rather good and the specimen is here used as a template for the overall shape of the skull in *Kronosaurus queenslandicus*.

Taphonomy

The skull is preserved with the mandible adducted to the cranium: the mandibular symphysis is ankylosed to the anterior rostrum, apparently in natural position. The anterior part of the skull is heavily weathered, with more weathering on the upper surface: the surface of the bone is rather poorly preserved, and only a small amount of matrix is covering the fossil in places. The anterior teeth are mainly preserved as external moulds or natural casts.

The rostrum and articulated anterior mandible were preserved in two modules, which had separated slightly: the gap between these runs through the M2 tooth positions in the transverse plane and both apposing broken faces are heavily weathered.

Superficial fractures in both these nodules show signs of weathering. The dorsal surface of the anterior and mid rostrum has been weathered so as to reveal the upper part of the nasal cavity, which appears to preserve a number of parallel, longitudinal structures that extend anteriorly to at least the Pmx3 tooth position.

Overall, the skull does not appear to have been exposed to any major distortion in the transverse axis: the obvious sedimentary compaction is in the vertical axis. The anterior rostrum appears to be largely free of vertical distortion, but the posterior rostrum has been pushed downwards. Around the position where the external nares should be, the dorsal surface of the rostrum is covered by matrix, and the teeth are here preserved as external moulds in the matrix surrounding the fragmentary mandibular ramus.

The posterior part of the skull, i.e. the orbital, temporal, and occipital region, is covered with more matrix than the anterior, and the bone is better preserved: this part of the skull appears to have been exposed to less weathering than the anterior part. Although all of the nodules preserving the posterior skull are extensively fractured, weathering along these fracture surfaces is minimal. The posterior-most teeth are also better preserved so that the original dentine/pulp structure can be discerned in the tooth roots. The bones of the orbital region, especially the postorbital wall, have been deformed vertically but otherwise appear to be in the correct relative positions.

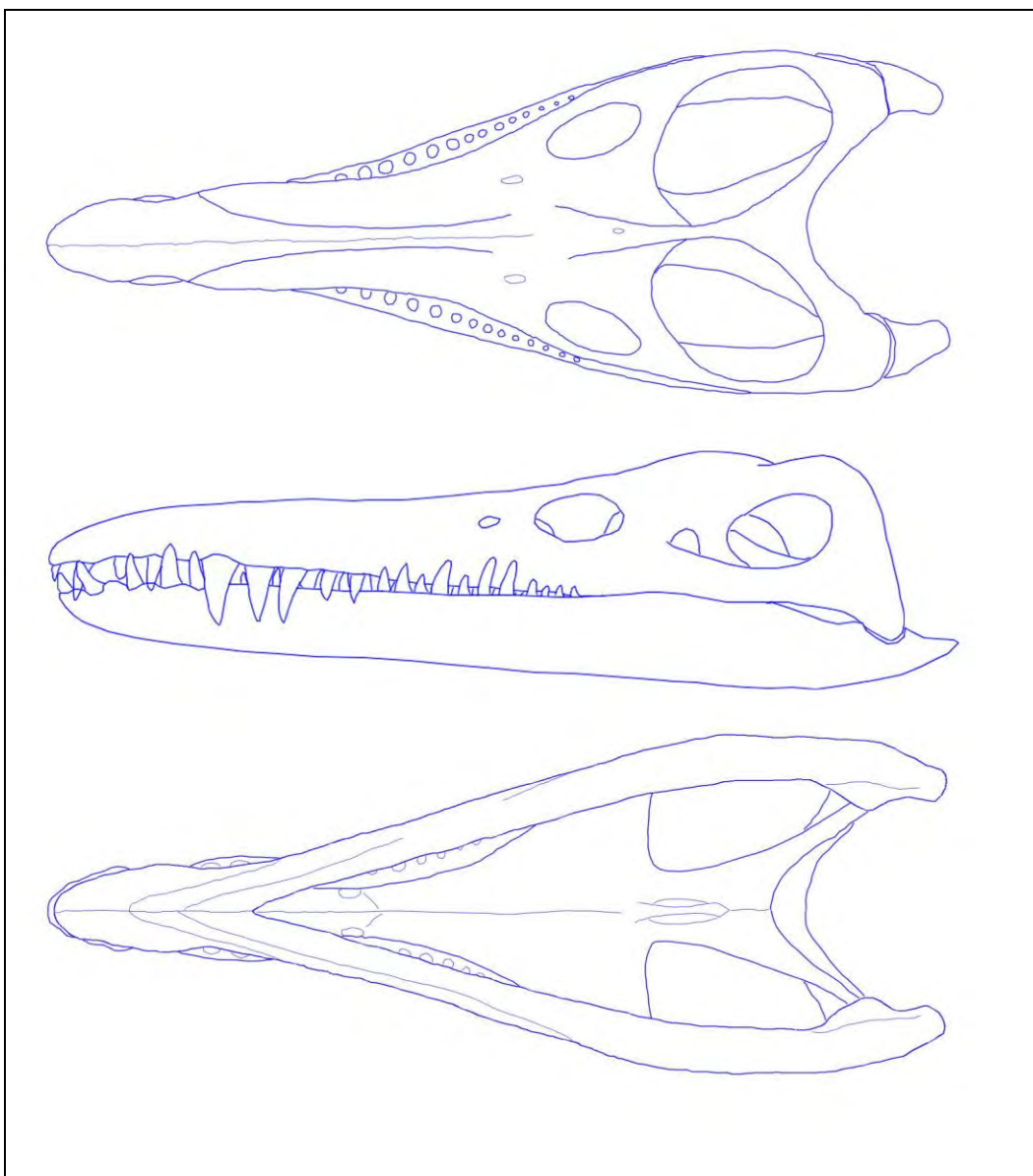


Figure 4-4: Preliminary reconstruction of the skull of *Kronosaurus queenslandicus*, made in 1997 and based largely upon the 'basic' photo-mosaic of QM F18827 shown in Figure 4-1.

The sagittal crest and posterior part of the parietals have been weathered but otherwise appear to be undeformed; likewise, the upper, posterior, and lateral parts of the squamosals are heavily weathered but otherwise unchanged, and the part of the dorsal squamosal arch that meets the parietals is surrounded by matrix (on the right side, the dorsal arch was broken during preparation). The external surface of the lateral wall of the braincase is exposed and slightly weathered: those of the left side remain covered by matrix. The zygomatic arches (lower temporal bars) are completely gone, as are the articular parts of the quadrates and the posterior mandible. The anterior cervical vertebrae are articulated with the occipital condyle. In

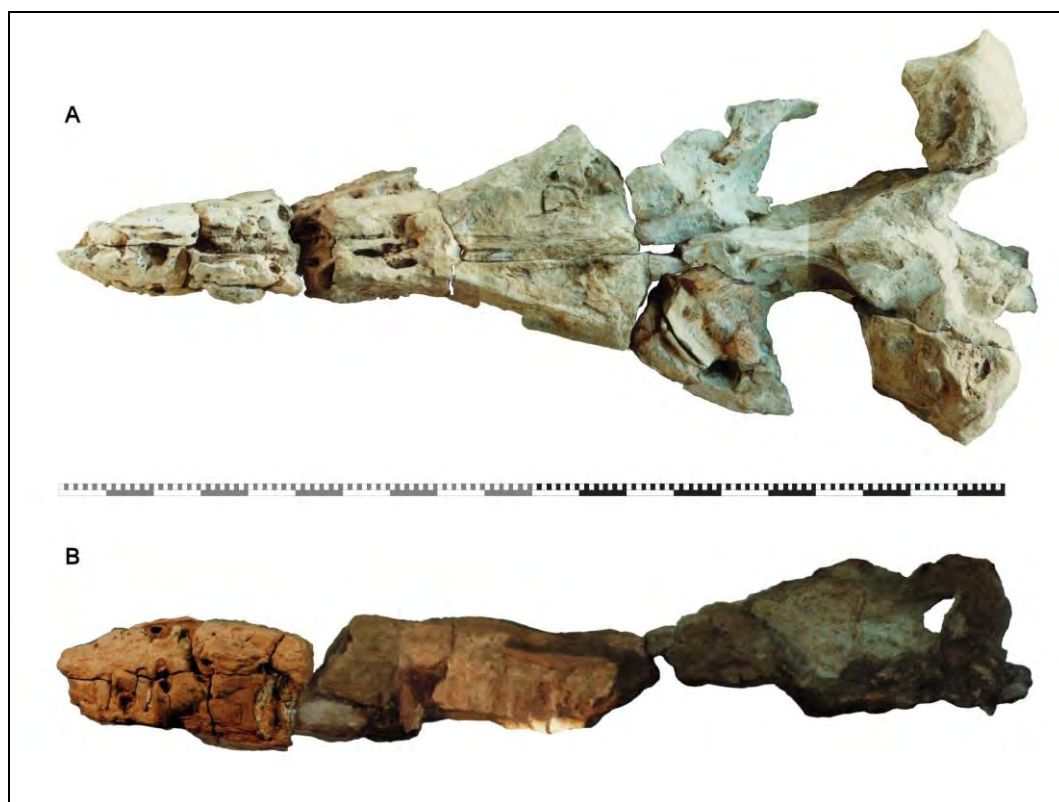


Figure 4-5: Photo-mosaic of QM F18827 in (A) dorsal and (B) left lateral views. Scale bar = 2 metres.

summary, the braincase and occiput appear to be largely unaffected by vertical compaction, although dorsal, lateral, and ventral surfaces are heavily weathered.

During preparation of the large block containing the braincase, some small ammonites were found within the matrix, as well as several inoceramid bivalves: these latter were lying on a thin layer of matrix covering the bone on the lateral surface of the left epipterygoid.

Methods

As part of initial attempts to prepare this specimen, it was assembled and photographed in 1997, using a Pentax MX SLR camera with a 55mm lens and 35mm film. A simple photo-mosaic (Figure 4-1) was used as the basis for a preliminary reconstruction of skull shape in *Kronosaurus queenslandicus* (Figure 4-4). For the dorsal view, the fragments of the mid-rami of the mandible were not assembled with the

rest of the skull; for the lateral view, the blocks containing the squamosals and the orbital regions were removed.

Because of the extensive weathering of the anterior part of the specimen, the fossil is fragile, and the 1997 photographs were used in the present analysis; re-photographing the specimen, without a suitable surface to assemble it on, was judged to pose a risk of further damage to the specimen. The photographs were processed in PaintShop Pro, and the masked fossil from each were then digitally assembled in a master file. Within the master file, the masked components were rescaled to provide the best match between adjacent surfaces. In the final photo-composite (Figure 4-5), the lateral image was scaled to the corresponding parts of the skull in dorsal view.

Results

From the photo-composites shown in Figure 4-5, landmarks for the reconstruction of the skull (Section 4.5) were traced and scaled to the dimensions of QM F10113 in dorsal (Figure 4-31) and lateral (Figure 4-34) views.

A detailed description of the osteology in this important specimen has yet to be completed. Some features of the morphology can be summarised:

- Each premaxilla bears four teeth. The sequence of occluded anterior teeth, from front to back, is; Pmx1, D1, Pmx2, D2, Pmx3, D3, Pmx4, D4, D5, M1, M2, M3.
- There is a short diastema in the upper jaw between Pmx4 and M1 tooth positions, at which point the enlarged D4 and D5 lower jaw teeth occlude the upper jaw.
- D4 and D5 are large, caniniform teeth. Immediately behind them M1, M2, and M3 are the largest teeth in the jaw: the total length of crown plus roots in these is approximately 30 cms, with the crowns forming 1/3 of the total length.
- The mandibular symphysis bears 6½ tooth positions. The anterior symphysis is expanded in a 'spatulate' region that bears 5 pairs of teeth. D6 and D7 are much smaller than the preceding teeth and lie

well medial to the line of D3-D5. The first three maxillary teeth occlude lateral to the line of D6 and D7 and the teeth of the anterior mandibular ramus.

- Behind the anterior three maxillary tooth positions, the upper jaw teeth decrease markedly in size. The mandibular ramus widens more rapidly than does the rostrum, so that the lower jaw teeth go from occluding well medial of M1-M3, to occluding on the labial side of the upper jaw teeth from about M5 back: this gives the jaw a definite 'under-bite' in the rear half of the tooth row.
- The teeth have crowns with a circular section and an ornament that is present around the entire circumference. The ornament consists of longitudinal, parallel ridges of varying lengths; shorter ridges are staggered between the longer ones.
- From the longitudinal structures exposed at the front of the nasal cavity by the weathering of the dorsal roof bone of the anterior rostrum, there appears to be a vomerine cavity lying between the tooth-bearing parts of the premaxillae.
- The overall shape of the anterior rostrum and adducted mandible is tall and narrow. The rostrum expands to the orbits rapidly from about the 8th maxillary tooth position. As noted above the line of the mandibles in this region lies well lateral of the upper jaw.
- The upper tooth row extends backwards to halfway along the lateral border of the orbits.
- On the right side, the lateral pterygoid preserves a definite buttress that has a triangular section when viewed laterally.
- The preserved cervical and pectoral vertebrae lack sub-central foramina.
- The Dorsal Cranial Length (DCL – anterior tip of the premaxillae to the rearmost part of the supraoccipitals) is 189 cm.

QM F10113

Specimen summary

Comprising a large quantity of articulated cranial and post-cranial material, this specimen is probably the largest fossil³ known from Australia and is one of the most complete fossils worldwide of a large pliosaur. It was collected in 1978 by Alan Bartholomai, from Toronto Park Station⁴: the geology is the Toolebuc Formation. It was donated to the Queensland Museum by the owner of Toronto Park, Marlin Entriken.

The specimen comprised several hundred fragments of fossil bone and matrix, of various sizes: it was assembled at the University of Queensland by the author from 1994–1998, with some additional assembly by Laurie Beirne and Kristen Spring at the Queensland Museum from 1998–2003. So far, a large a part of the skull and an articulated axial column, from the atlas to the anterior caudal region, as well as a two partial and two nearly complete propodials, have been assembled; there is still a significant amount of small fragments which have yet to be identified and assembled.

Despite the geographic and stratigraphic proximity to the Lucerne specimen (QM F18827), the matrix is noticeably different: it is an orange-red micritic limestone, and has extensive areas covered by a dark red mineral which appears to be siderite (iron carbonate), giving the fossil a distinctly red hue. The matrix is hard: limited mechanical and acid preparation were trialled on the block containing the mandibular symphysis, but the matrix was resistant to acid preparation and the hardness of the limestone was not suitable for extensive mechanical preparation. Overall, the specimen as been ‘degraded’ by weathered to a lesser extent than in QM F18827: weathering has exposed the bone surface, but the bone is still in relatively good condition, and there is little weathering evident along the fractured surfaces within the blocks. As with QM F18827, the summary of the morphology presented here has been based upon the exposure of the bone at the weathered exterior surfaces of blocks and the naturally fractured surfaces within them.

³ Fossils of larger animals – specifically, sauropod dinosaurs – are known, but from much less complete material.

⁴ Toronto Park neighbours Lucerne, to the north of Richmond. Both are owned by M. Entriken.

Because of the extensive preservation of both cranial and postcranial material, QM F10113 is an important specimen of *Kronosaurus queenslandicus* and offers much potential information on the cranial and postcranial anatomy of this species. It is regarded here as a key specimen for relating skull size to overall body proportions.

Taphonomy

As noted above, the specimen is remarkable for the articulation of the axial column from the skull to the sacral/ anterior caudal region. Although collection data is scant, if orientation can be deduced from the pattern of weathering, the weathering of the ventral surface of the vertebral column suggests that it was preserved with the ventral side up, i.e. the specimen appears to have been lying on its back. Given that the preserved parts of the vertebral column comprise a length of some five metres of fossil/matrix blocks, there was evidently only a small amount of displacement from the original position within the original bedding layers. However, the dorsal surface of the skull is more weathered than the ventral. In contrast to the situation with the trunk vertebrae, some of the contacts between consecutive blocks containing cervical vertebrae show extensive weathering, to the point where the original contacts have nearly been lost. It is possible that the head and anterior neck were preserved in one or more nodules that may have been separated from the rest of the fossil. Whether the skull is too large to have been ‘flipped’ by late-taphonomic processes is unknown, but this would explain the inverted weathering profile relative to the postcranium. Alternatively, the skull might have been flipped prior to burial, and has been weathered more or less in the position in which it was fossilised.

The specimen preserves an incomplete skull – although not as complete as QM F18827, the length of the cranium can be assembled from the premaxillae to the occiput and suspensoria. The anterior-most part of the rostrum, forward of the Pmx3 tooth socket, is missing. The posterior parts of the mandibles are articulated with the quadrates: however, the anterior mandibles were evidently displaced during preservation, as matrix covering the ventral (palatal) part of the rostrum preserved the imprints of a line of lower jaw teeth lying obliquely across the rostrum. Most of the mandibular rami are missing; only two large fragments are preserved, and these have not been located precisely, but the mandibular symphysis is incompletely

preserved: the anterior-most tip is missing, but the posterior halves of the D1 alveoli are preserved.

The dorsal roof bones of the anterior and mid rostrum are preserved to a point just in front of the position of the external nares, although a small part of the brow region between the orbits and including the parietal foramen is also present. The dorsal surface appears to have been deformed vertically and transversely relative to the palate – or, if the skull was preserved ventral side up, the palatal surface has been pressed down and sideways relative to the skull roof. The broken transverse faces of adjacent skull blocks preserve the cross section of the fossil bone in fine detail, including the thickness of the cortical bone (where unweathered) and the geometry of the trabeculae. The dorsal surface of the parietals have been almost completely removed, revealing the supraoccipital, and the lateral surfaces of the block containing the braincase and occiput have been heavily weathered. The occipital condyle appears to have been crushed vertically. Most of the squamosals have been weathered, but the contact between the quadrate and the quadrate ramus of the pterygoid has been preserved on the right side, as well as the glenoid region of the mandibles and part of the retroarticular process.

Large parts of the matrix close to the fossil bone contain extensive layers of inoceramid bivalves, although the distribution of these has not been charted. The pliosaur carcass may have settled on an existing inoceramid shell bed, or formed a hard surface for the colonisation of these bivalves (Henderson 2004), or both. The post-cranial blocks contain evidence of stomach contents, but no gastroliths (Chapter 8).

Methods

Following the relocation of the Queensland Museum fossil collections in 2003, the specimen was reassembled at the Hendra storage facility and photographed between 2005 and 2007 using digital cameras. Camera position was standardised as far as possible, by attachment of the camera tripod to a tall ladder as described above. Portions of the fossil were assembled in approximately 50 cm lengths at a time in a sand tray, and photographed in dorsal, ventral, and lateral views.

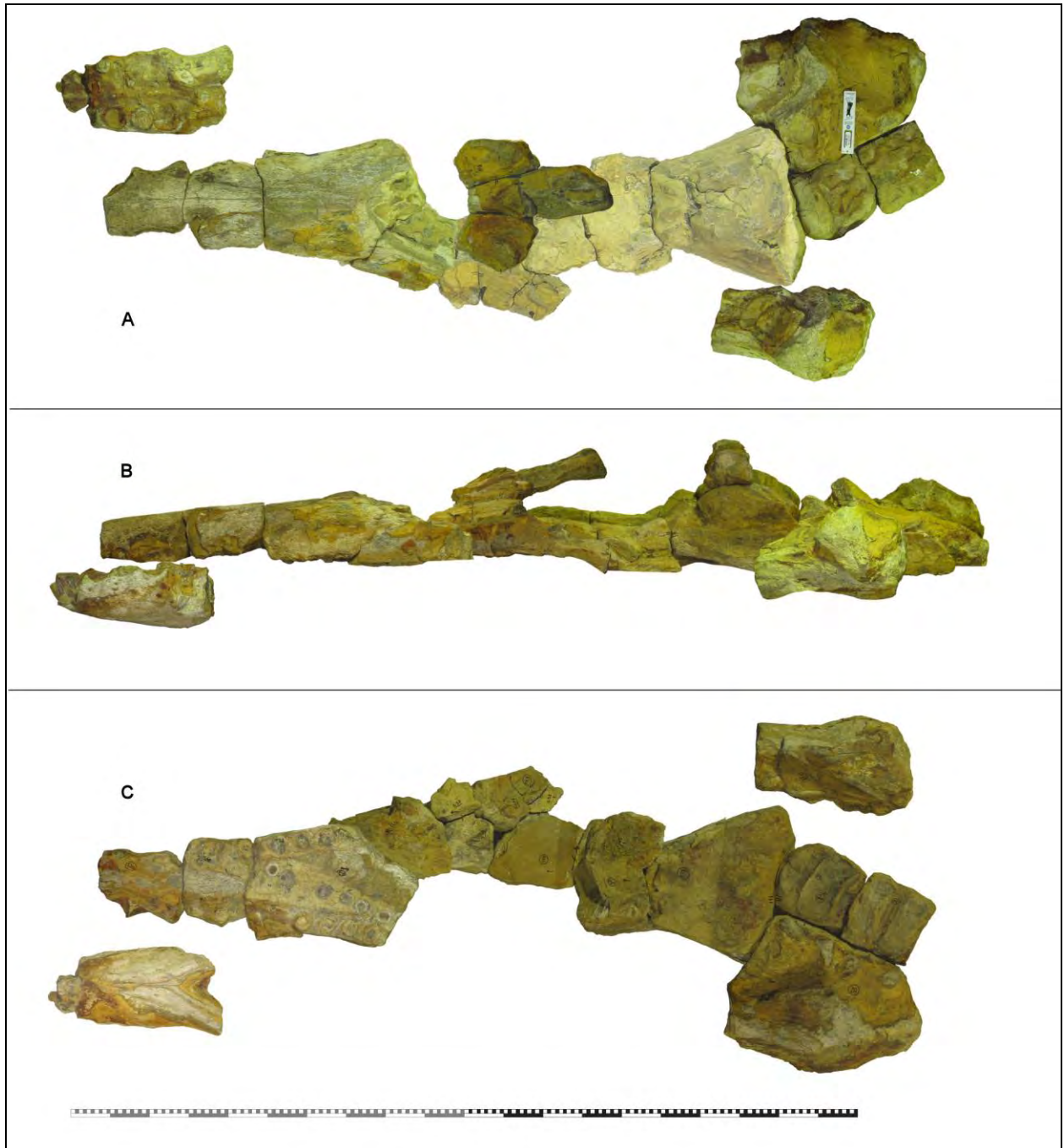


Figure 4-6: Photo mosaic of skull of QM F10113 in (A) dorsal, (B) left lateral, and (C) ventral view. The mandibular symphysis is shown to the right of the rostrum in the dorsal and ventral views: the block containing the left quadrate/articular is in approximate life position. Scale bar = 2 metres.

The dorsal shots were taken using; (1) a Canon Powershot A95, at 8mm focal length, and (2) a Canon Powershot A720, at 12–15mm focal length. Ventral shots of the skull were taken using an A95 at 23 mm focal length. Dorsal and ventral shots of the

symphysis, and the lateral shots of the skull, were taken using an A720 at 15mm focal length.

The fossils in each individual photograph were masked and combined into a master file using Paintshop Pro. Because camera height was kept constant for the dorsal and ventral shots, the need for rescaling different individual images within the photo-composites was minimised: however, scaling was more of an issue with the lateral shots because the camera had to be closer to the specimen, resulting in increased parallax in each image. The overall photo-composites within each master file were scaled from measurements taken directly from the specimens and which could be reliably replicated in the 2D images.

Results

The overall proportions of the skull can be seen in dorsal view (Figure 4-3). For the skull reconstruction, the quadrates and the brow roof were included in the photo-composite (Figure 4-6). Landmarks on the skull were traced for dorsal (Figure 4-32), lateral (Figure 4-35), and ventral (Figure 4-36, Figure 4-37) views for use in the overall 2D reconstruction of the skull (Figure 4-38).

Pending a thorough account of the osteology preserved in this specimen, the morphology can be summarised:

- The premaxillae tooth count is not known because the tip of the snout is missing. At the broken transverse face of the anterior rostrum, a tall, narrow cavity between the premaxillae and above the vomer can be seen, comparable to the vomerine cavity postulated for QM F18827.
- Although the very tip of the dentary is missing, the remains of the first pair of dentary teeth are preserved. The mandibular symphysis holds 6½ dentary tooth position, the anterior-most five being held in a spatulate expansion of the symphysis. D4 and D5 are the largest teeth in the anterior mandible.
- At the dorsal midline of the mandibular symphysis, there is a longitudinal ridge that has a blunt upper edge. This is obscured by

matrix in some places, but appears to run for the entire length of the mandible.

- Although only the roots of most teeth are preserved, some crowns remain. The ornament consists of sparse, heavy longitudinal ridges that are present around the entire circumference of the teeth. The teeth are circular in section.
- In the upper jaw, the diameter of the first three maxillary teeth alveoli are the largest in the jaw. There is a gap in the tooth row (i.e. a short diastema) between the first maxillary and the fourth premaxillary teeth, and the rostrum narrows slightly at the point where the premaxillary/maxillary suture contacts the lateral margin of the jaw.
- The skull roof is preserved in the mid rostrum, but is missing around the region of the external nares. The transverse section of the broken roof bone just anterior of the position of the nares reveals at least one element, in addition to the paired maxillae and premaxillae, forming the internal part of the dorsal median ridge.
- At the same broken surface (at the rear of the preserved mid-rostrum roof bone), the nasal cavity is filled with limestone matrix. In the upper part of the cavity, on each side of the midline, there is a circular region of different coloured matrix that has a 'flaky' appearance compared with the matrix in the rest of the cavity. The symmetry of these structures is striking; they may represent an infill of a soft tissue structure within the nasal cavity at a different time to the deposition of finer carbonate within the rest of the cavity.
- In the blocks that preserve the brow region of the skull roof between the orbits, the internal surface of the skull roof in front of the parietal foramen preserves a series of ventral flanges on either side of the midline. On each side of the midline suture, there is a pair of these flanges: the lateral one is larger than the medial, and they are aligned longitudinally but sloping medially as they project downwards. They each taper to a blunt point. With reference to the figure of the same region of *Peloneustes philarchus* in (Andrews 1911) – see Chapter 5), they are interpreted as ventral processes of the frontals.

- On either side of these, the internal surface of the skull roof is thickened to form a ventral ‘boss’ on the underside of the skull roof: although the orbital rim is not preserved, from their position these are positioned at the anterior medial corner of the orbit, and would be expected to be formed from a dorso-medial process of the prefrontals.
- At the front of the palate, the vomer forms a thick ventral element to the anterior rostrum. The position of the internal nares is obscured by matrix, but the preserved broken transverse surface of the palatal bones behind the position of the internal nares indicate that the palate is thick in the mid rostrum also.
- The parasphenoid is preserved in section at the front of the block that preserves the braincase and occipital condyle. The position of the epipterygoids and paroccipital processes can be identified on the same block: although these are all heavily weathered they do not appear to be deformed.
- Basal skull length (BSL) is estimated, from photo-composites and assuming that the missing portion of the anterior rostrum was similar to that of QM F18827, at 187.6 cm.

QM F51291

Specimen summary

Alex Cook discovered this specimen at the Geology Museum of James Cook University (Townsville) in 1996. Its history prior to this is uncertain: it was evidently collected from the Great Artesian Basin (GAB), but there is no collection data. The matrix is consistent with the Rolling Downs Group, specifically from the region around Dunraven Station to the north of Hughenden (A. Cook, pers. comm.), which is in the Toolebuc Formation.

The fossil is a weathered partial skull, preserving the orbital region of a pliosaur. The morphology is consistent with *Kronosaurus* material from the GAB, but the specimen does not preserve any diagnostic anatomy beyond being a member of the



Figure 4-7: QM F51291, in oblique right view. Note the dark red-brown sideritic matrix marking the sutures of the posterior dorsal median ridge on the upper surface,. At the antero-lateral margin of the orbit, the right lacrimal is clearly delineated by patent sutures from the prefrontal medially, the maxilla antero-laterally, and the jugal postero-laterally. Rule shows centimetres. Photograph by J. Scott.

Brachaucheniidae, and its specific assignment is assumed rather than demonstrated. If *Kronosaurus*, it represents a small animal, perhaps half the linear size of QM F18827 and QM F10113.

The fossil is preserved in a 'clean grey' micritic limestone matrix, with some part of the fossil bone covered by dark red-brown matrix, which consists of two types of mineral that appear to be pyrite and limonite. Various features within the fossil, including many of the sutures, are infused with pyrite, giving a marked visual contrast between the pale fossilised bone and the darker in-filled sutures (Figure 4-7).

The fossil has had some preparation since being accessioned by the Queensland Museum in 1996; mechanical removal of limestone matrix from the orbits and the

left post-orbital cavity, and mechanical plus acid preparation of a mass of the pyretic matrix that was covering the external surface of the bone between the orbits and external nares. The exposed bone has been consolidated with Paraloid™.

Although incomplete, the fossil is remarkable for the apparent lack of crushing and the quality of preservation of the orbital region and posterior rostrum, areas that are not often well preserved in pliosaur skulls (Chapter 3).

Taphonomy

All surfaces of the block have been weathered: the original skull was presumably fragmented from the rest of the skull some time ago and the fractured surfaces are extensively worn. The postorbital wall has been almost completely removed, and the posterior-lateral corners have only small remnants of bone – the shape of the orbits is here preserved in the matrix as a natural internal mould. The ventral surface appears to be more weathered than the dorsal.

Only the roots of the upper jaw teeth are preserved; the dentine is preserved as concentric layers of an opaque white mineral, while the pulp cavities are in-filled with carbonate matrix or recrystallised with calcite. Remnants of the adducted lower jaw teeth are ankylosed to the lateral margin of the upper jaw on the left side, either as fragments of dentine or imprints on small patches of matrix covering the upper jaw margin. There is a portion of a displaced tooth preserved in the matrix filling the left orbit. Parts of the palate, although weathered, are also covered in clumps of crystals which may also be calcite. The only intact surface bone is on the dorsal surface of the skull, between the antero-medial edge of the orbits and the external nares on both sides, where the fossil was originally covered with pyritic matrix: the preservation of the bone in these positions is excellent.

On first inspection, the specimen seems to be free of vertical compaction. The upper jaw tooth margins appear to be splayed slightly outwards – although this might be exaggerated by the removal of the crowns and distal parts of the roots – but other than that the specimen seems to preserve the three dimensional shape of the orbital region well. There are, however, several very localised depressions on the dorsal surface; one on each side of the brow, at the antero-medial corners of each orbit, and

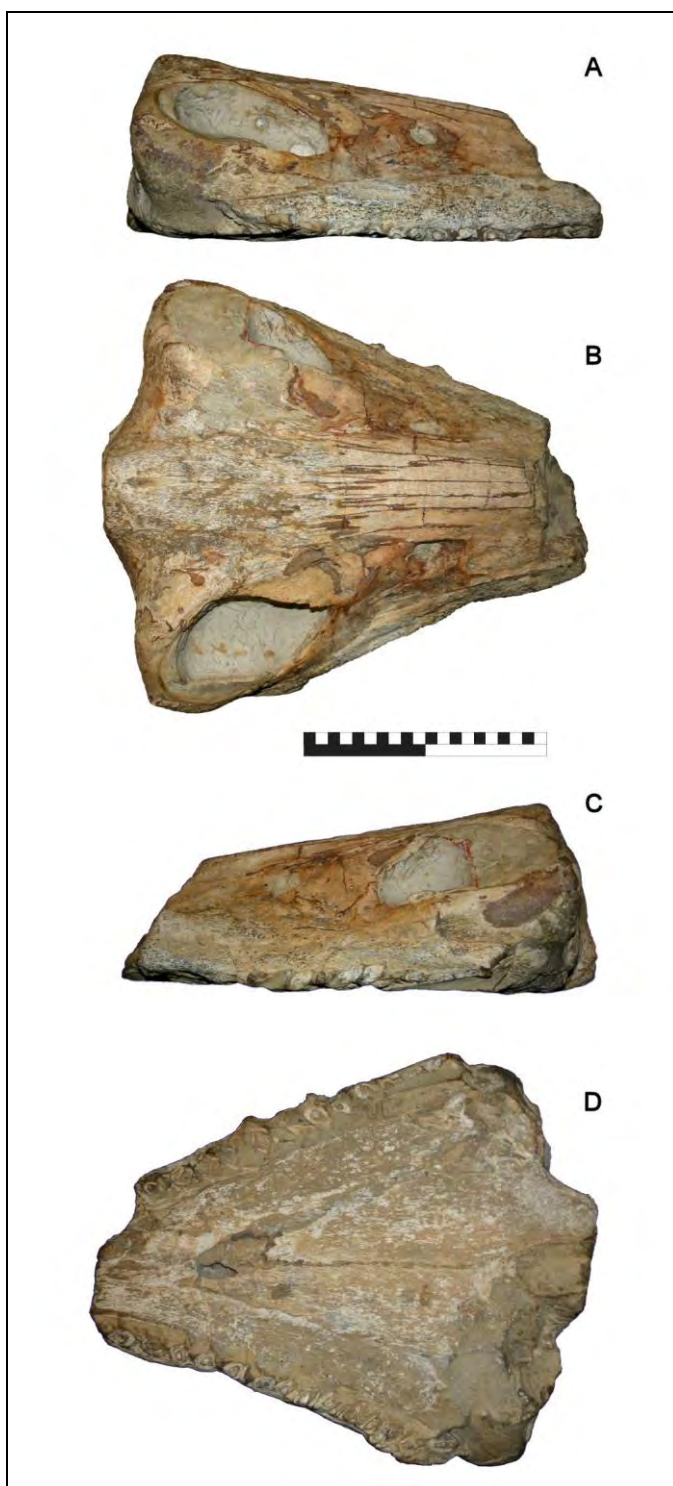


Figure 4-8: QM F51291, in (A) right lateral, (B) dorsal, (C) left lateral, and (D) ventral views. Scale bar = 20 cm. Original photographs by J. Scott.

another on the right postfrontal. The depressions are not symmetrical, and the surface bone within each is considerably damaged: with the two depressions at the antero-medial corners of the orbits, there is a definite boundary between the bone of the depressed fracture and the surface bone in front and the contrast in the



Figure 4-9: QM F51291, in dorsal view. See Figure 4-10 for interpretation. Original photograph by J. Scott.

appearance of the bone is marked. Each of the three depressed fractures are also partially filled with pyritic matrix (Figure 4-7, Figure 4-9, Figure 4-12).

Of the bone that was not covered in pyritic matrix, the surface of the dorsal median ridge is the least weathered; the outermost layer of compact bone has been removed, but the preserved surface is dense bone with very thin, longitudinal cavities. Further back, the brow region is extensively weathered, revealing larger trabecular cavities between the mineralised bone; the same is true of the lateral parts of the dorsal surface, and the ventral and postorbital surfaces. The trabecular cavities in all of

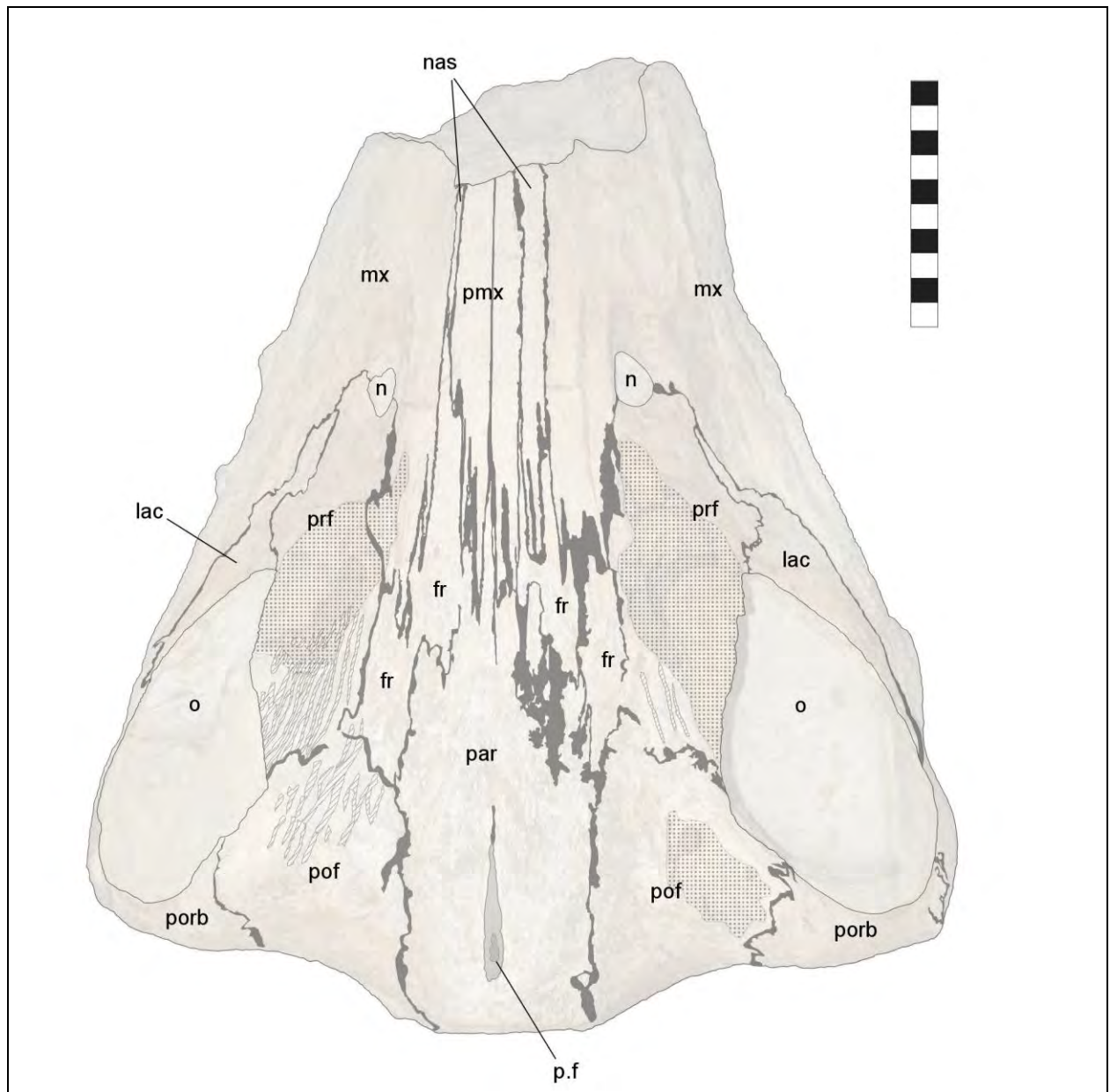


Figure 4-10: Interpretative diagram of Figure 4-9. Sutural surfaces shown as grey lines with solid in-fill. Labeled elements; parietals (par), frontals (fr), postfrontals (pof), postorbitals (porb), prefrontals (prf), lacrimals (lac), nasals (nas), maxillae (mx), and premaxillae (pmx). Labeled structures; orbits (o), external nares (n), parietal foramen (p.f). The lines shaded with diagonal stripes are the parallel structures in the supraorbital region: the three stippled areas indicate the regions of localised compression fractures (see text). Scale bar = 10 cm.

these are in-filled with grey limestone matrix: despite the weathering, sutural contacts can be traced as continuous layers of matrix which tend to have a slightly darker colour. On the lateral sides of the posterior rostrum, the maxilla bears a number of large foramina, aligned at a level near upper parts of the tooth roots, that run obliquely through the bone and which are in-filled with grey limestone. At the

anterior surface of the block, the nasal cavity is also in-filled with the grey limestone matrix.

Methods

The specimen was photographed by Jess Scott (University of Newcastle) using a Canon EOS 300D at various camera positions and focal lengths. Photographs were masked in PaintShop Pro.

Results

Figure 4-8 shows the specimen in dorsal, ventral, left lateral and right lateral views. Landmarks for use in compiling the skull reconstruction were traced on dorsal (Figure 4-32), lateral (Figure 4-34), and ventral (Figure 4-36) views.

A detailed description of the osteology in this remarkable specimen is under preparation. The preserved morphology can be summarised:

- The preserved external surface of the dorsal median ridge (DMR) is constructed from two pairs of elements that lie medial to the maxillae (Figure 4-9). By topological criteria, the median of these elements are the facial processes of the premaxillae, and the lateral elements are most likely to be the nasals; their presence has been noted by Druckenmiller and Russell (2008). The geometry of these elements is not symmetrical; the presumed left nasal much narrower than the left premaxilla, whilst the right nasal is of a similar width to the premaxilla.
- At the broken transverse anterior surface of the block, the two pairs of elements on the external surface of the DMR can be seen in cross section. Ventral to these, and apparently forming the internal surface of the DMR, are another pair of elements. The contacts between these and the surrounding premaxillae, nasals, and maxillae are clearly defined and are unequivocal (Figure 4-11). Their identity is at this point uncertain; they may represent anterior processes of the prefrontals or the frontals. Alternatively, from topology, i.e., lying

between the maxillae and nasals, they may be septomaxillae, but these elements have never been reported in the Plesiosauria.

- In anterior view, the nasal cavity has a hexagonal section, with the dentulous part of the maxilla forming a lower-lateral wall that is angled relative to the upper, nasal part of the maxilla. The ventral floor of the cavity is formed by the palate, and the upper horizontal roof by the internal surface of the DMR.
- The margins of the external nares are well preserved on both sides: they are formed from the maxillae anteriorly and the prefrontals posteriorly.



Figure 4-11: Oblique anterior view of QM F51291, showing close-up of the broken transverse section through the dorsal median ridge at the anterior surface of the block. The external elements of the dorsal median ridge are clearly separated from a pair of ventral elements. Original photograph by J. Scott.

- The orbital rim is completely preserved on both sides of the skull, although the compression fractures at the antero-medial corners have altered the shape of the margins slightly. There was evidently a supraorbital flange at this corner: this is better preserved on the left orbit. Along the weathered surface of each supraorbital flange, the faint remains of a series of parallel oblique-longitudinal grooves can be discerned (Figure 4-12).
- Although the postorbital wall has been largely removed by weathering on each side, the positions of the medial contact between parietal/frontal and postfrontal, and the more lateral suture between postfrontal and postorbital, can be seen on both sides. The position of the postorbital-jugal contact is indicated by small remnants of bone and a pyrite-filled suture at the postero-lateral corners of the orbital cavity.



Figure 4-12: Left side of QM F51291. Well preserved surface bone of the prefrontal (between the naris and orbit) contrasts with the roughed texture of a depression fracture of the supraorbital flange at the antero-medial corner of the orbit. Behind the flange, the weathered remains of parallel, longitudinal ridges can be seen near the dorso-medial apex of the orbital rim. The suture between the prefrontal and a ventro-lateral element – the lacrimal – is clearly marked in sideritic matrix: the more lateral contact between lacrimal and maxilla is in-filled with grey limestone. Original photograph by J. Scott.

- The brow region between the orbits preserves the heavily weathered surfaces of the parietals and frontals. These form strongly interdigitated contacts with the elements of the dorsal median ridge. The contacts between frontals, parietals, and prefrontals are difficult to make out, but the parietals appear to exclude the frontals from an external midline contact externally, although the latter likely contact internally (c.f. Andrews 1911).
- Lateral to the prefrontals, there is an element that makes up the antero-lateral margin of the orbit, and which is clearly separate from the maxilla and the jugal. From topology, it is identified as a lacrimal (Druckenmiller and Russell 2008): it is clearly visible on each side of the skull.
- The palatines contact each other along the midline in front of the long midline contact between the anterior parts of the pterygoids. The lateral surface of the pterygoids are heavily eroded and the extent of the ectopterygoids cannot be determined with confidence. The jugals, lacrimals, ectopterygoids, and pterygoids evidently contacted each other in the suborbital area and between them comprised the suborbital floor. There is no evidence of a sub-orbital fenestra. The midline contact along the ventral surface between the anterior pterygoids is weathered and the bone appears to have been thin at the midline, but there is no convincing evidence of an anterior palatal vacuity (‘anterior interpterygoid vacuity’ of Cruickshank 1994).
- The front of the inter-pterygoid vacuity, between the posterior rami of the pterygoids, is preserved: on the palatal surface, the anterior part of the parasphenoid can be seen where it contacts the pterygoids at the same point where the pterygoids meet in the midline at the front of the vacuity. At the posterior surface of the block, the parasphenoid can be seen in transverse section.
- The posterior rami of the pterygoids at the rear surface of the block can be seen to rise dorsally; on the left side, the anterior-most edge of the epipterygoid can be seen, along with its contact with the dorsal surface of the left pterygoid. The position of the dorsal part of the

anterior surface of the left epipterygoid appears to be preserved as a natural mould in the matrix infilling the post-orbital cavity, allowing the position of its contact with the left postfrontal to be discerned.

MCZ 1284

Specimen summary

Comprising an anterior rostrum ankylosed to an adducted anterior mandible, this specimen was collected from the Late Aptian Doncaster Formation of Grampian Valley Station, north of Richmond, by W. Schevill of the Museum of Comparative Zoology (MCZ), Harvard. The specimen was collected during 1931-2, at the same time as a larger and more famous specimen (MCZ 1285) that was recovered from the neighbouring property of Army Downs. White (1935) published an account of the skull material from the two Doncaster Formation MCZ specimens, but focused upon the material included in MCZ 1285.

Collection and preparation data has not been published, although records may exist in the Harvard University archives: some indeterminate material with the same catalogue number is held in the MCZ collection, but I was unable to identify what that represented, and it is not considered here. From the very weathered broken posterior surface, the main part of the specimen has been separated from the rest of the skull for some time prior to collection. The matrix is a dark grey, very hard micritic limestone. There is no obvious sign of manual removal of matrix, but the anterior-most part of the fossil was evidently cracked away from the rest and has been reattached using a dark grey putty; the same material has been used to consolidate some of the teeth on the left side. The rest of the fossil has been covered in a transparent lacquer. Unusually for large pliosaur body fossils from the Rolling Downs Group, the teeth are preserved, including large surfaces of enamel on the crowns.

The specimen is of particular interest because of the preservation of the anterior teeth and a complete premaxillary tooth count, as well as the mandibular symphysis: the dentition of the premaxilla and symphysis have been considered taxonomically relevant in several pliosaur taxa (e.g. Noè 2001, Noè et al. 2004, Tarlo 1960).

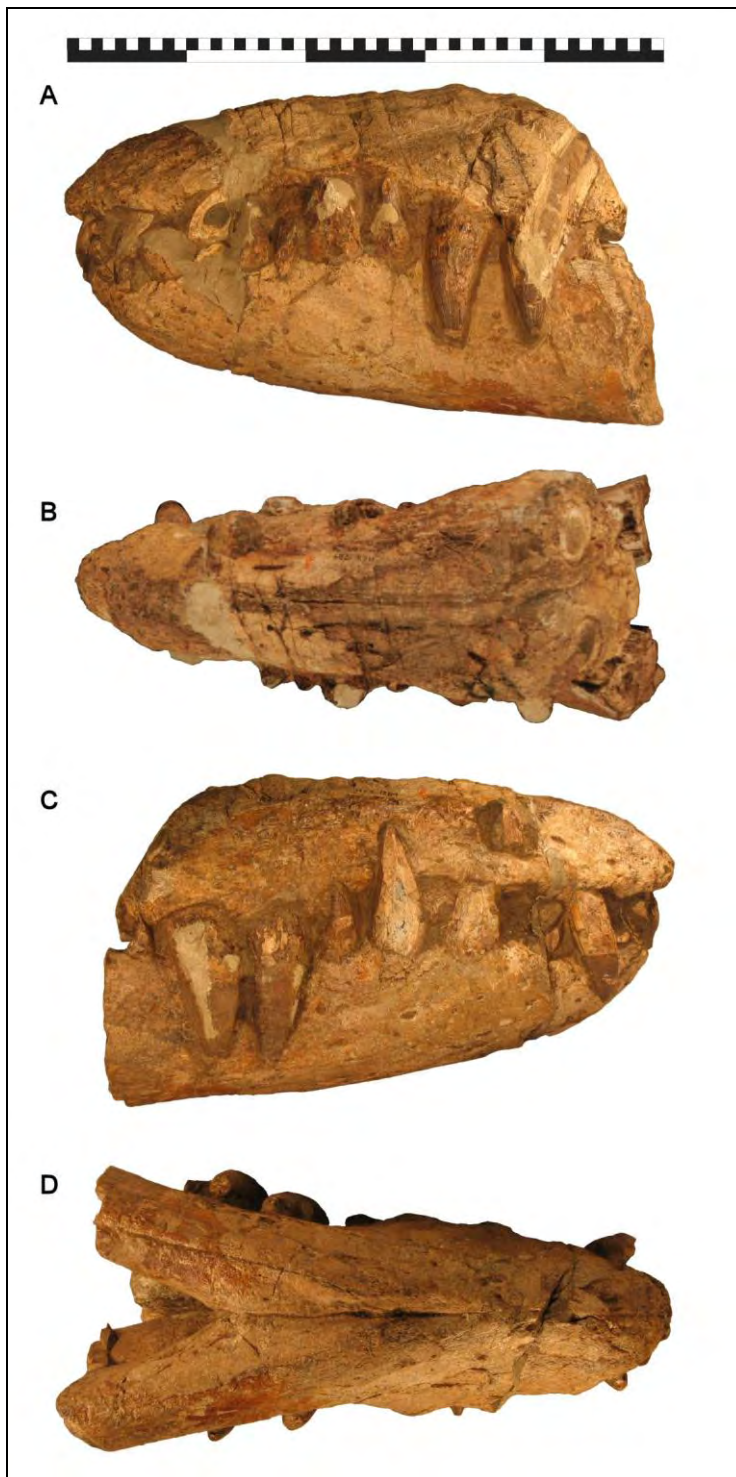


Figure 4-13: MCZ 1284 in (A) left lateral, (B) dorsal, (C) right lateral, and (D) ventral views. Scale bar = 50 cm.

Taphonomy

The broken transverse surface at the rear of the preserved jaws is heavily weathered, as is the dorsal surface, but the ventral surface of the mandibular symphysis is

reasonably well preserved. The jaws have been deformed in an oblique vertical axis; this is most obvious in posterior view (Figure 4-15), where the axis of deformation appears to have been from upper left to lower right. The eroded dorsal surface shows signs of the same longitudinal structures in the anterior nasal cavity as noted for QM F18827, and the remains of the premaxilla–maxilla suture can be discerned.

Some of the upper jaw teeth are partially out of their sockets. The division between the ornamented, enamel-covered crown and the paler surface of the dentine of the tooth roots lie some way from the bony margins of the tooth roots: The specimen appears to have been lying dorsal side up prior to burial. Presumably, the teeth started to slip out after the periodontal ligament and the cement decomposed.

The preserved enamel is fragile and is flaking away from the dentine, especially in the large anterior maxillary teeth.

Methods

The specimen was photographed whilst on loan from the MCZ. The orthogonal views were taken using a Canon Powershot A95 at 16 mm (lateral view) and 11 mm (ventral) focal length. Some earlier photographs taken using 35mm film were used for the dorsal view.

Results

The specimen is shown in dorsal, ventral, left, and right lateral view (Figure 4-13). Landmarks for use in the 2D reconstruction of the skull were traced for dorsal (Figure 4-32), lateral (Figure 4-35), and ventral (Figure 4-36) views.

The morphology as preserved can be summarised:

- The premaxillae each preserve four teeth. The tooth count of the mandibular symphysis cannot be determined precisely because it is adducted to the rostrum, but the spatulate anterior expansion bears five pairs of dentary teeth, as in QM F18827 and QM F10113, and the overall proportions of the symphysis are consistent with these.



Figure 4-14: Close-up of the right side of MCZ 1284, showing details of the ornament on the crowns of the (from left to right) D5, M1, and M2 teeth. Note that the ornament on the M1 tooth is finer than on the D5 crown. Note also the wear facet on the tip of D5.

- The sequence of teeth, from the tip of the snout, is; Pmx1, D1, Pmx 2, D2, Pmx 3, D3, Pmx 4, D4, D5, M1, M2: i.e., identical to the pattern in QM F18827. As with QM F18827 and QM F10113 specimen, the D4 and D5 are the largest teeth of the anterior mandible, while the M1 and M2 are the largest teeth preserved. The crowns of M1 and M2 are approximately 11 cm in length; the enamel bears an ornament consisting of longitudinal ridges (Figure 4-14). The teeth are circular in section, with no carinae.
- The tip of D5 on the left side appears to be worn: whether from occlusion, or a rework break, is uncertain. The tips of several other teeth are broken, although this may be taphonomic.
- At the broken posterior surface, the transverse section of the vomer can be seen (Figure 4-15): it is 'cupped' so that the ventral surface is convex and the dorsal (internal) surface is concave. It is possible that this shape has been exaggerated by the sedimentary distortion affecting the fossil, but it seems to at least partially reflect the true shape of the vomer at this point. There is a cavity above the vomer and between the medial internal surfaces of the premaxillae: this

cavity has the section of a tall, narrow triangle, and its dorsal edge is exposed by weathering of the dorsal surface of the fossil.

- The contact between dentary and splenial bones can be clearly seen along the ventral surface of the symphysis and anterior mandibular ramus on each side. At the posterior surface of the broken mandible, the matrix-filled Meckelian canal can be seen in the lower part of the rami: it is bounded by the splenial medially, the dentary ventrolaterally, and the underside of the dentary tooth row dorsally.



Figure 4-15: Posterior view of MCZ 1284, showing the taphonomic distortion of the fossil and the shape of the dorsal edge of the vomer, seen in transverse section on the rear surface of the block. The inner surfaces of the maxillae and vomer enclose a vomerine cavity, which is the anterior part of the nasal cavity.

QM F2446*Specimen summary*

In 1935 a large quantity of fossils were collected from the region of Telemon Station, west of Hughenden, by J. Edgar Young: this material includes a number of marine reptile fossils from the Toolebuc limestone, which are catalogued as QM F2446–F2455. The material includes two ichthyosaurs; most of the rest is identified in the catalogue as referable to *Kronosaurus*, but at least one (QM F2449) is referable to the Elasmosauridae. Some specimens may be catalogued under more than one number, reflecting uncertainty surrounding their collection. As identified by Longman (1935), there are two important specimens of *Kronosaurus* included within this material, each comprising partial skull material from what must have been large individuals; QM F2446, and QM F2454.

QM F2446 comprises a large block containing the anterior orbital region, as well as other fragmentary material, the most important of which is an apparently undistorted occipital condyle and partial braincase. The present account focuses upon the orbital block: this was figured by Molnar (1991 – reproduced here as Figure 4-16) who noted that its relatively flat profile was in contrast to that of the mounted skull of MCZ1285. Molnar interpreted the QM F2446 orbital block as being relatively free of crushing, and thus concluded that the two specimens may represent different taxa: since QM F2446 was collected from the same Albian strata as the holotype of *Kronosaurus queenslandicus*, whilst MCZ 1285 comes from the older Aptian Doncaster Formation, Molnar considered that QM F2446 belonged to the type species. Molnar's figure of skull proportions in *Kronosaurus queenslandicus*, based upon his interpretation of QM F2446, was repeated by Hampe (2005) in an examination of skull proportions in large pliosaurs.

The matrix is a hard, dirty, mid-grey micritic limestone. The orbital block from QM F2446 has been mechanically prepared, evidently by chisel, some time prior to the 1990s, to reveal the internal walls of the right orbit (Figure 4-18). The area around the right external nares has also been prepared. The surfaces of fossil bone visible at this time were consolidated with an unknown lacquer. Some further mechanical

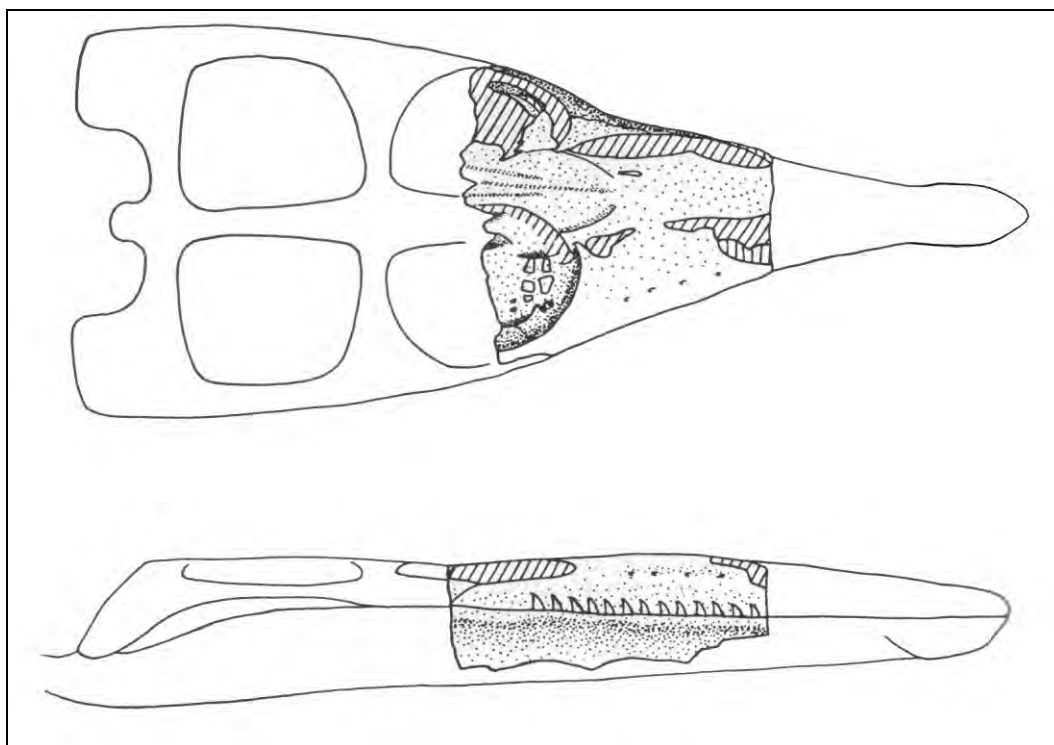


Figure 4-16: Reconstruction of *Kronosaurus queenslandicus* based upon QM F2446, reproduced from Molnar (1991).

preparation of the ventral surface of the right pterygoid, using pneumatic hand drills, was attempted in 1996-1998, and newly exposed bone was consolidated with Paraloid™.

The specimen preserves the pliosaur orbital region, an anatomical region that is poorly understood. The apparent large size of this individual is also of interest for attempts to describe maximum size in *Kronosaurus*.

Taphonomy

The block is extensively weathered on the dorsal surface. The lower jaws are preserved adducted to the cranium, but have been largely removed by weathering to the lateral surfaces of the block. The right side preserves only impressions and thin remnants of the lower jaw tooth row and the medial edge of the mandible bones: the left preserves more complete tooth roots and a substantial part of the surrounding bones of the lower jaw. The ventral surface of the cranium is covered in a thick layer of limestone matrix: the outer surface is discoloured to a red-brown, compared with

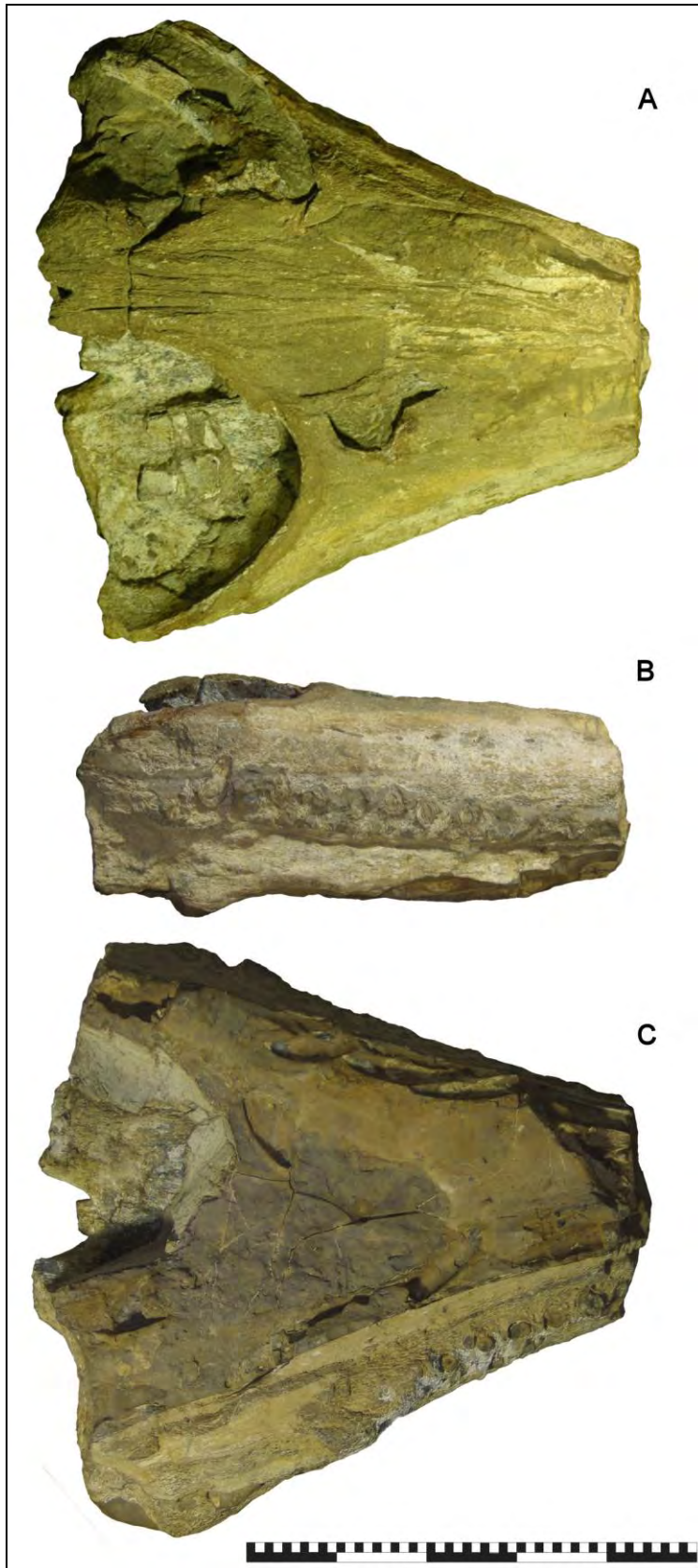


Figure 4-17: QM F2446 in (A) dorsal, (B) right lateral, and (C) ventral view. Scale bar = 50 cm.

the grey of the rest of the matrix, and preserves the impressions of disarticulated teeth, which have presumably fallen out from the upper jaw as the lower jaw teeth from these part of the skull are still in their sockets. Each impression forms a mould of one side of the tooth: some of these have thin layers of enamel and dentine attached (Figure 4-19). Given the heavy weathering of the dorsal surface of the block, and the presence of disarticulated upper jaw teeth below the cranium, the specimen appears to have been buried dorsal-side up. The current external surface of matrix covering the ventral surface may represent a layer of sediment close to or at the palaeo sea floor at the time that the specimen settled on the bottom.

The dorsal skull roof has been extensively weathered, and most of the original thickness of the roof bones seems to have removed. On both sides of the midline, the nasal part of the maxilla has been eroded so that the matrix-filled nasal cavity is revealed in places; this, combined with the original preparation of the right side in front of the orbits, makes precise location of the external nares difficult. The original height of the mid-nasal ridge has been almost completely removed. The inter-orbital brow region is sheared to the left; the midline of the roof, located by the preserved anterior end of the parietal foramen, lies approximately 10 cm to the left of the



Figure 4-18: Oblique dorsal view of the bones forming the antero-lateral wall of the right orbit in QM F2446. The lacrimal is visible in the centre of the image, bounded by the jugal (right), prefrontal (left) and ectopterygoid (below). A disarticulated sclerotic plate is visible in the middle of the lower half of the picture.



Figure 4-19: External mould of one side of a tooth, preserved in the matrix of the ventral surface of QM F2446. A thin layer of the fossilised enamel is adhered to the matrix in the region of the tooth crown. Scale on the edge of the rule closest to the tooth is in centimetres.

midline of the palate. Accompanying this shearing, the roof bone at the antero-medial corner of the left orbit is fractured so that the medial part of the orbit rim has been shifted sideways: the antero-lateral wall, marked by the eroded surface of the lacrimal and lateral part of the prefrontal, is not as displaced. On the right side, the bone of the antero-medial orbital rim has been pulled leftwards from the antero-lateral rim: the two parts are separated by a fracture, more or less in the sagittal plane, near the anterior apex of the rim. The displacement of the brow roof relative to the palate and lateral margins of the posterior rostrum appears therefore to have been a result of brittle rather than plastic failure: the taphonomic stage at which this failure occurred is as yet unknown.

Although heavily weathered, the skull roof preserves sutural contacts between its component elements as a matrix that has a slightly darker colour than the rest of the matrix surrounding the fossil. This matrix appears to have been slightly harder than the adjacent bone, as it has weathered slightly proud of the bone surface. The in-filled sutural layers are angled steeply, almost to the sagittal plane., and although erosion makes them difficult to interpret, the three dimensional relationships of the elements that formed the brow and its contact with the dorsal median ridge were evidently complex.

The left orbit is filled with matrix, and contains a large fragment of bone that is separate from the skull, and a large ammonite that has been recrystallised in calcite. The latter is lying nearly horizontally directly on top of the palatal bones that form the sub-orbital floor, and has been sectioned by the broken transverse surface at the rear of the block. On the suborbital floor of the right orbit, the disarticulated sclerotic plates of the right eye lie directly upon the dorsal surface of the palatal bones.

The broken transverse surfaces at front and rear of the block show some signs of weathering, although there is more at the rear than the front, which appears to have become only recently separated from the anterior rostrum.

Methods

The orbital block of QM F2446 was photographed in orthogonal views using a Canon Powershot A95 at 16 mm focal length for the ventral view, 14 mm for the lateral view, and a Nikon D70S at 48 mm focal length for the dorsal view.

Results

The orbital block of QM F2446 is shown in dorsal, ventral, and left lateral view in (Figure 4-17). Outlines tracing landmarks for use in the 2D skull reconstruction (Section 4.5) were traced for dorsal (Figure 4-31), lateral (Figure 4-34), and ventral (Figure 4-36) views.

Although heavily weathered and somewhat distorted, the specimen preserves several features of interest to an understanding of the orbital/ posterior rostral region of the cranium in *Kronosaurus*. A detailed description of the preserved osteology is in preparation; for the present study, the salient morphological features can be summarised:

- The specimen appears to preserve the suborbital/ posterior rostral part of the palate better than any other specimen of *Kronosaurus*, although the matrix which has thus far protected the bone obscures the morphology. Given the potential taphonomic information also

preserved in the matrix, careful consideration should be given to the curation of this specimen: in particular, non-destructive techniques (such as CT scanning) should be considered.

- At the broken anterior face of the block, the paired palatines can be seen in transverse section: these form a dorsally concave surface that is thinnest at the midline, where the bone is ~4 cm thick in the vertical axis. The midline contact is weakly interdigitate across the sagittal plane. The palatines contact the dentulous part of the maxilla laterally: there is no evidence of the anterior parts of the pterygoids at this point.
- The preserved part of the dorsal median ridge has been weathered, but the sutural contacts can be seen. Near the midline, there appear to be at least one pair of median elements (premaxillae?), which lie above a pair of ventral elements: this is consistent with the morphology preserved in QM F51291 and QM F10113.
- From the antero-medial orbital rim, the roof bones of the brow narrow anteriorly to the point where they contact the dorsal median ridge elements; in dorsal view, the impression is of a wedge-shaped structure. The anterior edge is interdigitate across the transverse plane, consistent with the strongly interdigitate contact that can be seen between the brow elements and the dorsal median ridge in QM F51291.
- The weathered surface of the brow between the anterior parts of the orbits appears to preserve a coronal section of the brow. At least three pairs of elements can be seen; from medial to lateral, a pair of elements that form the anterior rim of the parietal foramen and which may thus be the parietals, then the frontals, and most laterally the prefrontals. The contacts between these are nearly vertical (in the sagittal plane).
- At the preserved medial edge of the orbits, there is a surface of bone that slopes downwards and medially towards the palate; its lower edge is broken. The rim of the orbit is damaged, but in QM F51291 is formed by the prefrontal and postfrontal. The medial 'wall' visible in

QM F2446 may be the ventral flange of the frontal described for QM F10113.

- The preparation of matrix from the right orbit has exposed the bones forming the antero-lateral wall of the orbit. Although the taphonomic damage to the antero-medial part of the orbit makes interpretation more complex than might be expected from the excellent preservation of the lateral part, there appears to be a suture between the right prefrontal and the element that forms the lateral part of the anterior wall and which must be the lacrimal (Figure 4-18). The contact between the lacrimal and the jugal, which forms the lateral wall of the orbit, is marked by a layer of matrix: this contact can be followed on the dorsal surface of the roof bones in front of the right orbit for at least a few centimetres anteriorly, despite the weathering of this region, but anterior to this point is harder to discern, either because of weathering or fusion of the suture.
- Within the orbit, the postero-ventral edge of the lacrimal contacts an element that forms the lateral part of the sub-orbital floor and which, as it appears to be separate from the pterygoid, must be the ectopterygoid. At the medial part of the sub-orbital floor, there is a narrow, longitudinally running ridge on the dorsal surface of the pterygoid.
- The lateral part of the pterygoids are preserved in transverse section at the broken posterior edge of the block: here, they are thick and apparently form a robust lateral buttress of the pterygoid at this point. Medially, the anterior part of the inter-pterygoid vacuity is preserved, including the anterior tip of the parasphenoid and the junction between the anterior parts of the pterygoids and the posterior rami of the pterygoids that lie on each side of the vacuity. These latter were evidently robust structures: in transverse section at the broken rear surface of the block, the posterior pterygoid rami form a strong ventral keel and a smaller dorsal ridge.

QM F2454

Specimen summary

Collected as part of the same series of fossils as QM F2446 (see above), this specimen also comes from the Toolebuc Formation of Telemon Station, west of Hughenden (Longman 1935). QM F2455 is noted in the catalogue as perhaps representing parts of the same individual, but I have not been able to determine whether or not that is the case. QM F2454 comprises a large quantity of skull material from what appears to have been a very large pliosaur, including a block that preserves the occipital condyle and the braincase, and another comprising a partial quadrate that is ankylosed to the articulated glenoid of the mandible. Several large blocks, representing the orbital and posterior rostral region of the skull, can be assembled by 'click fit' of the broken surfaces, although a large number of fossil/matrix fragments have yet to be assembled.

The fossil is preserved in a mid-grey micritic limestone matrix similar to that of QM F2446. There has evidently been some preparation of the ventral side of some of the blocks preserving the rostral region. Along with the apparent large size of this individual, this specimen preserves some important features of the palate that have been partially revealed by this preparation.

Taphonomy

The skull is heavily compressed in the vertical axis by sedimentary compaction; the roof bones of the posterior rostrum are nearly touching the bones of the palate in most places. Although the lateral surfaces of the tooth margins are heavily weathered, many of the dorsal and ventral surface are comparatively well preserved and extensive areas of surface bone can be seen. Most of the broken surfaces show little signs of weathering and the fossil appears to have fragmented relatively recently prior to collection.

Methods

The blocks comprising the posterior rostrum and orbital region were assembled in a sand-tray and photographed in ventral and dorsal view, using a Canon Powershot

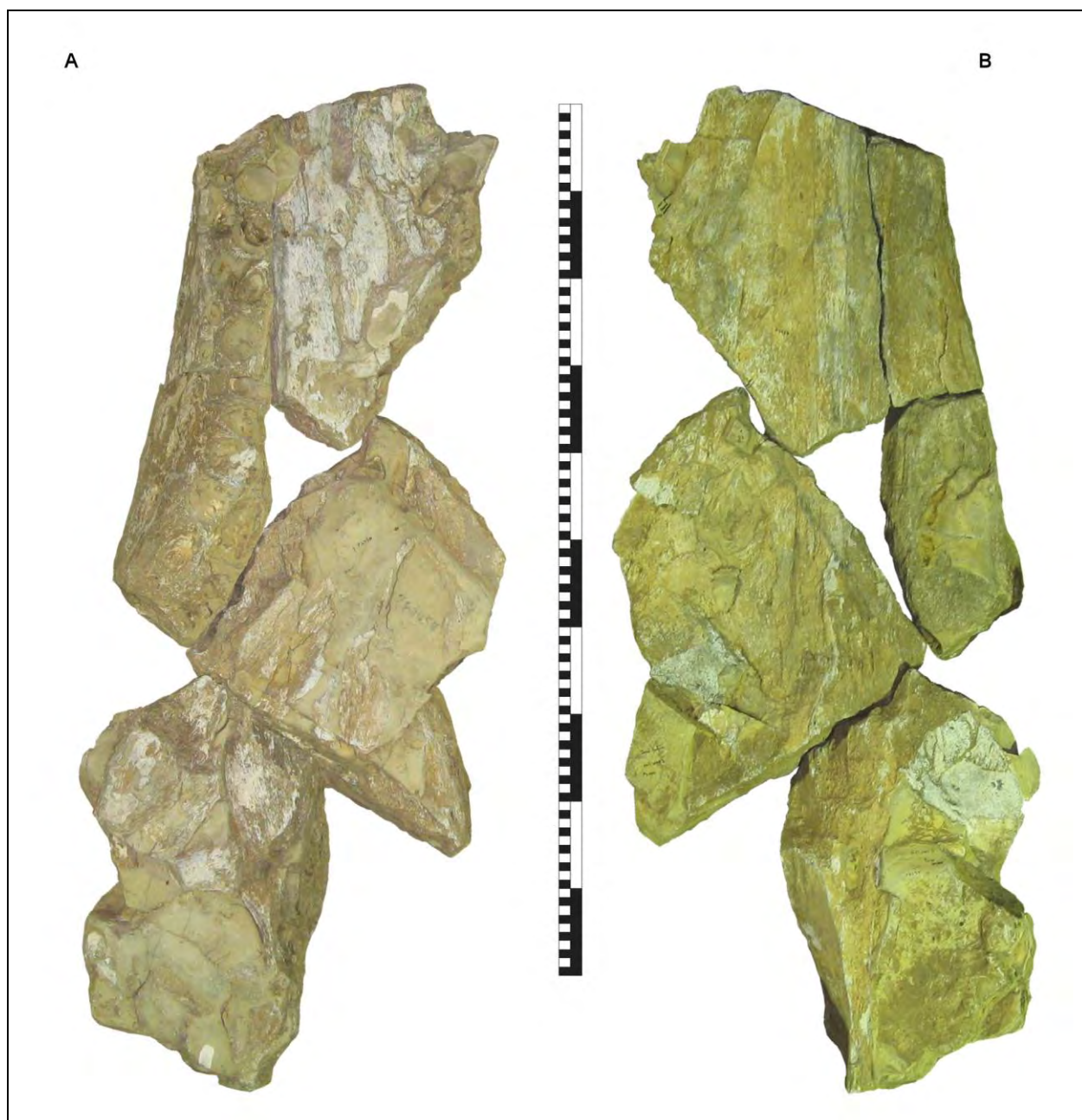


Figure 4-20: Assembled orbital and posterior rostral blocks of QM F2454 in (A) ventral and (B) dorsal view. Scale bar = 1 metre.

A720. The dorsal view was taken in a single shot at 8 mm focal length; the ventral views were photographed at 17 mm focal length and processed into a photo-mosaic.

Results

The specimen is shown in dorsal and ventral orthogonal views (Figure 4-20): landmarks for use in the 2D reconstruction were traced in dorsal (Figure 4-31) and ventral (Figure 4-36) views.

This specimen is both the largest and the most crushed of the *Kronosaurus* material collected from the Rolling Downs Group: however, it preserves many important anatomical features, particularly around the braincase. These will be the focus of future work; at present, the morphology can be summarised:

- The left internal naris is visible on the palate: although the internal nares are probably preserved in QM F10113 as well, they are obscured by matrix in that specimen, and QM F2454 is the only Queensland Museum specimen in which at least one of the internal nares is visible (Figure 4-21).
- The posterior-most part of the vomer is expanded in ventral view: the posterior edge approximates a semi-circle in outline, convex posteriorly. The front of the posterior expansion forms the posterior-medial edge of the naris; the medial and lateral borders are formed by the vomer and maxilla respectively, and the anterior border is not well preserved but is presumably formed from these two elements. The bone forming the postero-lateral border is cracked, but appears to have been part of the maxilla: the palatines, whose anterior edge is close to the naris, appear therefore to have been excluded from forming any part of the margin.
- At the midline between the preserved anterior parts of the palatines, immediately behind the vomer, is a long, narrow gap that is filled with matrix. Given the extensive taphonomic distortion of this specimen, it is uncertain whether this represents a real palatal vacuity.
- On the dorsal surface, the proximal part of the post-orbital bar is well preserved: the surface bone appears to be intact over a large part of this, and the contact between postfrontal, frontal, and prefrontal is clearly visible (more so than in any other specimen).
- The parietal foramen and sagittal crest are preserved without obvious crushing, but some weathering. The top of the crest narrows considerably: the preserved surface is a result of fragmentation, and there is no evidence that the actual surface of the crest was a blunt,

rounded upper edge. It is possible that the crest continued dorsally to form a tall, narrow crest, as can be seen in FHSM VP-321.

- The posterior rostrum is crushed and weathered: the mid dorsal ridge is not raised relative to the maxilla (i.e. there is no ridge preserved). In dorsal view, only one pair of elements between the maxillae are visible on the dorsal surface: these appear to be the facial processes of the premaxillae.



Figure 4-21: Close-up of block from QM F2454, showing front-most part of preserved palate. The block is oriented so the anterior is at the upper right. The left internal naris (i.n) is preserved, surrounded by the vomer (vom), left maxilla (l.max), and left palatine (l.pal). Between the left palatine and the right palatine (r.pal) is a longitudinal midline gap (mid): this may be a result of taphonomic distortion, or may indicate a real structure.

QM F18154

Specimen history

This specimen was found, and donated to the Queensland Museum, in 1990 by Charles Robinson at Canary Station, Boulia. Like many of the other specimens listed here, it derives from the Toolebuc Limestone: however, it is the only specimen from the Boulia region considered here. Boulia is several hundred kilometres south-west of the Richmond–Hughenden exposures of the Toolebuc; the preservation of marine reptile fossils from Boulia is characterised by a strong yellow/orange/red colouration of the fossils and carbonate matrix, and there is often extensive re-crystallisation of calcite which can replace the original fossil bone and make morphology difficult to interpret.

The specimen comprises a medium sized, incomplete skull and associated cervical and pectoral elements, including vertebral centra and the proximal heads of two propodials that are presumably humeri. It has not been prepared. Although it is strongly weathered, there appears to be little evidence of sedimentary compaction and for this reason the blocks containing the orbital region and posterior rostrum were included in the present study.

Taphonomy

The specimen is strongly weathered: there is no surface bone remaining on any of the surfaces of the fossil blocks. Extensive secondary crystal growth within the matrix and fossil bone has destroyed many morphological features, making interpretation of the osteology difficult. As noted above, however, the specimen appears to be largely free from the effects of sedimentary compaction.

The skull has fragmented into large blocks of fossil and matrix: the orbital and posterior-rostral region is preserved in two of these blocks. Soft tissue structures, specifically, the fronto-parietal sutures and the parietal canal, have been in-filled with a hard matrix and the weathering of the dorsal surface has removed the bone from around them: their smooth texture makes them stand out from the eroded parietal and circum-orbital bones. At the rear end of the block, the dorsal internal surface of the bottom of the parietal canal is preserved as an internal mould (Figure 4-23).

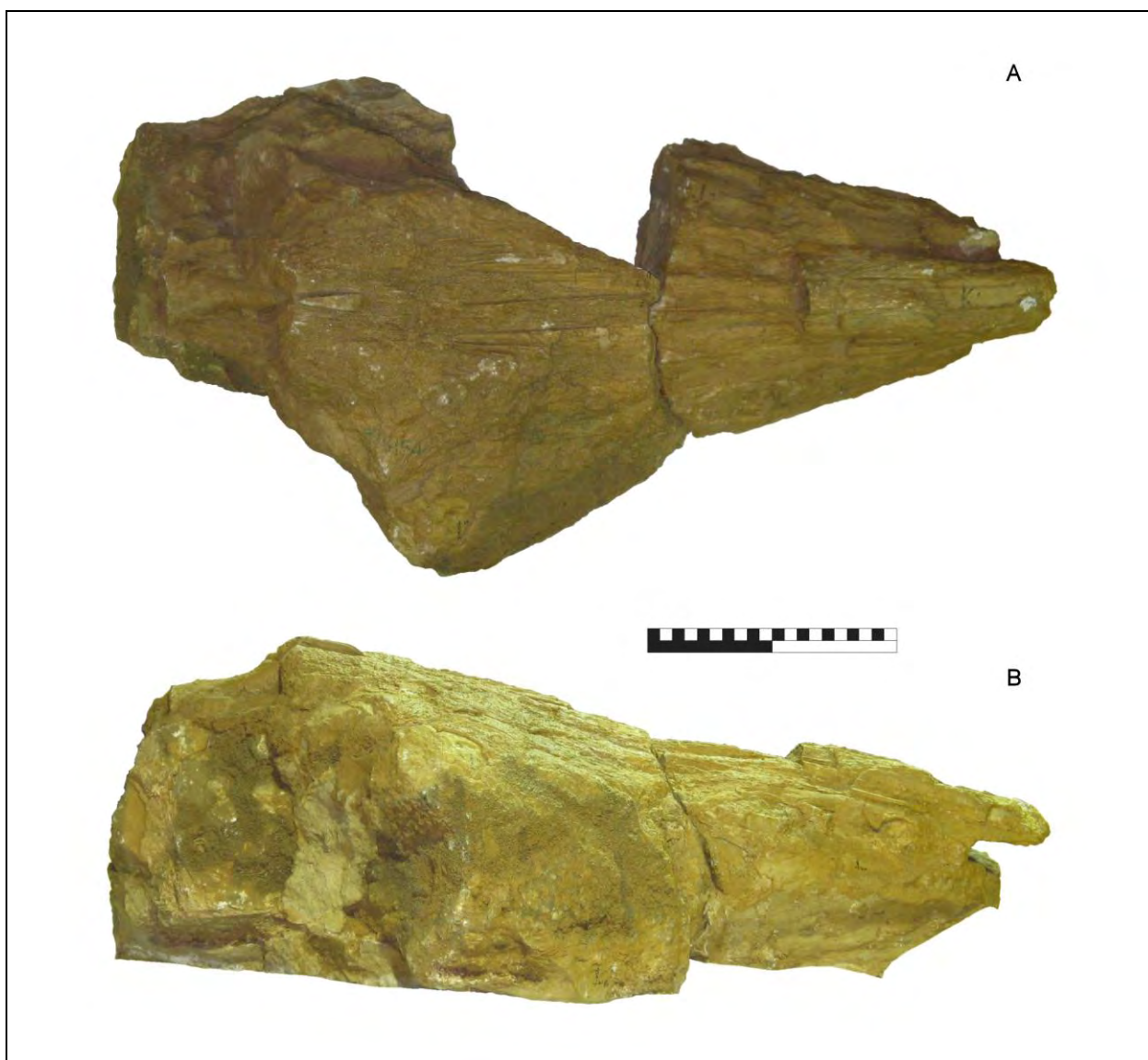


Figure 4-22: QM F18154 in (A) dorsal and (B) right lateral views. Scale bar = 20 cm.

Methods

The blocks comprising the orbital and posterior rostral region were photographed in dorsal and lateral orthogonal views using a Canon Powershot A720 at a focal length of 15 mm.

Results

The two blocks containing the orbital and posterior dorsal region of the cranium are shown in dorsal and right lateral view in Figure 4-22. Landmarks to be used in the



Figure 4-23: QM F18154: weathered surface of parietals in (top) dorsal and (below) oblique posterior view. Note the 'fan' shaped appearance of the anterior parietals, and the complex sutural surface with the underlying frontals/ prefrontals. In the oblique posterior view, the endocast of the parietal stalk is proud of the eroded margin of the parietal foramen; behind this, an endocast of the anterior brain can be seen at the rear edge of the block.

2D reconstruction of the skull were traced over the dorsal (Figure 4-31) and lateral (Figure 4-34) views.

The erosion and growth of secondary crystals make interpretation of the osteology in this specimen challenging. In the context of the present study, the most relevant morphological features are:

- The epipterygoids are preserved at the broken posterior surface of the larger block: they are somewhat weathered but the geometry of their anterior portion can be seen.
- The in-filled parietal canal preserves an endocast of the parietal stalk. The upper surface of the matrix in-fill lies approximately 1 cm above the surface of the surrounding eroded bone: it may represent the original position of the parietal foramen.
- The sutural surface preserved at the anterior margin of the parietals (i.e. in front of the parietal foramen) shows the complexity of the fronto-parietal contacts of the brow (Figure 4-23). On each side of the midline, the sutural surface is interdigitate in an oblique transverse plane, and also in the coronal plane. From above, the bone lying on top of the sutural surface makes the 'fan' shaped wedge that can be seen in the same region of QM F2446.
- The bone around the external nares is highly eroded: the margins of the nares can be made out, and are proportionately large, although this may have been exaggerated by weathering.

QM F52279

Specimen summary

This specimen was collected from Lydia Downs Station, north-west of Richmond, by Alan Bartholomai: it is from the Toolebuc Formation. Various fragments of skull were recovered, including a large block containing the orbital region of a small-medium sized individual. Remarkably, a series of vertebrae, from a large lamniform shark (S. Turner, pers. comm.) are preserved in the right orbit and alongside the posterior right jaw margin.

The matrix is a medium grained orange-red coloured micritic limestone with extensive coverings of a darker red sideritic mineral, i.e. very similar to that of QM F10113 (although the average grain size may be slightly larger in QM F52279). Throughout the matrix there are fragments of bivalve shell, mainly inoceramid, of various size and orientation. The cranium is distorted by sedimentary compaction, but preservation of the bone is good. The orbital block does not appear to have any components of the mandible adducted to or associated with it, although the right jaw margin is obscured matrix and it is possible that some parts of the mandible are preserved within that matrix. There has been no preparation of the specimen.

The preservation of the orbital region in this specimen, the intact external surface of bone on the dorsal skull roof, and the association with the shark vertebrae make this specimen of particular interest.

Taphonomy

The dorsal surface is almost entirely free of matrix, and the surface bone of the skull roof is eroded but preserves the external surface of the brow region reasonably well. The skull has been distorted by sedimentary compaction in the dorso-ventral and transverse axes, so that the roof of the skull is sheared sideways and down relative to the palate: the axis of compaction is from the dorsal right to the ventral left, and the midline of the brow has been folded down onto the left orbit.

The palate is still largely covered by matrix, except for the anterior part of the left pterygoid which is weathered posteriorly and has been completely removed anteriorly, leaving a natural mould of its dorsal (internal) surface on the matrix within the skull. The matrix on the ventral surface contains a large amount of inoceramid bivalve shell; most are small fragments with non-uniform orientation, but under the left orbit there are a few layers of larger remnants of shell which are parallel and which may be *in situ*. This, with the grain size of the carbonate matrix, suggests some amount of energy in the depositional environment, although the inoceramid shells may also have been bioturbated by arthropods (Henderson 2004). Where the left pterygoid has been broken and eroded, clumps of calcite crystals can be seen.

The matrix that in-fills the nutritive foramina in the palate is invariably the dark-red siderite: this is a diagenetic product of pyrite, and suggests the processing of nutrient-rich (in particular, iron) organic matter in a low-oxic environment by chemotrophic Bacteria and Archea (Chapter 3), as can be seen in the decomposition of Recent whale carcasses (Allison et al. 1991).

The broken anterior and posterior surfaces of the block are slightly weathered, suggesting that the fossil fragmented some time before discovery, but not so much that click-fits with adjacent fragments would be obscured if these were available. However, at the ventral rear-right corner of the block, there is a geometrically complex element lying behind the lateral process of the right pterygoid, i.e. in the lower temporal arcade. It has a complex shape, and the eroded and fractured surface makes interpretation difficult, but it appears to be a vertebra from the pliosaur, and is perhaps the fused atlas-axis.

In front of the right orbit, at the margin of the upper jaw, there are the remains of a small bone that appears to have been lying in contact with the skull roof at burial. It is mostly weathered away, but may have been a phalange.

The association of this fossil with the lamniform vertebrae is certainly of interest (Figure 4-25). Perhaps eight vertebrae are preserved; three in the right orbit of the *Kronosaurus*, and at least five next to the posterior margin of the upper jaw on the right, just lateral to the right orbit. Only the centra are preserved; these are disc-shaped, of a consistent diameter (~7 cm) and length (~2 cm), with shallow concave anterior and posterior faces and an ornamented outer surface consisting of longitudinal, parallel and evenly-spaced robust ridges. The vertebrae have been disturbed so that they are not all articulated, and although two vertebrae in the orbit and at least two at the jaw margin appear to be in natural sequence, there is some slippage between all of the vertebrae, and at three points the faces of adjacent vertebrae are at 90° to each other.

Preservation of stomach contents with reptile fossils from the Rolling Downs Group is not uncommon (McHenry et al. 2005; see also summary of QM F10113 above, and Chapter 8), and one of the factors supporting interpretation of association



Figure 4-24: QM F52279 in dorsal view. Scale bar = 20 cm.

between large reptile and smaller vertebrate and invertebrate fossils as evidence of trophic interactions is that the depositional environment of the Toolebuc and Doncaster Formations tend to be characterised by low energies, reducing the chances of non-trophic post-mortem association. In this context, it is perhaps tempting to interpret the association of the lamnid and the pliosaur in this fossil as representative of feeding relationships, although it is not immediately obvious who would have been feeding on whom: the size of the vertebrae suggest a large shark, perhaps 5 m or more and thus of a potentially similar size to the pliosaur. Arguing against the trophic interpretation, the actual stomach contents of the pliosaur are unknown: the shark vertebrae are preserved in association with the pliosaur's head. Of course, it is possible that pliosaur died with the shark in its mouth – fossil *Xiphactinus* are known from the Kansas Upper Cretaceous Niobrara Chalk with whole fossils of large fish stuck in their gullet, with an over-ambitious appetite being the presumed cause of death – but the shark vertebrae associated with QM F52279 do not actually lie within the buccal cavity: they are to one side of the jaw, and within the orbit. Given that the palate underneath the orbits is essentially closed, it is difficult to see how something originally held within the mouth could end up being fossilised within the orbit of a



Figure 4-25: Close up of right orbit of QM F52279, showing lamnid shark centra lying within the orbit and adjacent to the jaw margin. Rule on right side of image shows centimetres.

Kronosaurus. In view of the apparently high energy of the depositional environment for this fossil, and the relatively light weight of lamniform vertebrae, it may be possible that the association of shark and pliosaur in this case is not a result of trophic interactions, but instead of post-mortem taphonomic association (A. Cook, pers. comm.). The presence of a vertebrae from the pliosaur within the temporal region of the skull suggests that there was appreciable post mortem disturbance of the skeleton, to a degree not seen in the other specimens considered here.

Methods

The block containing the orbital region was photographed in dorsal view using a Canon Powershot A95 at a focal length of 10 mm.

Results

The specimen is shown in dorsal orthogonal view in Figure 4-24. Landmarks for use in the 2D skull reconstruction were traced in dorsal view (Figure 4-32).

The specimen preserves several anatomical features of interest, and the osteology it preserves warrants detailed description in future work. The matrix seems to be less

hard than in some other specimens, and may respond to mechanical preparation without damaging the fossil bone: if so, preparation of the palate would be of interest. The morphological features currently visible in the specimen can be summarised:

- The surface bone of the brow, in front of the parietal foramen and between the orbits, has a series of longitudinal ridges running between the parietal foramen and the interdigitate suture between the fronto-parietals and elements of the dorsal median ridge. These ridges may be a result of the taphonomic distortion affecting the fossil, but seem to represent a real morphology.
- The parietals form a pair of shallow ridges that enclose each side of the parietal foramen.
- The length of the interdigitations on the dorsal surface seems relatively shorter than those preserved on QM F51291.
- The dorsal median ridge forms a markedly distinct ridge from the surfaces of the maxilla on either side, as with QM F51291 but unlike QM F2454. At the anterior end of the preserved mid dorsal ridge, on the external surface there are clearly two elements between the midline and the left maxilla: these are interpreted as the premaxillae (medial) and nasal (lateral). The left nasal is narrow (in the transverse axis), but in transverse section at the broken face is deep (in the dors-ventral axis). The bones of the right side of the ridge are difficult to interpret because of crushing and weathering, but there do appear to be two elements between the midline and the part of the maxilla that forms the dorsal margin of the right naris; if so, then these are both larger than the corresponding elements of the left side. This may be an artefact of taphonomy, but asymmetry in the dorsal median ridge elements was noted for QM F51291.
- Ventral to the elements that form the external surface of the dorsal median ridge, on the broken anterior surface there is more bone lying dorsal to the matrix that in-fills the nasal cavity. This is of a much lower density than the elements that make up the dorsal surface, but

has a large section and is twice the height of the external elements.

Whether it is a single element, or a pair of bones, is unclear.

- The external nares are large, oval shaped structures. The cracking of the surface bone around them makes the osteology of their margins difficult to interpret, but the nares are separated from the dorsal median ridge and if the lateral external element of the ridge is indeed the nasal, this makes no contribution to the margin of the naris on either side; i.e. similar to the morphology of QM F51291.
- At the dorso-medial apex of the orbits, there is a strong supraorbital ridge: as with the dorsal median ridge, this seems to have resisted the crushing affecting the rest of the skull roof slightly better than the bones of the nasal walls. That the bone underlying the supraorbital ridge may have been supported by a boss of the prefrontal on the internal (ventral) surface of the skull roof is suggested by the preservation of QM F10113.
- The pterygoids develop a ventral keel, running longitudinally, just in front of the inter-pterygoid vacuity: this keel deepens posteriorly to form the ventral edge of the posterior ramus on each side of the vacuity, similar to the morphology preserved in QM F2446. On the dorsal side of the posterior ramus of the pterygoid, the epipterygoids form narrow columns that ascend to the medial part of the postorbital wall: they are oval in section, with a much greater diameter in the longitudinal (anterior-posterior) axis than in the transverse.
- The right pterygoid preserves some of the lateral pterygoid buttress underneath the postorbital wall, although the original shape of the buttress has been removed by weathering.
- The preserved right pterygoid and palatine, and the mould of the dorsal surface of the anterior part of the left pterygoid, preserve several large nutritive foramina. On the left side, these are preserved as raised 'bumps' in the smooth surface of the matrix: on the right side, they are in-filled with dark red, sideritic matrix.
- The anterior-most extent of the pterygoids appear to lie at the broken anterior edge of the block. At this surface, the contact

between the right palatine and maxilla can be seen in transverse section.

- On the broken left side of the block, the posterior part of the upper jaw margin has been fractured, revealing a parasagittal section of the skull just in front of the left orbit. The crescent shape of the ventral process of the prefrontal can be seen forming the medial part of the anterior orbital wall.

QM F1609

Specimen history

The holotype specimen, this is a fragment of the mandibular symphysis that was discovered by A. Crombie, a school teacher in Hughenden, several kilometers to the south of the town, and sent to the Queensland Museum in Brisbane in 1899. From the description of the location of the find, it is certainly from the Toolebuc Formation of the Hughenden area. Longman (1924) identified it as representing the jaw of a large pliosaur, and founded the name *Kronosaurus queenslandicus* upon this specimen.

Taphonomy and morphology

The specimen is a middle part of the fragmented symphysis: the anterior and posterior parts are missing. The dorsal, lateral, and ventral surfaces have been eroded, but the specimen shows no sign of sedimentary compaction. By comparison with more complete specimens of the mandibular symphysis in *Kronosaurus queenslandicus*, the fossil preserves the 3rd, 4th, and 5th dental alveoli on each side: several of the alveoli have been exposed by erosion, and some of the dentine layers of the tooth roots are adhered to the insides of the sockets. No crowns from mature teeth are preserved, but on the left side, posterior-medial to the mature alveolus, there is the tip of a replacement tooth visible at the broken posterior surface. The pulp cavities of D3 and D4 on the left side are large, and have been filled with recrystallised calcite. Although the dorsal surface is eroded, the midline preserves a median, longitudinal ridge of bone, as in QM F10113.

Remarks

The holotype specimen does not preserve the anatomical features that can be used to diagnose *Kronosaurus queenslandicus* (see Section 4.4 and Chapter 6), and is not diagnostic to species or even genus, although it can be identified as a large pliosaur. Given the highly fragmentary nature of the specimen, it is not included in the composite data used to create the 2D skull reconstruction (Section 4.5) however, a comparison with the dimensions of QM F10113 is used to provide an estimate of head size for the holotype (Section 4.6, Figure 4-45).

Discussion

Attempts to provide consistent orthogonal photography for the *Kronosaurus* specimens had mixed results. In particular, the logistical issues outlined in the opening section meant that many of the orthogonal images are affected by parallax distortion; this seems mainly to have affected the lateral images.

Whilst the dorsal and ventral surfaces of the specimens tend to be in a plane parallel to the long axis of the specimen and this orthogonal to the axis of each shot, the basic triangular shape of the skull means that the lateral surface approximates a plane at an oblique angle to the longitudinal axis. Thus, for a lateral photograph of the rostrum, the posterior part will lie much closer to the camera than the anterior part: this greatly accentuates parallax distortion, with the result that:

- (1) Scaling a lateral shot to the dorsal and ventral views by the dimensions of the midline will give a lateral image that appears much longer than the others. For this reason, the lateral views of some specimens (especially, MCZ 1284, QM F2446, and QM F51291) have been adjusted to make the size of the lateral edge consistent with the proportions of the dorsal/ventral views.
- (2) For QM F10113, limited room around the specimen meant that the camera was comparatively close when taking the lateral shots; this led to a large amount of parallax distortion of the resulting photo-composite.

There was more room around the assembled skull of QM F18827, leading to less distortion of the lateral photo-composite, and this view has been emphasised in the

construction of the skull reconstruction in lateral view below. Likewise, for all of the specimens, the proportions drawn in lateral view have been adjusted for consistency with the dorsal/ventral views prior to generating the composition (see below).

The orthogonal views provided for each specimen should therefore be treated as illustrative, rather than definitive records of the geometry in each specimen.

Experience with the *Kronosaurus* material suggests that, for large specimens, the use of photography to describe geometry is problematic. The best results will involve:

- A camera position >10 metres from the specimen, with the use of long focal lengths to reduce parallax.
- An emphasis on photographing the skull in one shot, rather than relying on photo-composites to describe skull geometry.
- Definition of an appropriate axis system so that orthogonal camera positions can be identified consistently and accurately.
- Excellent lighting, preferably with a telemetric flash system using two or more flash units set up close to the specimen.

The resolution of digital cameras is now good enough that photographing a two metre skull in one shot need not lead to unacceptable loss of detail. Likewise, good quality digital SLR cameras are not prohibitively expensive and can be used as the basis for a telemetric flash system; these should be standard equipment for palaeontological collections.

Lighting was a major issue with the photography of these specimens; the lighting in collection facilities is universally atrocious, and the use of compact cameras with an in-built flash limits the maximum distance of the camera from the specimen. In some cases, it was possible to increase this distance by using a combination of flash and long exposure (e.g. shutter speed of 1/6 seconds): this increases the contribution of ambient light to the image, allowing the camera to be placed further away from the specimen. For closer shots, it also counteracts the 'flattening' effect of using a single camera-mounted flash. On the flip side, using a slow shutter speed means that the image will reflect the quality of the ambient lighting: compare, for example, the dorsal and ventral shots of QM F2454, where the former was taken with a shutter

speed of 1/6th sec, and latter at 1/60th seconds. In the dorsal shot, the fossil has a very greenish hue, a result of the mercury lights used in that part of the collection facility. Likewise, the photographs of QM F10113 are much greener than the actual red colour of the specimen.

4.3 **Additional material: *Brachauchenius lucasi***

None of the specimens of *Kronosaurus* discussed here preserve complete crania or mandibles, and although between them the morphology of most of the skull can be reconstructed, certain parts of the skull are not preserved in any of the specimens. In particular, the size and shape of the zygomatic arch (lower temporal bar) is unknown, as is the sagittal crest. The overall shape of the mandible is also not preserved in any of the Queensland *Kronosaurus* material.

Each of these missing parts are important components of the overall geometry of the reconstructed skull, and to complete the 2D reconstruction of the skull in *Kronosaurus*, the morphology of the zygoma, sagittal crest, and mandible was reconstructed with reference to two well preserved skulls of the North America Turonian pliosaur *Brachauchenius lucasi*: In overall morphology *B. lucasi* is very similar to *Kronosaurus*, the two genera are closely related phylogenetically (Druckenmiller and Russell 2008, Hampe 2005, Ketchum 2008; *contra* O'Keefe 2001).

USNM 4989

Specimen summary

This specimen was recovered from the Niobrara Chalk of Kansas by Charles H. Sternberg in 1884 (Everhart, 2007): it ended up at the US National Museum where it was described by Williston, who made it the holotype of *Brachauchenius lucasi* Williston 1903. The osteology of this and another skull, from the Eagle Ford Shale of Texas (USNM 2361), was further described by Williston (1907). The stratigraphy of the specimen has been uncertain, but has recently been identified as early Middle Turonian in age (Schumacher and Everhart, 2005).

The specimen comprises a cranium and articulated mandible, together with an articulated axial series from the atlas to the 35th vertebra, and a large number of ribs but no appendicular elements. The ventral side of the specimen has been mechanically prepared and a mount of the specimen in ventral view was figured by

Williston (1907 – also reproduced in Everhart 2007). The quality of preservation of the bone on this ventral surface is excellent.

The specimen is included here primarily because it includes an articulated mandible that is complete except for the front end of the symphysis.

Taphonomy

The dorsal side of the skull is weathered; the weathering is progressively worse towards the anterior end of the skull and it appears that the missing tip of the rostrum and lower jaw is simply a result of these parts having eroded away completely prior to excavation. The skull has been compressed and sheared by sedimentary compaction: the midline has been forced down and to the right, and the axis of compression seems to have been from the upper left to lower right.

The right side of the rostrum is very weathered. Parts of the orbital and temporal regions are well preserved, in particular the brow, postorbital bars, the lateral side of the left orbital margin, and both zygomas. From the traces of mechanical preparation on the matrix in the orbital and temporal cavities, these appear to have originally been covered by matrix, which protected the bone from the weathering affecting the rest of the dorsal surface. The dorsal surface of the posterior parietals, squamosal arch, and suspensoria are all weathered.

Of the surfaces of bones that have been prepared, including the regions listed above, the lateral side of the left mandibular ramus, and the ventral surface of the palate and mandible, is very well preserved, with details of the surface bone and sutural contacts clearly visible.

Methods

The skull was photographed in dorsal and ventral view during a visit to the Smithsonian Institute in 1996, using a Pentax MX SLR 35mm film camera and a 55mm lens. The prints were juxtaposed to produce a composite of the whole skull for each view, and the composites scanned and digitally processed.



Figure 4-26: Skull of USNM 4989, the holotype specimen of *Brachauchenius lucasi*, in dorsal (left) and ventral (right) view. The photo-composites have been created simply by overlaying photographs of the anterior and posterior parts of the skull, with no digital manipulation beyond masking the fossil from the original images. Scale bar = 1 metre.

Results

The skull is shown in dorsal and ventral view (Figure 4-26). Tracings of the mandible in ventral view were used to help create the 2D geometry for the mandibular rami in the 2D reconstruction of the skull in *Kronosaurus queenslandicus* (Section 4.5, Figure 4-40).

The descriptions by Williston (1903, 1907) are thorough and little needs to be added here. Some morphological features can be summarised:

- The pterygoids form a lateral buttress (Figure 4-27), as with *Kronosaurus*. The buttress is at the posterior edge of the lateral part of the palate, which is formed by the pterygoid: the ectopterygoid lies immediately in front of the buttress. On the left side, the buttress is rounded in section and the lateral end appears to have a roughened surface that is penetrated by fossa or foramina: these may indicate a cartilaginous covering in life, comparable to the lateral edge of the pterygoid flange in extant crocodylians.
- The lower edge of the pterygoid buttress continues medially towards the inter-ptyergoid vacuity, where it turns posteriorly and forms the ventral keel of the posterior pterygoid ramus. Unlike the situation in *Kronosaurus*, the ventral keel does not run parallel with the lateral and medial edges of the ramus, but angles strongly medially as it runs back. The keel has quite a sharp, narrow edge, compared with the broader, rounder edge in QM F2446. At the posterior edge of the inter-ptyergoid vacuity, the keel ends abruptly with a rounded end that tapers to the broader surface of the posterior pterygoids. The difference in the morphology of the posterior pterygoids between *Brachauchenius lucasi* and *Kronosaurus queenslandicus* was noted by Carpenter (1996).
- The palatines contact at the midline in front of the anterior parts of the pterygoids, as with QM F51291. There is no evidence of a palatal vacuity (anterior inter-ptyergoid vacuity) or suborbital fenestrae.



Figure 4-27: Close-ups of USNM 4989. Top, oblique view of left orbit: the dark markings on the sutures and abbreviations for the circum-orbital bones may have been made by Williston. Below, ventral view of posterior skull, showing the angled ventral keels of the posterior processes of the pterygoids on either side of the inter-pterygoid vacuity. Lateral to these is the lateral pterygoid buttress on each side.

- The premaxillary and symphyseal tooth counts cannot be determined in this specimen, but the first three maxillary teeth are not enlarged caniniforms as is the case in *Kronosaurus queenslandicus* (QM F18827,

QM F10113, MCZ 1284). The dentition appears to be generally much more isodont than is the case in *Kronosaurus*, with less variation in size along the tooth rows.

- The teeth are circular in cross section and, as with *Kronosaurus queenslandicus*, lack carinae: the ornament consists of longitudinal ridges around the entire circumference of the crown (see Liggett et al, 2005). The ridges are larger and fewer than in *Kronosaurus queenslandicus*.
- The contacts of the jugal are well preserved anteriorly and can be discerned posteriorly. Similarly, the contacts of the postorbital and postfrontal can be made out on both sides. The matrix that is infilling the orbital and temporal cavities obscures the lower part of the post-orbital wall.
- On the lateral side of the anterior orbital margin, there is an element that forms the orbital margin that is clearly distinct from the maxilla laterally and the prefrontal medially (Figure 4-27). The sutural contacts between this element and the surrounding bones have been marked in a heavy dark substance (charcoal?), but are real nevertheless. The position, shape, and topological relationships of this element are very similar to the lacrimal identified in QM F51291. Williston (1907) noted the presence of a lacrimal in *Brachchauchenius*, based upon examination of the holotype and USNM 2361, but this interpretation was not followed by various subsequent workers and the absence of a lacrimal was eventually commonly identified as a feature of plesiosaurs (see Druckenmiller and Russell 2008 for summary).
- There have been differing interpretations of the osteology of the brow in *Brachchauchenius*: Williston (1907) thought that the parietals contacted the facial processes of the premaxillae at the midline interdigitated suture in front of the orbits, but Carpenter (1996) interpreted (on the basis of FHSM VP-321 – see below) that the frontals formed a midline contact in front of the parietals and thus forming the posterior part of the interdigitate suture with the

premaxillae. The surface bone of the bones in the brow region is reasonably well preserved, but the crushing affecting the skull makes the topology of elements difficult to interpret. It is possible to interpret the parietals as contacting the facial processes of the premaxillae: it is also possible to reconstruct the frontals as meeting along the midline in front of the parietals. On the question of the topology of the bones at the brow, this specimen appears ambiguous.

FHSM VP-321

Specimen summary

This specimen was discovered by Robert and Frank Jennrich in Russell County, Kansas, and collected by them and George F. Sternberg⁵ in 1950 (Schumacher and Everhart 2005). It comprises a complete skull and mandible from a large pliosaur: the Dorsal Cranial Length is 153.5 cm. Preservation of the bone is good and the surface is largely intact, but the skull has been considerably distorted by sedimentary compaction and in many places the bone is cracked in the manner typical of plesiosaur fossils preserved in shales. The matrix appears to have been a chalk, and was removed when the specimen was prepared for display by mounting in plaster. The specimen has been on display at the Fort Hays Sternberg Museum (Figure 4-28): recently, the plaster covering the ventral surface has been removed (M. Everhart, pers. comm.) to allow study of the palate, which is apparently well preserved. The locality has recently been re-located and identified as the Middle Turonian Fairport Chalk (Schumacher and Everhart 2005).

FHSM VP-321 is without question one of the best preserved large pliosaur skulls from any horizon worldwide, and yet it has received minimal attention in the scientific literature. Carpenter (1996) figured the skull and included a brief summary of its taxonomy and osteology (Figure 4-29). A detailed account of its osteology is under preparation by Bruce Schumacher, Ken Carpenter, and Mike Everhart (B. Schumacher, pers. comm.), and a recent phylogenetic analysis of the Plesiosauria included data from this specimen (Ketchum 2008): the latter found FHSM VP-321

⁵ The grandson of Charles H. Sternberg

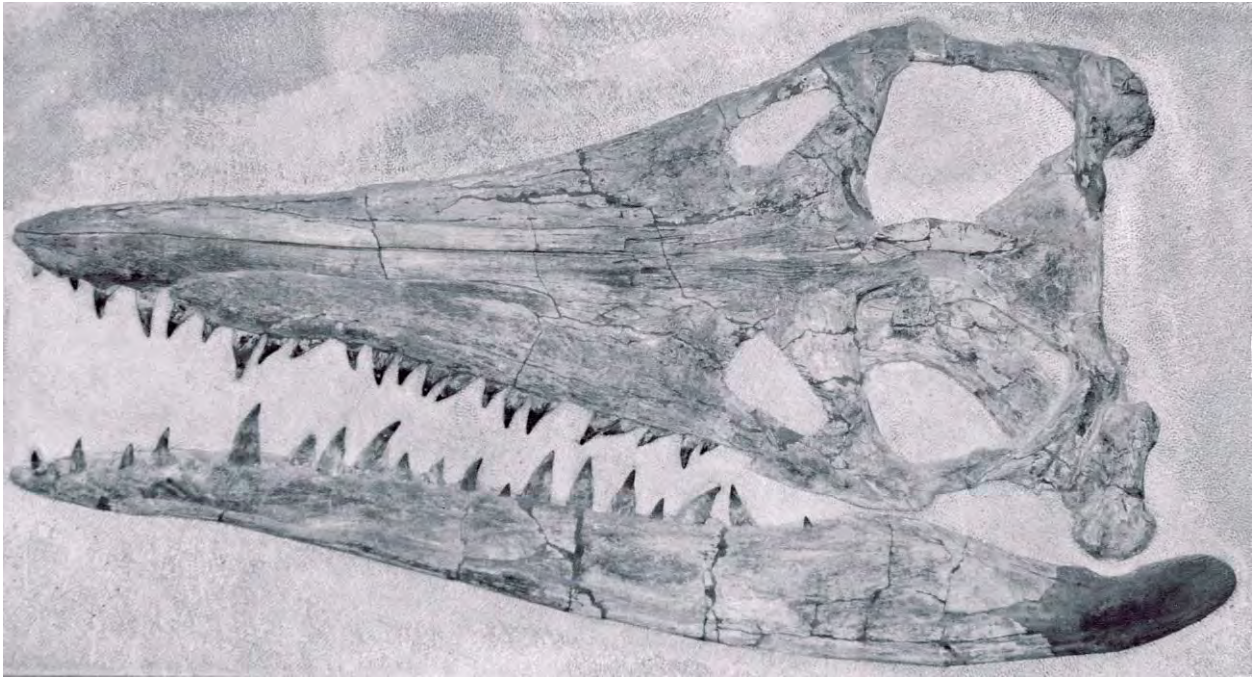


Figure 4-28: FHSM VP-321, photographed as mounted prior to 2008. Dorsal cranial length is 153.5 cm. Image courtesy of M. Everhart.

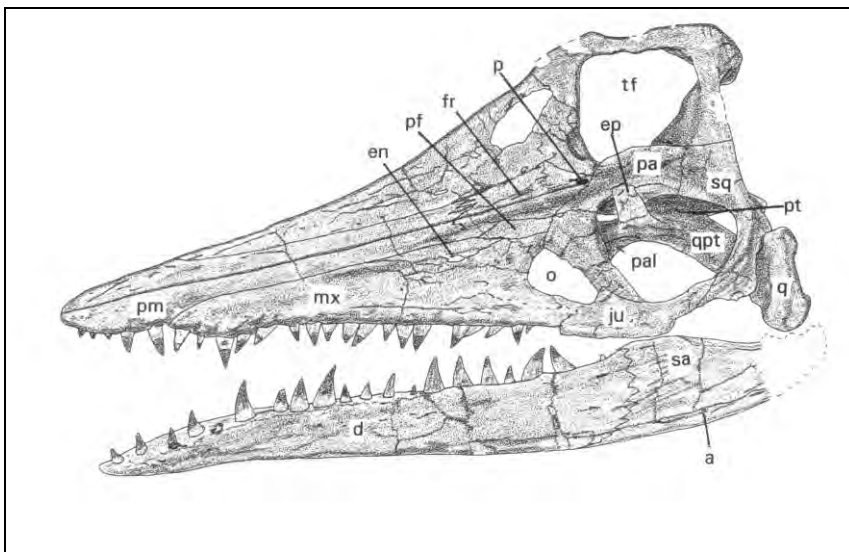


Figure 4-29: Interpretative diagram of FHSM VP-321, figured by Carpenter (1996). Legend; premaxilla (pm), maxilla (mx), external naris (en), prefrontal (pf), frontal (fr), parietal foramen (p), epipterygoid (ep), parietal (pa), temporal fenestra (tf), squamosal (sq), quadrate ramus of pterygoid (qpt), pterygoid (pt), quadrate (q), palate (pal), jugal (ju), dentary (d), surangular (sa), articular (a). The element interpreted by Carpenter as the prefrontal is here interpreted as the frontal (see Figure 4-30).

to form a sister group with a clade comprising *Kronosaurus queenslandicus* and *Brachauchenius lucasi*. Carpenter's (1996) referral of this specimen to *B. lucasi* is followed here, pending further examination of the taxonomy of the various specimens that have been referred to *Brachauchenius* (B. Schumacher, pers. comm.).

The specimen preserves two parts of the cranium that are missing in all of the *Kronosaurus* material examined for the present study; the zygomatic arch, and the dorsal edge of the sagittal crest. The preservation of this specimen, from a taxon closely related to *Kronosaurus queenslandicus*, also provides insights into the anatomy of the latter species.

Taphonomy

The specimen has been flattened by brittle and plastic deformation of the bone: the axis of deformation is from the dorsal left to ventral right. The degree of compaction is greater than for any of the *Kronosaurus* specimens detailed above except QM F2454, and greater than for USNM 4989, and the preservation of this specimen in chalk highlights the importance of the Rolling Downs limestone facies in the preservation of 3D morphology of pliosaur skulls.

The teeth have slid partly out of their sockets in both the cranium and the mandible, suggesting that the mandible was not articulated with the cranium prior to burial. The cranium and mandible are penetrated by a large number of cracks, reminiscent of the preservation of many specimens of pliosaur skulls from the Jurassic Oxford and Kimmeridge Clays (pers. obs.): the difficulties posed by such cracks for interpretation of sutural topology is well documented (see, for example, Noè 2001). In FHSM VP-321, many of the cracks are in-filled by a dark red-brown substance (Figure 4-30): missing parts of the specimen, such as the left retro-articular process, have been reconstructed using a similar material, and substance in the cracks appears thus to be a result of preparation of the specimen for display, rather than a matrix in-filling the cracks. Where unambiguous sutures are in-filled by matrix (e.g. the midline suture between the dorsal median ridge elements of the posterior rostrum), the matrix is a mid-grey colour, similar to the external surface of the bone.

The excellent preservation of the surface bone in this specimen reveals a range of different bone textures across the specimen. The surface bone of the mid-nasal ridge in the mid-rostrum is smooth, with very fine longitudinal striations. The lateral maxillae are penetrated by numerous nutritive foramina along the margins, in a line that seems to correspond with the depth of the tooth alveoli. The anterior parietals,

in front of the parietal foramen, bear a series of ridges running towards the interdigitate contact of the brow with the mid-dorsal ridge: on each side, these ridges are parallel to each other, and are oriented nearly parallel to the midline, but angle medially slightly as they run forward. The antero- and postero-medial rim of the orbit bears a rugose texture of bone, with a series of short parallel ridges: these appear to be more developed on the antero-medial edge and the supraorbital region. Each of these bring to mind features that can be observed in the various specimens of *Kronosaurus queenslandicus*: the smooth texture of the mid-dorsal ridge bone is hinted at in QM F2454, the nutritive foramina of the jaw margin can be seen in QM F10113, the long ridges of the anterior parietals are present in QM F52279, and the short ridges of the supraorbital region are present in QM F51291. However, FHSM VP-321 preserves an additional surface bone texture: in front of the orbits and in the brow region on the left side, there are a number of linear structures formed from slightly roughened lines of bone. These lines correspond with the interpreted sutural contacts of the lacrimal, prefrontal, frontal, and postfrontal in QM F51291 and other specimens of *Kronosaurus queenslandicus* described above, except for a region between the antero-medial corner of the orbit and the left external nares, where a wider area of bone carries this rugose texture. In some places there is a small amount of matrix marking the middle part of these rugose lines, but in others there is no consistent lie of matrix. Bone of this texture can be seen on the skulls of large crocodylians, where the nasals start to fuse with each other and with the surrounding rostral elements (pers. obs. of *Crocodylus porosus*). The lines of rugose bone in FHSM VP321 may thus represent the fusion of elements in a large adult animal.

Compared with the front part of the skull, which has an ellipsoid transverse section, the posterior part (occiput and suspensorium) is taller, wider, and has a more rectangular overall section. The oblique flattening of the skull has thus distorted the apparent dimensions of the posterior part to a greater extent than the anterior, because of the way in which 'box-like' sections collapse under oblique forces: this is an important aspect for reconstructions of overall skull shape and dimensions.

Methods

The specimen was photographed by Mike Everhart (FHSM) as mounted, during my visit to the Fort Hays Sternberg Museum in 2004, using a Nikon E4300 camera. The

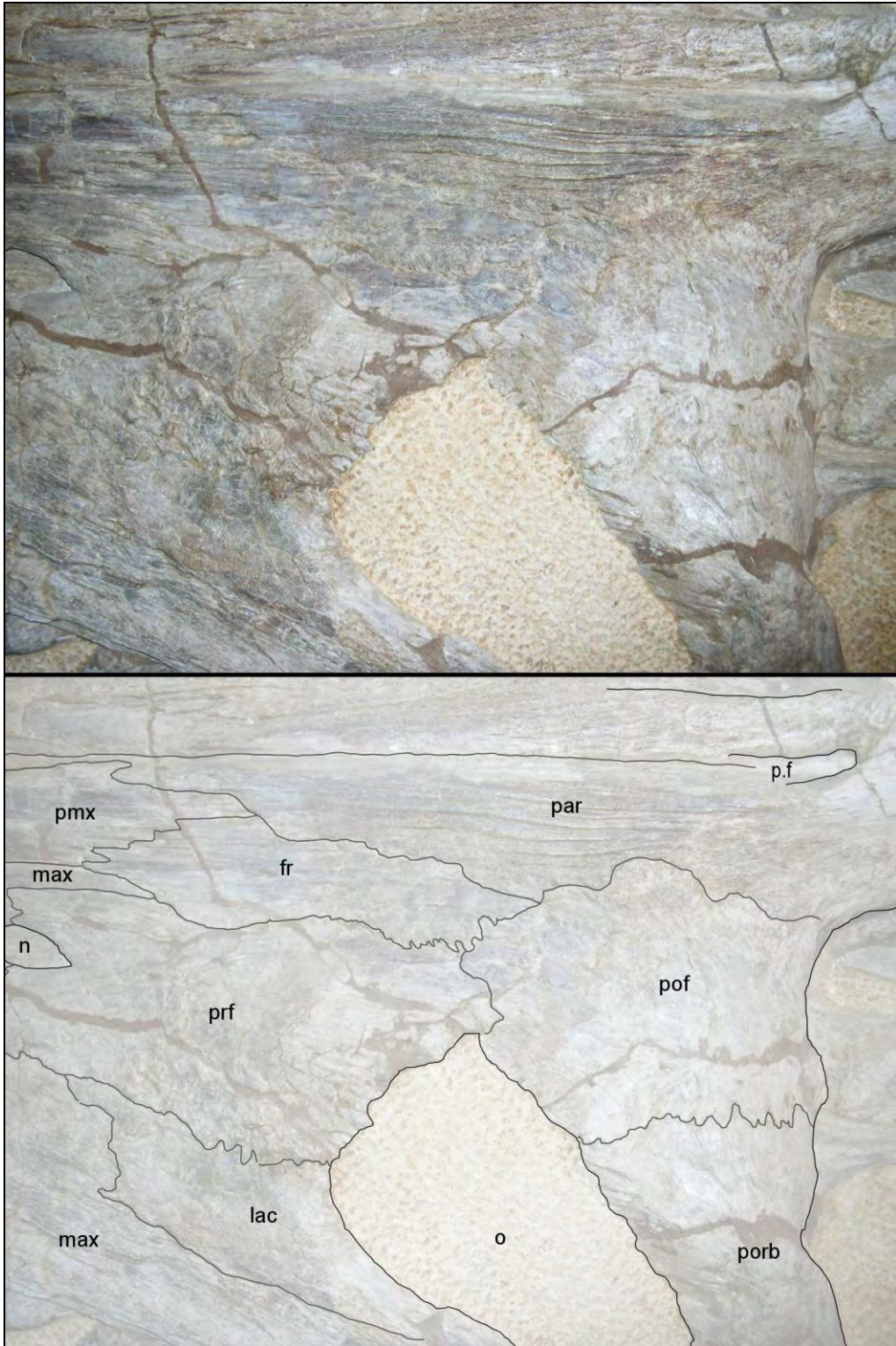


Figure 4-30: Close-up of the left circum-orbital region of FHSM VP-321 (top), showing interpretation of osteology (below). Labels; premaxilla(pmx), maxilla (max), lacrimal (lac), prefrontal (prf), frontal (fr), postfrontal (pof), postorbital (porb), parietal (par), orbit (o), external naris (n), parietal foramen (p.f). The midline suture between the anterior parts of the parietals is visible running anteriorly from the parietal foramen. Photograph by M. Everhart.

dorsal view of the whole skull (Figure 4-28) was supplied by Mike Everhart from previous photographs of the specimen.

Results

The specimen is shown in oblique dorsal view (Figure 4-28). Because of the taphonomic distortion of the specimen, it is of limited use for reconstruction of 3D morphology, but preserved many detailed features very well, including the zygomatic arch and the sagittal crest. The specimen certainly deserves a thorough study of its osteology – pending this, the relevant morphological features can be summarised:

- The sagittal crest is a very tall structure that rises sharply from immediately behind the parietal foramen. It is also very thin: at the point where it is broken in USNM 4989, QM F18827, and QM F2454, it is no wider than the remaining part of the crest in those specimens. Given this, it is apparent that the sagittal crest in USNM 4989, and in *Kronosaurus queenslandicus*, may have been considerably taller than is suggested from the preserved portion.
- The zygomatic arch (lower temporal bar) is gracile compared with the lateral part of the postorbital wall immediately in front of it. There is a definite ‘step’ in the lateral margin of the cranium from the postorbital wall to the zygoma: the latter has a consistent thickness until it approaches the suspensorium, where it flares rapidly to the contact with the squamosal. The exact geometry is complicated by the crushing of this specimen, but does provide a basis for the reconstruction of this region in *Brachauchenius* and, by extension, *Kronosaurus queenslandicus*.
- There are five pairs of premaxillary teeth: four crowns on the left side can be seen in Figure 4-28, and the Pmx 1 alveolus is empty (pers. obs.). The mandibular symphysis carries 6½ teeth: as mounted, the large tooth at the rear of the symphysis is sitting between two empty alveoli and appears to have been placed there during preparation. There is an expanded spatulate anterior part of the symphysis, which bears five tooth alveoli: although the degree of lateral expansion is

not as marked as in specimens of *Kronosaurus queenslandicus*, this may be a result of the compaction affecting FHSM VP-321.

- The teeth are round in section, lack carinae, and have a series of heavy longitudinal ridges ornamenting the crown, i.e. they are very similar to the teeth of USNM 4989. The ornament is heavier, and there are less ridges around the circumference of the skull, than in *Kronosaurus queenslandicus*.
- As with the holotype (USNM 4989), the dentition is much more isodont than in *Kronosaurus queenslandicus*: the teeth that, in *K. queenslandicus*, are enlarged caniniforms (D4-5, and M1-3) are not notably larger than their respective neighbours.
- The depth of the mandibular ramus in the middle and posterior regions is considerable greater than at the symphysis, although the degree to which this may have been exaggerated by taphonomic distortion is unknown.
- The left quadrate appears to have been disarticulated and is lying on top of the left squamosal.
- The interdigitate suture between the brow and dorsal median ridge is shorter, in the anterior-posterior axis, than the corresponding structure in specimens of *Kronosaurus queenslandicus* such as QM F51291. This might represent a difference between the two taxa or, as suggested by the preservation of QM F52279, may indicate that the extent by which the serrate processes of the bones at this contact is less at the external surface than in the underlying bone: the *Kronosaurus* material largely preserves sections through the suture, rather than the true external surface.
- If the interpretation of the contacts around the anterior orbits and brow region outlined above is correct – i.e., the sutures are partly fused in many places, then the topology of the circum-orbital elements is as follows (c.f. Figure 4-30):
 - The postfrontal-postorbital contact on the left side is clear, but is less clear on the right side where it is obscured by cracks.

- On both sides of the skull, the edges of the lacrimal are clearest at the lacrimal-prefrontal contact and the anterior lacrimal-maxilla contact. The more posterior part of the lacrimal-maxilla contact is barely visible on the left side.
- The maxilla-prefrontal contact is difficult to distinguish on both sides: it may arise from the dorso-posterior margin of the orbit and run medially and posteriorly towards the anterior part of the frontals, as in QM F51291.
- The frontal-parietal contact is clear at the left antero-lateral edge of the parietal. From the widest point of the parietals, at the triple junction between frontal, postfrontal, and parietal, the frontal-parietal runs forward and medially. By the anterior-most part of the parietal, the parietal is narrow and the frontals thus almost meet in the midline of the external surface, but the narrow contact between parietals and the facial processes of the premaxillae excludes the frontals from midline contact.

Discussion

The interpretation of circum-orbital osteology provided here differs from that of Carpenter (1996), who considered that the frontals in FHSM VP-321 specimen do meet at the midline, in front of the parietals, and that the frontals thus form all of the interdigitate contact with the elements of the median dorsal ridge. From Carpenter's figure (Figure 4-29), however, it appears that he interpreted the frontal to be prefrontal; this means that his interpretation of the frontals contacting at the midline is actually describing the anterior processes of the parietals. Ketchum's (2008) interpretation of the frontal-parietal sutures in FHSM VP-321 is similar to the interpretation of this study, and to Williston's interpretation of the USNM specimens (Williston 1907).

Ketchum (2008) provided a comprehensive phylogenetic analysis of the Plesiosauria that focused upon the Pliosauridae (*sensu* Andrews 1913) and Brachaucheniiidae (*sensu* Hampe 1992). For the brachaucheniiids, Ketchum's analysis recognised *Kronosaurus queenslandicus* (in the sense used in Section 4.2 of the present study), *Brachauchenius lucasi* (comprising USNM 4989 and USNM 2361), and FHSM VP-321 as Operational

Taxonomic Units (OTUs – see Druckenmiller and Russell, 2008): these three OTUs were found to constitute a terminal clade within the Pliosauridae. The congruence of this topology with Hampe's (1992, 2005) use of Brachaucheniidae Williston, 1925 makes the Brachaucheniidae a valid higher taxon by the criteria (monophyly) employed in current systematics. However, as a family level name, its position within the Pliosauridae means that it can be recognised as a sub-family, with the suffix emended to 'inae': Although Williston did not coin this name directly, under the ICZN principle of coordination the author of a family level taxon is considered the simultaneous author of subfamily and superfamily taxa, and thus the clade recovered by Ketchum (2008) comprising the OTUs of *Kronosaurus queenslandicus*, *Brachauchenius lucasi*, and FHSM-VP321 can be designated as the Brachaucheniinae Williston, 1925 (*sensu* Ketchum, 2008).

Within the Brachaucheniinae, Ketchum (2008) found FHSM VP-321 to be the sister OTU to the clade comprising *Kronosaurus queenslandicus* and *Brachauchenius lucasi* (the latter OTU comprising USNM 4989 and USNM 2361). In Ketchum's analysis, this topology is supported by quantitative and qualitative characters; the former concerned mainly with overall skull proportions, the latter with circum-orbital bone topology (Ketchum, pers. comm.). In one of the circum-orbital characters – the topology of the anterior part of the frontal on the external surface of the skull roof – the interpretation of the osteology in FHSM VP-321 differs from that made here, but the preservation of this region in this specimen makes interpretation difficult. However, as argued above, it is likely that the taphonomic distortion of FHSM VP-321 has altered the overall proportions of the skull, and Ketchum's (2008) results underline the need for accurate reconstruction of skull proportions and interpretation of circum-orbital topology in any taxonomic review of the various specimens that have been assigned to *Brachauchenius*.

4.4 **The taxonomy of cranial material referred to *Kronosaurus queenslandicus* Longman (1924)**

“*A species is what a competent taxonomist says it is*”

C. Tate Regan (1926)

The alpha taxonomy of a species – i.e., which specimens can be realistically assigned to that species, and how that species can be consistently distinguished from its close relatives – is of fundamental importance to palaeontology and this study is no exception. For the ultimate aim of this section – producing a reconstruction of skull geometry of *Kronosaurus queenslandicus* – identifying the range of specimens that can be used as a basis for that reconstruction is a critical component.

Despite the importance of alpha taxonomy to scientific analyses of biological form, consistent definitions of what constitutes a species remains an unsolved problem in biology. Different disciplines have tended to emphasise different guises of the species concept; thus, the ongoing debate between the proponents/ users of the biological (genetic) species concept, the evolutionary (phylogenetic) species concept, the ecological species concept, etc. (Nelson 1999). Because each of these requires data from physiology, behaviour, genetics, and observed ecology, none of them are applicable to fossil taxa and for this reason palaeontology still uses a (slightly) more formalised version of the concept used by Linnaeus, the morphological species concept⁶, to identify species of fossils.

As the name suggests, the morphological species concept groups individual fossil specimens into species based upon observed similarities/ consistencies in morphology. Of course, similarity is often in the eye of the beholder, and there is plenty of opportunity for subjectivity in the designation of morphological species. As Regan’s observation suggests, the experience and even the personality of the person

⁶ Recent debates on the use of phenetic vs. cladistic approaches to taxonomic systems relate to the construction of higher taxa: genera, families, etc. Both approaches use the species as the fundamental unit of taxonomy and, in palaeontology, these are largely determined by applying various criteria of morphological similarity / congruence.

making the taxonomic assignments often comes into play (Regan 1926): some workers are by nature ‘splitters’, others ‘lumpers’⁷. However, despite the inherent subjectivity of species level taxonomy, in practice taxonomists achieve a remarkable level of consistency in alpha taxonomy, even when working within different species concepts (Froese 1999).

In addition to making the areas of subjectivity consistent, or at least explicit, several criteria can be applied to the alpha taxonomy of fossils which offer, in theory, the potential to quantify the most common sources of variation. These sources can be summarised;

- Individual variation: at a fundamental level, each organism within a population is a unique combination of genetics, developmental history, environmental context. As a consequence, morphological variation between individuals in a population is to be expected and is of course widespread, with very few exceptions.
- Ontogenetic variation: the structure of every organism changes significantly over the course of its life cycle, or ontogeny. This variation is both qualitative (e.g. infant deer don’t have antlers) and quantitative (adults are larger than juveniles). In osteology, ontogenetic variation often affects the relative size of different bones, the complexity of the structures they form, and the extent to which different elements are ossified, or fused with neighbouring elements.
- Allometric variation: this is a special case of the quantitative aspects of individual and ontogenetic variation, where the relative proportions of structures depend upon the organism’s absolute size; for example, larger deer can have proportionally larger antlers. Specific structures of amniote crania that are often subject to allometric variation include the size and shape of the orbits. Allometry is contrasted with isometric variation, where the change in size of a shape is in proportion to the overall size of the organism.
- Polymorphic variation: in many species, individuals can be grouped into two or more ‘morphs’ which can be consistently identified above background rates of individual and ontogenetic variation. The most familiar form of this variation is sexual dimorphism.

⁷ In the spirit of at least making areas of subjective judgment explicit, I confess to being a ‘lumper’.

- Geographic variation: the range of morphologies seen within a group of organisms may correlate with geographical populations as a result of evolutionary processes. This may be closely related to true inter-specific variation (c.f. allopatric models of speciation).

These affect all neontological and palaeontological species: however, there are some additional sources of variation that are specific to fossils:

- Taphonomic variation: almost all fossils are subject to this to some degree. Depending on how the organism died, the specifics of the sedimentary environment in which it was buried, the structural/ tectonic environment of the rock unit after lithification, the details of erosion, exposure, and weathering, and how the specimen was collection, curated, and prepared, there is the potential for enormous variation of fossilised morphology, even if the original morphology was relatively consistent. As emphasised in this study, accounting for taphonomic variation is a major part of palaeontological research.
- Stratigraphic variation: if the detailed stratigraphic context of a range of specimens is unavailable, then any temporal variation in morphology (Darwinian evolution) may be ‘time-averaged’ (i.e., missed).

Distinguishing these from genuine inter-specific variation is a challenge for taxonomy. Quantitative approaches can potentially sort through this array of variation: morphometric plots of different skull measurements, for example, can be used to identify the range of allometric variation present and, if sample size is sufficient, can statistically identify if more than one class of allometric curve is present (e.g. Ketchum 2008). An alternative use of this approach is to quantify the range of variation present in a well studied extant species (e.g. Busbey 1995), and then to use this as a context for assessing the variation between the fossil specimens. Even if, as is the case with pliosaurs, there are no closely related extant taxa available, the range of typical variation in comparable species can still be informative: for pliosaurs, crocodylians and delphinid odontocetes might constitute useful comparisons. Where the sample of specimens comprise reasonably complete specimens, basic metrics can provide useful data (e.g. skull length vs. skull width, or rostral proportions – see Busbey 1995), but geomorphometric approaches can offer

more comprehensive quantitative descriptions of the underlying variation (Milne and O'Higgins 2002, O'Higgins and Jones 1998, Wroe and Milne 2007), even when the specimens are not complete.

There are, however, two problems with applying quantitative techniques such as those to the alpha taxonomy of the specimens referred to *Kronosaurus queenslandicus*. Firstly, the total of eight specimens preserving cranial material is not sufficiently large for robust statistical analysis. Secondly – and perhaps even more critically – the taphonomic distortion of these specimens is likely to swamp any taxonomic signal in the observed range of morphological variation: although this assessment has not been tested, a sensitivity analysis of the relevant data is beyond this analysis and must remain a topic for future study.

The assessment of the alpha taxonomy presented here thus focuses upon qualitative variation in the morphology of the specimens, and uses a 'null hypothesis' approach: the observed morphological variation is considered to indicate the presence of more than one species only if it cannot be reasonably attributed to (1) taphonomy, (2) ontogenetic variation, or (3) individual variation.

Taxonomic context

The purpose of alpha taxonomy is to determine the species to which a specimen can be assigned: it must thus provide a basis for diagnosing one species from any other (usually, related) species. Amongst workers within a particular group, certain morphological features are often emphasised in establishing the alpha taxonomy of that group.

In the case of *Kronosaurus queenslandicus*, the overall taxonomic context is provided by the Brachaucheniidae and Pliosauridae. For these, cranial features that have been used to underpin taxonomies include; the size and shape of the mandibular symphysis (Noè et al. 2004, Tarlo 1960), the premaxillary tooth count (Tarlo 1960), the presence of carinae/ cross-sectional shape of tooth crowns, the distribution and morphology of ornament on the tooth crowns (Noè 2001), and the osteology of circum-orbital bones (Ketchum 2008).

As a member of the Brachaucheniidae, the most closely related species to *K. queenslandicus* are *Kronosaurus boyacensis* Hampe 1992, and *Brachauchenius lucasi* Williston 1903. With reference to those cranial features that have been used to distinguish different species of Pliosauridae, these two are both characterised by:

- the possession of a short mandibular symphysis with 6–7 pairs of dentary teeth in the symphyseal region
- teeth lacking carinae and circular in cross-section;
- a tooth crowns that bear ornament around their entire circumference.

In addition, Hampe (1992) described *Kronosaurus boyacensis* as possessing 5 pairs of premaxillary teeth, a count that matches that of *B. lucasi* (FHSM VP-321). However, given the preservation of the *K. boyacensis* holotype specimen, where the jaws are tightly adducted, and the potential importance of premaxillary tooth counts in the genus-level taxonomy of pliosaurs (see below and Chapter 6), this feature of *K. boyacensis* warrants confirmation.

At present, *Kronosaurus boyacensis* and *Brachauchenius lucasi* can be distinguished on the basis of;

- The extent of the variation in tooth size (anisodonty) along the tooth row: *K. boyacensis* has strongly developed anisodonty, with anterior caniniform teeth that are much larger than the teeth of the posterior tooth row – in *B. lucasi* the variation in tooth size is much less and the dentition is more or less isodont.

Published descriptions of tooth ornament morphology do indicate potential difference between these species (Hampe 1992, Liggett et al. 2005), but as tooth ornament morphology can also vary between teeth at different positions in the tooth row (pers. obs., MCZ 1284, FHSM VP-321), the use of quantitative variation in ornament to distinguish species should preferably be made within the context of a comprehensive description of the variation in morphology within and between specimens, using techniques such as those illustrated by Forrest and Oliver (2003) to illustrate ornament morphology.

Alpha taxonomy of specimens referred to K. queenslandicus

With respect to the features discussed above (taxonomic context), the range of morphology preserved in the specimens described in Section 4.2 above can be summarised:

Premaxillary tooth count

QMF 18827 and MCZ 1284 preserves 4 pairs of teeth in the premaxillae. The premaxillary tooth count is not completely preserved in any other specimens.

Mandibular symphysis

The symphysis is 'short', bearing 6½ pairs of teeth, with an expanded 'spatulate' anterior part that bears 5 pairs of teeth, in QM F18827, QM F10113, and MCZ 1284.

Anisodonty

All specimens that preserve the anterior part of the rostrum (QM F18827, QM F10113, MCZ 1284) exhibit extreme anisodonty, with large caniniform teeth in the anterior maxilla occluding with much smaller dentary at the very rear part of the symphysis (note that, in QM F10013, tooth size is inferred from alveolar diameter). In QM F18827 and QM F10113, the upper jaw caniniforms are at the first three maxillary positions: in MCZ 1285, only the first two maxillary teeth are preserved but the relative and absolute dimensions are similar to the other specimens. Immediately in front of the maxillary caniniforms, the three tooth positions of the rear part of the spatulate section of the symphysis (D3-D5) are also large caniniforms: the alternation of large teeth in the upper and lower jaws has been termed 'festooning' and can be found in several reptilian taxa that display extreme anisodonty (modern examples include the large species of *Crocodylus*). The large D4 and D5 teeth occlude between the Pmx4 and M1 tooth positions, at the short diastema present in the upper jaw where the maxilla and premaxilla contact at the jaw margin. The enlargement of D4-5 may be related to the absence of the 5th pair of premaxillary teeth: the majority of pliosaurids and *Brachauchenius* possess 5 pairs of premaxillary teeth, where the 5th pair occlude between D4 and D5. A comparable situation may be found in *Crocodylus*, where all species have 5 pairs of premaxillary teeth, except for adult *C. porosus* and

some *C. niloticus*: in these species, the very large D1 tooth occludes through the front of the upper jaw, obliterating the Pmx2 tooth in early ontogeny.

In the posterior tooth row (QM F18227, QM F2446, QM F2454, QM F51291), the anisodonty is much less developed, and, in this part of the tooth row, these specimens exhibit isodonty.

Tooth shape and ornamentation

Teeth are poorly preserved in most of the specimens that preserve cranial bone. However, tooth morphology is preserved in some specimens, notably as moulds in the matrix covering some of the specimens. In all instances where tooth morphology is preserved, the crowns are circular in section and lack carinae (QM F18827, QM F10113, MCZ 1284, QM F2446, QM F51291).

The ornament consists of longitudinal ridges: as no parts of preserved crowns lack this ornament, it appears to have been distributed around the entire circumference of the tooth. On each tooth, the ridges have a broadly consistent density so that, as the circumference of the tooth increases from the tip to the base, additional ridges appear *de novo* (rather than by bifurcations of the longer ridges) in the ‘valleys’ between the longer ridges, as described for *Brachauchenius lucasi* by Liggett et al. (2005). In the specimens described here, the ridges are numerous on each tooth and can be classed as ‘fine’ (QM F18827, QM F10113, MCZ 1285, QM F2446). This pattern contrasts with the fewer, heavier ridges figured for *Brachauchenius lucasi* (Liggett et al, 2005) and *Kronosaurus boyacensis* (Hampe, 1992): however, fossils of isolated teeth collected from the Rolling Downs Group and currently held in private collections (pers. obs.) suggest that the number and relative size of the ridges can vary more than is apparent from the specimens considered here, and the potential of tooth ornament morphology as a distinguishing feature amongst brachaucheniids requires further study.

Circum-orbital bone topology

These features exhibit variation between specimens. A lacrimal is preserved as a separate element, with patent sutures around most of its perimeter, in QM F51291.

In QM F2446, the sutures are patent at the anterior orbital wall and, on the dorsal surface of the posterior rostrum, immediately in front of the orbital rim, but cannot be distinguished reliably forward of this. A lacrimal may be present in QM F52279, but crushing of this specimen obscures interpretation. The relevant part of the skull is not well preserved in, QM F18827, QM F18174, and QM F2454, and is not preserved in QM F10113 or MCZ 1284.

A nasal is present, as the lateral surface element of the posterior part of the dorsal median ridge, in QM F51291 and QM F52291. It is not present in QM F10113 or QM F2454, and preservation obscures interpretation in QM F 18827, QM F18174 and QM F2446. The relevant part of the skull is not preserved in MCZ 1284.

The dorsal median ridge also incorporates an internal, ventral element (QM F10113, QM F52279) or pair of elements (QM F51291, QM F2446). Preservation hinders interpretation in QM F18827 and QM F18174.

Discussion

The alpha taxonomy here involves two related questions; (1) how many species are represented between the specimens considered, and (2) how can this/these species be distinguished from close relatives?

Where preserved, anterior (premaxillary and symphyseal) tooth counts are consistent between specimens, as is the morphology of the symphysis. The pattern of anisodonty appears also to be consistent; well developed anteriorly, poorly developed posteriorly. Tooth crown morphology and ornament is also consistent. In all of the specimens considered, the lack of these features in any one is a result of incomplete/poor preservation, rather than the presence of alternative morphological states.

The variation described for the circum-orbital bones is of the order used by some authors to distinguish between species of pliosaurid (see Ketchum, 2008). However, variation in the ossification of the sutures of the lacrimal and dorsal median ridge are here interpreted as the result of ontogenetic processes, rather than indicating inter-specific variation; the smaller specimens preserve more elements, consistent with

patterns of osseous fusion known in extant amniotes (see Section 4.6 for estimates of size between specimens). In particular, the smallest specimen (QM F51291) preserves the largest number of elements, and the largest specimen (QM F2454) also preserves the lesser number of elements in the dorsal median ridge, while another large specimen (QM F2446) apparently displays partial fusion of the lacrimal.

Since the observed variation is interpreted as either taphonomic or ontogenetic, there is no evidence of more than one species for the specimens considered here, and previous referral of these specimens to *Kronosaurus queenslandicus* Longman 1924 is supported. This includes MCZ 1284 (as far as is known given the fragmentary nature of this specimen), which is of potential interest given that this specimen derives from a older horizon, the Aptian Doncaster Formation, than the others, which are all from the Albian Toolebuc Formation and are thus 10–12 million years younger.

On the basis of the cranial material, the *Kronosaurus queenslandicus* specimens can be distinguished from *Brachauchenius lucasi* on the basis of the premaxillary tooth count and the pattern of anisodonty, and possibly on the basis of tooth ornamentation. Premaxillary tooth count apparently separates *K. queenslandicus* from *K. boyacensis*, although the premaxillary tooth count in *K. boyacensis* requires confirmation⁸. The pattern of anisodonty is not sufficient to distinguish *Kronosaurus queenslandicus* from *Kronosaurus boyacensis*, although these two species can be distinguished on the basis of postcranial characters (Chapter 6), and potentially on the basis of tooth ornamentation.

⁸ The issue of the actual premaxillary tooth count in *Kronosaurus boyacensis* is important. Hampe (1992) specified a count of five; however, photographs of the holotype specimen suggest that the tooth-bearing margins of the anterior rostrum are not well preserved: five is in any case a very common premaxillary tooth count for large pliosaurs. That the Late Barremian – Early Albian Colombian fauna included a large pliosaur with a premaxillary tooth count of four is demonstrated by an as-yet undescribed specimen, that has been interpreted as c.f. *Kronosaurus* (M. Gomez, pers. comm. – see Chapter 1). Either these represent two different species, or Hampe’s count of five for *K. boyacensis* is inaccurate.

In the context of traditional pliosaur taxonomy, premaxillary tooth counts have tended to correspond with genus-level distinction between species; examples of species with differing premaxillary tooth counts being placed within the same genus are very rare. If *Kronosaurus boyacensis* is found to have five premaxillary teeth, then this feature may warrant placement in a genus separate to *Kronosaurus queenslandicus*. Alternatively, if *K. boyacensis* is found to have premaxillary tooth count of four, then the list of cranial features that can distinguish *K. boyacensis* from *K. queenslandicus* is reduced to potential (but as yet unconfirmed) differences in tooth ornamentation, although at present the two species can be distinguished on the basis of post-cranial features (Chapter 6).

Type material and nomenclatural status

The holotype specimen of *Kronosaurus queenslandicus* is QM F1609, from the Toolebuc Formation, which does not preserve any diagnostic features (see Section 4.2). As there is no indication of more than one taxon of large pliosaur from the Toolebuc Formation, the holotype can be assumed to represent the same species as the more complete specimens discussed above. In particular, QM F18827 preserves all of the features – premaxillary tooth count, mandibular symphysis, tooth shape and ornamentation, anisodonty of the tooth row, vertebral centra morphology – that can separate the Toolebuc Formation large pliosaur taxon from all other currently described species of pliosaur except *Kronosaurus boyacensis*. QM F10113 preserves a number of these features (a notable and potentially important exception is the premaxillary tooth count), and also preserves postcranial features which can distinguish it from *K. boyacensis*. Either of these two specimens may be appropriate candidates for the name-bearing specimen for *Kronosaurus queenslandicus*. Under the International Committee of Zoological Nomenclature (ICZN) rules, re-allocation of the type specimen for a species, on the grounds that the holotype has not been lost or destroyed, but is non-diagnostic, requires a petition to the ICZN committee. It is recommended that this action be taken in order to retain *Kronosaurus queenslandicus* Longman 1924 as a valid species.

4.5 **A (2D) reconstruction of skull anatomy in *Kronosaurus queenslandicus***

Reconstructions of skull morphology are an important part of the interpretation of fossils. Unless preservation is pristine, the reconstruction requires a level of inference beyond an interpretative diagram of a skull: the reconstruction must allow for distortion, weathering, and missing pieces, and seeks to represent the morphology of the skull in life. Where taphonomy has had minimal effects of the skull, this can be a straightforward process, but for the majority of vertebrate skull fossils – and for most specimens older than Pleistocene in age – the final reconstruction requires the judgement of the palaeontologist and in effect represents a hypothesis of form. It is an area of palaeontology where the science and the art of the discipline merge.

Despite a wealth of material, there have been few attempts to provide skull reconstructions for pliosaur species in the 130 years since the suborder was formally named. Andrews (1895) provided a reconstruction of *Peloneustes philarchus* in addition to the excellent interpretative diagrams he prepared for *Peloneustes*, *Liopleurodon*, and *Simolestes* (Andrews, 1913). Williston (1907) offered a partial reconstruction of *Brachachaenius lucasi*, and Linder (1913) also supplied a reconstruction for *Peloneustes*, but for much of the 20th Century attempted reconstructions of pliosaur skulls were few: Newman and Tarlo (1967) provided a reconstruction of an unnamed large pliosaur (which may have been based upon *Stretosaurus* Tarlo, 1959 – see Chapter 6) that included a skull, but until the 1990s very little else appeared in the scientific literature. This was in marked contrast with other groups of fossil vertebrates, in particular Mesozoic archosaurs, for which many reconstructions of skull anatomy were provided, especially following the start of the ‘Dinosaur Renaissance’ of the 1970s (Bakker 1975, Paul 1988). It is of course likely that the lack of attempted skull reconstructions for pliosaurs was symptomatic of a general lack of palaeontological interest in this group, but given that studies of functional morphology tend to start – not finish – with reconstructions of the morphology in life, it is possible that the lack of attempted reconstructions contributed to a dearth of at least one major type of palaeontological research on the group.

The situation changed somewhat in the 1990s, with increased levels of research activity on the Plesiosauria (leading to observations of a ‘Plesiosaur Renaissance’) and the publication of skull reconstructions for *Rhomaleosaurus zetlandicus* (Taylor 1992), *Kronosaurus boyacensis* (Hampe 1992), *Pliosaurus brachyspondylus* (Taylor and Cruickshank 1993), and ‘*Rhomaleosaurus*’ *megacephalus* (Cruickshank 1994) amongst others. Noè (2001) included high quality reconstructions of *Liopleurodon ferox*, *Simolestes vorax*, and *Pachycostasaurus dawni*, and Druckenmiller (2002) reconstructed the skull in *Edgarosaurus muddi*, while Ketchum (2008) has provided an updated reconstruction for the skull of *Peloneustes philarchus*, and Smith and Dyke (2008) have reconstructed cranial and postcranial anatomy in *Rhomaleosaurus*.

The use of the term ‘two-dimensional’ to describe these skull reconstructions refers, in this context, not to the number of views presented, but to the techniques used to generate the reconstructions. A reconstruction of a skull in the any two of the coronal, sagittal, and transverse planes may allow the reader to mentally construct a basic three-dimensional understanding of the morphology, but each of these views can be produced using 2D or 3D techniques. The difference between these is simply the medium used to generate the reconstruction: with 2D techniques, the reconstruction is drawn on paper or in a 2D computer graphics program (such as CorelDraw, Photoshop, PaintShop Pro, etc), whilst 3D reconstructions are made in a three dimensional medium such as modelling clay, or a 3D computer graphics/design package such as AutoCAD or Rhino. Note that 3D reconstructions can be (and often are) represented in 2D output, such as drawings, photographs, computer screens, or print-outs. When only two-dimensional output is required, distinguishing between 2D and 3D techniques can seem academic, but when 3D output is required these differences can be important (see Chapter 5).

The aim of this section is to produce a 2D reconstruction of skull morphology in *Kronosaurus queenslandicus*, using the morphological information presented in the previous section.

Methods

As outlined above, the skull of *Kronosaurus queenslandicus* is represented by a number of specimens that preserve some features of the skull anatomy very well. Conversely,

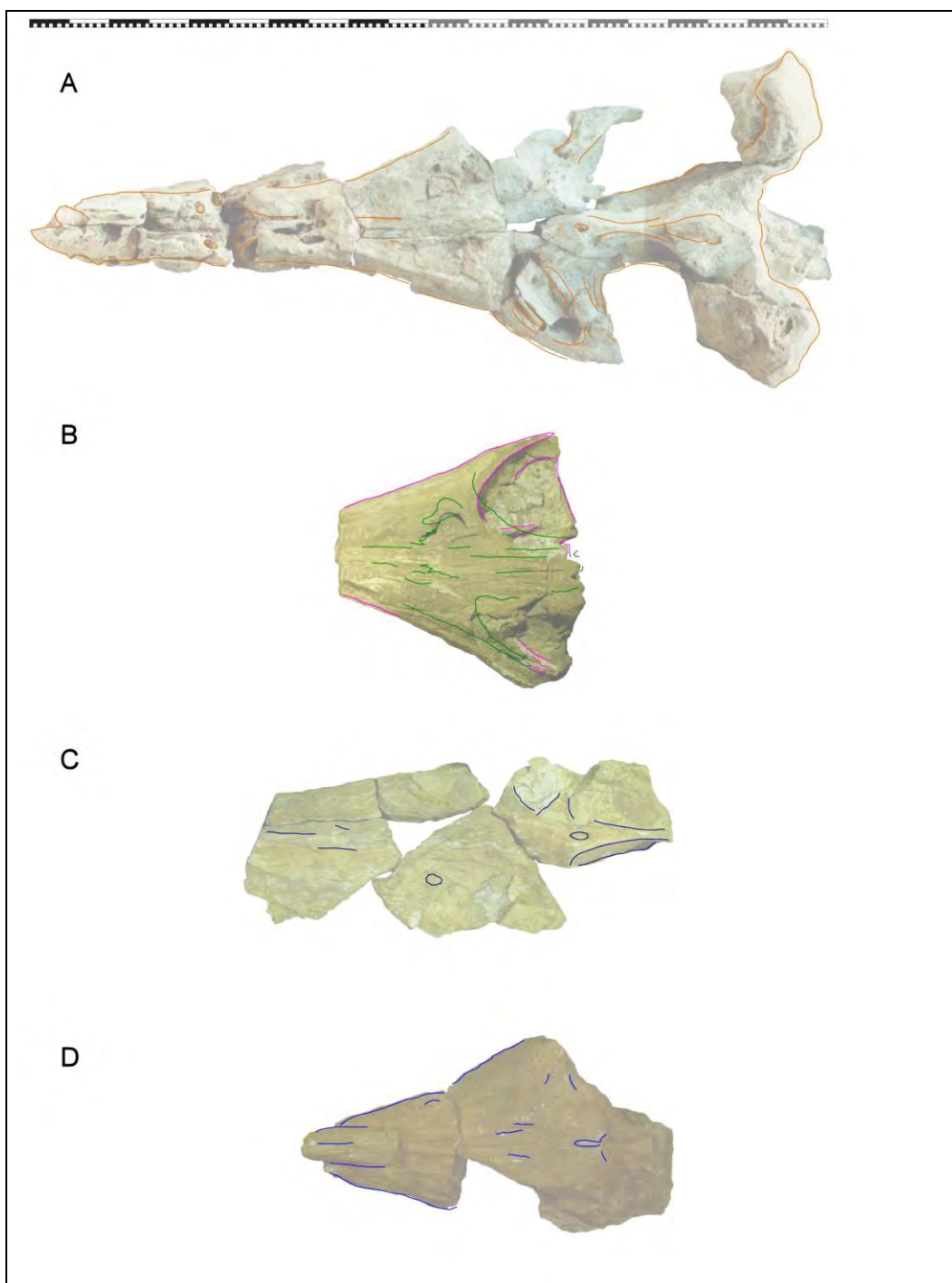


Figure 4-31: Traced landmarks/ outlines for specimens of *Kronosaurus queenslandicus* in dorsal view: (A) QM F18827, (B) QM F2446, (C) QM F2454, (D) QM F18154. Note that specimens have been rescaled to the dimensions of QM F10113. Scale bar = 2 metres.

no one specimen preserves the entire skull, and all of the specimens discussed above have been affected by one or more of the taphonomic processes of sedimentary compaction, fragmentation, and erosion. The taphonomy of these specimens presents challenges for generating reconstructions of the skull in *K. queenslandicus*.

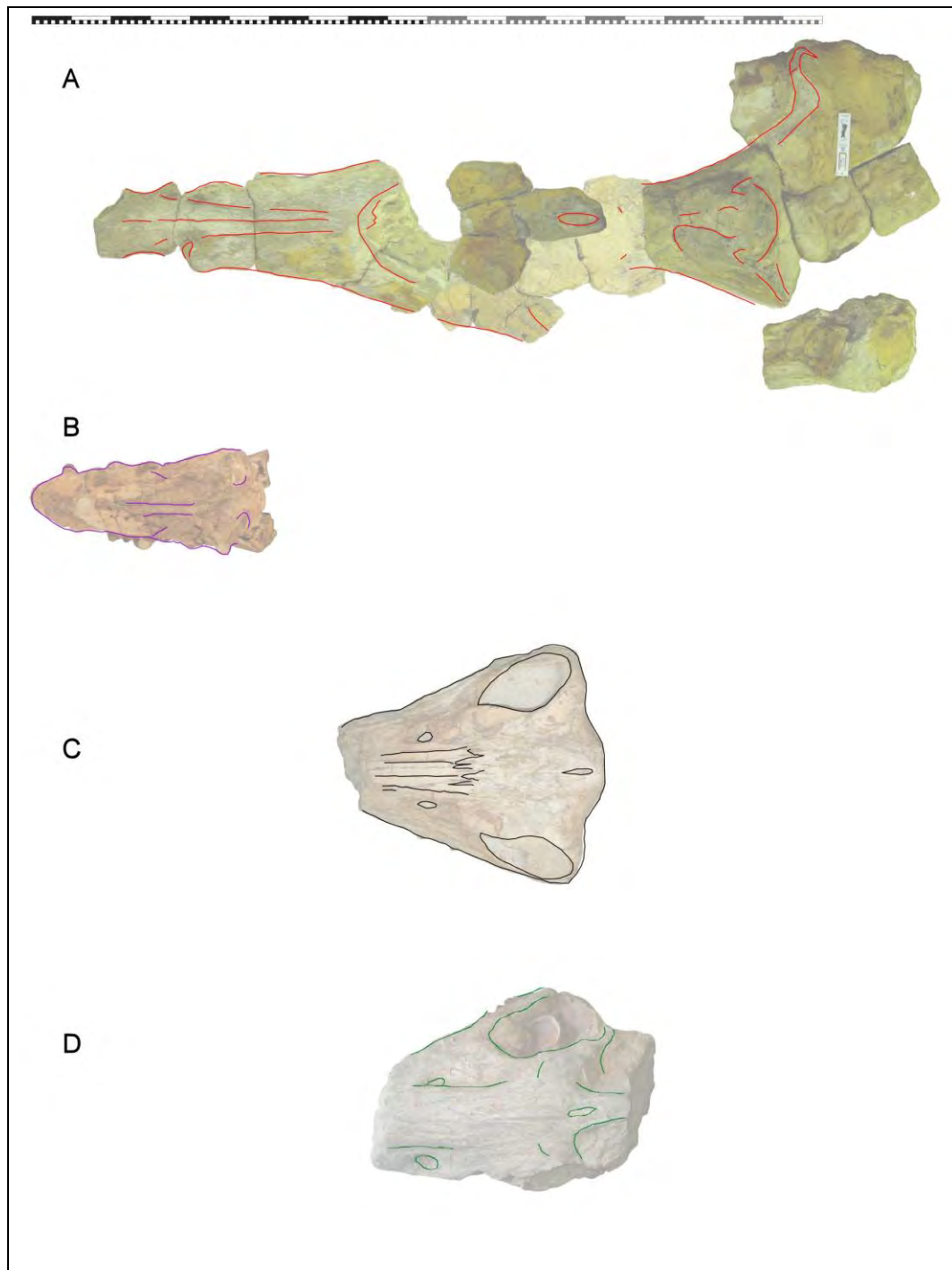


Figure 4-32: Traced landmarks/ outlines for specimens of *Kronosaurus queenslandicus* in dorsal view, scaled to the dimensions of QM F10113: (A) QM F10113, (B) MCZ 1284, (C) QM F51291, (D) QM F52279. Scale bar = 2 metres.

In a recent analysis of *Peloneustes philarchus*, Ketchum (2008) compiled data from 18 specimens, several of which preserve complete or nearly complete skulls. The skull material formed the basis for an updated reconstruction of skull anatomy in this species: although Ketchum did not detail her methods, it appears that the high

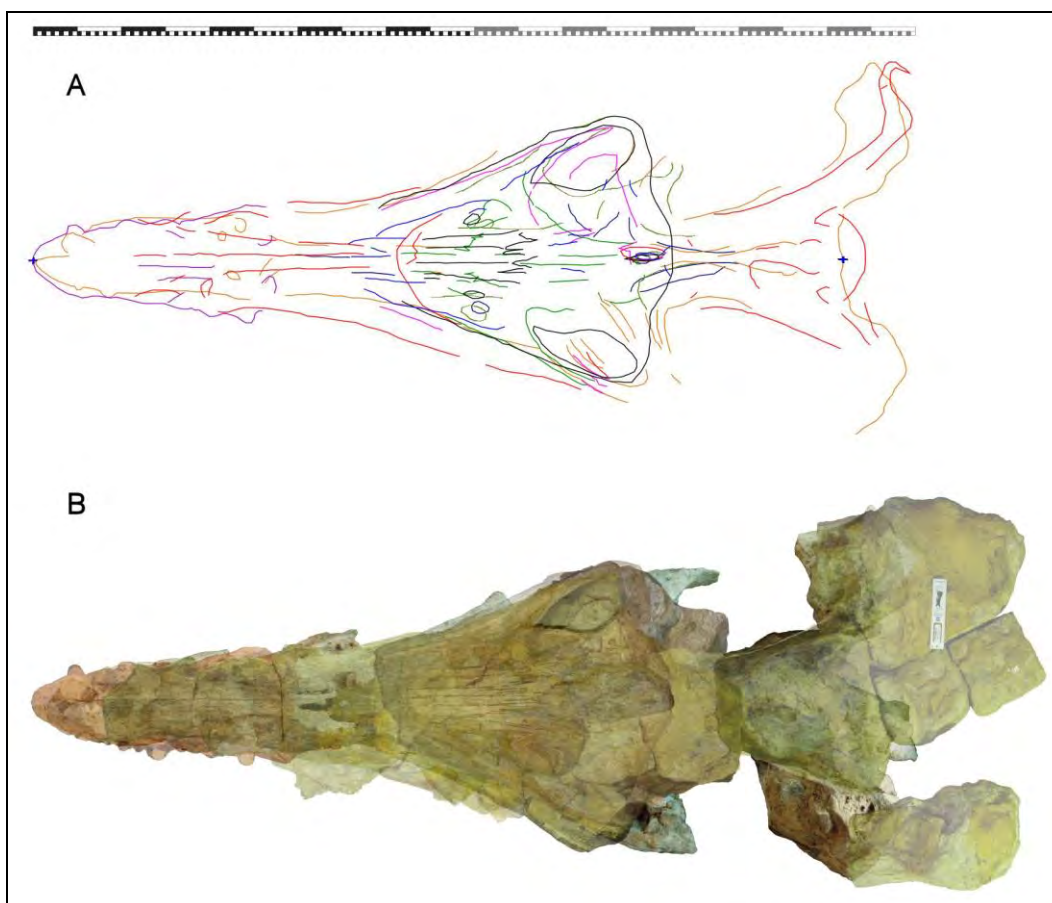


Figure 4-33: Combined (A) traced landmarks/ outlines, and (B) images for specimens in dorsal view, rescaled to the dimensions of QM F10113. Scale bar = 2 metres.

quality interpretative diagrams she prepared for several of the skulls provided an adequate basis for the reconstruction. For example, she provided interpretative diagrams for five crania in a variety of dorsal, lateral, and ventral views. Many of the specimens are preserved in the shale beds that characterise the host unit, the Oxford Clay, and exhibit a high degree of dorso-ventral compaction (see Chapter 3), but one specimen is preserved in a pyritic nodule and appears free from compaction: the interpretative diagram from this specimen (BMNH R4058) was apparently sufficient to provide the data in the dorso-ventral axis required to ‘un-compress’ the other specimens and generate reconstructions of the skull in the sagittal, coronal, and transverse planes. Noè (2001) used a similar approach in providing a reconstruction of *Liopleurodon ferox* from numerous specimens, and of *Simolestes vorax* from a smaller number of specimens: again, in the case of the latter species, the preservation of one of the specimens in a pyritic nodule provided the necessary data in the dorso-ventral axis.

From the high quality of the reconstructions produced by Noè (2001) and Ketchum (2008), this approach evidently works very well when a number of complete specimens are available. This is not the case, however, for the *Kronosaurus* material available for the present study, and a slightly different approach was used.

For each of the specimens of *Kronosaurus* considered in the previous section (except for the holotype, QM F1609), basic outlines of landmarks, sufficient to capture overall skull geometry and which were considered to be minimally affected by taphonomy, were traced over each of the orthogonal views provided for those specimens. For example, outline/landmarks were traced for the lateral and dorsal views of QM F18827, but not the ventral view because it has not yet been possible to assemble the specimen to show the ventral view, whilst for QM F18827 the ventral part of the skull is obscured by matrix, but useful geometry is visible in lateral and dorsal orthogonal views. For QM F2454, the extensive dorso-ventral crushing of the skull means that the lateral view is of limited use, but the dorsal and ventral views do record useful geometry and were included. A key part of this approach is to concentrate on the geometry of the overall shape of the skull, such as orbital rims and rostral margin, and major landmarks such as the external nares and the parietal foramen, rather than attempting to capture every osteological detail, or the edge of each fossil block. This means that, for each specimen, less lines are drawn than would be expected in a more typical interpretative diagram of the specimen. The tracings were done as vector graphics overlays of the processed photographs presented for Section 4.2, using the layering functions of PaintShop Pro.

The traced outlines for the dorsal, lateral, and ventral views of each specimen were then combined into three master files (one file for each view), with the traced outlines for each specimen held as separate layers. Each of these layers was then rescaled to the linear dimensions of a single specimen which was thus used as a template for the resulting reconstructions. The template specimen selected was QM F10113, as it preserves a large proportion of the skull, can be imaged in dorsal, lateral, and ventral views, and is indicated by preliminary analysis to represent an 'adult' size.

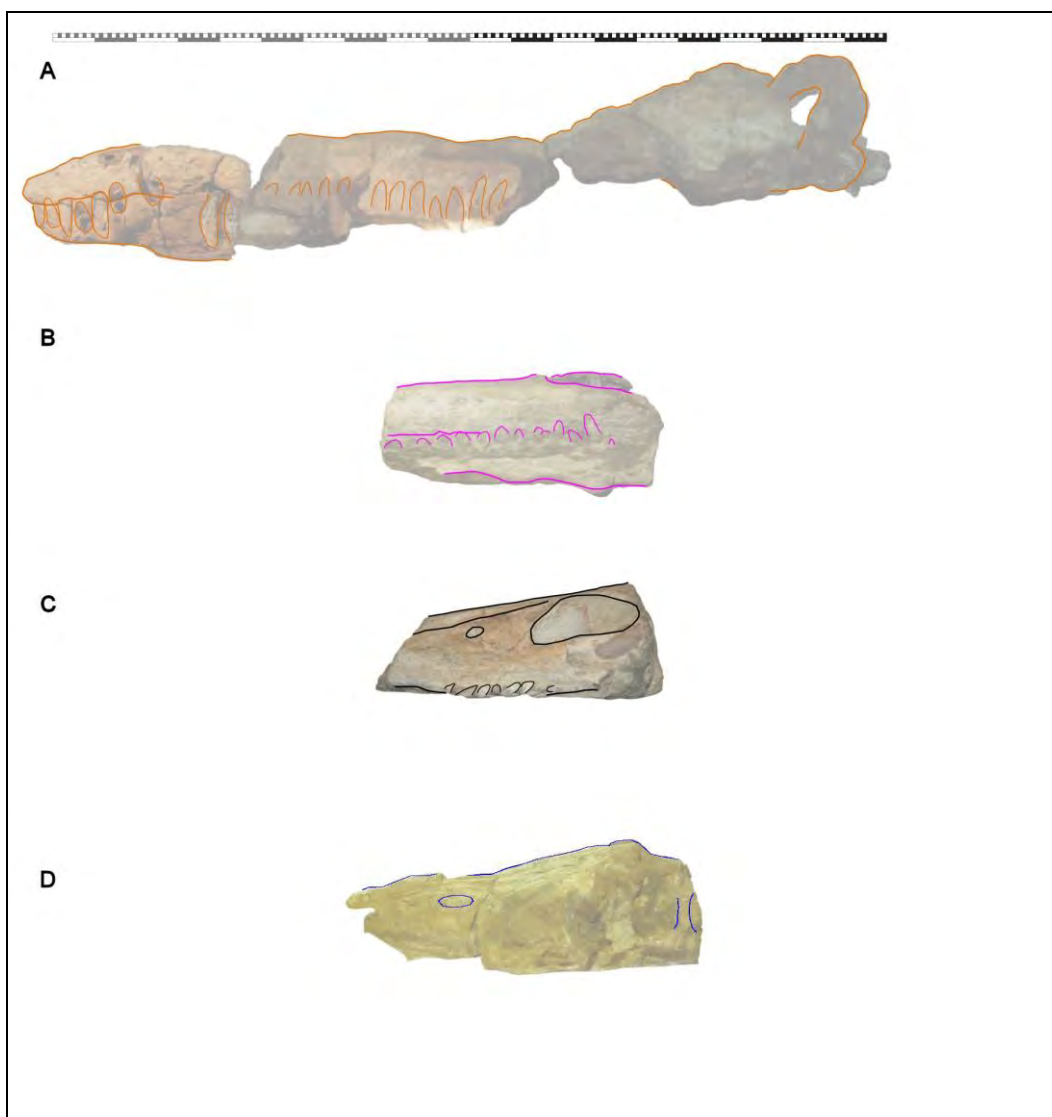


Figure 4-34: Traced landmarks/ outlines for specimens of *Kronosaurus queenslandicus* in lateral view, rescaled to the dimensions of QM F10113: (A) QM F18827, (B) QM F2446, (C) QM F2454, (D) QM F18154. Scale bar = 2 metres.

The outline/landmarks of the other specimens were rescaled to the dimensions of the traced outlines of the template specimen (QM F10113) according to one of the following criteria:

1. Dorsal Cranial Length (DCL): the distance (measured in the sagittal plane) between the anterior rostral tip and the rear-most extent of the supraorbital/parietals at the midline of the dorsal skull roof.
2. Distance between the external nares and the parietal foramen (pf-n): This was measured as the longitudinal (anterior-posterior) component of the linear distance between the centre of the parietal foramen and the centre of the external

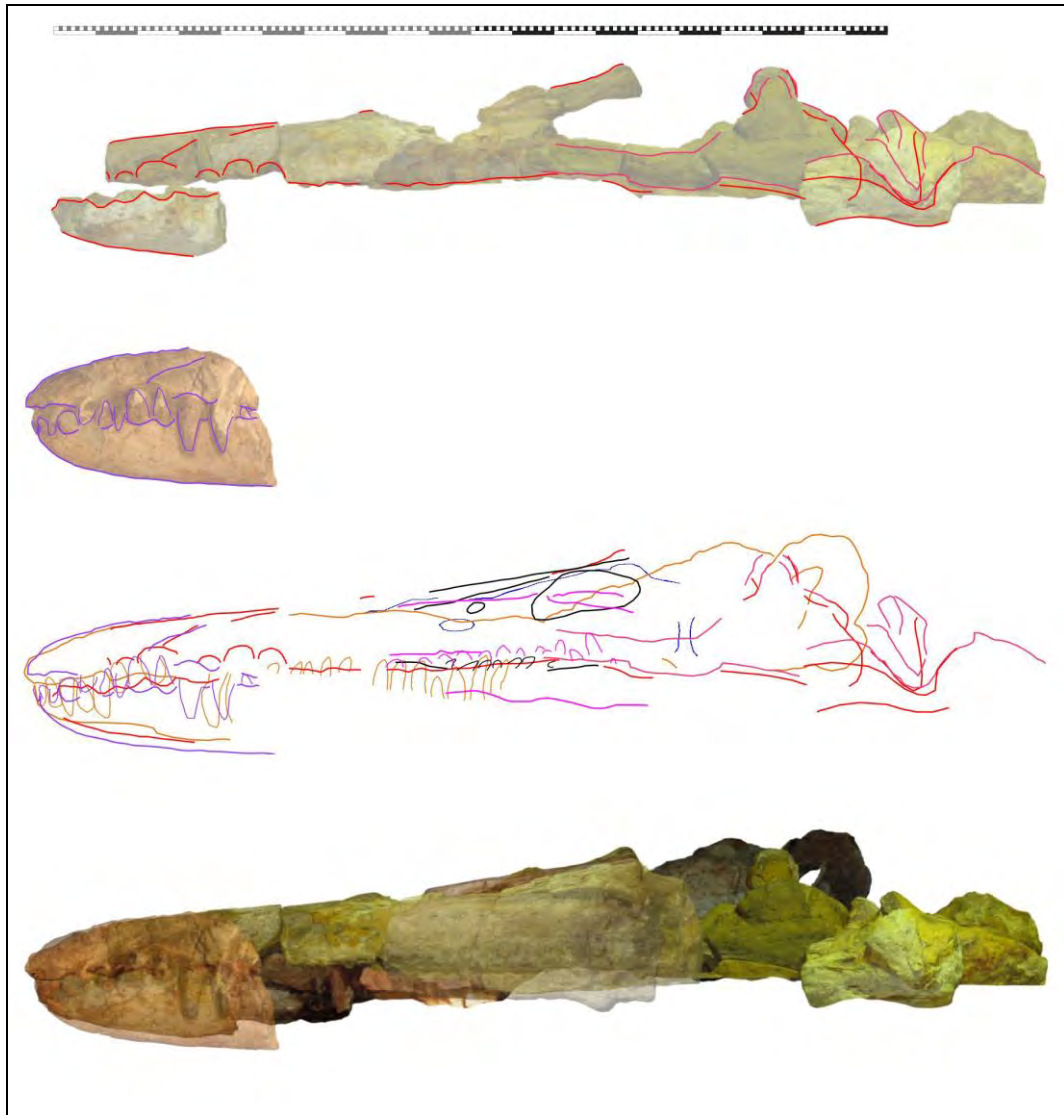


Figure 4-35: Traced landmarks/ outlines for specimens of *Kronosaurus queenslandicus* in lateral view, scaled to the dimensions of QM F10113: (A) QM F10113, (B) MCZ 1284, (C) combined outlines, (D) combined images. Scale bar = 2 metres.

naris. Where this distance differed for the left and right naris, the mean value was used.

3. Snout–M1 tooth length (s-M1): measured as the longitudinal component of the distance from the anterior rostral tip to the first maxillary tooth. Where the tooth was preserved *in situ*, the measurement was made to the middle part of the base of the crown: where the tooth was absent, it was made to the centre of the alveolus.

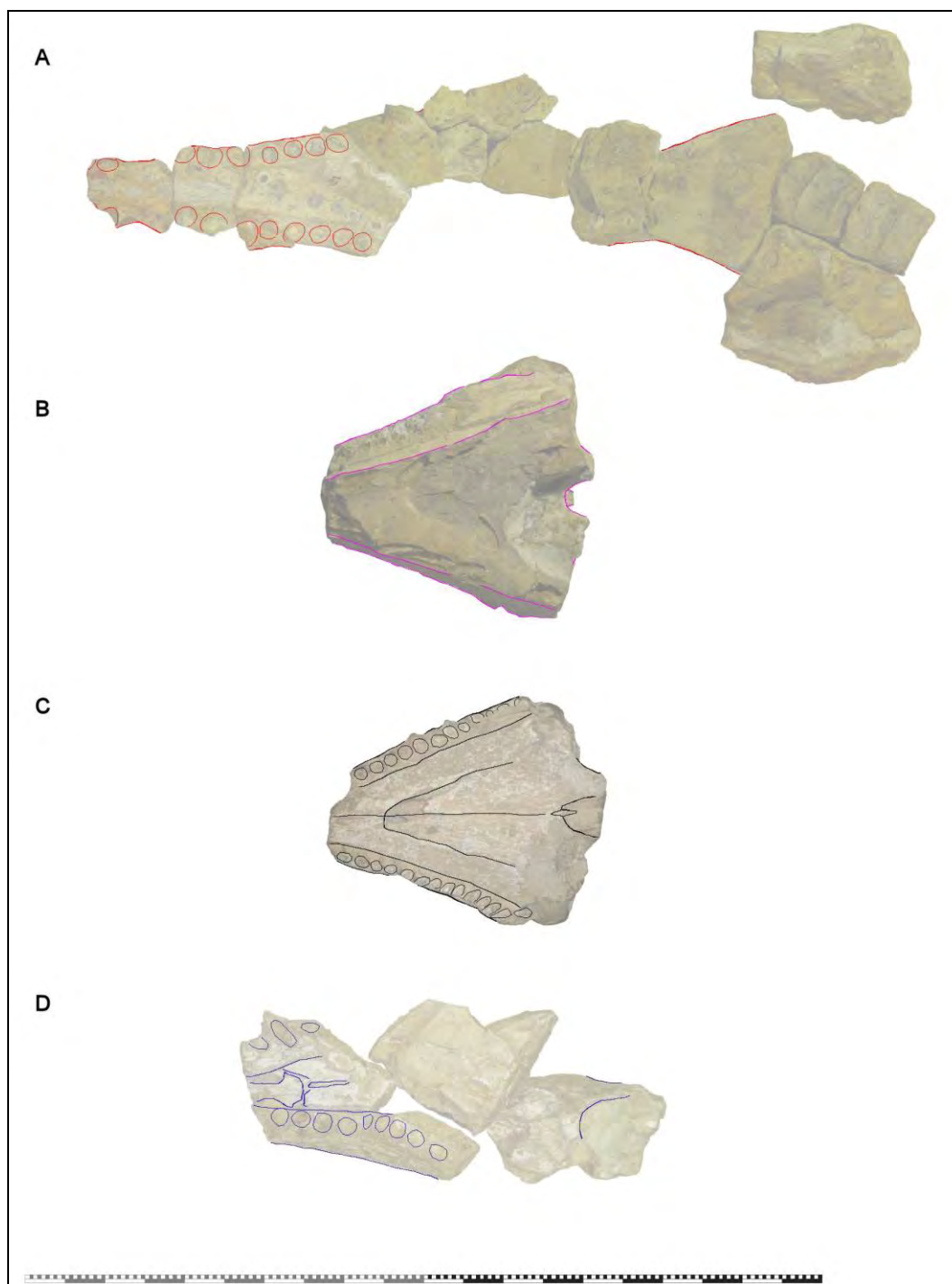


Figure 4-36: Traced landmarks/ outlines for specimens of *Kronosaurus queenslandicus* in ventral view, rescaled to the dimensions of QM F10113: (A) QM F10113 (cranium), (B) QM F2446, (C) QM F51291, (D) QM F2454. Scale bar = 2 metres.

4. Maximum Symphyseal Width (MSW): the maximum width (in the transverse axis) of the expanded part of the anterior part of the mandibles. In *Kronosaurus queenslandicus*, this is generally at, or near, to the D4 tooth position.

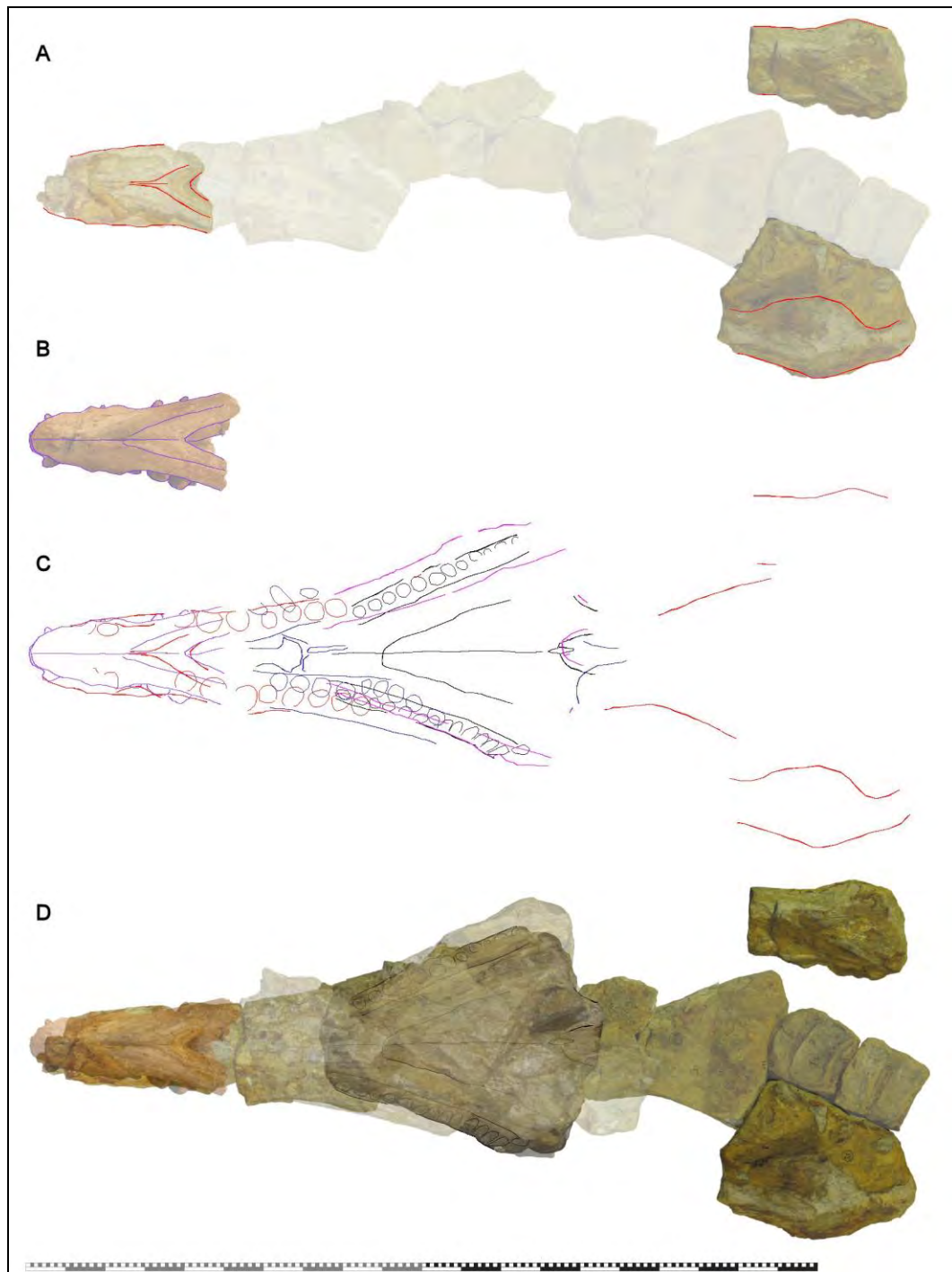


Figure 4-37: Traced landmarks/ outlines for specimens of *Kronosaurus queenslandicus* in ventral view, rescaled to the dimensions of QM F10113: (A) QM F10113 (mandible), (B) QM F2446, (C) combined outlines, (D) combined images. Scale bar = 2 metres.

Note that two of these metrics – DCL and s-M1 – require preservation of the anterior tip of the premaxillae. These are missing in QM F10113, which preserves the premaxillae only to the Pmx3 alveolus. The position of the anterior tip of the premaxillae was restored by comparison with QM F18827 and MCZ 1284: the

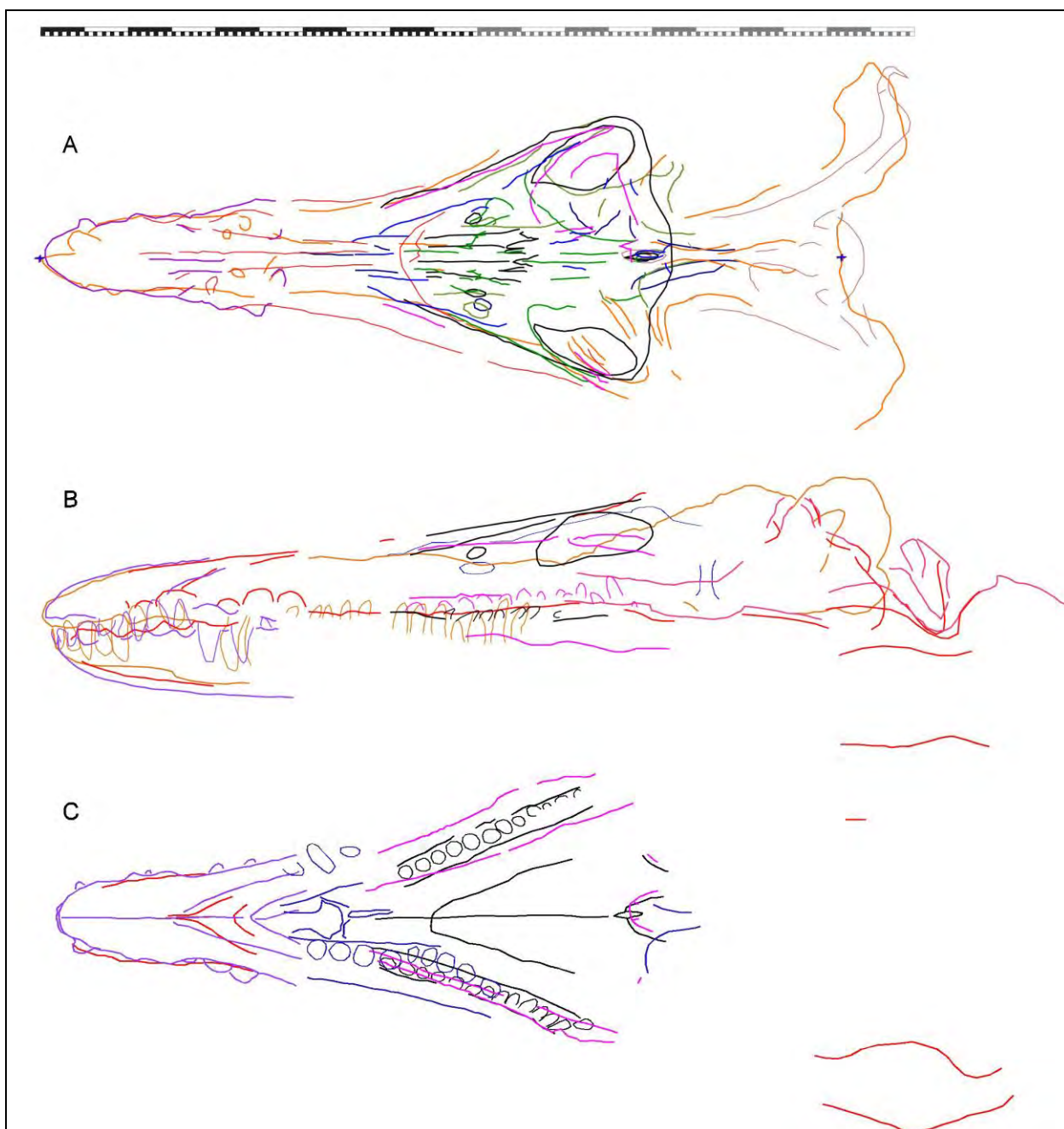


Figure 4-38: Combined outlines for specimens of *Kronosaurus queenslandicus*, rescaled to the dimensions of QM F10113; (A) dorsal, (B) lateral, (C) ventral views, Scale bar = 2 metres.

preservation of most of the mandibular symphysis in QM F10113 allowed the anterior rostral tip to be reconstructed with a high degree of confidence. The estimates of DCL and s-M1 for QM F10113 were then based upon this reconstruction of the anterior rostrum.

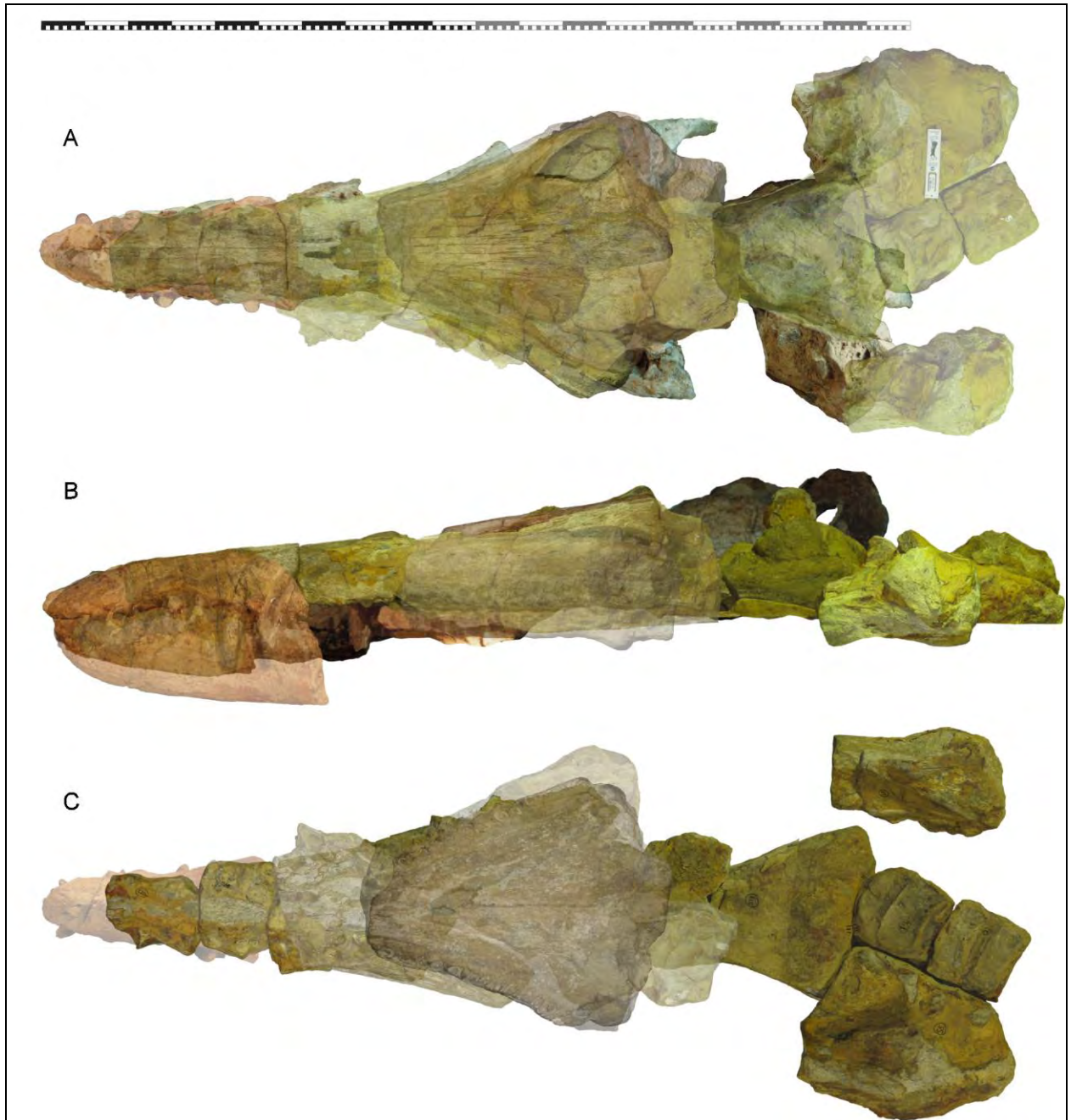


Figure 4-39: Combined images for specimens of *Kronosaurus queenslandicus*, rescaled to the dimensions of QM F10113; (A) dorsal, (B) lateral, (C) ventral views, Scale bar = 2 metres.

Once the outlines from multiple specimens were aligned and displayed to a consistent scale, the dorsal, lateral, and ventral outlines (Figure 4-38) were printed and reconstructed outlines and major features of the skull were drawn by hand for each view. The drawn reconstructions were then scanned and vector outlines traced over them so that a 2D vector version of each was generated; vector reconstructions were prepared separately for the cranium and mandible, and the dorsal and ventral

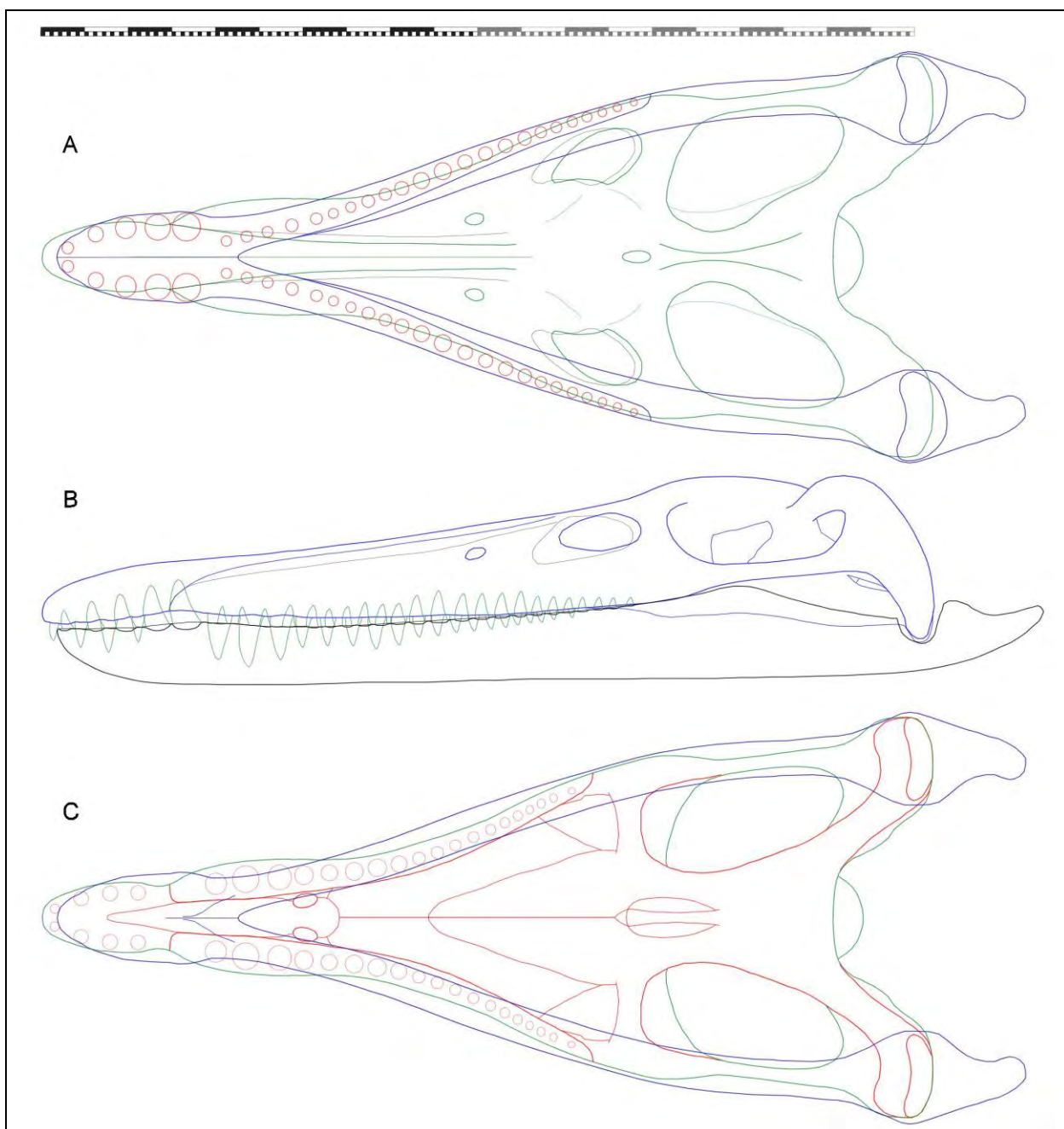


Figure 4-40: Vector outlines created for the skull of *Kronosaurus queenslandicus*, based upon the traced landmark/ outlines shown in Figure 4-38 and scaled to the dimensions of QM F10113, in (A) dorsal, (B) lateral, and (C) ventral view. In (A) and (B), the faint lines of the orbits and dorsal median ridge indicate proportions based upon QM F51291. Scale bar = 2 metres.

views were forced to bilateral symmetry. The proportions of the reconstructions in dorsal, ventral, and lateral view were aligned as much as possible. For the parts of the skull not well preserved in any of the *Kronosaurus queenslandicus* material – the zygoma, the sagittal crest, and the overall geometry of the mandibular rami – the

shape of these in USNM 4989 and FHSM VP-321 specimens of *Brauchauchenius lucasi* were used to generate the outlines.

The various specimens of *Kronosaurus queenslandicus* included in this analysis encompass between them an appreciable range in body size – enough that some allometric variation should be expected. For amniotes, allometric variation in the size and shape of the orbits is documented in numerous taxa, and the preserved morphology of the orbits in QMF 51291, compared with QM F18827, suggests that this may be the case between the smaller and larger specimens in this analysis. Similarly, the dorsal median ridge appears to be proportionally broader in QM F51291 than in QM F10113 and QM F2454. To provide an initial visual description of possible allometric variation in *K. queenslandicus*, the reconstructions included two versions of the geometry of the orbits and dorsal median ridge; for the orbits, the outline was based upon QM F51291 and QM F18827, and for the dorsal median ridge on QM F51291 and QM F10113.

Specimen	comparative measurement	BSL (cm)
QM F1609	MSW (0.7)	131.3
MCZ 1284	s-M1 (0.88)	165.1
QM F2446	pf-n (1.2)	225.1
QM F2454	pf-n (1.24)	232.6
QM F10113	-	187.6
QM F18154	pf-n (0.88)	165.1
QM F18827	DCL (1.06)	198.9
QM F51291	pf-n (0.64)	120.1
QM F52279	pf-n (0.7)	131.3

Table 4-2: Calculated basal skull lengths (BSL) for *Kronosaurus queenslandicus* specimens preserving skull material, based upon comparison with QM F10113. Criteria used for comparative measurement (see text for definitions); MSW, maximum symphyseal width; s-M1, snout-M1 tooth distance; pf-n, distance between parietal foramen and external nares; DCL, dorsal cranial length. Numbers in brackets indicate scaling ratios with QM F10113. Species listed in chronological order of specimen registration.

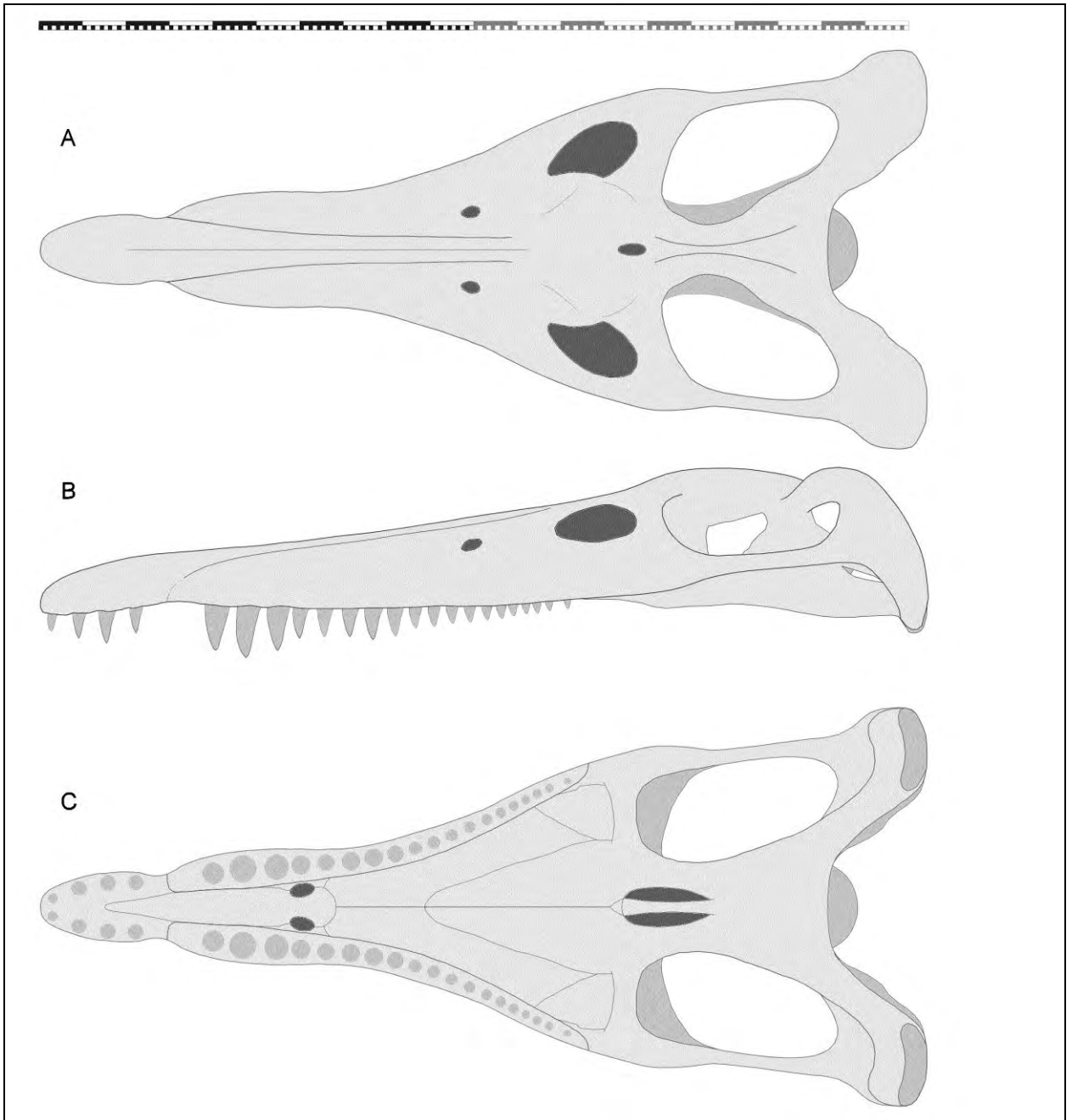


Figure 4-41: 2D reconstruction of the cranium in *Kronosaurus queenslandicus*, based upon the vector outlines shown in Figure 4-40 and scaled to the dimensions of QM F10113, in (A) dorsal, (B) lateral, and (C) ventral view. Proportions of orbits and dorsal median ridge are shown for 'adult' sized skull. Scale bar = 2 metres.

Results

The traced outlines for the *Kronosaurus queenslandicus* specimens detailed in Section 4.2 are shown for the dorsal (Figure 4-31, Figure 4-32), lateral (Figure 4-34, Figure 4-35, and ventral (Figure 4-36, Figure 4-37) images.

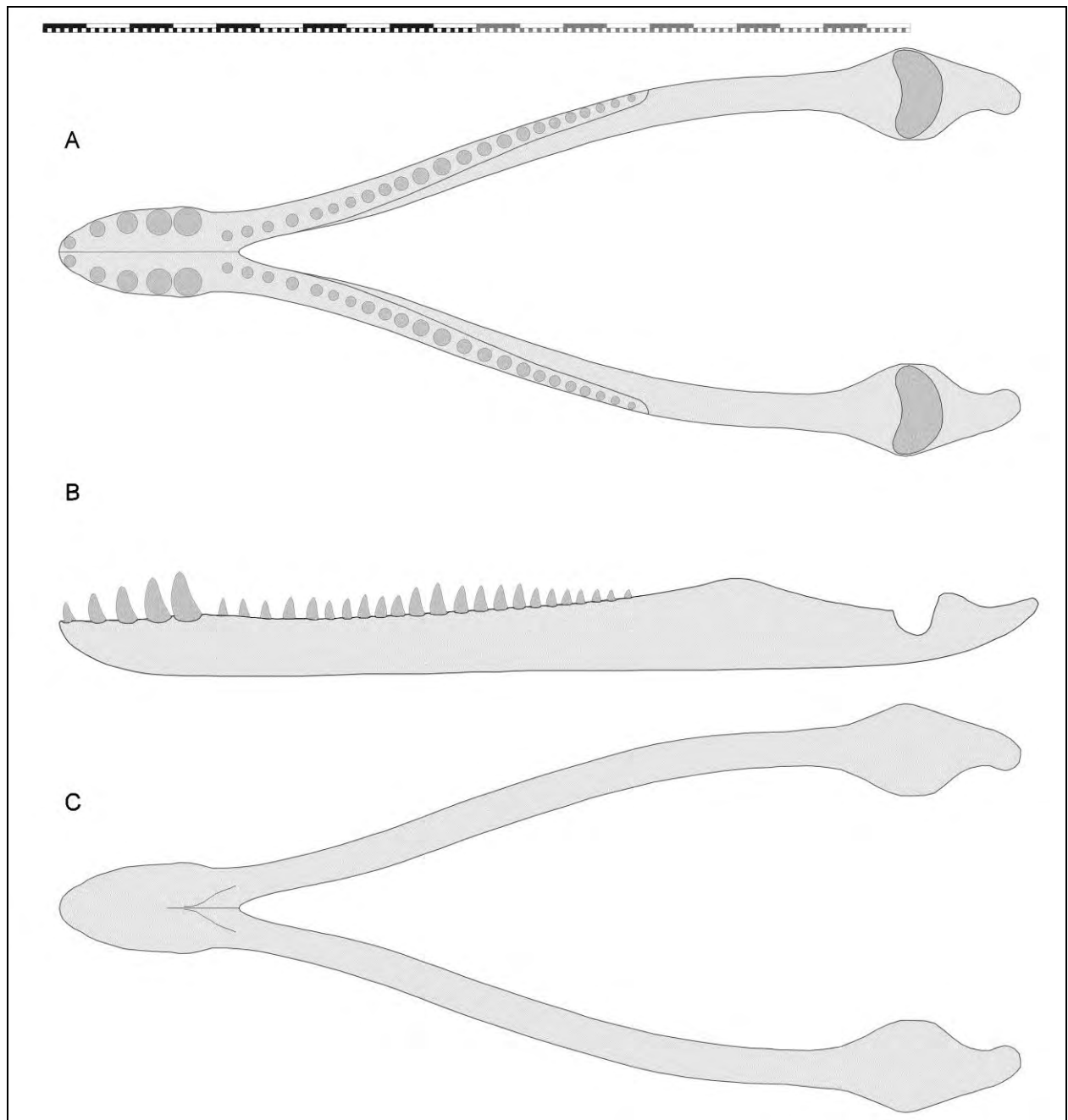


Figure 4-42: 2D reconstruction of the mandible in *Kronosaurus queenslandicus*, based upon the vector outlines shown in Figure 4-40 and scaled to the dimensions of QM F10113, in (A) dorsal, (B) lateral, and (C) ventral view. Scale bar = 2 metres.

Table 4-2 shows the scaling factors calculated for each specimen and lists the specific criteria used to rescale each to the dimensions of QM F10113. The rescaled outline/landmarks for all applicable specimens were then overlain and aligned with each other for each of the dorsal (Figure 4-33, Figure 4-38), lateral (Figure 4-35, Figure 4-38), and ventral (Figure 4-37, Figure 4-38) views. Although not directly used

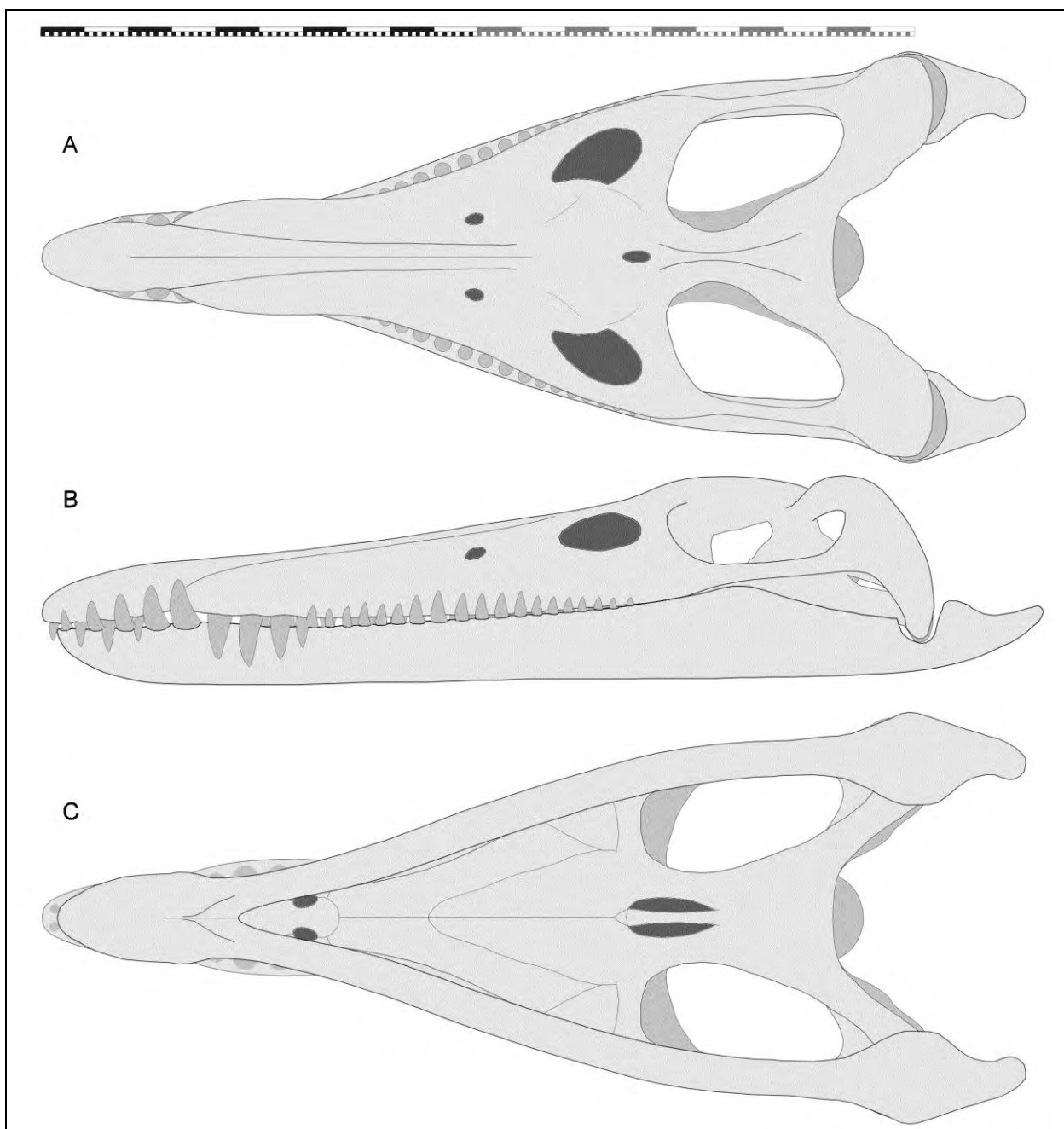


Figure 4-43: 2D reconstruction of articulated cranium and mandible in *Kronosaurus queenslandicus*, from an overlay of the reconstructions shown in Figure 4-41 and Figure 4-42, in (A) dorsal, (B) lateral, and (C) ventral view. Note the ‘underbite’ of the lower jaw teeth in the posterior half of the tooth row. Scale bar = 2 metres.

to generate the skull reconstruction, rescaling and aligning the orthogonal photographs of each specimen as per their respective outline/landmarks provides a composite impression of overall preserved skull morphology in *K. queenslandicus*.

The outlines from Figure 4-38 provided the basis for the reconstructions of the skull in dorsal, lateral, and ventral view as described above. The reconstructed vector outlines are shown in Figure 4-39: For the dorsal and lateral views, the ‘adult’ geometry of the orbital margin and dorsal median ridge are shown as heavy lines, while the respective geometry reconstructed from QM F51291 is shown as fine lines (Figure 4-39A, B).

From the reconstructed vector outlines, reconstructions of the cranium (Figure 4-41), mandible (Figure 4-42), and articulated skull (Figure 4-43) were prepared.

Discussion

Given the potential for taphonomic, ontogenetic, allometric, and individual variation between the eight specimens of *Kronosaurus queenslandicus* used to generate the reconstructions presented here, it would be surprising if there were no details of the reconstructed morphology affected by uncertainty or even contradictory evidence. Specific issues affecting this reconstruction are as follows:

1. The preserved depth of the symphysis and mandibular ramus in QM F10113 is proportionally less than that preserved in MCZ 1285 and FHSM VP-321.
2. The width of the rostrum is proportionally greater, and the height lesser, in QM F10113, compared with QM F18827 and MCZ 1285.
3. The position of the epipterygoids appears to be more posterior in QM F10113 and QM F18154 than in QM F51291.

In the case of the rostral proportions and epipterygoid position, I tried to create a geometry that ‘averaged’ the differences specified above. However, with the depth of the mandible, I emphasised the data from QM F10113 because both MCZ 1284 and FHSM VP-321 have been subjected to taphonomic distortion, whereas the symphyseal and articular parts of QM F10113 show no obvious signs of sedimentary compaction.

Some additional aspects of the reconstruction deserve mention:

- The zygomas are consistent with FHSM VP-321 (i.e., gracile).

- The height of the sagittal crest is conservative: it is reconstructed as being less tall than in FHSM VP-321.
- The overall shape of the mandibular rami, as viewed in the coronal plane, is consistent with the data from QM F2446, QM F18827, QM F51291.

Note that the reconstruction does not account for allometric variation in the morphological criteria used to rescale the outline/landmarks, and this is likely to be an additional, and important, source of error. In particular, most of the specimen data was rescaled with reference to the distance from the parietal foramen to the external nares (pf-n), and as this measurement is largely one of the length of the orbital region, allometric variation in orbital dimensions will therefore affect this measurement. This aspect of the reconstruction should be a focus for future attempts to update the reconstructed skull geometry in *Kronosaurus queenslandicus*.

Reconstructed skull anatomy of Kronosaurus queenslandicus

Structural

Kronosaurus queenslandicus is reconstructed as having a relatively elongate, moderately tall vaulted rostrum with a distinct dorsal median ridge. The large caniniform teeth are arranged in the forward part of the tooth row: there are four pairs of premaxillary teeth. The mandibular symphysis is short, bearing 6 ½ tooth positions, with 5 large teeth held in the expanded anterior spatulate part of the symphysis. The three anterior-most maxillary teeth occlude just behind the large D4 and D5 teeth of the lower jaw, resulting in a strong festooning (undulation in the line of the tooth tips along the tooth row) in the anterior part of the rostrum. In the posterior part of the tooth row, the dentition is less anisodont, and the teeth of the lower jaw occlude well lateral of the upper jaw, resulting in a pronounced ‘under bite’.

The orbits are oriented to face dorsally, laterally, and anteriorly. The temporal fenestrae are very large, but there is no anterior palatal vacuity or suborbital fenestrae. The braincase and occiput lie more or less in line with, or posterior to, the

dorsal skull roof, unlike the situation in *Liopleurodon ferox* (Noè, 2001) and *Peloneustes philarchus* (Ketchum, 2008). The suspensoria are reconstructed as sloping backwards to the quadrate-articular joint, rather than vertically.

Osteology

The lacrimals are present in smaller individuals, but tend to fuse in large adult specimens. The prefrontals are large and make up the antero-medial margin of the orbits and the posterior margin of the nares: the dorsal process of maxilla separates the naris from the dorsal median ridge and the frontals. The frontals are excluded from orbital margin by contact between the postfrontals and prefrontals: the frontals are also excluded from midline contact on the dorsal surface of skull roof by contact between the parietals and the facial processes of the premaxillae. The topology of the parietals, frontals, and prefrontals in brow region of skull is three-dimensionally complex.

The dorsal median ridge is formed from at least two pairs of elements at the dorsal surface – the premaxillae and the nasals – and apparently one pair of elements internally, which may be anterior processes of a brow element, possibly the frontals. The nasals and premaxillae fuse in adults, but the ventral elements remain separate.

Remarks

Almost all pliosaur crania are affected by substantial taphonomic variation – in addition, significant allometric variation is likely to be present. In the present study, criteria to account for these have been stated but remain largely subjective. Quantitative models of the taphonomic processes – in particular sedimentary compression – that affect pliosaur skulls from different strata worldwide would enable retrodeformation (Boyd and Motani 2008) of key specimens: some suggestions on a potential program for this line of research are made in subsequent chapters of this thesis.

In pliosaur palaeontology, the complexity of sutural morphology – and ontogenetic variation therein – has been largely analysed outside of a biologically relevant paradigm that could help to interpret complex or preservationally problematic

morphology: very little account is given to the biology of sutural contacts in extant reptiles in the interpretation of sutures in pliosaurs, although functional aspects of sutural morphology have been investigated for other extinct taxa such as theropods (Rayfield 2005). In particular, the pattern of fusion of sutures in relevant extant species, such as crocodylians and turtles, is poorly documented. Sutures do not necessarily fuse synchronously in extant taxa (pers. obs. of *Crocodylus porosus*), and sutural fusion is not limited to very early or very late stages of ontogeny, but can instead be correlated with the biomechanical context of feeding behaviours in adults (Snively et al. 2006). A basic consideration of the possible functional aspects of sutural morphology would suggest that the patency/ fusion of sutures should be expected to depend on the demands of (a) growth, or (b) redirection of strain fields around the skull (Moazen et al. 2009). The dorsal median ridge of the pliosaur cranium is positioned in the part of the skull that is predicted, by basic beam-theory mechanics, to be the site of significant mechanical strain during feeding in a meso- or longirostrine form: it should therefore be of no surprise that this region experiences profound ontogenetic variation in the patency of sutures. Likewise, the presence of the orbits has fundamental and far reaching consequences for the transmission of mechanical loads through the middle part of the skull: and yet, attempts by some workers to document the persistence of elements in the mid-nasal or circum-orbital region of pliosaur skulls have been ignored by others on the basis of limited but contradictory data, with apparently little consideration of the potential for variation in ontogenetic stage or biomechanical context (see Druckenmiller and Russell 2008 for summary).

Accurate reconstruction of skull anatomy in fossil forms requires careful attention to potential taphonomic and ontogenetic processes. The lack of attention given to pliosaur palaeontology through most of the 20th Century is being redressed, but current uncertainty in many aspects of pliosaur palaeobiology – compare, for example, the differing results in the phylogenies presented by Druckenmiller and Russell (2008) and Ketchum (2008) – underscores the need for a comprehensive account of the effects of these processes upon the preservation of cranial anatomy in this group.

4.6 **Size estimates of the different *Kronosaurus* specimens**

Size is a fundamental trait of organisms: in the present context, the size of the specimens provides the context for discussion of ontogenetic variation and the ecology of the species through its life cycle.

The scaling factors calculated for the various specimens in Section 4.5 (Table 4-2) were used to calculate basal skull length (BSL) for each specimen, by comparison with the reconstructed BSL in QM F10113. To illustrate the variation in skull lengths, dorsal views of the specimens were aligned with scaled outlines of the skull (Figure 4-44, Figure 4-45).

The results illustrate both the range in the size of the individual animals represented by the specimens, and also some of the potential problems with the use of the parietal foramen – external nares (pf-n) measurement as a scaling metric between specimens. For example, the reconstructed skull length of QM F2446 is somewhat larger than what might be estimated on the basis of the preserved width of this specimen, even allowing for the taphonomic distortion of the skull roof (Figure 4-44). A similar problem may affect the reconstructed length of QM F2454 (Figure 4-45). The potential for allometric variation of the orbital region of the skull is discussed above: as the reconstructions of skull length in the specimens discussed here do not account for allometric variation, these estimates should be regarded as preliminary and should be the focus of further investigation.

The palaeobiological implications of the range of body sizes amongst these specimens is considered further in Chapter 6.

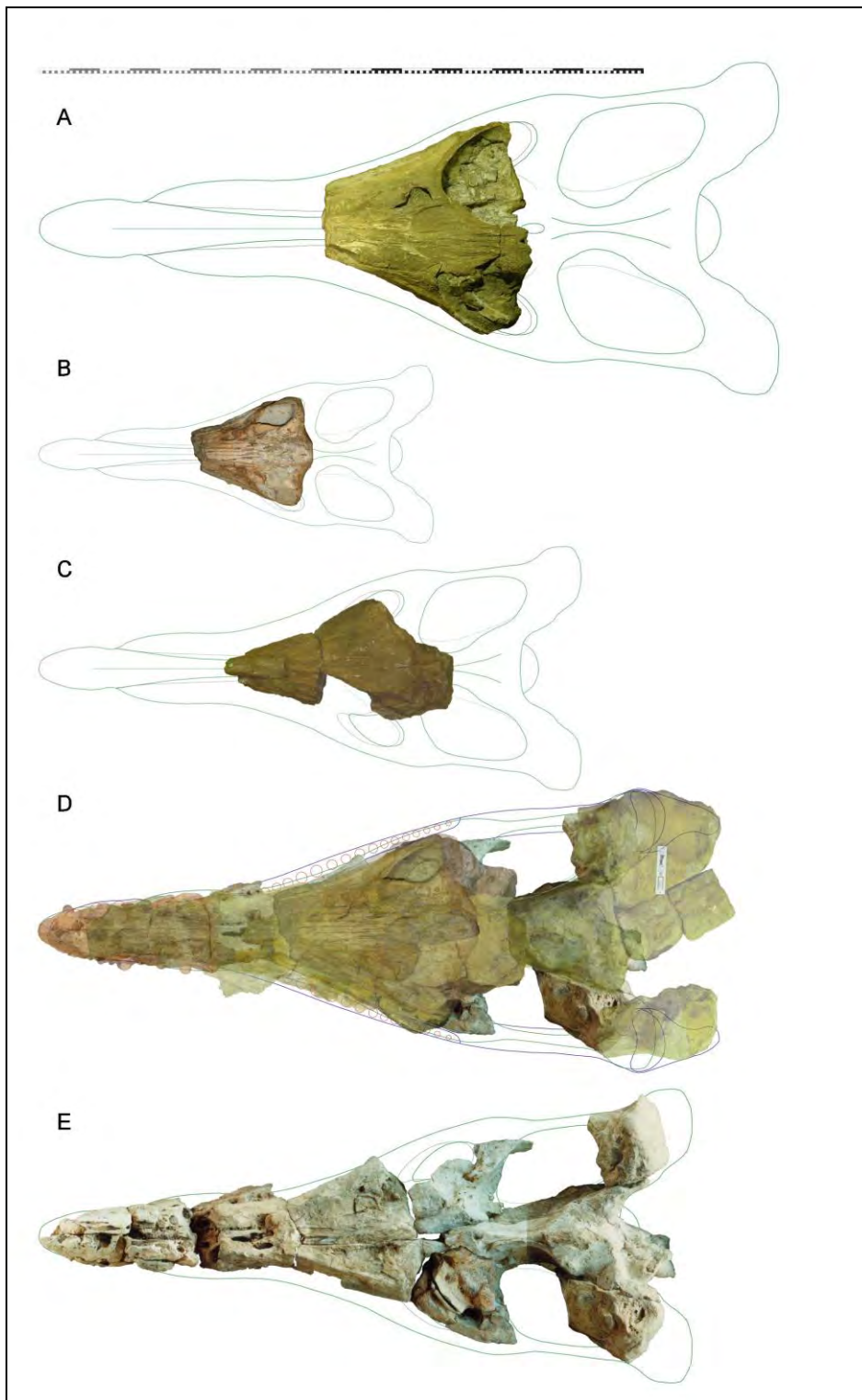


Figure 4-44: Dorsal view of *Kronosaurus queenslandicus* specimens, shown to scale: (A) QM F2446, (B) QM F51291, (C) QM F18154, (D) composite images scaled to QM F10113, (E) QM F18827. Scale bar = 2 metres. Outlines show calculated skull lengths for each specimens (see text, Table 4-2).

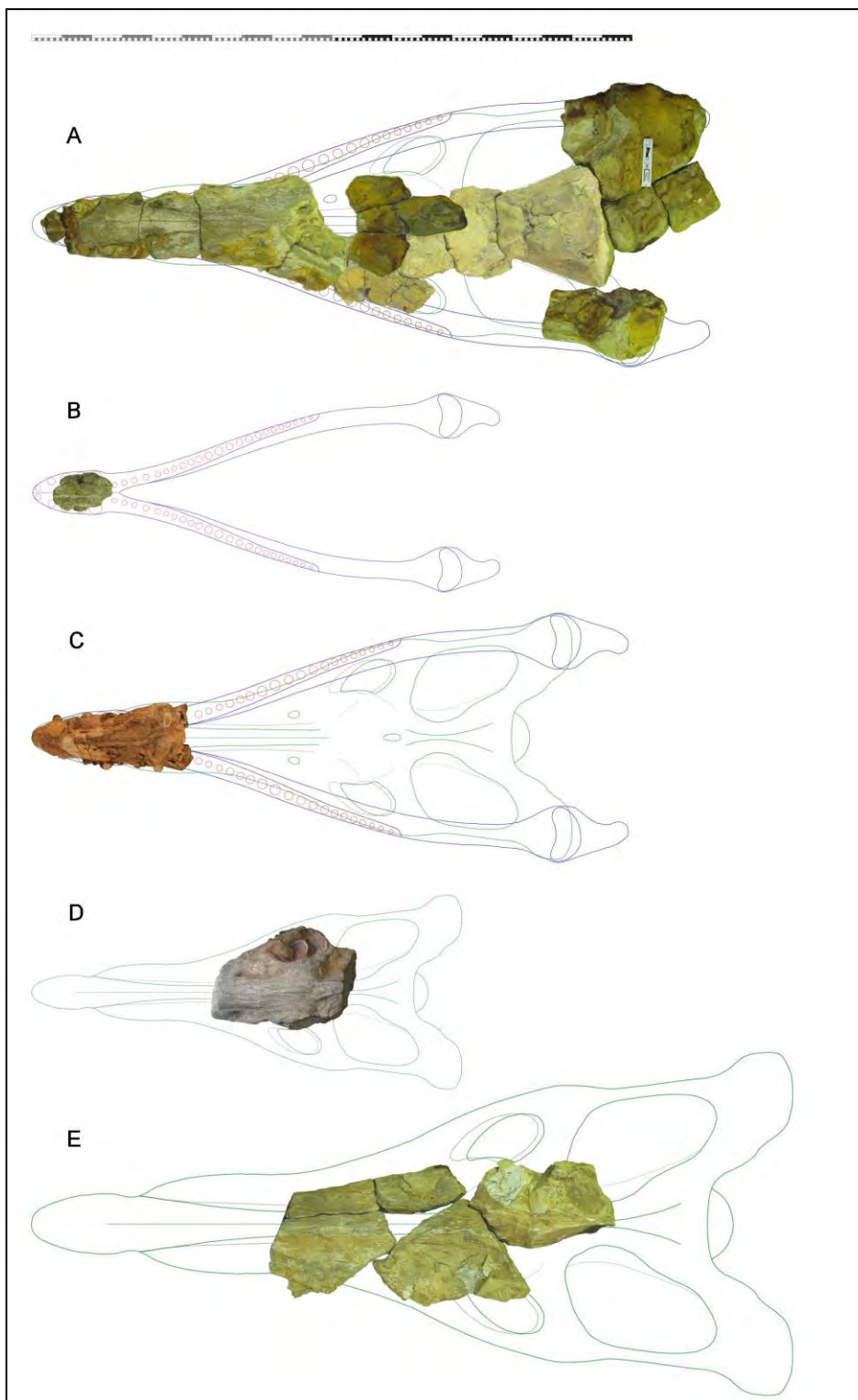


Figure 4-45: Dorsal view of *Kronosaurus queenslandicus* specimens, shown to scale: (A) QM F10113, (B) QM F1609, (C) MCZ 1284, (D) QM F52279, (E) QM F2454. Scale bar = 2 metres. Outlines show calculated skull lengths for each specimens (see text, Table 4-2)

4.7 References

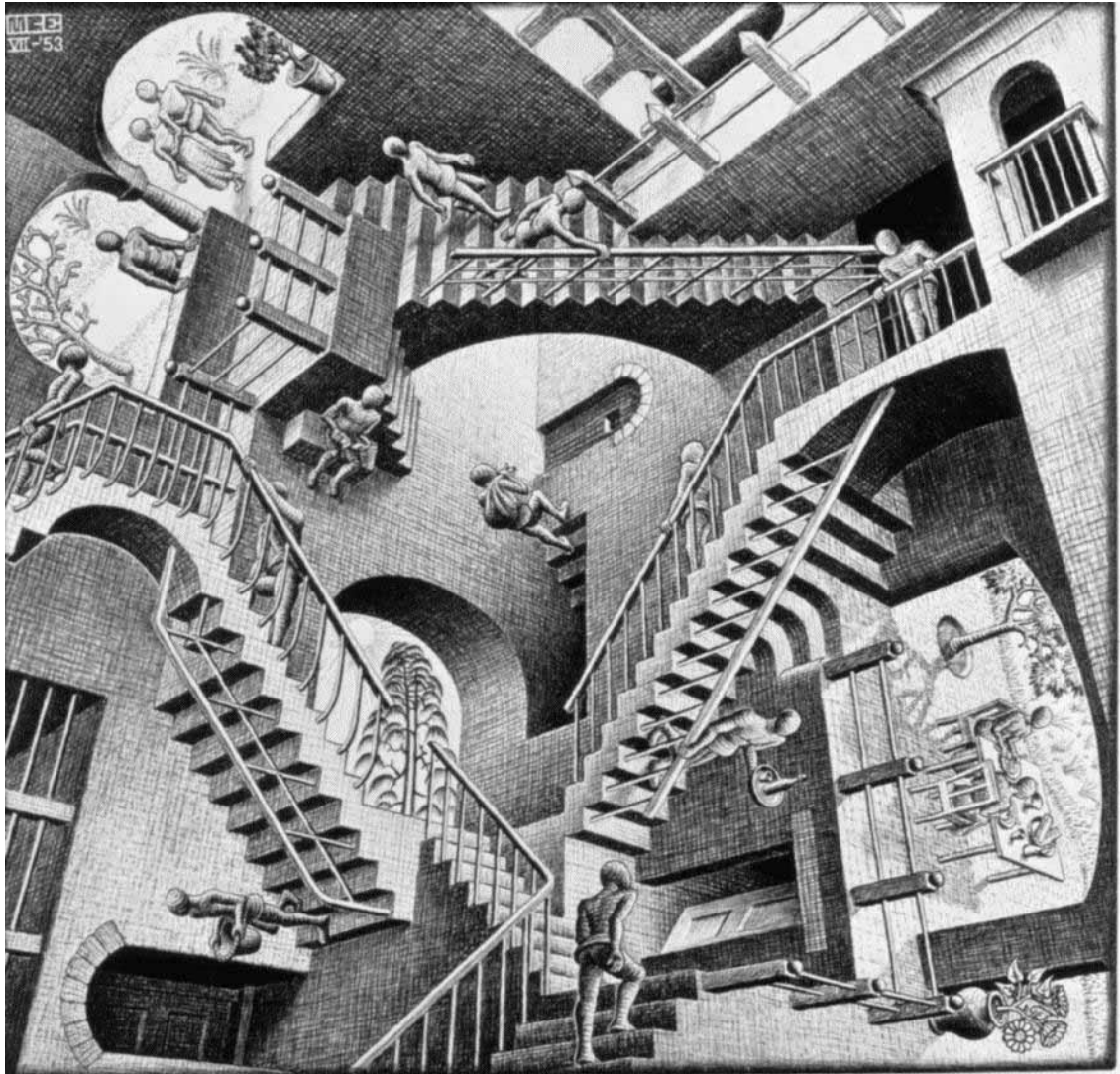
- Allison, P. A., C. R. Smith, H. Kukert, J. W. Deming, and B. A. Bennett. 1991. Deep-water taphonomy of vertebrate carcasses; a whale skeleton in the bathyal Santa Catalina Basin. *Paleobiology* 17(1):78-89.
- Andrews, C. W. 1895. On the structure of the skull of *Peloneustes philarcus*, a pliosaur from the Oxford Clay. *Annals and Magazine of Natural History* 16(6):242-256.
- Andrews, C. W. 1911. On the Structure of the Roof of the Skull and of the Mandible of *Peloneustes*, with some remarks on the Plesiosaurian Mandible generally. *Geological Magazine* 8(4):160-164.
- Andrews, C. W. 1913. A descriptive catalogue of the Marine Reptiles of the Oxford Clay, Part II. BM(NH), London.
- Bakker, R. T. 1975. Dinosaur Renaissance. *Scientific American* 232:58-78.
- Boyd, A. A., and R. Motani. 2008. Three-dimensional re-evaluation of the deformation removal technique based on "jigsaw puzzling". *Palaeontologica Electronica* 11(2):7A:7p.
- Busbey, A. B. 1995. The structural consequences of skull flattening in crocodylians. Pp. 173-192. *In* J. Thomason, ed. *Functional morphology in vertebrate paleontology*. Cambridge University Press, Cambridge.
- Carpenter, K. 1996. A review of short-necked plesiosaurs from the Cretaceous of the Western Interior, North America. *Neues Jahrbuch für Geologie und Paläontologie Abhandlungen* 201:259-287.
- Conybeare, W. D. 1824. On the Discovery of an almost perfect skeleton of the Plesiosaurus. *Transactions of the Geological Society, Second Series* 1:381-389.
- Cruikshank, A. R. I. 1994. Cranial anatomy of the Lower Jurassic pliosaur *Rhomaleosaurus megacephalus* (Stutchbury) (Reptilia: Plesiosauria). *Philosophical Transactions of the Royal Society, London B* 343:247-260.
- Druckenmiller, P. S. 2002. Osteology of a plesiosaur from the Lower Cretaceous (Albian) Thermopolis Shale of Montana. *Journal of Vertebrate Paleontology* 22:29-42.
- Druckenmiller, P. S., and A. P. Russell. 2008. A phylogeny of Plesiosauria (Sauropterygia) and its bearing on the systematic status of *Leptocleidus* Andrews, 1922. *Zootaxa* 1863:1-120.
- Everhart, M. J. 2007. Historical note on the 1884 discovery of *Brachauchenius lucasi* (Plesiosauria; Pliosauridae) in Ottawa County, Kansas. *Transaction of the Kansas Academy of Science* 110:255-258.
- Forrest, R., and N. Oliver. 2003. Ichthyosaurs and plesiosaurs from the Lower Spilsby Sandstone Member (Upper Jurassic), north Lincolnshire. *Proceedings of the Yorkshire Geological Society* 54(4):269-275.

- Froese, R. 1999. The good, the bad, and the ugly: A critical look at species and their institutions from a user's perspective. *Reviews in Fish Biology and Fisheries* 9:375-378.
- Hampe, O. 1992. Ein grosswuchsiger Pliosauridae (Reptilia: Plesiosauria) aus der Unterkreide (oberes Aptium) von Kolumbien *Courier Forsch.-Inst. Senckenberg* 145:1-32.
- Hampe, O. 2005. Considerations on a *Brachauchenius* skeleton (Pliosauroida) from the lower Paja Formation (late Barremian) of Villa de Leyva area (Colombia). *Mitt. Mus. Nat.kd. Berl., Geowiss. Reihe* 8:37-51.
- Henderson, R. A. 2004. A Mid-Cretaceous Association of Shell Beds and Organic-rich Shale: Bivalve Exploitation of a Nutrient-Rich, Anoxic Seafloor Environment. *Palaios* 19:156-169.
- Ketchum, H. F. 2008. The anatomy, taxonomy, and systematics of three British Middle Jurassic pliosaurs (Sauropterygia: Plesiosauria) and the phylogeny of Plesiosauria. Unpublished Ph.D. Thesis. University of Cambridge.
- Liggett, G. A., K. Shimada, C. Bennett, and B. A. Schumacher. 2005. Cenomanian (Late Cretaceous) reptiles from northwestern Russell County, Kansas. *PaleoBios* 25:9-17.
- Linder, H. 1913. Beiträge zur Kenntnis der Plesiosauria-Gattungen *Peloneustes* und *Pliosaurus*. Nebst Anhang: Über die Beiden Ersten Halswirbel der Plesiosauria. *Geologische und Palaeontologische Adhandlungen* 11:339-409.
- Longman, H. A. 1924. A new gigantic marine reptile from the Queensland Cretaceous. *Memoirs of the Queensland Museum* 8:26-28.
- Longman, H. A. 1935. Palaeontological Notes. *Memoirs of the Queensland Museum* 10(5):236-239.
- McHenry, C. R., A. G. Cook, and S. Wroe. 2005. Bottom-Feeding Plesiosaurs. *Science* 310:75.
- Milne, N., and P. O'Higgins. 2002. Inter-specific variation in *Macropus* crania: form, function, and phylogeny. *Journal of Zoology* 256:523-535.
- Moazen, M., N. Curtis, P. O'Higgins, M. Jones, S. Evans, and M. J. Fagan. 2009. Assessment of the role of sutures in a lizard skull - a computer modelling study. *Proceedings of the Royal Society Series B* 276:39-46.
- Molnar, R. E. 1991. Fossil Reptiles of Australia. Pp. 605-701. *In* P. Vickers-Rich, J. M. Monaghan, R. F. Baird, and T. H. Rich, eds. *Vertebrate Palaeontology of Australasia*.
- Nelson, J. S. 1999. Editorial and introduction: The species concept in fish biology. *Reviews in Fish Biology and Fisheries* 9:277-280.
- Newman, B., and L. B. Tarlo. 1967. A Giant Marine Reptile From Bedfordshire. *Animals* 10(2):61-63.

- Noè, L. F. 2001. A Taxonomic and Functional Study of the Callovian (Middle Jurassic) Pliosauroida (Reptilia, Sauropterygia). Unpublished PhD Thesis. University of Derby.
- Noè, L. F., D. T. J. Smith, and D. I. Walton. 2004. A new species of Kimmeridgian pliosaur (Reptilia; Sauropterygia) and its bearing on the nomenclature of *Liopleurodon macromerus*. Proceedings of the Geologists' Association 115:13-24.
- O'Higgins, P., and N. Jones. 1998. Facial growth in *Cercocebus torquatus*: an application of three dimensional geometric morphometric techniques to the study of morphological variation. Journal of Anatomy 193:251-272.
- O'Keefe, F. R. 2001. A cladistic analysis and taxonomic revision of the Plesiosauria (Reptilia: Sauropterygia). Acta Zool. Fennica 213:1-63.
- Paul, G. S. 1988. Predatory Dinosaurs of the World. Simon and Schuster, New York.
- Rayfield, E. J. 2005. Aspects of comparative cranial mechanics in the theropod dinosaurs *Coelophysis*, *Allosaurus* and *Tyrannosaurus*. Zoological Journal of the Linnean Society 144:309-316.
- Regan, C. T. 1926. Organic Evolution. Pp. 75-86. Rep. 93rd Meet. Brit. Assoc. Adv. Sci., 1925.
- Schumacher, B. A., and M. J. Everhart. 2005. A stratigraphic and taxonomic review of plesiosaurs from the old "Fort Benton Group" of Central Kansas: a new assessment of old records. Paludicola 5(2):33-54.
- Smith, A. S., and G. J. Dyke. 2008. The skull of the giant predatory pliosaur *Rhomaleosaurus cramptoni*: implications for plesiosaur phylogenetics. Naturwissenschaften DOI 10.1007/s00114-008-0402-z.
- Snively, E., D. M. Henderson, and D. S. Phillips. 2006. Fused and vaulted nasals of tyrannosaurid dinosaurs: implications for cranial strength and feeding mechanics. Acta Palaeontologica Polonica 51:435-454.
- Tarlo, L. B. 1959. *Stretosaurus* gen. nov., a giant pliosaur from the Kimmeridge Clay. Palaeontology 2(1):39-55.
- Tarlo, L. B. 1960. A review of the Upper Jurassic pliosaurs:. Bulletin of the British Museum (Natural History), Geology series 4:145-189.
- Taylor, M. A. 1992. Functional anatomy of the head of the large aquatic predator *Rhomaleosaurus zetlandicus* (Plesiosauria, Reptilia) from the Toarcian (Early Jurassic) of Yorkshire, England. Philosophical Transactions of the Royal Society, London B 335:247-280.
- Taylor, M. A. D., and A. R. I. Cruickshank. 1993. Cranial anatomy and functional morphology of *Pliosaurus brachyspondylus* (Reptilia: Plesiosauria) from the Late Jurassic of Westbury, Wiltshire. Philosophical Transactions of the Royal Society London. B 341:399-418.
- White, T. 1935. On the skull of *Kronosaurus queenslandicus* Longman. Boston Soc. Natural History, Occ. Papers 8:219-228.

- Williston, S. W. 1903. North American Plesiosaurs (Part 1). Field Columbian Museum, Publ. 73, Geological Series 2(1):1-79.
- Williston, S. W. 1907. The skull of *Brachauchenius*, with special observations on the relationships of the plesiosaurs.
- Williston, S. W. 1925. The Osteology of the Reptiles. Harvard University Press, Cambridge, Mass.
- Wroe, S., and N. Milne. 2007. Convergence and remarkably consistent constraint in the evolution of carnivore skull shape. *Evolution* 61:1251-1260.

5. Form (3-D)



Relativity, M. Escher, 1953. Being able to draw an object in two dimensions does not necessarily mean that it can exist in three.

(c) 2009 The M.C. Escher Company - the Netherlands. All rights reserved. Used by permission.
www.mcescher.com.

“His pattern indicates two-dimensional thinking”.

Mr Spock, Star Trek: The Wrath of Khan, 1982.

5.1 **Adventures in the third dimension**

We live in a 3-D world, and yet by convention we communicate in two dimensions or less. In terms of the way that information is conveyed, written text is a one dimensional medium, and when we do seek to augment our paper-based communiqués we do it with 2-D pictures. We are so used to this, and so proficient at communicating information in this way, that we hardly even notice it.

Inevitably, there are particular concepts that do not lend themselves to conventional one- and two-dimensional media. With these we struggle, but it seems that our ability to explore these concepts is not limited by any innate inability to comprehend data in dimensions greater than two – in our daily lives we continuously process the world in three spatial and one temporal dimensions. We understand 3-D data when it is presented to us, but our ability to communicate the same data has been limited to what can be represented on paper: a maximum of two dimensions allowed. Even with the increasing use of computers, information is still predominately conveyed in one or two dimensional formats. Of course, one possibility offered by computers is to store and represent data in 3-D formats: this allows us to not just communicate 3-D data better with others, but to explore it ourselves.

For the vast majority of fossils, 3-D data is critical to their interpretation: this is presumably one of the reasons that curated collections of specimens are considered to be much more important than the text and pictures produced to describe them, and why time spent in collections physically examining specimens is still a vital part of many forms of palaeontological research. Ironically, given the importance of the 3-D data format for palaeontology, the source data is often in poor three dimensional shape, thanks to the vagaries of taphonomy. Pliosaur skulls, as we have seen in Chapter 3, are an excellent example of this problem. Given the importance of 3-D data, palaeontology as a discipline has been at the forefront of developing and using new computer based tools for managing and analysing data in a 3-D format. This chapter focuses on two of these tools; the application of CT scanning techniques to

Form (3-D)

3-D modelling of fossil specimens, and the integration of 3-D scan data with 2-D reconstructions to produce a 3-D reconstruction of a fossil species- in this case, *Kronosaurus queenslandicus*. The 3-D scan data is from QM F51291: this preserves the orbital region of the skull, for which the anatomy is poorly known for pliosaurs (Chapter 3). It also appears to be largely free of taphonomic distortion, and can therefore serve as a 3-D template for the creation of skull geometry in the orbital region. The 2-D reconstructions are those produced in Chapter 4.

5.2 Reconstructing 3-D morphology direct from CT

The degree of difficulty in converting Computed Tomography (CT) data into a 3-D computer model depends, in addition to the software available, on the peculiarities of the individual CT scan. The raw output from a CT scan is a series of greyscale bitmaps, each bitmap corresponding to an X-Ray slice of a certain thickness through the scanned object: medical CT scanners, such as the Toshiba Aquilion scanner used in the current work, arrange these bitmaps in a format called DICOM¹ which preserves information on the slice dimensions and the distance between each slice, the contrast settings, and specimen (usually, a ‘patient’) identifier data. As a form of X-Ray scan, the CT collects data on the structural geometry and density² of the specimen being scanned: for each slice, the resolution of this data corresponds to the individual pixel size of the output bitmap. A typical CT slice is shown in Figure 5-1: the darkest pixels represent scan regions with the lowest density (i.e. CT attenuation), the whitest being those with the highest attenuation and thus the highest density.

A key part of CT imaging is the contrast settings chosen for the resulting output. Figure 5-2 shows the same slice shown in Figure 5-1, but at four different contrast settings. In medical CT, these contrast settings are referred to as a ‘window’ of Hounsfield Units³ (HU), and are specified by two numbers: the ‘W’ number (‘width’) denotes the HU range of the image, and the ‘L’ number (‘location’) denotes the middle HU value of the range.

In order to create a 3-D computer model from the CT scan, the imaging software being used must be able to convert the image stack (i.e. the array of 2-D bitmaps) from the CT output into a 3-D data array. To do this, the imaging software turns the

¹ Digital Imaging and Communications in Medicine;

² More specifically, the CT scan records X-ray absorbance (sometimes referred to as CT attenuation), not true density. Since denser materials tend to be more radio-opaque, i.e. they absorb a greater amount of X-Ray radiation, there is a quantitative correspondence between X-ray absorbance and true density: unfortunately, the relationship is non-linear (Figure 5-3) and varies with different types of material and individual scanners. In the DICOM format, X-Ray absorbency is quantified as Hounsfield Units³ (HU).

³ Named after Godfrey Hounsfield, who received a Nobel Prize for his work on developing CT scanning. The Hounsfield Range is set so that the CT attenuation of distilled water at Standard Temperature and Pressure (STP) is 0 HU, and the CT attenuation of air at STP is -1000 HU.

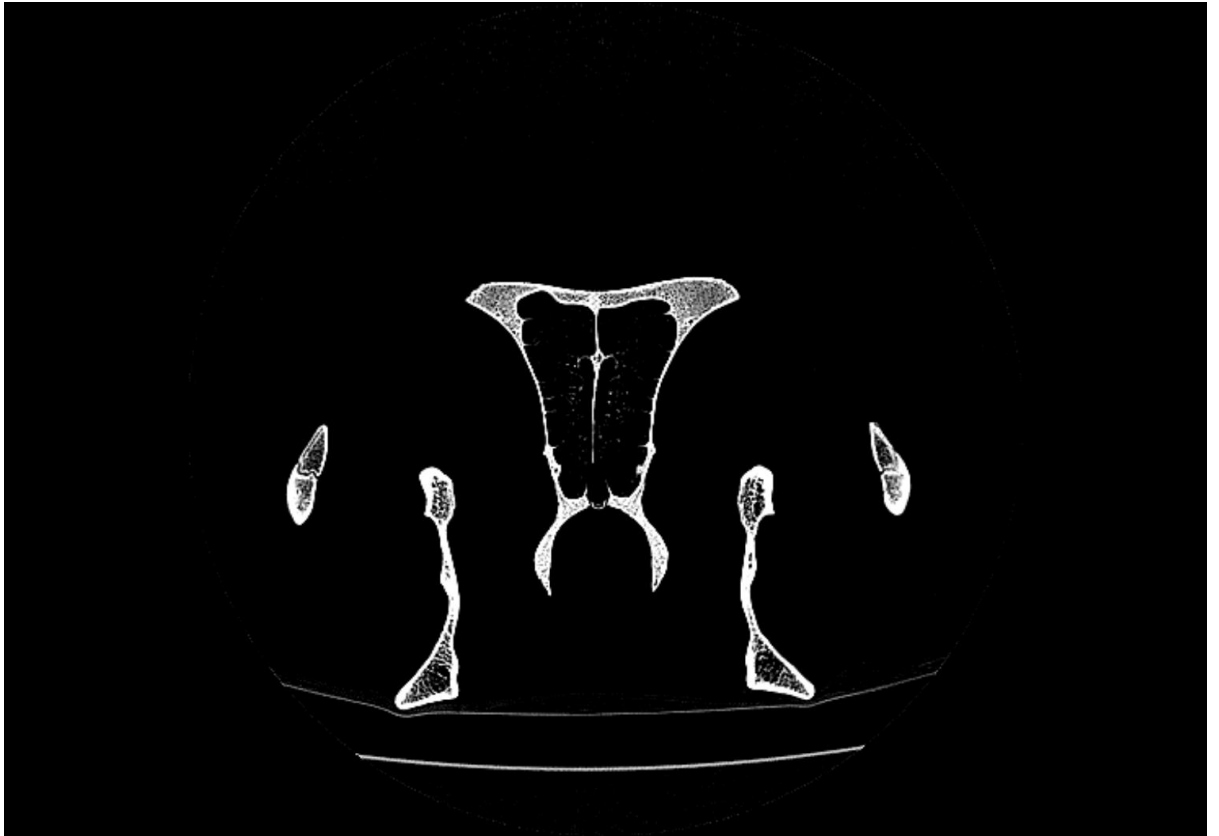


Figure 5-1: An example of a single slice from the CT scan of a lion skull, taken by the Toshiba Aquilion 16 scanner at the Newcastle Mater Misericordiae Hospital. Different grey-scale values in the bitmap correspond to different densities (as measured by CT attenuation), with black indicating the lowest density and white the highest. The contrast settings for this image were L300, W2000 (for explanation see text).

2-D pixels of the CT bitmaps into a 3-D voxel⁴: the centre of each voxel is assigned a coordinate in the X,Y, and Z axes, as well as a HU value. The X and Y coordinates are simply taken from the horizontal and vertical coordinates of the original pixel in the relevant bitmap, while the Z coordinate corresponds with the position of that bitmap slice within the whole array. The length of the voxel in the Z axis is equivalent to the inter-slice distance⁵ from the CT scan: the actual slice can be visualised as passing through the middle of the voxel in the Z axis. By organising the

⁴ The name 'voxel' denotes representation of a volume; i.e. the 3-D equivalent of a pixel.

⁵ Perhaps counter-intuitively, this is not the same as the slice thickness for the scan. The slice thickness refers to the volume of the specimen for which X-Ray attenuation is compressed into a single 2-D slice: the image representing the slice is thus showing the X-Ray shadow of the volume upon a 2-dimensional area, in the same way that a traditional X-Radiograph is an image of the X-Ray shadow of an entire object. The slice thickness is quite independent of the distance between slices, and in certain circumstances a radiographer will set the slice thickness to a value greater than the inter-slice distance so that there is a substantial overlap in the volumes represented by neighbouring slices. In any case, the relevant information for establishing the Z coordinates of a voxel is the inter-slice distance.

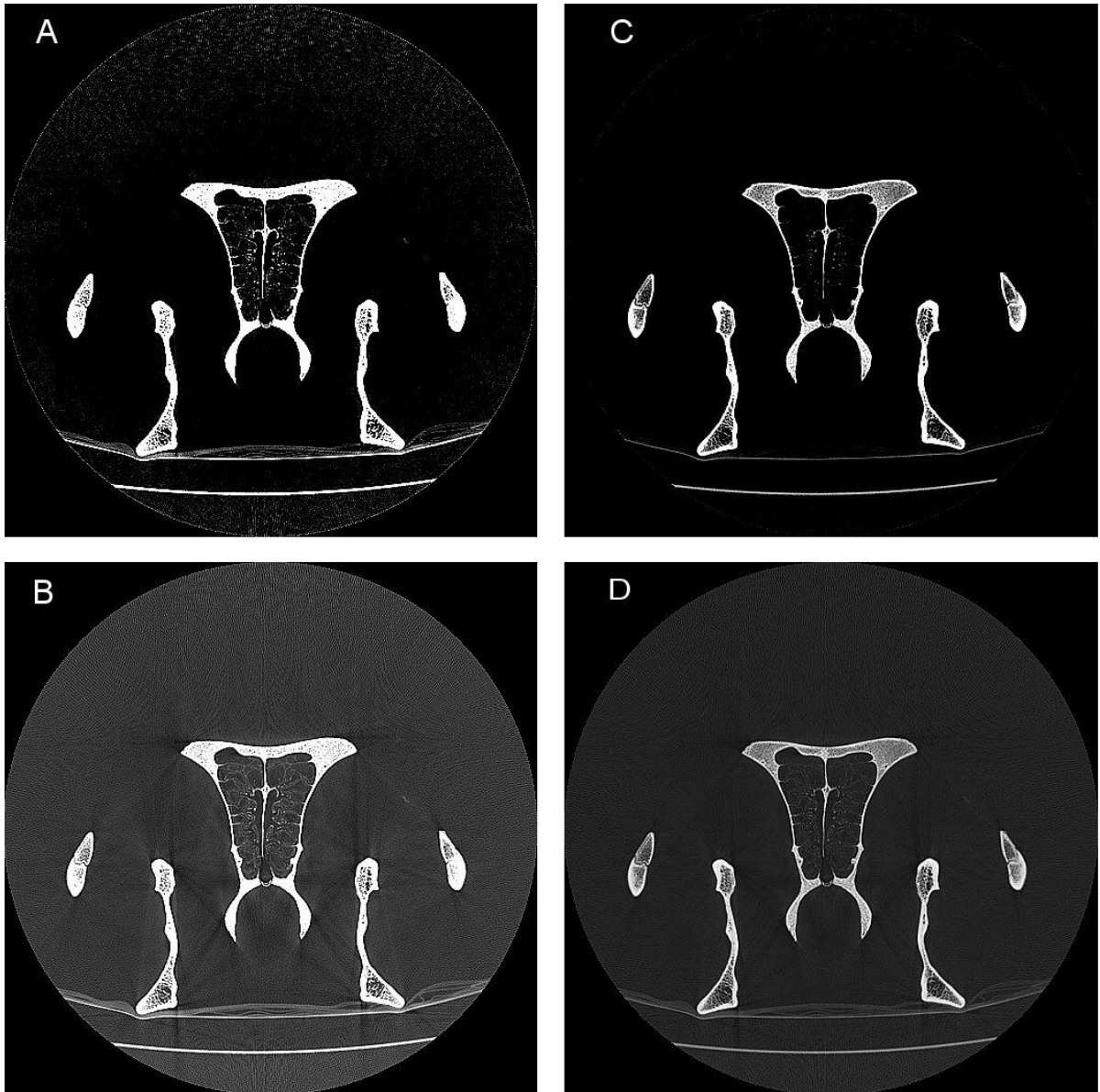


Figure 5-2: Scan output of the same slice shown in Figure 5-1, at different contrast settings. In **A**, L is set at -600 HU, W at 600: pixels that are black thus indicate an HU of -900 [$-600 - (600/2)$] or less, whilst white pixels indicate an HU of -300 [$-600 + (600/2)$] or more. Intermediate densities are shown by greyscale values that correspond to the specific HU, with the greyscale range being 256: thus, a pixel with a greyscale value of 128 indicates -600HU, and a greyscale of 64 indicates -450HU. Recall that the HU of water is 0, and that of air is -1000. Note that both spongy and cortical bone have HU values much greater than 0 and therefore show as pure white (greyscale 256) at this setting. **B**; L-600 W1600: the Hounsfield Range is therefore -1400 to +200, and even air is shown as grey pixels (also visible are the lines showing the refraction of the X-Ray beam by the specimen). **C**; L300 W2000: the Hounsfield Range is -700 to +1300, (as in Figure 5-1) and spans the range of typical spongy bone and thus shows spongy bone as a shade of grey, but cortical bone as white – this setting is commonly used as a preset for imaging osteological features. **D**; L400 W4000: the Hounsfield Range is -1600 to 2400, and even some pixels showing cortical bone have a greyscale value less than 256.

Form (3-D)

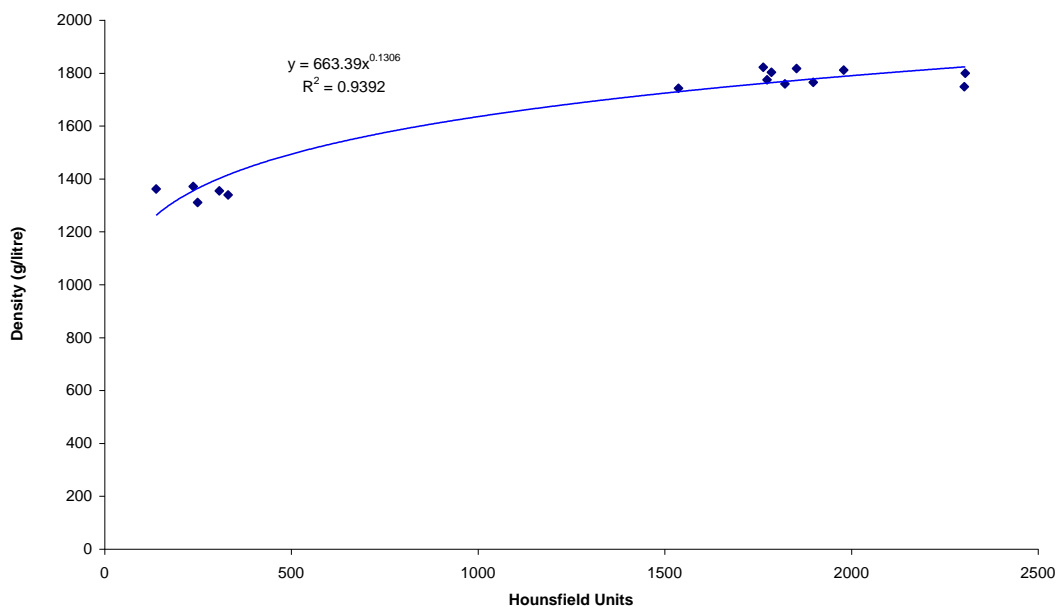


Figure 5-3: The relationship between Hounsfield Units and true density, as measured on samples of a bovine rib bone. The best fit line is a power function (the equation shown on the chart). The bimodal distribution corresponds to spongy (~350 HU) and cortical (~1500–2400 HU) bone from the same rib. Data from McLellan (2007).

CT data in this way, the imaging software can present the volume in three different orthogonal views: an example is shown in Figure 5-4. The imaging software is then used to create a ‘mask’⁶ designating the voxels in the array that form a structure of interest: the mask can be created automatically on the basis of greyscale value, or manually by editing each slice as one would edit a photograph in a 2-D graphics application. From the mask the software creates a 3-D object which can then be converted into one of the standard 3-D modelling formats and exported to an application, such as Finite Element (FE) Analysis software, that deals with 3-D models.

When processing CT software from non-fossil material, processing the data into a 3-D object can be straightforward: if the scan is of a ‘dry’ specimen (i.e. one lacking soft-tissues) as in Figure 5-1, then the contrast between the bone and the air

⁶ This part of the process is often termed ‘segmentation’; but the process is very similar to creating the masks used by 2-D graphics applications such as Photoshop.

surrounding is substantial and a mask generated from voxel greyscale values will reliably distinguish bone from air with minimal need for manual editing. Creating

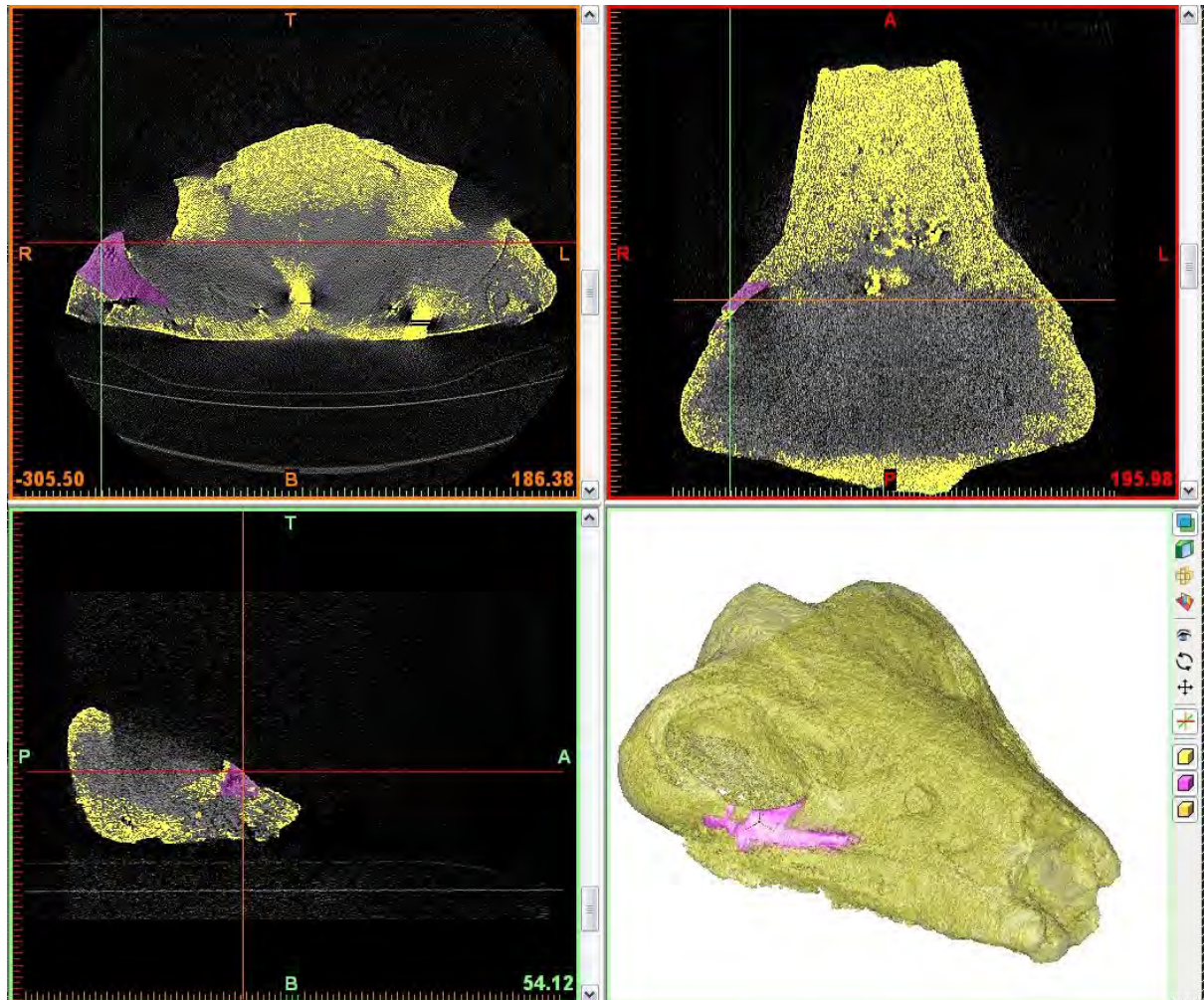


Figure 5-4: Screenshot from 3-D image processing software (MIMICS). The upper left, lower left, and upper right windows show CT slices for a fossil specimen (QMF51291) in axial, transverse, and coronal views respectively (T, B, R, L, A, P = Top, Bottom, Right, Left, Anterior, Posterior respectively). The coloured pixels denote ‘masks’, which can be created from greyscale values or by manual editing of each slice as (one would edit a bitmap in a 2-D graphics application). Multiple masks can be created, and once processed by the software form the basis for 3-D ‘objects’, which are shown in the lower right window, the yellow and purple shapes corresponding to the coloured pixels in the orthogonal views.

masks from wet scans, where the dense bone is surrounded by soft-tissues, is usually not quite so straightforward, but the differences in HU values between the hard- and soft-tissues is generally sufficient to allow the hard parts (for example) to be masked without too much difficulty (Figure 5-5).

The situation with fossilised bone can be rather different⁷, especially with the limestone matrix typical of the material dealt with here. In terms of mineralogy, the



Figure 5-5: CT scan slice of a wet specimen of a saltwater crocodile *Crocodylus porosus*, showing the soft-tissues (in medium shades of grey) surrounding bone (which shows as a light-grey). Although the contrast is not quite as great as with the scan of a dry specimen in Figure 5-1, masking this scan data is not difficult.

bone is very similar to the surrounding limestone matrix and this is reflected in similar CT attenuation, resulting in very low contrast between the bone and the matrix in the output images. Perhaps even more serious are the consequences of the solidity of the limestone nodule containing the fossil: the energy dosage used by

⁷ Although geologically young specimens that are preserved in caves or tar-pits, where the fossilised bone is not directly surrounded by a mineralised matrix, can preserve good contrast between the bone and surround medium and thus present little challenge for masking.

medical CT scanners is designed to minimise the radiation exposure to living patients, and as humans are basically bags of soft-tissue with some internal mineralised structures, usable images can be obtained with far lower energy levels than are used, for example, with industrial CT scanners. Even a relatively small limestone nodule such as QM F51291 (Figure 5-6) contains far more mineral across its width than any human, and the overall absorbance of the X-Rays is so great that any internal structures become almost lost in noise.

These problems are illustrated in Figure 5-7: standard tube settings fail to produce a usable image, irrespective of the contrast settings used to view the image. Using higher X-Ray tube energies gives a better result (Figure 5-8), but even at the maximum dosage that can be obtained from a medical CT scanner, the contrast between fossil rock and bone is not sufficient to allow a good mask to be automatically generated from voxel greyscale values. In order to produce a 3-D object, each slice must then be edited by hand – a process that can take hundreds of hours.



Figure 5-6: QMF51291, a limestone nodule containing the fossilised orbital and posterior-facial region of a small *Kronosaurus queenslandicus*. Scale bar shows 300 mm.

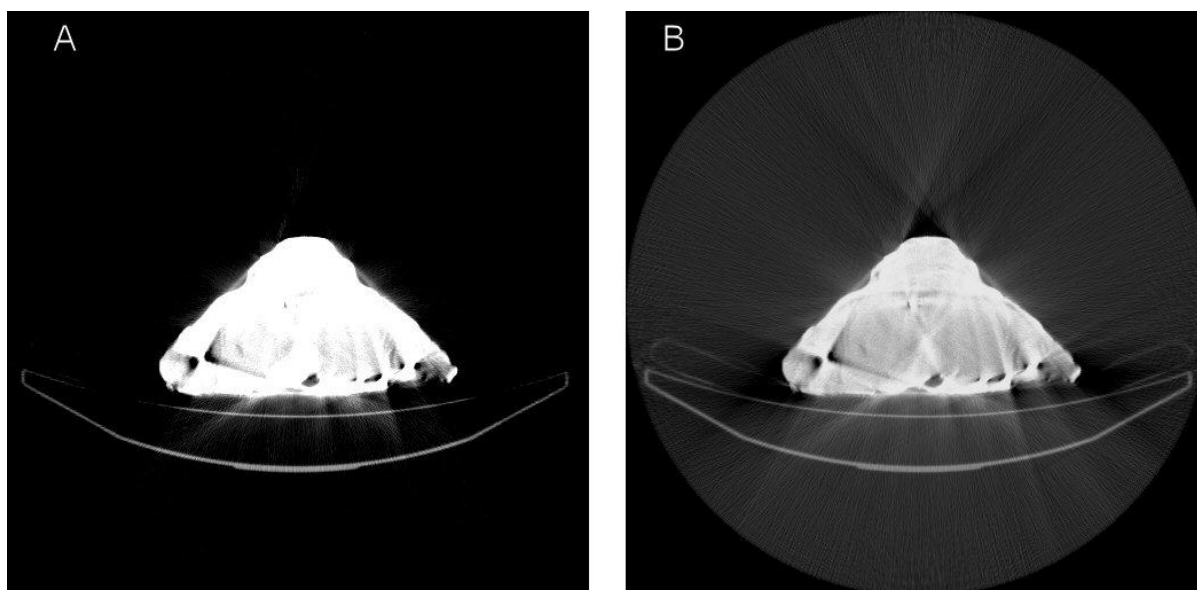


Figure 5-7: CT scan of QMF51291, a limestone nodule containing fossil bone, showing a slice taken through the anterior margin of the external nares (see Figure 5-6) at a typical level of X-Ray dosage for medical CT (see Table 1). A; image viewed at L300 W2000 (the optimum settings for viewing bone in biological specimens): B; image viewed at L400 W4000. Contrast between fossilised bone and matrix is totally obscured in A. At the settings used in B, the boundary between bone and matrix can be discerned in places (e.g. the underside of the dorsal median ridge, between the dorso-lateral concavities of the nares), but the image is dominated by refraction artefacts from large crystals (most likely calcite) within the nodule. Total absolute absorbance of the X-Rays across the specimen is so great that contrast between bone and fossil is mostly below noise-level variation and significantly less than the signal from the refraction artefacts.

Methods

A series of CT scans was performed on QM F51291 between November 2005 and October 2007, on a Toshiba Aquilion 16 scanner. Initially, the aim was simply to establish whether or not a usable scan could be obtained, but initial results were so poor that several attempts were made at different X-Ray tube and contrast settings. The best imaging results were obtained at the scanner's maximal tube settings (Table 1) – although the energies were such that the specimen had to be scanned in two sections to prevent the tube from overheating. The two sections were the anterior and posterior portions of the nodule, with some overlap, although the very front and very back of the block were omitted.

The specimen was scanned along the longitudinal ('axial') axis; care was taken to keep the specimen's alignment as consistent as possible between the scans of the two different sections. In each scan, scaling was set to maximise resolution, and the scan diameter of the narrower anterior section was much less than that of the posterior

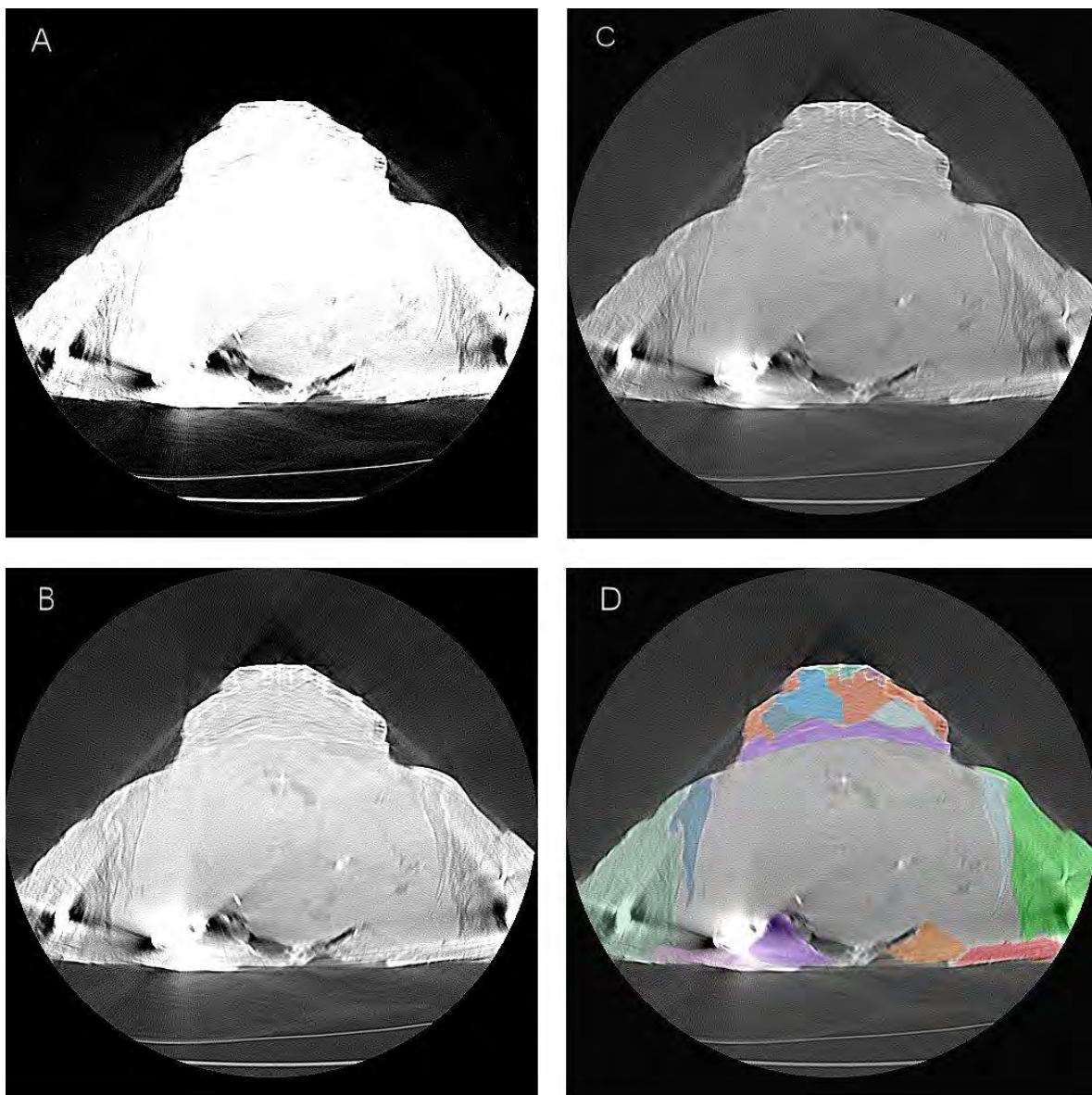


Figure 5-8: CT images of QMF51291, through approximately the same region as shown in Figure 5-7, but at higher X-Ray tube energies (see ‘maximum’ settings in Table 1). A, L300 W2000; B, L400 W4000; C, D, L800 W6000. Unlike the scan shown in Figure 5-7, the contrast between fossilised bone and matrix is discernable at the settings in B, but the settings in C and D give the best contrast. Refraction artefacts from large crystals (probably calcite) are swamping the imaging of bone and matrix in the lower left side of the specimen (as viewed): smaller crystals are visible in the central part of the nodule and give substantially less distortion. Note also a faint series of concentric circles visible at the middle of the block: these are an artefact of the scanner’s geometry. Lines of white corresponding to siderite deposition along sutural contacts can be clearly seen in the dorsal median ridge in C; D shows an interpretation of different elements in various colour overlays. At the energies used here, a scan of the whole nodule would overheat the X-Ray tube and the specimen was therefore scanned in sections.

section. In particular, the observed complexity of the osteology of the dorsal median ridge (as viewed externally) led to a focus on scanning this region at the best possible resolution, which resulted in some cropping of the lateral margins of the specimen in the scan of the anterior section.

	Typical medical CT	Maximum dosage
Peak voltage	120 kVp	135 kVp
Exposure time	500 ms	1500 ms
X-Ray current	140 mA	250 mA
Exposure	70	375

Table 1: CT scanner settings for the Toshiba Aquilion 16 scanner used in the present study. The ‘typical’ settings were used to generate the images shown in Figure 5-1 and Figure 5-2: similar settings were used to generate the images of QMF51291 shown in Figure 5-7. The images shown in Figure 5-8 were taken at the ‘maximum’ settings. kVp, peak kiloVolts; ms, milliseconds; mA, milliAmps.

At the maximum tube energy settings, the contrast between fossilised bone and the limestone matrix was discernable by eye through most of the block, although results were better at the anterior end where the nodule is thinner and overall X-Ray absorption is therefore lower (Figure 5-9), and in slices minimally affected by refraction artefacts caused by crystals within the nodule. Nevertheless, the contrast was not sufficient for automated masking techniques based upon voxel greyscale values, and each slice was masked manually. The 3-D imaging software used to

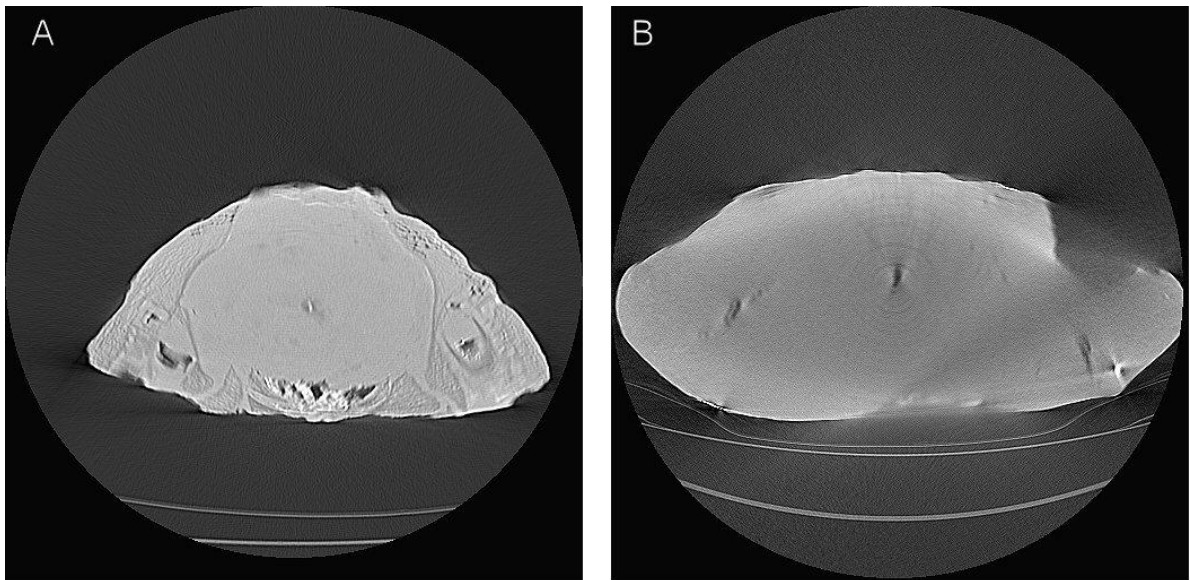


Figure 5-9: CT slices through anterior (A) and posterior (B) portions of QMF51291. X-Ray tube settings are identical to those used to produce Figure 5-8, contrast settings are as in Figure 5-8C, D. The nodule is much thicker in the posterior part, and X-Ray absorbance is so great that the contrast between bone and matrix is extremely difficult to make out – the region at the dorsal edge of the block in B is the inter-orbital bar (‘brow’), which is expected to have a detectable thickness of dorsal roof bone. Contrast this with the scan of the much thinner anterior part of the block (A), where the bone can easily be discerned from the matrix, and even fine details of trabecular bone structure are visible. For an idea of the nodule overall shape, see Figure 5-4 and Figure 5-6.

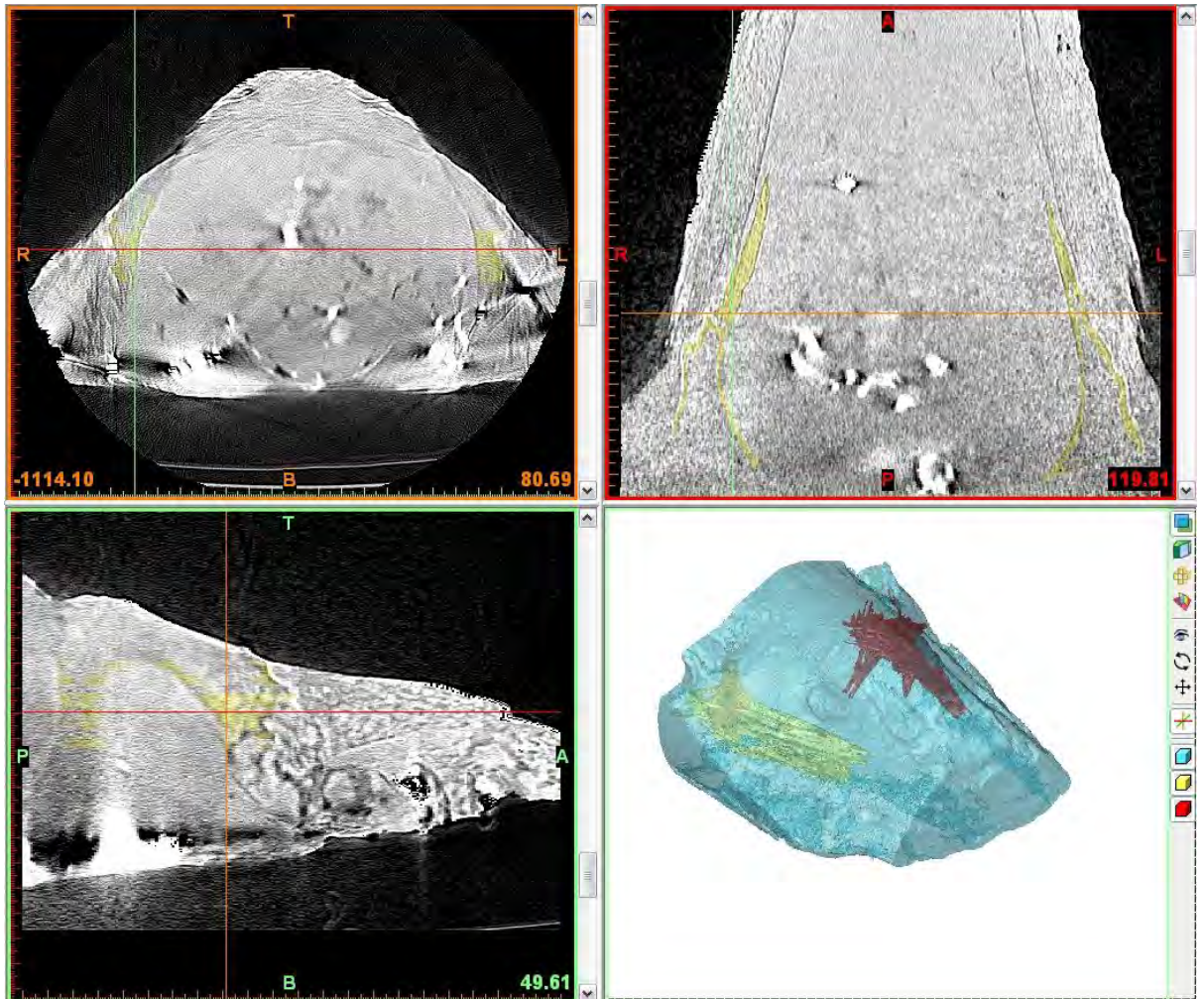


Figure 5-10: Manual editing of CT slice data direct in MIMICS, using raster image editing tools. The structure of interest is coloured in using 'brush strokes' of the mouse (or other pointing device): in the example shown here, the prefrontal bones are being coloured in a yellow mask. In each slice, the outline of the element must be carefully defined (no going over the edges!): an enclosed shape can be filled in using the 'fill' function, but any gaps will result in the whole screen turning yellow. Mistakes must be corrected using an 'eraser' tool. The mask is used to create a 3-D object: the incomplete mask for the prefrontals is shown in the lower right screen, lying within the shape of the anterior part of the nodule. One of the major difficulties is keeping a consistent edge to the masked structure between adjacent slices – hence the 'layered' appearance of the 3-D objects – and because of this, each object usually needs to be edited in each one of the 3 orthogonal views. The image shown here represents 50 – 100 hours work, and is a long way from being completed, even for a single pair of elements.

convert the CT data into 3-D objects (MIMICS) includes editing tools that are similar to the raster-based pixel editing tools in many 2-D graphics applications ('paintbrush', 'eraser', 'fill', etc.), but I found that producing an acceptable result by raster based editing of each slice was very time-consuming – the process is akin to the children's exercise of colouring-in a drawing without going over the lines or leaving any white space (Figure 5-10). The task is made even more difficult by the use

of a computer mouse instead of a pencil, although I did obtain better results with a WACOM graphics tablet and stylus. As someone with a very basic level of drawing skills, however, I find vector⁸ based editing of bitmaps to be much easier than raster based techniques, and after some time spent attempting to edit the scan directly in MIMICS, I exported the CT dataset as a series of JPEG files into Paint Shop Pro v.8, a 2-D graphics package, and edited it slice by slice using vector editing tools. The original CT dataset was composed of 269 slices for each scan section: these were combined by a ‘multi-view’ function using the scanner’s proprietary image processing software into a series of 71 axial slices for each of the anterior and posterior scans.

Within Paint Shop Pro, slices were handled in separate raster layers, and masks created in overlying vector layers (Figure 5-11). For the purposes of the present study, the separation of individual elements is not necessary – the FE model that will be created at the end of this process cannot incorporate the effects of sutures, and thus the bone will be modelled as a single structure – but, as discussed above, QM F51291 preserves the osteology of the mid-orbital and posterior facial region of a large pliosaur better than any specimen I am familiar with, and has the potential to offer important insights into this particular anatomical mystery. Future work will re-examine the osteology of this specimen in more detail, and so masks were created for individual elements wherever possible; subsequent combining of these into a single mask of the bone for FEA is a simple step.

The vector mask layers were then exported as a series of bitmaps. The mask bitmaps were imported back into MIMICS, and were used to create 3-D objects corresponding to the masked bone in each section. The mask bitmaps for each section were initially handled in two different MIMICS files, as each represent scans taken at different spatial dimensions and alignment; once the required 3-D objects were created, they were exported as STL files into a single new MIMICS file, aligned manually, and merged using the ‘Boolean’ function.

⁸ Vector-based tools are those that allow you to define a line, for example, by specifying a series of points which the line must pass through, rather than by the digital ‘brush’ strokes used in raster tools. Ergonomically, it is much easier to define a point through a single mouse-click than it is to draw a line with a smooth drag of the mouse (or, at least, for me it is). A line created in this way can be edited simply by moving, deleting, or rotating the vector control point, rather than using ‘brush strokes’ from an eraser and then a paintbrush tool, and the line can be converted into a Bézier curve if required. Line thickness, colour, and transparency can be controlled fully: similar levels of control apply to ‘infills’ of any closed curve.

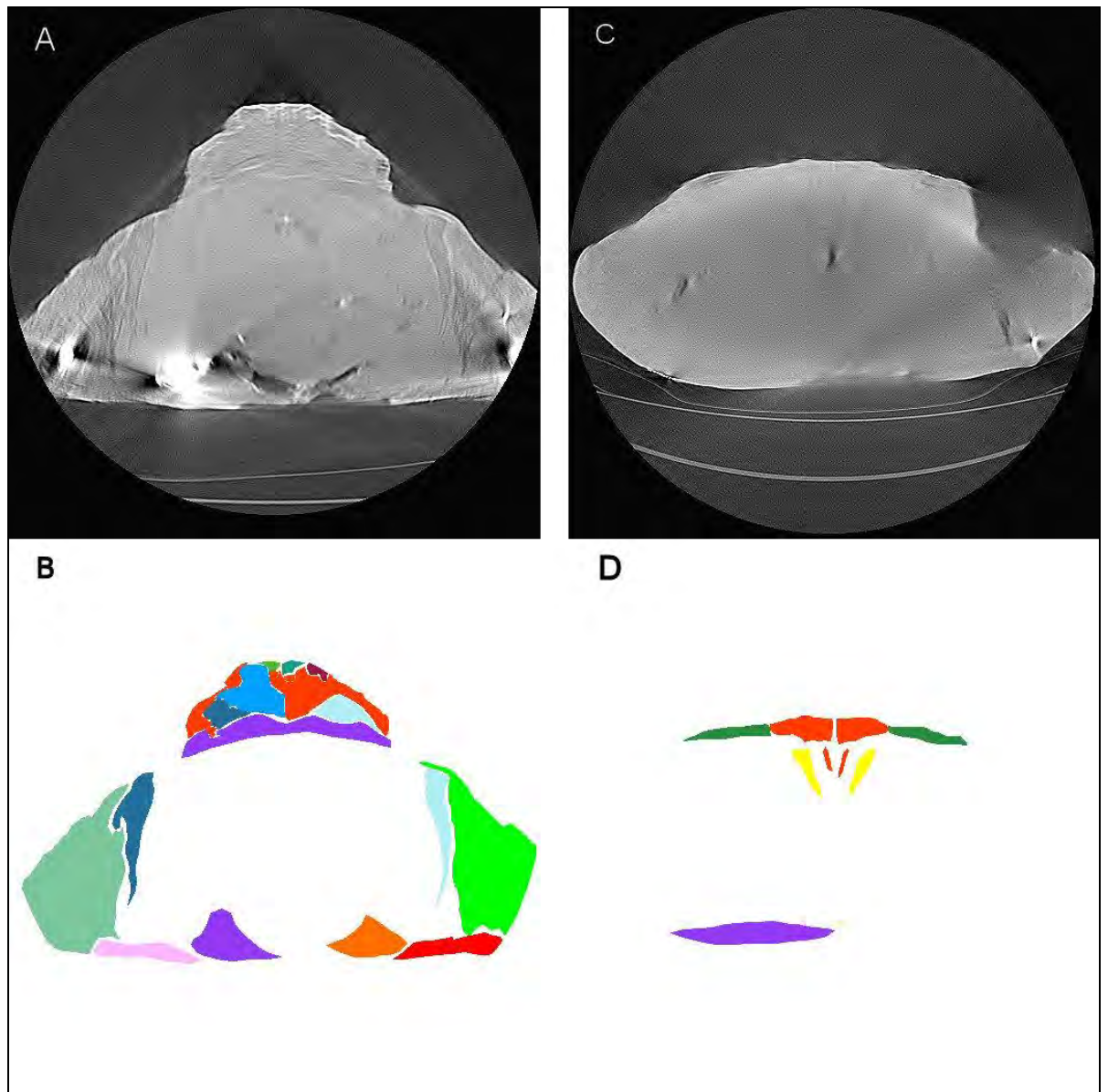


Figure 5-11: Examples of CT slices from QMF51291 that have been masked using a vector graphics tool. A, B; CT slice and mask for a slice from anterior section scan. C, D; CT slice and mask for a slice from posterior section scan. Note that the poor contrast in C means that the bones are masked in D with rather less confidence – and greater reliance on inference from surface topology – than is the case in B. The vector mask for each bone is defined by a ‘filled’ vector curve fitted to the edge of each element in each slice; MIMICS imports these as greyscale bitmaps, but as long as each colour converts to a different greyscale value the ‘thresholding’ function (where raster masks are created in MIMICS on the basis of voxel greyscale values) can automatically create masks for each element and convert these to 3-D objects. For the present study, data on individual elements is not required, and the 3-D objects were merged (into a single 3-D object for all of the fossil bone) before export into the next stage of data conversion: the osteology of individual elements as imaged by CT will be the subject of future work, for which these masks will form the basis.

The specimen was scanned again in October 2007 at low X-ray tube energies and using the FC61 (soft-tissue) algorithm⁹ for data reconstruction; this allowed the surface geometry of the whole nodule to be defined as a separate 3-D object into which the details of the internal anatomy gleaned from the earlier scans could be positioned. This object was imported (as an STL file) into the MIMICS file containing the masked geometry from the two earlier, high-power scans, and manually aligned with these.

The 3-D objects thus created in MIMICS are not of sufficient quality to import directly into FE software and give meaningful results – and in any case they only represent part of a whole skull. But they can be used to provide an accurate template of the external and internal geometry of this part of the skull in a 3-D CAD application, such as Rhinoceros v.4 (Rhino). The CAD application can then be used to integrate this template with the geometry data produced from the 2-D reconstructions in Chapter 4, allowing a 3-D CAD model of the whole skull to be created that incorporates the internal geometry of the orbital region (something that is very difficult to achieve using only 2-D drawings). That model – which is now a 3-D reconstruction of the pliosaur skull, rather than a model of any particular specimen – can then be exported into an FE application and form the basis of a Finite Element Analysis (FEA).

The 3-D objects corresponding to the masked bone and the whole nodule were exported in STL format, and imported into a Rhino file containing geometry created from the 2-D reconstructions of *Kronosaurus queenslandicus*. The details of this stage of the process are given in Section 5.3.

⁹ The raw data from the CT scan is processed (by the computer workstation controlling the scanner) into bitmap slices using a reconstruction algorithm to determine contrast: this is separate to the ‘windowing’ (i.e. setting L and W values) described earlier, and once the algorithm has been set for a CT dataset it cannot be altered. A variety of different algorithms are available to maximise contrast, based upon the tissue type of interest; the most basic choices are between ‘soft-tissue’ and ‘bone’ algorithms. As the name suggests, ‘bone’ algorithms maximise contrast for scans where hard parts are of interest, which is the case in nearly all of the scans performed in this work. However, these algorithms tend to introduce artefacts at boundaries between materials of very different X-Ray absorbance, such as the external surface of the specimen (a boundary between carbonate rock and air): examples of these ‘beam-hardening’ artefacts can be seen at the edge of the nodule in Figure 5-7, Figure 5-8, and Figure 5-9. The soft-tissue algorithm is less prone to beam-hardening, and when an accurate external surface is required this is a better option. The scanner can create a hard-tissue and soft-tissue scan dataset from the same raw data (there is no need to scan twice), but once each dataset is created they remain separate entities. The FC-61 algorithm referred to in the text is specific to Toshiba scanners: each manufacturer uses their own system to designate different algorithms.



Figure 5-12: QMF51291, seen in oblique external view (above) and modelled from CT data in MIMICS (below). The shape of the nodule containing the fossil bone is shown as transparent red and is based upon a low energy, ‘soft-tissue’ scan (see text) – the bone is shown in various colours. The CT data is consistent with the external view in many respects: for example, the lacrimal bone (shown in orange) forms the anterior margin of the orbit and is clearly distinct from the surrounding elements; the prefrontal (light blue) forms the posterior margin of the nares and the anterior-medial margin of the orbit, and shares a clearly visible suture with the maxilla (yellow) immediately below the nares; and the jugal (dark red) has an anterior process that separates the posterior part of the lacrimal from the maxilla. The junction between the anterior and posterior scanned-sections can be seen running through the middle of the lacrimal in the transverse plane, and the posterior-lateral part of the anterior section has been clipped. Several elements making up the dorsal median ridge can be distinguished at the front of the nodule, but are harder to distinguish behind the nares and have not been masked separately. The frontals and parietals forming the skull roof of the brow (inter-orbital region) are difficult to distinguish and have not been masked separately – they are shown together in red. Similarly, the dorso-posterior process of the maxilla has not been separated from these in the brow region. The postfrontal (dark green) can be distinguished from the frontal and prefrontal bones in some slices, but not in others.

Results

Figure 5-12 shows screen output from MIMICS of the 3-D objects generated from the masks of the bone and whole nodule of QM F51291, together with a photograph of the external surface. Various elements can be seen as separated masks; however, elements were only masked separately where the separation between them was clearly visible, and in parts of the brow region the junction between frontal and parietal bones could not be identified without difficulty – in such case, the bones were masked together.

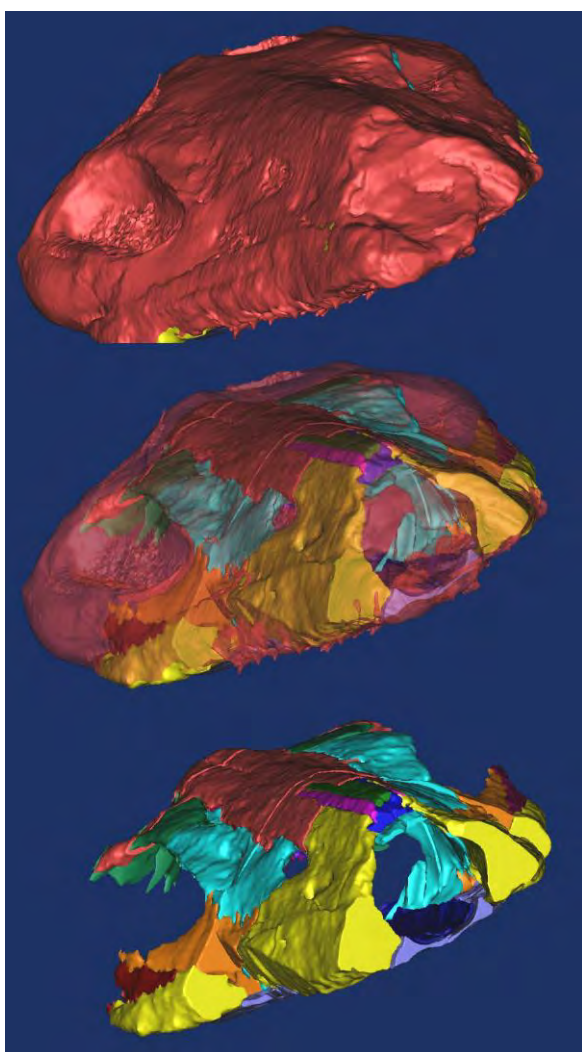


Figure 5-13: Anterior-oblique view of QMF51291 3-D objects, showing the whole nodule (top), the relation of the fossil bone to the external surface of the nodule (middle), and the fossil bone isolated from the matrix (bottom). There are a number (4 pairs) of separate external and internal elements making up the dorsal median ridge, visible at the front of the model – published descriptions state that this structure is made up only of the premaxillae. Through the nasal cavity at the front of the model, the descending process of the left prefrontal (light blue) can be seen contacting the palate and thus forming the medial part of the internal anterior orbital wall.

In anterior view (Figure 5-13), the hexagonal section of the nasal cavity can be seen – the dentulous (tooth-bearing) part of the maxilla is thick and forms a strong buttress to the bones of the palate. The depth of the dorsal median ridge is also clear: it is formed from at least four pairs of elements, an observation in marked contrast to descriptions of other pliosaur specimen that identify the premaxillae as the only bones involved with this structure. Also visible, through the nasal cavity, is a strong descending process of the left prefrontal bone, which forms a broad contact with the palate and thus makes up a robust pillar connecting the dorsal and palatal roof bones of the skull antero-medial to the orbit – a pattern that brings to mind the similarly positioned prefrontal pillar of crocodilians (Iordansky 1973).

The anatomy of the prefrontal suggests a bone of greater complexity – and perhaps structural import – than has been generally realised. In external view, it consists of the smooth exterior surface that lies behind the nares and forms the antero-medial margin of the orbit, including a posterior-dorsal process that gives this margin a

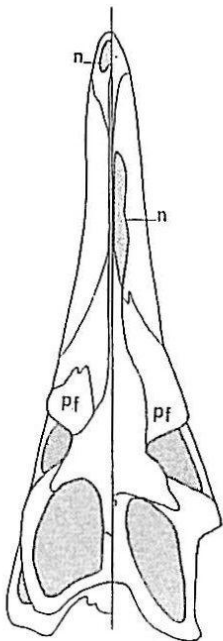


Figure 5-14: Skull profiles of the marine crocodile *Metriorhynchus* (left side) and the mosasaur *Clidastes* (right side), showing convergence in overall skull proportions. The position of the external nares (n) is characteristic of each group. Note the supraorbital flange formed by the prefrontal (pf) in each taxon: a similar structure (albeit lesser developed) is evident in QMF51291. From (Langston 1973)[original figures from Andrews (1913) for *Metriorhynchus*, and Russell (unreferenced) for *Clidastes*].

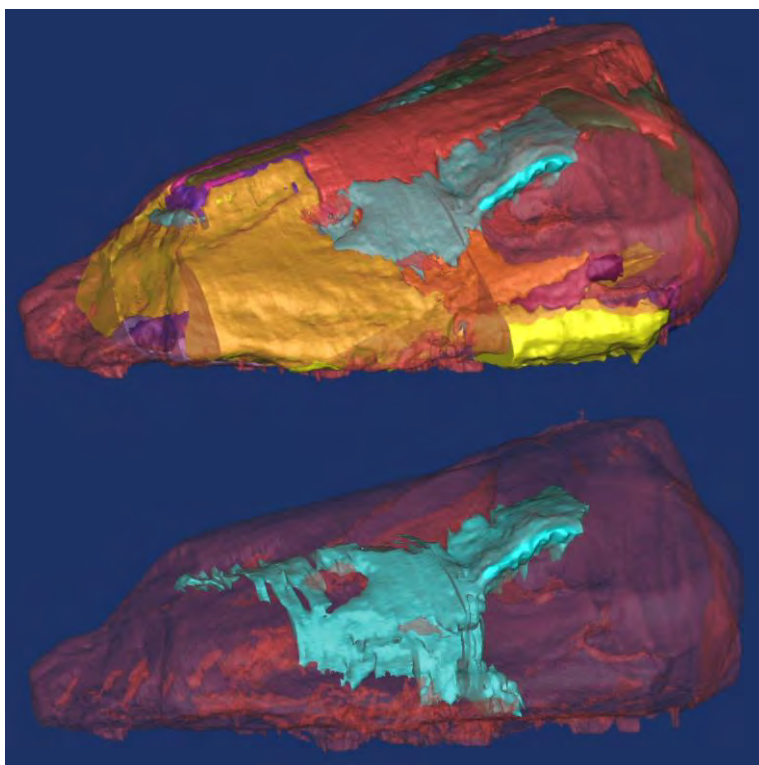


Figure 5-15: 3-D objects constructed from CT scan data of QMF51291 in left lateral-oblique view, showing the various elements of the skull (top) and the left prefrontal (bottom) in relation to the whole nodule (shown as transparent red). The contrast between the portion of the prefrontal bone (light blue) visible externally, apparent in the top image, and the extent of the whole bone (bottom) was unexpected. From the central part of the bone that forms the external surface of the skull posterior to the orbits, the element sends (1) a robust postero-dorsal process that forms a supra-orbital ridge and underlaps the frontal-parietal mid-orbital brow; (2) a broad posterior-medial process that meets the palate and forms the medial part of the cupped anterior-orbital wall; (3) a thin anterior process, lying medial to the maxilla in front of the nares, and which can be seen in Figure 5-8 and Figure 5-11; and (4) a dorsal anterior process that underlies all of the other elements of the dorsal median ridge. The latter, and the extent of its relations with the more ventral anterior process, is difficult to make out and it is possible that it is a separate element rather than part of the prefrontal: however, the first three processes can each be seen clearly in the CT data. This hitherto unseen anatomy of the pliosauroid prefrontal may reflect the structural importance of this bone in bracing the facial, orbital, and palatal parts of the skull.

pronounced supra-orbital flange or ridge reminiscent of a structure visible in metriorhynchid crocodiles and mosasaurs (Figure 5-14). However, the CT data shows that it is a far more extensive bone than suggested by its external surface (Figure 5-15): from the central portion that lies between the nares and orbit and which forms the exterior surface of the skull in this region, a total of four processes extend;

Form (3-D)

1. A postero-dorsal process extends beyond the externally-visible supra-orbital flange and forms a thick, extensively underlapping contact with the frontal-parietal bones of the brow.
2. The orbit has a concave anterior wall running from its dorsal anterior margin to the palate; the medial part of this wall¹⁰ is formed by a ventro-medial process of the prefrontal, which makes a robust contact with the pterygoid.
3. An anterior process of the prefrontal extends, as a thin flange lying medial of the maxilla, in front of the external nares and forms the upper part of the lateral wall of the nasal cavity for a short distance.
4. An antero-dorsal process also extends forward of the nares and appears to form the dorsal roof of the nasal cavity, underlying the other elements of the dorsal median ridge.

The exact relations of the antero-dorsal process (4) with the other bones of the dorsal median ridge, and even the anterior process of the prefrontal (3) are difficult to make out. Whether this bone is truly part of the prefrontal is not certain: in CT it appears to be of a relatively low density, with an irregular inner surface.

As stated earlier, the osteological details of QM F51291 are not the primary focus of this work: nevertheless, it is clear that these processes (that the first three are truly part of this element is fairly clear) are potentially of structural and hence biomechanical significance. With its position at the anterior-medial corner of the orbit, the prefrontal is of particular importance to the structural connections between the facial and circum-orbital parts of the skull. The robust processes that brace the roof bones of the brow with the palate around the edge of the orbit are obvious candidates for ‘mechanically important’ features; while the extensively overlapping (‘scarf’) joints formed by the two anterior processes with the various bones of the face are also of interest from a structural perspective.

The CT also resolves the issue of the morphology of the ventral surface of the dorsal roof bones of the brow (Figure 5-16). On the basis of the preserved morphology of another specimen (QM F2446), I had previously hypothesised that the ventral

¹⁰ The more lateral part is formed by the lacrimal.

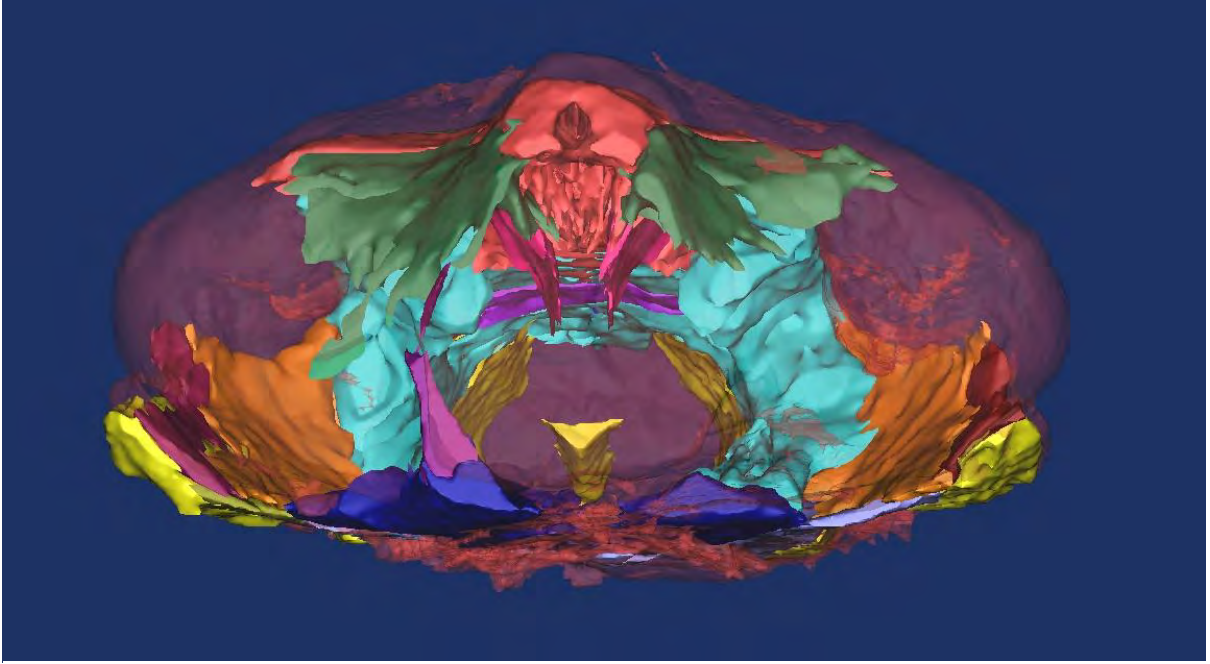


Figure 5-16: Posterior view of the 3-D objects created from the CT scan of QMF51291. Note the position of the parasphenoid (yellow, ventral mid-line structure, with triangular cross-section). From the skull roof above the parasphenoid, a pair of thin descending processes can be seen (magenta): these are similar to the ventral processes of the frontals described by Andrews (1911) for *Peloneustes* in this region of the skull. To the left of the parasphenoid, the epipterygoid (purple) can be seen as a vertical strut between pterygoid (dark blue) and the postfrontal (dark green). The extensive anterior wall of the orbits can be seen on each side of the skull, formed by the lacrimal (orange) and the prefrontal (light blue).

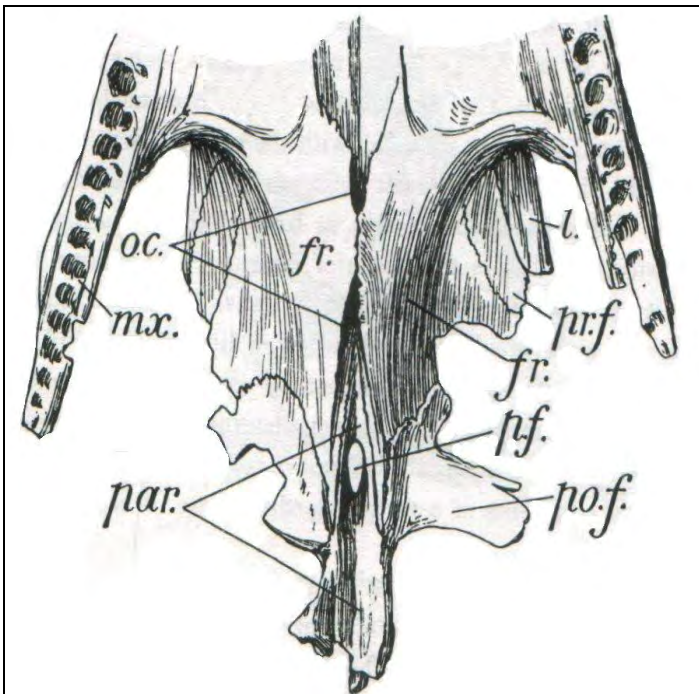


Figure 5-17: Part of the skull roof of *Peloneustes philarchus*, reproduced from Andrews (1911). The original caption read; “Fig. 1. Inner face of the middle portion of the skull roof in *Peloneustes philarchus*. (About one-third natural size.) *fr.* frontals; *l.* lachrymal; *mx.* maxilla; *o.c.* channel enclosed by the downgrowths of the frontals; *par.* parietals; *p.f.* pineal foramen; *po.f.* post-frontal; *pr.f.* pre-frontal.” Note the use of a variant spelling of ‘lacrimal’.

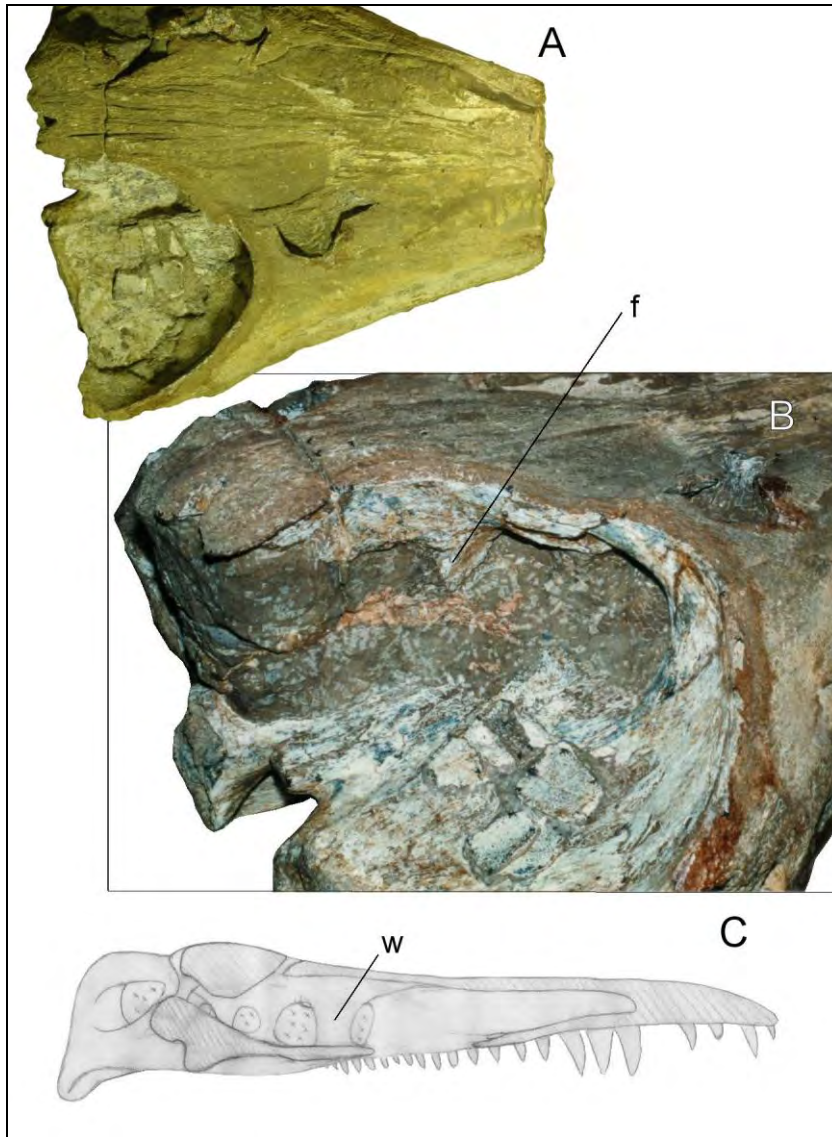


Figure 5-18: QMF2446 in (A) dorsal, (B) right oblique views. The view in B is taken from the right postero-lateral corner of the specimen, looking medially and slightly anteriorly into the right orbit: the palatal bones of the suborbital floor can be seen in the foreground. The structure marked 'f' is interpreted, on the basis of the structures visible in Figure 5-16 and reported for *Peloneustes* in Figure 5-17, as the ventral flange of the frontal. A 1997 reconstruction of skull anatomy in *Kronosaurus queenslandicus* (C), showing the left side of the skull following a sagittal section, erroneously interpreted the structure marked 'f' as the upper part of a broken medial orbital wall, which is marked 'w'.

surface of the inter-orbital roof bones were connected to the underlying pterygoid in a thin, vertical wall situated on the medial edge of the orbit (Figure 5-18). However, the CT of QM F51291 does not indicate any such structure. The thickness of the nodule in this region means that the contrast between bone and matrix is particularly poor: however, the section of the bones of the brow can be made out, and instead of a wall there is a thin, elongated ventral flange that is parallel with the longitudinal axis

and angled ventro-medially, but which does not contact the palate; as such, it brings to mind Andrew's illustration of the ventral parts of the paired frontal bones underneath the parietal foramen in *Peloneustes philarchus* (Figure 5-17) and, as he suggested, these structures may serve to form the lateral walls of the olfactory canal (Andrews 1911, 1913). They are not of any obvious structural significance to the mechanics of the skull in this region.

Discussion

Although not the primary focus of the present study, the CT-based models show several osteological features that are likely to be of interest. In particular, the presence of a lacrimal as a separate element, apparent in external view, is also clear from the CT data: given the various opinions on the presence or absence of this element within the Plesiosauria discussed above (Chapter 3), this is an interesting result. This observation is simply one example of the value of this specimen, and this approach, to resolving some of the current questions surrounding plesiosaur anatomy.

The use of CT data to complement traditional methods of studying osteology is not without its own problems, however. With fossils such as these, preserved in large carbonate nodules, contrast between bone and matrix is poor. In the thicker parts of the nodule the anatomy cannot be resolved with confidence, and the complex three-dimensional pattern of contacts between the bones of the dorsal median ridge is also problematic. The data collected here is just the start of detailed study of this remarkable specimen: further information will come from (1) continued study of the CT dataset, and (2) additional scans at even higher tube energies, perhaps using industrial CT scanners. The potential for synchrotron scanning to image this specimen should also be considered. Whether or not additional CT data becomes available, the main task in resolving the details of the anatomy is to cross-check masks such as those generated here (from axial views of the scans) against coronal and parasagittal views of the dataset; masks that are consistent between these will have the highest probability of accuracy.

To generate images capable of providing high quality osteological data will thus require further work. For our present purposes, however, we are less interested in

Form (3-D)

capturing the details of each individual bone, and more concerned with describing the external and internal geometry of the skull bones preserved in this specimen. The masks created from the CT data here, and the 3-D objects generated from them, are considered sufficient for this task. Although they are not precisely smooth – note the ‘stepped’ and ‘jagged’ appearance of the 3-D objects in Figure 5-15 and Figure 5-16 – they are sufficient to provide a template for a CAD approach to defining the geometry of the skull bones in this region (Figure 5-19). That process is detailed in the following section.

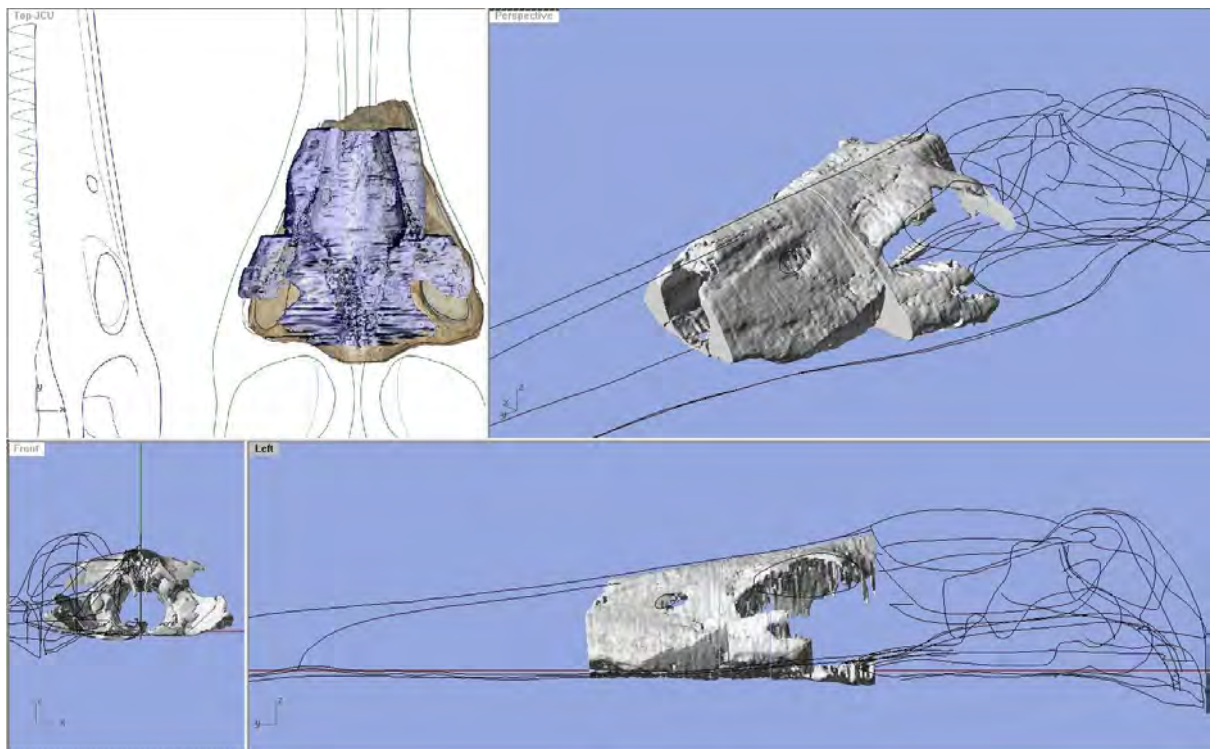


Figure 5-19: Mesh of the masked fossil bone from QMF51291 viewed in Rhinoceros v4.0, in dorsal (upper left), posterior (lower left), left lateral (lower right), and oblique (upper right) views. The mesh was created by merging the 3-D objects shown above and exporting from MIMICS as a stereolithography (.STL) file. The black lines visible in the posterior, lateral, and oblique views are 3-D geometry created from 2-D reconstructions and overlain photographs (visible in the dorsal view).

5.3 **Combining 2-D reconstructions and CT data into a 3-D model of the skull**

Palaeobiological analyses are making increasing use of complex, three-dimensional modelling to generate and test hypotheses (Plotnick and Baumiller 2000, Rayfield 2007): the emerging use of these computer-based tools heralds a new phase of studies that are broadly linked under the umbrella of functional morphology (Jenkins et al. 2002, McHenry et al. 2007, Moreno et al. 2008, Preuschoft and Witzel 2005, Rayfield 2005, Rayfield et al. 2007, Rayfield et al. 2001, Snively and Russell 2002, Witzel and Preuschoft 2005, Wroe 2007, Wroe et al. 2007a). From a technical perspective, the most complex models have been based upon high-resolution CT imaging data of extant species, where specimens are structurally pristine (Wroe et al. 2007b). CT data offers considerable advantages for the construction of high resolution models, including the ability to incorporate multiple material properties into a 3-D mesh on the basis of bone density, and thus create heterogeneous models.

Because of the complex geometry that is created when CT data is processed by an application such as MIMICS or AMIRA, the resulting 3-D model is tightly defined by the original specimen. This is of course not a problem when the original specimen is in good condition, but is more of an issue when the specimen has been deformed or broken, as is often the case with fossils. If overall deformation is low, and only small parts of the original structure are missing, the 3-D model can be ‘patched up’ by assuming symmetry and creating the missing geometry from the mirror side of the skull; this approach works if relatively minor parts of the fossil are missing (McHenry et al. 2007, Wroe 2007). In particular, Pleistocene fossils from peat/ tar pits or cave deposits generally exhibit very low levels of sedimentary deformation and are often remarkably complete and well preserved: in the cases of the *Smilodon fatalis* skull modelled by McHenry et al. (2007) and the *Thylacoleo carnifex* skull modelled by Wroe (2007), the creation of high resolution, heterogeneous 3-D models involved little more work than is typically required for equivalent models of Recent specimens.

Much fossil material, however, exhibits some degree of distortion, or is too fragmented for a simple mirror of a contra-lateral part to be effective. Even relatively low levels of taphonomic distortion are a minor issue for studies of osteology, but

have a potentially major effect on structural geometry. Three-dimensional meshes that are constructed directly from scan data of these will include all of the fossil's imperfections, but the complexity of the mesh means that it will be difficult to correct these. There has been some work on 'retro-deformation' techniques that use algorithms and the assumption of original symmetry to correct for plastic and brittle deformation (Boyd and Motani 2008), but these techniques are in early stages of development and have yet to be used to create an 'undistorted' FE model from a distorted fossil. An alternative approach is to create the geometry for the FE model manually, but this is time-consuming for low resolution meshes (Daniel and McHenry 2001, McHenry et al. 2006) and is effectively impossible for high resolution meshes.

Traditional palaeontology includes the production of 2-D reconstructions which represent the undeformed morphology of a fossil species: an early example is the reconstruction of the pliosaur *Peloneustes* by Andrews (1895). Experienced palaeoartists can create sculptures of fossils that effectively represent a hypothesis of the undeformed geometry of that species (for example, Brian Cooley's reconstruction of the skull in a specimen of *Tyrannosaurus rex*; E. Snively, pers. com.), and a 3-D scan of such a sculpture can be used to generate a 3-D model, although these are necessarily homogeneous (c.f. Chapter 2).

As detailed in Chapter 4, the fossil skull material for *Kronosaurus* is either fragmentary or deformed and in most cases is both. Two largely complete skulls are known; QM F18726 and QM F18827. The former is deformed in the transverse and vertical axes, and is still covered in limestone matrix: although it possibly preserves important osteological details, and should thus be a focus of future study, it has not been included in the present analysis. QM F18827 is deformed in the vertical axis, but from visual inspection deformation in the two horizontal axes (longitudinal and transverse) appears to be minimal. QM F18827 is largely complete, with the exception of the zygomatic arches and posterior parts of the mandible: however, the dorsal surface of the rostrum is heavily weathered. Deformation in the vertical axis is not uniform along the fossil; the anterior rostrum appears not to be deformed, but the posterior rostrum and medial parts of the orbital region are noticeably

compacted. The braincase and occiput appear to be largely unaffected by vertical compaction.

QM F10113 appears to have a similar pattern of preservation: deformation is mainly in the vertical axis (although the brow between the orbits has been sheared laterally slightly relative to the palate), and affects the posterior rostrum and orbital region more than the anterior rostrum and braincase. However, the skull in QM F10113 is less complete than in QM F18827. All of the other skull material listed in Chapter 4 is very incomplete; QM F18154 shows little evidence of deformation but is heavily weathered and diagenetically altered, QM F52279, QM F2446 and QM F2454 are heavily distorted, QM F1609 (the holotype) is an undistorted fragment of mandible but, in addition to being fragmentary, is heavily weathered. MCZ 1284 is slightly more complete than the holotype, but is slightly distorted and is weathered. Only QM F51291 shows no apparent signs of sedimentary compaction, but it is fragmentary and weathered.

It is thus apparent that attempts to recreate skull geometry directly from these specimens would have to contend with the problems of deformation, fragmentation, and weathering. Given current technology, this cannot be achieved through the direct editing or manipulation of 3-D scan data. In order to generate a 3-D model of the skull in *Kronosaurus queenslandicus*, therefore, a different approach is required.

In 3-D design, geometry is usually defined by the user, rather than imported from scans of pre-existing structures. Different software applications use different techniques to achieve this goal: Parametric modellers, such as ProEngineer and SolidWorks, create the 3-D geometry directly: complex shapes are typically created by manipulating simpler precursors. Other packages, such as Rhino and AutoCAD, use a 2-D based approach to create the 3-D geometry; objects are generated in one orthogonal plane, as in a 2-D graphics design package such as CorelDraw, and can then be manipulated in one of the other two orthogonal planes: this step adds a third dimension to the created geometry. In practical terms, what this means is that 2-D plans for a structure (such as the plan and elevation views for a building) can be used as a template for creating 3-D geometry. For example, an outline of a structure can be traced from the plan view: this creates an object within the CAD application. The

same object can then be viewed in elevation, and the control points for the object edited so that they align with elevation drawing for the building.

The same process can be applied to 2-D reconstructions of fossil structures such as a skull. The following is simply an example; starting with 2-D diagram of the skull in dorsal view, a line is traced corresponding to the outline of the skull. In Rhino, geometry is created by creating objects; an object consisting only of lines is termed a 'curve'. The curve is created as a vector, i.e. it is defined by the position of control points, which can be manipulated. The same curve used to define the outline of the skull in dorsal view can then be manipulated in lateral view, using the 2-D diagram of the same skull in lateral view as a template. Once the curve has been aligned with the appropriate outlines of the lateral view, the result is a 3-D geometry of the skulls' outline; this stage can be achieved quite quickly (Figure 5-20).

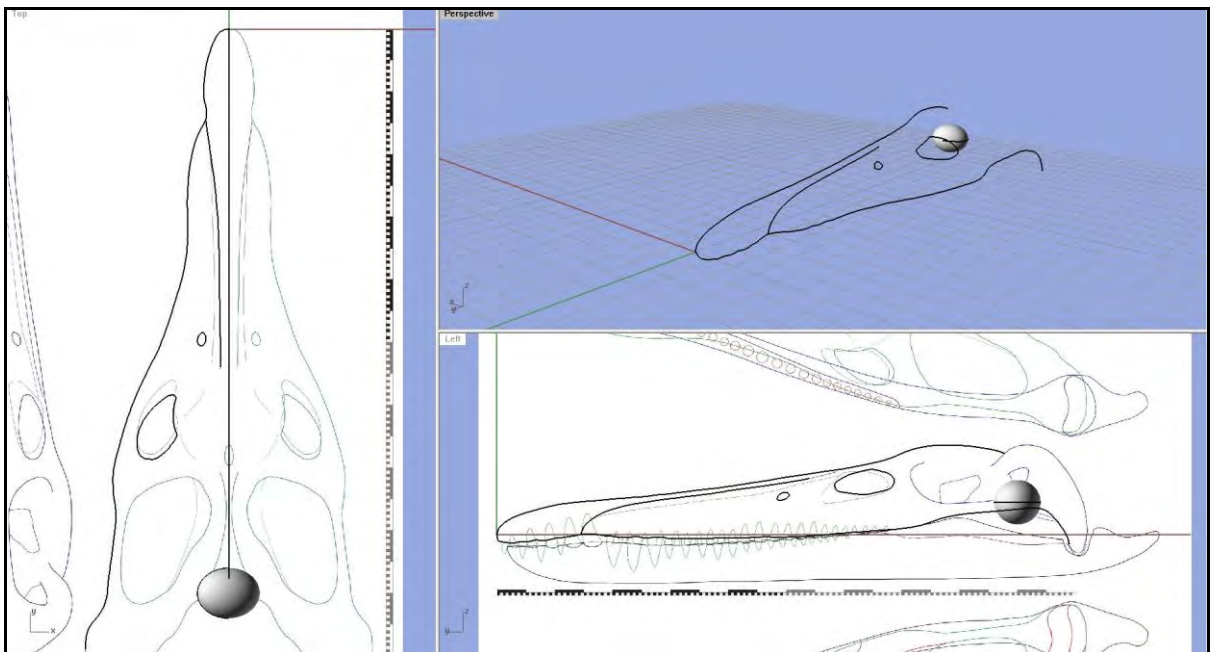


Figure 5-20: Generation of NURBS curves in three dimensions from 2-D drawings, using Rhino. A curve is traced over a drawing of the skull in dorsal view (left). The same curve is aligned to the respective part of the drawing in lateral view (right, lower): the result is a 3-D curve (right, upper). The spheroid represents the position of the occipital condyle.

Simply creating an outline of the skull in 3-D is only the start of the process, however. A 3-D FE model is more than a collection of curves in three dimensions – in the same way that a wire basket and a bowl can share the same overall geometry, but have very different properties, a 3-D object must fulfil a particular set of requirements before it can form an FE model. To go from a series of 3-D curves to an FE model requires two major steps; firstly, the object must be constructed from surfaces, not lines; and secondly, the surfaces created by CAD must form a contiguous surface that completely enclose a volume. This second requirement is often referred to as having a ‘water tight’ surface, the analogy being that, if the volume enclosed by the surface was to be filled with water, the water would not leak out. A volume enclosed by a surface that is not ‘water tight’ cannot be used to generate an FE model: this will be examined in more detail below.

In Rhino, all that is required to generate a CAD surface is three or four intersecting lines; three for a triangle, four for a quadrilateral¹¹. The lines do not have to be straight: the surface is interpolated from the intersecting geometry of lines, so that a curve in one or more of the lines will be reflected in the resulting surface (Figure 5-21). By using a series of curves arranged in an intersecting pattern, a set of surfaces can be generated which approximate the surface of even a complex biological structure such as a skull. The resolution that can be achieved depends upon how many curves are used and how finely the shape of each curve matches the original geometry.

A water-tight volume has one surface that connects to itself with no free edges; viewed thus, a skull is simply a distorted torus. However, it is easier to model the skull by considering it to be formed from internal and external surfaces that are joined. The internal surface lines the major cavities of the skull; the nasal cavity, the orbits, and the endocranial space. In these regions, the skull can be conceived as a mostly closed, hollow structure connected to other parts of the skull. In pliosaurs, the concept of an internal surface is less useful in the temporal arcade and the suspensorium: these are more open structures – like a ‘space frame’ – and the concept of internal and external surfaces is less helpful.

¹¹ There are lots of ways to make surfaces in Rhino – the procedure described here concerns forming surfaces from edge curves.

Form (3-D)

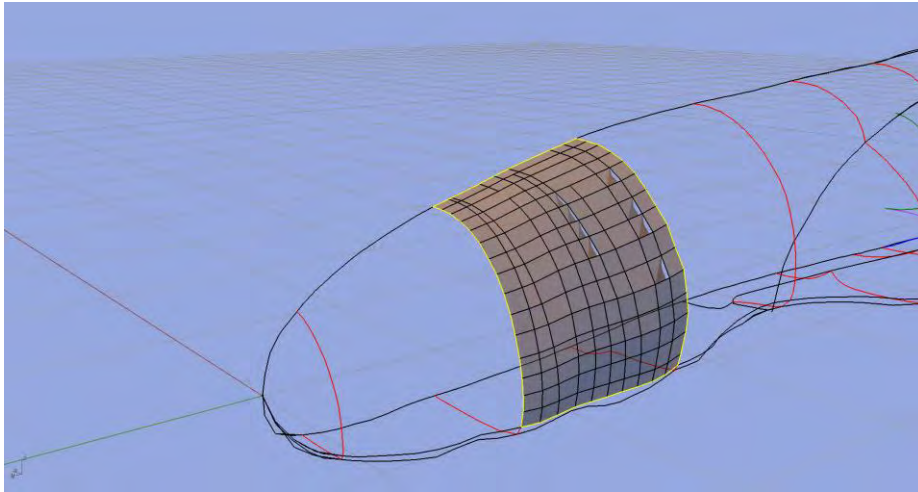


Figure 5-21: A NURBS polysurface, generated from edge curves (yellow lines) in Rhino. Three or four intersecting curves are sufficient to generate a surface that interpolates the geometry of each edge curve.

In the mandible, the internal surface is the Meckelian canal, which connects with the external surface at the adductor fossa. In the cranium, the internal surface of the nasal cavity connects with the external surface of the rostrum at the internal and external nares. If anterior palatal vacuities are present, these form another connection between the two surfaces. The internal surface of the nasal region is continuous with the internal surface of the orbital region, which can be considered to comprise of the orbits and the interorbital region: here, the internal and external surfaces connect around the orbital margins and the sub-orbital fenestrae (if present). The internal surface of the orbits connect with the (external) surface of the open temporal arcade via the postorbital fenestrae. In the median part of the orbital region, the internal surface of the interorbital ('sphenethmoid') region connects with the anterior ('sphenoid') part of the brain cavity. In terms of the ossified parts, the internal surface of the brain cavity connects with the external surface at five major points; (1) anteriorly, with the inter-orbital region: the dorsal part of this region is the olfactory canal; (2) dorsally, at the parietal foramen via the parietal canal; (3) antero-laterally, with the temporal arcade, behind the epipterygoids; in life, most of the unossified space here may be closed by the laterosphenoid cartilage, although the proötic foramen is an important opening in the lateral wall of the braincase through which the trigeminal nerve emerges; (4) ventrally, via the inter-pterygoid vacuity on either side of the parasphenoid, although this space may be closed in life by cartilage; (5) posteriorly, via the foramen magnum. There are in addition numerous smaller

foramina that connect the endocranial cavity with other parts of the head; in addition to the passages for the carotid arteries and jugular veins, many of these are the cranial nerve foramina, which are very important to osteological studies of the braincase, but which will not be considered here as they are unlikely to be critical structurally.

The space enclosed by these surfaces is, of course, the volume occupied by the bone (with some minor contributions from sinuses) in the skull. The thickness of this volume, seen for example in the rostrum, corresponds with the thickness of the bone in a CT scan of that same region. A CT slice is a 2-D slice: in 2-D, the internal and external boundaries of the bony nasal wall are internal and external edges, and these edges can be used to generate the curves which help to define the geometry of the respective surfaces. In fact, this is an important part of using CAD to build skull geometry: for relatively simple shapes, manipulating objects in two of the three orthogonal planes is all that is required. However, for the skull, objects need to be manipulated in all three orthogonal views. Also, since the skull has only one plane of symmetry, multiple views are required for two of the planes. Details of these are provided below.

The aim of this part is to create a 3-D model of the cranium and jaws in *Kronosaurus queenslandicus* that is suitable for conversion into a FE model

Methods

The dorsal, ventral, and left lateral reconstructions presented in Chapter 4 were imported as bitmaps into a Rhino file with 1 cm grid. Each bitmap was scaled 1:1, and the origin aligned to the anteriormost tip of the premaxillae. The axis system was: transverse axis, X; longitudinal axis, Y, dorso-ventral (vertical) axis, Z. The 3-D model was initially created with the same alignment as the 2-D reconstructions in Chapter 4: after surface meshing, the model was rotated so that the basal skull axis¹² was aligned in the Y axis (this required a downwards rotation of the posterior of the skull of 3° in the YZ plane, about the centre of the skull). All the measurements provided in the Results section below are taken with the latter alignment.

¹² A longitudinal axis that passes through the midlines of the anteriormost tip of the premaxillae and the posteriormost apex of the occipital condyle.

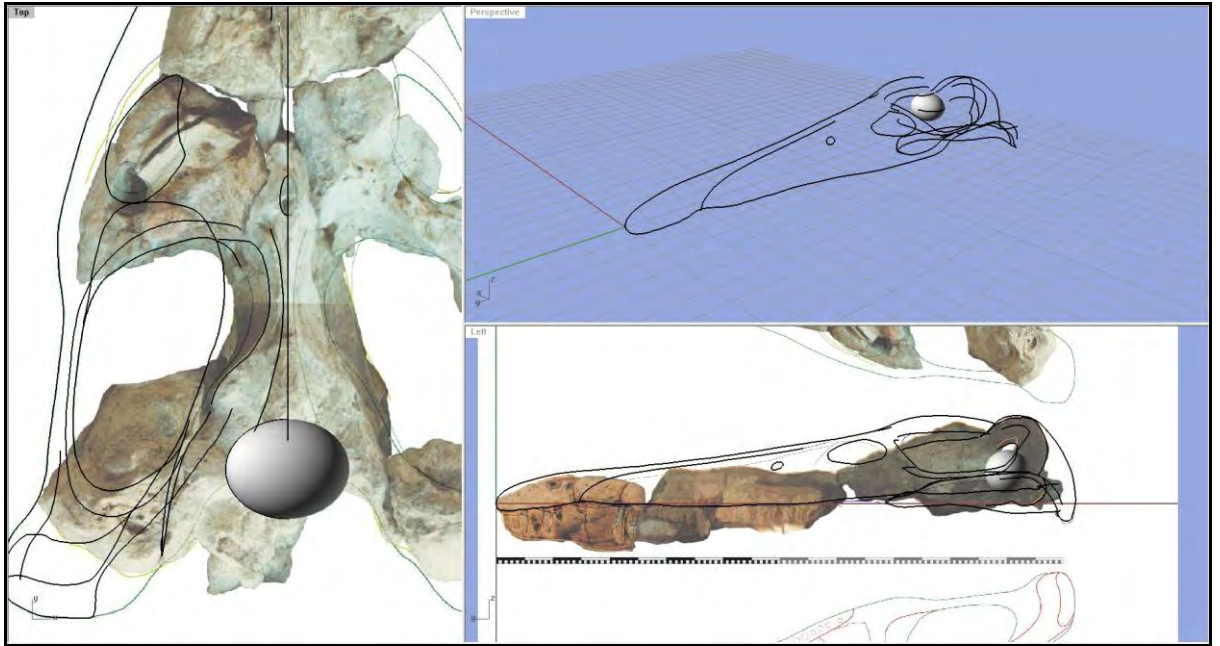


Figure 5-22: Axial curves in the *Kronosaurus queenslandicus* 3-D model. Tracing lines over photographs of the fossils augments the curves traced from the 2-D reconstruction; here, the geometry of the braincase is being created using photos of QM F18827.

NURBS¹³ curves were traced from the dorsal, ventral, and lateral reconstruction bitmaps, these ‘axial’ lines defined the overall shape and proportion of the left side of the skull (Figure 5-20, Figure 5-22). Transverse curves were created at regular 10 cm intervals throughout the model, with additional transverse curves in regions of complex geometry such as the orbital region. Surfaces were created by the intersection of ‘transverse’ and ‘axial’ lines. Only the tooth margins were modelled: no attempt was made to model the teeth.

For both the cranium and mandible, curves for the entire structure were completed before the creation of surfaces. In areas of complex geometry around the orbital region, such as the anterior wall of the orbits and the external nares, additional axial lines were traced from sections of the CT data for QM F51291 (see below).

The axial lines of the posterior region of the skull were defined with reference to the figure provided by White (1935) of that part of MCZ 1285 in posterior view (Figure 5-23).

¹³ Non-Uniform Rational B-Spline – a particular class of shape function that can be represented mathematically.

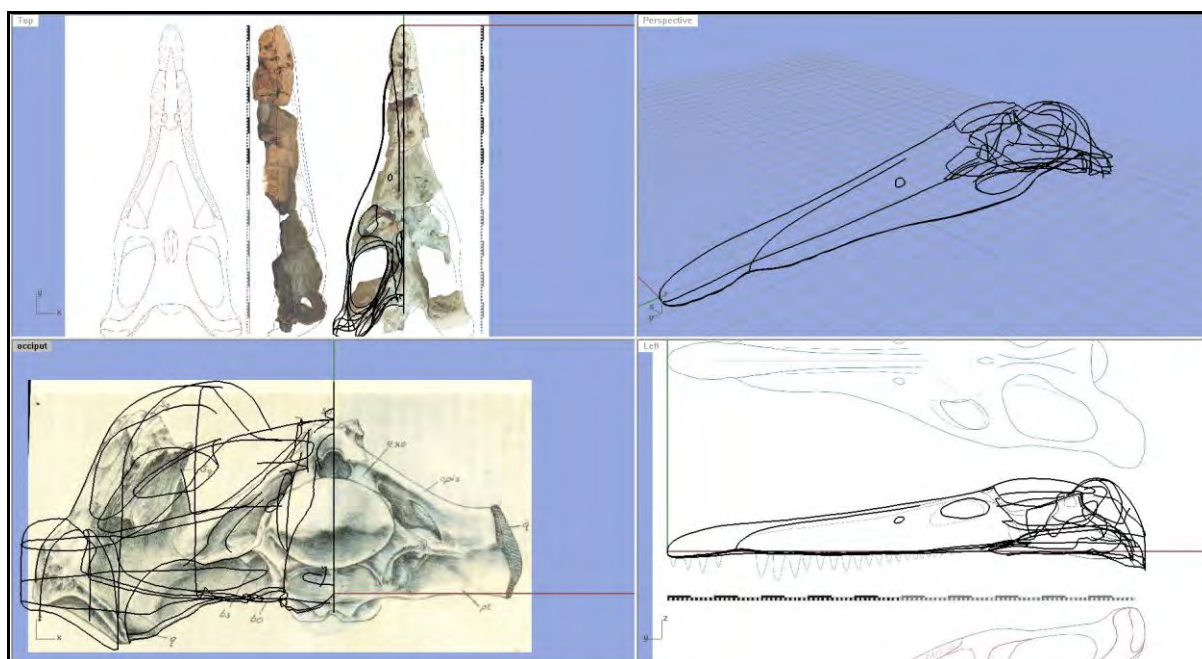


Figure 5-23: ‘Axial’ curves for the suspensorium were partly based upon a figure of the rear of the skull in MCZ 1285 (lower left – from White, 1935) prior to the incorporation of that fossil into the ‘Harvard mount’ (see Chapter 6).

Internal geometry and transverse lines

Anterior and mid rostrum: Natural breaks in the rostrum of QM F10113 provided sections of the rostrum at four locations in front of the orbital margins (Figure 5-24). From photographs of each of these sections, outlines of the bones were traced (Figure 5-25): these were then imported into Rhino and used to trace transverse curves at the respective points along the rostrum (Figure 5-26). As the 2-D reconstructions were created to the size of QM F10113, the imported bitmaps were scaled 1:1. The broken surfaces are irregular, but for the purposes of model construction were assumed to lie exactly in the transverse plane. The transverse curves were adjusted to fit the axial lines at each of these sections, in effect retro-deforming the preserved geometry of the rostral sections so that these were consistent with the overall reconstructed skull shape (i.e., the 2-D reconstructions). As part of this process, the geometry created for the model (i.e., the left side of the skull) incorporated the original geometry from both sides of the fossil through mirroring of the traced outline.

Axial lines representing the internal geometry were interpolated from the geometry of the transverse curves.

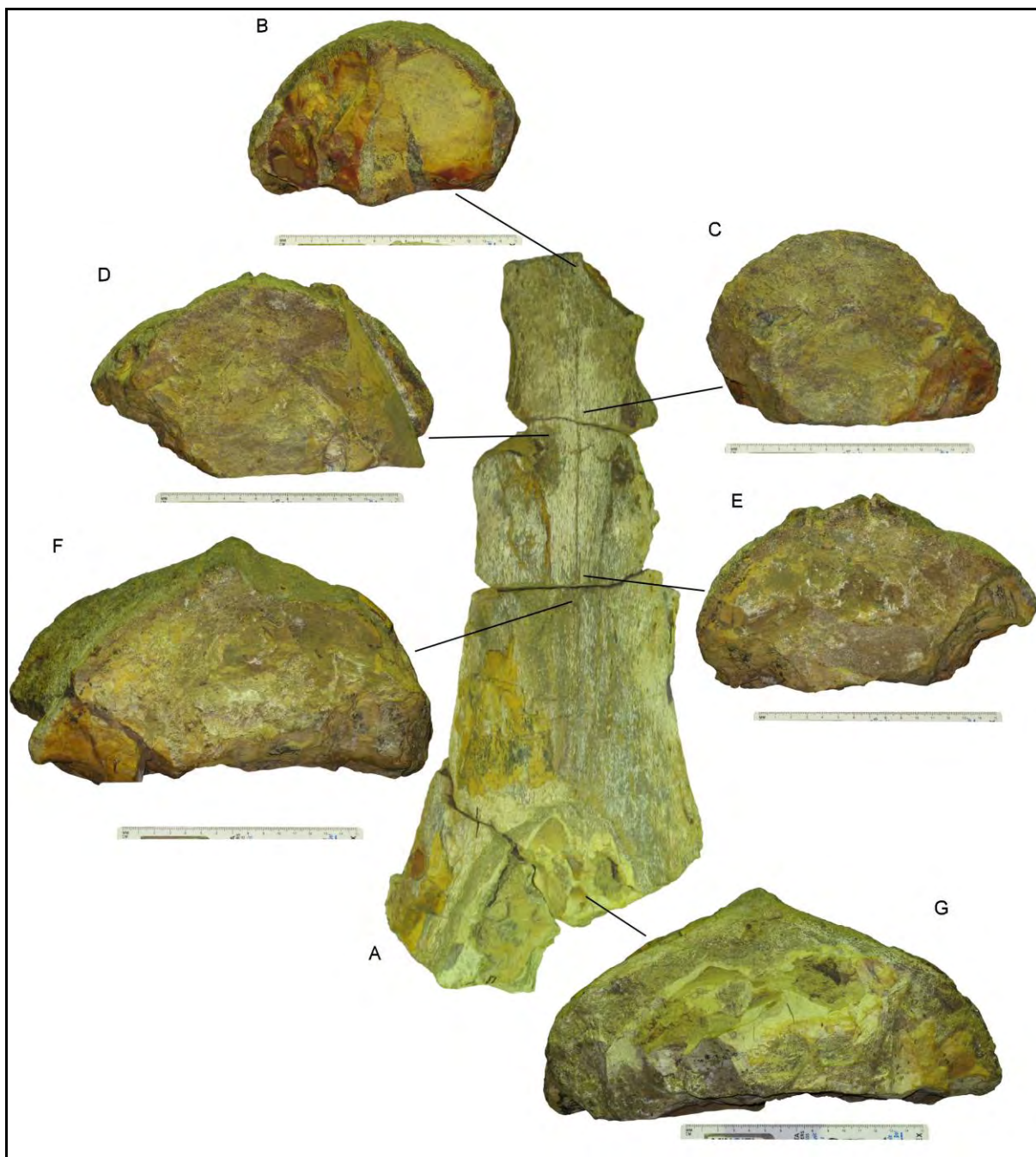


Figure 5-24: Rostral sections in QM F10113. A, dorsal view of four blocks comprising the anterior to mid rostrum: the anterior end is at the top of the page. B–G, transverse faces of the three anterior blocks. B, anterior face of S20; C posterior face of same. D, anterior face of SC65; E, posterior face of same. F, anterior face of S19; G, posterior face of same. Transverse faces are shown to the same scale; the rule shown under each is 15 cms. The dorsal view of the rostrum (A) is not to scale.

Posterior rostrum and orbital region: The 3-D objects of the fossil bone and the whole block, created from CT scan data of QM F51291 (see Section 5.2 above), were imported into the Rhino file. In creating the 2-D reconstruction (Chapter 4), this specimen had been rescaled to the size of QM F10133: the 3-D objects were similarly

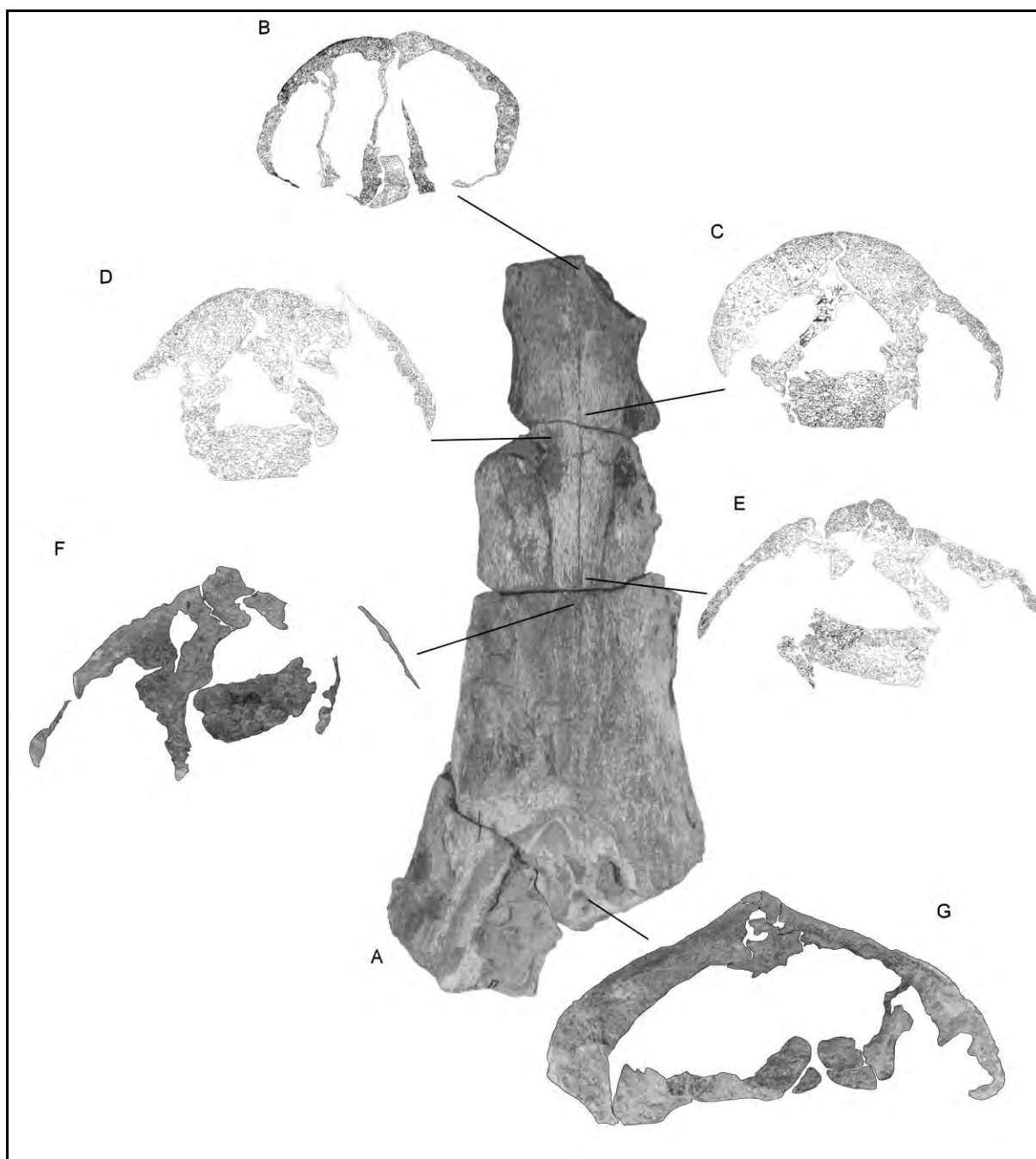


Figure 5-25: Interpretation of Figure 5-24; A–G refer to the same parts of QM F10113 as Figure 5-24. B–G show the preserved bone in approximately transverse section at each respective face. For B–E, the bone was traced from photographs; in F and G, outlines of the bone were used to mask parts of the photograph.

rescaled and oriented. The objects were then sectioned at each of the 10 cm transverse intervals, and the edges of the 3-D object at each section were traced on the respective transverse plane: these sections were then used to create idealised geometry in each transverse plane (Figure 5-27).

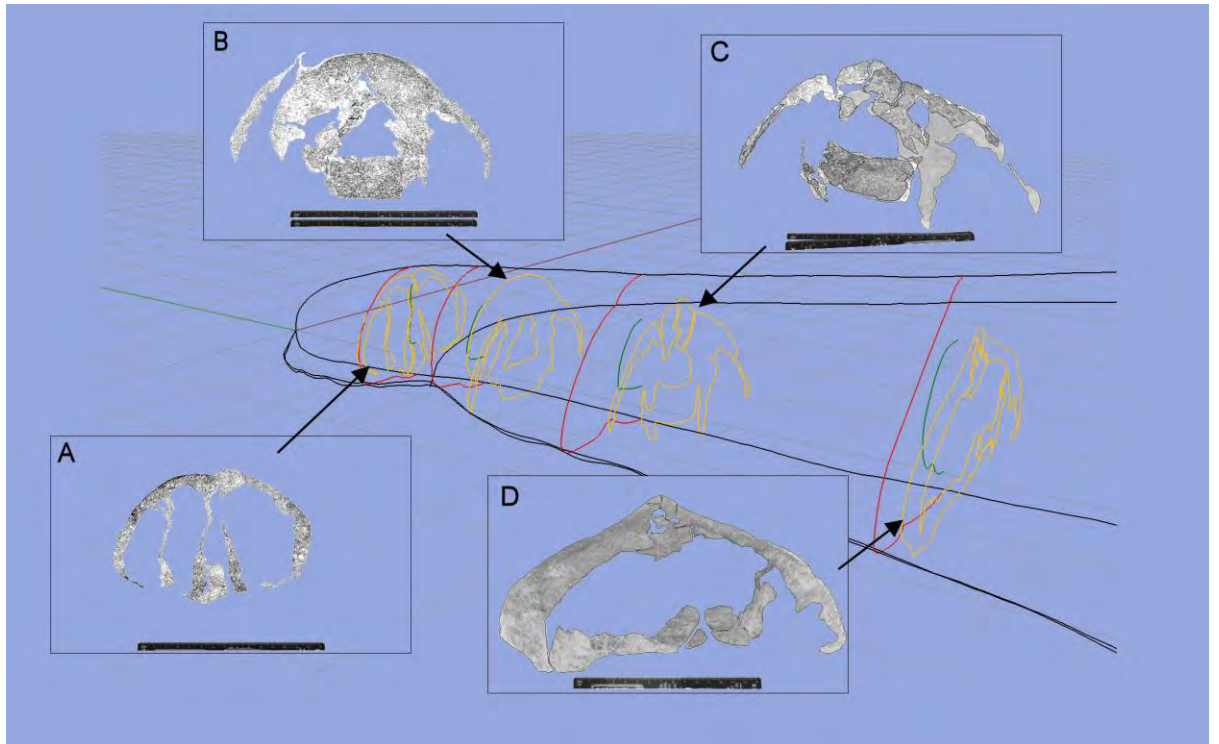


Figure 5-26: Creating the geometry for the transverse curves of the anterior/mid rostrum in the 3-D model. The diagrams of the rostral sections from Figure 5-25 are imported into Rhino and used to trace outlines of the bone (orange lines) in the transverse plane. The three anterior rostral blocks of QM F10113 (Figure 5-24, Figure 5-25) preserve four transverse sections; A shows the anterior face of block S20 ('B' in Figure 5-24 and Figure 5-25). B shows the section preserved at the posterior face of S20 and the anterior face of SC65 ('C' and 'D' respectively in Figure 5-24 and Figure 5-25). C shows the section preserved at the posterior face of SC65 and the anterior face of S19 ('E' and 'F' respectively in Figure 5-24 and Figure 5-25); D shows the posterior face of S19 ('G' in Figure 5-24 and Figure 5-25). In B and C, the images of the posterior face have been mirrored and aligned to the image of the anterior face, giving a composite image (hence the two scale bars in these). The traced outlines at each section are then used to create idealised geometry for the external (red) and internal (green) edges; these are fitted to the axial lines created from the 2-D reconstructions of the skull (Figure 5-20, Figure 5-22).

Rescaled to QM F10113, the QM 51291 objects spanned the transverse sections at the 90, 100, 110, 120, 130, and 140 cm intervals. Because of the complexity of the geometry around the nares and orbits, additional transverse sections were made at 98, 106, 113, 116, 125, 136, 137, and 144 cm along the Y (longitudinal) axis. Sections of the 'fossil bone' 3-D object provided the internal and external geometry of the fossil at each slice; sections of the original block provided additional information on structures preserved as natural moulds; principally, the posterior-lateral internal 'corners' of the orbits.

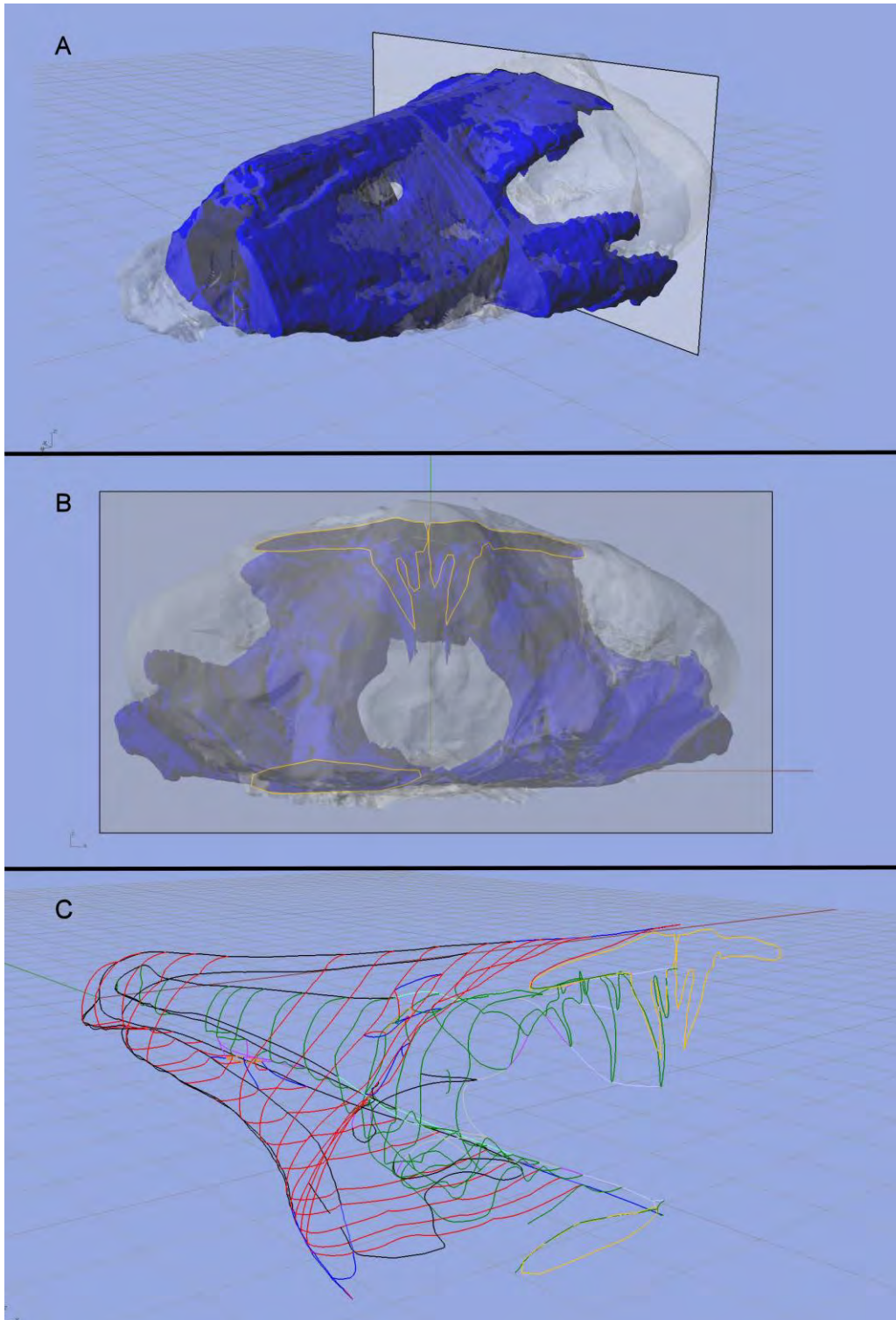


Figure 5-27: Transverse curves for the posterior rostrum and orbital region, based upon the geometry of the 3-D object created from CT scan data of QM F51291: the dark blue object is the model of the fossil bone, the translucent white object represents the whole block of fossil and matrix. A, the 3-D object is sectioned in the transverse plane; the section shown here is at $Y = 130$ cm in the *Kronosaurus queenslandicus* model. B, the outline of the bone at that section (orange line) is traced at that plane. C, the traced outline is used to create idealised geometry of external and internal edges at that section, as in Figure 5-26.

QM F51291 appears to be largely unaffected by sedimentary compaction (Chapter 4), but is weathered and, at several points of the brow, exhibits depressed fractures. In creating the geometry for the model, the transverse curves were adjusted to fit the axial lines at each section, as described above for the anterior rostrum; mostly, this involved restoring 'weathered' bone rather than retro-deforming distorted geometry.

In addition to the transverse curves, the QM F51291 3-D objects were sectioned in the sagittal and coronal planes, and axial lines delineating the internal and external surfaces created from these sections. In particular, the internal axial lines were essential for the creation of the complex internal geometry of the anterior orbital region.

Suborbital region: QM F51291 preserves the geometry of the sub-orbital floor of the palate, but the external surface has been largely eroded. QM F2446 preserves the external surface, including the lateral pterygoid buttress, but the palate in this specimen is still largely obscured by matrix. The posterior view of QM F2446 does show a section of the sub-orbital floor and the bones surrounding the inter-ptyergoid vacuity, and this was used to reconstruct the geometry of the transverse curves representing the external surfaces at 136, 137, and 140 cm along the Y axis (i.e. immediately in front of the post-orbital wall).

Postorbital wall: QM F51291 preserves the internal geometry of the anterior face of the postorbital wall, including the boundaries of the postorbital fenestrae. A diagram of the posterior view of the fossil block, with the interpretation from left and right sides mirrored, was used to create the geometry of the postorbital wall (Figure 5-28).

Braincase: The geometry of the braincase and temporal arcade (except the zygomatic arches) was based mainly on photographs of QM F18827, which appears to preserve the structures between the epiptyergoids and the occipital condyle with minimal distortion (but some erosion). The 2-D reconstruction was itself largely based upon these photographs and thus already incorporated the external geometry as far as it could be described without 3-D scanning. Additional data on the external morphology of the otic region came from QM F10113 and QM F2446.

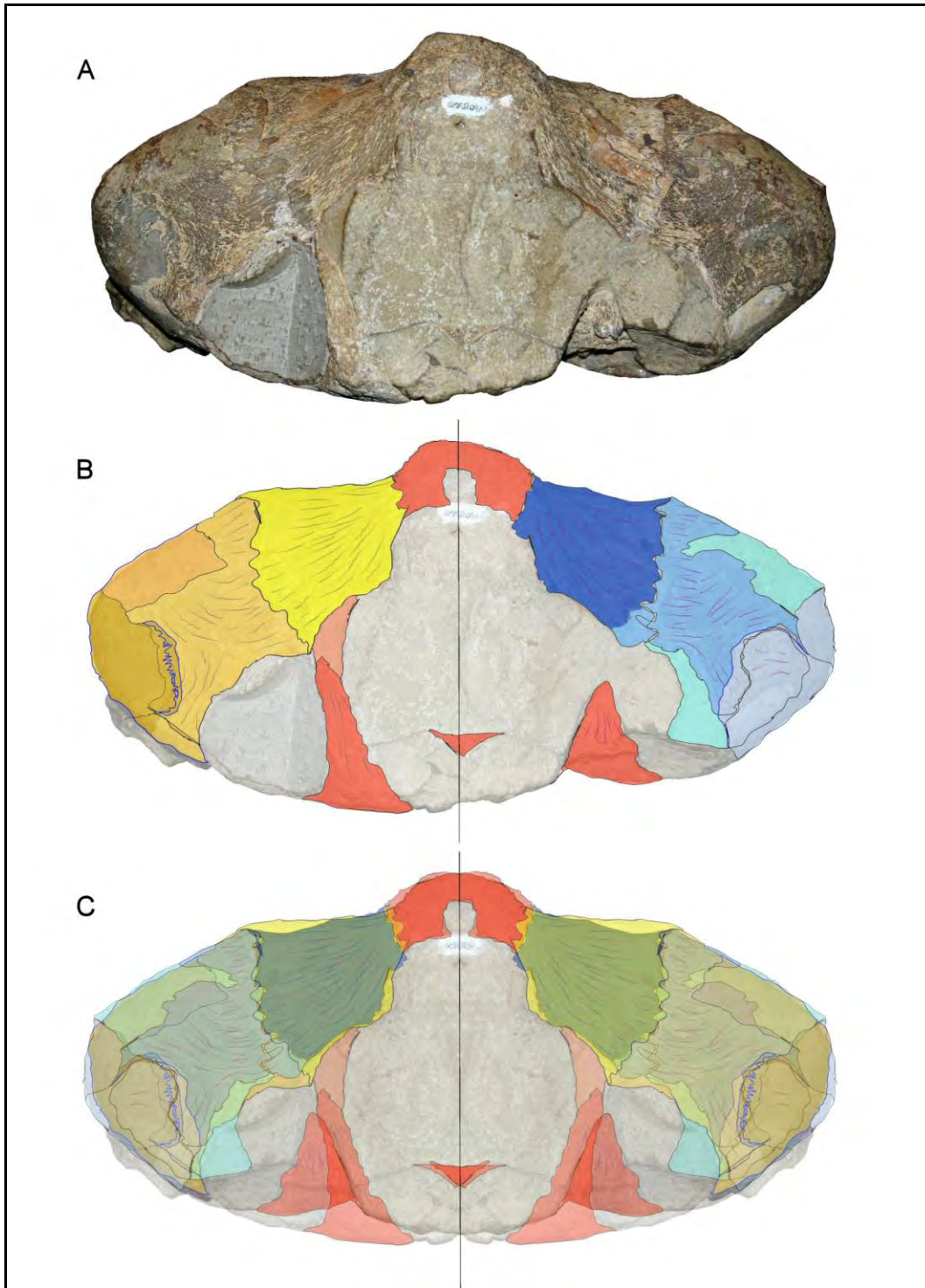


Figure 5-28: QM F51291 in posterior view. A photograph of the specimen (A) forms a basis for diagrammatic interpretation of the preserved bone (B); this is mirrored around the midline (C) to provide a guide for the geometry of the postorbital wall, anterior epipterygoid, and the postorbital fenestra. Note that, in (B), the transverse surface of the broken right pterygoid (red) lies forward of the equivalent surface on the left, in effect providing the geometry for transverse curves at two positions along the longitudinal axis.

The internal geometry of the endocranial cavity was reconstructed with reference to published descriptions of the braincase in other pliosauroid taxa (Carpenter 1997, Cruickshank 1994, Noè et al. 2003), and to unpublished CT data of a pliosaur braincase from the Upper Cretaceous of Texas (MCZ 2446; McHenry, in prep.). The parietal stalk was based upon the preserved endocast in QM F18154.

Occiput and suspensorium: Several of the Queensland Museum specimens (QM F18827, QM F10113, QM F2446) preserve the occipital condyle and associated elements of the posterior braincase, and these were included in the geometry of the axial curves via the 2-D reconstructions of the skull (e.g. Figure 5-22). Transverse lines for these were created based upon interpolation from photographs of these specimens. The paroccipital process is not preserved well in any of the QM material, and geometry for this was based upon White's figure of the occipital region of MCZ 1285 (White 1935). Geometry for the squamosal arch, quadrate, and quadrate ramus of the pterygoid was based upon White's (1935) figure in addition to the preservation of QM F18827, QM F10113, and QM F2454 (Figure 5-23).

Mandible: As described in Chapter 4, no specimen of *Kronosaurus queenslandicus* preserves an intact mandible. The 2-D reconstruction of the mandible interpolates data from a number of specimens which preserved incomplete parts, in particular QM F18827, QM F10113, QM F51291, QM F2454, QM F2446, and MCZ 1284, and the axial lines for the mandible were generated from the 2-D reconstruction.

Transverse lines for the external and internal geometry were created from the preserved sections of the mandible in QM F0113; the mandibular symphysis, two sections of the ramus, and the articular region including the glenoid and the incomplete retro-articular process. The symphysis and the articular regions could be located precisely: however, the two sections of the mandibular ramus do not click fit with any other parts of the fossil, and cannot be located precisely. They were positioned so that their vertical dimensions gave the best fit to the axial lines generated from the 2-D reconstruction, and the pattern of the tooth alveoli was consistent with that of the 2-D reconstruction. Together with the anterior and posterior surfaces of the symphysis, and the anterior surface of the articular, this gave seven transverse sections; at 12, 46.4, 68.3, 78.8, 95.6, 122.8, and 175.9 cms in the Y

axis. In both cases, the vertical dimension of the ramus fragments exceeded that of the 2-D reconstruction: the depth of the ramus was thus increased in the 3-D model, although not to the maximum extent that could have been restored on the basis of these fragments.

The internal geometry of the mandible comprises the size and shape of the Meckelian canal. This was traced from photographs of each of the transverse surfaces of the parts of the mandible detailed above. Because of the uncertainty surrounding the detailed morphology of the mandible in *Kronosaurus queenslandicus*, the internal geometry was simplified in the model. With the exception of the symphysis and the ventral surface of the articular, each of the preserved parts of the mandible in QM F10113 has been subjected to significant erosion of the external surfaces; these were restored as described for the orbital region above.

In addition to the transverse curves created from the surfaces of the broken parts of the mandible, transverse curves were created for sections at the glenoid fossa and the base of the retro-articular process; at 200.2 and 213 cm in the Y axis respectively. No internal geometry is required at these sections: external geometry was interpolated from photographs of the block containing the left articular and quadrate of QM F10113.

Only one specimen, QM F2454, preserves the coronoid process and the adductor fossa, albeit as a weathered and incomplete fragment. Photographs of this specimen were used to create the external geometry of the coronoid process via the 2-D reconstruction (Chapter 4). The adductor fossa is the place at which the internal and external surfaces of the mandible join; the complex morphology of this region was interpolated from photographs of QM F2454.

Polysurfaces and meshes

NURBS polysurfaces were created from the axial and transverse curves for the cranium and mandible using the 'edge curves' function in Rhino (Figure 5-29A, B); as described above, this allows a polysurface to be created from 3 or 4 NURBS curves (see Figure 5-21). Because the geometry of the surface is interpolated from the geometry of the respective edge curves – for example, undulations in the edge curves

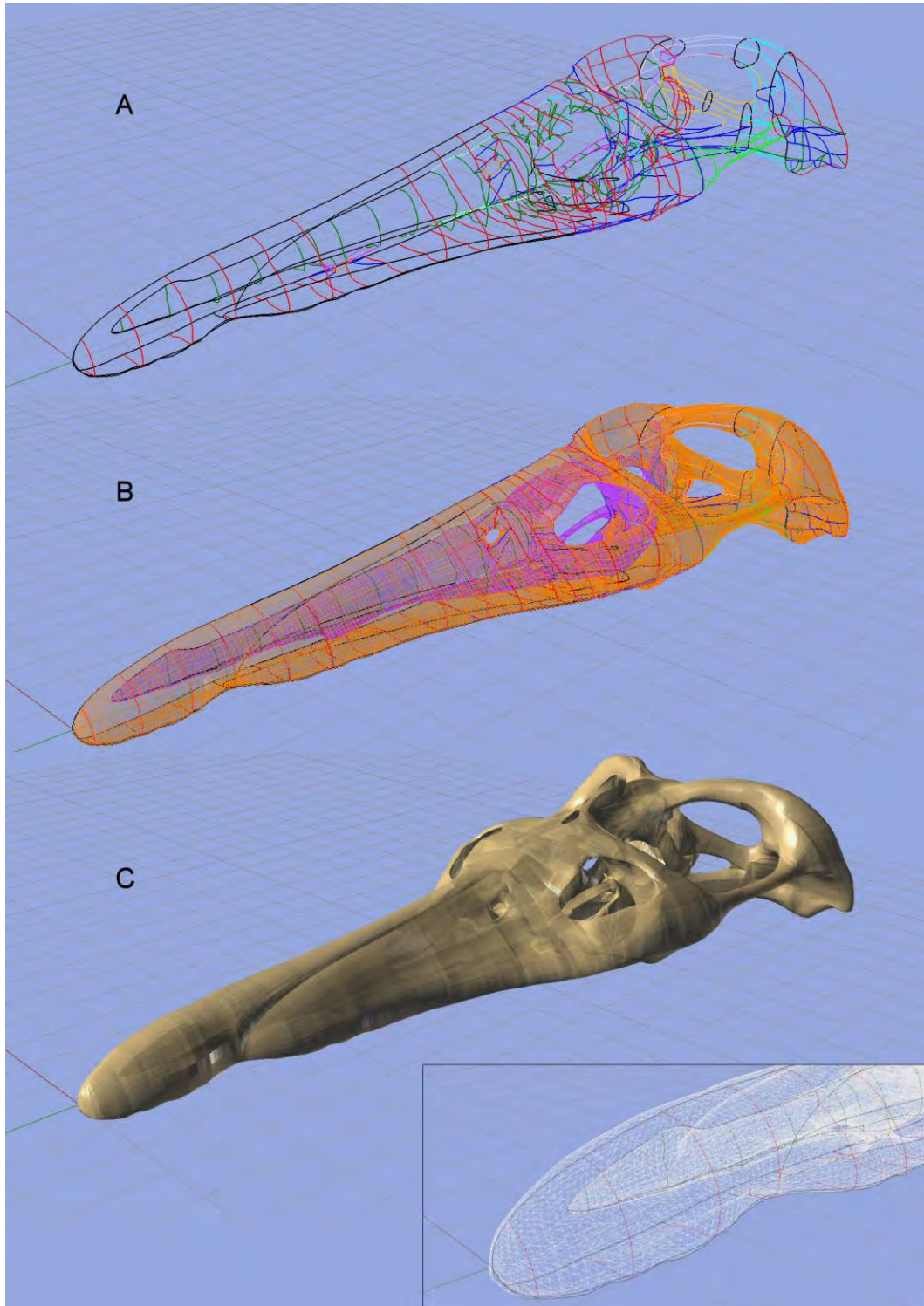


Figure 5-29: Surface meshing the 3-D model of the cranium. A, the final model consisting of axial and transverse NURBS curves. B, surface model of NURBS polysurfaces; each polysurface is created at the intersection of the curves in A. The internal surface (purple) can be seen behind the external surface (orange). C, Surface mesh created from the NURBS polysurfaces, mirrored to give the whole cranium, and rendered to give a 'solid' appearance. The mesh is actually composed of straight-edged triangles (insert – compare with Figure 5-21).

are reflected by undulations in the resulting polysurface – the degree to which the polysurfaces reflect the desired geometry of the modelled object(s) depends in part on the ‘resolution’ of the curves, i.e. how well the curves model the actual geometry of the original object, and how many curves are used. This requirement led to more complex parts of the skull, for example, the orbital region, being modelled with a larger number of curves.

The polysurfaces form the template for the mesh that is eventually used to generate the FE model (see below). For this process to produce a workable result, the different polysurfaces should align as closely as possible, i.e. adjacent polysurfaces should share at least one edge. Gaps between adjacent polysurfaces – for example, created by the shared edge being modelled by two similar but non-identical NURBS curves – will produce imperfections in the mesh that will decrease the resulting quality of the FE model, or even prevent successful FE modelling. For this reason, all curves representing a shared edge between polysurfaces were modelled as precisely as possible. Where a single edge of one polysurface contacts only one adjacent polysurface, this is relatively straightforward: however, where two (or more) polysurfaces will need to contact a single edge, the original NURBS curves must be aligned with precision.

Modelled in this way, a single NURBS polysurface is not necessarily a flat surface, and for a biological structure such as a skull flat surfaces are rare. Each surface in the *Kronosaurus queenslandicus* skull model includes at least one order of curve. Meshes, however, have no curved surfaces: each surface in a mesh is flat, and curved surfaces in a modelled object are approximated by the use of numerous small, tessellated mesh surfaces: junctions between adjacent mesh surfaces are angled slightly to match the curves of the original object. Because of the need for tessellation, meshes are usually comprised of triangles or quadrilaterals (Figure 5-29C).

The NURBS polysurfaces were converted to a low resolution, triangle-based mesh. The meshes for the left sides of the cranium and mandible were each mirrored about the sagittal plane (Figure 5-29C) and then exported as separate STL files. The STL files for the cranium and mandible were imported into a MIMICS project, and the

mesh optimised for export into FEA using the remeshing algorithms within MIMICS.

The mesh produced by Rhino and modified by MIMICS describes only the surface geometry; it is thus referred to as a 'surface' mesh. FEA, in contrast, requires a 'solid' mesh, where the triangles (in this case) of the surface mesh are simply the external faces of three dimensional tetrahedral elements, and most of the elements lie inside the external surface in a volume entirely filled by tessellated elements. A solid mesh, therefore, typically contains many more elements than a surface mesh does triangles. Resolution of the remeshed cranium and mandible were determined by a desired final resolution of ~1.5 million elements in the FE model; previous experience indicated that the remeshed STL objects should be approximately 130,000 and 50,000 triangles for the cranium and mandible respectively.

Results

The finalised 3-D model of the left side of the skull of *Kronosaurus queenslandicus* comprised ~1,000 NURBS curves for the cranium and ~220 curves for the mandible. These required the manual creation and manipulation of ~10,000 and 2,350 control points respectively, although more than these were involved in the creation of the models. Overall, the process required the equivalent of at least three months of full-time work.

Structural morphology

The creation of a 3-D model of a complex structure such as a fossilised skull requires detailed data on the original structure of the modelled object, as is shown above. However, the process also illuminates many aspects of the structure's morphology that are difficult to represent in traditional 2-D media. Because the aim of the process is to produce a model that has structural integrity within FEA, it also makes assumptions and uncertainties concerning the original structure explicit in a way that traditional descriptions do not always manage. These are summarised here.

Anterior nasal / vomerine cavity: the presence of a cavity anterior to the position of the internal nares is suggested by eroded dorsal surfaces of the premaxillae in QM F18827 and MCZ 1284. The creation of a closed end of the nasal cavity anterior to the transverse section at $Y = 20$ cm, based upon the preserved morphology of the anterior-most transverse section of QM F10113, requires a tall, thin section of the cavity at this point (Figure 5-29, Figure 5-30).

Lateral (maxillary) walls of nasal cavity: Anterior to the external nares, the maxilla forms a thick lateral wall to the nasal cavity. In the model, the thickness of the maxilla (normal to the external surface of the point) is 2.73 cm at a point 10 cm in front of the nares ($Y = 90$ cm), at about the same dorso-ventral height as the nares – similar to direct measurement of the equivalent bone in QM F10113 (2.72 cm), even though the external and internal surfaces of the model at this point were interpolated from different specimens. At the same coordinate in the Y (longitudinal) axis, the maximum width of the dentulous part of the maxilla, measured in the coronal plane where the internal surface of the maxilla contacts the dorsal surface of the palate, is 11.1 cm.

Dorsal median ridge: In the model, the geometry of this structure was based upon the CT data from QM F51291. Measured in transverse section at $Y = 90$ cm, the modelled dorsal median ridge (DMR) is 5.3 cm high at the midline. The planar width from the premaxilla-maxilla suture to the midline at this point is 2.9 cm. Equivalent measurements from QM F10113 are 5.0 and 2.6 cm respectively. The larger dimensions of the DMR in the model may reflect allometry in this structure, with it being proportionally larger in the smaller QM F51291 specimen (see Chapter 4).

Palate: Behind the internal and external nares, the dorsal (internal) surface of the palate carries a longitudinal ridge at the contact between the palatine and the pterygoid; from CT of QM F51291, the ridge appears to be formed by the dorso-lateral edge of the pterygoid. The dorsal apex of the ridge is sharpened (not rounded), and may support a soft-tissue structure within the nasal cavity. It extends posteriorly to the medial part of the palate in between the orbits (Figure 5-30, Figure 5-31).

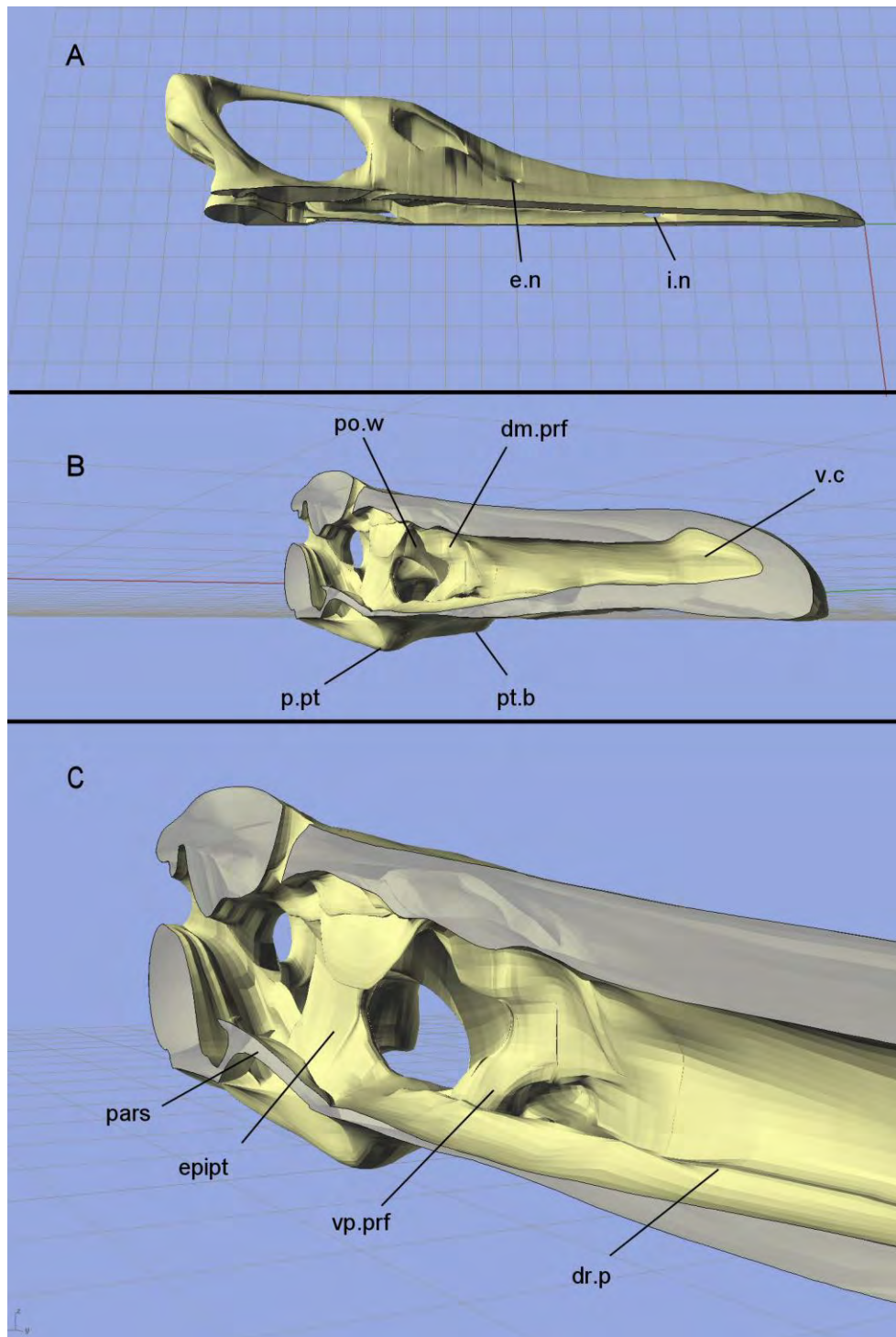


Figure 5-30: Geometry in the 3-D surface model of the half-cranium in *Kronosaurus queenslandicus*. A, oblique dorsal view, showing the positions of the internal (i.n) and external (e.n) nares. B, the model in oblique anterior view, showing internal and external structures; vomerine cavity (v.c), lateral buttress of the pterygoid (pt.b), posterior ramus of the pterygoid (p.pt), dorso-medial process of the prefrontal (dm.prf), and the postorbital wall (po.w). C. Close up of (B), showing the ventral process of the prefrontal (vp.prf), the dorsal ridge of the palate (dr.p), the epipterygoid (epipt), and the parasphenoid (pars). Surface of the bone is in gold, the sagittal section of the bone is shown as partially opaque grey surface. The grid is 10 cms.

For most of its width across the floor of the nasal cavity, the palate is thick and robust. However, the pterygoid thins towards the midline, and the bone at the midline of the palate is comparatively thin, especially in the posterior rostral and orbital region of the palate (Figure 5-30, Figure 5-31). Although there is no evidence for a midline anterior palatal vacuity (sometimes termed an anterior inter-pterygoid vacuity), it is possible that the thinness of the bone along the midline, coupled with weathering/ taphonomic distortion, may resemble such a structure, as appears to be the case with QM F2454.

Evidence for a robust lateral pterygoid/ ectopterygoid buttress in the sub-orbital region is preserved in QM F2446 and QM F18827, although the precise morphology remains unclear. The buttress is a blunt, robust ridge (Figure 5-30B, Figure 5-31C) with an inverted triangle section as viewed laterally. In the model, this structure has a minimum thickness (in the vertical axis) of 3.8 cm: viewed posteriorly, the ventral edge angles upwards at approximately 10° to the horizontal as it runs laterally.

Orbital region: As modelled, the maximum diameter of the orbital margin is 21.1 cm in the longitudinal (Y) axis and 14.4 cm in the transverse (X) axis. The longest diameter of the orbit is angled antero-medially, so that the maximum diameter is 22.6 cm. There is a prominent supraorbital ridge in along the anterior half of the medial border. In most amniotes, the orbital dimensions are significantly negatively allometric: as the geometry of the orbits was based upon the preservation of QM F51291, which is a much smaller specimen than QM F10113, any allometry in orbital size between these specimens will mean that the orbits in the model are proportionally too large.

At the front of each orbit, the lacrimal and prefrontal form a strong anterior wall that separates the orbital and nasal cavities (Figure 5-31B). The 'central' part of the prefrontal makes up the medial part of the lateral wall of the posterior rostrum; a descending process from this part runs ventrally, posteriorly, and slightly medially to form a robust pillar connecting the rostral roof with the palate (Figure 5-30C, Figure 5-31B). Lateral to this, the lacrimal forms a smooth, concave antero-medial wall to the orbital cavity that forms a broad connection between the anterior margin of the orbit, the palate, and the lateral wall of the orbit. In front of the lacrimal component

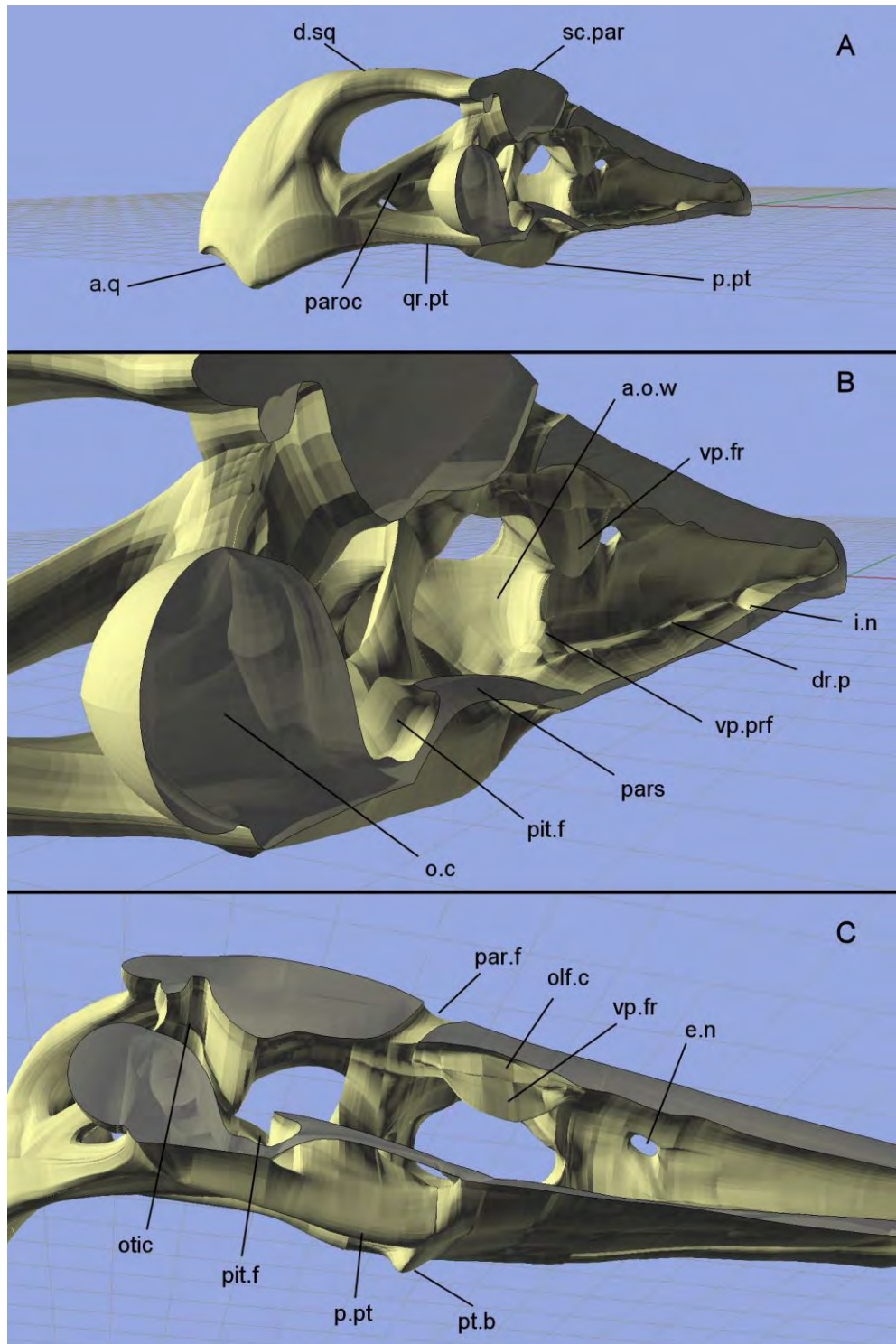


Figure 5-31: 3-D model of half-skull shown in Figure 5-30. A, oblique posterior view, showing the suspensorium, comprising the dorsal arch of the squamosal (d.sq), the paroccipital process (paroc), the quadrate ramus of the pterygoid (qr.pt) and the articular face of the quadrate (a.q). The sagittal crest of the parietal (sc.par) is also shown. B, internal-posterior view of endocranium, showing the anterior orbital wall (a.o.w), ventral process of the frontal (vp.fr), pituitary fossa (pit.f) and occipital condyle (o.c). C, internal-ventral view, showing internal otic region of endocranium (otic), parietal foramen (par.f), and the hypothesised position of the olfactory canal (olf.c – see Figure 5-17). Other labels as for Figure 5-30.

of the anterior orbital wall, the posterior-lateral extremity of the nasal cavity appears to form a 'blind' space.

From the 'central' part of the prefrontal, a dorsal-medial process runs posteriorly and medially and underlaps the roof bones of the brow region between the orbits, giving the appearance of a thickened 'knob' of bone on the internal surface of the supraorbital region (Figure 5-30B). On the median part of the brow, there are two pairs of thin ventral processes that descend from the internal surface of the skull roof: these are aligned longitudinally and are present along the whole length of the inter-orbital region. The more lateral process is the larger, but they do not contact any bony structures and may be involved with the support of soft-tissue structures associated with the olfactory canal (Figure 5-31).

Postorbital region: The orbital cavities are separated from the temporal arcade dorsally and medially by a postorbital wall formed by the postfrontals and postorbital bones. A postorbital fenestra connects the orbital cavity with the temporal arcade; the fenestra lies in the ventro-medial part of the post-orbital region. It is bordered medially by the epipterygoid, which forms a robust pillar connecting the pterygoid ventrally with the parietal dorsally. As modelled, the fenestra has a maximum diameter of 14.1 cm vertically and 10.3 cm in the transverse axis: its geometry is interpolated entirely from the preserved remnants of the postorbital wall in QM F51291.

The epipterygoid itself is modelled as a near-vertical column with an ovate section (Figure 5-30C): the diameter of the section at the narrowest point is 8.0 cm in the longitudinal axis and 4.6 cm in the transverse. This section may be proportionally more elongate than in the original skull: the anterior edge was interpolated from QM F51291, while the posterior edge was interpolated from QM F18154, and thus any errors in scaling these specimens to the overall dimensions of QM F10113, or allometric variation between these two specimens, may have exaggerated the epipterygoid's dimensions. The 'laterosphenoid' fenestra, between the epipterygoid and the proötic, may be larger in the model than the same space is in QM F10113.

On the palatal surface, the inter-pterygoid vacuity (= posterior inter-pterygoid vacuity of other authors) is bordered on each side by a robust posterior process of the pterygoid (Figure 5-30B, Figure 5-31). The process has a strong keel on the ventral surface: in transverse section at the maximum width of the inter-pterygoid vacuity, the posterior process has a transverse diameter of 7.5 and a depth, from the junction with the overlying epipterygoid, of 7.9 cm. The geometry of the pterygoid process at this point is interpolated principally from QM F2446.

Zygomatic arch: The contact between jugal and postorbital bones at the posterior-lateral corner of the orbit forms the forward part of the zygomatic bar: this has been modelled as a smoothly tapering junction that rapidly decreases in diameter posteriorly (Figure 5-33). As modelled, the minimum diameter of the zygomatic arch, which forms the lateral margin of the temporal arcade, is 3.7 cm in height and 3.2 cm in width. Posteriorly, the jugal is modelled as forming a smooth join with the squamosal dorsally and medially, but a sharper junction ventrally. The geometry of the zygomatic arch, and its contacts with the postorbital wall anteriorly and the suspensorium posteriorly, is based upon the preserved morphology of two specimens of *Brachauchenius lucasi*; USNM 4989 and FHSM VP-321 (Chapter 4).

Parietals: The parietal foramen is an elongate, ovoid structure 6.8 cm long and 2.5 cm wide. It is enclosed by the parietals, which form a raised lip around its sides; this lip is deeper at the rear and grades posteriorly to the sagittal crest. The parietal canal runs from the foramen on the dorsal surface, downwards and backwards towards the anterior braincase; its diameter decreases slightly as it runs backwards. At the rear of the foramen, the parietal is 7.3 cm thick in the vertical axis: its maximum depth, at the apex of the sagittal crest, is 13.5 cm as modelled, with approximately 4.3 cm of that consisting of the narrow crest (Figure 5-31C). In some taxa of pliosaurs, the rearmost part of the parietals form an expanded, triangular 'roof' to the supraoccipitals, but this does not appear to be the case in *Kronosaurus queenslandicus* (Figure 5-33), although no specimens preserve this part of the skull well. At the posterior edge of the parietals, there is a midline bulge, convex posteriorly, that may indicate the attachment of the nuchal ligament with the occipital surface of the skull (c.f. Carpenter 1997): this can be seen on QM F18827. In the longitudinal axis, this

bulge extends to $Y = 182.5$ cm: it is thus well in front of the rear apex of the occipital condyle, which is at $Y = 187.3$ cm.

Anterior braincase: The parasphenoid is modelled largely from the preservation of QM F51291, although when this was scaled to the full size of the model its dimensions were much larger than the sections preserved in QM F2446 and QM F10113, suggesting that this element is also subject to negative allometry. The parasphenoid forms an arched beam running from the basisphenoid forwards to the middle part of the pterygoids (Figure 5-30C, Figure 5-31); the contact with the pterygoids at the front edge of the inter-pterygoid vacuity is more or less in line (in the longitudinal axis) with the anterior edge of the parietal foramen on the skull roof (Figure 5-33). In section, the parasphenoid is an inverted triangle with a strongly concave upper edge; the lateral borders form sharp edges that may support soft-tissue structures. At its narrowest point, the parasphenoid as modelled has a transverse diameter of 1.9 cm: the section is 1.8 cm high.

The inter-pterygoid vacuity is a large opening enclosed by the posterior processes of the pterygoids laterally (Figure 5-31C, Figure 5-33) and bounded by the parasphenoid dorsally (see above). In ventral view, it has a ‘tear-drop’ shape: it is 26.2 cm long and 9.0 cm wide. It is closed posteriorly by the midline contact of the posterior pterygoid rami underneath the posterior braincase. The geometry of the inter-pterygoid vacuity in the model is based upon QM F2446 and QM F51291 anteriorly, and White’s (1935) figure of MCZ 1285 posteriorly.

At the posterior part of the inter-pterygoid vacuity, the ventral surface of the parasphenoid curves downwards to join the pterygoids. The lateral edges of the parasphenoid expand laterally and contact the internal surface of the lateral wall of the braincase (Figure 5-31B): this contact is 6-7 cm above the contact with the pterygoids. Between these contacts, the parasphenoid appears to form the anterior wall of a deep fossa, which from its position appears to be the pituitary fossa (Figure 5-31B, C). The thickness of the pterygoids underneath this fossa is 1.7 cm.

Otic region: The opisthotic and proötic bones form thick lateral walls of the posterior braincase. In life, these contain the otic cavities of the inner ear, but these

were not modelled here. The robust form of these bones suggest that they may have structural importance in bracing the parietals with the basisphenoid; as modelled, the lateral wall of the braincase in the otic region is between 1.7 and 4.2 cm thick.

The paroccipital process is modelled as a robust structure, oriented sharply posteriorly and slightly ventrally as it runs laterally from the lateral wall of the posterior braincase (Figure 5-31A, Figure 5-33). It is deeper than wide: in transverse section normal to its own long axis, it has been modelled as 2.3 cm wide by 4.1 cm tall. This may be too small; the geometry in the model was based upon White's (1935) figure of MCZ 1285, but the weathered remnants of the paroccipital process in QM F10113 may indicate that it was larger.

Suspensorium: The dorsal arch of the squamosal rises from the dorso-lateral face of the posterior parietals, and is angled laterally, posteriorly and dorsally before arching downwards towards the quadrates. The narrowest part of the arch is at its dorsal apex, where, measured normal to its own long axis, it is 5.5 cm high and 7.0 cm wide, with an ovate cross section. The lateral part of the arch, where the squamosal is contacted by the paroccipital process, the quadrate ramus of the pterygoid, the jugal, and the quadrate, is massive (Figure 5-31A): below the point where it contacts the jugal, it forms a curved wall, with the concave edge facing forwards and the convex edge backwards, that is more or less vertical but slopes slightly backwards as it descends to the articular face of the quadrate (Figure 5-33).

The quadrate ramus of the pterygoid is a robust process that angles posterior-laterally from the posterior part of the pterygoids, where these contact on the midline behind the inter-pterygoid vacuity. The narrowest part of the ramus is, measured normal to its own long axis, 4.0 cm wide and 5.4 cm tall. This geometry has been interpolated from White's (1935) figure of MCZ 1285, although, as with the paroccipital process, the remnants of the process in QM F10113 may indicate a more robust structure.

At the base of the condylar surface, the quadrate is 14.6 cm in the transverse (X) axis, and 5.5 cm in the longitudinal (Y) axis at the apex of its curved vertical surfaces. The articular face is inclined so that, from the medial to the lateral edge, it rises sharply dorsally and laterally, i.e. the medial part is lower than the lateral (Figure 5-33). This

geometry is based upon White's (1935) figure of MCZ 1285 (Figure 5-23), although it needs to be confirmed in other specimens – QM F0113 and QM F2454 may each preserve the articular face of the quadrate, but in both it is still in articulation with the glenoid fossa of the mandible and thus the articular surface is obscured.

Occiput: Although mostly preserved as an ovate hemi-spheroid, with the transverse radius approximately equal to the longitudinal but exceeding the vertical radius, the occipital condyle appears to be particularly prone to taphonomic distortion and is often altered by sedimentary compaction. In one specimen, QM F2446, it is preserved as a hemisphere, with all radii approximately equal, and it is modelled closer to this shape here: the vertical radius is 8.0 cm, the transverse 8.5 cm, and the longitudinal radius is 6.9 cm.

Mandible: The morphology of the mandibular symphysis is visible in external view of the structure in QM F10113. The rami are both broken just behind the rear of the symphysis¹⁴, allowing the dimensions of the anterior part of the Meckelian canal to be seen at the broken transverse surfaces: the canal is 5.5 cm tall at this point (Y = 46 cm). The Meckelian canal runs along the bottom part of the mandible, which can be conceived as a hollow beam that houses tooth sockets in its upper portion.

The thickness of the bone surrounding the Meckelian canal was approximated from the transverse surfaces of the mandibular rami fragments of QM F10113. At the anterior part of the ramus (Y = 68 cm) the medial wall is 1.5 cm thick and the lateral 1.3 cm. The ventral 'floor' of the ramus is somewhat thicker, 2.9 cm. More posteriorly (Y = 123 cm), at a position just in front of the adductor fossa, the medial wall narrows to 0.6 cm, while the lateral wall is 1.3 cm; the ventral floor is here 2.1 cm thick.

Most other relevant dimensions can be measured directly in external view. The glenoid fossa is modelled as a deep, saddle shaped fossa that qualitatively matches the shape of the apposite quadrate condyle, except that that the fossa is nearly as deep in

¹⁴ This appears to be a consistent weak point in pliosaur mandibles – in many fossils, the rami are broken at this same point. It also appears to be a weak point in 3-D (i.e. rapid prototyped) models of crocodylian skulls.

the lateral part as in the medial: this emphasised the need for re-examination of the morphology of the articular surface of the quadrate.

Meshing

The meshes of the cranium and mandible that were generated from the polysurfaces created in Rhino were imported into MIMICS as described in the Methods above. Within the ‘remeshing’ module, the meshes were ‘smoothed’ and the number of triangles ‘reduced’, using default settings, before being ‘auto-remeshed’. In the auto-remesh function, the total number of triangles in the surface mesh are determined by the input values for triangle edge length.

Overall, the imported meshes were of poor quality and required several iterations of this remeshing process before a mesh suitable for solid-meshing in Strand was produced. The final remeshed surface mesh that was exported in Strand was auto-remeshed to a maximum triangle edge length of 1.3 mm (equivalent to 1.3 cm on the original model as MIMICS reduced the size of the imported STL meshes – this is possibly a confusion of units by the software). The final remeshed surface meshes exported from MIMICS into Strand were 117,036 triangles for the cranium and 81,012 triangles for the mandible. These were converted within Strand7 (Release 2.3) into solid meshes, comprising 940,455 and 450,563 elements respectively.

The repeated smoothing and reducing iterations within the MIMICS remesher led to inevitable losses of geometry, most notably around the thin sagittal crest, which was ‘smoothed’ from a taller, thin crest with a smoothly convex upper edge to a lower, thicker crest with a rough upper surface. The junction between the facial processes of the premaxillae and the dorsal part of the maxilla was also smoothed out somewhat (Figure 5-32). The extent of the smoothing was not considered sufficient to alter structural properties of the skull models by any substantial margin.

The surface mesh created in Rhino also had a number of problematic vertices, particularly around the upper surface of the dorsal arch of the squamosal, and the junction between the postorbital wall and the upper part of the epipterygoid.



Figure 5-32: 3-D surface mesh of the skull in *Kronosaurus queenslandicus*. A, surface mesh of the cranium produced from Rhino. B., Surface mesh of cranium, remeshed in MIMICS. C, remeshed cranium (B) overlain on original mesh (A): areas in red show where the original geometry has been altered. In particular, the top of the sagittal crest has been lost, and the edge of the dorsal median ridge of the rostrum (marked by the suture between the premaxilla and maxilla) has been smoothed. In (C), the surface mesh of the mandible is shown at reduced opacity; the geometry of the Meckelian canal can be seen.

Discussion

The 3-D solid meshes of the cranium and mandible of *Kronosaurus queenslandicus* (Figure 5-33, Figure 5-34, Figure 5-35) may be the highest resolution models attempted for biological objects using essentially manual CAD techniques – a significant achievement. However, it is important to identify the areas in which this model can be improved in future work.

Firstly, the model is based upon a generic reconstruction of the morphology of an extinct form that is represented by numerous incomplete and distorted fossil specimens. As such, it is necessarily imperfect. Although the 2-D and 3-D reconstructions were generated with the aim of being as objectively accurate as possible, given the nature of the material it is impossible to eliminate subjective input by the researcher from this process: in fact, without that subjective input it would be impossible to create either the 2-D reconstruction or the 3-D model. These should be seen, therefore, not as definitive blueprints of the skull anatomy of *Kronosaurus queenslandicus*, but rather as an idea, or even a hypothesis, of cranial form in this species based upon one person's experience with the relevant fossil material. I have attempted to make the input data and my assumptions as explicit as possible – nevertheless, from a philosophical perspective the reconstructions are as much a result of an artistic process as they are a scientific one, and this should be acknowledged explicitly. Of course, involving art should not – and does not – take away from the scientific value of the work: much of our scientific understanding of morphology is dependent upon the artistic input used in creating reconstructions of fossil anatomy, whether this is done directly by the palaeontologist researching the fossil, or by a professional palaeoartist. The artistic component of the process is here acknowledged and embraced.

That said, there are also problems with the input data used to generate the reconstruction. The morphology preserved by the various specimens that I have used to generate these 2-D and 3-D models is highly variable: the potential sources of that variation are taphonomic, allometric, sexual dimorphism, intra-specific, and inter-specific. Inter-specific variation may indeed be important because not all of the cranial material used here can be confidently assigned to *Kronosaurus queenslandicus*, although it is most likely all *Kronosaurus*: this principally affects the two MCZ

specimens (see Chapter 6). Given the size difference between some of the specimens (e.g. QM F10113 and QM F51291), there is almost certain to be allometric variation: indeed, potential instances of this are noted above. Whether sexual dimorphism applies to this material is as yet unknown, but it is of course highly likely that intra-specific variation does: for example, the width of the anterior rostrum in QM F10113 appears to exceed that of the similarly sized QM F18827 and to be proportionally greater than that of MCZ 1284. However, in generating these models I have assumed that all of the variation is taphonomic: it is probable that a large portion of it is, but of course this source of variation is extremely difficult to account for in generating a model of the original, undistorted anatomy, and inevitably some subjective errors have crept in. However, that assumption – that the variation is all taphonomic – can and should be tested. The development of new tools that can quantitatively account for taphonomic distortion will provide the means to accurately retro-deform each fossil, eliminating a major source of the present subjectivity. No doubt it will be possible in future work to generate a far more accurate model of the cranial anatomy in *Kronosaurus queenslandicus*. In the meantime, the model presented here must be considered a preliminary but workable account: like the lines of average rainfall in a climate map of a continent, however, it likely defines by its creation an entity that never actually existed¹⁵.

As artificial as it may be, the construction of a 3-D model does provide a test of Escher's paradox, i.e. can the shape that is represented in the two dimensional medium exist in three dimensions? For a 3-D model to exist, the geometry must pass the test of 3-D integrity. There were several instances of this during the construction of the 3-D model, involving structures that are poorly preserved in the fossil specimens. The 2-D reconstructions of these were based upon equivocal direct evidence, and yet the restored geometry was found to be three-dimensionally valid: this provides a basic test of the reconstructed morphology. Examples of this included the shape and position of the postorbital wall and fenestra and the quadrate ramus of the pterygoid. In other cases, the reconstructed 2-D geometry needed to be altered to produce an integrated 3-D model; this particularly affected the restored geometry of the posterior dorsal surface of the skull, i.e. the parietal crest and the dorsal arch of

¹⁵ A farming acquaintance, whose property is near the threshold '8 inches' annual rainfall isocurve in western New South Wales, once observed that the only annual total of rainfall he had never seen was 8 inches.

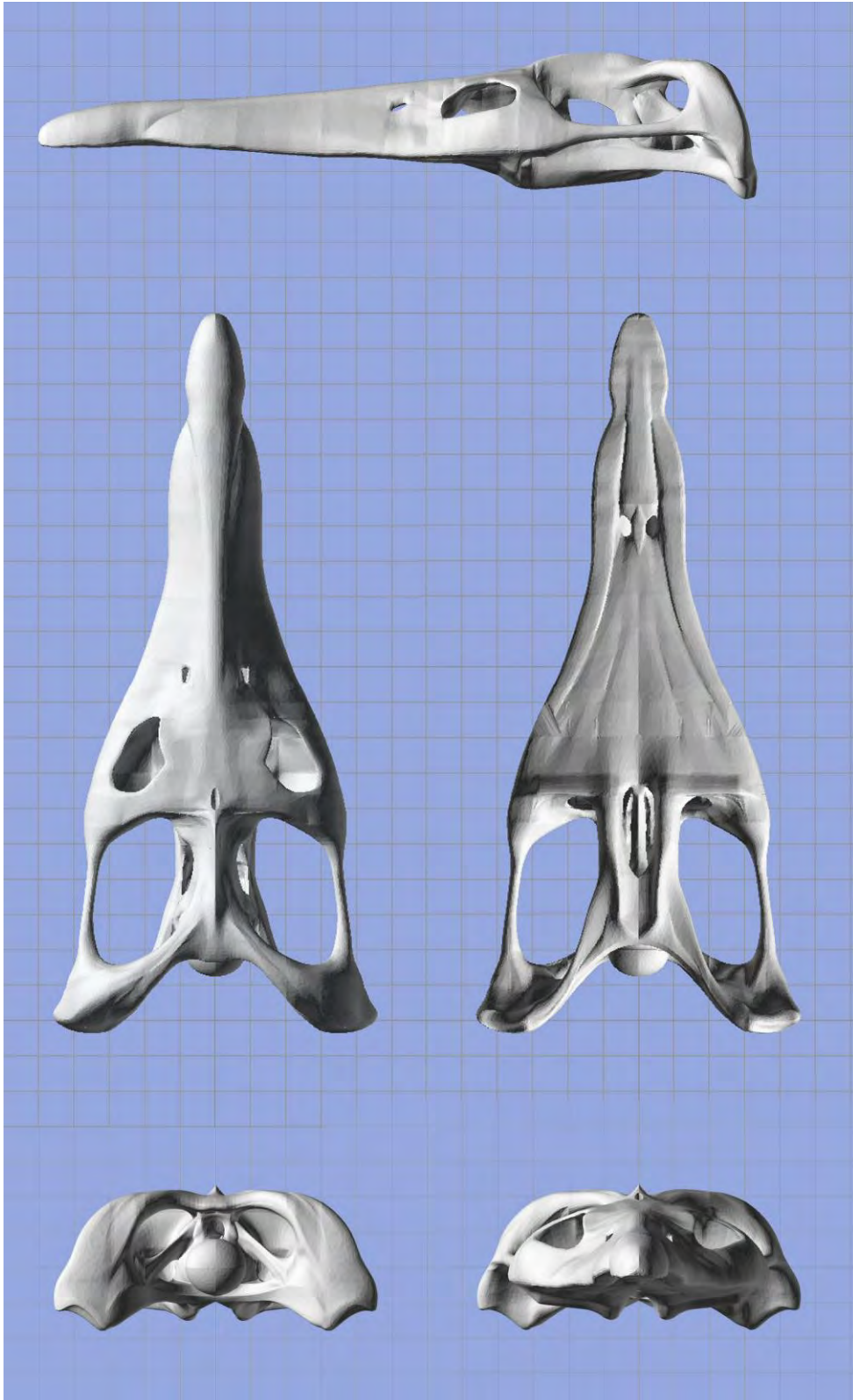


Figure 5-33: The cranium of *Kronosaurus queenslandicus*, shown as a rendered surface mesh produced in Rhino. Clockwise, from top; left lateral, ventral, anterior, posterior, and dorsal views. Grid is 10 cm.

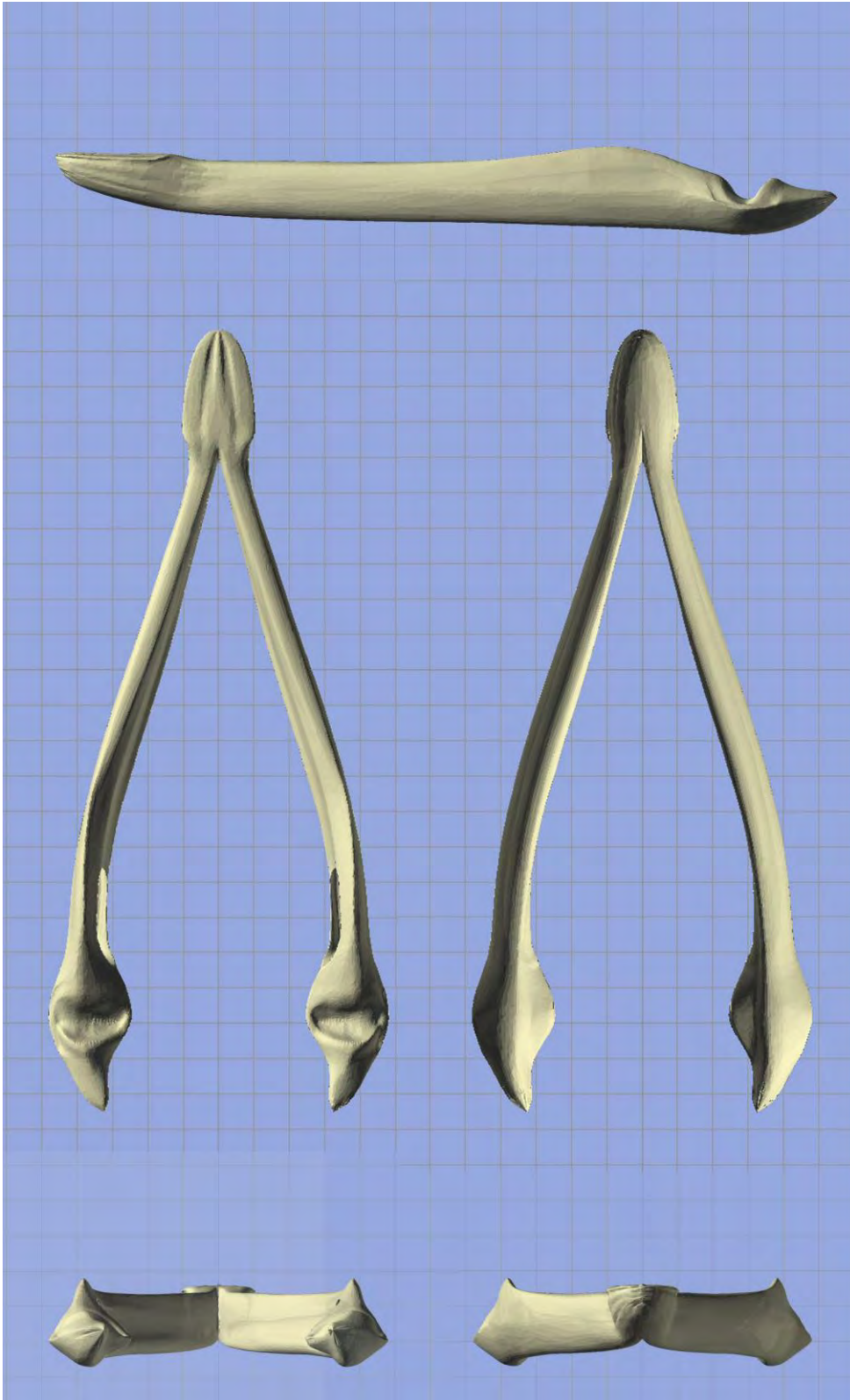


Figure 5-34: The mandible of *Kronosaurus queenslandicus*, shown as a rendered surface mesh produced in Rhino. Clockwise, from top; left lateral, ventral, anterior, posterior, and dorsal views. Grid is 10 cm.

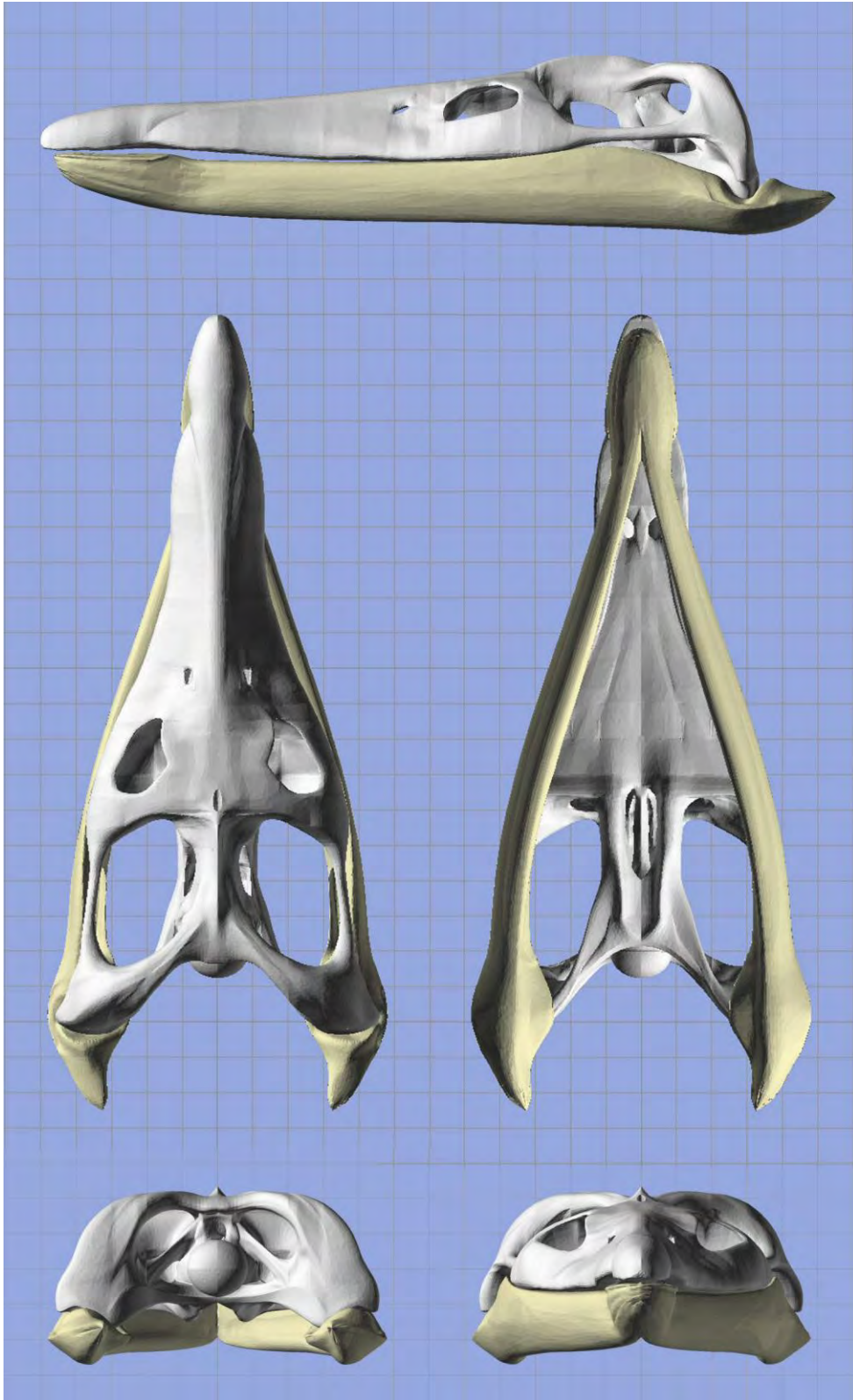


Figure 5-35: The cranium and mandible models from Figure 5-33 and Figure 5-34, shown in articulation.

the squamosal (Figure 5-36). It is likely that 3-D modelling will be especially useful in refining the morphology of the tooth row, when this is included at some future time; an 'Escher' test of the tooth rows included in the 2-D reconstruction (Figure 5-36) might show that, as drawn, the teeth of the upper and lower jaws would be mal-occluded and would prevent the mouth from being closed.

Even though the tooth crowns were not included in the 3-D model, the tooth roots were modelled indirectly as I assumed that the tooth sockets in the upper and lower jaws were solid, i.e. effectively filled by the roots. This raises the question of the mechanical role of the tooth roots and the alveoli within skulls: does the tooth row act as a solid beam of variable density/ material properties (McHenry et al. 2006), or does the geometry of the tooth sockets minimise the mechanical role of teeth that are not directly involved with a bite? This is an interesting question for future research.

Considerably uncertainty surrounds the morphology of the mandible, as a consequence of its poor preservation in most of the relevant specimens. However, an opportunity to improve understanding of the mandible's morphology lies with a QM F18827, which preserves many sizeable fragments of the mandible in articulation with the cranium: the present work did not incorporate data from these. Another specimen, QM F18726, appears to preserve a complete mandible, but no data from this specimen was included here for logistical reasons. Also, my focus has tended to be more on the cranial morphology of the specimens, and it would certainly be possible to extract more thorough anatomical data on the preserved parts of the mandible in QM F2446, QM F2454, and QM F10113 than I have been able to do here.

In practical terms, the creation of geometry from photographic data is useful for general shapes, but can be less satisfactory for specific details. It is possible that input of 3-D data directly from the fossil specimen, as was done here for QM F51291, would lead to greater accuracy in the reconstructed geometry. In particular, 3-D data on the braincase, occiput, and suspensorium from QM F18827, QM F10113, and QM F2446 would be particularly valuable. For the reasons outlined in Section 5.2, the larger specimens may be logistically difficult to CT scan, but other methods of

Form (3-D)

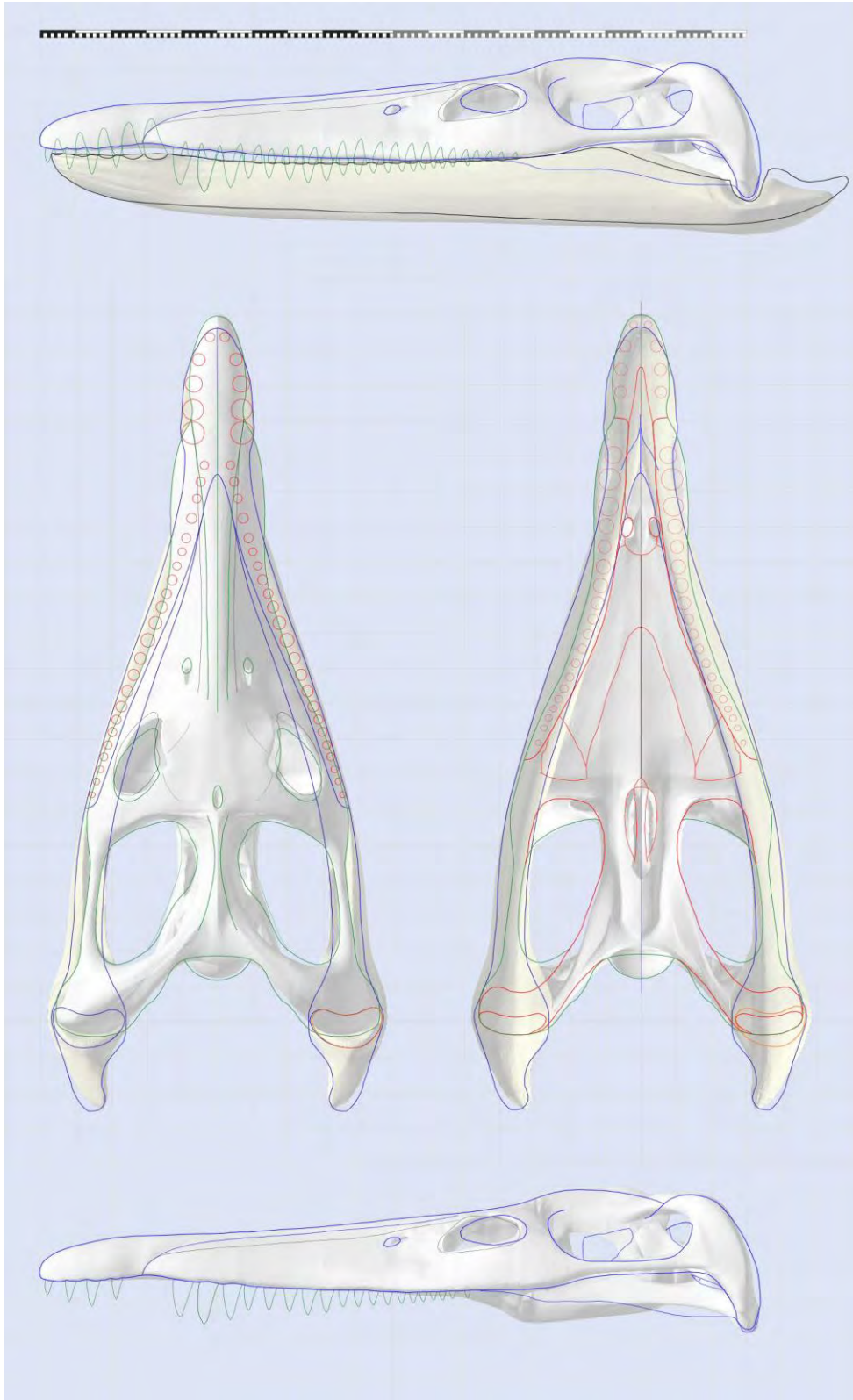


Figure 5-36: Comparison of 2-D and 3-D reconstructions of *Kronosaurus queenslandicus*. The 3-D models of the cranium and mandible (Figure 5-33, Figure 5-35) have been overlain with the 2-D reconstructions from Chapter 4. In various places, the 3-D geometry has been altered to produce a workable 3-D model, notably around the rear of the cranium and mandible. The depth of the mandible has been increased in the 3-D model, while the 2-D model failed also to capture the geometry of the posterior process of the pterygoids.

capturing 3-D geometry, such as 3-D optical scanning, could potentially be applied to these.

The 3-D modelling processes also emphasise some of the problems that result from using photographic data to create geometry. When the 3-D object created from the CT scan of QMF 51291 (Section 5.2) was aligned to the photograph of the fossil in dorsal view, it was impossible to align all parts; even in a single plane, the 3-D object has different planar proportions to the photograph. In the end, I assumed that, in a 35mm photograph, the axis of the image with the shortest side is subject to less optical distortion, and aligned the 3-D object according to width rather than length. The result (Figure 5-37) highlights the distortion that is inherent in photography: of

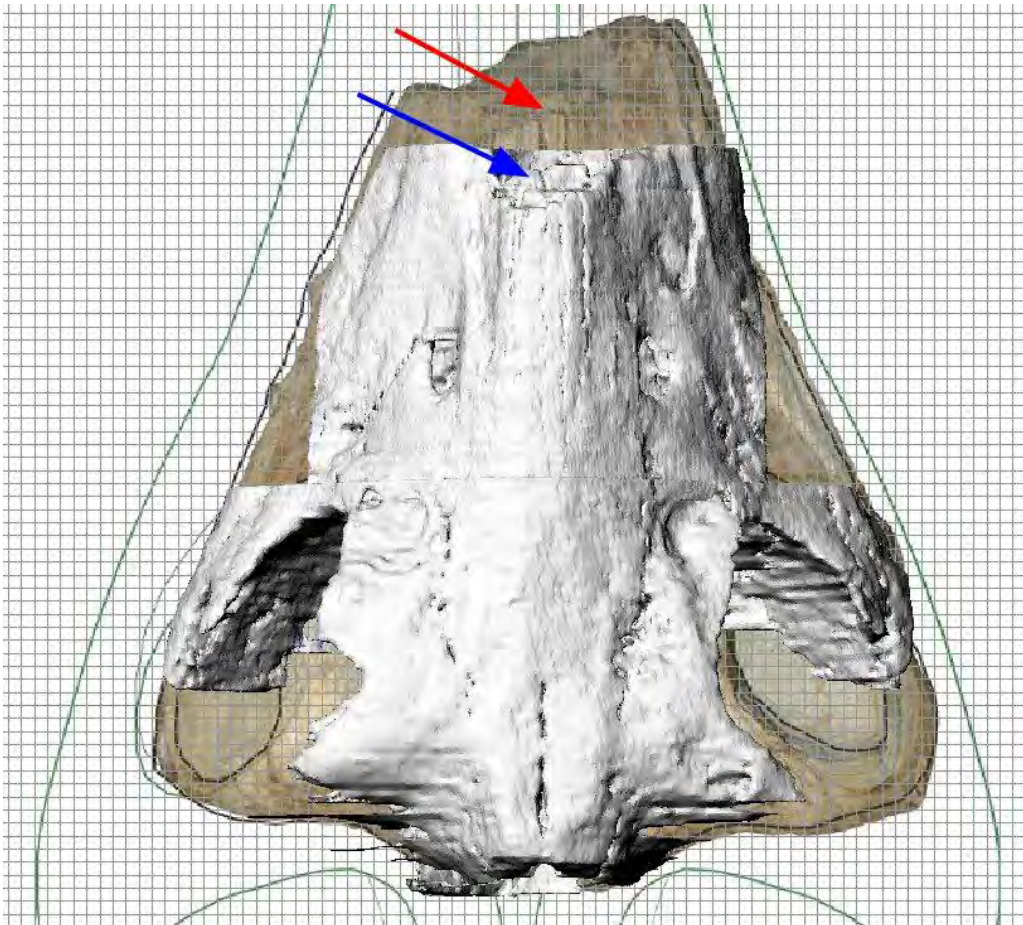


Figure 5-37: 3-D object of fossil bone in QM F51291, overlaid on a bitmap of the photograph of that specimen combined with the 2-D reconstruction in dorsal view. The 3-D object has been aligned with the width of the specimen in the photograph: the antero-dorsal corner of the dorsal median ridge in the photograph (red arrow) is some distance in front of the equivalent point in the 3-D object (blue arrow). Grid = 1 cm.

course, this problem affects the 2-D reconstruction of the skull produced in Chapter 4 because this is entirely based upon photographic data.

The quality of the mesh created in Rhino was poor compared to the meshes that can be generated directly from CT data. In part, this is probably due to the simple fact that CT data is a direct representation of structures that exist in real 3-D space, whilst the CAD-generated geometry is not, and parts of the latter may not exist for the simple reason that such shapes don't exist in Nature – a particular form of Escher's spatial paradox. In particular, the front of the mandibular symphysis and the rear of the retro-articular process had some of the worst geometry in the model, likely a result of the uncertainty surrounding mandibular morphology (see above). Some of the problematic geometry, on the upper surface of the dorsal arch of the squamosal, and at the 'corner' where the epipterygoid joins the postorbital wall, is in hindsight the result of high aspect-ratio polysurfaces, and these could be improved by adjusting the NURBS curves used to create them. In addition, some of the edges of the polysurfaces did not match in the manner specified as being important above (see Methods), particularly in the model of the cranium, because of difficulties in perfectly aligning the control points of adjacent NURBS curves. Rhino does have a set of functions that allow control points to be 'snapped' to each other, but I discovered these only after the skull mesh had been completed. Such are learning curves.

5.4 **Conclusions**

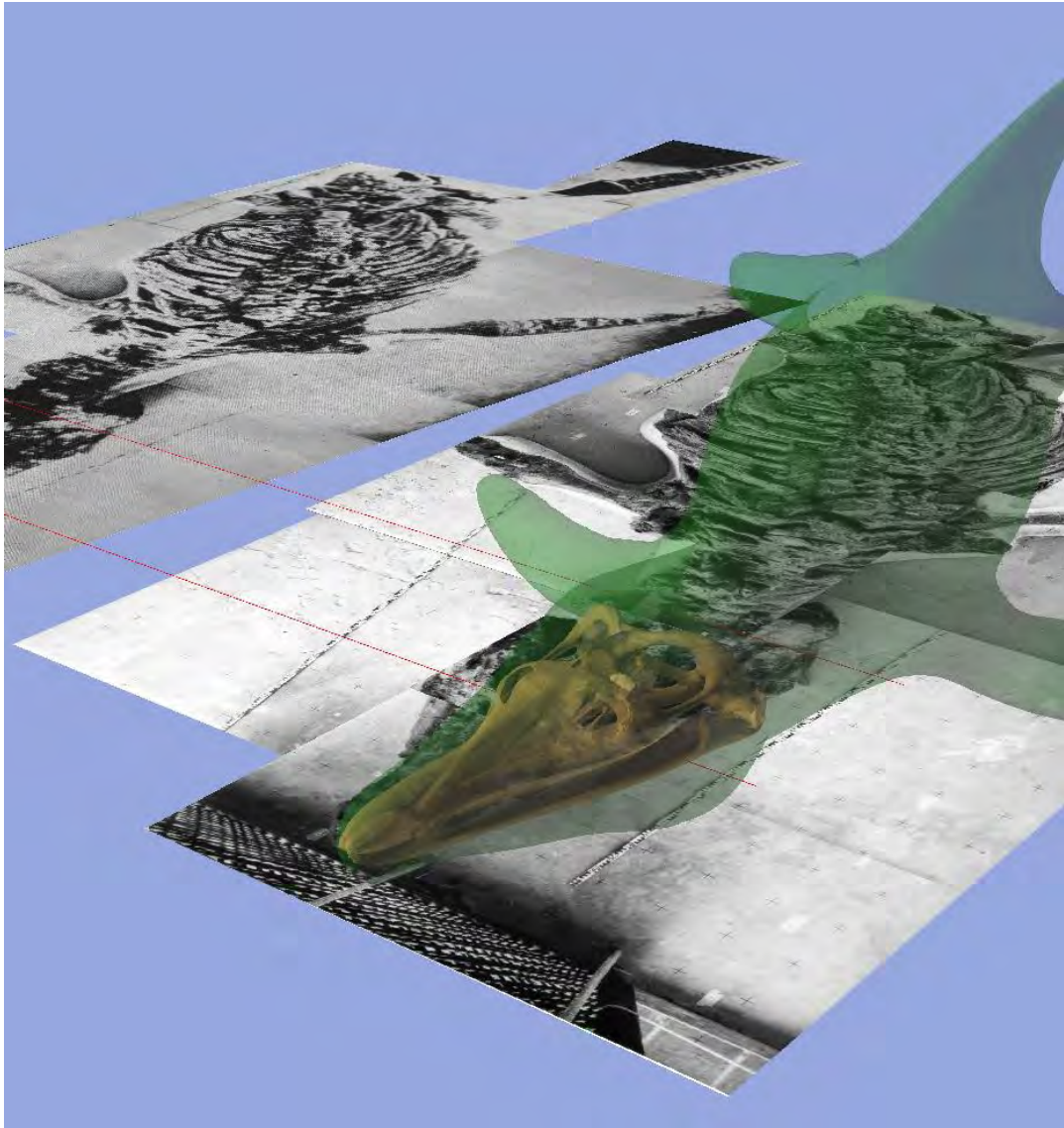
- (1) CT scanning of fossils, even those preserved in dense matrix such as limestone, can reveal details of anatomy in a non-destructive manner. The success of CT depends upon the power available for the X-Ray tubes, the dimensions and mineral composition of the fossil, and the ability of the image processing software to filter artefacts and reveal contrast between fossil bone and matrix. Contrary to expectations, minerals formed from iron salts do not adversely affect the CT scan, but large crystals cause significant artefacts – for fossils preserved in carbonate rocks, secondary calcite crystals are therefore a significant hurdle.
- (2) Imaging of CT data from fossils has much lower contrasts than images of ‘wet’ specimens; automatic masking algorithms do not work and it is usually necessary to mask the data by hand. For this, vector based tools may be preferable to raster based tools.
- (3) 3-D models based on direct scans of specimens can be combined with conventional 2-D reconstructions of fossil morphology to produce 3-D models using CAD techniques. The resulting mesh is suitable for analysis using 3-D engineering techniques, such as FEA (Finite Element Analysis) and Computational Fluid Dynamics (CFD).
- (4) The model produced here is the first 3-D model of the skull in a pliosaur and may be the first high resolution model of a vertebrate skull produced from CAD techniques. As such, it represents a novel approach for reconstructing the 3-D geometry of fossil taxa. The ability to create high resolution 3-D models from species represented only by distorted and/or fragmentary material (i.e. the majority of vertebrae fossils) may prove a useful technique for palaeobiological analysis and communication.

5.5 References

- Andrews, C. W. 1895. On the structure of the skull of *Peloneustes philarcus*, a pliosaur from the Oxford Clay. *Annals and Magazine of Natural History* 16(6):242-256.
- Andrews, C. W. 1911. On the Structure of the Roof of the Skull and of the Mandible of *Peloneustes*, with some remarks on the Plesiosaurian Mandible generally. *Geological Magazine* 8(4):160-164.
- Andrews, C. W. 1913. A descriptive catalogue of the Marine Reptiles of the Oxford Clay, Part II. BM(NH), London.
- Boyd, A. A., and R. Motani. 2008. Three-dimensional re-evaluation of the deformation removal technique based on "jigsaw puzzling". *Palaeontologica Electronica* 11(2):7A:7p.
- Carpenter, K. 1997. Comparative cranial anatomy of two North American Cretaceous plesiosaurs. Pp. 191-216. *In* J. M. Calloway, and E. L. Nicholls, eds. *Ancient Marine Reptiles*. Academic Press.
- Cruikshank, A. R. I. 1994. Cranial anatomy of the Lower Jurassic pliosaur *Rhomaleosaurus megacephalus* (Stutchbury) (Reptilia: Plesiosauria). *Philosophical Transactions of the Royal Society, London B* 343:247-260.
- Daniel, W., and C. McHenry. 2001. Bite force to skull stress correlation: modelling the skull of *Alligator mississippiensis*. Pp. 135-143. *In* G. Grigg, F. Seebacher, and C. Franklin, eds. *Crocodylian biology and evolution*. Surrey Beatty, Chipping Norton.
- Iordansky, N. N. 1973. The skull of the Crocodylia. Pp. 201-262. *In* C. Gans, ed. *Biology of the Reptilia*, vol. 4. Academic Press, New York.
- Jenkins, I., J. J. Thomason, and D. B. Norman. 2002. Primates and engineering principles: applications to craniodental mechanisms in ancient terrestrial predators. *Senckenbergiana Lethaea* 82:223-240.
- Langston, W. J. 1973. The crocodylian skull in historical perspective. Pp. 263-289. *In* C. Gans, ed. *Biology of the Reptilia*, vol. 4. Academic Press, New York.
- McHenry, C. R., P. D. Clausen, W. J. T. Daniel, M. B. Meers, and A. Pendharkar. 2006. The biomechanics of the rostrum in crocodylians: a comparative analysis using finite element modelling. *Anatomical Record*, 288A:827-849.
- McHenry, C. R., S. Wroe, P. D. Clausen, K. Moreno, and E. Cunningham. 2007. Supermodeled sabercat, predatory behavior in *Smilodon fatalis* revealed by high-resolution 3-D computer simulation. *Proceedings of the National Academy of Sciences* 104(41):16010-16015.
- McLellan, F. 2007. Density, CT attenuation, and strength in bovine bone samples. University of Newcastle, Unpublished Hons. Thesis.
- Moreno, K., S. Wroe, P. D. Clausen, C. R. McHenry, D. C. D'Amore, E. J. Rayfield, and E. Cunningham. 2008. Cranial performance in the Komodo dragon (*Varanus komodoensis*) as revealed by high-resolution 3-D finite element analysis. *Journal of Anatomy* 212:736-746.

- Noè, L. F., J. Liston, and M. Evans. 2003. The first relatively complete exoccipital-opisthotic from the braincase of the Callovian pliosaur, *Liopleurodon*. *Geological Magazine* 140(4):479.
- Plotnick, R. E., and T. K. Baumiller. 2000. Invention by Evolution: Functional Analysis in Paleobiology. *Paleobiology* 26(4):305-323.
- Preuschoft, H., and U. Witzel. 2005. Functional Shape of the Skull in Vertebrates: Which Forces Determine Skull Morphology in Lower Primates and Ancestral Synapsids? *Anatomical Record* 283A:402-413.
- Rayfield, E. J. 2005. Aspects of comparative cranial mechanics in the theropod dinosaurs *Coelophysis*, *Allosaurus* and *Tyrannosaurus*. *Zoological Journal of the Linnean Society* 144:309-316.
- Rayfield, E. J. 2007. Finite Element Analysis and Understanding the Biomechanics and Evolution of Living and Fossil Organisms. *Annual Review of Earth and Planetary Sciences* 35:541-576.
- Rayfield, E. J., A. C. Milner, V. B. Xuan, and P. G. Young. 2007. Functional Morphology of Spinosaur 'Crocodile-Mimic' Dinosaurs. *Journal of Vertebrate Paleontology* 27(4):892-901.
- Rayfield, E. J., D. B. Norman, C. C. Horner, J. R. Horner, P. M. Smith, J. J. Thomason, and P. Upchurch. 2001. Cranial design and function in a large theropod dinosaur. *Nature* 409(6823):1033-1037.
- Snively, E., and A. Russell. 2002. The tyrannosaurid metatarsus: bone strain and inferred ligament function. *Senckenbergiana Lethaea* 82:35-42.
- White, T. 1935. On the skull of *Kronosaurus queenslandicus* Longman. *Boston Soc. Natural History, Occ. Papers* 8:219-228.
- Witzel, U., and H. Preuschoft. 2005. Finite-Element Model Construction for the Virtual Synthesis of the Skulls in Vertebrates: Case Study of *Diplodocus*. *Anatomical Record* 283A:391-401.
- Wroe, S. 2007. High-resolution 3-D computer simulation of feeding behaviour in marsupial and placental lions. *Journal of Zoology* 274:332-339.
- Wroe, S., P. Clausen, C. McHenry, K. Moreno, and E. Cunningham. 2007a. Computer simulation of feeding behaviour in the thylacine and dingo: a novel test for convergence and niche overlap. *Proceedings of the Royal Society Series B* 274:2819-2828.
- Wroe, S., K. Moreno, P. Clausen, C. McHenry, and D. Curnoe. 2007b. High-resolution computer simulation of hominid cranial mechanics. *The Anatomical Record* 290A:1248-1255.

6. Size



Modelling body size in large pliosaurs: a 3D model of a *Kronosaurus queenslandicus* skull has been aligned with a life reconstruction of a pliosaurid. The models have been scaled to high resolution photographs of *Kronosaurus boyacensis* provided by Oliver Hampe, and can then be used to provide estimates of skull and body volume in that species. The image in the background is taken from a figure (scanned at lower resolution) in Hampe (1992).

“You’re gonna need a bigger boat”.

Roy Scheider, *Jaws*, 1975.

6.1 **Rumours, myths, and measurements: previous estimates of body size in large pliosaurs**

The scientific study of large pliosaurs dates to the mid 18th Century and the discovery of very large (total length of crown and root exceeding 30 cms) trihedral teeth that were referred to *Pliosaurus* by Owen (1840). Further finds indicated the presence of very large marine reptiles in the Middle and Late Jurassic of England (Phillips 1871), whose carnivorous nature was inferred from the morphology of the teeth. In 1895 the remains of a large plesiosaurian were reported from the Jurassic of Wyoming and nominated as the holotype of a new species, *Cimoliosaurus rex* (Knight 1895): the species was subsequently referred to its own genus *Megalneusaurus*, and was characterised as “the largest known example of the order Sauropterygia” (Knight 1898: 378). Rediscovery of the type locality indicates *Megalneusaurus* to have been part of the Oxfordian Sundance fauna (Wahl et al. 2007).

Longman (1924) named *Kronosaurus queenslandicus* on the basis of a jaw fragment from the Albian (Early Cretaceous) Toolebuc Formation, near the town of Hughenden in central-west Queensland; subsequent finds of propodial heads (Longman 1930) from the same general area indicated that *Kronosaurus* was a very large animal, exceeding Knight’s *Megalneusaurus* in size on the basis of propodial proportions, although Longman declined to provide an estimate of absolute body size. The overall body proportions of *K. queenslandicus* were reconstructed with reference to *Peloneustes* (Longman 1932).

Longman’s claim of extreme body size for *Kronosaurus* was confirmed soon after, when a Harvard Museum of Comparative Zoology (MCZ) expedition lead by W. Schevill collected two specimens of *Kronosaurus* from the Aptian Doncaster Formation north of Richmond (which is approximately 110 km west of Hughenden). The specimens – a portion of snout and anterior jaw (MCZ 1284), and the articulated cranial and post-cranial remains of a large individual (MCZ 1285) were collected and shipped to Harvard in 1931-32; White (1935) described the skull material and

reconstructed the length of the skull in MCZ 1285 at 3.9 m. Additional material was collected by J.E. Young from the Toolebuc Formation near Hughenden and brought to the Queensland Museum (QM) in 1935: Longman mentioned these specimens (including QM F2446 and QM F2454) as further evidence of large size in *Kronosaurus* (Longman 1935).

Tarlo (1957) described the discovery of a large pliosaur from the Kimmeridge Clay (Kimmeridgian – Late Jurassic) of Stretham in Cambridgeshire, which he referred to *Pliosaurus macromerus* Phillips 1871. Soon after, the Harvard Museum completed a mounted reconstruction of MCZ 1285, which was described by Romer and Lewis (1959): with a restored total length (TL) of 12.8 metres, the ‘Harvard *Kronosaurus*’ became the benchmark for large pliosaur size. Tarlo (1959) provided additional information on the Stretham specimen, including a humerus and femur for which the lengths were given as 840 mm (reconstructed) and 960 mm (measured) respectively. In addition, Tarlo claimed that the specimen was distinct from *Pliosaurus* and referred *P. macromerus* to a new genus, *Stretosaurus* (Tarlo 1959). Tarlo also noted the mandible of another Kimmeridgian pliosaur (OUM J.10454; from Cumnor: hence referred to as the ‘Cumnor mandible’) as 3 m long and interpreted it thus; “Without doubt it belongs to the largest Pliosaur ever recorded, somewhat exceeding the size of the Cretaceous *Kronosaurus*” (Tarlo 1959: 51), but did not attempt to estimate body size. He considered the Cumnor mandible to belong to *Stretosaurus macromerus*.

Another find of a large pliosaur was reported by Newman and Tarlo (1967): the specimen, from Stewartby in Bedfordshire, was apparently donated to the Natural History Museum (NHM), although Newman and Tarlo provided no details of catalogue numbers, stratigraphy, or even taxonomy. The brick pits at Stewartby are listed as producing fossils of *Cryptocleidus* (Forrest 2008), which would suggest that they may be part of the Callovian Oxford Clay (Brown 1981). Although incomplete, the Stewartby pliosaurs preserves the hindquarters (as well as a fragment of snout): Newman and Tarlo reconstructed the hind limb span at 21 feet (6.4 m), and the overall length as 36 feet (10.97 m). In the same paper, they produced a reconstruction of a large pliosaur of unspecified species (Newman and Tarlo 1967), although Tarlo (who later published as Halstead) seemed to imply that the

reconstruction was partly based upon the Stretham specimen (which he also sunk into *Liopleurodon* – Halstead 1989).

Molnar (1991) compared QM F2446, collected by Young from the Toolebuc in 1935, with the mounted Harvard specimen. He stated that the QM specimen may represent a larger individual, but that the MCZ specimen may be a different species. He also noted that *Stretosaurus* was larger.

McHenry et al. 1996¹ reidentified an isolated vertebra (PETMG R272 – previously identified as from a sauropod dinosaur) from the Oxford Clay near Peterborough as a pliosaur cervical vertebra: by comparison with the Harvard *Kronosaurus* mount, they estimated the length at between 15-18 m. However, the assumption of accuracy in the Harvard mount (see below), and the identity of the Peterborough vertebra, have been questioned (A. Cruickshank, pers. comm.): the vertebra may well belong to a sauropod after all, although consensus has not been reached on this matter (D. Naish, pers. comm.).

From the mid 1990s popular accounts of pliosaurs started to give the maximum length of *Liopleurodon ferox* from the Oxford Clay as 25 m and, by analogy with the largest extant balaeopterid whales, a body mass of 150 tonnes (Ellis 2003, Martill and Naish 2000). Buchy et al. (2003) reported the remains of a large pliosaur from the Kimmeridgian of Mexico, and by comparison of vertebral dimensions with a mounted specimen of *L. ferox* (at the Universität Tübingen) estimated a total length of 15 metres: they further claimed the Mexican material represents a juvenile, on the criterion of lack of fusion of neural arches to the vertebral centra (Brown 1981).

Recent finds from a Kimmeridgian marine reptile locality at Svalbard, in the Norwegian Arctic, include the remains of very pliosaurs (P. Druckenmiller, pers. comm.) and have renewed public speculation of the upper limits of body size in pliosaurs: although there are as yet no published accounts in the scientific literature, initial reports appear to indicate an animal at least as large as *Megalneusaurus rex*. A recent review of pliosaur systematics (Smith and Dyke 2008) states a maximum size of 17 m for the Plesiosauria, although only one of the sources cited for this figure

¹ This was presented to the 40th Annual meeting of the Palaeontological Association: McHenry, Martill, Noè, and Cruickshank; *Just when you thought it was safe to go back into the water: the biggest pliosaur yet.*

(Buchy et al. 2003) actually provide an estimate of absolute body size, and that is 15 m.

Measurements of body size

For any organism, body mass is fundamentally linked to its biomechanical, physiological, and ecological characteristics (Schmidt-Nielsen 1975) in a way that other measurements of body size, such as length, are not. Body mass is therefore regarded as an important ecological variable (Wroe et al. 2004), although it is also subject to both high levels of variation between individuals (and even within an individual's own adult life-span), and measurement error due to the logistical challenges of measuring mass in intact specimens (Wroe et al. 2003). Inferring body mass in specimens represented only by skeletal remains is especially problematic.

Total length can be measured more easily on live and museum specimens, and can even be measured in fossils given excellent preservation, and various workers have compiled datasets that allow the predication of body mass from total length (Farlow et al. 2005, Greer 1974, Hurlburt et al. 2003). Body length has the additional advantage of being less prone to fluctuation for individuals, and where studies focus on animals with similar overall body shape total length may be a superior metric of body size for many purposes. Between animals of different body shape it is less suitable and where used as a primary measurement the data should be converted to body mass before making quantitative comparisons: this will necessarily involve error, which should be quantified (Meers 2002).

For most reptiles, however, a significant proportion of the total length is in the tail, but only the proximal tail carries any bulk and so measurable variation in tail length – which can occur between related species, between individuals of the same or different sex, or even within an individual's life-time if the tail is damaged – may not necessarily involve significant changes in body mass. Conversely, a model that predicts body mass on the basis of total length will exaggerate differences in tail length because of the cubic relationship between length and volume. These problems can be avoided if snout-vent length is used as a primary measure of size: variation in tail length does not affect this measurement, which encompasses the part of the body that carries most of the bulk. Snout-vent length can also be easier to measure, as it does not require the tail to be held straight (this can be a logistically

difficult in the field) or even present (in the case of museum specimens and/or fossils), and is a standard measurement of body size in herpetology (Tucker et al. 1996, Webb and Messel 1978). As with measurements of total length, quantitative analyses that convert snout-vent length to body mass should indicate the range of statistical error (Webb and Messel 1978).

Estimating body size from incomplete remains

With fossils, complete specimens of large species are extremely rare, and estimates of body size often involve comparing measurements from partial skeletons with the corresponding segments of the few relevant specimens that are complete enough to indicate body size. For pliosaurs, parts that are common as fragmentary fossils are teeth, skulls, vertebrae, and limb propodials. Each of these presents advantages and problems as a basis for inferring body size.

Intact teeth are reasonably common in the fossil record: as reptiles replace their teeth continuously, one animal may produce a large number of teeth over its life-time. The structural and chemical differences between teeth and bone can also lead to good quality preservation of teeth in sedimentary environments where bone preservation is poor (pers. obs). Set against this, tooth size is a difficult predictor of body size because, in large pliosaurs, tooth size varies markedly along the tooth row, meaning that the tooth must be located in its correct anatomical position before it can be used to infer body size. However, in reptiles with pseudo-heterodont dentition, tooth form does not vary within the tooth row sufficiently to allow the position of the tooth to be precisely inferred from its morphology as is the case with mammals (although in large pliosaurs posterior teeth can often be distinguished from anterior teeth). That reptile jaws usually contain several teeth in replacement phase is an additional complication. Assumptions that isolated teeth represent the smallest in the jaw will bias estimates of body size upwards, and vice versa.

Although not as common as palaeontologists might wish, nearly intact fossilised skulls² are more common than fossils of the entire animal and many palaeoecological studies have used skull dimensions as a robust predictor of body size [see, for

² i.e. sufficiently well preserved to derive at least one of the standard cranial measurements – see Methods.

example, Van Valkenburgh (1990) for carnivoran mammals; Hurlburt et al. (2003) and Farlow et al. (2005) for crocodylians; Myers (2001) for marsupials]. Skull length can be a robust predictor of body size for animals with similar skull shapes: however, rostral proportions are commonly labile and influenced by a species' ecology, and so measurements of skull length are problematic when applied to species with differing rostral proportions [e.g. felids vs. canids (Wroe et al. 2005), or different species of *Crocodylus* (Farlow et al. 2005)]. Within carnivoran families certain species can be relatively small headed whilst others have relatively large heads (e.g. feline vs. pantherine cats – Wroe et al. 2005), further complicating prediction of body size from cranial dimensions. Some workers consider skull width to be a more consistent predictor of body size amongst related species (M. Meers, pers. comm.), although skull width can also vary with ecologically significant factors, in particular bite force (Wroe et al. 2005). Overall skull proportions can also vary considerably with ontogeny: this is well documented in the early growth from hatchling/infant through juvenile to young adult stages in all amniotes (Thompson 1992), but in addition some reptiles display a further growth phase during adulthood in which the skull becomes very robust – i.e. width, height and bone thickness increase much faster than skull length – a growth pattern that has been termed 'macrocephalic' (Cann 1998, Georges et al. 2002) and which has been observed in crocodylians (Webb and Messel 1978; pers. obs.) and chelid turtles (Cann 1998). This growth pattern may be linked to late ontogeny and an increase in overall body mass for a small increase in length, but may not affect all adults within a population (Georges et al. 2002, Legler 1981). Cranial metrics that are not directly linked to functional aspects of feeding ecology, but instead to features of the Central Nervous System (CNS) have been used successfully for some groups: CNS proportions might be expected, *a priori*, to scale with body size, and have been used to infer palaeobiology in fossil taxa (Griffin 1995). Wroe et al. (2003) used endocranial volume to predict body size in the fossil marsupial *Thylacoleo*. Notwithstanding these potential complications, for species, or groups of species, that have consistent head proportions, skull dimensions can be useful predictors of body size (Farlow et al. 2005, Hurlburt et al. 2003).

The axial skeleton has an obvious and direct connection with body size, and isolated vertebrae, or series of vertebrae, are a tempting subject for estimates of body size. Many of the accounts of fragmentary pliosaurs cited above list vertebral

measurements where possible. Motani et al. (1996) have shown that in ichthyosaurs, variation in total length is achieved, not by changing the number of segments, but through the modification of each segment's length. This implies that the ratio of vertebral length to diameter should provide a useful indicator of body size in species where the relationship between vertebral and overall dimensions is well understood.

However, one of the problems that makes isolated teeth a difficult predictor of body size also applies to vertebrae; their size changes along the axial column, and whilst the gross morphology of a vertebra can be used to locate it to broad regions of the column (i.e. neck, trunk, tail), plesiosaur vertebrae are far less variable along the column than are e.g. those of terrestrial mammals: locating an isolated plesiosaur vertebra precisely is difficult to achieve on the basis of morphological features.

Because the vertebrae do vary in size throughout the column, however, inaccuracies in locating the vertebrae will lead to inaccuracies in estimates of body size. Brown (1981) showed that the ratio of central length to diameter (termed the Vertebral Length Index, or VLI) in the plesiosauroid *Cryptocleidus* displayed a consistent pattern that could be used to locate isolated vertebrae more precisely than is possible on the basis of qualitative morphological criteria alone. However, he also demonstrated that the pattern of VLI along the column changes with ontogeny. VLI has been a useful concept for the study of isolated vertebrae in some groups of plesiosaurians, such as the Elasmosauridae of the North American Cretaceous, thanks largely to the study of numerous well preserved and nearly complete specimens for which vertebral dimensions have been documented and can serve as a reference dataset (Welles 1943, 1952). As yet, a comparable dataset that be used to study isolated vertebrae in large pliosaurs is lacking.

In terrestrial mammals, fundamental biomechanical principals predict that limb proportions will scale allometrically with body size, but minimal proximal limb circumference (MPLC) has been used to estimate body size in fossil and living species of mammals (Anderson et al. 1985) and reptiles (Erickson et al. 2004). For aquatic species, the situation is more complex: Farlow et al. (2005) found femur length to be a robust predictor of body size in crocodylians, although Meers noted that humeral features predicted to be of biomechanical importance (and to thus scale allometrically) actually scaled isometrically in crocodylians (Meers 2002). O'Keefe and

Carrano (2005) showed that paddle size scales with negative allometry for plesiosaurs, a feature noted by Kear (2007) for leptocleidid plesiosaurs. For incomplete fossils, however, propodial dimensions are more relevant than overall limb proportions; plesiosaur propodials are robust elements and are often preserved, and would thus make useful indicators of body size if the relationship between propodial dimensions and body size could be documented.

Prediction of body size in large pliosaurs

Despite the scientific and popular interest in the question of size in pliosaurs, quantitative descriptions of body proportions in complete or nearly complete specimens are rare and the lack of an anatomical ‘template’ with which to compare less complete material has hindered a methodical approach. Historically, absolute estimates of size were avoided until the Harvard mount of *Kronosaurus queenslandicus* provided a value for size in this taxon: since 1959 many of the estimates for size in other large specimens, of various species, have been made by comparison with this mount. However, the accuracy of the Harvard reconstruction has been called into question (e.g. Carpenter 1996), potentially affecting those estimates.

Given the importance of body size to discussions of a species’ palaeoecology, the present study required an estimate of body size in *Kronosaurus queenslandicus*. To this end the body proportions of two specimens, referred to *K. queenslandicus* and preserving significant postcranial material (MCZ 1285, QM F10113), were documented. A further three specimens of Cretaceous pliosaur that preserve most of the axial column in articulation were included to provide a comparative dataset, with the aim of generating body size estimates from less complete material. This data can also be used, albeit with caution, to provide estimates for some Jurassic pliosaur material.

6.2 Material and Methods

Cretaceous material

Five specimens of Cretaceous large pliosaur preserve significant cranial and postcranial material; USNM 4989 (*Brachauchenius lucasi*), QM F10113 and MCZ 1285

(*Kronosaurus queenslandicus*), the holotype of *Kronosaurus boyacensis* (Hampe 1992), and a new specimen of *Brachauchenius* from Villa de Leyva, Colombia (*Brachauchenius* sp., Hampe 2005).

Measurement data was generated by direct examination (QM F10113, MCZ 1285, USNM 4989) and from published descriptions [Williston (1903, 1907) for USNM 4989; Romer and Lewis (1959) for MCZ 1285; Hampe (1992) and Hampe and Leimkuhler (1996) for *Kronosaurus boyacensis*; Hampe (2005) for *Brachauchenius* sp. Villa de Leyva]. A combination of direct measurement and photographic techniques (see below) were used to document dimensions of axial elements.

For skull material, four principal measurements were used, allowing specimens of differing preservation to be documented; Basal Skull Length (BSL – also known as basal condylar length – Wroe et al. 2005), Dorsal Cranial Length (DCL – Tucker et al. 1996), Jaw–Quadrate/Articular distance (JQA – Erickson et al. 2003), Mandibular Length (ML). Of these, BSL, DCL, and JQA are planar, while ML is taken along the longitudinal axis of the mandibular ramus.

Estimates of body mass require a model of the relationship between length and volume in the taxa under study; previous workers have used scale models of life reconstructions to achieve this for extinct species (Alexander, 1989). For this method to produce useful results, the model chosen must be as realistic as possible.

Numerous scale models of pliosaurs are available commercially: for this study, I used the British Museum (Natural History) model, labelled ‘A PLIOSAUR (*Liopleurodon*)’, and made by Invicta Plastics Ltd (hereafter, the ‘BMNH model’ – see below and Figure 6-1). Although it is based upon the body proportions of a large pliosaurid, and the five specimens that form the primary focus of this study are brachaucheniiids, the BMNH model is notable for its excellent quality, presumably achieved in part through consultation with scientific staff at the Natural History Museum in London (A. Cruickshank, pers. comm.). Scale models of brachaucheniiids are commercially available, specifically of *Kronosaurus* – however, these are obviously influenced by the Harvard mount of MCZ 1285 which, as detailed below, is of doubtful accuracy. The BMNH model is here considered, based upon preliminary examination of the body proportions in brachaucheniiids, to be a more realistic reconstruction.

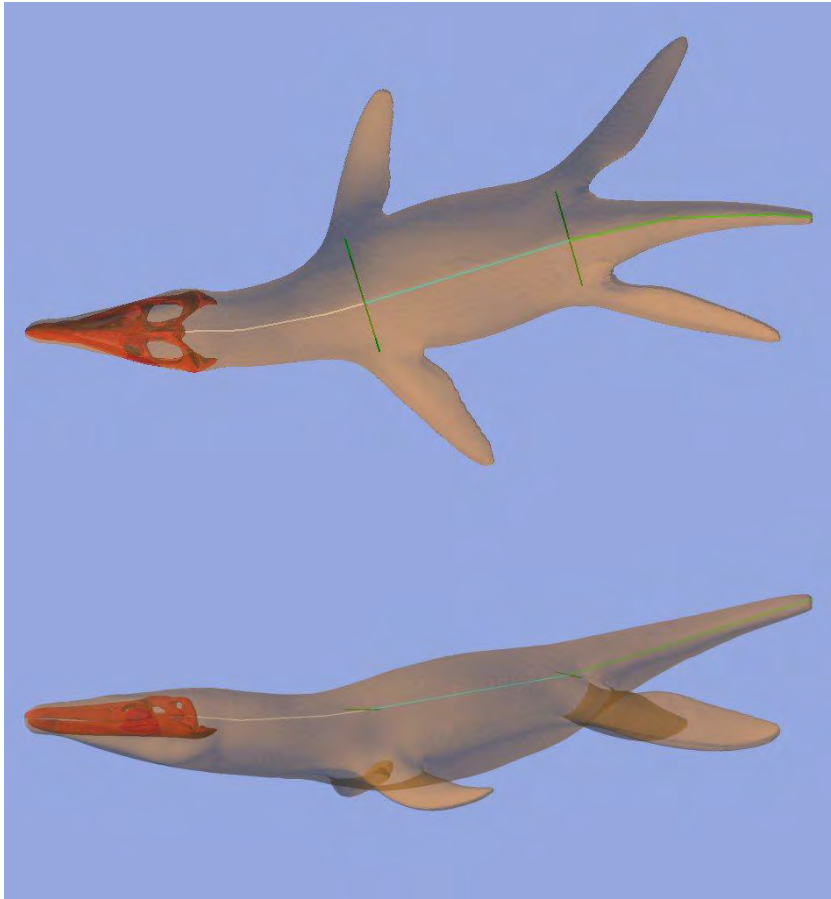


Figure 6-1: BMNH model of a pliosaur (Invecta Plastics Ltd) in (top) dorsal and (bottom) lateral view. The model has been imaged from CT data in Rhino (v.4) and is displaced at reduced opacity. The 3D skull model of *Kronosaurus queenslandicus* (Chapter 5) has been scaled to fit the sculpted head region of the BMNH model and is overlain on the model image. Beams representing the neck, torso, and tail have been aligned to the approximate geometry of the axial column. Junctions between neck, torso, and tail have been determined through placement of the shoulder and hip joints: these are identified in the dorsal view (dark green transverse lines) – see text.

Comparison between skeletal material and life reconstruction models requires reliable reference points that can be accurately determined for each. For this study, total length cannot be used because none of the five brachaucheniid specimens preserve tails. As discussed above, snout-vent length does not require the preservation or mention of a tail, but this measurement is based in part upon soft-tissue anatomy and cannot be directly applied to fossils. Hurlburt et al. (2003) used the position of the ischium as a proxy for vent position in crocodylians, facilitating the comparison of snout-vent data from live specimens with a skeletal-based equivalent in fossils. Four of the five brachucheniid specimens preserve the pelvic girdle; however, to allow comparison with the features that can be observed on the BMNH model, the

position of the hip joint (acetabulum) was used as the relevant pelvic measurement, as this could be inferred with a high degree of confidence from the position of the hind limbs in the BMNH model. In articulated specimens, the position of the hip joint can be readily identified from the position of the femoral head when the latter is preserved – on the basis of QM F10113 and the holotype of *Kronosaurus boyacensis*, the hip joint was taken as being in line with the joint between first and second sacral vertebrae, allowing an estimate of snout–hip distance to be made for specimens where the position of the femoral head could not be determined directly. For all of the brachaucheniid material included in this study, estimates of body size involved scaling the measured volume of the BMNH model by the third power of the ratio of snout–hip length in the specimen to snout–hip length of the model (see below).

To allow estimates of body proportions, measurement data was used to estimate the size of four regional segments in each specimen; head, neck, torso, and tail. The junction of head and neck was defined as the position of the atlanto-occipital joint, and that of torso and tail by the position of the hips as outlined above. Similarly, the junction of neck and torso was defined as the position of the shoulder joint (glenoid), identified in both QM 10113 and the holotype of *K. boyacensis* as corresponding with the joint between second and third pectoral vertebrae (see below): this permitted the shoulder joint's position to be identified on the other specimens.

Measurements of vertebral centra comprised length, width, and height, as far as logistically possible given preservation. However, these do not include the distance of the intervertebral joints, which is an important component of axial column length. Measurements from USNM 4989, which preserves most vertebrae in articulation, were used as a basis for inferring intervertebral joint size from vertebral dimensions alone.

The data for the five brachaucheniid specimens formed a basis for body size estimates of additional, less complete brachaucheniid specimens, in particular the specimens of *Kronosaurus queenslandicus* that preserve cranial material (Chapter 3).

Jurassic material

Although more numerous and widespread, Middle and Late Jurassic specimens of large pliosaurs are typically less complete than the five brachaucheniid specimens listed above. As yet, measurements of snout–hip length based on articulated specimens are not available. In contrast to the preservation of several rhomaleosaurid pliosaurs from the Early Jurassic, and the five brachaucheniid pliosaurs from the Cretaceous, there may not be any specimens of Middle – Late Jurassic pliosaurids from which such measurements could be taken. Several specimens of Callovian pliosaurids, in particular a NMH specimen of *Peloneustes philarchus* (Andrews 1910b) and an unnumbered specimen of *Liopleurodon ferox* on display at the Universität Tübingen Museum (Noè 2001) preserve complete or nearly complete axial columns, but I do not have quantitative data on body proportions in these and I am not aware of any published records.

Given the uncertainties surrounding the postcranial dimensions of Jurassic pliosaur material, detailed estimates of body size were confined to specimens preserving at least one of the four metrics of skull size listed above. The specimens (and sources) were; *Liopleurodon ferox* NHM R2680 (Andrews 1913); *Pliosaurus brachyspondylus* BRSMG Cc332 ('Westbury #2' skull, direct measurement); *Pliosaurus macromerus* NHM R39362 (photo. measurement); *P. macromerus* OUM J. 10454 (Tarlo 1959, Noè et al. 2004); *Pliosaurus portentificus* SEKC K1, (Noè et al. 2004). These were compared with two models of body segment proportions in Jurassic pliosaurids – the BMNH model, and a reconstruction by Newman and Tarlo (1967) – to provide a range of estimates of snout-hip lengths for these taxa. Body mass was estimated by comparing snout–hip length estimates with data from the BMNH model as described above.

Several less complete specimens, which have been the basis for discussion of the largest pliosaurid taxa, were compared with respective sections of the brachaucheniid material to provide some (very cautious) estimates of possible body size in these specimens. However, these estimates are subject to high degrees of uncertainty, and should be taken as indicative – they are provided only to help provide a context for some of the previous speculation of body size in the very largest pliosaurs.

Comparative models of pliosaurid body proportions

BMNH model

A three-dimensional computer model of this scale life-model was generated from CT data using protocols described in Chapter 4. The computer model was imported (via STL format) into a CAD package (Rhino v4), which allowed a precise estimate of volume (Table 6-1). A 3-D scaled copy of *Kronosaurus queenslandicus* skull model produced in Chapter 5 was fitted, as accurately as possible, to the external features of the head visible in the BMNH model (Figure 6-1), allowing an estimate of skull dimensions in the BMNH model. The junction between head and neck was taken as the posterior surface of the 3-D skull model's occipital condyle. The position of the neck-torso and torso-tail junctions were delineated by lines joining the estimated positions of the shoulder and hip joints respectively. Beams following the estimated line of the axial column between each junction point (Figure 6-1) allowed head, neck, torso, and tail length to be measured directly in the CAD software (Table 6-1).

Newman and Tarlo 'Stretosaurus' reconstruction

This reconstruction, apparently based upon the Stewartby and Stretham specimens (see above), was published in Newman and Tarlo (1967), although the artist is not credited (Figure 6-2). From vertebral counts of the different body segments and general proportions of the skull it undoubtedly represents a large pliosaurid, perhaps 'Stretosaurus' (*Pliosaurus macromeris*). It is referred to herein as the 'Newman and Tarlo Stretosaurus' reconstruction, or the 'Stretosaurus' reconstruction. The total length of the reconstructed pliosaur was given as '36 feet' (10.97 metres), identical to

	head	neck	torso	snout-hip	tail	TL	volume (litres)
BMNH model	42.4	48.2	57.5	148.1	68.0	216.0	0.094387
Newman & Tarlo 'Stretosaurus'	2,396	1,891	2,642	6,929	3,417	10,346	9,672

Table 6-1: Measurements of body proportions from the BMNH model (Figure 6-1) and the 2D reconstruction of a large pliosaurid (Newman & Tarlo 'Stretosaurus', 1967 – Figure 6-2). Volume in the Newman & Tarlo 'Stretosaurus' reconstruction is calculated by scaling the BMNH model volume according to snout-hip length. Linear measurements are given in mm – for the Newman and Tarlo 'Stretosaurus' model these are scaled to the total length (including soft tissues – see Figure 6-2) of '36 feet' (10,973 mm) given for the reconstruction. See text for explanation of the different anatomical regions, and the methods used to measure these and volume.

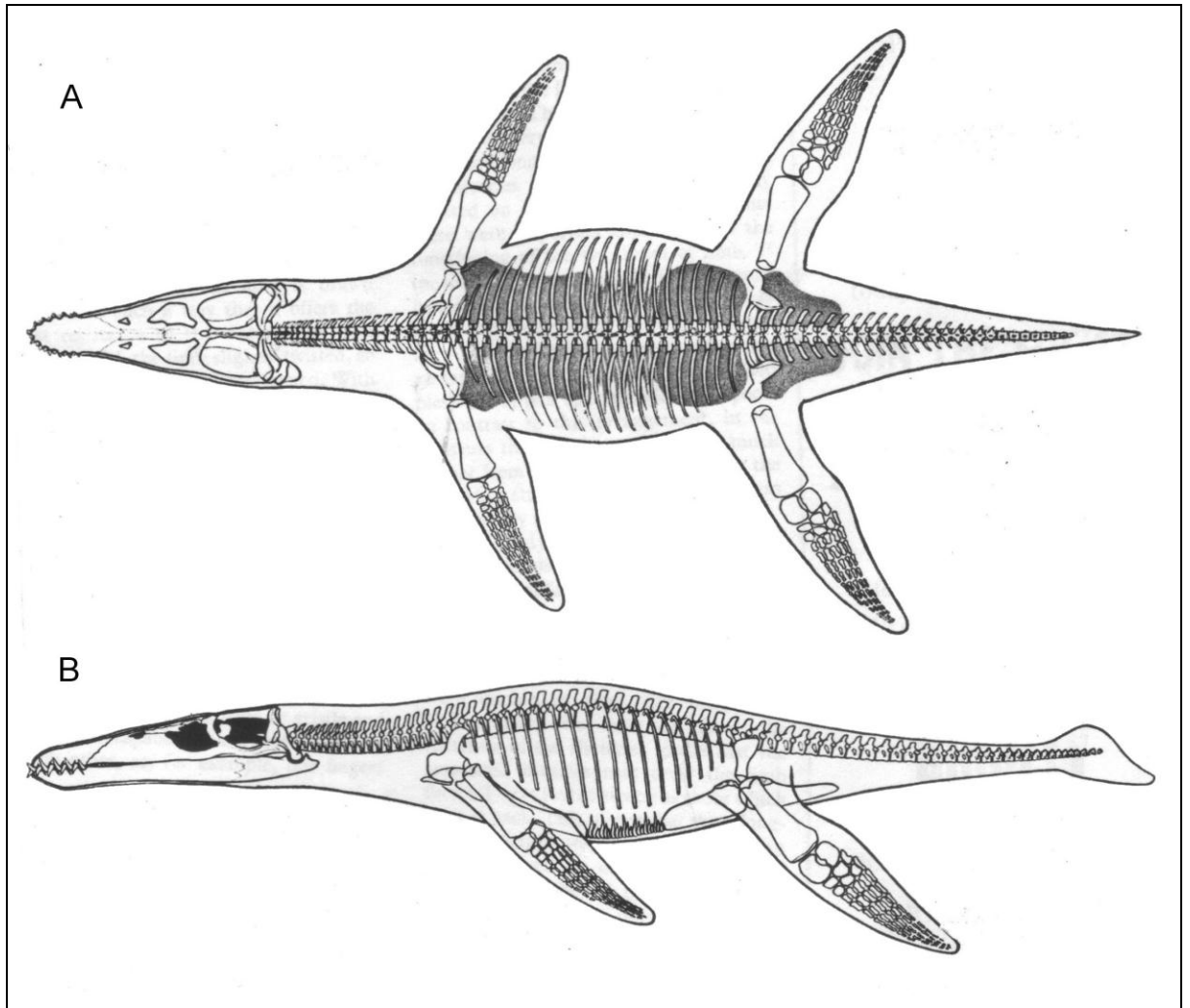


Figure 6-2: Reconstruction of the Jurassic pliosaur ‘Stretosaurus’, in (A) dorsal and (B) lateral view (from Halstead and Newman, 1967).

the estimate Newman and Tarlo provided for the Stewartby animal and apparently similar to the dimensions of the Stretham specimen. Body proportions were derived from measurement of the distances between the anterior snout, atlanto-occipital joint, glenoid, acetabulum, and terminal caudal vertebrae, as described above (Table 6-1).

Taxonomic context

Plesiosaurian taxonomy has recently been the subject of several studies, and as such has been in a state of some flux (Druckenmiller and Russell 2008a). The recognition of brachaucheniid pliosaurs as a separate group to the pliosaurids, however, was made by Andrews, who observed that Williston’s referral of *Brachauchenius lucasi* to the Pliosauridae “would exclude the type species from the family” (Andrews 1913: 2).

Andrews went on to state that “Probably the North-American reptiles corresponding to the Pliosaurus of Europe will be found to constitute a distinct family, in which the characteristics common to the two groups are the consequence of parallel modifications”. Williston was evidently persuaded by this, as he later erected the Family Brachaucheniiidae for the genus *Brachauchenius* (Williston 1925).

Longman’s creation of *Kronosaurus* preceded Williston’s creation of the new family, and all of the early literature on *Kronosaurus queenslandicus* compares the material with the pliosaurids of the Jurassic, especially *Peloneustes*. The first study to group *Kronosaurus* with *Brachauchenius* was that of Hampe (1992): Hampe’s referral of *Kronosaurus boyacensis* to the Brachaucheniiidae was subsequently accepted by Carpenter (1996). However, the validity of the Brachaucheniiidae *sensu* Hampe (1992) was challenged by O’Keefe who, in the first comprehensive cladistic analysis of plesiosaurians, recovered *Kronosaurus* as a basal pliosaurid and *Brachauchenius* as a derived member of the Pliosauridae, despite their stratigraphic proximity (O’Keefe 2001). Subsequent cladistic analyses – in particular Druckenmiller (2006), who used data from first-hand observation of the *K. queenslandicus* material discussed below – have failed to support O’Keefe’s result, however, and the most recent studies that include both *Brachauchenius* and *Kronosaurus* have found these to be sister taxa with respect to other large pliosaurs [H. Ketchum, pers. com.; Smith and Dyke (2008)]. As such, Williston’s Brachaucheniiidae continues to be phylogenetically and taxonomically relevant.

Smith and Dyke (2008) found the *Kronosaurus*+*Brachauchenius* clade to be basal to a clade containing *Pliosaurus* and other species of Middle and Late Jurassic pliosauroids traditionally considered as pliosaurids (*Peloneustes*, *Liopleurodon*, and *Simolestes*). Their results also suggest that the brachaucheniids and the Jurassic ‘pliosaurids’ form a clade that is phylogenetically distinct from the other traditionally recognised pliosauroid families, i.e. the Rhomaleosauridae (Nopsca 1928), Polycotylidae (Cope 1869), and Leptocleididae (White 1940): moreover, all of the traditional families were found to be monophyletic and thus taxonomically valid (Smith and Dyke 2008). However, Smith and Dyke indicated that they considered the Brachaucheniiidae to be a subset of the Pliosauridae, despite there being no requirement from the topology of their tree for this taxonomy of the Cretaceous forms. Although they did not detail the

specifiers for the families listed in their results, they are in effect considering the Pliosauridae to comprise of *Pliosaurus*+*Brachauchenius*: however, *Brachauchenius* has not generally been considered a member of the Pliosauridae since Andrew's monograph on the Callovian pliosaurids referred to above (Andrews 1913).

It is argued here that the information content of the family level taxonomy of pliosauroids is maximised if the Brachaucheniidae (Williston 1925) is defined as *Brachauchenius*+*Kronosaurus*, with *Pliosaurus* as an external specifier, while the Pliosauridae (Seeley 1874) can be defined as *Pliosaurus*+*Simolestes*, with *Rhomaleosaurus* as an external specifier (see Section 6.6 below). This definition of each family would retain the traditional context of each family, subject to the major branches of the tree topology recovered by Smith and Dyke (2008) being accepted as valid. Should future studies find that *Brachauchenius* and *Kronosaurus* do not form a natural group with respect to *Pliosaurus*, the Brachaucheniidae would become redundant. Similarly, if future analyses establish that *Simolestes* is topologically closer to *Rhomaleosaurus* than to *Pliosaurus*, then either the Rhomaleosauridae would (as the more recently created family) become subsumed as a tribe of the Pliosauridae, or the definition of the Pliosauridae should be emended to exclude the rhomaleosaurids. Given present knowledge of pliosauroid phylogenetics, however, the definitions for the Brachaucheniidae and Pliosauridae proposed above would allow the members of these two families of large pliosaurs to be placed in an evolutionary and ecological context – without the need for terminology such as ‘non-brachaucheniid pliosaurids’ to specify the *Simolestes*+*Pliosaurus* group, as would be required under the system presented by Smith and Dyke (2008). In the present work, the vernacular terms ‘pliosaurid’ and ‘brachaucheniid’ are used consistent with the definitions for these families proposed here³, applied to the tree topology of Smith and Dyke (2008).

³ Note added In Press: Clarification of the data matrices used by Smith and Dyke (2008) and Ketchum (2008) (H. Ketchum, pers. comm.) suggests that the topology recovered by Ketchum (2008), i.e. with *Kronosaurus* and *Brachauchenius* forming a sister group within the Pliosauridae, but exclusive of any of the ‘traditional’ members of the Pliosauridae, i.e. *Pliosaurus*, *Peloneustes*, and *Liopleurodon*, and *Simolestes*, may be robust. This result is similar to that recovered by Druckenmiller and Russell (2008a), although they did not include *Brachauchenius* in their analysis. In this case, the concept of the Brachaucheniidae argued here is still valid: it need only be adjusted to the rank of Subfamily and thence becomes Brachaucheniinae Williston (*sensu* Ketchum 2008) by the ICZN Principle of Coordination. It is still a useful taxon, as it would then differentiate the derived Cretaceous forms from the Jurassic forms; the presence of *Pliosaurus* as an external specifier ensures that, should *Brachauchenius* and *Kronosaurus* be found to be pliosaurids, but not especially closely related to each other, the taxon would become redundant. Pending further clarification of these issues, the present study uses the terms ‘pliosaurid’

A note on anatomical nomenclature of plesiosaur vertebrae

Traditional classification of plesiosaur vertebrae is a modified version of nomenclature for other groups. In reptiles, the vertebrae of the neck are characterised by the attachment of the ribs to the centrum, whilst the ribs of the trunk region attach to the neural arch, often via enlarged transverse processes (Romer 1956). Isolated vertebrae can thus be identified to major regions of the axial skeleton by (amongst other features) the morphology of the rib attachment, even when the ribs themselves are not preserved.

Although there is, as yet, no formal standard of anatomical nomenclature for reptiles, the convention for most reptilian groups is to refer to the neck vertebrae, with the costal facets located on the centrum, as cervical vertebrae (or ‘cervicals’), and the vertebrae of the trunk, where the ribs articulate with the transverse process born by the neural arch, as dorsal vertebrae (‘dorsals’). Sacral vertebrae are defined as those vertebrae that carry the sacral ribs (which in turn articulate with the illia), and like the cervicals can be identified by the location of the costal facet on the centrum (the sacral rib facets tend to be more robust than their cervical counterparts).

At the anterior end of the trunk, there is usually a transition region where, if you look at successive vertebrae from anterior to posterior along the column, the costal facets gradually move up from the centrum to the neural arch. The region where the facet is located partly on the centrum and partly on the arch is referred to as the ‘pectoral shift’ (Romer 1956): in different groups, the number of vertebrae including in the pectoral shift varies, but is typically between two and five. In most groups, these vertebrae are categorised as part of the dorsal series; however, in plesiosaurs the convention is to identify them as ‘pectorals’, and they are categorised separately to the cervical and dorsal vertebrae [see, for example, Brown (1981), Welles (1943, 1952)].

Where the ribs are preserved with the vertebrae, plesiosaur pectoral vertebrae often carry long ribs similar to those of the dorsals. In addition, the most posterior cervical vertebrae often bear ribs that are much longer than the short, stout ribs typical of the

and ‘brachaucheniid’ in the manner defined above, i.e., to denote the Mid–Late Jurassic (pliosaurid) and Cretaceous (brachaucheniid) large pliosauroids respectively.

anterior and middle cervical series. These posterior cervical ribs can be as large as the pectoral ribs, or can be of a length that is intermediate between the pectoral and typical cervical ribs (Figure 6-3).

Although this nomenclatural convention, being based entirely on the morphology of the rib facets on the vertebrae and making no reference to the morphology of the ribs themselves, allows isolated vertebrae to be allocated to major regions of the axial column, it is a poor foundation for describing the functional anatomy of the post-cranial anatomy of plesiosaurs. The recognition of a sternum in plesiosaurs (Nicholls and Russell 1991 – see also description of USNM 4989 below) allows a functional classification of vertebrae that bear the ribs that are part of the sternal ‘basket’: as with mammals and most other reptiles, these vertebrae and their ribs can be termed ‘thoracic’, as the presence of a rib cage defines the thorax. The thoracic ribs can be recognised by their ‘cup-like’ distal ends, which contrast with the tapered ends of lumbar ribs: in life, these concave distal facets of the thoracic ribs were attached to the costal cartilages, which in turn attached to the sternum.

In front of the thoracic region, the enlarged ribs of the posterior cervical region have tapered distal ends that show no signs of having been attached to cartilaginous sections. These have been termed ‘prothoracic’ ribs by Evans and McHenry⁴, although this term has been used to describe the anterior thoracic vertebrae and ribs in crocodylians (Salisbury and Frey 2001), which do articulate with the sternal basket, and to avoid potential confusion the elongated ribs anterior to the thoracic region should be given a different term, such as ‘prethoracic’ (M. Evans, pers. comm.). The ribs of the lumbar region have a similar, tapered distal end (M. Evans, pers. comm.).

As stated above, the traditional terminology for vertebral regions in plesiosaurs is useful in that it can be applied to vertebrae that are separated from their corresponding ribs. However, it is functionally ambiguous. A terminology that recognises prethoracic, thoracic, and lumbar regions of the axial column (hereafter referred to as the ‘Evans & McHenry’ system) would have advantages for the study

⁴ Work in progress. A preliminary account of specimens interpreted as having taphonomic consistency with the Nichols and Russell model of pectoral morphology was presented to the 2006 SVP/PCA meeting in Paris: M. Evans & C.R. McHenry, *A basket full of ribs: the anatomy of the trunk region in plesiosaurs*.

Traditional	cervical		pectoral		dorsal		sacral	caudal
costal facet location	centrum		centrum + neural arch		neural arch		centrum	centrum
Example 1	brevicostal-cervicals	prethoracico-cervicals	prethoracico-pectorals	thoracico-pectorals	thoraco-dorsals	lumbo-dorsals	sacral	caudal
Example 2	brevicostal-cervicals		brevicostal-pectorals	prethoracico-pectorals	thoraco-dorsals	lumbo-dorsals	sacral	caudal
rib morphology	short, tapered ends		elongated, tapered ends	elongated, cupped ends		elongated, tapered ends	short, cupped ends	short, tapered ends
Evans & McHenry	(brevicostal) cervical		prethoracic	thoracic		lumbar	sacral	caudal

Table 6-2: Proposed nomenclatural system for anatomical regions in plesiosaurs, based upon work in progress by M. Evans and myself. The system accepts the presence of a sternum (Nicholls and Russell, 1991) and thus a thorax in plesiosaurs. Because the Evans & McHenry system focuses upon the length of the ribs and their connection (or lack thereof) to the sternum, it is essentially a system based upon the morphology of the distal ends of the ribs. In contrast, the Traditional system focuses upon the position of the rib attachment to the vertebrae and is thus a function of the morphology of the proximal end. As such, it is possible to use a hybrid nomenclatural system to describe the regional postcranial morphology in different specimens (Example 1 and Example 2): this system conveys maximal information at a small cost to word-length, and is flexible enough to encompass all conceivable permutations of rib morphology.

of functional morphology in plesiosaurs, but requires excellent preservation of vertebrae and ribs. Note that the two classifications do not correspond consistently in different groups of plesiosaur; in some specimens, the pectoral vertebrae might all be thoracic, whilst in others they might include individual vertebrae with prethoracic ribs, thoracic ribs, and even ‘cervical-type’ short (‘brevicostal’) ribs. As the traditional system focuses upon the details of the proximal attachment of the rib, whilst the Evans & McHenry system focuses upon the morphology of the distal end, there is the potential to use a hybrid system for the nomenclature of the postcranial regional anatomy. Such a hybrid system would have the dual advantages of maximising the information content of the terms, and being flexible enough to be applicable to all conceivable combinations of vertebral and rib anatomy (Table 6-2).

6.3 Results

Brachauchenius lucasi: USNM 4989

The holotype specimen of *Brachauchenius lucasi* Williston (1903) includes a nearly complete skull (the tip of the snout is missing) preserved with 35 vertebrae (Figure 6-3): most of the elements are articulated, with some minor slippage between the anteriormost cervicals and the posterior dorsals. As such, it provides a rare opportunity to document the intervertebral distances in a specimen of brachaucheniid plesiosaur.

The vertebral dimensions and intervertebral gaps were measured directly (Table 6-3). Skull length has been estimated by comparison with a complete skull at the Fort-Hays Sternberg Museum (FHMS VP-321 - Figure 6-4) on the basis of the planar distance from the external nares to the parietal foramen.

Estimates of body proportions are shown in Table 6-4. The estimate of head length includes the intervertebral gap between the occipital condyle and the atlas. The positions of the shoulder and hip joints (in the sagittal plane) are assumed to be in line with the p2-p3 and s1-s2 vertebral joints respectively (c.f. QMF 10113 and *K. boyacensis* holotype) – see Methods, and results for these specimens below.

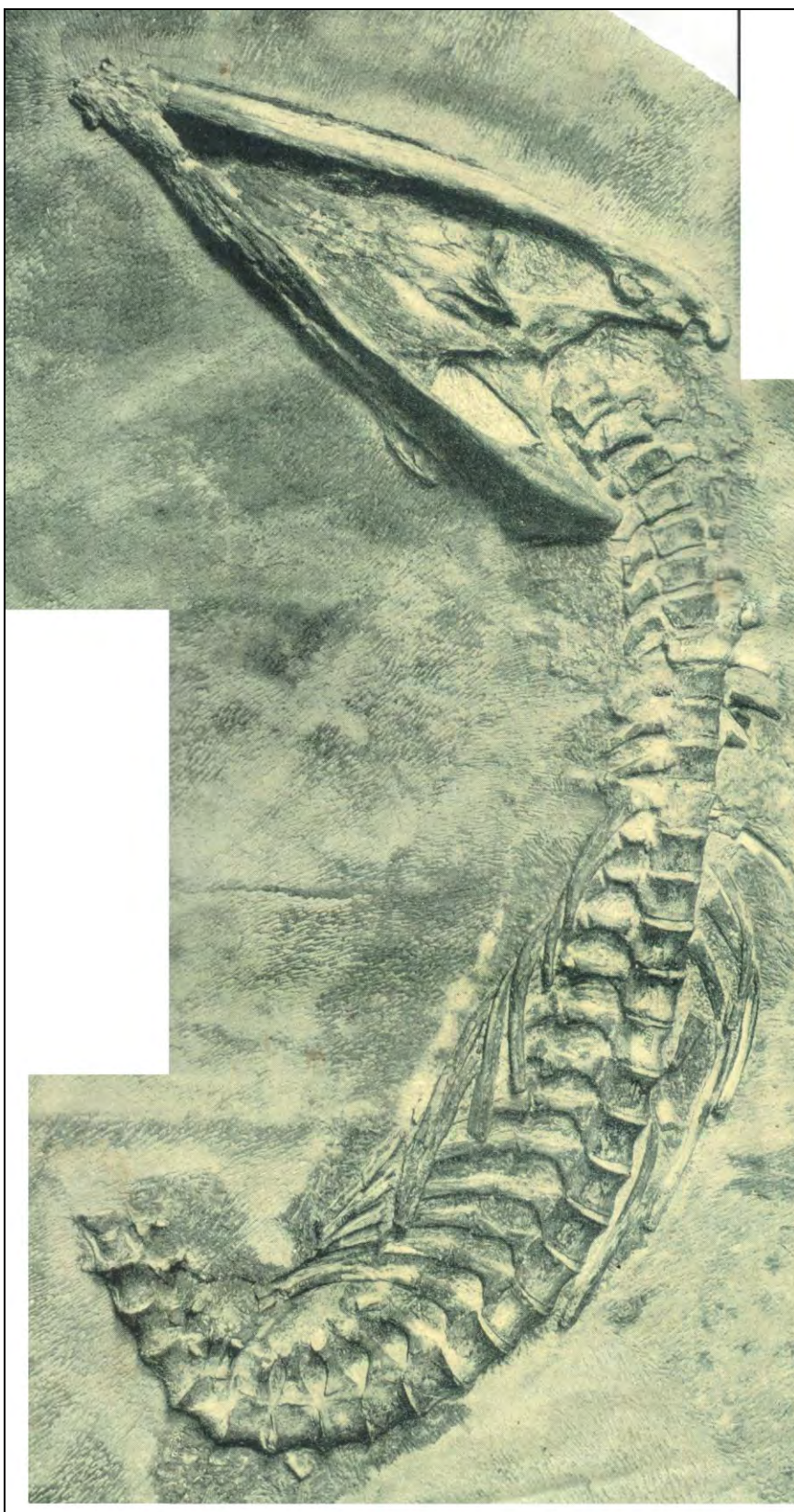


Figure 6-3: USNM 4989: holotype of *Brachauchenius lucasi* Williston, 1903. The specimen preserves a partial skull (the tip of the snout, including most of the dentulous parts of the premaxillae and the mandibular symphysis, has been lost) and an articulated vertebral column comprising 35 vertebrae (v1 and v2 are fused). The vertebrae lack sub-central foramina, as is typical for brachaucheniiids (from Williston, 1907).

Size

Axial element	interp. (trad.)	cent. length (mm)	centrum width (mm)		post-centrum gap (mm)	Region
			ant	post		
skull		1045	-	-	10	head
v1	atlas (c1)	44	-	-	-	neck
v2	axis (c2)	44	92	77	10	neck
v3	c3	44	(83)	(76)	12.5	neck
v4	c4	41	84	76	18	neck
v5	c5	45	78	79	14	neck
v6	c6	43	83.5	79	13	neck
v7	c7	46	87	86	11	neck
v8	c8	47	87	86	9	neck
v9	c9	(47)	(87)	(87)	12	neck
v10	c10	48	87	87	16	neck
v11	c11	47	84	88	14.5	neck
v12	c12	56	89	87	10	neck
v13	c13	53	(89)	87	9	neck
v14	p1	60	90	87	10	neck
v15	p2	62	90	88	10	neck
v16	p3	67.5	87	86	8	torso
v17	d1	72	91	88	6.5	torso
v18	d2	70	82	91	6	torso
v19	d3	73	87	89	9	torso
v20	d4	72	85	84.5	7	torso
v21	d5	72	88	89.5	7	torso
v22	d6	76.5	90	84	9	torso
v23	d7	75	84	85	10	torso
v24	d8	75	88	84	7	torso
v25	d9	72	86	84	7	torso
v26	d10	76	85	82	7	torso
v27	d11	73	84	78	7	torso
v28	d12	74	85	83	7.5	torso
v29	d13	78	82.5	78	7.5	torso
v30	d14	72	80	(84)	7.5	torso
v31	d15	77	78	76	8	torso
v32	d16	72	76	80	8	torso
v33	d17	70	78	78	7.5	torso
v34	d18	68.5	77	76	6	torso
v35	d19	79	75	78	5	torso
(v36)	(s1)	(79)	-	-	-	torso

Table 6-3: Measurements and interpretation of axial skeleton elements in USNM4989 (holotype of *Brachuchenius lucasi* Williston, 1903). Figures in brackets are estimates. The specimen does not preserve V36 – an estimate of its centrum length has been included to facilitate an estimate of torso length (p3–s1) in this specimen. The distance of gaps refer to the inter-vertebral gaps at the posterior end of the respective vertebrae.

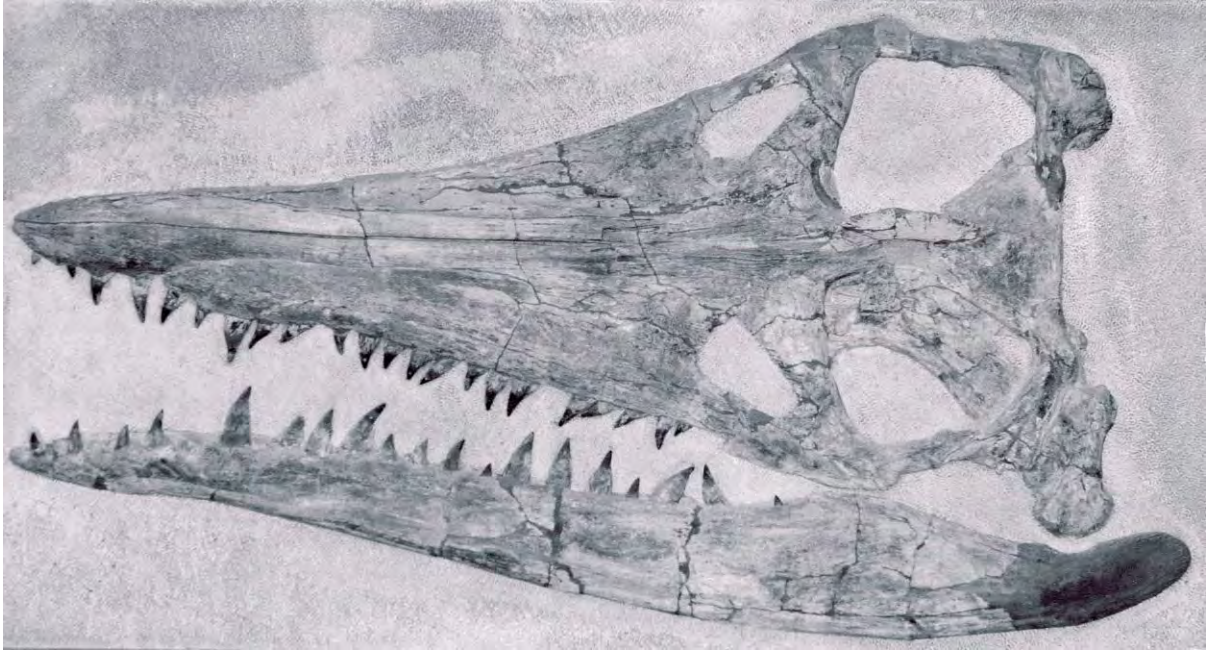


Figure 6-4: *Brachauchenius lucasi* FHSM VP-321.(photograph courtesy of M. Everhart).

The assumption of a presacral vertebral count of 35 in this specimen is based upon comparison with articulated brachaucheniid specimens: in addition to USNM 4989, there are three known specimens of brachaucheniid pliosaurs; these are described below. Each one of these is a large headed, short necked pliosaur with a compact torso; presacral counts in two of these (QMF 10113, *K. boyacensis* holotype) are close to 35 (see below), and the body proportions in the third specimen (*Brachauchenius* sp. VL – for which a dorsal vertebrae count is not yet available) are very similar (compare Figure 6-15 with Figure 6-7). However, this evidence is not in itself conclusive, and it is of course to be hoped that new specimens of *B. lucasi* will be described that resolve the question of vertebral counts in this species.

head	neck	torso	snout-hip	tail	TL	volume (litres)
1,055	896	1,691	3,642	1,671	5,313	1,404

Table 6-4: Estimates of body proportions in USNM 4989. Linear measurements are given in mm. Head length is based upon BSL and includes the distance between the occipital condyle and the atlas vertebrae. The torso and snout-hip lengths have been estimated by including assuming that all pre-sacral vertebrae are preserved in this specimen, and estimating a length of 79 mm for the first sacral vertebra. Tail length and volume are estimated by scaling from the BMNH model (Table 6-1) by snout-hip length: linearly in the case of lengths, by the third power in the case of volume.

If future discovery of *Brachbauchenius lucasi* specimens eventually show this species to have had 35 presacral vertebrae, the anatomical inferences that can be drawn from the taphonomy of USNM 4989 are of interest. The specimen is missing both pectoral and pelvic girdles and limbs, the gastralia, the ribs from the posterior part of the dorsal column, and the sacral and caudal limbs and vertebrae: essentially, the posterior and ventral part of the body. The specimen is remarkable for the apparent lack of disturbance to the preserved parts – displacement between adjacent vertebral elements is minimal – so it would appear that the missing parts are unlikely to have been removed after the specimen sunk to the sea-floor. The specimen was preserved dorsal-side up, so the ventral torso elements have not been removed by erosion. If the missing elements dropped away from the carcass while afloat (Chapter 3), then we can surmise that the connection between the pelvic girdle, sacral ribs, and sacral vertebrae may have been stronger than the connection between the sacral vertebrae and the posterior dorsals. The gastralia are likely to have tightly associated with the superficial layers of the abdominal musculature, and were lost along with the ventral parts of the torso and pelvis.

Ribs are preserved, on both sides, along the vertebral column as far back as vertebra (v)24. Posterior to this, only the broken proximal ends of the right ribs attached to v25 and v26 are present (Table 6-5, Figure 6-3). All the preserved ribs are articulated to their respective vertebrae – the arrangement of the large ribs in the anterior part of the torso seems to indicate that they settled gently onto the underlying remains with a minimum of displacement. The contrast between the preservation of these ribs, and the absence of the ribs from the posterior trunk, is remarkable.

Traditionally, plesiosaurs have been assumed to lack a sternum (Storrs 1991), but this interpretation has been challenged (Nicholls and Russell 1991) and in the light of that debate the preservation of the rib cage in USNM 4989 is of interest. Whatever the organisation of the anterior vs posterior region of the trunk, something evidently kept the anterior trunk ribs closely associated to the vertebral column whilst the ribs were lost from the posterior trunk. The presence of a sternum, connected to the ossified ribs via costal cartilages (as in most other groups of amniotes) would certainly fulfill this taphonomic role. The distal ends of most of the preserved ribs is

a flattened, concave facet of exactly the morphology that would be expected if the rib was joined to a more distal component: the most parsimonious interpretation of USNM 4989 seems therefore to be that a sternum was present, and that the trunk ribs preserved in the specimen articulated with the sternum via costal cartilages. Furthermore, the articulations between sternum and thoracic ribs appear to have persisted for longer than the connection between the axial skeleton and the appendicular skeleton of the pectoral region, which has been lost. The inference of a sternum in USNM 4989 has important implications for understanding of the functional anatomy of the postcranium in plesiosaurs: in addition, anatomical nomenclature for these reptiles will need to accommodate recognition of thoracic and lumbar regions of the trunk (see above).

The anatomical nomenclatural system outlined above (and shown in Table 6-2) can be applied to this specimen thus (Table 6-5): the anteriormost vertebrae (v2–v13)⁵ have the costal facet entirely upon the centrum and are thus cervical vertebrae under the traditional definition. Vertebra 2 to v9 bear short cervical ribs; they are therefore brevicostal-cervicals. Vertebra 10 and v11 bear ribs that are slightly elongated relative to anterior cervicals, and which have tapered ends rather than the expanded distal ends that give plesiosaur cervical ribs a characteristic ‘hatchet’ appearance, but are still considered to be brevicostal cervicals. The ribs on v12 are missing (right) and broken (left), so their length is unknown, but the rib facet on the vertebral body is of a larger diameter than the preceding segments. It is interpreted here as a brevicostal-cervical. Vertebrae 13 and v14 bear elongated ribs: the distal ends are not as well preserved as on some of the adjacent ribs, but are not gradually tapered as is the case with the ribs on v11. Neither are they definitely cupped in the way that the ribs on v15 are. These vertebrae may thus be prethoracics – v13 is a cervical (as defined traditionally), so it would be a prethoracico-cervical, and v14 a prethoracico-pectoral. The ribs on v15–v24 have cupped distal ends, and as v15 and v16 are pectorals these two are thoracico-pectorals, whilst v17–v24 are thoracico-dorsals. Vertebra 25 bears a robust rib, but the distal end is broken – it may be a thoracico-dorsal. Only the proximal ends of the right ribs on v26 and v27 are preserved. No vertebrae posterior to v27 preserve any trace of ribs.

⁵ The atlas vertebra, v1, does not have a rib.

Axial element	t.p. length	rib			Traditional	hybrid	Evans & McHenry
		dist. d	length	prox. d			
v1	-	-	-	-	cervicals	brevicostal cervicals	brevicostals (cervicals)
v2	-	32	61	27			
v3	-	39	59	29			
v4	-	47	72	28.5			
v5	-	39	61	31			
v6	-	45	69	30			
v7	-	38	56*	30			
v8	-	50	78	31			
v9	-	40	72	29			
v10	-	12	92	29			
v11	-	14	101	29			
v12	-	-	-	34			
v13	-	17	224	37	pectorals	prethoracico- cervical	prethoracics
v14	47	16	260	?		prethoracico- pectoral	
v15	60	22	381	45	dorsals	thoracico- pectorals	thoracics
v16	71	34	400	40			
v17	77	30	465	37			
v18	90	28	445	39			
v19	88	21	380	35			
v20	82	16	390	35			
v21	82	18	360	34			
v22	82	?	300*	30			
v23	82	?	270*	33			
v24	83	17.5	325	34.5			
v25	75	14.5	270	34			
v26	85	-	-	29			
v27	82	-	-	28	thoracico- dorsal ?	thoracic?	

Table 6-5: Measurements of ribs and transverse processes, and anatomical nomenclatural systems, for the axial column in USNM 4989. Transverse process (t.p.) length and rib length measured as the chord between the proximal (prox.) and distal (dist.) ends; rib diameter (d.) measured at proximal and distal ends in approximately the coronal plane. For explanation of the 'Traditional', 'Evans & McHenry', and 'hybrid' anatomical nomenclatural system see Table 6-2 and text.

At present, the specimen has not been prepared from the surrounding matrix.

Because the specimen preserves the vertebrae and ribs in articulation, physical removal of the matrix may not be desirable; however, given the specimen's size and

the nature of the matrix, it would be suitable for CT scanning – this would help to further clarify some of the remaining question of axial skeleton morphology, and help to establish a nomenclatural and functional model for postcranial anatomy in brachaucheniid pliosaurs.

***Kronosaurus queenslandicus*: QM F10113**

The skull of this specimen (see Chapter 4) is associated with a vertebral column that is mostly articulated from the anterior cervicals to the sacrals. Parts of the limb girdles and two nearly complete propodials (left humerus and left femur) are also preserved. The postcranial skeleton of this specimen is the subject of ongoing study: measurements for the cervical series are provided in Table 6-6.

Axial element	Interpretation	length (mm)	width (mm)	post-centrum gap (mm)	Region
skull		1876		18	head
v1	atlas	(80)	202.4*	-	neck
v2	axis	90	195.4*	20	neck
v3	c3	83	185	24	neck
v4	c4	72	175	32	neck
v5	c5	58	178	18	neck
v6	c6	68	168	21	neck
v7	c7	(69.5)	180	17	neck
v8	c8	71	185	14	neck
v9	c9	80	187	20	neck
v10	c10	(86)	172	29	neck
v11	c11	92	173	28	neck
v12	c12	81	174	14	neck
v13	c13	92	167	16	neck
v14	p1	106	153	18	neck
v15	p2	101	130	16	neck
v16	p3	121	159	14	torso
v17	d1	-	155	-	torso

Table 6-6: Measurements and interpretation of axial skeleton in QM F10113. Figures in brackets are estimates: all widths measured at the anterior face of the respective centra, except the atlas and axis (*) which were measured at the posterior part. Lengths were measured along the ventral size of the centrum. ‘Post-centrum gap’ is the intervertebral distance succeeding the respective vertebrae, calculated from data from USNM 4989 (Table 6-3).



Figure 6-5: Photo-mosaic of QM F10113 in ventral view, showing post-cranial skeleton laid out on a flat surface. The photo-mosaic of the skull (see Chapter 4) has been superimposed onto the front of the cervical series. The scale bar next to the skull is 2 metres.

For the purposes of obtaining an estimate of occipital-hip length the fossil was laid out on a flat surface and photographed with the blocks placed together as closely as possible without damaging the fractured surfaces (Figure 6-5). This artificially increases the apparent length of the axial column in two ways; firstly, because of the gaps between adjacent blocks, and secondly because the three dimensional nature of the contacts between adjoining blocks is flattened out. A comprehensive account of the post-cranial geometry in this specimen could involve placing the blocks in three-dimensionally correct ‘click fit’ contact, supported by a flexible but strong substrate (such as sand) – this work is planned for the near future.

	head	neck	torso	snout-hip	tail	TL	volume (lites)	humerus (length)	femur (length)
photo-mosaic	1,894	1,584	2,359	5,837	2,679	8,516	5,781	-	-
measurement	-	1,516	-	-	-	-	-	650	900

Table 6-7: Estimates of body proportions in QM F10113. Linear measurements are given in mm, head length calculated as for USNM 4989 (Table 6-4). The photo-mosaic method (Figure 6-5) used here slightly over-estimates length compared to direct measurement (compare figures for the neck region, and see text).

The data presented in Table 6-7 represents an initial attempt to quantify body size in this specimen. The blocks containing the left pectoral girdle and humerus are articulated with the vertebral column, allowing the position of the shoulder joint to be identified as lying in line with the p2-p3 intervertebral joint. The length of the neck and torso regions were measured in Rhino; the distances of the larger gaps between blocks were subtracted from the overall measurements to give corrected estimates of body region length. Comparing the photo-mosaic estimate of neck length with the direct measurements taken for the c1-p2 vertebrae shown in Table 6-6 (these latter including the estimated intervertebral gaps calculated by comparison with USNM 4989) suggests that the photo-mosaic measurements are indeed slight overestimates of actual length (Table 6-7).

The cervical count for this specimen can be accurately determined as 13 vertebrae. The presacral count has yet to be determined precisely, because the vertebrae in the pelvic region are partially obscured by matrix, and which one of the vertebrae is the

Size

Axial element	Interpretation (Hampe)	length (mm)	width (mm)	post-centrum gap (mm)	Region
skull		2399		23	head
v1	atlas	(90)	-	-	neck
v2	axis	(90)	-	20	neck
v3	c3	69	194	20	neck
v4	c4	72	197	32	neck
v5	c5	80	212	25	neck
v6	c6	78	-	24	neck
v7	c7	86	-	21	neck
v8	c8	89	210	17	neck
v9	c9	86	234	22	neck
v10	c10	83	219	28	neck
v11	c11	81	248	25	neck
v12	c12	82	275	15	neck
v13	p1	102	-	17	neck
v14	p2	88	-	14	neck
v15	p3	99	-	12	torso
v16	d1	(141.5)	-	13	torso
v17	d2	184	-	16	torso
v18	d3	(161)	-	20	torso
v19	d4	138	-	13	torso
v20	d5	131	-	13	torso
v21	d6	130	-	15	torso
v22	d7	127	-	17	torso
v23	d8	127	-	12	torso
v24	d9	132	-	13	torso
v25	d10	129	-	12	torso
v26	d11	132	-	13	torso
v27	d12	137	-	14	torso
v28	d13	131	-	13	torso
v29	d14	124	-	13	torso
v30	d15	124	-	13	torso
v31	d16	124	-	14	torso
v32	d17	122	-	13	torso
v33	d18	120	-	11	torso
v34	d19	117	174	7	torso
v35	?s1	117	-	7	torso
v36	?s2	116.5	-	6	tail
v37	s3	116	172	6	tail
v38	s4	107	178	5	tail
v39	s5	120	174	6	tail

Table 6-8: Measurements and interpretation of the axial skeleton of the holotype specimen of *Kronosaurus boyacensis*. Measurements are taken from Hampe (1992), except: Hampe did not provide lengths for v1, v2, v16, and v18 – these have been estimated by comparison with QM F10113 (for v1 and v2), or as averages of adjacent vertebrae (v16 and v18); Hampe listed skull length (DCL) as 2,360 mm; the length in the table is BSL, calculated from the proportions of DCL:BSL in the 3-D model of *K. queenslandicus*; the post-centrum gap is the intervertebral distance between a vertebra and the adjacent posterior segment, calculated from the proportions of post-centrum gap to centrum length in USNM 4989. Region is assigned on the basis of the location of the shoulder and hips joints, ascertained from photographs of this specimen (Figure 6-7, Figure 6-8).

first sacral (as diagnosed by rib facet morphology) is not clear. However, the presacral count in this specimen is either 35, or is very close to that number.

***Kronosaurus boyacensis*: holotype specimen⁶**

Discovered in 1977, this is the most complete specimen of a large pliosaur that I am aware of. It was initially assigned to *Kronosaurus* pending more detailed study (Acosta et al. 1979): Hampe concluded that it represented a new species and established the name *Kronosaurus boyacensis* upon this specimen (Hampe 1992). The specimen has not been physically moved since its discovery: it is on display *in situ* in a purpose-built facility, and is preserved with dorsal surface upwards.

The specimen appears to be quite weathered in places – the skull roof bones are poorly preserved – and the overall appearance of the fossil bone is similar to the preservation of many of the *Kronosaurus queenslandicus* specimens from the central Great Artesian Basin. This, and the *in situ* display of the specimen, presents logistical difficulties for detailed descriptions of the osteology – conversely, the fact that the specimen seems to have been preserved with a minimum of post-mortem displacement of the skeletal elements presents an excellent opportunity to document the body proportions of this pliosaur. Hampe used photogrammetric techniques to detail the position and dimensions of the major elements (Hampe and Leimkuhler 1996), in addition to recording the linear dimensions of the main parts of the axial skeleton (Hampe 1992). Photogrammetric work is especially useful for the present purposes of establishing body size in brachaucheniid pliosaurs: given the potential problems with using photography to establish dimensions and proportions in large specimens (see Chapter 4), it also provides the opportunity to test different photographic techniques against measurements taken manually.

Measurements of the skull and vertebral column, listed in Hampe (1992), are shown in Table 6-8. Note that Hampe did not provide measurements of intervertebral gaps - these are calculated from the proportions of centrum length to succeeding gap in USNM 4989 (see above). Also, Hampe provided a measurement of 2360 mm for

⁶ I have not been able to find a collection number for this specimen.

Interp.	head	neck	torso	snout-hip	tail	TL	volume (litres)	humerus	femur
Direct 1	2,422	1,454	3,019	6,895	3,165	10,060	9,531	799	977
Direct 2	2,214	1,454	3,019	6,688	3,069	9,757	8,695	-	-
Photo 1	2,214	1,503	2,689	6,406	2,940	9,346	7,642	796	980
Photo 2	2,220	1,515	2,674	6,410	2,942	9,351	7,655	858	981
Photo 3	2,766	1,733	3,110	7,608	3,492	11,100	12,803	934	1,173
Photo 4	2,630	1,701	3,125	7,456	3,422	10,879	12,052	876	1,102

Table 6-9: Body proportions in *K. boyacensis* holotype specimen, showing the results of differing measurement methods. Note that the head measurement is based upon estimates of BSL, and includes the calculated intervertebral distance between the occiput and the atlas vertebra. Linear measurements in mm.

skull length, measured from the anterior tip of the premaxillae to the posterior-most part of the supraoccipital. This measurement is very similar to dorsal cranial length (DCL): I have assumed it is equivalent, and estimated basal skull length (BSL) from the ratio of BSL:DCL in *K. queenslandicus* (see Chapter 4, 5). Estimates of body segment length in *K. boyacensis*, based on Hampe's measurements, are shown in Table 6-9 ('Direct 1'). The measurement of DCL provided by Hampe indicates a very large skull, 127% the length of the skull of QM F10113. However, the measurements of the neck and torso regions are 118% of the equivalent dimensions in QM F10113. The position of the supraoccipital, as interpreted by Hampe, appears to lie in line with the quadrates and directly above the position where, according to his determination of the position of the axis vertebra (which I agree with), I would expect the neural spine of the atlas. In QM F10113, QM F18827 and *Brachyuchenius lucasi* the position of the supraoccipital lies well in front of the line of the quadrates, and it is possible that Hampe has interpreted the supraoccipital in *K. boyacensis* as lying somewhat behind its actual position, leading to an inflated estimate of skull length. The measurement of BSL derived from the photogrammetric data (Photo 1) is 118% of BSL in QM F10113, which is comparable to the proportional difference in neck+torso for these two specimens. To allow for the possibility that Hampe's skull measurement is too long, Table 6-9 lists a second estimate of body proportions, where Hampe's measurements of vertebral dimensions are taken together with the skull measurements derived from photogrammetry ('Direct 2').



Figure 6-6: *Kronosaurus boyacensis*, 'Photo 1': diagram of the holotype specimen constructed from photogrammetric data (from Hampe and Leimkuhler 1996).

Table 6-9 summarises these estimates based upon Hampe's measurements (Direct 1 and Direct 2), compared with four different sets of measurements that are derived from photographic interpretation of the specimen. The first of these (Photo 1) is based upon the photogrammetric output shown in Hampe and Leimkuhler (1996 – reproduced as Figure 6-6). The second (Photo 2) is based upon a photo-mosaic of some of the high quality photographs⁷ used in the photogrammetric study of the specimen: I have aligned these photos so that that the features of the concrete floor

⁷ Kindly provided by Olivier Hampe.

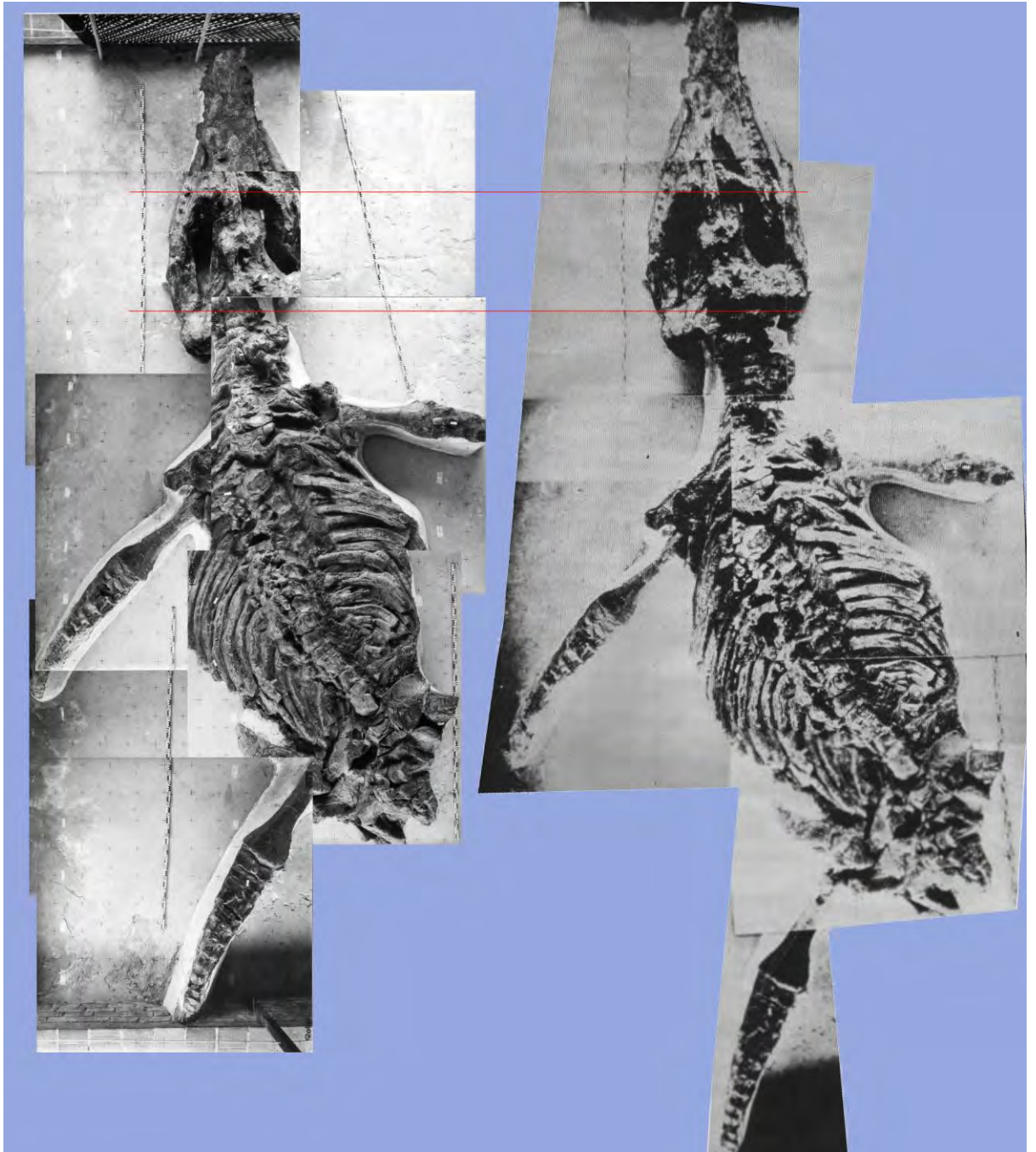


Figure 6-7: *Kronosaurus boyacensis*; 'Photo 2' (left) and 'Photo 3' (right) reconstructions. Compare with Figure 6-6 and Figure 6-8 – see text for explanation.

on which the specimen sits are aligned as well as possible⁸ (Figure 6-7). The third (Photo 3) is based upon the figure of the specimen (again, constructed by photo-

⁸ I have assumed that all of these photos were taken at the same height above the floor, and the camera was translated but not rotated in the horizontal plane. However, it is likely that this assumption may not be completely accurate for some of the photographs.

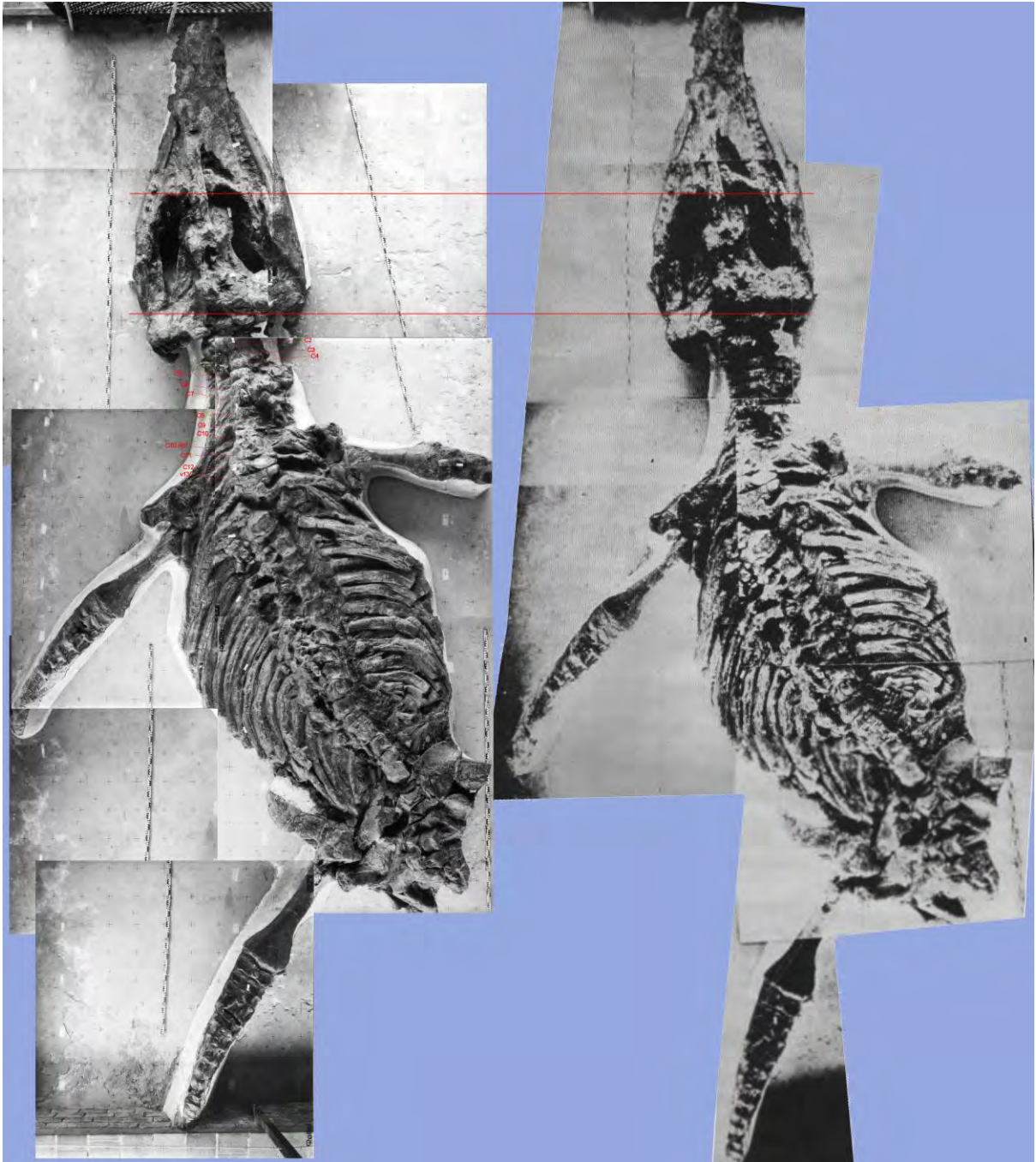


Figure 6-8: *Kronosaurus boyacensis*; 'Photo 4' (left) and 'Photo 3' (right) reconstructions. Compare with Figure 6-6 and Figure 6-7 – see text for explanation.

mosaic methods) provided in Hampe (1992) (Figure 6-7, Figure 6-8). The fourth method (Photo 4) uses the same photographs as Photo 2, but aligns them with respect to the fossil bone (Figure 6-8), which appears to have been approximately $\frac{1}{2}$ metre above the floor.

Evaluation of measurement methods

Photogrammetric vs. direct measurements: Estimated Total Length based upon direct measurement is 9.8–10.1 metres: the photogrammetric image gives measurements that are slightly less, around 9.3 metres. There are several candidates source of this variation: in addition to measurement error during direct measurement, scaling errors when importing bitmaps into Rhino, and measurement errors in Rhino, three points are worth considering:

1. The intervertebral gaps in the *K. boyacensis* holotype may be less than calculated here – this would bring the Direct measurements closer to the Photo 1 measurement. To my knowledge, the scaling patterns of inter-vertebral distance has not been quantified in any large reptile, but it would be no surprise if this feature is allometric. Given the differences in size between this specimen and the specimen from which they have been calculated (USNM 4989), allometric and inter-specific variation may account for the discrepancy between Direct 1 / 2 and Photo 1. This source of error can be eliminated by measurements of intervertebral distance taken directly from the specimen, but these data are not yet to hand.
2. The Photo 1 measurements shown here are all taken in the horizontal plane, but the direct measurements were presumably taken in the long axis of each measurement: the Photo 1 estimate would therefore be expected to be an underestimate of actual length. This discrepancy can be addressed through 3D analysis of the photogrammetric data collected by (Hampe and Leimkuhler 1996).
3. Hampe gives the length of the 17th vertebrae (d2) as 184 mm – this is considerably more than the measurements provided for both the 15th and 19th vertebrae. Compounding this, measurements for the vertebrae immediately adjacent to v17 were not provided by Hampe; and because these are estimated in Table 6-8 by averaging the measurements for their neighbouring vertebrae, the large measurement for v17 leads to comparatively large estimates for v16 and v18. If Hampe's measurement for v17 is an error, its effect on the estimate of body size will thus be exaggerated: for example, a measurement of 140 mm for v17 leads to a decrease of nearly 100 mm for torso and thus snout-hip length. For present purposes, it is assumed that Hampe's measurement of v17 is accurate, and it is included in the Direct measurements shown in Table 6-9.

Photographic methods: Comparing the results of the different photographic methods, the Photo 2 results closely resemble Photo 1, but the Photo 3 and Photo 4 give much larger estimates (Table 6-9, Figure 6-9, Figure 6-10). Assuming that the photogrammetric methods of Photo 1 are the most accurate, it is clear that aligning photo-mosaics by the reference plane of the scale bar gives more accurate results than aligning the photo-mosaic by the fossil. However, size estimates of the

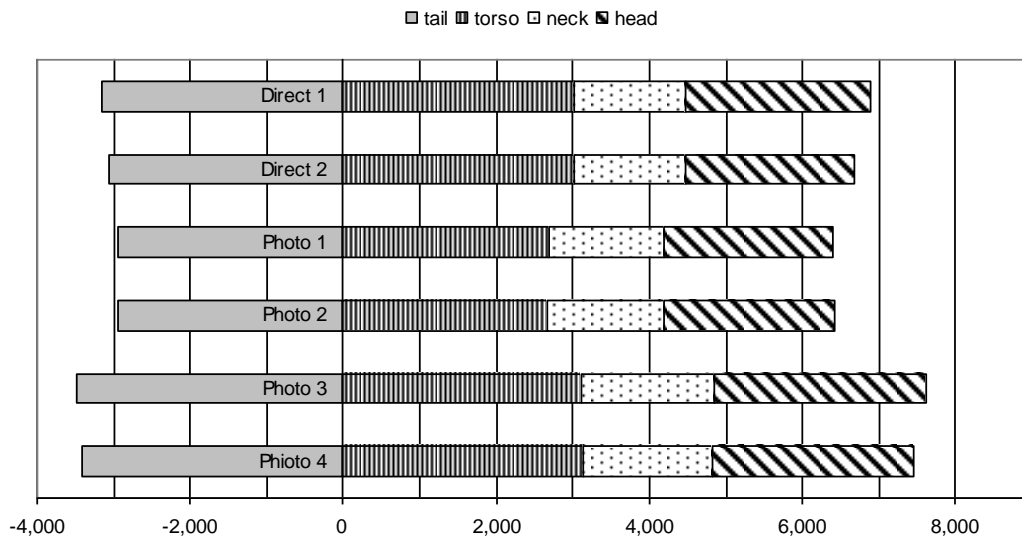


Figure 6-9: Body segment lengths (in mm) in *Kronosaurus boyacensis*.

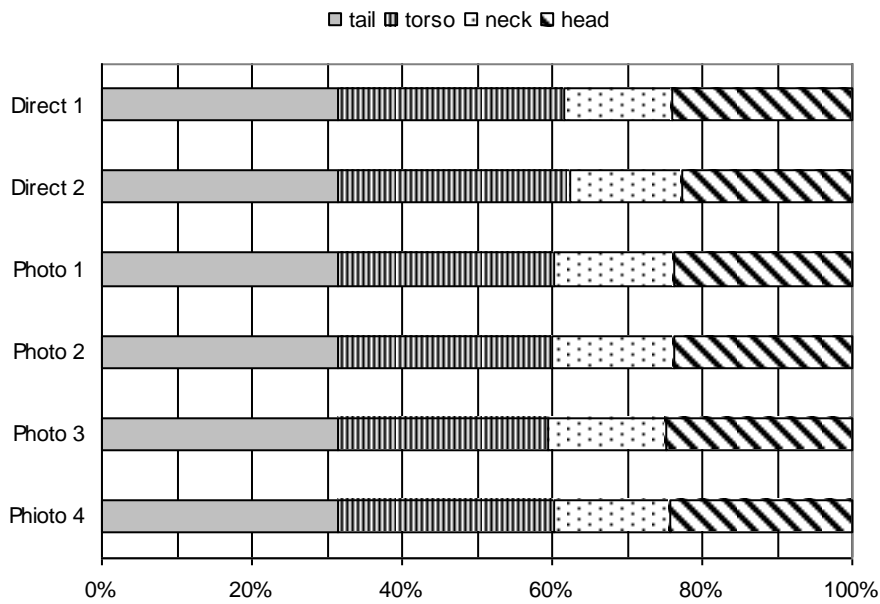


Figure 6-10: Body segment proportions in *K. boyacensis*.



Figure 6-11: The Harvard *Kronosaurus* (MCZ 1285), on display at the Museum of Comparative Zoology.

propodials are affected differently. For the humerus the Photo 2, Photo 3, and Photo 4 measurements all gave inflated results, while Photo 1 was very similar to the direct measurement provided by (Hampe 1992). For the femur, in contrast, the Photo 2 estimate was closer to that of the Photo 1 and Direct measurements, whilst the Photo 3 and Photo 4 estimates were inflated. This is likely a consequence of the humerus being visible in a single one of the frames used to produce the photo-mosaic, whilst the femur, like the whole skeleton, spans several overlapping frames (Figure 6-7, Figure 6-8).

Kronosaurus queenslandicus: MCZ 1285

Collected from the Aptian Doncaster Formation north of Richmond in 1931-2 by a Harvard University expedition led by W. Schevill, this specimen is historically important thanks to being mounted on display at the Museum of Comparative Zoology (MCZ) in Harvard since 1959. There are two relevant published accounts; an initial account of the cranial material (White 1935), and a summary of the postcranial skeleton (Romer and Lewis 1959). Evidently, the specimen includes a considerable amount of cranial and postcranial material: however, when placed on display the fossil was augmented with plaster to the extent that the original fossil material is difficult to discern, and earning the specimen the nickname 'Plasterosaurus' (Ellis 2003).



Figure 6-12: 'Kronosaur', Doug Henderson, 1989. This illustration is heavily influenced by the mount of MCZ 1285 at the Harvard Museum of Comparative Zoology. Used with permission.

The specimen is responsible for some extreme estimates of body size in *Kronosaurus*. White erroneously stated that the skull was 3720 mm in length, and gave the imperial equivalent of 9 feet 8 inches for this measurement – this latter is often given as the length for the skull in *Kronosaurus* in popular accounts. However, 3720 mm equates to 12 feet 2 inches: the metric equivalent of 9ft 8 inches is 2946 mm, which is much closer to the length of the skull in the mounted exhibit (the mandible is 2616 mm long). Following completion of the mount in 1959, the Total Length (TL) of the specimen was measured at 12.8 metres (Romer and Lewis 1959): at that time, the longest measurement for a pliosaur known, and taking into account the robust build of pliosaurs, leading to widespread acceptance of *Kronosaurus* as being the largest carnivorous reptile in the fossil record. This reputation persisted, despite the reports of the Cumnor mandible referred to *Stretosaurus* (Tarlo 1959), until the reconstruction of a total length of 18 metres in *Mosasaurus hoffmani* (Lingham-Soliar 1995). The largest marine reptile currently known is the Triassic ichthyosaur *Sbonisaurus sikanniensis* (Nicholls and Manabe 2004).

Compared with the reconstructed body shape in the Jurassic pliosaurids *Peloneustes*, *Pliosaurus* and *Liopleurodon*, the Harvard mount depicts an animal with a very large skull, short neck, and a long, barrel-like torso (Figure 6-11). Taken together with the robust parietal crest restored as part of the mount in 1959 (but which was not incorporated in White's original reconstruction of the skull), these body proportions of the Harvard mount have led to reconstructions of *Kronosaurus* as a rather more 'whale-like' than other large pliosaurs (e.g. Doug Henderson, 'Kronosaur', 1989 - Figure 6-12).

With the assistance of the MCZ, I was able to make detailed observations of this specimen in 1996. Those observations are summarized here, in two stages: firstly, an evaluation of how well the specimen as mounted agrees with the account published by Romer and Lewis (Table 6-10); and secondly, an assessment of the likely accuracy of the mount (Table 6-11, Table 6-13).

There are several discrepancies between Romer and Lewis' description and the specimen as mounted. There are no records of modifications to the mount since it was completed – thus, Romer and Lewis' account seems simply to have contained a number of errors, mainly concerning the position in the axial column of artificial vertebrae that were included to mitigate what were believed to be gaps in the fossil as collected. Romer and Lewis counted 46 preserved vertebrae – the mounted specimen actually contains the remains of 45, including cervicals, pectorals, dorsals, sacrals, and caudals. The posterior part of the tail is missing: the most posterior vertebrae in the mount that contains fossil material is the ninth caudal, which is the 56th vertebrae (v56) in the axial column of the mount. Forward of this point, 11 of the vertebrae in the mount are entirely artificial.

The rationale for the inclusion of these artificial vertebrae was evidently the presence of gaps between consecutive blocks as they were collected in the field. It is clear from Romer and Lewis' description of the specimen that they believed it to have been *in situ* prior to collection:

“The specimen had been entombed, in an articulated state, dorsal surface up, in a limestone matrix. In recent times, however, the skeleton had been

Description by Romer & Lewis (1959)	Observations on mounted specimen
<i>"Anteriorly, vertebrae 1-5 were found in position behind the skull"</i>	Agreed; these vertebrae seem to be well preserved
<i>"Following a short gap, 4 further vertebrae were present in another block.....interpolation of 3 vertebrae between the first and second series appears reasonable, and we shall consider the second series to include vertebrae 9-12".</i>	Again, that matches up with the mounted specimen - vertebrae 6, 7, and 8 are completely artificial, followed by four vertebrae that can be seen to contain original fossil material.
<i>"An isolated neural spine and arch appears...to have occupied a short gap following vertebra 12"</i>	This corresponds with what can be seen on the mount - vertebra number 13 is an artificial centrum, but the neural arch and spine contains fossil material.
<i>"The next block contained vertebrae 14-16. It was necessary to break up, in the field, the large mass containing the pectoral girdle region. This caused two further gaps, the first of which can be accurately determined to involve one segment; the second, following a series of 5 vertebrae - presumably 18-22 - seems certainly to have been occupied by 3 vertebrae".</i>	The mounted specimen does not correspond with this. In the mount vertebrae 14 to 17 contain fossil material, but vertebra 18 is completely artificial. There are then five vertebrae which contain fossil material, which are vertebrae 19 to 23 on the mount. Following that there are indeed three fake vertebrae.
<i>"There follows a series of 4 vertebrae, our numbers 26-29".</i>	Because of the miscount of vertebrae 14-17 (Romer and Lewis count them as 14-16), they is still one vertebra out in his count - the first vertebra of this series is number 27. But there are actually three vertebrae in this series, not four, so the last one is indeed number 29. The mistakes have, thus far, 'cancelled each other out'.
<i>"Behind this is a block with 2 vertebrae separated by gaps fore and aft. The first gap is of a length appropriate for 2 vertebrae; the second gap is short, but because of the imperfect nature of the vertebra behind it, it is uncertain whether a segment should be intercalated here, as we have done in the mount"</i>	This agrees with the mounted specimen. There are two artificial vertebrae (30 and 31), followed by two containing fossil material (32, 33), followed by another artificial one (34).
<i>"Back of this point, an unbroken series of vertebrae, which we have restored as numbers 35-43 can be traced to a point close to the puboischiadic suture on the underlying pelvic girdle. Here 1 vertebra is definitely missing, followed by vertebrae 45-48, found above the ischium, and 49-50 close behind them. Three further adjacent blocks contain 4 vertebrae and parts of the centra of 3 others, bringing the total as restored to this point to 57 vertebrae".</i>	Again, there is a discrepancy between Romer and Lewis' description and what can be seen on the mounted specimen. On the mount the unbroken series of vertebrae is comprised of numbers 35 to 44. Despite the fact that they were so definite about number 44 being missing, it is number 45 that is missing on the mount. Following vertebra 45, on the mount, there are 11 vertebrae that contain some fossil material - thus the last vertebrae that I could identify as containing fossil bone on the mount is vertebrae number 56, not number 57 as stated by Romer and Lewis. All the vertebrae after this point are fake.

Table 6-10: Published descriptions (from Romer & Lewis, 1959 – quoted passages are from page 4 of that reference) compared with personal observation of the mounted *Kronosaurus* specimen MCZ 1285. There are some discrepancies between the published account and the actual mount.

subject to erosion, so that it consisted essentially of a series of limestone nodules, freed from the underlying strata and nearly completely buried in the soil. Skull, neck, trunk and part of the tail were contained in a linear series of 15 nodules of varied size. Of these, the first had been displaced and overturned; the others, however, appear to have undergone little or no displacement. Erosion had destroyed much of the outer parts of the nodules so that, for example, most of the superficial bones of the skull had been destroyed, part or all of the neural spines had vanished, and the girdles, ribs, and abdominal armor were incomplete. Erosion had, further, destroyed some of the contacts between successive blocks, *but because of their seemingly undisturbed position, interpolation of materials once filling the gaps can be made with considerable confidence.* No trace of the pectoral limbs was preserved. The pelvic limbs were present in normal articulation, extending out on either side from the large block containing the pelvic region, but even the femora were badly weathered and the more distal regions of the ‘flippers’ were very poorly preserved”.

Romer & Lewis (1959: pp1-2) (my italics).

This interpretation of the specimen’s taphonomy is in contrast to typical marine reptile fossils in the Rolling Downs group (Chapter 3), where fossil-containing nodules ‘float’ to the top of the soil horizon from the underlying host bedrock layer, a process that involves both vertical and horizontal displacement of the nodules (c.f. the “Brazil-nut effect” – see discussion in Chapter 3). Romer and Lewis’ description of the nodules as being free from underlying bedrock is telling, because given this it is very unlikely that the nodules were still *in situ* with respect to the bedding layers by the time that they were excavated. When accompanied by weathering of the original contact surfaces between adjacent nodules, the displacement of the blocks can make the exact spatial relationships between the nodules difficult to discern. Because of the preparation of this specimen, which included complete removal of the fossil bone from the matrix, and the lack of documentation of the original appearance of the nodules collected in the field, it is impossible to establish whether adjacent nodules ever preserved contacts in this specimen. However, contact between adjacent nodules is preserved in comparable specimens from the Richmond area, such as QM F10113, and given that Romer and Lewis’ reconstruction of ‘missing’ vertebrae in the

Axial element	Mount interpretation	length (mm)	width (mm)	height (mm)	post-centrum gap (mm)	region	CRM interp 1
skull		2210	-	-	21	head	
v1	atlas	91.5	175*	235	-	neck	atlas
v2	axis	91.5	276	-	21	neck	axis
v3	c3	101	178	176	29	neck	c3
v4	c4	95.5	195	279	42	neck	c4
v5	c5	96	190	176	30	neck	c5
v6	(c6)	96	186	180	29	neck	c6
v7	(c7)	96	-	-	23	neck	c7
v8	(c8)	96	-	-	23		
v9	c9	96	-	-	18	neck	c8
v10	c10	101.5	-	-	26	neck	c9
v11	c11	109	-	-	36	neck	c10
v12	c12	107	-	-	33	neck	c11
v13	c13	106	-	-	19	neck	c12
v14	c14	96	-	-	16	neck	c13
v15	p1	109	-	-	18	neck	p1
v16	p2	118.5	190	197	19	neck	p2
v17	p3	123	192	193	15	torso	p3
v18	(d1)	124	-	-	11		
v19	d2	121	172	192	10	torso	d1
v20	d3	133	160	198	16	torso	d2
v21	d4	139.5	158	192	14	torso	d3
v22	d5	137	162	208	13	torso	d4
v23	d6	129	162	201	15	torso	d5
v24	(d7)	137	-	-	18		
v25	(d8)	135	-	-	13		
v26	(d9)	129	-	-	13		
v27	d10	144	165	204	13	torso	d6
v28	d11	141	165	214	14	torso	d7
v29	d12	140	165	216	14	torso	d8
v30	(d13)	142	-	-	14		
v31	(d14)	135.5	-	-	14		
v32	d15	135	175	210	14	torso	d9
v33	d16	146	171	206	16	torso	d10
v34	(d17)	140	-	-	15		
v35	d18	148	177	210	13	torso	d11
v36	d19	146	163	197	9	torso	d12
v37	d20	137	164	205	7	torso	d13
v38	d21	137	169	197	7	torso	d14
v39	d22	136	167	195	7	torso	d15

Axial element	Mount interpretation	length (mm)	width (mm)	height (mm)	post-centrum gap (mm)	region	CRM interp 1
v40	d23	136	161	188	6.80	torso	d16
v41	d24	134.5	151	190	6.73	torso	d17
v42	d25	136.5	155	187	6.83	torso	d18
v43	d26	140	154	189	7.00	torso	d19
v44	s1	135	150	182	6.75	torso	s1
v45	(s2)	133	-	-	6.65		
v46	s3	129	146	182	6.45	tail	s2
v47	s4	138	140	177	6.90	tail	s3
v48	cd1	125	138	174	6.25	tail	cd1
v49	cd2	125	143	175	6.25	tail	cd2
v50	cd3	127	166	178	6.35	tail	cd3
v51	cd4	108.5	172	176	5.43	tail	cd4
v52	cd5	111	179	162	5.55	tail	cd5
v53	cd6	120	187	172	6.00	tail	cd6
v54	cd7	110	183	169	5.50	tail	cd7
v55	cd8	123	172	175	6.15	tail	cd8
v56	cd9	110	177	170	5.50	tail	cd9

Table 6-11: Measurements and interpretation of the mounted specimen MCZ 1285. Lengths are taken on centra ventral surfaces; widths and heights at posterior centra faces except where marked * (anterior face). Vertebrae shown in parentheses ('Mount interpretation' column) are completely artificial. Head length is measured as BSL, pst-centrum gaps calculated by comparison of centra lengths with USNM4989 (see text). 'CRM interp 1' column shows the interpretation of vertebral counts favoured in this analysis (see text). Intervertebral gaps and body region calculated as for QMF10113 and the *K. boyacensis* holotype (see Table 6-6, Table 6-8 and text).

gaps between adjacent nodules was made without direct experience of the field conditions applying to this specimen, the following interpretation of MCZ 1285 is made with the assumption that most, if not all, of the 11 restored 'missing' vertebrae are not valid. Instead, the specimen is reconstructed with comparison to the preserved vertebral counts in USNM 4989, QM F10113, and the holotype of *Kronosaurus boyacensis*.

The mount restores a total of 8 additional, artificial vertebrae in the dorsal series, leading to a dorsal count of 26 vertebrae (Table 6-11). Note that the 'dorsal' vertebrae in this context does not include the three pectoral vertebrae which, identified on the basis of the position of the transverse process on the centrum and

neural arch (as for USNM 4989), are here identified as v14-v16 of the mounted specimen⁹. If all eight of these artificial vertebrae are assumed to be invalid, the adjusted dorsal count is then 19 (Table 6-11, ‘CRM 1’ and ‘CRM 2’), the same number interpreted for the dorsal series in USNM 4989. Hampe also listed 19 dorsal vertebrae for the holotype of *K. boyacensis*, although he indicated some uncertainty on the nature of the vertebrae that he listed as the first two sacrals – if either one or both of these are in fact dorsals *K. boyacensis* could potentially have 20 or 21 dorsal vertebrae. QM F10113 apparently preserves an entire dorsal series, but vertebrae in the pelvic region are somewhat obscured by matrix the exact location of the first sacral vertebrae in this specimen is yet to be determined. Romer and Lewis stated that the first dorsal (v18) could be accurately determined to be missing due to the dynamiting of the large pectoral block in the field – if this interpretation is accepted, then the minimum dorsal count for MCZ 1285 is 20 (Table 6-12).

The cervical series preserves 11 vertebrae which, when added to the three cervical vertebrae restored in the mount, gives a cervical count of 14 – higher than the equivalent in QM F10113 and USNM 4989, which both have 13 cervicals, and the holotype of *K. boyacensis*, which Hampe interpreted as having 12 cervicals. If MCZ 1285 is restored with two ‘missing’ cervical vertebrae, then the count matches QM

Interp.	cervicals	pectorals	dorsals	Total presacrals
Mount	14	3	26	43
CRM 1	13	3	19	35
CRM 2	12	3	19	34
CRM 3	13	3	20	36

Table 6-12: Four different interpretations of presacral vertebral counts in MCZ 1285; ‘Mount’, for specimen as mounted, including 33 preserved and 10 restored vertebrae. ‘CRM 1’, ‘CRM 2’, ‘CRM 3’, interpretations, accepting two, one, and three of the restored vertebrae as valid respectively (see text). Reconstructed body proportions for each of these is shown in Table 6-13.

⁹ Romer and Lewis identified v13 and v14 of the mount as pectoral vertebrae, although they did not specify how they were defining these terms. Because of the restoration of the specimen, it is difficult to be precise about which vertebrae in the mounted specimens are the three pectorals – assuming, of course, that MCZ 1285 does have three pectoral vertebrae, as do the other brachaucheniid specimens discussed in this chapter.

F10113 and USNM 4989 – if with one, it matches *K. boyacensis*. Assuming that all three of the restored cervical vertebrae are unwarranted, however, gives a cervical count of 11, which is outside the range described for brachaucheniids thus far.

The interpretation of MCZ1285 preferred here is ‘CRM 1’, with 13 cervicals, 3 pectorals, and 19 dorsals. This interpretation depends upon one of the restored cervical vertebrae as being unwarranted: circumstantial support for this comes from comparison with USNM 4989, where the proximal end of the rib on v12 indicates is of similar appearance and relative size in its proximal portion to that preserved on v13 of the MCZ 1285 mount: v14 of the MCZ1285 mount would thus, by analogy with USNM 4989, be a prothoracico-cervical, equivalent to v13 in USNM 4989, leaving v14-v16 as the pectoral vertebrae. The accuracy (or not) of this interpretation will be more certain once the pectoral vertebrae in other specimens of brachaucheniid – in particular, USNM 4989, QM F10113, RMFM R236 (see below), and the *K. boyacensis* holotype – have been described more fully, and at that point it would be worth re-visiting the anatomy of the pectoral region in MCZ 1285. The

Interp.	head	neck	torso	snout-hip	tail	TL	volume (litres)	femur length
Mount	2,231	1,989	4,285	8,506	3,904	12,409	17,888	1,060
CRM 1	2,287	1,870	3,156	7,312	3,356	10,668	11,366	960
CRM 2	2,256	1,751	3,156	7,163	3,288	10,451	10,684	-
CRM 3	2,308	1,870	3,291	7,469	3,428	10,897	12,113	-

Table 6-13: Estimates of body proportions for MCZ1285, using three different interpretations of the specimen. ‘Mount’; using measurements direct from the specimen as mounted (45 prescral vertebrae, i.e. accepting all the artificial vertebrae as real. ‘CRM 1’, assuming 13 cervical and 35 presacral vertebrae, as for USNM 4989 and QM F10113 (i.e. that of the artificial vertebrae in the mount, only ‘v6’ and ‘v7’ are legitimate). ‘CRM 2’, assuming 12 cervical and 34 presacral vertebrae, as for the holotype specimen of *Kronosaurus boyacensis* (i.e. that of the artificial vertebrae in the mount, only ‘v6’ is legitimate); ‘CRM 3’, assuming 13 cervical vertebrae and that Romer & Lewis’ reconstruction of ‘v18’ in the mounted specimen is legitimate. For ‘CRM 1’, ‘CRM 2’, and ‘CRM 3’, head length was estimated by making several predictions based upon comparison of different sections of the axial column with QMF10113, and taking the mean value of those predictions – the small variations in reconstructed neck and torso length produce slight variations in estimated head length. Femur length shown for ‘CRM 1’ is minimum length, based upon data from Romer & Lewis (1959). Linear measurements in mm; body sections defined as for QM F10113 and *Kronosaurus boyacensis* holotype (see Table 6-11).

details of the pectoral region anatomy are important because they affects the likely cervical vertebrae count for the specimen, an issue that potentially has taxonomic significance in addition to its bearing on estimates of size in this specimen.

It is important, however, not to assume that vertebral counts in plesiosaurians are invariable. In vertebrates, the Hox gene-controlled segment patterning is subject to variation between individuals, and even in organisms with conservative cervical vertebrae counts, such as mammals, a natural range of variation exists: for example, humans occasionally show one cervical segment more or less than the usual count of seven¹⁰ (Williams and Warwick 1980). The development of remarkably long necks in several families of plesiosaurians is likely to have involved a relaxing of the Hox gene regulation that constrains variation in vertebral counts in other groups of vertebrate, and intraspecific variation in cervical counts has been noted in members of the ultra long-necked family Elasmosauridae (Welles 1952). Interestingly, the specific pattern of Hox gene expression in plesiosaurian necks, as measured through recurring patterns of variation in centrum length between adjacent vertebrae within the cervical series, may be taxonomically significant (R. Forrest, pers. com.): patterns of vertebral dimension are known to be linked to phylogeny in cetaceans (Buchholtz 2007).

Given the verifiable vertebral counts in the other brachaucheniid specimens listed above, the most parsimonious interpretation is of MCZ 1285 is that the specimen as preserved is missing at least one and perhaps two cervical vertebrae, but is missing no more that one dorsal vertebrae and is possibly missing none. Given the taphonomy context of large vertebrate fossils from the Rolling Downs Group, the presence of gaps between the positions of adjacent nodules in the field is not considered to be sufficient evidence for the restoration of additional vertebrae. The result is an estimate of body length for MCZ 1285 that is considerably less than that reconstructed by Romer and Lewis: some of the different permutations of various cervical and dorsal counts for MCZ 1285 are shown in Table 6-12, and estimates of the body proportions based on these in Table 6-13, Figure 6-13 and Figure 6-14.

¹⁰ Apparently, a result of the rib on the seventh vertebrae forming a connection with the sternal basket and thus being classified as a thoracic.

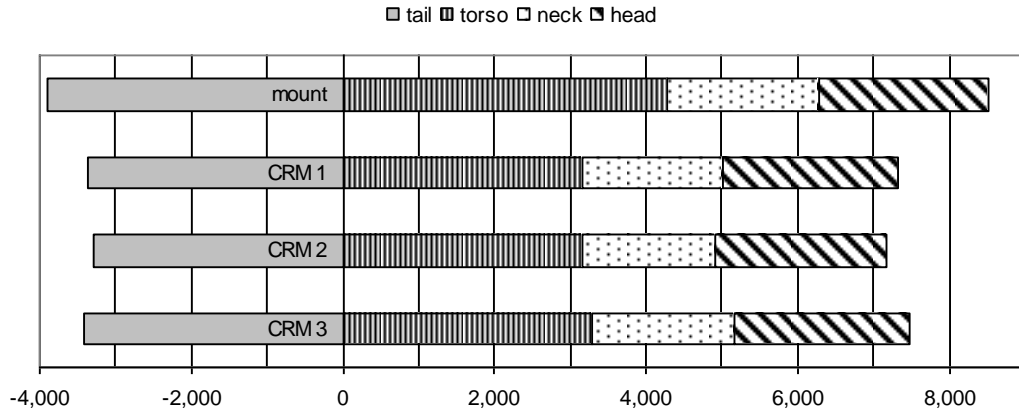


Figure 6-13: Body segment lengths (in mm) in MCZ 1285, according to differing interpretations of the preserved specimen. See Table 6-12, Table 6-13 and text for explanation.

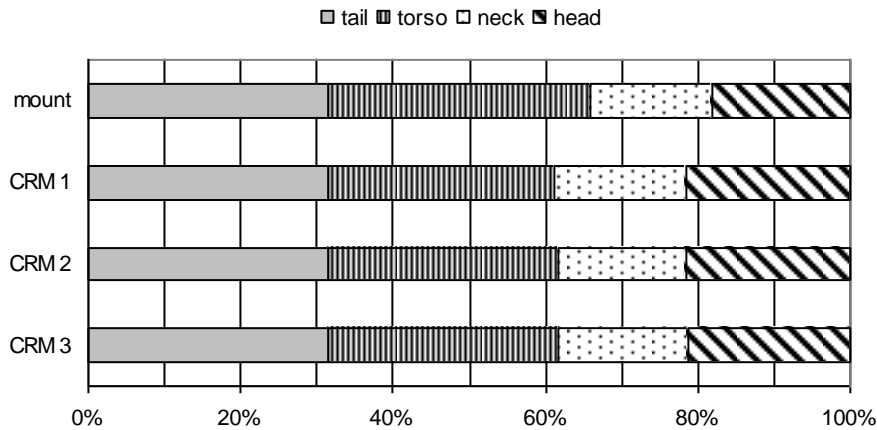


Figure 6-14: Body segment proportions in MCZ1285, for the data presented in Figure 6-13.

An uncritical acceptance of the mounted specimen gives a total length (TL) of 12.4 metres (compare with Romer & Lewis’ reconstructed length of 12.8 metres, which appears to include a proportionally longer tail), and a volume of 17.9 m³ (equating to 17.9 tonnes if a density of 1,000 kg/m³ is assumed). In contrast, the most generous of the revised interpretations (CRM 3) gives a TL of 10.9 metres and a volume of 12.1 m³, whilst the most conservative (CRM 2) gives a TL of 12.5 metres and a volume of 10.6 m³. Although not as large as initially reconstructed, MCZ1285 nevertheless represents a large individual, with a TL of 10.5–10.9 metres and a body mass of 10.6–12.1 tonnes.

***Brachauchenius* new species (*Villa de Leyva*).**

This specimen, from the Late Barremian (Early Cretaceous) of Colombia, was described by Hampe (2005) as an as yet unnamed new species of *Brachauchenius*. The overall appearance of the fossil as preserved (Figure 6-15) is similar to the holotype specimen of *Kronosaurus boyacensis*, although the new specimen is considerably smaller. Hampe referred it to *Brachauchenius*, despite the stratigraphic gap between this specimen and the Turonian (Late Cretaceous) *B. lucasi*, and the geographic and stratigraphic proximity of the new specimen to *K. boyacensis*, apparently on the basis of the cervical vertebrae count (13 in this specimen, compared with 13 in USNM 4989 and 12 in *K. boyacensis* – note, however, that the *K. queenslandicus* specimen QM F10113 has 13 cervical vertebrae)¹¹. No catalogue number is listed for this specimen: it is herein referred to as *Brachauchenius* sp. VL (*B. sp. VL*), following Hampe (2005).



Figure 6-15: *Brachauchenius* sp. VL. (from Hampe 2005). Note the compact body form and the superficial similarity of anatomy and preservation to the holotype specimen of *Kronosaurus boyacensis* (Figure 6-6, Figure 6-7, Figure 6-8).

¹¹ As noted earlier, it is possible that vertebral counts can be over-emphasised in plesiosaurian taxonomy.

Hampe provided measurements for the cervical series; these are shown in Table 6-14. The skull is largely complete but is missing the snout: Hampe reconstructed skull length as 120 cm but did not specify which measurement of skull length was being applied. By comparison with reconstructed skull length in *B. lucasi*, the BSL of this specimen is estimated at 1120 mm, which is longer than the BSL for USNM 4989. However, the cervical series is shorter than USNM 4989, suggesting that these specimens may have noticeably different body proportions. As yet, the extent of intra-specific variation in axial column proportions in pliosaurs is poorly understood, and whether this difference can be interpreted as support for Hampe's assertion that the Villa de Leyva specimen represents a new taxon remains an open question.

Table 6-15 shows two reconstructions of body proportions for this specimen: one based on extrapolating torso length by comparing the BSL estimate with USNM4989, the other by comparing neck length. Which of these is more accurate needs to be determined from further study of the specimen, which preserves the

Axial element	Interpretation (Hampe)	length (mm)	width (mm)	post-centrum gap (mm)	Region
skull		1120	-	11	head
v1	atlas	(43)	99	-	neck
v2	axis	(36)	106	8	neck
v3	c3	33	107	9	neck
v4	c4	46	83	20	neck
v5	c5	36	84	11	neck
v6	c6	39	94	12	neck
v7	c7	38	96	9	neck
v8	c8	37	94	7	neck
v9	c9	50	103	13	neck
v10	c10	43	104	14	neck
v11	c11	44	107	14	neck
v12	c12	49	117	9	neck
v13	c13	56	117	10	neck
v14	p1	58	-	10	neck
v15	p2	60	-	10	neck

Table 6-14: Measurements and interpretation of axial skeleton in *Brachauchenius* sp. VL. Figures in brackets are estimates; data from Hampe (2005). 'Post-centrum gap' is the intervertebral distance succeeding the respective vertebrae, calculated from data from USNM 4989 (Table 6-3). Skull length is reconstructed by comparison with USNM 4989 (Figure 6-3) and FHSM VP-321 (Figure 6-4).

Interp.	head	neck	torso	snout-hip	tail	TL	volume (litres)
B. sp. VL #1	1,131	823	1,538	3,492	1,603	5,095	1,238
B. sp. VL #2	1,131	823	1,813	3,767	1,729	5,496	1,554
B. sp. VL (mean)	1,131	823	1,676	3,630	1,666	5,296	1,396

Table 6-15: Estimated body proportions in *Brachauchenius* sp. VL, by comparison of neck length (B. sp. VL #1) and BSL (B. sp. VL #2) with USNM 4989; input values in bold. The proportions of skull and neck lengths are different to those reconstructed for USNM 4989, leading to different estimates of body size: in the absence of direct measurements of torso length, the two different estimates of torso length (and hence snout-hip, tail, and total lengths) have been taken as the average of the #1 and #2 estimates (B. sp. VL (mean)) for the purposes of analysis and discussion.

presacral series in articulation. A third reconstruction, based upon the mean values of these two, is used in the comparative plots discussed below.

Hampe also supplied measurements for the propodials – the specimen preserves a complete humerus and femur (Table 6-16). QM F10113 and the *K. boyacensis* holotype also preserve complete fore- and hind-propodials, and in each of these the humerus is shorter than the femur. However, in QM F10113 the humerus is 72% of the length of the femur, while in *K. boyacensis* it is 82% of the femur’s length. The relative lengths in the B. sp. VL specimen are more similar to *K. boyacensis* (81%): the relative propodial lengths in *B. lucasi* are unknown. These are the only three brachaucheniid specimens that preserve a complete humerus and femur, and although it is impossible to undertake statistical tests of hypotheses of allometric relationships with such a restricted dataset, the available specimens provide no support to the hypothesis that propodial length scales isometrically with body length (Figure 6-16). This in turn suggests that propodial length should be used with caution as a basis for estimates of body length in this group of pliosaurs.

	snout-hip	humerus	femur	humerus/femur
QM F10113	5,837	650	900	0.72
<i>K. boyacensis</i>	6,688	799	977	0.82
B. sp. VL (mean)	3,630	666	820	0.81

Table 6-16: Propodial lengths for the three specimens of brachaucheniid that preserve an intact humerus and femur.

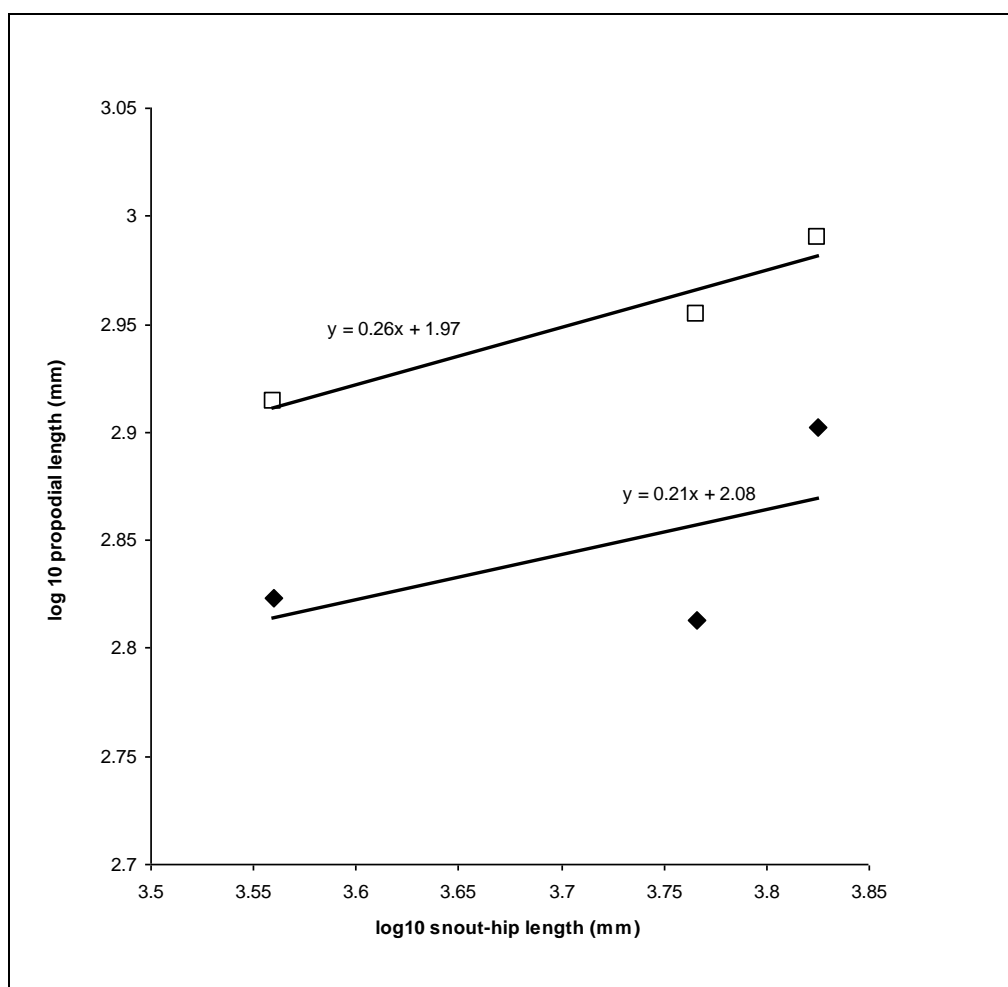


Figure 6-16: Log-log plot of propodial length to snout-hip length (data in mm) in three specimens of brachaucheniid (QM F10113, holotype specimen of *Kronosaurus boyacensis*, *Brachauchenius* sp. VL). Open squares, femuri; closed diamonds, humeri. Linear regressions for the femuri and humeri data points are shown to illustrate the apparent allometric relationship between propodial length and body length, but are each based on only three data points and are not intended to indicate statistically significant relationships

Other brachaucheniid specimens

Using the five specimens considered above as a template, body size in various other brachaucheniid specimens can be estimated. Table 6-17 shows estimates for the specimens containing that have been referred to cranial material that have been referred to *Kronosaurus queenslandicus* (Chapter 4), in addition to a large, complete skull of *Brachauchenius lucasi* (FHSM VP-321 - Figure 6-4) and a series of vertebrae on display at the Richmond Marine Fossil Museum¹² (RMFM R236).

¹² Known as 'Kronosaurus Korner' in publicity materials.

specimen	taxon	comparative specimen	comparative measurement	snout-hip	TL	volume (litres)
FHSM VP-321	<i>B.l.</i>	USNM 4989	DCL (1.37)	4,978	7,860	3,587
RMFM R236	<i>K.q</i>	MCZ 1285 (CRM 1)	l p1-p3 (0.97)	7,066	10,309	10,256
QMF 52279	<i>K.q</i>	K.q model/ QMF 10113	pf-n (0.7)	4,070	5,938	1,960
QMF 51291	<i>K.q</i>	K.q model/ QMF 10113	pf-n (0.64)	3,711	5,414	1,486
QMF 18827	<i>K.q</i>	K.q model/ QMF 10113	DCL (1.06)	6,159	8,986	6,793
QMF 18154	<i>K.q</i>	K.q model/ QMF 10113	pf-n (0.88)	5,113	7,460	3,886
QMF 2454	<i>K.q</i>	K.q model/ QMF 10113	pf-n (1.24)	7,239	10,561	11,027
QMF 2446	<i>K.q</i>	K.q model/ QMF 10113	pf-n (1.2)	6,998	10,210	9,964
MCZ 1284	<i>K.q</i>	QMF 10113	s-M1 (0.88)	5,129	7,483	3,922
QMF 1609	<i>K.q</i>	QMF 10113	MSW (0.7)	4,084	5,958	1,980

Table 6-17: Estimated body lengths for specimens of *Brachauchenius lucasi* (*B.l.*) and *Kronosaurus queenslandicus* (*K.q.*) specimens. All specimens listed are represented by cranial material, except for RMFM R286. ‘Comparative measurement’ lists the measurement upon which the body length estimate is based: DCL, Dorsal Cranial Length; pf-n, parietal foramen–nares planar distance; s-M1, snout to M1 tooth distance; MSW, maximum Mandibular Symphysis Width; l p1–p3, aggregate length of the pectoral vertebrae. For incomplete cranial material referable to *K. queenslandicus*, the *K. queenslandicus* skull model (Chapter 5), which is based upon the dimensions of QM F10113, was used for measurements of DCL and pf-n as these cannot be measured directly from QM F10113. Numbers in brackets (‘comparative measurement’ column) indicate the ratio of the specimen measurements to those of the respective comparative specimen.

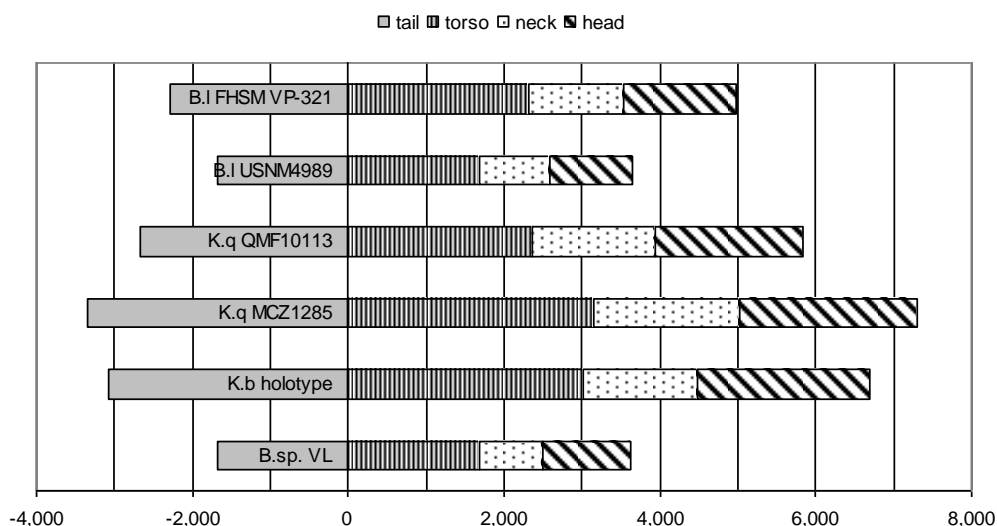


Figure 6-17: Body segment lengths (in mm) in brachaucheniid specimens, in stratigraphic order. This chart uses the 'Direct 2' interpretation of *K. boyacensis*, and the 'CRM 1' interpretation of MCZ1285 (see text).

The *B. lucasi* specimen FHSM VP-321 was compared with USNM 4989 on the basis of DCL (which was reconstructed in USNM 4989 by comparison with FHSM VP-321 on the basis of nares – parietal foramen distance). Figure 6-17 shows the reconstructed body segment length of FHSM VP-321, in comparison with the five more complete brachaucheniid specimens detailed above.

Body lengths in the *K. queenslandicus* specimens were derived by assuming isometry with MCZ 1285 (in the case of RMFM R236) and QM F10113 (for all the other specimens). The cranial material was compared with QM F10113 on the basis of Dorsal Cranial Length (DCL), the planar distance from the tip of the premaxillae to the centre of the alveolus for the first maxillary tooth (s-M1), the width of the mandibular symphysis across the position of the 4th dentary teeth alveoli (MSW), and the mean planar distance from the centre of the external nares to the centre of the parietal foramen (n-pf). RMFM R236 was compared with MCZ 1285 on the basis of aggregate vertebral length for the p1-d3 vertebrae (using the CRM 1 interpretation of MCZ 1285). The estimates of body segment lengths for these specimens are shown in Figure 6-18.

QM F2137 preserves two very large proximal heads from plesiosaurian propodials (Longman 1930): although weathered, they are 98-113% of the size of the femori heads in *K. boyacensis* (Hampe 1992). QM F33574, from the Aptian Doncaster Formation preserves a series of lumbar vertebrae and gastralia from a large brachaucheniid. Specific size estimates for these specimens have not yet been attempted.

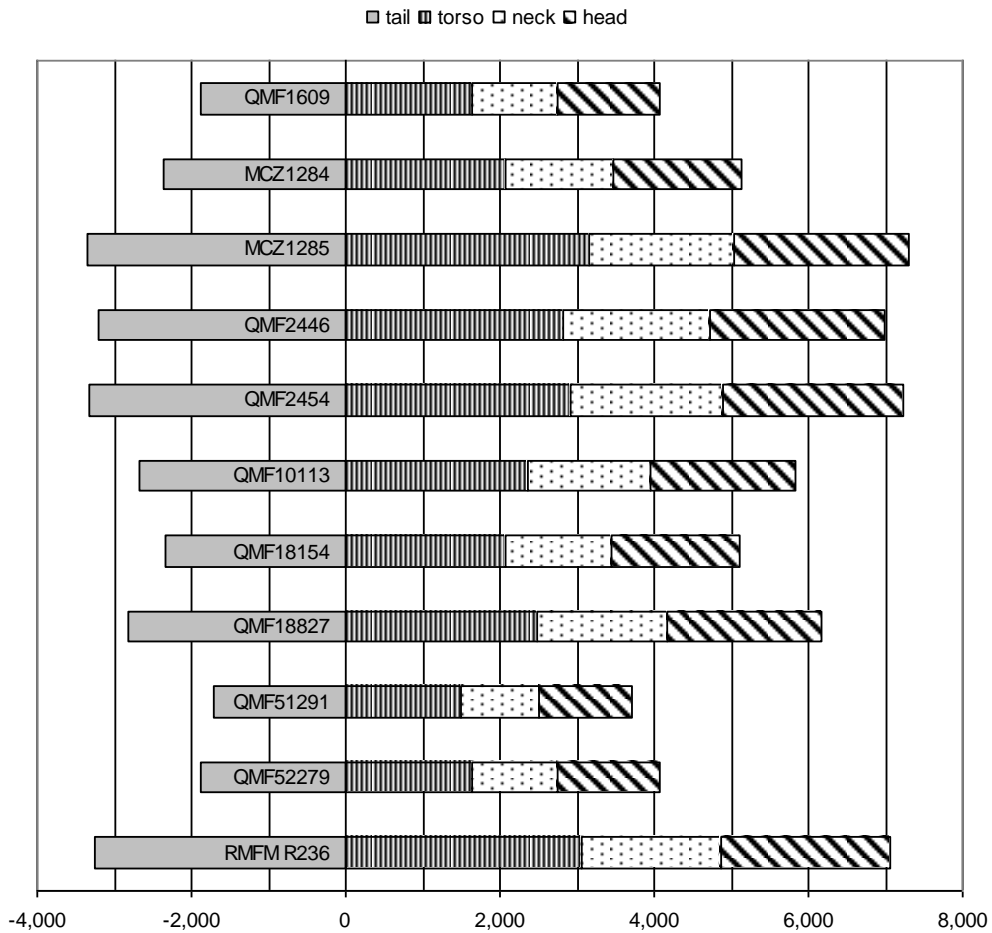


Figure 6-18: Body segment lengths (in mm) in *K. queenslandicus* specimens. See text and Table 6-17 for explanation of body size estimates.

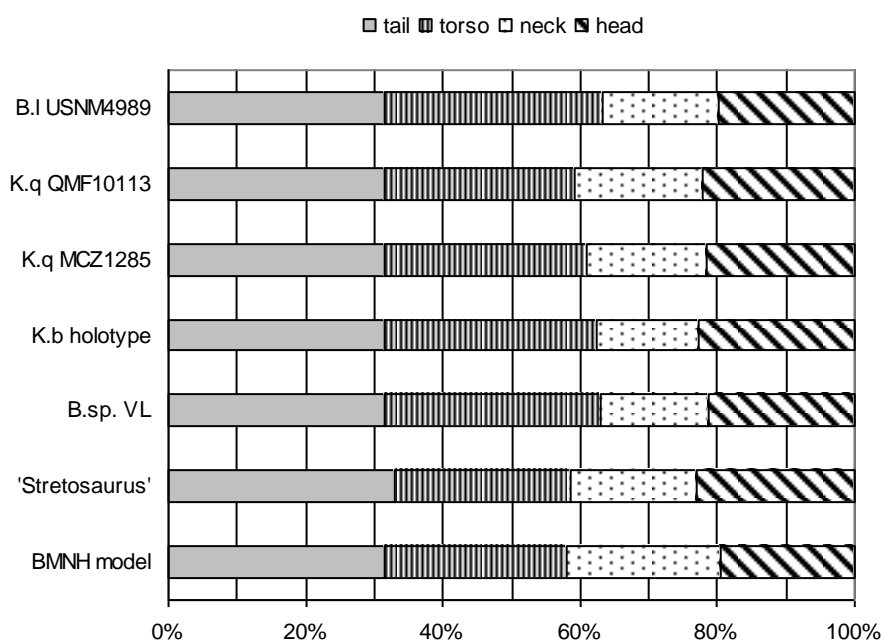


Figure 6-19: Body segment proportions in Jurassic and Cretaceous pliosaurids; *Brachauchenius lucasi* (B.l), *Kronosaurus queenslandicus* (K.q), *Kronosaurus boyacensis* (K.b), *Brachauchenius* sp. VL (B.sp. VL), Newman and Tarlo 'Stretosaurus' reconstruction, BMNH model. See text for explanation.

Body size in Jurassic pliosaurids

To provide a potential range for body size estimates, the two models used to estimate pliosaurid body proportions (the BMNH model, and the Newman and Tarlo 'Stretosaurus' reconstruction – see Methods) represent somewhat different interpretations of pliosaurid anatomy: the BMNH model has a shorter head and longer neck than the Newman and Tarlo pliosaur, which has a head that is relatively larger (as a proportion of snout to hip length) than any of the five brachaucheniid specimens analysed here (Figure 6-19). As 'small headed' and 'large headed' models of pliosaurids, their use as templates will, respectively, provide large and small estimates of body size from cranial measurements: these can be used to establish plausible upper and lower limits to the range of body size for each specimen.

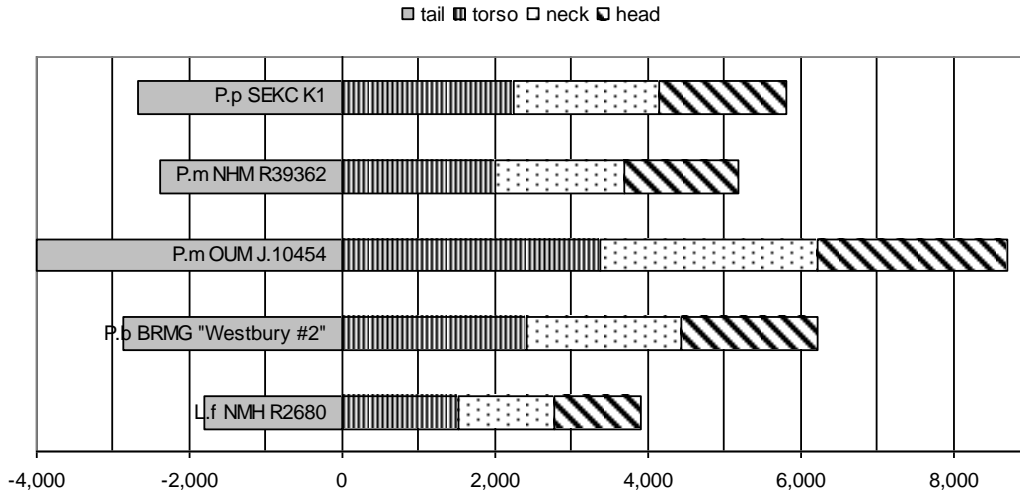


Figure 6-20: Jurassic pliosaurid specimens: estimates of body segment lengths (in mm) scaled according to BMNH model (see Table 6-18 for specimen abbreviations).

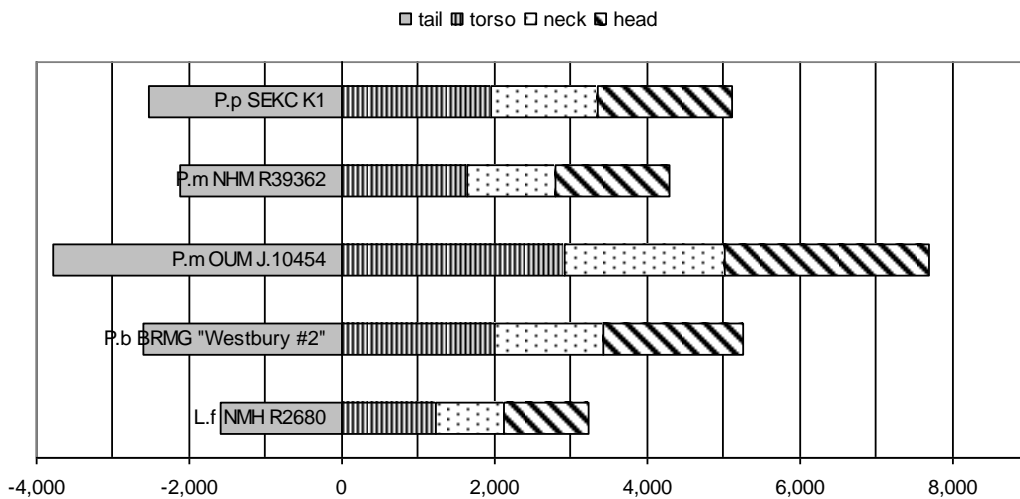


Figure 6-21: Jurassic pliosaurid specimens: body segment lengths (in mm), scaled according to 'Stretosaurus' reconstruction (Halstead and Newman 1967) – see Table 6-18 for specimen abbreviations.

Figure 6-20 shows the estimated body segment length for the five pliosaurid specimens represented by substantially intact skull material, when scaled by the BMNH model. Each estimate of Total Length is 110% - 117% of the corresponding estimate based upon the Newman and Tarlo pliosaur reconstruction (Figure 6-21): the variation in this range is a result of the differences in the relative proportions of the cranial measurements (BSL, JQA, ML) between the two models (Table 6-18).

Specimen	Taxon	BSL	DCL	JQA	ML	snout-hip	TL	volume (litres)
Scaled by BMNH model								
	BMNH model	42.4	41.7	44.9	50.9	148.1	216.0	0.094387
NHM R2680	<i>L. ferox</i>	1,120			1,344	3,909	5,703	1,736
BRSMG Cc332	<i>P. brachyspondylus</i>	1,785		1,890	2,142	6,229	9,088	7,026
OUM J.10454	<i>P. macromerus</i>	2,499			3,000	8,722	12,726	19,291
NHM R39362	<i>P. macromerus</i>	1,485			1,782	5,181	7,560	4,044
SEKC K1	<i>P. portentificus</i>	1,666			2,000	5,815	8,484	5,716
Scaled by 'Stretosaurus' reconstruction (Newman & Tarlo, 1967)								
	'Stretosaurus'	2,396	2,460	2,493	2,704	6,929	10,346	9,672
NHM R2680	<i>L. ferox</i>	1,120			1,264	3,239	4,836	988
BRSMG Cc332	<i>P. brachyspondylus</i>	1,816		1,890	2,049	5,253	7,842	4,213
OUM J.10454	<i>P. macromerus</i>	2,659			3,000	7,689	11,479	13,213
NHM R39362	<i>P. macromerus</i>	1,485			1,675	4,293	6,410	2,301
SEKC K1	<i>P. portentificus</i>	1,773			2,000	5,126	7,653	3,915

Table 6-18: Estimates of body size in selected large Jurassic pliosaurs. For each specimen, estimates based upon scaling by (1) BMNH model, and (2) 'Stretosaurus' reconstruction (Newman & Tarlo, 1967; Figure 6-2) are shown. For each specimen, skull measurements used to calculate body size are shown in bold: all other measurements are calculated by comparison with (1) or (2). Skull measurements for BMNH model are derived by fitting the 3D *Kronosaurus queenslandicus* skull to the model (Figure 6-1). Sources for skull measurements: *Liopleurodon ferox* NHM R2680 (Andrews 1913); *Pliosaurus brachyspondylus* BRSMG Cc332 ('Westbury #2' skull, direct measurement); *Pliosaurus macromerus* NHM R39362 (photo measurement); *Pliosaurus macromerus* OUM J.10454 (Tarlo 1959, Noè et al. 2004); *Pliosaurus portentificus* SEKC K1 (Noè et al. 2004). See text for discussion, and Figure 6-22 for comparison with Cretaceous brachaucheniid specimens. Linear measurements in mm. Abbreviations for skull measurements: BSL, basal skull length; DCL, dorsal cranial length; JQA, jaw to quadrate-articular, ML, mandible length – see text for definitions.

The largest specimen of pliosaurid, OUM J.10454 (*Pliosaurus macromerus* – the Cumnor mandible) is larger than any of the estimates for the brachaucheniid specimens (Figure 6-22), irrespective of whether the BMNH model or the Newman and Tarlo 'Stretosaurus' is used to establish body length. As the BMNH model is understood to better represent the body proportions of pliosaurid pliosaurs, the former estimate is preferred.

A. Vertebral measurements, scaling factors with comparative specimens

		length	width	height
measurement	PETMG R272	112	252.5*	219*
scaling factors	MCZ1285	1.17	1.33	1.24
	QMF 10113	1.93	1.42	
	<i>K. boyacensis</i>	1.40	1.19	

B. Comparative estimates of snout hip-length

snout-hip (comparative)	Estimated by:	length	width	height
7,312	MCZ1285	8,530	9,717	9,098
5,837	QMF 10113	11,271	8,279	
6,688	<i>K. boyacensis</i>	9,363	7,965	

C. Range of estimates of body size for PETMG R272

		snout-hip	TL	volume
from 'vertebral width' measurements	min	7,965	11,621	14,691
	mean	8,654	12,626	18,840
	max	9,717	14,177	26,670

Table 6-19: Estimates of body for PETMG R272 ('Peterborough vertebra'). **A**; Dimensions for R272, taken by direct measurements (*, average of measurements for anterior and posterior faces), and the calculated scaling factors of those measurements from equivalent measurements of the c5 vertebrae from three specimens of large brachaucheniid. **B**; Various estimates of snout-hip length by comparison of length, width, and height measurements with the three brachaucheniid specimens. Figures to the left of the comparative specimens numbers are snout-hip lengths for those respective specimens. **C**. The minimum, maximum, and mean of the estimates of snout-hip length in PETMG R272 by comparison with c5 width; TL and volume are calculated with reference to the BMNH model. All lengths in mm, volume in litres.

For less complete material indicating possibly larger specimens, results are based upon comparison with several candidate comparative specimens. The 'Peterborough vertebra' (PETMG R272), when compared by centrum width with the 5th cervical vertebra (c5) of QM F10113, MCZ 1285, and *K. boyacensis* holotype, is from an animal of an estimated 11.6–14.2 metres (mean estimate, 12.6 m) TL and 14.7–26.7 tonnes (mean, 18.8 tonnes) mass (Table 6-19). A similar method of comparison between the 1st dorsal (d1) of the Aramberri specimen and that of QM F10113, MCZ 1285, RMFM R236, and the *K. boyacensis* holotype gives a wide range of body size estimates, from 7.2–12.4 m TL and 3.6–17.8 tonnes body mass: the mean of the estimates made on the basis of centrum width is 11.7 m TL and 14.9 tonnes mass (Table 6-20).

A. Vertebral measurements, scaling factors with comparative specimens

		length	width	height
measurement	Aramberri	105	200	220
scaling factors	MCZ1285	0.87	1.16	1.15
	<i>K. boyacensis</i>	0.74		
	QMF 10113	0.87	1.29	
	RMFM R236	0.84		

B. Comparative estimates of snout hip-length

snout-hip (comparative)	Estimated by:	length	width	height
7,312	MCZ1285	6,345	8,502	8,378
6,688	<i>K. boyacensis</i>	4,963		
5,837	QMF 10113	5,065	7,531	
7,066	RMFM R236	5,935		

C. Range of estimates of body size for Aramberri specimen

		snout-hip	TL	volume
	min	4,963	7,240	3,553
	mean	6,674	9,737	8,642
	mean (by width)	8,016	11,696	14,976
	max	8,502	12,404	17,865

Table 6-20: Estimates of body size in the Aramberri specimen (Buchy et al., 2003). **A.**, Dimensions for the vertebra interpreted as d1 in the Aramberri specimen, from measurements given in Buchy et al. (2003), and the calculated scaling factors of those measurements from equivalent measurements of the d1 vertebrae from four specimens of large brachaucheniid. For the Aramberri specimen, length was taken as 105 mm, *contra* Buchy et al. (2003) – see text¹³. **B.** Estimates of snout-hip length, from comparison with the four brachaucheniid specimens. Figures to the left of the comparative specimens numbers are snout-hip lengths for those respective specimens. **C.** The minimum, maximum, mean of the estimates of snout-hip length in Aramberri specimen, by comparison with the various d1 dimensions in the comparative specimens: the mean of the estimates based on comparison of centrum width is also given ('mean by width'); TL and volume are calculated with reference to the BMNH model. All lengths in mm, volume in litres.

The large symphysis in the NHM collections has no catalogue number; it is referred to here as the 'NHM symphysis'. It bears 5 teeth in the symphyseal region; less than the 6½ symphyseal teeth in *Liopleurodon ferox* (Noè 2001) and *Pliosaurus macromeris*

¹³ Buchy et al. indicate that, for their 6th and 7th centra (here regarded as P3 and D1 respectively), "the length of the centra ranges from 90 to 105 mm, increasing cranially" (Buchy et al. 2003; p275). However, centrum length generally increases posteriorly (caudally) through the pectoral and anterior dorsal series in pliosaurs (see data presented above). In Table 6-20, the larger of these two lengths (105 mm) is taken here as the length of their 7th centrum (D1) for comparative purposes – this provides the more generous estimate of body size in the Aramberri specimen.

(pers. obs. of NHM R339362, Noè et al. 2004), but similar to the number in *Simolestes vorax* (Noè 2001). In the proportions of maximum symphyseal width to midline symphyseal length, the value for the NHM symphysis (0.75) exceeds *L. ferox* (0.45) and *P. macromerus* (0.47), but is less than *S. vorax* (1.02) (Table 6-21).

Body length estimates for the NHM symphysis were produced by comparison with *Liopleurodon ferox* and *Simolestes vorax*, using data on the mandibular proportions in these from (Noè 2001). Size estimates based upon 'Liopleurodon' skull proportions used the BMNH model as a template. *Simolestes* has a shorter skull for its width that does *Liopleurodon*; body size estimates of the NHM symphysis based on '*Simolestes*' skull proportions assumed that, for a given post-cranial length, skull length in *Simolestes* is 85% that of *Liopleurodon*. Size estimates were made by deriving an estimate of JQA for the NHM symphysis, and then scaling by the '*Liopleurodon*' (unmodified) or the '*Simolestes*' (modified) versions of the BMNH model accordingly. Estimates of JQA, and hence body size, were made by scaling from the respective models according to symphyseal length and symphyseal width (Table 6-21).

As the proportions of symphysis length: width in the NHM symphysis are intermediate to those of *L. ferox* and *S. vorax*, the estimate based upon *L. ferox* symphysis width greatly exceeded that based on length, and for estimates based on symphyseal dimensions in *S. vorax* the situation was reversed. There is considerable uncertainty in the estimates, which range from 9.1–15.1 metres (TL) and 7.1–32.4 tonnes (body mass).

The Stretham specimen of *Pliosaurus macromerus* is, judging from the femoral measurements provided by Tarlo (1959), of a similar size to large specimens of *Kronosaurus*. Tarlo listed femoral length in the Stretham specimen as 960 mm, which is slightly less than the equivalent measurement in the *K. boyacensis* holotype (Table 6-9, Table 6-16), and a total length of between 9–11 m seems reasonable for this specimen given the uncertainty surrounding the scaling of propodial elements in pliosaurids. Newman and Tarlo (1967) estimated the hindlimb span for the Stewartby pliosaur at 21 feet (6.2 m), which is very similar to the estimated hind-limb span in the *K. boyacensis* holotype (estimated from Figure 6-6) and this specimen also appears

Size

source	comparative specimen	symphysis width	symphysis length	JQA	ML	symp w/l
photo measurement	NHM symphysis	325	430	-	-	0.75
reconstruction (Noe, 2001)	<i>S.vorax</i>	164	160	910	1,027	1.03
reconstruction (Noe, 2001)	<i>L.ferox</i>	146	322	1,416	1,561	0.45
NHM R39362 (photo measurement)	<i>P. macromerus</i>	163	340	-	-	0.48

Size estimates for ‘NHM symphysis’

comparative specimen	compared by:	BSL	JQA	snout-hip	TL	volume
<i>Simolestes vorax</i>	symphysis width	1,701	1,801	6,682	9,887	9,895
	symphysis length	2,314	2,450	9,091	13,452	24,923
<i>Liopleurodon ferox</i>	symphysis width	2,970	3,145	10,366	15,124	32,384
	symphysis length	1,787	1,893	6,237	9,100	7,055

Table 6-21: Size estimates for the ‘NHM symphysis’: Top; measurements for the NHM symphysis and comparative specimens; ‘symp w/l’ is width: length ratio for each mandibular symphysis. Bottom; size estimates for the ‘NHM symphysis’ based upon comparison of symphysis length and width with *Simolestes vorax* and *Liopleurodon ferox*. All lengths in mm, volume in litres: data for *Simolestes vorax* and *Liopleurodon ferox* measured from figured reconstructions of maximum size in Noe (2001).

to represent a pliosaur of 9–11 m total length. The taxonomic identity of this ?Callovian specimen is, however, uncertain (see discussion of ‘NHM symphysis’ below).

Knight gave conflicting results (and identifications) of the propodial bone preserved with the holotype specimen of *Megalneusaurus rex*: it was first identified as a femur of 1200 mm length (Knight 1895), and then as a humerus of 990 mm (Knight 1898). Assuming that the later measurement is the correct one, the estimate of body size in *Megalneusaurus* depends on the true identity of the propodial. If it is a femur, then *M. rex* is a large pliosaur, perhaps between 11–12 m TL by comparison with *K. boyacensis*. If the propodial is a humerus, then *M. rex* is a very large pliosaur, perhaps the largest known: however, the measurements of vertebral centra provided by (Knight 1895) are not obviously larger than those of the large *Kronosaurus* specimens detailed above, and the propodial is here assumed to be a femur.

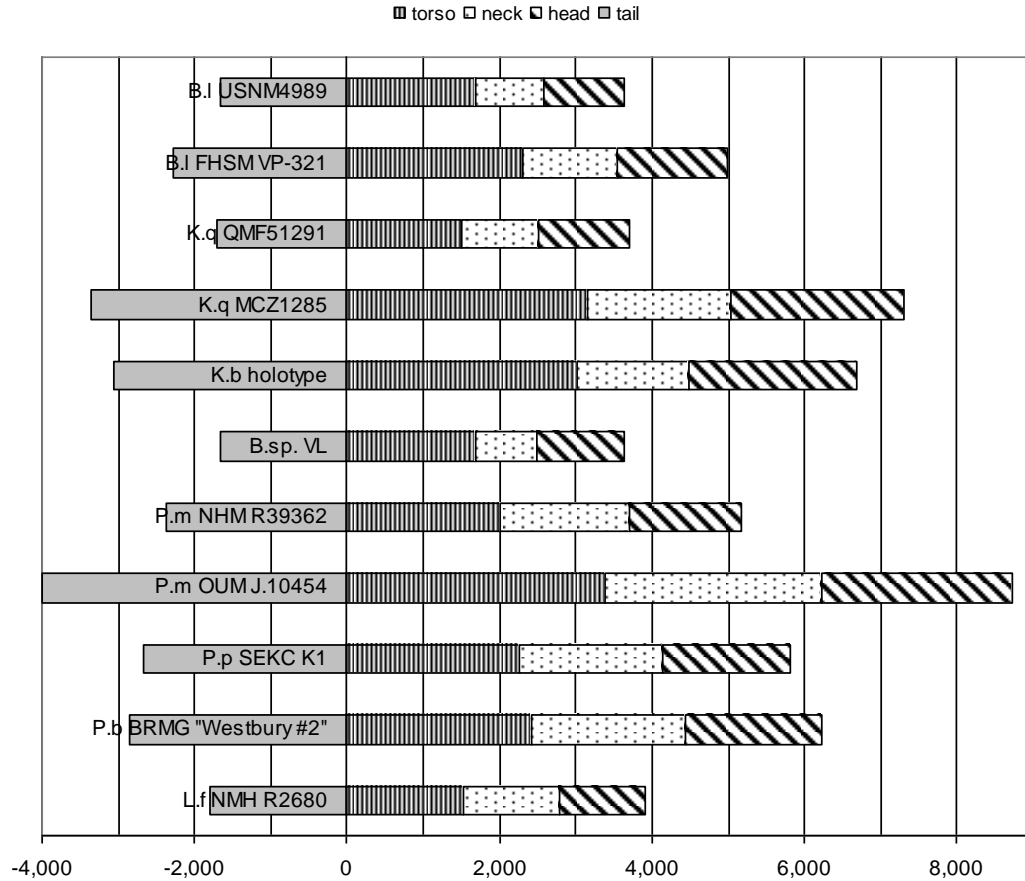


Figure 6-22: Body segment lengths (in mm) in Jurassic and Cretaceous pliosaurs. Includes smallest and largest specimens of species where applicable (*Brachauchenius lucasi*, *Kronosaurus queenslandicus*) and both specimens of *Pliosaurus macromeris* discussed herein. Included taxa; *Brachauchenius lucasi* (B.l), *Kronosaurus queenslandicus* (K.q), *Kronosaurus boyacensis* (K.b), *Brachauchenius* sp. VL (B.sp. VL), *Pliosaurus macromeris* (P.m), *Pliosaurus portentificus* (P.f), *Pliosaurus brachyspondylus* (P.b), *Liopleurodon ferox* (L.f).

The uncertainty inherent in estimates of body size based upon fragmentary material is high, and various techniques produce a range of estimates (Table 6-19, Table 6-20, Table 6-21). The pattern of variation of body size across a taxonomic group should preferably be based upon more complete specimens that include substantial portions of the cranial and/or post-cranial skeleton, and the currently known extent of this range for large pliosaurid and brachaucheniid pliosaurs is shown in Figure 6-22.

These show that the largest pliosaur specimen known from non-fragmentary remains is OUMJ.10454 (the ‘Cumnor mandible’), currently referred to *Pliosaurus macromeris* (Noè et al. 2004), which is here estimated (by comparison with the BMNH model) to have been 12.7 m in Total Length, with a body mass of 19.2 tonnes. Of the estimates

for fragmentary specimens given above, this size is exceeded only by taking the maximum estimates calculated for PETMG R272 and the 'NHM symphysis', although as discussed below those maximum estimates are of doubtful validity. The Aramberri specimen is estimated to be a smaller individual than the Cumnor specimen, even using a maximal estimate of size in the former for comparison.

6.4 Discussion

Limitations of this analysis

The attempts to reconstruct body size in this study are subject to a number of constraints. For the five brachaucheniid specimens that preserved significant cranial and postcranial remains, the estimates of body mass from length are based upon only one body form; and that is derived from a family of pliosaurs (the Pliosauridae) with different body proportions to the group that is the primary focus of this work, the Brachaucheniidae. None of the brachaucheniid fossils analysed here are preserved with complete tails, which is another potential source of error, although the emphasis on paraxial locomotion in plesiosaurs means that tail length is unlikely to be a critical component of body size in this group.

The additional *Kronosaurus queenslandicus* specimens included in the size estimates, i.e., those including mainly cranial material (Chapter 4), represent animals from a number of size classes. However, body size in these has been estimated by assuming isometry with the more complete specimens. Moreover, the smaller specimens preserve incomplete skulls, and overall skull length in these was reconstructed by assuming isometry with more complete material from larger animals. In particular, dimensions from the circum-orbital region and the anterior snout were used to reconstruct skull length in the less complete specimens, and isometry was assumed in all cases. However, the eye and the orbits is known to be strongly allometric in all amniotes, and the observable growth pattern of the anterior snout in large species of living crocodylians (see below) suggests that dimensions of the mandibular symphysis and tooth-bearing parts of the premaxillae may also be strongly allometric. Future

attempts to refine body size estimates in this material should account for the pattern of allometric growth in the skull of *Kronosaurus*.

Estimates of body lengths in the five Jurassic pliosaurids represented by good skull material are made with the assumption that the proportion of head size to body size lies within the range delineated by the BMNH model and the Newman and Tarlo 'Stretosaurus' model. For estimates based on the BMNH model, errors in fitting the 3D model of the *Kronosaurus queenslandicus* skull to the overall body shape will greatly affect predictions of body size in these taxa (this problem does not apply to the estimates of brachaucheniid specimens, because those are based upon comparisons of snout-hip length). The proportions of the four principle metrics of skull length in these pliosaurids (BSL, DCL, JQA, ML) are assumed to be as for the *K. queenslandicus* model; this is likely to be another source of error. Quantitative data on the relationship between skull size and that of major regions of the postcranium in large pliosaurids would allow better estimates of body size in these taxa.

To the estimates of body size for the very large, partial pliosaurid material, all of the above points of uncertainty apply, in addition to several more. Estimates made on incomplete series of vertebrae, or even a single vertebrae, are subject to the natural variation of vertebral dimensions and should be used with caution. The dimensions of individual vertebrae can be affected by taphonomic processes, in particular sedimentary compaction, and when size estimates are extrapolated from single elements small errors can be greatly magnified. The same applies to any allometric variation than is not accounted for in scaling models; as yet, the allometry of the axial skeleton in pliosaurids and brachaucheniids is undocumented. In addition to all of these, the size estimates for isolated pliosaurid vertebrae are herein made in comparison with brachaucheniids, a family known to have different proportions of the axial column (viz, a shorter neck). However, any estimates based upon more complete pliosaurid material requires extrapolation over at least an order of magnitude of body mass, a leap that means even small errors in the estimate of allometric or intraspecific variation will produce a large range of results.

The patterns of variation within closely related marine reptile groups has been documented in ichthyosaurs, where vertebral counts are conservative but vertebral proportions, in particular length, vary in step with overall body length (Motani et al. 1996). Pliosaurids and brachaucheniids have similar vertebral counts in the torso, but differ markedly in the cervical series; however, the extent of variation in vertebral shape that accompanies this has not been documented. The estimates presented here of the very large pliosaurid specimens, that are based on vertebral material, are made with an emphasis on vertebral width as a correlate of body size, but the validity of this has not been tested and for the present the most relevant aspect of these estimates is the large range that is produced from different comparisons. It is likely that data on the correlation of body size with various parameters of vertebral morphology from living large marine amniotes such as cetaceans would be useful in identifying the most relevant aspects of vertebral shape (Buchholtz 2001). The possibility of osteological indicators of CNS morphology, e.g. neural arch dimensions of the pectoral vertebrae as an indicator of brachial plexus size (Griffin 1995), as correlates of body size could also be examined in the extant groups of marine amniote.

Limb bone dimensions do correlate with body size, and where the scaling relationships between e.g. propodial dimensions and body size have been quantified, various studies have applied this to terrestrial mammals (Anderson et al. 1985), terrestrial reptiles (Erickson et al. 2004), and aquatic archosaurs such as crocodylians and phytosaurs (Farlow et al. 2005, Hurlburt et al. 2003). Pliosaurian propodials are massive elements that tend to preserve well in the fossil record, and some specimens indicate very large animals. However, even though the scaling of limb size in plesiosaurs appears to be negatively allometric (Kear 2007, O'Keefe and Carrano 2005), the relationship has not been quantified for propodial elements in pliosaurs and thus body size estimates based upon these must remain qualitative. Where a propodial from a fragmentary specimen appears to significantly exceed the known size range from more complete material, estimates should be especially cautious. A complicating factor is that, in pliosaurids and brachaucheniids, gross morphology of the humerus and femur is very similar and if preservation is not excellent they can be difficult to distinguish: however, the humeri in both families are always smaller than

the femora, being 70-85% of the length of the femora (Andrews 1913; Table 6-16). Thus the estimated body size, qualitative or quantitative, of a propodial of uncertain anatomical identity will depend greatly on whether it is identified as a fore- or hind-limb element.

In vertebrates, the morphology of the rostrum and anterior mandible is variable amongst related species, to a much greater extent than are vertebrae and limb elements. This variation is correlated with inter-specific differences in feeding ecology and can be a useful feature for species level taxonomy: the corollary is that estimation of head and body size from fragmentary remains of the anterior jaw depends to a very large extent on accurate taxonomy identification of the specimen in question. This is further complicated by allometric growth of the head skeleton, in particular the macrocephalic growth of large adults that has been demonstrated in crocodylians and turtles (Cann 1998, Legler 1981, Webb and Messel 1978). The possibility of macrocephalic growth pattern in pliosaurs is raised by the NHM symphysis; however, this specimen is very incomplete and of uncertain taxonomy, factors which also create considerable uncertainty about the body size of that animal. The taxonomy of this specimen, and the possibility of macrocephaly in other pliosaur specimens, warrant further study.

Quantifying error in body size estimates

In living animals of a given body length, body mass is subject to variation within individuals, between individuals, and between species, all of which cause statistical error for estimates of body mass based upon body length. Estimates of body mass in large marine organisms are also subject to considerable measurement error for logistical reasons.

Error in body mass estimates cannot be quantified directly in fossil groups. Further, this study uses a single model of body length to body mass, which does not allow any statistical evaluation of error in these estimates. Statistical error in body mass prediction has been calculated for crocodylians (Farlow et al. 2005, Webb and Messel 1978); pliosaurids and brachaucheniids have a more compact body form, and

quantitative error in body mass estimates may correspond with that of fusiform shaped taxa, such as odontocetes, pinnipeds, penguins, lamnids, and scombroids.

An alternative, and perhaps complementary, approach would be to construct several plausible ‘flesh’ reconstructions of different species of taxa and examine the variation of the resulting volumes for given lengths. However, this would be preferably based upon a robust understanding of postcranial anatomy in pliosaurs; current knowledge is still facing some fundamental questions (Nicholls and Russell 1991).

The error of body length predictions from fragmentary specimens can be quantified directly in fossil groups by comparing such specimens with more complete examples of the same taxon, but such data has yet to be compiled for pliosaurs. Complete (or nearly complete) specimens that are preserved in natural articulation are especially valuable for work of this kind, and such specimens do exist for brachaucheniids: three of the five specimens considered in detail in this study are preserved in this fashion, and the preservation of the fourth (QM F10113) can be reconstructed with confidence (work in progress). It is likely that MCZ1285 was preserved in natural articulation, but the data required to reconstruct this was lost when the specimen was prepared. In addition to the brachaucheniids mentioned, there are several rhomaleosaurid (Cruickshank 1994, Owen 1838, Smith and Dyke 2008, Storrs and Taylor 1996) and polycotyloid (Druckenmiller 2006, Druckenmiller and Russell 2008b) specimens that could be serve as a basis for the statistical analysis of the relationship between various skeletal elements and overall body length. In contrast, only two specimens of pliosaurid appear to have been complete and articulated when collected – a specimen of *Peloneustes phylarchus* (Andrews 1910b) and the mounted specimen of *Liopleurodon ferox* at the Universität Tübingen Museum, (Noè 2001) – but these have been removed from their matrix and thus data on e.g intervertebral joint distance has been lost (although they are still valuable comparative specimens). The rarity of complete and articulated pliosaurid specimens is perhaps surprising given the fossiliferous units from which they are known, especially the Callovian Oxford Clay and the Kimmeridgian Kimmeridge Clay: however, given the softer matrix characterising these units, specimens were historically collected by removal from the matrix, and the manual excavation of ‘brick pit’ quarries, that led to an abundance of

finds in the 19th Century, has been replaced by mechanical excavation. The value of specimens that are preserved in articulation should ideally be a factor in the decisions of how to excavate/prepare complete or nearly complete pliosaur fossils.

The present study does not attempt to analyse error in body length estimates statistically; however, where different methods produce a range of estimates for a specimen, these have been given.

Taphonomy

In this study, interpretation of a once-articulated specimen (MCZ 1285) is assisted by comparison with a specimen that is still preserved with some taphonomic data intact (USNM 4989); this illustrates the importance of taphonomic data in studies of body size. Good taphonomic data relating to the postcranial anatomy remains intact (but as yet uncollected or unpublished) for QMF 10113, the holotype of *K. boyacensis*, and the *Brachauchenius* sp. VL specimen.

Estimates of body size based on skeletal material depend on, amongst other things, accurate measurement of intervertebral distances; these can comprise up to 20% of the total length of the axial column (Finch and Freedman 1986). Intervertebral distances are preserved in USNM 4989, and this data is used as a basis for extrapolation of body lengths in other specimens. However, the fossil only preserves the intervertebral distances at the time of burial, which include any post-mortem change in the dimensions of the joints, such as can be reasonably expected in synovial joints exposed to a hypertonic medium. The extent of likely preburial change in intervertebral joint distances could be assessed through an actuo-palaeontology approach to the taphonomy of modern carcasses on the sea-floor (Schäfer 1972).

The taphonomy of pliosaur specimens is important for other reasons. The fact that all of the articulated brachaucheniid specimens discussed in this paper are missing the tail may have implications for reconstructions of the caudal soft-tissue anatomy, as long as the taphonomic circumstances of each specimen can be documented. As discussed above, the preservation of USNM 4989 may have implications for

understanding of post-cranial anatomy in plesiosaurians, in particular the presence (or not) of a sternum and thoracic region of the trunk (Nicholls and Russell 1991), which in turn has importance for interpretation of body proportions and functional anatomy in the group as a whole. However, the specimen was collected in the late 1880s without the documentation that is now considered necessary for taphonomic interpretation of a specimen; the possibility that the missing trunk elements were quarried before the specimen could be recovered substantially reduces the confidence that be placed in taphonomy based interpretations of this specimen (Everhart 2007). Future collection and studies of articulated pliosaur specimens should be conscious of the need to maximise the taphonomic data recovered; new technologies, such as photogrammetry and 3D scanning, can potentially be invaluable for this type of work.

Body proportions in brachaucheniids: taxonomic implications

One of the aims of this work is to address some of the uncertainty in the species level taxonomy of the Brachaucheniidae, in particular *Kronosaurus queenslandicus*. Currently, two valid species of *Kronosaurus* are recognised; *K. queenslandicus*, the genotype, described from Albian and Aptian strata of Queensland, Australia; and *K. boyacensis*, known from the Aptian of Colombia.

The holotype of *Kronosaurus queenslandicus* is QM F1609 (Longman 1924), from the late Albian Toolebuc Formation: the specimen is a jaw fragment from a large pliosaur but is not diagnostic to a genus or species level. However, the Toolebuc Formation has produced numerous fossils from large pliosaurs, including cranial and postcranial material: at present, there is no evidence that more than one taxon of large pliosaur is present in the Toolebuc fauna (Chapter 4), and this material can be confidently assigned to *Kronosaurus queenslandicus* Longman. On the basis of the cranial material, *Kronosaurus queenslandicus* can be distinguished at the genus level from all other valid pliosaurs (Chapter 4). One specimen (QM F10113) preserves significant portions of the cranial and postcranial skeleton, and this is largely articulated.

Kronosaurus boyacensis is known from a single articulated specimen (Hampe 1992, Hampe and Leimkuhler 1996). Erosion of the specimen has obscured the finer

details of cranial osteology, but the specimen can be distinguished from the Toolebuc specimens of *Kronosaurus queenslandicus* on the basis of the post cranial anatomy and, if the premaxillary tooth count in *K. boyacensis* (i.e., five – Hampe 1992) is confirmed¹⁴, upon cranial characters also. Hampe (1992) listed 12 cervical vertebrae for *K. boyacensis*, in contrast to the 13 preserved in QM F10113. The proportions of the head: neck: body length in *K. boyacensis* appear to be different from those of QM F10113 (Figure 6-19), although this depends in part upon which reconstruction of body segment lengths in *K. boyacensis* is preferred (Figure 6-10), underlining the importance of continued study in this specimen. In addition, the proportion of humerus to femur dimensions is markedly different between the two taxa: *K. boyacensis* has a longer humerus relative to femur length (Table 6-16). The two species can be distinguished from other large pliosaurids on the basis of cranial features, including overall cranial proportions and the morphology of the teeth, and also on the basis of post-cranial anatomy and proportions. They can be distinguished from *Brachauchenius*, on the basis of cranial morphology, but the question of whether their generic assignment is taxonomically valid may hinge upon confirmation of the premaxillary tooth count in *Kronosaurus boyacensis* – if *K. boyacensis* does have five premaxillary teeth (Hampe 1992) then it may be appropriate to separate it from *Kronosaurus queenslandicus* at the genus level (see Chapter 4, Section 6.6 below).

Hampe (1992) reported possible pachyostosis in the ribs of *K. boyacensis*, a feature which has been cited as an additional point of difference between the two species of *Kronosaurus*. The terminology surrounding the geometry of osteo-histology and anatomy has historically been used inconsistently, especially between zoologically and medically oriented workers: Gray and colleagues offer a standardised terminology aimed at marine mammals, which will be followed here (Gray et al. 2007). As defined by Gray et al, pachyostosis involves component of overall bone geometry ('robust' or 'massive' bone) and histology (thickened cortical layer of bone). Hampe did not examine the histology of the ribs, and his comments about pachyostosis referred to

¹⁴ I don't wish to labour this point – Hampe's description of *K. boyacensis* is thorough and I have no good reason to doubt any aspect of it. It is simply that the exact premaxillary tooth count has significant potential importance to the species and genus taxonomy of the Early Cretaceous brachaucheniids (Section 6.6 below) and, based upon my own experience with specimens of *Kronosaurus queenslandicus* that seem to exhibit similar preservation to the holotype of *K. boyacensis* (Chapter 4), this feature cannot always be discerned with confidence.

massive external appearance of the ribs (O. Hampe, pers. comm.). It is entirely possible that the ribs show thickened cortical layers as well, but for the time being this remains unexamined. The ribs in *K. queenslandicus* are not histologically pachyostotic, but are large as viewed externally (pers. obs. of QM F10113): whether they are as robust as those in *K. boyacensis* requires morphometric data that has not been collected. It therefore remains unknown to what degree Hampe's report of pachyostosis in *K. boyacensis* can be used to distinguish the two species, although this is an obvious point of interest for future research. Pachyostotic histology has been reported in other pliosaurs – *Liopleurodon ferox* (Andrews 1913), *Pachycostasaurus dawni* (Cruickshank et al. 1996) – and in several extant marine mammal taxa, notably sirenians (Domning and Buffrénil 1991), the beluga whale *Delphinapterus* (Brodie 1989), the dense beaked whale *Mesoplodon densirostris* (MacLeod 2002), and the sea otter *Enhydra lutris* (Gray et al. 2007), as well as the extinct archaeocete *Basilosaurus* (Buffrénil et al. 1990).

In addition to the specimens of *Kronosaurus queenslandicus* known from the Albian Toolebuc Formation of Queensland, material from large pliosaurs has been collected from the underlying Aptian Doncaster Formation (Romer and Lewis 1959, White 1935 – see Chapter 3). On the basis on preserved cranial and post-cranial features, the Doncaster material is referable to *Kronosaurus*. That the Doncaster material represents the Brachaucheniidae is shown by the lack of sub-central foramina on the vertebrae, a state which in pliosaurs is known only for *Brachauchenius* and *Kronosaurus* (and is hence diagnostic of the Brachaucheniidae). The premaxillae bear four teeth (MCZ 1284), as with the *Kronosaurus queenslandicus* material known from the Toolebuc Formation and which, in a large pliosaur, diagnoses the material to at least the genus *Kronosaurus* (see Section 6.6). In none of the features that can distinguish sympatric pliosaur taxa in other faunas – tooth crown ornamentation, premaxillary tooth count, morphology of the mandibular symphysis – can the Albian and Aptian Queensland material be distinguished. Detectable variation between the Doncaster and Toolebuc material is, as far as can be determined, within the range of ontogenetic and/or taphonomic variation (Chapter 4). However, although one of the Doncaster Formation specimens (MCZ 1285) preserves extensive postcranial material, it does not preserve any of the post-cranial features that can be used to differentiate *K.*

queenslandicus from *K. boyacensis*, i.e. both fore and hind propodials, or a complete complement of cervical vertebrae. MCZ1285 seems once to have preserved a complete cervical series, but the information required to specify an accurate count has been lost due to the way that the specimen was collected and prepared. Molnar (1991) stated that MCZ 1285 represented a different species to the Toolebuc material on the basis on differences in cranial proportions, but these differences are undoubtedly a result of taphonomy (Chapter 4). The MCZ specimen is the largest specimen of *Kronosaurus* known, but some of the Albian material (QM F2454, QMF 2446) is in a similar size class and body size cannot distinguish between the two sets.

In the context of present knowledge, the referral of the Aptian Doncaster Formation *Kronosaurus* material to *K. queenslandicus* is made (1) on the basis of the description of five premaxillary teeth in *K. boyacensis* (Hampe 1992), and (2) with respect to the shared geography of the Queensland material. Stratigraphically, however, the Doncaster *Kronosaurus* material is closer to the Late Barremian–Early Aptian *K. boyacensis* from Colombia. An emphasis of geographic over stratigraphic correlation may not be a biologically realistic premise; an apex marine predator of the size of *Kronosaurus* can reasonably be expected to have a cosmopolitan distribution, as do modern large carnivorous odontocetes and lamnids such as *Physeter*, *Orcinus*, *Pseudorca*, *Carcharodon*, and *Isurus*. Further, during the Early Cretaceous, Colombia and Australia were at opposite sides of the Gondwanan supercontinent; although the break up of the continent had commenced in the Jurassic, and several of the Gondwanan terrestrial faunas may have been isolated by the Aptian, the shallow marine environments of the different component of Gondwana were still largely contiguous, so that even if *Kronosaurus* was restricted to continental shelf environments there were no major oceanic basins that would have isolated an Australian from a Colombian population.

The Aptian horizon from which *Kronosaurus boyacensis* is known is slightly older than the Queensland Doncaster Formation, which may indicate that the two forms were not biologically continuous: *K. boyacensis* is known from the Late Barremian–Early Aptian Middle Paja Formation of the Villa de Leyva region (Hampe 2005), which correlates stratigraphically with the Late Barremian–Early Aptian inundation of the

Great Artesian Basin (Early Aptian Sea – Chapter 3), whilst the Doncaster *Kronosaurus* material is from Mid–Late Aptian marine strata that represent a subsequent transgressive episode (Late Aptian Sea). However, the Doncaster and Toolebuc *Kronosaurus* specimens are separated by a stratigraphically greater distance. Furthermore, the Doncaster and Toolebuc *Kronosaurus* specimens are actually separated by geography as well as stratigraphy; between the Doncaster and Toolebuc Formations are at least two regression/ transgression cycles (Chapter 3), meaning that there could not have been an endemic population of *Kronosaurus* within the Great Artesian Superbasin over that time span.

It is possible that further, detailed study of the *Kronosaurus* specimens detailed in this study – QM F10113, MCZ 1285, and the *K. boyacensis* holotype – can further resolve the question of the species level taxonomy of the Doncaster Formation *Kronosaurus* material. In particular, the premaxillary tooth count of *K. boyacensis* needs confirmation, and current uncertainties surrounding the morphology of the cervical and pectoral vertebrae and ribs could be of particular relevance; it is also possible that more detailed study of the cranial and dental specimens of each may be taxonomically useful. Histological study of the ribs may allow species level differences to be identified, in line with Hampe’s description of the ribs in *K. boyacensis*, and these could also allow the taxonomic identity of the Doncaster material to be resolved. For the present, the assignment of the Doncaster Formation *Kronosaurus* specimens to *Kronosaurus queenslandicus* is maintained, pending the results of future examination, as this taxonomy reflects the most parsimonious interpretation of the available data.

Jurassic pliosaurids

For the pliosaurids represented by intact cranial material, the estimates presented above indicate that most specimens are smaller than the large adult *Kronosaurus* specimens, but that one specimen – OUM J.10454, the ‘Cumnor mandible’ – was significantly larger and is thus the largest known pliosaur represented by intact material. Precise estimates of body size in these pliosaurids depend on the model of head size to body size used. Given that cervical series counts in pliosaurids (18–22; Andrews 1913) are known to considerably exceed those of the brachaucheniids (12–

13), it is entirely possible that the BMNH model, with a relatively longer neck and shorter head (Figure 6-19) is a more realistic model for pliosaurids than is the Newman and Tarlo ‘Stretosaurus’ model. There is a tendency, within the popular media and even in the scientific literature, to emphasise the upper range of body size estimates in reports, and this can produce a systematic bias in accounts of body size in charismatic but enigmatic groups such as pliosaurs. Despite the need to avoid this bias, it is likely that the body size estimates of the pliosaurids that are based upon the BMNH model are more accurate than those based on the Newman and Tarlo ‘Stretosaurus’ model; the Cumnor mandible thus appears to represent a pliosaur that was up to 12.7 metres long and 19.3 tonnes mass. *Pliosaurus brachyspondylus* may have reached lengths of 9.1 metres and a mass of 7.0 tonnes, comparable to known adult body size in *Kronosaurus*. The specimen of *Liopleurodon ferox* is the smallest of the pliosaurid taxa analysed here: although specimens that are larger than NHM R2680 are known (Noè 2001), it is a smaller taxon than *Pliosaurus brachyspondylus*.

Mega-pliosaurs?

Prior to the present analysis, the largest published length for a pliosaur known from substantial remains was Romer and Lewis’ figure of 12.8 metres for the MCZ specimen of *Kronosaurus* (Romer and Lewis 1959). Even though the reconstructed length of this specimen has herein been reduced to 10.5–10.9 metres, the Cumnor mandible represents an animal of a similar length to Romer and Lewis’s reported figure and 12–13 m can be considered as the upper range of body size that can be reconstructed on the basis of substantially complete cranial or post-cranial remains. As has been mentioned above, there has recently been speculation that some fragmentary fossils from the Middle–Late Jurassic may represent pliosaurs that exceeded have 12.8 metres in length, here termed ‘mega-pliosaurs’¹⁵. Coincidentally, under the BMNH model, this total length corresponds with a body mass of almost exactly 20 tonnes.

Potential mega-pliosaurs are stratigraphically limited from the Callovian to the Tithonian. Five are discussed here; the Aramberri specimen, the Peterborough

¹⁵ A term first used by Darren Naish (<http://dml.cmnh.org/2001Feb/msg00827.html>)

vertebrae, the NHM symphysis, the holotype of *Megalneusaurus rex*, and the recently discovered Svalbard material.

The Aramberri specimen (Kimmeridgian) preserves a series of posterior cervical to pectoral vertebrae and a propodial head, and is unquestionably pliosauroid; on the basis of the sub-central foramina preserved on the vertebrae it can be excluded from the Brachaucheniidae and is most likely a pliosaurid. It is certainly large: the dimensions given by Buchy et al. (2003) for the vertebrae reconstructed here as the first dorsal exceed the comparable dimensions of the *Kronosaurus* specimens examined in the present work. For a specimen such as the Aramberri material, however, there are two significant problems; (1) known pliosaurid specimens that could potentially serve as an anatomical template for size estimates are significantly smaller than the Aramberri specimen (the problems with extrapolation of body size over orders of magnitude are considered above); (2) the only fossils that can serve as useful templates, and which are from specimens not too much smaller than the Aramberri specimen, i.e., *Kronosaurus*, are from a family known to have different vertebral proportions to pliosaurids. On the basis of reported vertebral length, the Aramberri specimen is smaller than the large *Kronosaurus* specimens; however, the vertebral width and height of the Aramberri specimen are considerably greater than in any of the *Kronosaurus* specimens, and scaling by these produces size estimates of 11.7–12.2 metres total. Accepting that, between species with different vertebral counts, comparing the diameter of individual vertebrae produces more reliable estimates than comparing vertebral length (see above), the Aramberri specimen therefore seems to represent a very large pliosaur, but not one that is larger than the more reliable size estimate for the Cumnor mandible. The status of the Aramberri specimen as a ‘mega-pliosaur’ is thus subject to question.

Buchy et al. (2003) estimate total size in the Aramberri specimen at 15 metres, on the basis of scaling from a much smaller specimen of *Liopleurodon ferox*. The potential problems of this approach cannot be over-estimated. Further, they claimed that the Aramberri specimen represented a juvenile ontogenetic stage, citing lack of fusion of the neural arches to the centra. However reliable this character may be in other groups of reptiles, its validity as an indicator of ontogenetic stage in pliosaurids and

brachaucheniids is doubtful. Very few pliosaurid and no brachaucheniid vertebrae have the neural arches fused to the centra (pers. obs.); unless all of the large *Kronosaurus* specimens are interpreted as juveniles, it appears that this particular feature is paedamorphic in large pliosaurs and that claims that the Aramberri specimen is a juvenile are misplaced.

Unlike the Aramberri specimen, the Peterborough vertebra (Callovian) may not represent a pliosaur: the overall shape of the centrum is consistent with that of a pliosaur cervical, but the sub-central foramina and the costal facets are of a divergent morphology to the typical state in pliosaurids. It is, however, a very large element, exceeding the Aramberri specimen in diameter, and as pectoral/ anterior dorsals are always larger than cervicals from the same animal, if it is a pliosaur it is undoubtedly from a larger animal than the Aramberri specimen. Exactly how much larger is uncertain – unlike the Aramberri specimen, an isolated pliosaur cervical vertebra is very difficult to place accurately in the cervical series and, cervical vertebrae vary more than do those of the pectoral region. Comparison with the width of anterior cervical vertebrae of *Kronosaurus* suggest a size of 11.6–14.2 metres (14.6–26.7 tonnes), with a mean estimate of 12.6 metres and 18.8 tonnes. If the Peterborough vertebrae is a pliosaur, it might thus (taking the maximal estimate) represent a true mega-pliosaur (i.e. > 20 tonnes). However, the identification of this fossil remains in dispute; it is considered here to be, on balance, too likely to be a sauropod to warrant status as a confirmed mega-pliosaur.

The NMH symphysis (Callovian) is certainly more pliosauroid, but there is little information other than been collected from the Oxford Clay. It is of the ‘short symphysis’ type (Noè 2001, Noè et al. 2004, Tarlo 1960) but beyond that its taxonomy is difficult. The marine fauna from the host unit, the Oxford Clay, is perhaps the best studied of any worldwide: if the NHM symphysis represents a large individual from a species already described from the Oxford Clay, present knowledge suggests either *Simolestes vorax* or *Liopleurodon ferox*. Of the other pliosaurs known from that fauna, *Peloneustes* has a much longer symphysis, while symphyseal length in *Pachycostasaurus dawni* is unknown (Noè 2001). Alternatively, the NMH mandible indicates a ‘short’ symphysis species known thus far from different strata, such as the

Kimmeridgian *Pliosaurus macromerus*. All of these candidate species can be distinguished on the basis of the ornament and morphology of the tooth crowns, but no teeth are preserved with the NHM symphysis. For ‘short symphysis’ extant crocodylians, symphyseal tooth counts are consistent within species for individuals across all size classes (pers. obs.), indicating that this feature does not vary ontogenetically. Symphyseal tooth count is considered to be a robust taxonomic character in pliosaurs (Noè et al. 2004): by this criterion, NMH mandible is perhaps therefore more likely to represent *Simolestes vorax* than *Liopleurodon ferox* or *P. macromerus*, although *Pachycostasaurus* remains a logical possibility.

However, the proportions of the symphysis are somewhat different to that of *Simolestes*, or indeed of any other pliosaur known from the Callovian-Kimmeridgian. In addition to being absolutely large, the NHM symphysis is massive: for its length, it is very robust. The ‘macrocephalic’ growth pattern seen in some modern crocodylians and turtles has not, as yet, been documented in pliosaurs, but the NHM symphysis suggests that very large individuals may have shared this growth pattern. Assuming, that this is the case, we should expect to see that the proportions of the symphysis are relatively wider in a macrocephalic adult, compared with a smaller individual of the same species. By this logic, the NHM symphysis could possibly be *Liopleurodon ferox* or *Pliosaurus macromerus*, but not *Simolestes vorax*. Conversely, if symphyseal tooth counts are taxonomically robust, then the NHM symphysis is neither *L. ferox* or *P. macromerus*. It appears on balance to represent a different taxon to any of these.

Most large pliosaurs have head proportions broadly similar to *Liopleurodon* or *Pliosaurus*. Assuming that the NHM symphysis is from a macrocephalic adult of a similarly proportioned taxon, and that, in macrocephalic specimens, body length will correlate with jaw length (or part thereof), rather than jaw width or height, the best estimate for body size in this taxon is that based on comparison with symphyseal length in *Liopleurodon*, i.e. a TL of 9.1 m and a body mass of 7.1 tonnes. However, in macrocephalic individuals, overall girth of the body may increase for little or no proportional increase in length, and this weight estimate is likely to be conservative. The estimate based upon mandible width in *Liopleurodon* can be excluded as a logical

possibility; the mean of the remaining estimates is 10.8 m TL and 14 tonnes body mass.

As shown above, the Stretham (Kimmeridgian) and Stewartby (Callovian) specimens each represent animals similar in size to large *Kronosaurus*, underlining the consistency of the 10 – 11 m range of total length as the upper limit for most well preserved pliosaurs in the Middle – Late Jurassic and the Early Cretaceous. The holotype of *Megalneusaurus rex* (Oxfordian) comprises a series of vertebrae and limb elements: the propodial is reconstructed as 990 mm long, slightly larger than any propodial known from *Kronosaurus* and larger than the femur of the Stretham specimen (and, probably, the Stewartby specimen). The allometry of pliosaur propodials is not sufficiently known to allow quantitative estimates of body size; qualitative estimates of size in *M. rex* depend upon whether the propodial is a humerus or a femur. If a femur, it is a large pliosaur, possibly 11–12 m TL or slightly larger. If a humerus, it is a very large pliosaur, perhaps the largest known. However, the vertebral dimensions described by (Knight 1895) are not obviously larger than those of *Kronosaurus*: in all likelihood, the propodial is a femur and *Megalneusaurus rex* is a pliosaur slightly larger than the largest *Kronosaurus* and the Stewartby and Stretham pliosaurs. The same logic applies to size estimates based upon early reports of the Svalbard pliosaur (Tithonian – P. Druckenmiller, pers. comm.).

There seems, therefore, to be no strong evidence for pliosaurs that exceeded 20 tonnes. Of the specimens considered above, the only possibility for a pliosaur longer than 12.8 m is the Peterborough vertebrae, and that by taking the upper estimate of size for the specimen. The doubtful taxonomic assignment of this specimen casts further doubt on that specimen. There is, however, convincing evidence for pliosaurs in the 10–20 tonne size range; not only from the fragmentary material claimed to indicate mega-pliosaurs, but the more reliable Cumnor mandible as well, and the larger specimens of *Kronosaurus* are at the lower end of this scale. Historically, *Kronosaurus* has been the benchmark for body size in large pliosaurs. Between the original and revised lengths of body size in *Kronosaurus* (12.8–10.8 m respectively), there is a potential size class for pliosaurs that may have been very large, i.e. between

10 and 20 tonnes. From the evidence available to date, it appears that mega-pliosaurs remain a myth, but that very large pliosaurs were a reality.

Ecological implications of very large pliosaurs

In palaeobiology, body size is one of the principal predictors of the ecological options available to a species (Meers 2003). The data presented here suggests that pliosaurid and brachaucheniid pliosaurs dominated the apex predator guild from the Callovian to the Turonian, with a body size of under 10–11 tonnes for much of this time, but with the largest pliosaurs reaching up to 20 tonnes in the Kimmeridgian and perhaps the Callovian.

This pattern should be placed within a macroevolutionary context. Pliosaurids and brachaucheniids were not, on average, noticeably the largest marine carnivore groups of the Mesozoic. The larger species of a related group, the Lower Jurassic rhomaleosaurids, reached 1–10 tonnes (although nearer the lower end of that scale). The ichthyosaurs *Cymbospondylus* (Middle Triassic) and *Temnodontosaurus* (Early Jurassic) were carnivores in the 1–10 tonne range [by comparing reported body lengths from McGowan (1991) with length–weight data for balaenopterids]. By comparison of TL with modern crocodylians, the largest mosasaurs *Tylosaurus* and *Mosasaurus* (Late Cretaceous) may have weighed up to 30 tonnes, although given the likely ‘eel-like’ body form of these taxa this must be considered a maximum estimate and a range of 10–15 tonnes is perhaps more likely. The largest Mesozoic marine reptile of all was the Late Triassic *Sbonisaurus*, which reached 21 m and perhaps 40–50 tonnes, although adults of this taxon was edentulous and were presumably teuthivores rather than carnivores (Nicholls and Manabe 2004). Other than *Sbonisaurus*, and the hypothesised mega-pliosaurs, all the marine reptiles of the Mesozoic were less than 20 tonnes and the majority of apex carnivores appear to have been between 1–10 tonnes.

A similar pattern holds for the Cainozoic. One of the earliest large carnivorous whales was the Eocene archaeocete *Basilosaurus*, which reached 20 m total length but, because of a relatively elongate body plan may not have exceeded (or even achieved) 10 tonnes. Since the Eocene, the largest carnivores were the sperm whales, in

particular the killer sperm whales (Miocene: 1 to 5 tonnes; Bianucci and Landini 2006, Hampe 2006), ziphiid whales (5–10 tonnes, Miocene-Recent), the lamnid shark *Isurus hastalis* (Miocene: up to 2 tonnes; Nyberg et al. 2006), and the modern orcinine killer whales (between 1 and 10 tonnes; Klinowska 1991). The only exception to this pattern, for predators, was the giant lamnid shark *Carcharocles megalodon* (Miocene; ~50 tonnes; Nyberg et al. 2006, Wroe et al. 2008) and the modern sperm whale *Physeter macrocephalus* (50 tonnes; Trites and Pauly 1998), although the later is principally a teuthivore rather than a carnivore. In addition to these, a large number of modern, and fossil, species regularly exceed 20 tonnes (with many exceeding 50 tonnes), but these are all planktonivorous: mostly, the mysticete whales (Tershy 1992), but also the whale shark *Rhincodon* (Chen et al. 1999).

Since the start of the Mesozoic, the ecological pattern of large body size in marine vertebrates can be summarised; most of the species that exceed 20 tonnes are planktonivores (mostly Recent), or, less commonly, teuthivores (one Recent, one Late Triassic). Leaving aside the pliosaurs, all of the large carnivores are less than 20 tonnes (and the majority of these are less than 10 tonnes), with one exception: *C. megalodon*.

How might a hypothetical mega-pliosaur, or the very large pliosaurs that were between 10 and 20 tonnes, fit within this pattern? The overwhelming majority of >20 tonne marine vertebrates have been, or are, planktonivores, but planktonivory is a highly specialised niche and the largest pliosaurs show no apparent features that indicate a capacity for this trophic role. Only three of the above listed species definitely exceed 20 tonnes and are not planktonivores: two of these are/were teuthivores (*Shonisaurus* and *Physeter*), and one was a carnivore (*Carcharocles*). Exactly the same pattern holds for non-pliosaurs in the 10–20 tonne range: all are/were planktonivores, with possible exception of *Basilosaurus* and the largest mosasaurs if these species was larger than 10 tonnes. This pattern suggests that, if the largest pliosaurs were not planktonivores, then they were either teuthivores similar to *Shonisaurus* and *Physeter*, giant carnivores like *Carcharocles*, or comparable to the largest mosasaurs and archaeocetes (depending on the actual mass of those).

Very large pliosaurs as megatooth analogues?

Carcharocles is understood to have specialised on mysticete whales (Wroe et al. 2008), i.e. it had access to a prey base of animals that were as large or larger than itself. It is unlikely that the very large pliosaurs of the Jurassic were in a similar position; for most of the Mesozoic, the apex carnivores of each chronofauna have been the largest members of their ecosystems, a pattern that is in contrast to that of the Neogene. The only potential exception to this pattern is the presence of the large pachycormid teleost *Leedsichthys*, which may have reached up to 16 m and exceeded 20 tonnes, in the marine fauna of the Callovian Oxford Clay: intriguingly, this is one of the very few palaeofaunas that may also have included pliosaurs in the 10–20 tonne size range (Liston 2004, 2007). However, whether or not the large pliosaurs regularly preyed upon *Leedsichthys* is unclear (Liston 2007), and as outlined above, the evidence for pliosaurs exceeding 10 tonnes in the Oxford Clay is in any case equivocal. Kimmeridgian pliosaurs were undoubtedly larger than 10 tonnes (although they appear not to have exceeded 20 tonnes): but *Leedsichthys*, or any similar sized species, is not known from the Kimmeridgian. The evidence for very large pliosaurs as *Carcharocles* analogue, i.e. a specialised giant carnivore of marine megafauna, appears to be thin.

Deep-diving fish and squid eaters?

The modern giant odontocete *Physeter macrocephalus* is a specialist predator of mesopelagic and bathypelagic ecosystems (Watwood et al. 2006). These systems are based upon pelagic plankton production and the various species of cnidarians, crustaceans, fish and cephalopods that consume the plankton (Tierney et al. 2002). They are distributed throughout the pelagic realm, but are not uniformly distributed, being often concentrated by topological variation of the seafloor such as shelf edges, sea-mounts, and ocean trenches (Claridge 2006): horizontal distribution is also non-uniform. In some cases planktonivorous fish and squid can form aggregations that are dense enough to give a ‘false-bottom’ reading in oceanographic sonar, leading to their alternative name, the ‘deep scattering layer’. Myctophids (‘lanternfish’) are a particularly important component of the deep-scattering layer and are known for the nocturnal vertical migrations of many species to epipelagic depths.

Meso- and bathypelagic fish and squid are exploited by a range of larger predators, including many species of teleosts (such as the scombroids *Thunnus* and *Xiphias*), sharks (e.g. *Prionace*, *Alopias*), leatherback turtles (*Dermochelys*), penguins (*Aptenodytes*), phocids (*Mirounga*, Lobodontinae), and cetaceans (*Ziphiidae*, Delphinidae, Kogiidae, *Physeter*). Amniote predators of meso/bathypelagic systems must dive several hundred or even thousand metres to forage; in addition to various physiological specialisations exhibited by all deep diving species, body size plays an important role in determining maximum foraging depth. For each group, the deepest divers all tend to be the largest members of their respective clade (Schreer and Kovacs 1997). *Physeter* is the largest and deepest diving member of the meso/bathypelagic predator guild, and is able to exploit parts of this ecosystem that are inaccessible to smaller predators; it shows a preference for squid but also consumes fish (Clarke et al. 1993). Evidence for deep diving behaviour in ichthyosaurs (Motani et al. 1999), combined with interpretation of edentulous ichthyosaurs as teuthivores (Nicholls and Manabe 2004), suggest that *Sbonisaurus* was a deep diving meso/bathypelagic predator analogous to *Physeter* (Motani 1999, 2005, Schreer and Kovacs 1997).

Modern marine carnivores never exceed 10 tonnes. Given that a similar pattern holds – with the notable exception of *Carcharocles* – for fossil marine ecosystems in the Cenozoic and most of the Mesozoic, it may be that 10 tonnes is close to the upper limit of body size that is viable for marine carnivores¹⁶. It is possible that the very large pliosaurs of the Callovian–Kimmeridgian were able to circumvent this limit by accessing meso/bathypelagic ecosystems, and that, as with *Physeter* and *Sbonisaurus*, their very large body size increased their efficiency as deep diving predators. Note that published records of stomach contents in pliosaurs indicate that cephalopods were a consistent component of pliosaurid diets (Cicimurri and Everhart 2001); notably in the large species *Megalneusaurus rex* (Wahl et al. 2007), and also in *Simolestes vorax* (Martill 1992) and *Peloneustes philarchus* (Andrews 1910a). If very large pliosaurs were meso/bathypelagic predators, then their rarity in the fossil

¹⁶ This interpretation depends on the assumption that *Basilosaurus* and the largest mosasaurs, such as *Tylosaurus* and *Mosasaurus*, are not significantly larger than 10 tonnes. Although these taxa are much longer than any pliosaur, they have a highly elongate body form and their mass, in proportion to body length, is likely to be even lower than in balaenopterids or crocodylians. Any further work on the macroevolutionary patterns outlined here will need more reliable estimates of body shape in these taxa. Even if they do exceed 10 tonnes, the implications of their elongate form for locomotor mechanics may preclude them from the ecomorphs occupied by pliosaurs and lamnids.

record might thus be linked to facies bias; non-shelf habitats are infrequently preserved compared with shelf and epicontinental facies, and the apparent absence of very large pliosaurs in the Cretaceous may reflect the distance of the Australian and American sites from deep water environments. Alternatively, it is possible that the brachaucheniids did not exploit this niche: whether morphological differences between pliosaurids and brachaucheniids, such as the lack of sub-central foramina in the latter, reflect differences in deep-diving ability is at this point unknown.

Geriatric giants?

Within evolutionary science, there is often a focus on adaptive interpretations of morphological traits, including body size, such as the scenarios presented above. However, it is important not to assume that every trait exhibited by an organism is a result of adaptive processes, not only because evolutionary biology should be subject to the testing and self-correction that characterises science, but because it is unlikely that every feature of every organism can be described as adaptive (Gould and Lewontin 1979). In this context, it is important to remember that, while body size is certainly an important part of a species' ecology, the very largest individuals within a population are the extreme results of that species' growth trajectory but do not necessarily represent the selective pressures that have determined mean body size of that population. If the largest animals are of a size class that is very rare within a population, the relevance of those animals to recruitment within the population may be questionable, particularly if those animals only achieve extreme large size at very old ages. If the reproductive activity within the populations is dominated by animals of smaller size, then the large size of the largest individuals may be a pleiotropic effect of the growth trajectory of that species, rather than an adaptation to a specific ecological niche.

Within the living crocodylians, there is some circumstantial evidence that very large individuals may have been both very old and rare. Several museum collections worldwide contain crocodylian specimens from the 'colonial' era of wildlife collection, when exceptionally large individuals were targeted. In particular, the NHM collection contains two unnumbered skulls, of a *Crocodylus porosus* and a *Tomistoma schlegelli*, that are considerably larger than the range considered typical for

current members of these species (pers. obs., Figure 6-23). Both exhibit extreme macrocephaly, and the *Tomistoma* skull may be the largest of any extant crocodylian in any collection. Reptiles are characterised by indeterminate growth, and these individuals may represent extremely large individuals of advanced age. Animals of comparable size are unknown in modern populations, presumably as a result of hunting in the 19th and 20th Centuries. Although these individuals may have been large enough to have qualitatively different ecologies to more typical conspecifics –



Figure 6-23: Various crocodylian skulls in the NHM collection, including very large, macrocephalic skulls of *Crocodylus porosus* (second skull from top; the skull to its left is a medium sized adult) and *Tomistoma schlegelli* (third from top: the skull at bottom is from a medium-large adult). The difference in snout proportions and overall size between the macrocephalic specimens and more typical conspecifics is striking.

the giant *Tomistoma* specimen in particular may have been able to exploit large terrestrial mammals, rather than the fish and small tetrapods considered typical for this species – their contribution to their respective populations is difficult to estimate. In any case, an attempt to characterise the ecology of *Crocodylus porosus* and *Tomistoma schlegelli* with emphasis upon these individuals may produce a biased analysis. Arguments that seek to explain the evolution of these large forms within an adaptive context may be misleading if the largest individuals are not reproductively relevant, and the size of the very largest individuals may be a pleiotropic consequence of growth parameters that are under selective pressure at other ontogenetic stages.

Like crocodylians, the great whales have been subject to considerable hunting effort over the past 200 years and it is likely that, in addition to having had considerably larger population sizes, the largest individuals of most species were larger than the maximum sizes seen in current populations. Sperm whales have attracted much attention in this regard: large bulls today are typically up to 18 metres and 50 tonnes (Trites and Pauly 1998), but historical records from the whaling era indicate much larger animals, perhaps exceeding 70 tonnes (Berta et al. 2006). The discrepancy between current maximum and historical record sizes is likely to indicate as much about the effects of industrial whaling on the population, and the logistical difficulties of measuring maximum body size in a gigantic, pelagic animal, as potential differences in the ecology of 50 tonne vs 130 tonne male *Physeter*. However, published growth curves for *Physeter macrocephalus* indicate that males, unlike females, exhibit non-deterministic / non-asymptotic growth over much of their life span (Berta et al. 2006, Lockyer 1981), suggesting an important and intriguing possible parallel with large crocodylians and very large pliosaurids.

If 20 tonne Callovian to Kimmeridgian pliosaurs simply represent very old individuals, then we should predict that they represent species known more commonly from smaller specimens. In the case of the Cumnor mandible, this appears to be the case: *Pliosaurus macromeris* is known from several specimens, including the Stretham specimen, but they are each much smaller than the ~20 tonnes reconstructed for the Cumnor mandible. However, other very large Kimmeridgian pliosaurs, such as the Aramberri specimen and the Svalbard specimen,

cannot at this stage be identified to species. The taxonomic affinities of the Callovian specimens, i.e. the NHM mandible, the Peterborough vertebrae, and the Stewarby specimen, remain uncertain. The holotype material of the Oxfordian *Megalneusaurus rex* is undiagnostic and the validity of this taxon is currently uncertain: it may represent a taxon that is better known from other horizons. All of the large other pliosaur specimens known thus far represent animals close to 10 tonnes or less: this body size has been a remarkably consistent upper limit for marine carnivores since the Middle Triassic, breached only by the Miocene lamnid shark *Carcharocles megalodon* and possibly, depending on further refinements of body size estimates, *Basilosaurus* and the largest mosasaurs.

6.5 Conclusions

1. *Kronosaurus* was one of the largest pliosaurs, but was smaller than previous reconstructions. The Harvard specimen (MCZ 1285) may be the largest known.
2. *K. queenslandicus* can be distinguished from *K. boyacensis* on the basis of post-cranial and perhaps cranial characters; they are each valid taxa.
3. The question of whether the Queensland Aptian *Kronosaurus* material is taxonomically equivalent to the holotype of *Kronosaurus queenslandicus* (with which it is geographically consistent), or instead with *Kronosaurus boyacensis* (to which it is stratigraphically closer) remains, but currently available evidence supports its referral to *Kronosaurus queenslandicus* Longman 1924.
4. The biggest Jurassic pliosaurs were larger than *Kronosaurus*.
5. Variation in body size estimates should be noted; otherwise estimates tend to ratchet upwards (a process that has been dubbed ‘Godzillisation’ by Forrest (2008); for example, the length estimates for the Aramberri specimen given in Buchy et al. (2003) (15 m) with the figure (17 m) given in Smith and Dyke (2008).
6. Currently, the Cumnor mandible OUM J.10454 (*Pliosaurus macromerus*) is the largest pliosaur known. There is no convincing evidence that pliosaurs ever exceeded 12.8 m TL / 20 tonnes mass. Specimens that may have been between 12 and 20 tonnes are, with present knowledge, restricted to between the Callovian and the Kimmeridgian.
7. Claims of juvenile ontogenetic stage in the Aramberri specimen – and hence an implication of larger size in ‘adults’ – contradict the observed vertebral morphology of all Cretaceous large pliosaur material.
8. For most of the fossil record since the Middle Triassic, the largest marine carnivores at most times, including pliosaurs, can be compared with orcinine odontocetes (killer whales), i.e. 5 to 10 tonnes.
9. The Callovian–Kimmeridgian pliosaurs that were between 10–20 tonnes are considered to be either (a) deep diving predators analogous to *Physeter*, or (b)

very rare, and possible old, individuals of species that were more commonly <10 tonne carnivores. Planktonivory, or giganto-carnivory analogous to that reconstructed for *Carcharocles megalodon*, are not considered likely for 10–20 tonne pliosaurs. The pattern is complicated by the possibility that *Basilosaurus* and the largest mosasaurs exceeded 10 tonnes, highlighting the need for refined estimates of body size in these ‘eel-like’ taxa.

10. Estimates of body size in large pliosaurs provided here can be refined by study of skull allometry within *Kronosaurus queenslandicus*, and postcranial anatomy for the Jurassic pliosaurids.
11. Taphonomy is important in marine reptile palaeobiology (Lingham-Soliar and Plodowski 2007). Further study of the taphonomy of pliosaurid and brachaucheniid skeletons is needed. In particular, given the loss of data that occurs when the specimen is removed, skeletons should be documented thoroughly before excavation, preferably using 3D scanning / photogrammetric techniques (Hampe & Leimkuhler 1996).
12. The taphonomy of USNM 4989 is interpreted as being consistent with the Nicholls & Russell model of plesiosaur pectoral anatomy; however, the interpretation of thoracic ribs in this specimen is made from rib morphology in addition to inference from taphonomy: the taphonomic data in this specimen is not pristine (Everhart 2007).

6.6 Taxonomic summary

Based upon the morphology of the specimens discussed in this chapter and in Chapter 4, the taxonomy of currently accepted brachaucheniid taxa is given below. The families Brachaucheniidae and Pliosauridae are defined under monophyletic criteria, and diagnosed using available morphological data. Note that this taxonomy is based upon morphotypic logic rather than the topology of a phylogenetic analysis (which has not been attempted in this thesis); however, a taxonomy should be consistent with the consensus of phylogenetic analyses and the taxonomy proposed below is therefore subject to testing by phylogenetic analysis. This taxonomy is, at time of writing, consistent with the topologies of the most recently available phylogenetic analyses of the taxa in question (Druckenmiller 2006, Druckenmiller and Russell 2008a, Ketchum 2008, Smith and Dyke 2008).

The question of whether the Brachaucheniidae Williston 1925 form a subfamily within the Pliosauridae depends upon whether the topology of Ketchum (2008), or that of Smith and Dyke (2008), is supported by future analyses. For the time being, I have adopted the conservative position and retained the Brachaucheniidae at the family level, but should Ketchum's (2008) result prove to be supported by the consensus of future work then this taxon would simply become the Subfamily Brachaucheniinae Williston (*sensu* Ketchum 2008), without the need for altering the definitions offered below, and requiring only minor alteration to the diagnosis and content of the Pliosauridae.

Brachaucheniidae Williston, 1925

Revised definition: *Kronosaurus* + *Brachauchenius*, ex. *Pliosaurus*.

Revised diagnosis: Single headed cervical ribs; vertebral centra lack nutritive foramina on the ventral surface (sub-central foramina); 12–13 cervical vertebrae; very large skull (BSL >30% of snout-hip length); no sub-orbital fenestrae; conical teeth lacking carinae; tooth ornament = strong, longitudinal ridges, more or less evenly spaced around circumference of crown; short mandibular symphysis (6 ½ pairs of functional alveoli); humeri 70-85% of femora length; neural arch facets on anterior dorsal vertebrae are elongate, rectangular shaped (not oval) in dorsal view.

Stratigraphic range: Late Barremian–Turonian.

Distribution: N. America, S. America, Australia.

Kronosaurus Longman, 1924

Type species: *Kronosaurus queenslandicus* Longman, 1924

Diagnosis: Brachaucheniid with strongly anisodont dentition, and M1-M3 enlarged to fangs; posterior cranial roof does not extend posterior to occipital condyle.

Kronosaurus queenslandicus Longman, 1924

Diagnosis: Four pairs of premaxillary teeth*; mandibular symphysis has expanded spatulate region bearing five pairs of teeth; D4 and D5 teeth occlude between Pmx4 and M1*; 13 cervical vertebrae; length of humerus is ~70% of length of femur.

Holotype specimen: QM F1609 (Toolebuc Fm, Queensland)

Referred specimens: QM F10113, QM F18827, QM F2446, QMF 2454, QM F51291, QM F52279, QM F18154, QM F18726, QM F2137, RMFM R236 (Toolebuc Fm, Queensland); MCZ1284, MCZ1285, QM F33574 (Doncaster Fm, Queensland).

Note: QM F1609 is not diagnostic to genus or species. QM F18827 preserves the cranial features that diagnose *Kronosaurus queenslandicus* and thus constitutes a suitable name-bearing specimen. QM F10113

preserves the post-cranial features that are here taken as representative of *Kronosaurus queenslandicus*.

Kronosaurus boyacensis Hampe, 1992

Diagnosis: Five pairs of premaxillary teeth*; 12 cervical vertebrae; length of humerus is ~80% of length of femur.

Holotype specimen: The holotype is an unnumbered, nearly complete specimen on display at the Villa de Leyva, Colombia.

* These characters are all linked to the premaxillary tooth count, and their status as taxonomic characters as listed here depends upon the accuracy of Hampe's report of five premaxillary teeth in *K. boyacensis* (Hampe 1992 – see Chapter 4 and Discussion above). If the premaxillary tooth count in *K. boyacensis* is confirmed as five, then this may prove constitute grounds to place *K. boyacensis* into a separate genus to *K. queenslandicus*, as pliosaur taxonomy typically places species with differing premaxillary tooth counts into separate genera. However, if the premaxillary tooth count in *K. boyacensis* is actually four, then;

- a premaxillary tooth count of four becomes a genus level character for *Kronosaurus*, rather than a species level character for *K. queenslandicus*, and
- *K. boyacensis* remains a valid taxon, diagnosable from *K. queenslandicus* on the basis of post-cranial anatomy, but the species level identity of the Aptian Doncaster Fm *Kronosaurus* material (MCZ 1284, MCZ 1285, QM F33574) becomes problematic – this material does not preserve any of the post-cranial anatomy that would then allow it to be diagnosed to *K. boyacensis* or *K. queenslandicus*, and it would therefore be referred to *K. queenslandicus* on the basis of geographic correlation (see Discussion above).

Brachauchenius Williston, 1903

Diagnosis: Combination of five pairs of premaxillary teeth **and** anisodonty weakly developed or absent; mandibular symphysis lacks enlarged ‘spatulate’ region; posterior skull roof extends well posterior of occipital condyle. Liggett et al. (2005) have noted a unique configuration of metapodial elements.

Included species: *Brachauchenius lucasi* Williston, 1903 (type species). Hampe (2005) has referred a new, unnamed species from the Barremian of Villa de Leyva, Colombia to *Brachauchenius* (*Brachauchenius* sp. VI).

Notes: The Brachaucheniidae may form a taxon within the Pliosauridae, depending on the consensus of recent and current work (Ketchum 2008). Should the placement of the clade containing *Kronosaurus* + *Brachauchenius* be found to lie within the *Pliosauridae*, i.e. the tree topology recovered by Ketchum (2008), within a clade defined by *Pliosaurus* + *Simolestes* (see below), and without including any of the traditional Middle–Late Jurassic pliosaurid taxa, i.e. *Liopleurodon*, *Peloneustes*, *Pliosaurus*, *Simolestes*, then the Brachaucheniidae Williston 1925 would become the Subfamily Brachaucheniinae Williston (*sensu* Ketchum 2008) according to the ICZN Principle of Coordination.

Pliosauridae Seeley, 1874

Definition: *Pliosaurus* + *Simolestes*, ex. *Rhomaleosaurus*

Diagnosis: Skull BSL <30% of snout-hip length; 18–22 cervical vertebrae; some or all cervical ribs are ‘double headed’; sub-central foramina present; sub orbital fenestrae present; ? anterior pterygoid vacuity; humerus is 70–85% of femur length; neural arch facets on anterior dorsal vertebrae are oval shaped in dorsal view.

Composition (currently recognised genera): *Pliosaurus*, *Liopleurodon*, *Pachycostasaurus*, *Peloneustes*, *Simolestes*, ?*Megalneusaurus*, ?*Plesiopleurodon*, ?*Polyptychodon*.

Range: Callovian – Tithonian, ?Cenomanian/Turonian.

Distribution: Europe, North America.

Notes: *Megalneusaurus* may not be a valid taxon. The Cretaceous taxa *Plesiopleurodon* and *Polyptychodon* have been assigned to the Pliosauridae, but this taxonomy has not been extensively tested phylogenetically [although Ketchum (2008) recovered *Plesiopleurodon* as a polycotylid]; if these taxa are found not to belong to the Pliosauridae then the known range of that family is restricted to Callovian–Tithonian.

Pliosauroida, c.f. Pliosauridae/Brachaucheniidae: Kaim et al. (2008) have reported a ‘pliosaurid’ from the Turonian of Japan: depending upon the taxonomic affinities of this specimen, the range of either the Brachaucheniidae or the Pliosauridae is therefore extended to the Late Cretaceous of the North-West Pacific.

6.7 References

- Acosta, C., G. Huertas, and P. Ruiz. 1979. Noticia preliminar sobre el hallazgo de un presunto *Kronosaurus* (Reptilia: Dolichorhynchopidae) en el Aptiano Superior de Villa de Leiva, Colombia. *Lozania (Acta Zoologica Colombiana)* 28:1-7.
- Anderson, J. F., A. Hall-Martin, and D. A. Russell. 1985. Long-bone circumference and weight in mammals, birds, and dinosaurs. *Journal of Zoology (London)* 207:53-61.
- Andrews, C. W. 1910a. A descriptive catalogue of the marine reptiles of the Oxford Clay. Part 1. *Brit. Museum Nat. Hist. London*.
- Andrews, C. W. 1910b. Note on a mounted skeleton of a small pliosaur, *Peloneustes philarchus* Seeley. *Geological Magazine Lond.* 7:110-112.
- Andrews, C. W. 1913. A descriptive catalogue of the Marine Reptiles of the Oxford Clay, Part II. *BM(NH), London*.
- Berta, A., J. L. Sumich, and K. M. Kovacs. 2006. *Marine Mammals: Evolutionary Biology*. Academic Press, Burlington.
- Bianucci, G., and W. Landini. 2006. Killer sperm whale: a new basal phystereroid (Mammalia, Cetacea) from the Late Miocene of Italy. *Zoological Journal of the Linnean Society* 148:103-131.
- Brodie, P. F. 1989. The White Whale *Delphinapterus leucas* (Pallas, 1776). Pp. 119-144. *In* S. H. Ridgeway, and R. Harrison, eds. *Handbook of Marine Mammals, Volume 4*. Academic Press, London.
- Brown, D. S. 1981. The English Upper Jurassic Plesiosauroidea (Reptilia) and a review of the phylogeny and classification of the Plesiosauria. *Bulletin of the British Museum (Natural History), Geology series* 35(4):253-347.
- Buchholtz, E. A. 2001. Vertebral osteology and swimming style in living and fossil whales (Order: Cetacea). *Journal of Zoology, London* 253(175-190).
- Buchholtz, E. A. 2007. Modular Evolution of the Cetacean vertebral column. *Evolution & Development* 9(3):278-289.
- Buchy, M., E. Frey, W. Stinnesbeck, and J. G. López-Oliva. 2003. First occurrence of a gigantic pliosaurid plesiosaur in the late Jurassic (Kimmeridgian) of Mexico. *Bul. Soc. géol. Fr.* 174(3):271-278.
- Buffrénil, V., A. Ricqles, C. E. Ray, and D. P. Domning. 1990. Bone histology of the ribs of the archaeocetes (Mammalia: Cetacea). *Journal of Vertebrate Paleontology* 10:455-466.
- Cann, J. 1998. *Australian Freshwater turtles*. Beaumont Publishing, Singapore.
- Carpenter, K. 1996. A review of short-necked plesiosaurs from the Cretaceous of the Western Interior, North America. *Neues Jahrbuch für Geologie und Paläontologie Abhandlungen* 201:259-287.

- Chen, C. T., K. W. Liu, and S. J. Young. 1999. Preliminary report on Taiwan's whale shark fishery. *In* S. L. Fowler, T. Reid, and F. A. Dipper, eds. Elasmobranch biodiversity, conservation and management. Proc. Int. Seminar and Workshop in Sabah, Malaysia. IUCN, Gland, Switzerland.
- Cicimurri, D. J., and M. J. Everhart. 2001. An elasmosaur with Stomach Contents and Gastroliths from the Pierre Shale (Late Cretaceous) of Kansas. *Transactions of the Kansas Academy of Science* 104(3-4):129-143.
- Claridge, D. E. 2006. Fine-Scale Distribution and Habitat Selection of Beaked Whales (unpublished M.Sc. thesis). University of Aberdeen.
- Clarke, M. R., H. R. Martins, and P. Pascoe. 1993. The diet of sperm whales (*Physeter macrocephalus* Linnaeus 1758) off the Azores. *Philosophical Transactions of the Royal Society of London, Series B* 339:67-82.
- Cope, E. D. 1869. Extinct Batrachia, Reptilia, and Aves of North America. *Transactions of the American Philosophical Society* 14:1-252.
- Cruikshank, A. R. I. 1994. Cranial anatomy of the Lower Jurassic pliosaur *Rhomaleosaurus megacephalus* (Stutchbury) (Reptilia: Plesiosauria). *Philosophical Transactions of the Royal Society, London B* 343:247-260.
- Cruikshank, A. R. I., D. Martill, and L. F. Noè. 1996. A pliosaur (Reptilia, Sauropterygia) exhibiting pachyostosis from the Middle Jurassic of England. *Journal of the Geological Society London* 153:873-879.
- Domning, D. P., and V. Buffrénil. 1991. Hydrostasis in the Sirenia: Quantitative data and functional interpretations. *Marine Mammal Science* 7:331-368.
- Druckenmiller, P. S. 2006. Early Cretaceous plesiosaurs (Sauropterygia: Plesiosauria) from northern Alberta: palaeoenvironmental and systematic implications. PhD Thesis, University of Calgary.
- Druckenmiller, P. S., and A. P. Russell. 2008a. A phylogeny of Plesiosauria (Sauropterygia) and its bearing on the systematic status of *Leptocleidus* Andrews, 1922. *Zootaxa* 1863:1-120.
- Druckenmiller, P. S., and A. P. Russell. 2008b. Skeletal anatomy of an exceptionally complete specimen of a new genus of plesiosaur from the Early Cretaceous (Early Albian) of northeastern Alberta, Canada. *Palaeontographica Abt. A* 283:1-33.
- Ellis, R. 2003. *Sea Dragons: predators of the prehistoric oceans*. Kansas University Press.
- Erickson, G. M., A. K. Lappin, and K. A. Vliet. 2003. The ontogeny of bite-force performance in American alligator (*Alligator mississippiensis*). *Zool Lond* 260:317-327.
- Erickson, G. M., P. J. Makovicky, P. J. Currie, M. A. Norell, S. A. Yerby, and C. A. Brochu. 2004. Gigantism and comparative life-history parameters of tyrannosaurid dinosaurs. *Nature* 430:772-775.
- Everhart, M. J. 2007. Historical note on the 1884 discovery of *Brachauchenius lucasi* (Plesiosauria; Pliosauridae) in Ottawa County, Kansas. *Transactions of the Kansas Academy of Science* 110:255-258.

- Farlow, J. O., G. R. Hurlburt, R. M. Elsey, A. R. C. Britton, and W. Langston. 2005. Femoral Dimensions and Body Size of *Alligator mississippiensis*: Estimating the Size of Extinct Mesoeucrocodylians. *Journal of Vertebrate Paleontology* 25(2):354-369.
- Finch, M. E., and L. Freedman. 1986. Functional morphology of the vertebral column of *Thylacoleo carnifex* Owen (Thylacoleonidae: Marsupialia). *Australian Journal Zoology* 34:1-16.
- Forrest, R. 2008. The Plesiosaur Site. www.plesiosaur.com.
- Georges, A., M. Adams, and W. McCord. 2002. Electrophoretic delineation of species boundaries within the genus *Chelodina* (Testudines: Chelidae) of Australia, New Guinea, and Indonesia. *Zoological Journal of the Linnean Society* 134:401-421.
- Gould, S. J., and R. C. Lewontin. 1979. The spandrels of San Marco and the Panglossian paradigm: a critique of the adaptationist programme. *Proceedings of the Royal Society Series B* 205:581-598.
- Gray, N., K. Kainec, S. Madar, L. Tomko, and S. Wolfe. 2007. Sink or Swim? Bone Density as a Mechanism for Buoyancy Control in Early Cetaceans. *Anatomical Record* 290: 638-653.
- Greer, A. E. 1974. On the Maximum Total Length of the Salt-Water Crocodile (*Crocodylus porosus*). *Journal of Herpetology* 8(4):381-384.
- Griffin, E. B. 1995. Functional interpretation of spinal anatomy in living and fossil amniotes. Pp. 235-248. In J. J. Thomason, ed. *Functional Morphology in Vertebrate Paleontology*. Cambridge University Press, Cambridge.
- Halstead, L. B. 1989. Plesiosaur locomotion. *Journal of the Geological Society London* 146:37-40.
- Hampe, O. 1992. Ein grosswuchsiger Pliosauridae (Reptilia: Plesiosauria) aus der Unterkreide (oberes Aptium) von Kolumbien *Courier Forsch.-Inst. Senckenberg* 145:1-32.
- Hampe, O. 2005. Considerations on a *Brachauchenius* skeleton (Pliosauroida) from the lower Paja Formation (late Barremian) of Villa de Leyva area (Colombia). *Mitt. Mus. Nat.kd. Berl., Geowiss. Reihe* 8:37-51.
- Hampe, O. 2006. Middle/late Miocene hoplocetine sperm whale remains (Odontoceti: Physeteridae) of North Germany with an emended classification of the Hoplocetinae. *Fossil Record* 9(1):61-86.
- Hampe, O., and C. Leimkuhler. 1996. Die Anwendung der Photogrammetrie in der Wirbeltierpalaontologie am Beispiel eines *Kronosaurus*-Fundes in Kolumbien. *Mainzer geowissenschaftliche Mitteilungen* 25:55-78.
- Hurlburt, G. R., A. B. Heckert, and J. O. Farlow. 2003. Body mass estimates of Phytosaurs (Archosauria: Parasuchidae) from the Petrified Forest Formation (Chinle Group: Revueltian) Based on Skull and Limb Bone Measurements. In Z. E. Ziegler, A. B. Heckert, and S. G. Lucas, eds. *Paleontology and Geology of the Upper Triassic (Revueltian)* Snyder

- Quarry, New Mexico. New Mexico Museum of Natural History and Science Bulletin 24, Albuquerque.
- Kaim, A., Y. Kobayashi, H. Echizenya, R. G. Jenkins, and K. Tanabe. 2008. Chemosynthesis-based associations on Cretaceous plesiosaurid carcasses. *Acta Palaeontologica Polonica* 53(1):97-104.
- Kear, B. P. 2007. A juvenile pliosauroid plesiosaur (Reptilia: Sauropterygia) from the Lower Cretaceous of South Australia. *Journal of Paleontology* 81(1):154-164.
- Ketchum, H. F. 2008. The anatomy, taxonomy, and systematics of three British Middle Jurassic pliosaurs (Sauropterygia: Pleiosauria) and the phylogeny of Plesiosauria. Unpublished Ph.D. thesis. University of Cambridge.
- Klinowska, M. 1991. Dolphins, porpoises and whales of the world. The IUCN Red Data Book. IUCN, Gland.
- Knight, W. C. 1895. A new Jurassic plesiosaur from Wyoming. *Science* 2(449).
- Knight, W. C. 1898. Some new Jurassic vertebrates from Wyoming. *American Journal of Science* 4:378-381.
- Legler, J. M. 1981. The taxonomy, distribution, and ecology of Australian freshwater turtles (Testudines: Pleurodira: Chelidae). *National Geographic Society Research Reports* 13:391-404.
- Liggett, G. A., K. Shimada, C. Bennett, and B. A. Schumacher. 2005. Cenomanian (Late Cretaceous) reptiles from northwestern Russell County, Kansas. *PaleoBios* 25:9-17.
- Lingham-Soliar, T. 1995. Anatomy and functional morphology of the largest marine reptile known, *Mosasaurus hofmanni* (Mosasauridae, Reptilia) from the Upper Cretaceous Upper Maastrichtian of the Netherlands. *Philosophical Transactions of the Royal Society of London* 347:155-180.
- Lingham-Soliar, T., and G. Plodowski. 2007. Taphonomic evidence for high-speed adapted fins in thunniform ichthyosaurs. *Naturwissenschaften* 94:65-70.
- Liston, J. J. 2004. An overview of the pachycormiform *Leedsichthys*. Pp. 379-390. *In* G. Arratia, and A. Tintori, eds. *Mesozoic Fishes 3 – Systematics, Paleoenvironments and Biodiversity*.
- Liston, J. J. 2007. A Fish Fit For Ozymandias?: The Ecology, Growth and Osteology of *Leedsichthys* (Pachycormidae, Actinopterygii). PhD Thesis, University of Glasgow.
- Lockyer, C. 1981. Estimates of growth and energy budget for the sperm whale, *Physeter catodon*. *FAO Fish Series* 5(3):489-504.
- Longman, H. A. 1924. A new gigantic marine reptile from the Queensland Cretaceous. *Memoirs of the Queensland Museum* 8:26-28.
- Longman, H. A. 1930. *Kronosaurus queenslandicus* A gigantic Cretaceous Pliosaur. *Memoirs of the Queensland Museum* 10(1):1-7.

- Longman, H. A. 1932. Restoration of *Kronosaurus queenslandicus*. *Memoirs of the Queensland Museum* 10(2):98.
- Longman, H. A. 1935. Palaeontological Notes. *Memoirs of the Queensland Museum* 10(5):236-239.
- MacLeod, C. D. 2002. Possible functions of the ultradense bone in the rostrum of Blainville's beaked whale (*Mesoplodon densirostris*). *Canadian Journal of Zoology* 80:178-184.
- Martill, D. 1992. Pliosaur stomach contents from the Oxford Clay. *Mercian Geologists* 13(1):37-42.
- Martill, D., and D. Naish. 2000. *Walking with Dinosaurs: The Evidence*. BBC Books.
- McGowan, C. 1991. *Dinosaurs, Spitfires and Sea Dragons*. Harvard University Press.
- Meers, M. B. 2002. Cross-sectional geometric properties of the crocodylian humerus: an exception of Wolff's law? *Journal of Zoology* 258:405-418.
- Meers, M. B. 2003. Maximum Bite Force and Prey Size of *Tyrannosaurus rex* and Their Relationships to the Inference of Feeding Behavior. *Historical Biology* 16(1):1-12.
- Molnar, R. E. 1991. Fossil Reptiles of Australia. Pp. 605-701. *In* P. Vickers-Rich, J. M. Monaghan, R. F. Baird, and T. H. Rich, eds. *Vertebrate Palaeontology of Australasia*.
- Motani, R. 1999. Phylogeny of the Ichthyopterygia. *Journal of Vertebrate Paleontology* 19:472-495.
- Motani, R. 2005. Ichthyosauria: evolution and physical constraints of fish-shaped reptiles. *Annual Review of Earth and Planetary Sciences* 33:395-420.
- Motani, R., H. You, and C. McGowan. 1996. Eel-like swimming in the earliest ichthyosaurs. *Nature* 382:347-48.
- Myers, T. J. 2001. Marsupial body mass prediction. *Australian Journal of Zoology* 49:99-118.
- Newman, B., and L. B. Tarlo. 1967. A Giant Marine Reptile From Bedfordshire. *Animals* 10(2):61-63.
- Nicholls, E. L., and M. Manabe. 2004. Giant Ichthyosaurs of the Triassic - a new species of *Shonisaurus* from the Pardonet Formation (Norian: Late Triassic) of British Columbia. *Journal of Vertebrate Paleontology* 24(4):838-849.
- Nicholls, E. L., and A. P. Russell. 1991. The plesiosaur pectoral girdle: the case for a sternum. *N. Jb. Geol. Palaont. Abh.* 182:161-185.
- Noè, L. F. 2001. A Taxonomic and Functional Study of the Callovian (Middle Jurassic) Pliosauroida (Reptilia, Sauropterygia). Unpublished PhD Thesis. University of Derby.

- Noè, L. F., D. T. J. Smith, and D. I. Walton. 2004. A new species of Kimmeridgian pliosaur (Reptilia; Sauropterygia) and its bearing on the nomenclature of *Liopleurodon macromerus*. *Proceedings of the Geologists' Association* 115:13-24.
- Nopsca, F. 1928. The genera of reptiles. *Palaeobiologica* 1:163-188.
- Nyberg, K. G., C. N. Ciampaglio, and G. A. Wray. 2006. Tracing the ancestry of the Great White Shark, *Carcharodon carcharias*, using morphometric analysis of fossil teeth. *Journal of Vertebrate Paleontology* 26(4):806-814.
- O'Keefe, F. R. 2001. A cladistic analysis and taxonomic revision of the Plesiosauria (Reptilia: Sauropterygia). *Acta Zool. Fennica* 213:1-63.
- O'Keefe, F. R., and M. T. Carrano. 2005. Correlated trends in the evolution of the plesiosaur locomotor system. *Paleobiology* 31(4):656-675.
- Owen, R. 1838. A description of Viscount Cole's specimen of *Plesiosaurus macrocephalus* Conybeare. *Quarterly Journal Proc. Geol. Soc. London* 2:663-666.
- Owen, R. 1840. Report on British fossil reptiles. Report of the British Association for the Advancement of Science 9:43-126.
- Phillips, J. 1871. *Geology of Oxford and the valley of the Thames*. Clarendon Press, Oxford.
- Romer, A. S. 1956. *Osteology of the Reptiles*. University of Chicago Press, Chicago.
- Romer, A. S., and A. D. Lewis. 1959. A mounted skeleton of the giant plesiosaur *Kronosaurus*. *Brevoria Museum of Comparative Zoology* 112:1-15.
- Salisbury, S. W., and E. Frey. 2001. A biomechanical transformation model for the evolution of semi-spheroidal articulations between adjoining vertebral bodies in crocodylians. Pp. 85-134. In G. C. Grigg, C. E. Franklin, and F. Seebacher, eds. *Crocodylian Biology and Evolution*. Surrey Beatty & Sons, Chipping Norton.
- Schäfer, W. 1972. *Ecology and Palaeoecology of Marine Environments*. The University of Chicago Press.
- Schmidt-Nielsen, K. 1975. *Animal Physiology*. Cambridge University Press, London.
- Schreer, J. F., and K. M. Kovacs. 1997. Allometry of diving capacity in air-breathing vertebrates. *Canadian Journal of Zoology* 75(3):339-358.
- Seeley, H. G. 1874. Note on some of the generic modifications of the plesiosaurian pectoral arch. *Quarterly Journal of the Geological Society of London* 30:436-449.
- Smith, A. S., and G. J. Dyke. 2008. The skull of the giant predatory pliosaur *Rhomaleosaurus cramptoni*: implications for plesiosaur phylogenetics. *Naturwissenschaften* 95(10): 975-980.

- Storrs, G. W., and M. A. Taylor. 1996. Cranial anatomy of a new plesiosaur genus from the Lowermost Lias (Rhaetian/Hettangian) of Street, Somerset, England. *Journal of Vertebrate Paleontology* 16(3):403-420.
- Storrs, G. W. 1991. Anatomy and relationships of *Corosaurus alcovensis* (Diapsida: Sauropterygia) and the Triassic Alcova Limestone of Wyoming. *Bulletin of the Peabody Museum of Natural History* 44:1-151.
- Tarlo, L. B. 1957. The scapula of *Pliosaurus macromerus* Phillips. *Palaeontology* 1(3):193-199.
- Tarlo, L. B. 1959. *Stretosaurus* gen. nov., a giant pliosaur from the Kimmeridge Clay. *Palaeontology* 2(1):39-55.
- Tarlo, L. B. 1960. A review of the Upper Jurassic pliosaurs. *Bulletin of the British Museum (Natural History), Geology series* 4:145-189.
- Tershy, B. R. 1992. Body Size, Diet, Habitat Use, and Social Behaviour of Balaenoptera Whales in the Gulf of California. *Journal of Mammalogy* 73(3):477-486.
- Thompson, D. W. 1917. *On Growth and Form*. Cambridge University Press.
- Tierney, M., M. Hindell, and G. S. 2002. Energy content of mesopelagic fish from Macquarie Island. *Antarctic Science* 14(3):225-230.
- Trites, A. W., and D. Pauly. 1998. Estimating mean body masses of marine mammals from maximum body lengths. *Journal of Zoology* 76:886-896.
- Tucker, A. D., C. J. Limpus, H. I. McCallum, and K. R. McDonald. 1996. Ontogenetic Dietary Partitioning by *Crocodylus johnstoni* during the Dry Season. *Copeia* 1996(4):978-988.
- Van Valkenburgh, B. 1990. Skeletal and dental predictors of body mass in carnivores. Pp. 181-205. *In* J. Damuth, and B. J. MacFadden, eds. *Body size in mammalian paleobiology: Estimation and biological applications*. Cambridge University Press, Cambridge.
- Wahl, W. R., M. Ross, and J. A. Massare. 2007. Rediscovery of Wilbur Knight's *Megalneusaurus rex* site: new material from an old pit. *Paludicola* 6(2):94-104.
- Watwood, S. L., P. J. O. Miller, M. Johnson, P. T. Madsen, and P. L. Tyack. 2006. *Journal of Animal Ecology*. 2006 75:814-825.
- Webb, G. J. W., and H. Messel. 1978. Morphometric Analysis of *Crocodylus porosus* from the North Coast of Arnhem Land, Northern Australia. *Australian Journal of Zoology* 26:1-27.
- Welles, S. P. 1943. Elasmosaurid Plesiosaurs with description of new material from California and Colorado. *Memoirs of the University of California* 13(3):125-254.
- Welles, S. P. 1952. A review of the North American Cretaceous Elasmosaurs. *University of California Publications in Geological Sciences* 29(3):46-144.
- White, T. 1935. On the skull of *Kronosaurus queenslandicus* Longman. *Boston Soc. Natural History, Occ. Papers* 8:219-228.

- White, T. 1940. Holotype of *Plesiosaurus longirostris* Blake and the classification of the plesiosaurs. *Journal of Paleontology* 14:451-467.
- Williams, P. L., and R. Warwick, eds. 1980. *Gray's Anatomy*, 36th Edition. Churchill Livingstone, Philadelphia.
- Williston, S. W. 1903. North American Plesiosaurs (Part 1). *Field Columbian Museum, Publ. 73, Geological Series 2(1):1-79.*
- Williston, S. W. 1907. The skull of *Brachauchenius*, with special observations on the relationships of the plesiosaurs.
- Williston, S. W. 1925. *The Osteology of the Reptiles*. Harvard University Press, Cambridge, Mass.
- Wroe, S., M. Crowther, J. Dortch, and J. Chong. 2004. The size of the largest marsupial and why it matters. *Proceedings of the Royal Society, London, Series B (Suppl.)* 271:S34-S36.
- Wroe, S., D. R. Huber, M. Lowry, C. McHenry, K. Moreno, P. Clausen, T. L. Ferrara, E. Cunningham, M. N. Dean, and A. P. Summers. 2008. Three-dimensional computer analysis of white shark jaw mechanics: How hard can a great white bite? *J. Zoology Online*.
- Wroe, S., C. McHenry, and J. Thomason. 2005. Bite club: comparative bite force in big biting mammals and the prediction of predatory behaviour in fossil taxa. *Proceedings of the Royal Society of London, Series B* 272:619-625.
- Wroe, S., T. Myers, F. Seebacher, B. P. Kear, A. Gillespie, M. Crowther, and S. W. Salisbury. 2003. An alternative method for predicting body-mass: The case of the marsupial lion. *Paleobiology* 29:404-412.

